

SUMMARY OF SKYLAB S-193

ALTIMETER ALTITUDE RESULTS

(NASA-TM-X-69355) SUMMARY OF SKYLAB S-193
ALTIMETER ALTITUDE RESULTS (NASA) - 324 p HC
\$9.25 CSCL 05B

N75-21776

Unclass
20301

G3/43

by: J.T. McGoogan and C.D. Leitao

National Aeronautics and Space Administration

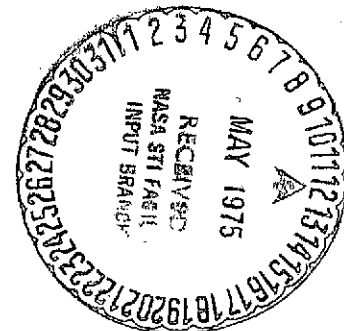
Wallops Flight Center

Wallops Island, Va. 23337

and: W.T. Wells

Wolf Research and Development Corp.

Riverdale, Md. 20840



NATIONAL AERONAUTICS AND SPACE ADMINISTRATION

WALLOPS FLIGHT CENTER

WALLOPS ISLAND, VIRGINIA 23337

February 1975

1. Report No. NASA TM X-69355		2. Government Accession No.		3. Recipient's Catalog No.	
4. Title and Subtitle SUMMARY OF SKYLAB S-193 ALTIMETER ALTITUDE RESULTS				5. Report Date February 1975	
				6. Performing Organization Code	
7. Author(s) J. T. McGoogan & C. D. Leita, (NASA Wallops Flight Center, Wallops Island, Va.) W. T. Wells (Wolf Research and Development Corp., Riverdale, Md.)				8. Performing Organization Report No.	
				10. Work Unit No.	
9. Performing Organization Name and Address National Aeronautics and Space Administration Wallops Flight Center Wallops Island, Virginia 23337				11. Contract or Grant No.	
				13. Type of Report and Period Covered Technical Memorandum	
12. Sponsoring Agency Name and Address National Aeronautics and Space Administration Washington, D.C. 20546				14. Sponsoring Agency Code	
15. Supplementary Notes					
16. Abstract This document presents the SKYLAB S-193 altimeter altitude results in a concise format for further use and analysis by the scientific community. The altimeter mission and instrumentation is described. The altimeter processing techniques and values of parameters used for processing are included. The determination of reference orbits is discussed and the tracking systems utilized for the results in this document are tabulated. Techniques for determining satellite pointing are presented and a tabulation of pointing for each data mission included. The geographical location, the ocean bottom topography, the altimeter determined ocean surface topography and the altimeter automatic gain control history is presented. Finally, some typical applications of this data are suggested.					
17. Key Words (Suggested by Author(s)) Geodesy, Geoids, Oceanography, Tectonics, Petrology, Topography, Gravimetry, Geology, Earth Planetary Structure, Geophysics				18. Distribution Statement Unclassified - Unlimited STAR Category 43	
19. Security Classif. (of this report) Unclassified		20. Security Classif. (of this page) Unclassified		21. No. of Pages 323	
				22. Price*	

ACKNOWLEDGEMENTS

These experimental results would not be possible without the work of many individuals, we wish to acknowledge those persons who have made particularly important contributions. First, L. S. Miller of Applied Science Associates, Apex, North Carolina, has provided leadership and assistance in every phase of this experiment from design concept through data analysis. In this document he has directly contributed to the understanding and quantifying of the time bias and sea surface bias errors. The waveform results are based on work of G. S. Hayne, and G. S. Brown also of Applied Sciences Associates.

B. S. Yapple and D. L. Hammond of NRL have made substantial contributions throughout the planning and hardware phases of the program. At NASA Goddard Space Flight Center, we are grateful to I. Salzberg for supplying the S-band data used in orbit determination and J. G. Marsh for furnishing the geoid model that was used for altimeter comparisons. Over the past several years, E. L. Hofmeister and T. Godby at General Electric Company, Utica, New York (the altimeter contractor) have provided valuable discussions of the altimetry hardware design characteristics. We wish to thank the NASA Johnson Space Center personnel and, in particular, N. M. Hatcher and C. K. Williams (deceased) for assistance in mission planning and in data acquisition.

Other contributions have come from NASA Wallops Flight Center personnel. In particular R. G. Forsythe has been instrumental in making the waveform processing software operational and has provided assistance in the processing of the data.

TABLE OF CONTENTS

	Page
INTRODUCTION	1
Purpose	1
Scope	1
MISSION DESCRIPTION	2
INSTRUMENT DESCRIPTION	3
DATA PROCESSING	4
MODE CHANGE CORRECTIONS.	6
ORBIT DETERMINATION	11
POINTING DETERMINATION	45
Analysis of Waveform Trailing Edge.	45
Analysis of Tracking Response and AGC	47
Pointing Data Summary	51
ERROR BUDGET	59
Instrument Errors	59
Pointing.	65
Sea Surface	65
Atmosphere.	65
Orbit Error	66
System Accuracy	66
DATA SUMMARY	69
RESIDUALS AND BOTTOM TOPOGRAPHY.	81
AUTOMATIC GAIN CONTROL	231
APPLICATIONS	307
Correlation with Ocean Floor Topography	308
Geological Structure.	308
Current Detection	308
Long Arc Analysis	309
Geoid Construction	313
Altitude Data Filtering	319
REFERENCES	323

PRECEDING PAGE BLANK NOT FILMED

INTRODUCTION

Purpose

The purpose of this document is to present the SKYLAB S-193 altimeter altitude results in a concise format for further use and analysis by the Scientific Community. Therefore, extreme care has been used to preserve the integrity of this data. The instrument and processing techniques are described for the users benefit. In addition, errors and techniques required to use these measurements in geodetic applications are discussed.

Scope

The data contained in this report has been obtained from all three SKYLAB missions (SL-2, SL-3, SL-4). No attempt is being made to present a complete analysis of all the data or to suggest the proper interpretation. However, some suggestions that might be useful to the data user are made and it is hoped that these will be helpful. All results included are based on work done at Wallops Flight Center.

MISSION DESCRIPTION

The SKYLAB altimeter was the first of a series of satellite altimeters planned over the next decade devoted primarily to geodesy and oceanography [1]. This paper will describe the design criteria and the role of the operating modes of the SKYLAB instrument. The sensor technology to be gained by this instrument is described along with the status of results. Some of the present and possible near future applications for the data are presented and some of the current capabilities for fulfilling these applications are mentioned. In addition the prime objectives related to altimetry in the NASA Earth and Ocean Physics Program are highlighted. Throughout this paper an effort is made to show how the SKYLAB mission fits into the overall program.

The S-193 altimeter experiment was conceived to develop satellite altimeter sensor technology for a series of altimeter missions including GEOS-C (1975), SEASAT-A (1978) and SEASAT-B (1980's). The long term objectives of satellite altimetry were stated in the 1969 Williamstown study [2] on Solid Earth and Ocean Physics and the 1972 Earth and Ocean Physics Applications Program (EOPAP) report. These studies call for development of a synoptic satellite altimeter exhibiting 10 cm accuracy with at least 1° (100 km) spatial resolution.

As one can readily see the goals are not merely the development of instrumentation but must include the techniques required to make the whole satellite system perform to the requirements. Models were developed for mean waveshapes, radar cross sections (σ_0), pointing, sea state, and time correlation. In addition, a system error budget was developed. The SKYLAB altimeter experiment was designed with system flexibility oriented so that experience with various possible error sources might be obtained. For example, pointing effects were studied by moving the antenna, footprint and bandwidth were studied by varying pulsewidth and bandwidth. Time correlation was studied by varying pulse spacing with a double pulse transmission. Return signals from conventional and pulse compression transmission techniques are also compared.

INSTRUMENT DESCRIPTION

Geometrically the instrument system consisted of a space platform (the SKYLAB satellite) and a radar altimeter oriented to make vertical (nadir) measurements of the distance from the satellite to the ocean surface. While the SKYLAB orbit (440 km height, eccentricity .001 and inclination 50°) was not an ideal reference system for long arc geodetic measurements, it did represent an excellent test bed for altimeter sensor development and short arc topography measurements. The low orbit, payload weight, and size capacity made it possible to build a radar system with good signal-to-noise and instrument versatility and flexibility. Therefore, the S-193 altimeter system was optimized to provide a variety of measurements under various operating parameters. Within the hardware [1,2] five basic modes were developed to perform various pre-set data taking and calibration operations to gather data needed to design improved altimeters for future space missions. Basically, the five experimental modes can be summarized as follows: (For more detail see Table 2.)

TABLE 1. SKYLAB ALTIMETER MODES

<u>Mode</u>	<u>Unique Features</u>	<u>Prime Data Generated</u>
1. Pulse Shape	.5° Step in Antenna Position Wide Receiver Bandwidth	Sample and Hold Altitude AGC
2. σ_0 (Radar-Cross-Section)	12 db Step (AGC Calibration) Antenna Position 0°, 1/2°, 15.6°, 8°, 3°, 1.5°, 0°	Sample and Hold AGC
3. Time Correlation	Two Pulsewidths Double Pulse Operation Spacings 1, 19.2, 76.8, 153.6, 408.6, 819.1 (Micro Seconds)	Sample and Hold Altitude
5. Pulse Compression	Three Pulsewidths 10 ns 10 ns (compressed) 100 ns	Sample and Hold AGC Altitude
6. Nadir Alignment	Slow Spiral Drive	AGC

The most important measurements provided by the altimeter consist of altitude, waveforms and Automatic Gain Control voltage (AGC). The altitude measurements are made approximately 8 times per second with a 2 Hz bandwidth tracking system. The spatial footprint (spot size) was about a 3 km radius for the narrow pulse operation which represents a two dimensional filter for topography mapping missions. Wide pulse operation represents about an 8 km radius filter.

The waveforms were sampled by eight moveable sample-and-hold gates placed at regular intervals on the return signals. These gates can sample the return waveform 100 times per second and can be utilized for wave height and antenna pointing angle estimation.

The AGC is available approximately 4 times per second and is useful to calibrate the above waveforms and to detect clouds, rain and other anomalies which affect signal strength.

DATA PROCESSING

The PCM analog tape was converted by NASA Johnson Space Center to a digital format and both editing and decommutation were performed (see JSC TR 524 documentation). In addition, the airlock module time (AMT) of each frame of data was converted to GMT. The raw altimeter two-way range bit data (20 bits) was converted to measured altitude bit data (21 bits) by making the 21st high order bit a one if the 20th high order bit was a zero. Finally, the following algorithm was used to convert bits to kilometers [1]:

$$A_m = [(21 \text{ bits}) \times BW + ID] \times (C/2)$$

where: BW = bit weight, 2.5×10^{-9} sec/bit,
 ID = estimate of the internal system delay
 40×10^{-9} sec for SL-2, 3
 -195×10^{-9} sec for SL-4, and
 C = speed of light, 299792.5 km/sec.

A processed digital tape with frame GMT, measured altitude and other altimeter measurements, statuses and housekeeping data was sent to approved investigators.

After the tape was received from Johnson Space Center, it was converted to a format compatible with Wallops Honeywell 625 Computer. Then, the following algorithm was used to preprocess the altitude data:

$$A_c = A_m - (ID \times \frac{C}{2}) + (PMICM - MICDS3) + MC-R$$

where A_c = corrected altitude,
 A_m = measured altitude provided by Johnson Space Center

$ID \times \frac{C}{2}$ = correction to remove internal system delay correction
 made by Johnson Space Center,
 PMICM = premission internal system calibrate measurement broken
 down as follows:
 2624000 ns base delay
 -95 ns {calibrate vs data path difference (-85 ns)
 {rectangular vs triangular pulse difference (-10 ns)
 2623905 ns
 MICDS3 = measurement obtained in MODE 1, calibration Data Step 3
 (altitude calibrate mode used to gather). This measured
 approximately 2624105 ns, (data on altimeter aging effects).
 MC = error caused by switching pulsewidths, bandwidths, and pointing
 with certain modes and submodes, and
 R = tropospheric refraction correction.

The magnitudes of the different corrections vary. For example, the system inflight calibration correction obtained was approximately 30 m with an uncertainty of less than 20 cm detected in evaluating the third term in the algorithm. The pulsewidth/bandwidth correction varies from 0 to 103 ns (0-16 m) depending on the mode and submode used, and the pointing angle correction being used in Mode 1 is approximately 13 ns (2 m). The refraction model,

$$R = \frac{2.77(N)}{328.5 (.026) + \sin E},$$

assumes a constant surface refractivity of 340 N units, and E is 90 degrees when looking at nadir. This results in a correction of 2.79 m.

Unified S-Band (USB) data was used to estimate orbital parameters. The orbital elements are used as initial conditions to integrate an orbit from which altimeter measurement residuals are calculated. The residuals are the differences between the altimeter measurements to the sea surface and the calculated altitude from the spacecraft to the ellipsoid. Finally, the altitude residuals, and both the GEM 6 geoid and ocean bottom topography along the subsatellite track were merged and plotted for further analysis. Figure 1 illustrates the data flow.

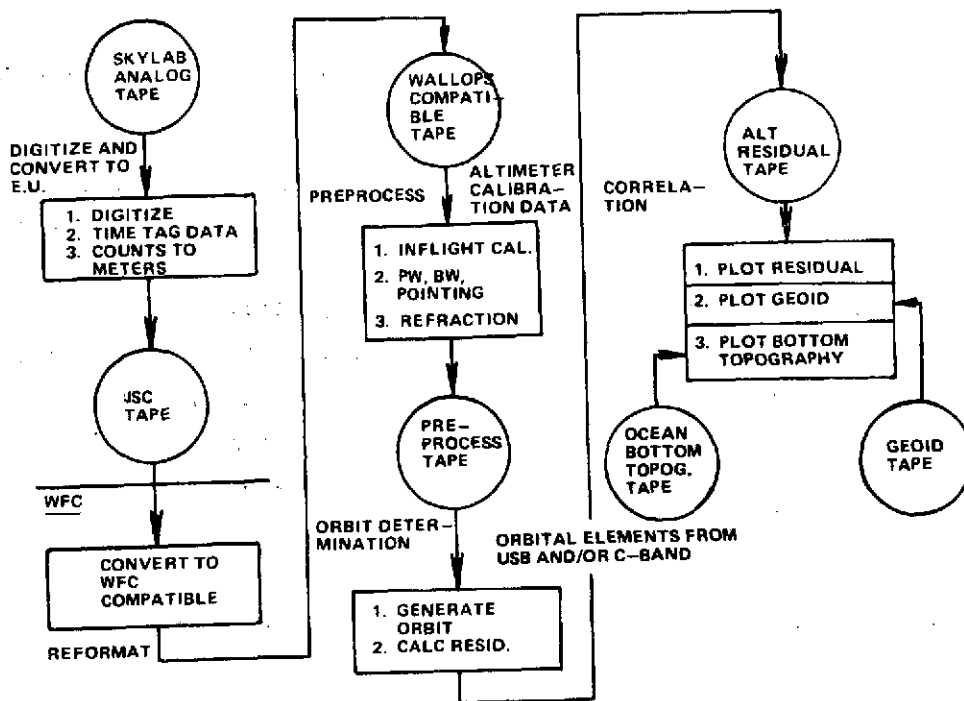


Figure 1 Skylab Altitude Data Flow

MODE CHANGE CORRECTIONS

Mode change corrections are applied during automatic processing to correct for pulsewidth, bandwidth, and other operating parameter changes that cause altitude bias. The corrections utilized were based on pre-mission measurements. These corrections were not sufficient because the mission operating parameters were slightly different from the pre-mission conditions. For example, satellite pointing errors often changed the radar return waveforms significantly. Therefore, the best mode change corrections were felt to be available from the data itself. These were obtained by differencing the mean residuals on each side of a known mode change. It should be noted that mode changes should not produce a bias from data pass to data pass since all altimeter modes start out with the same basic operating parameters. Any altimeter bias noted from pass to pass is probably due to pointing errors, and the correction for this effect is discussed in the Pointing Determination Section.

To assist the user of the results in this report, a set of typical mode times sequences is supplied in Table 2. If one suspects that an altitude jump is due to a mode change, the appropriate AGC plot should be examined for sharp change in signal level. In addition, these changes in signal level can be aligned with the Table 2 events to confirm a mode change.

ORIGINAL PAGE IS
OF POOR QUALITY

Table 2
Altimeter Modes

MODE 1 PULSE SHAPE EXPERIMENT														
TRANSMITTER				ANT.	RECEIVER		SIGNAL PROC.	SQUARE LAW SAMPLING						TYPICAL RUNNING TIME SEC.
SUB-MODE	PULSE MODE	FREQ. GHz	PULSE WIDTH NSEC.	POINTING ANGLE DEGREES	IF FILTER BANDWIDTH MHz	CAL. PATH ATTN. dB	ALTITUDE TRACK OR COUNTER	# OF SAMPLE POSITIONS	# OF S&H GATES PER POSITION	S&H GATE SPACING NSEC.	RETURNS SAMPLED PER FRAME	# OF FRAMES OF DATA	# OF SAMPLES OBTAINED	
(0) DAS-1	Single-250 pps	13.9	100	Sub-Satellite	10	N/A	Alt. Track	3	8	25	104	50	41,600	52.00
(1) DAS-2	"	"	"	"	100	"	"	"	"	"	"	61	50,752	63.44
(2) DAS-3	"	"	"	0.431° Pitch	"	"	"	"	"	"	"	61	50,752	63.44
(3) CDS-1	"	"	"	N/A	"	*	Alt. Counter	2	"	"	"	7	5,824	7.28
(4) CDS-2	"	"	"	"	10	*	"	"	"	"	"	5	4,160	5.2
(5) CDS-3	"	"	"	"	"	*	Alt. Track	"	"	"	"	5	4,160	5.2

NOTES: • 1 Frame = 1.04 SEC. (192 INCL 2 DUMMY +)
 • DATA/TOTAL FRAMES: 172/192 (1 END OF MODE FRAMES)
 • TOTAL RUNNING TIME FOR DATA FRAMES: 178.88 SEC
 • TOTAL MODE RUNNING TIME: 199.68 SEC. (INCL. DUMMY + ECM FRAMES)
 • SAMPLE GATE POSITIONS RELATIVE TO THE TRACKER POSITION ARE INDEXED BY S²M.

* W/G Attenuation
 nominal = 119 ± 1 dB
 S-193 SN1 Atten. = 118.49 dB

Table 2
Altimeter Modes (Continued)

MODE 2 CROSS-SECTION EXPERIMENT														
TRANSMITTER				ANT.	RECEIVER		SIGNAL PROC. SQUARE LAW SAMPLING							
SUB-MODE	PULSE MODE	FREQ. GHz	PULSE WIDTH NSEC.	POINTING ANGLE DEGREES	IF FILTER BANDWIDTH MHz	CAL. PATH ATTEN. dB	ALTITUDE TRACK OR COUNTER	# OF SAMPLE POSITIONS	# OF S&H GATES PER POSITION	S&H GATE SPACING NSEC.	RETURNS SAMPLED PER FRAME	# OF FRAMES OF DATA	# OF SAMPLES OBTAINED	TYPICAL RUNNING TIME SEC.
(0) DAS-1	Single-250 pps	13.9	100	Sub-Satellite	10	N/A	Alt. Track	3	8	25	104	10	8,320	10.4
(1) DAS-2	"	"	"	0.431°	"	"	Disabled, held at DAS-1 Range	1	"	"	"	30	24,960	31.2
(2) DAS-3	"	"	"	15.6°	"	"	"	"	"	"	"	30	24,960	31.2
(3) DAS-4	"	"	"	7.564°	"	"	"	"	"	"	"	30	24,960	31.2
(4) DAS-5	"	"	"	2.652°	"	"	"	"	"	"	"	30	24,960	31.2
(5) DAS-6	"	"	"	1.3°	"	"	"	"	"	"	"	30	24,960	31.2
(6) DAS-7	"	"	"	Sub-Satellite	"	"	Alt. Track	3	"	"	"	7	5,824	7.28
(7) CDS-1	"	"	"	N/A	"	** (~130dB)	Alt. Counter	2	"	"	"	7	5,824	7.28
(8) CDS-2	"	"	"	"	100	** (~130dB)	"	3	"	10	"	7	5,824	7.28
(9) CDS-3	"	"	"	"	"	* (~119dB)	"	"	"	"	"	7	5,824	7.28

NOTES: • 1 FRAME = 1.04 SEC.
 • DATA/TOTAL FRAMES: 167/191 (INCLUDES 2 DUMMY + 1 EOM FRAMES)
 • TOTAL RUNNING TIME FOR DATA FRAMES: 173:68 SEC.
 • TOTAL MODE RUNNING TIME = 198.64 (INCLUDING DUMMY & EOM FRAME)
 • SAMPLE GATE POSITIONS RELATIVE TO THE TRACKER POSITION ARE INDEXED BY S²M.

** Internal ALT + W/G Attenuation in Cal Submodes
 nominal = (11 ± 1)dB + (119 ± 1)dB
 S-193 SMI Atten = 10.6 ± dB + 118.49 dB = 129.09 dB
 * W/G Attn in Cal Submode = 119 ± 1dB (nominal)
 S-193 SMI Attn = 118.49 dB
 ‡ 10.8 dB @ -20°C & +50°C

ORIGINAL PAGE IS
OF POOR QUALITY

Table 2
Altimeter Modes (Continued)

MODE 3 TIME CORRELATION EXPERIMENT														
TRANSMITTER				ANT.	RECEIVER		SIGNAL PROC.	SQUARE LAW SAMPLING						TYPICAL RUNNING TIME SEC.
SUB-MODE	PULSE MODE	FREQ. GHz	PULSE WIDTH NSEC.	POINTING ANGLE DEGREES	IF FILTER BANDWIDTH	CAL. PATH ATTEN. dB	ALTITUDE TRACK OR COUNTER	** # OF SAMPLE POSITIONS	# OF S&H GATES PER POSITION	S&H GATE SPACING NSEC.	RETURNS SAMPLED PER FRAME	# OF FRAMES OF DATA	# OF SAMPLES OBTAINED	
(0) CDS-1	DUAL-250 pulse pairs/sec	13.9	100	N/A	100	*	Alt. Counter	6	4	25	208	23	19,136	23.92
(1) CDS-2	"	"	20	"	"	*	"	8	"	10	"	25	20,800	26.0
(2) CDS-3	Single 250 pps	"	100	"	10	*	"	2	8	25	104	3	2,496	3.12
(3) DAS-1	"	"	"	Sub-Satellite	"	N/A	Alt. Track	3	"	"	"	16	13,312	16.64
(4) DAS-2	DUAL-250 pulse pairs/sec	"	"	"	100	"	"	8	4	"	208	25	20,800	26.0
(5) DAS-3	"	"	20	"	"	"	"	16	"	10	"	98	81,536	101.92
(6) CDS-4	"	"	100	N/A	"	*	Alt. Counter	6	"	25	"	20	16,640	20.8
(7) CDS-5	"	"	20	"	"	*	"	8	"	10	"	25	20,800	26.0

* W/G Attenuation in Cal Submodes

nominal = 119 ± 1 dB

S-193 SW1: Attn = 118.49 dB

NOTES: * 1 FRAME = 1.04 SEC.

• DATA/TOTAL FRAMES 139/238 (238 INCL. 2 DUMMY + 1 EOM)

• TOTAL RUNNING TIME FOR DATA FRAMES: 144.56 SEC.

• TOTAL MODE RUNNING TIME = 247.52 SEC (INCL DUMMY & EOM FRAMES)

• PULSE PAIRS IN SM'S 0,1,4,5,6 & 7 HAVE PULSE SEPARATIONS 819.25, 409.65, 153.65, 76.85, 19.25, 1.05 MSEC IN CONSECUTIVE ORDER INDEXED BY THE S³M.

• SAMPLE GATE POSITIONS RELATIVE TO THE TRACKER POSITION ARE INDEXED BY THE S⁴M.

** Number of sample positions are doubled for Dual Pulse SMs (i.e. Start of each S&H group is considered a gate position)

Table 2
Altimeter Modes (Continued)

MODE 5 PULSE COMPRESSION - 20 NANOSECOND EXPERIMENT														
SUB-MODE	TRANSMITTER			ANT.	RECEIVER		SIGNAL PROC.	SQUARE LAW SAMPLING						TYPICAL RUNNING TIME SEC.
	PULSE MODE	FREQ. GHz	PULSE WIDTH NSEC.	POINTING ANGLE DEGREES	IF FILTER BANDWIDTH MHz	CAL. PATH ATTEN. db	ALTITUDE TRACK OR COUNTER	# OF SAMPLE POSITIONS	# OF S&H GATES PER POSITION	S&H GATE SPACING NSEC.	RETURNS SAMPLED PER FRAME	# OF FRAMES OF DATA	# OF SAMPLES OBTAINED	
(0) DAS-1	Single-250 pps	13.9	100	Sub-Satellite	10	N/A	Alt. Track	3	8	25	104	16	13,312	16.64
(1) DAS-2	"	"	130 (PC)	"	100	"	"	4	"	10	104	99	82,368	102.96
(2) DAS-3	"	"	20	"	"	"	"	"	"	"	104	51	42,432	53.04
(3) CDS-1	"	"	"	N/A	"	*	Alt. Counter	2	"	"	104	7	5,824	7.28
(4) CDS-2	"	"	130 (PC)	"	"	*	"	3	"	"	104	7	5,824	7.28
(5) CDS-3	"	"	100	"	10	*	"	2	"	25	104	5	4,160	5.20

NOTES: • 1 FRAME = 1.04 SEC.
 • DATA/TOTAL FRAMES: 166/188 (188 INCL. 2 DUMMY & 1 EOM FRAMES)
 • TOTAL RUNNING TIME FOR DATA FRAMES: 172.64 SEC.
 • TOTAL MODE RUNNING TIME: 195.52 SEC (INCL DUMMY + EOM FRAME)
 • SAMPLE GATE POSITIONS ARE INDEXED BY S²M

* W/G Attenuation in Cal Submodes
 nominal = 119 ± 1 dB
 S-193 SN 1 Attn = 118.89 dB

NADIR ALIGN														
(0) N/A	Single-250 pps	13.9	100	Scanning	10	N/A	Free to Track *	N/A	N/A	N/A	N/A	192	None	199.68

* TRACKING NOT REQUIRED FOR MODE SEQUENCING TO OCCUR

NOTE: 1 FRAME = 1.04 SEC. MODE RUNNING TIME = 202.8 SEC. (INCL. 2 DUMMY & 1 EOM FRAME)

ORBIT DETERMINATION

Analysis and evaluation of the SKYLAB altimeter data can best be accomplished by reducing the measurements to quantities which can be compared with independently derived data. Since the ocean surface, except for tidal and wind effects, follows an equipotential surface, it is convenient to derive an estimate of the geoid height from the altimeter altitude measurements. These can then be compared with an independent determination of the geoid height. The relationship between geoid height (h_g) and satellite altitude measurements is given by:

$$h_g = h_s - h_a - \Delta h$$

Where h_s = satellite height above a reference spheroid obtained from the satellite orbit determined from tracking data,

h_a = satellite altitude measured by the altimeter,

and

Δh = dynamic ocean effects of tides, winds and currents.

The relationship of these quantities is shown in Figure 2.

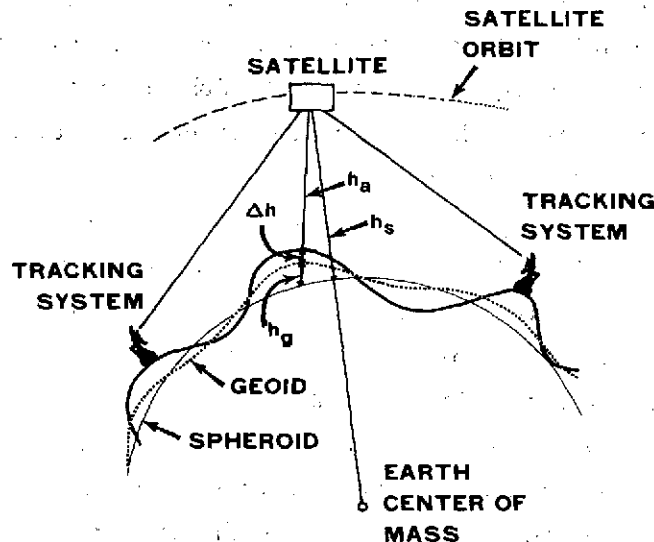


Figure 2 The Determination of Geoid Heights From Altimeter Data

It is obvious from this relationship that any radial orbit errors will propagate directly into errors in geoid heights determined from the data. Therefore, for analysis and evaluation of the SKYLAB altimeter data it was necessary to obtain the most accurate orbit possible from the available tracking data.

Several factors make the determination of accurate SKYLAB orbits a difficult task. The altitude of the SKYLAB orbit was approximately 440 KM and its effective area was 293 square meters with a mass of 87,441 kg. These factors meant that atmospheric drag has a large effect on the satellite orbit. In addition, thrusting is used for spacecraft maneuvers both before and after the altimeter data is acquired. The tracking data was provided by the Goddard Space Flight Center, unified S-Band System (USB) with some C-Band support. The USB system is a worldwide system, but due to workload and scheduling every station did not track at every opportunity, and hence the density of tracking data was sometimes sparse in the vicinity of an altimeter data take.

Error analyses have shown [3] that in order to minimize systematic error effects due to drag, thrusting and geopotential errors, the length of arc fitted should be kept as short as possible. The arc length necessary to be able to determine an orbit with reasonably low error depends on the available tracking coverage. Experience has shown that this can vary from 2 hours (SL-2 Pass 6) to 25 hours (SL-2 Pass 4). The difference in the effects of systematic errors on these two orbits is estimated to be less than a meter due to drag on the 2 hour orbit and 50 meters on the 25 hour orbit.

The tracking station locations and other relevant constants used for orbit determination are presented in Table 3. The gravity field used was the complete GEM-1 model described in [4]. The tracking data used for each orbit is summarized on pages 17 to 44. Table 3 on the following page entitled "Orbit Comparisons for SKYLAB" illustrates the success of this approach to orbit determination for altimeter data analysis. The table compares the GEM-1 short arc results with two day orbital fits using the GEM-6 model and additionally with the model used by Johnson Space Center to obtain SKYBET (SKYLAB Best Estimate of Trajectory Computer Program) orbits. The Johnson Space Center model is a very truncated five term gravity model which is adequate for operational orbits but clearly inadequate for detailed altimeter data analysis.

For each orbit obtained, a comparison error analysis was performed. The effects of station location errors, gravity model errors and refraction errors were calculated and propagated into effects on the calculated satellite altitude. The maximum value during an altimeter data take was used as an orbit quality number. This orbit quality number is listed on the "Pointing Correction Summary Tables."

For short data spans, radial orbit errors can introduce a bias and tilt in a geoid obtained from the altimeter observations. As an illustration, Figure 3 shows the altimeter geoid obtained from two different orbits with different arc lengths and different amounts of tracking data.

While some of the differences between the altimeter geoid and the GEM-6 geoid can be explained by orbit error, there are others which could be due to medium wavelength GEM-6 geoid errors. Figure 4 illustrates such a case with two segments of altimeter data in an area northwest of Australia.

<u>LOCATION</u>	<u>GEODETTIC LATITUDE</u>			<u>EAST LONGITUDE</u>			<u>SPHEROID HEIGHT</u>	<u>ABBREVIATION</u>
	DEG	MN	SECONDS	DEG	MN	SECONDS	(METERS)	
GOLDSTONE, California	35	20	29.647	243	7	35.0	928.6	GDS
TEXAS, Corpus Christie	27	39	13.0	262	37	16.9	- 36.4	TEX
BERMUDA ISLAND	32	21	5.0	295	20	31.9	- 22.4	BDA
MADRID, Spain	40	27	19.9	355	49	53.5	824.5	MAD
HONEYSUCKLE, Australia	-35	-35	- 0.0	148	58	40.1	1141.3	HSK
HAWAII ISLAND	22	7	34.1	200	20	5.4	1145.6	HAW
CANARY ISLAND	27	45	52.4	344	21	57.8	190.2	CYI
CARNARVON, Australia	-24	-54	-23.7	113	43	32.0	16.8	CRO
GUAM ISLAND	13	18	38.1	144	44	12.5	125.3	GWM
MERRITT ISLAND, Florida	28	30	29.7	279	18	23.8	- 54.8	MIL
ASCENSION ISLAND	- 7	-57	-17.2	345	40	22.5	538.2	ACN

CONSTANTS USED FOR ORBIT DETERMINATION

Semi Major Axis = 6378155.00 meters

Flattening = 1./298.255

Drag Coefficient = 2.0000

Reflectivity = 1.500

Satellite Cross Sectional Area = 293.3 m²

Satellite Mass (Kilograms) = 87440 Kg

TABLE 3. TRACKING STATION LOCATIONS AND ABBREVIATIONS USED FOR ORBIT DETERMINATION

Y M D
73 09 13

	GEM 1 SHORT ARC	GEM 6 2 DAY ARC ORBIT 1	GEM 6 2 DAY ARC ORBIT 2	HOUSTON GRAV 2 DAY ARC ORBIT 1	HOUSTON GRAV 2 DAY ARC ORBIT 2
		<u>COMPUTED</u>	<u>SKYLAB ALTITUDE</u>	(METERS)	
19 ^h 43 ^m	431616.2	431628.6	431597.9	431678.6	431680.6
44 ^m	891.1	902.1	873.0	958.7	962.6
45 ^m	432120.8	432130.2	432102.7	432193.0	432198.8
46 ^m	278.7	314.5	288.7	383.2	390.7
47 ^m	451.9	457.9	434.0	532.2	541.5
48 ^m	560.3	564.7	542.8	644.5	655.5

DIFFERENCES FROM GEM 1 SHORT ARC

19 ^h 43 ^m	12.4	-18.3	62.4	64.4
44 ^m	11.0	-18.1	67.6	71.5
45 ^m	9.4	-18.1	72.2	78.0
46 ^m	7.7	-18.1	76.4	83.9
47 ^m	6.0	-17.9	80.3	89.6
48 ^m	4.4	-17.5	84.2	95.2

TABLE 4. ORBIT COMPARISONS FOR SKYLAB

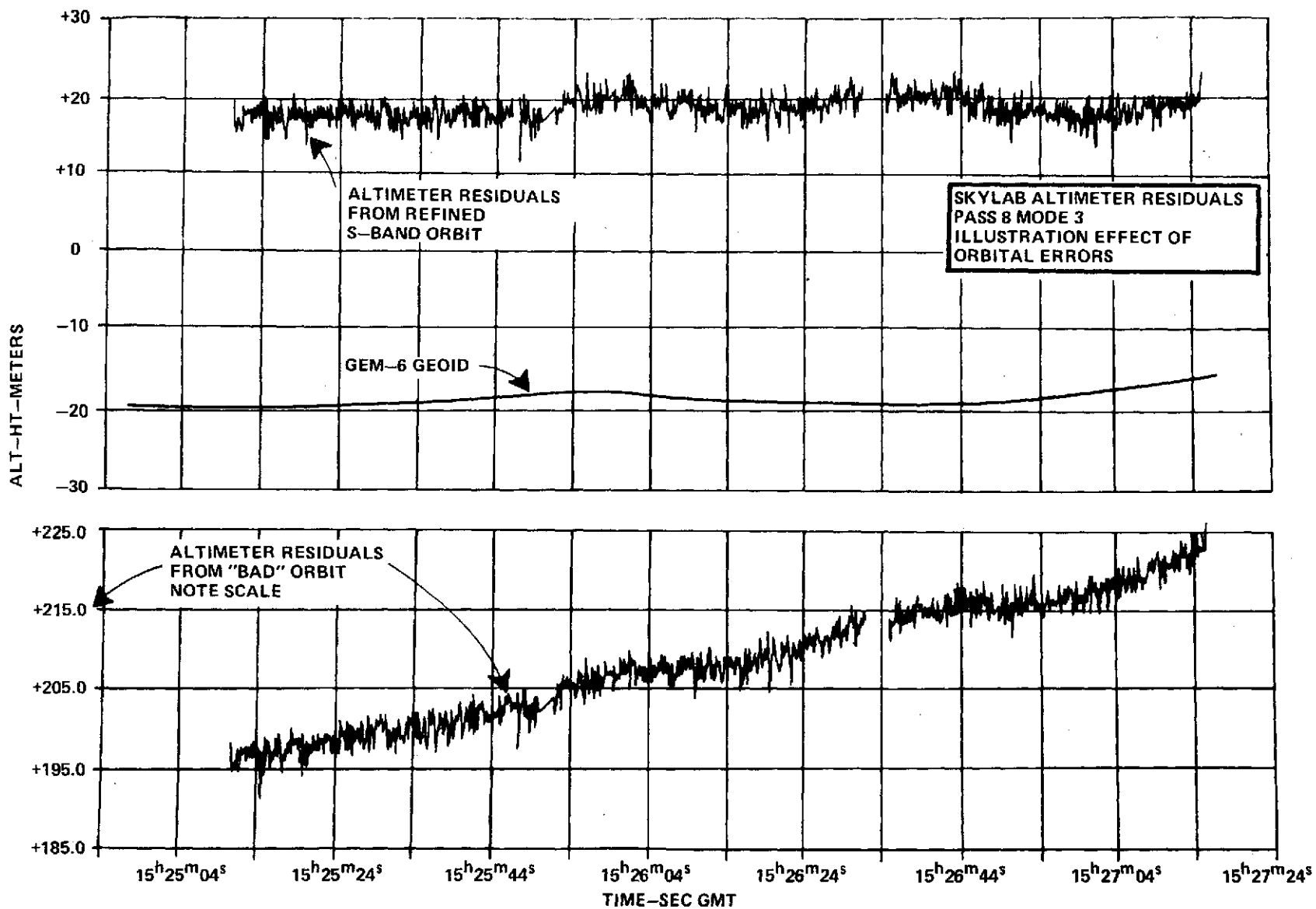


FIGURE 3. ILLUSTRATION EFFECT OF ORBITAL ERRORS

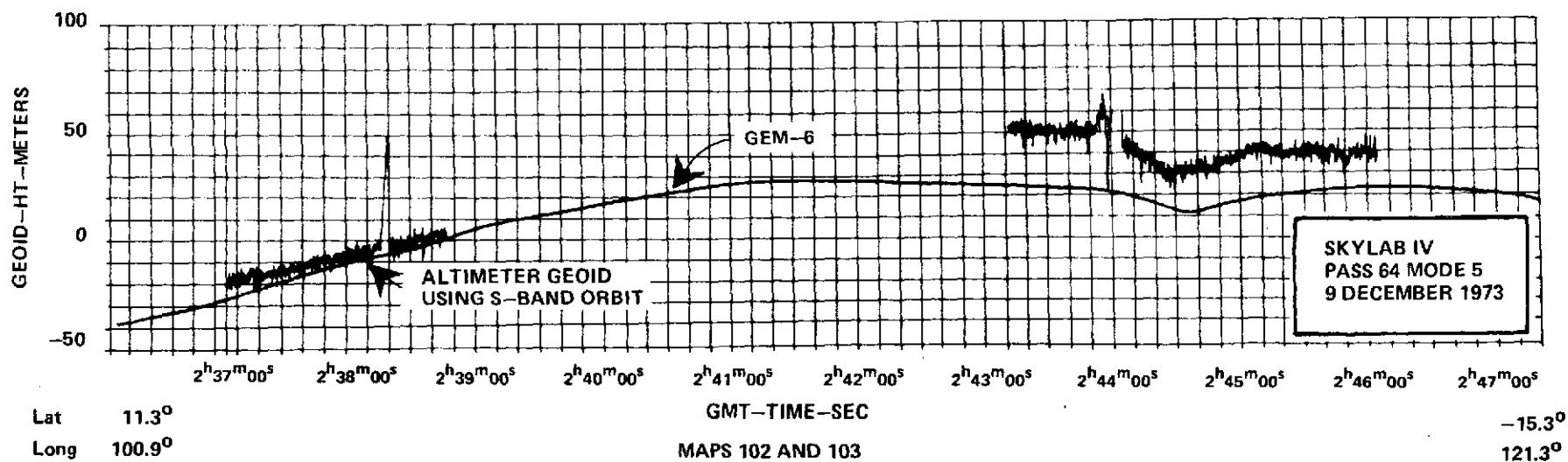


FIGURE 4. COMPARISON OF GEM-6 GEOID AND ALTIMETER GEOID FOR 2 DATA SEGMENTS OF PASS 64

ORIGINAL PAGE IS
OF POOR QUALITY



ARC LENGTH FOR ORBIT DETERMINATION $0^h 33^m$
TRACKING SCHEDULE AND ALTIMETER DATA TAKES
SL-2 PASS 1 30 MAY 1973
MAP 1



ARC LENGTH FOR ORBIT DETERMINATION $0^h 13^m$
TRACKING SCHEDULE AND ALTIMETER DATA TAKES
SL-2 PASS 2 2 JUNE 1973
MAP 2

Timeline of the 15h to 16h period showing tracking data availability and altimeter on status for GDS, TEX, and MIL.

Legend:

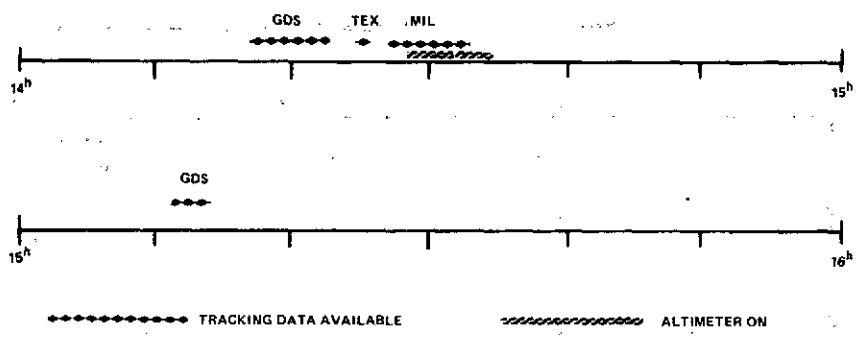
- TRACKING DATA AVAILABLE
- ▨ ALTIMETER ON

Timeline details:

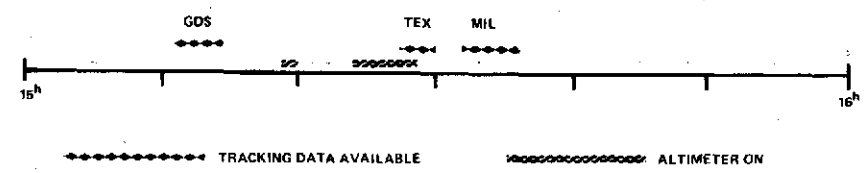
- GDS:** Tracking data available from 15:00 to 15:10.
- TEX:** Tracking data available from 15:00 to 15:05.
- MIL:** Tracking data available from 15:05 to 15:15. Altimeter on from 15:10 to 15:15.

MAP 5

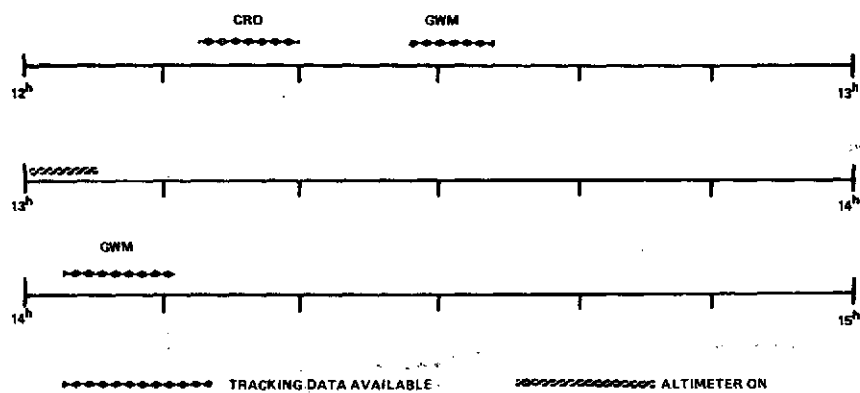
ORIGINAL PAGE IS
OF POOR QUALITY



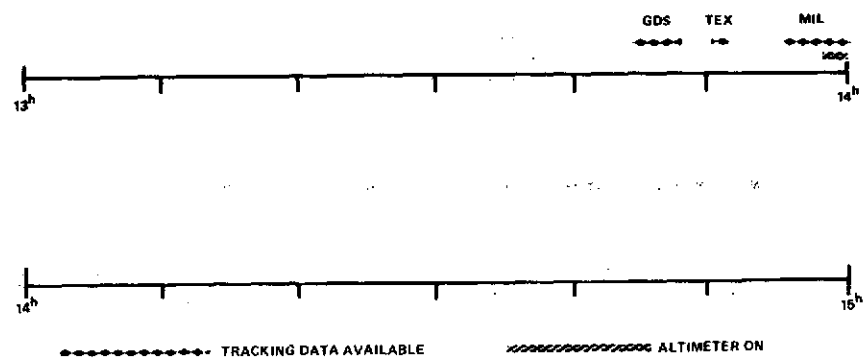
ARC LENGTH FOR ORBIT DETERMINATION 0^h59^m
TRACKING SCHEDULE AND ALTIMETRY DATA TAKES
SL-2 PASS 7 10 JUNE 1973
MAPS 6, 7, 8



ARC LENGTH FOR ORBIT DETERMINATION 0^h17^m
TRACKING SCHEDULE AND ALTIMETRY DATA TAKES
SL-2 PASS 8 11 JUNE 1973
MAPS 9 AND 10

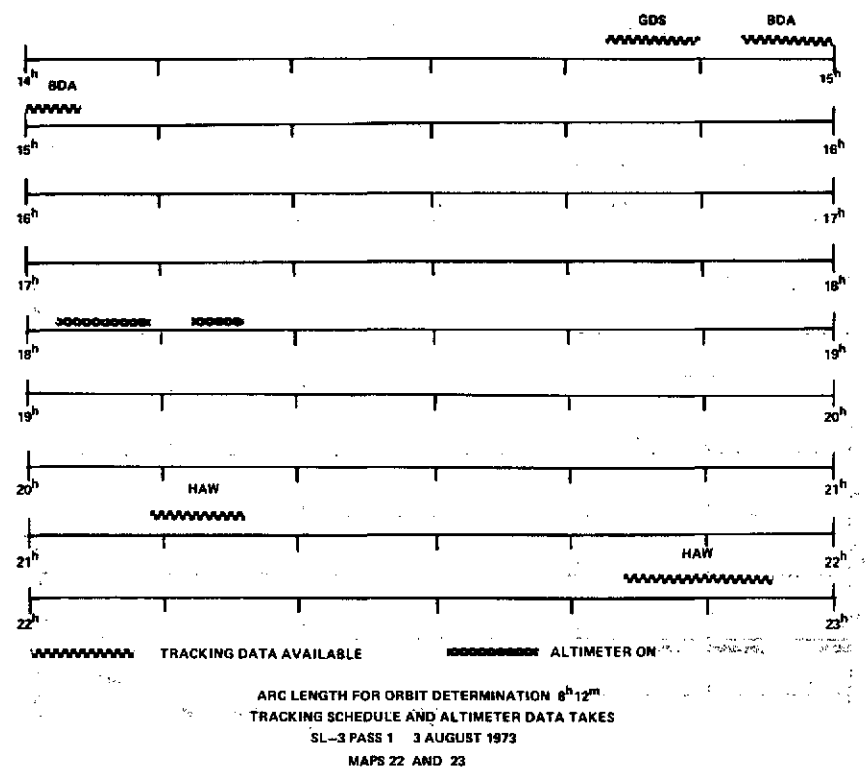
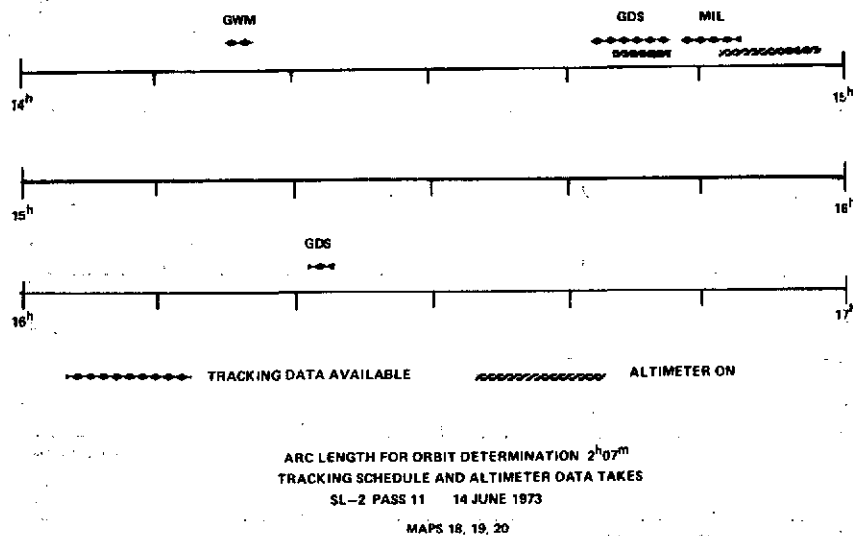


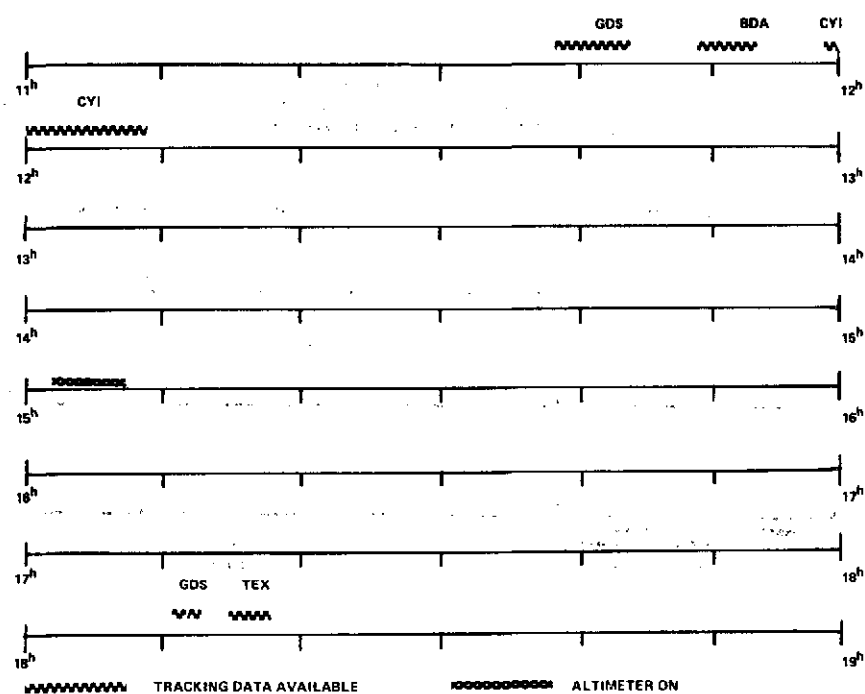
ARC LENGTH FOR ORBIT DETERMINATION 2^h0^m
 TRACKING SCHEDULE AND ALTIMETRY DATA TAKES
 SL-2 PASS 9 12 JUNE 1973
 MAPS 11, 12, 13



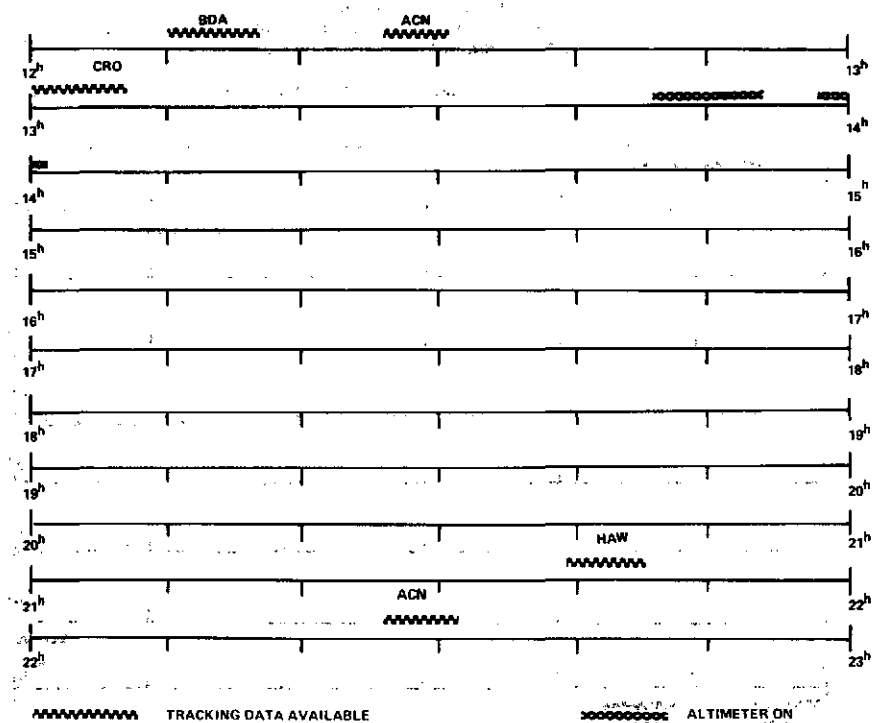
ARC LENGTH FOR ORBIT DETERMINATION 0^h17^m
 TRACKING SCHEDULE AND ALTIMETRY DATA TAKES
 SL-2 PASS 10 13 JUNE 1973
 MAPS 14 AND 15

ORIGINAL PAGE IS
OF POOR QUALITY



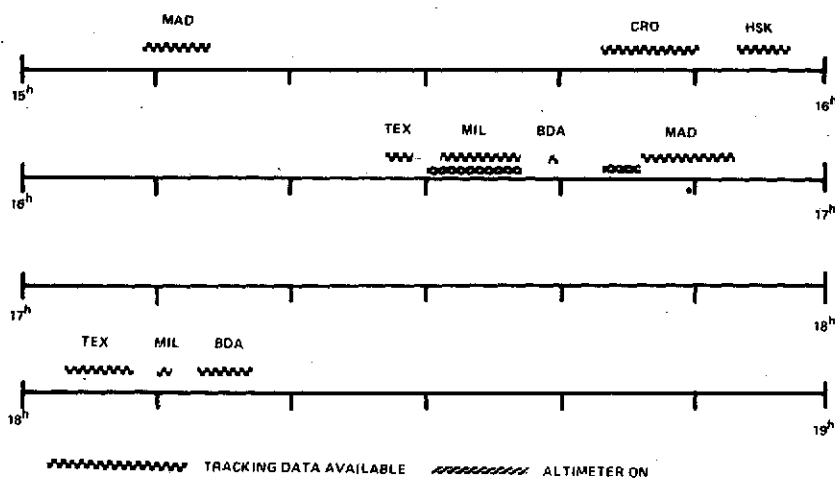


ARC LENGTH FOR ORBIT DETERMINATION 6^h20^m
 TRACKING SCHEDULE AND ALTIMETER DATA TAKES
 SL-3 PASS 3 5 AUGUST 1973
 MAP 26

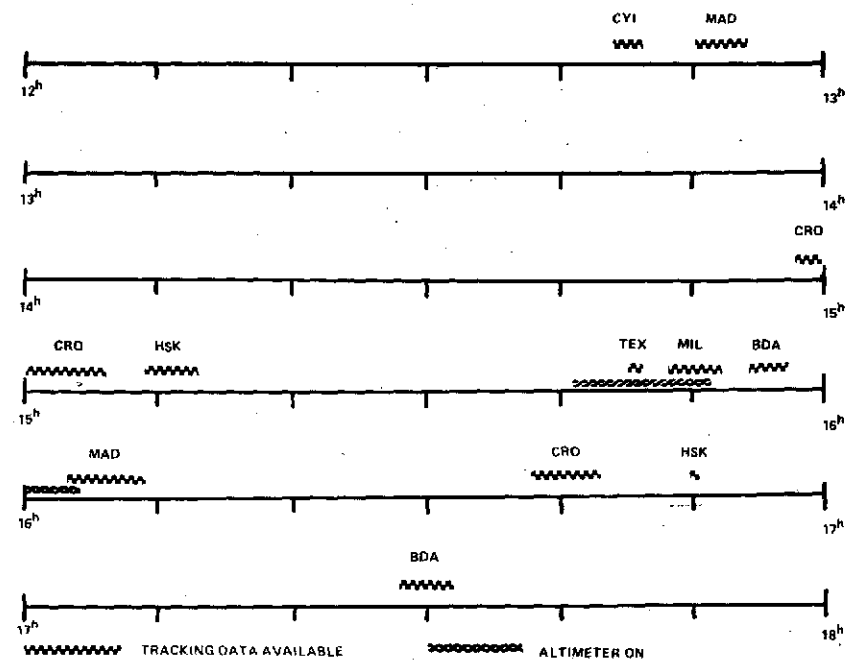


ARC LENGTH FOR ORBIT DETERMINATION 10^h20^m
 TRACKING SCHEDULE AND ALTIMETER DATA TAKES
 SL-3 PASS 6 9 AUGUST 1973
 MAPS 28, 29, 30

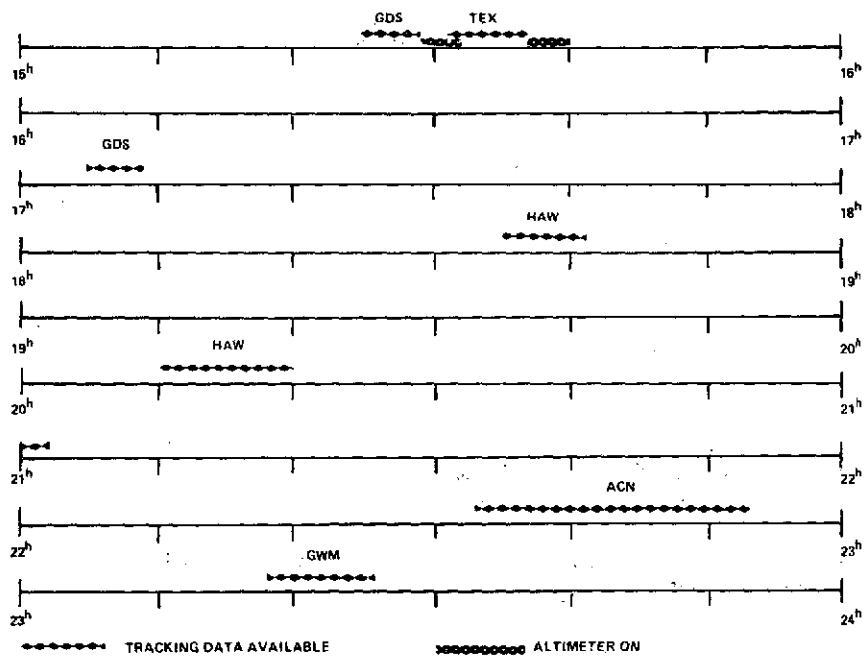
ORIGINAL PAGE IS
OF POOR QUALITY



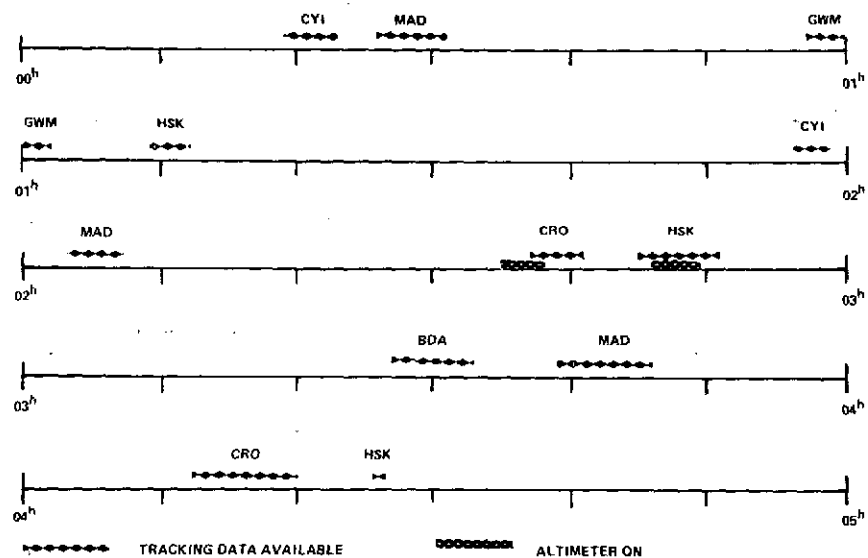
ARC LENGTH FOR ORBIT DETERMINATION 3^h08^m
 TRACKING SCHEDULE AND ALTIMETER DATA TAKES
 SL-4 PASS 78 08 JANUARY 1974
 MAPS 127, 128, 129



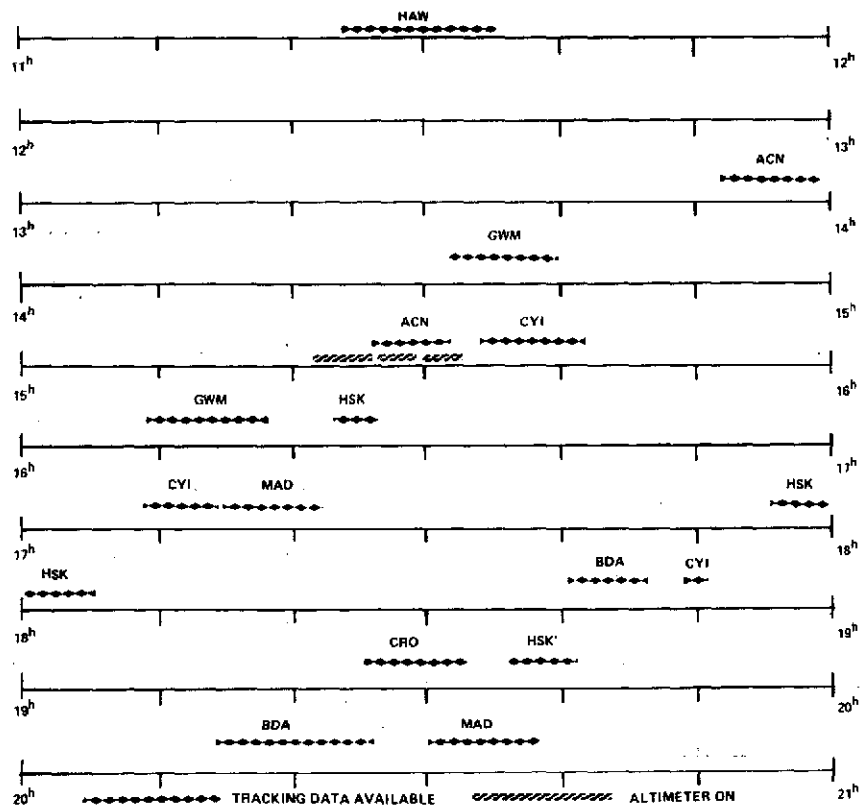
ARC LENGTH FOR ORBIT DETERMINATION 4^h48^m
 TRACKING SCHEDULE AND ALTIMETER DATA TAKES
 SL-4 PASS 79 09 JANUARY 1974
 MAPS 131, 132, 133, 134



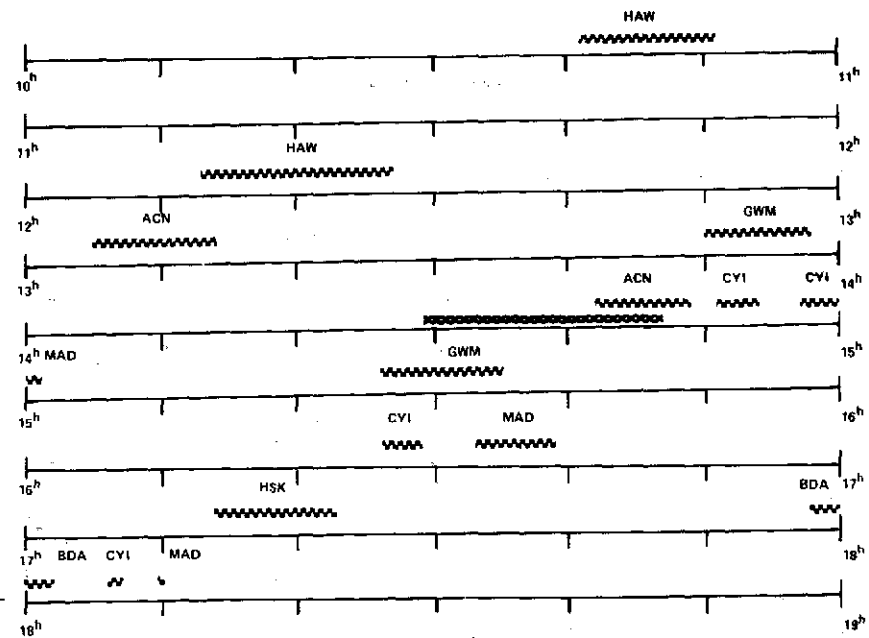
ARC LENGTH FOR ORBIT DETERMINATION 8^h01^m
 TRACKING SCHEDULE AND ALTIMETER DATA TAKES
 SL-3 PASS 7 11 AUGUST 1973
 MAPS 31 AND 32



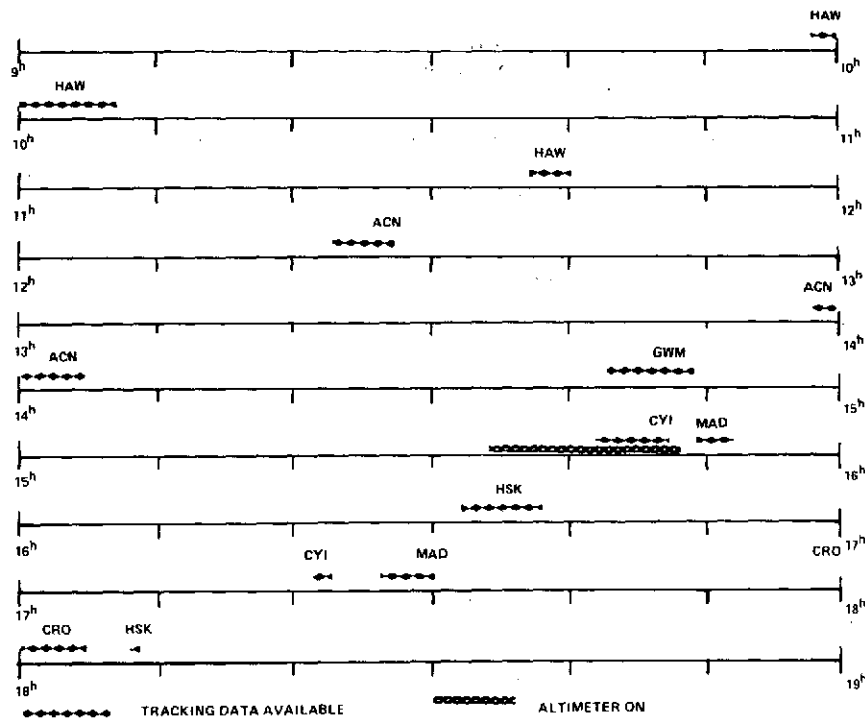
ARC LENGTH FOR ORBIT DETERMINATION 3^h07^m
 TRACKING SCHEDULE AND ALTIMETER DATA TAKES
 SL-3 PASS 8 12 AUGUST 1973
 MAPS 33 AND 34



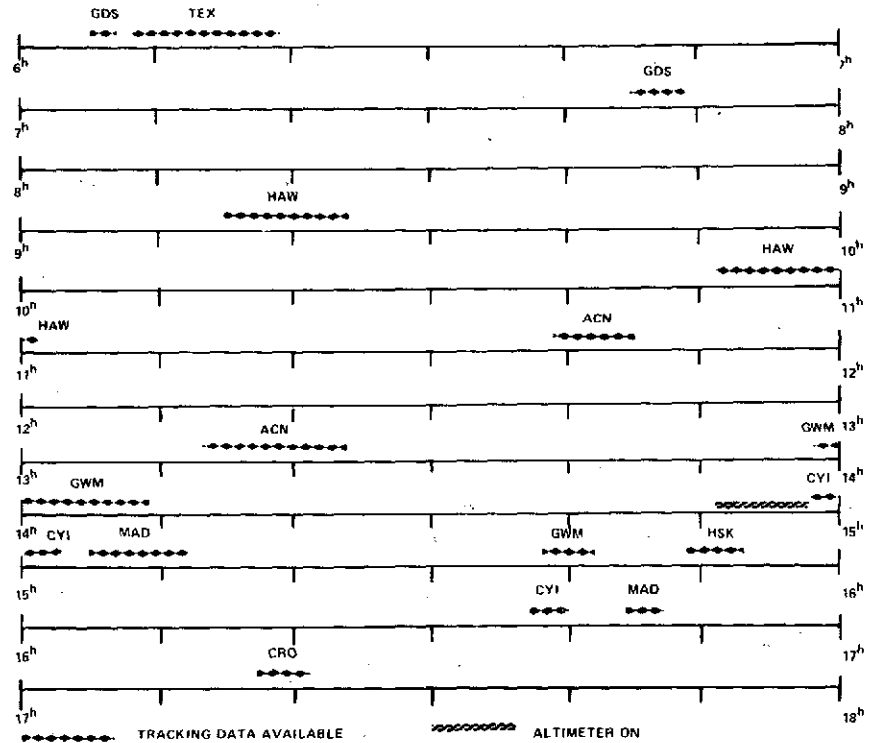
ARC LENGTH FOR ORBIT DETERMINATION 9^h14^m
 TRACKING SCHEDULE AND ALTIMETER DATA TAKES
 SL-3 PASS 10 1 SEPTEMBER 1973
 MAPS 35, 36, 37



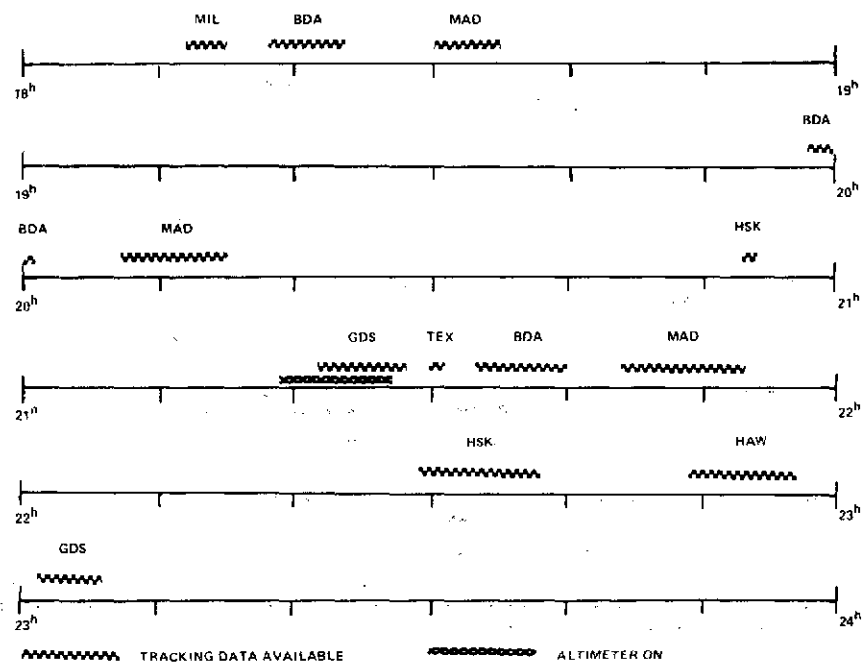
ARC LENGTH FOR ORBIT DETERMINATION 7^h29^m
 TRACKING SCHEDULE AND ALTIMETER DATA TAKES
 SL-3 PASS 11 2 SEPTEMBER 1973
 MAPS 38, 39, 40, 41, 42



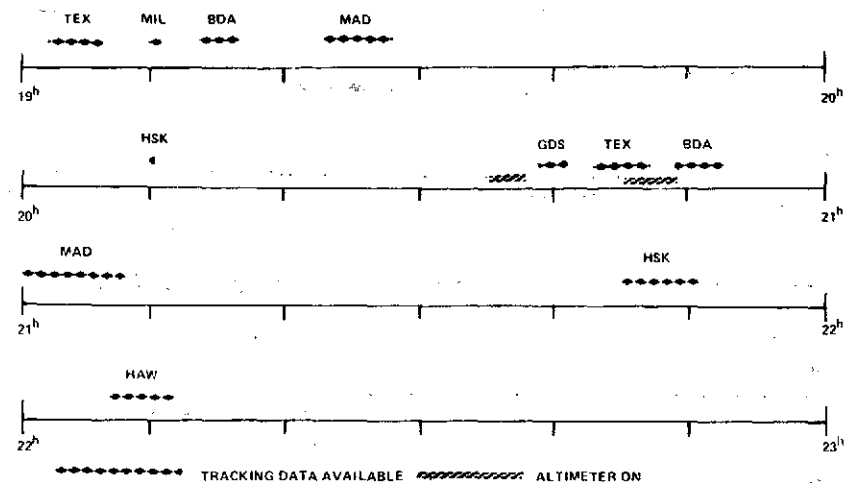
ARC LENGTH FOR ORBIT DETERMINATION 8^h16^m
 TRACKING SCHEDULE AND ALTIMETER DATA TAKES
 SL-3 PASS 13 3 SEPTEMBER 1973
 MAPS 43, 44, 45



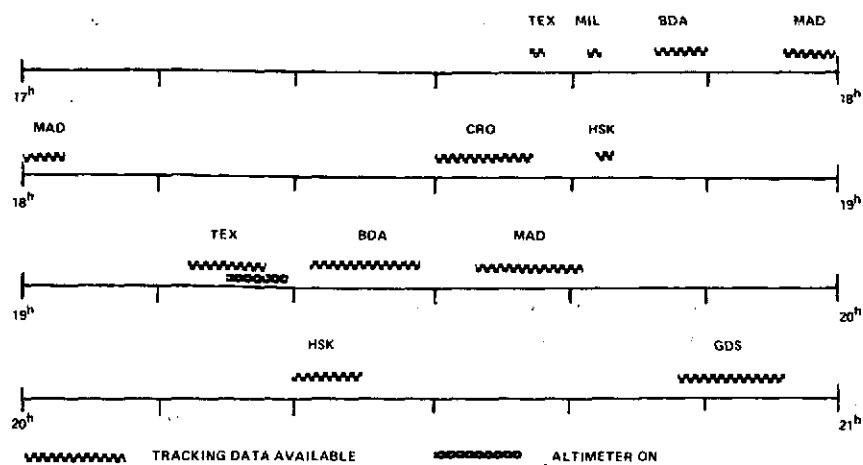
ARC LENGTH FOR ORBIT DETERMINATION 11^h16^m
 TRACKING SCHEDULE AND ALTIMETER DATA TAKES
 SL-3 PASS 14 04 SEPTEMBER 1973
 MAPS 46 AND 47



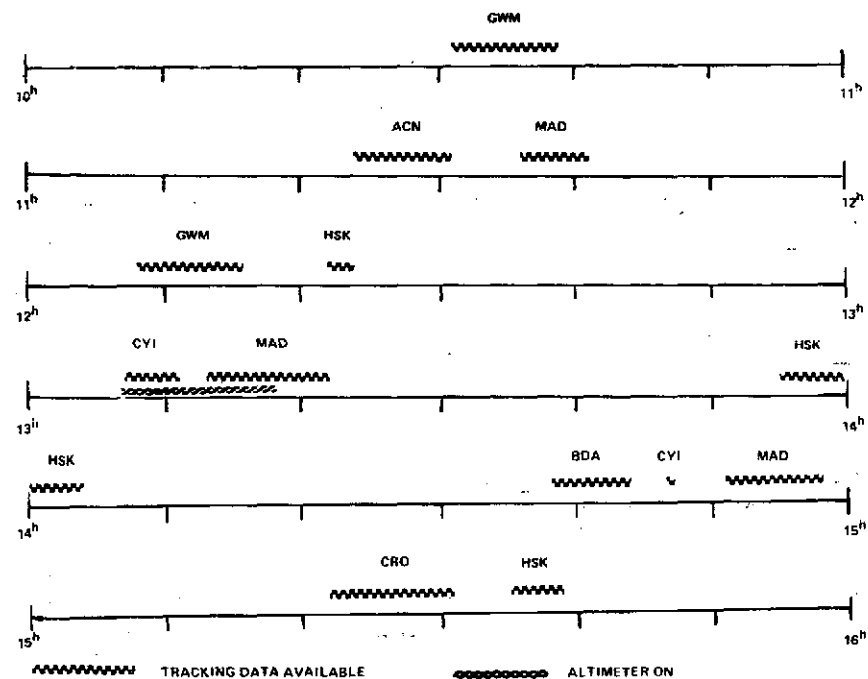
ARC LENGTH FOR ORBIT DETERMINATION 4^h49^m
 TRACKING SCHEDULE AND ALTIMETER DATA TAKES
 SL-3 PASS 16 6 SEPTEMBER 1973
 MAPS 48 AND 49



ARC LENGTH FOR ORBIT DETERMINATION 3^h10^m
 TRACKING SCHEDULE AND ALTIMETER DATA TAKES
 SL-3 PASS 17 7 SEPTEMBER 1973
 MAPS 50 AND 51

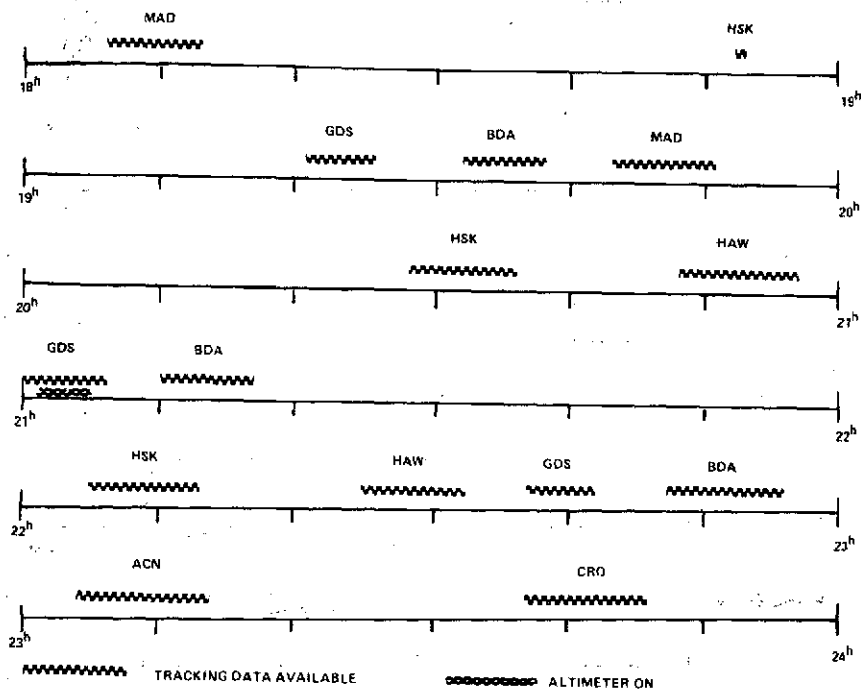


ARC LENGTH FOR ORBIT DETERMINATION $3^{\text{h}}16^{\text{m}}$
 TRACKING SCHEDULE AND ALTIMETER DATA TAKES
 SL-3 PASS 18 9 SEPTEMBER 1973
 MAP 52

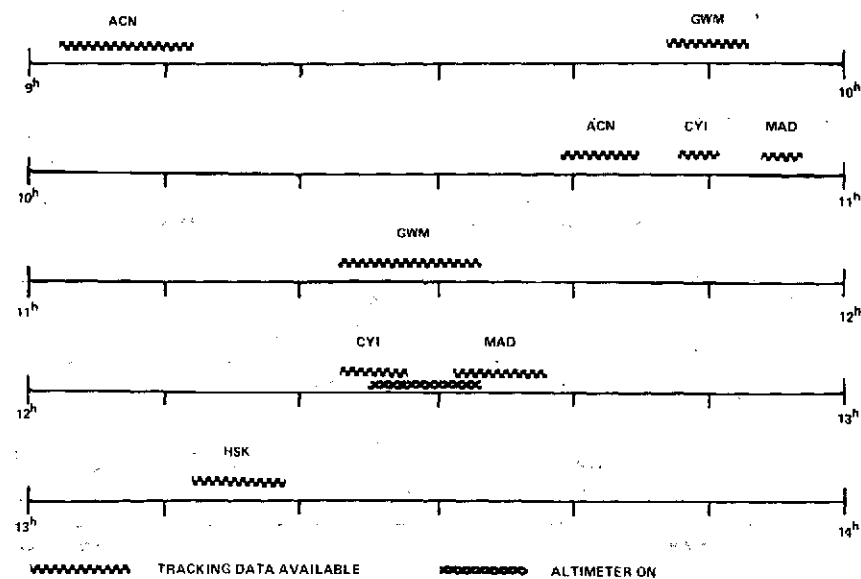


ARC LENGTH FOR ORBIT DETERMINATION $5^{\text{h}}08^{\text{m}}$
 TRACKING SCHEDULE AND ALTIMETER DATA TAKES
 SL-3 PASS 21 11 SEPTEMBER 1973
 MAPS 54, 55, 56

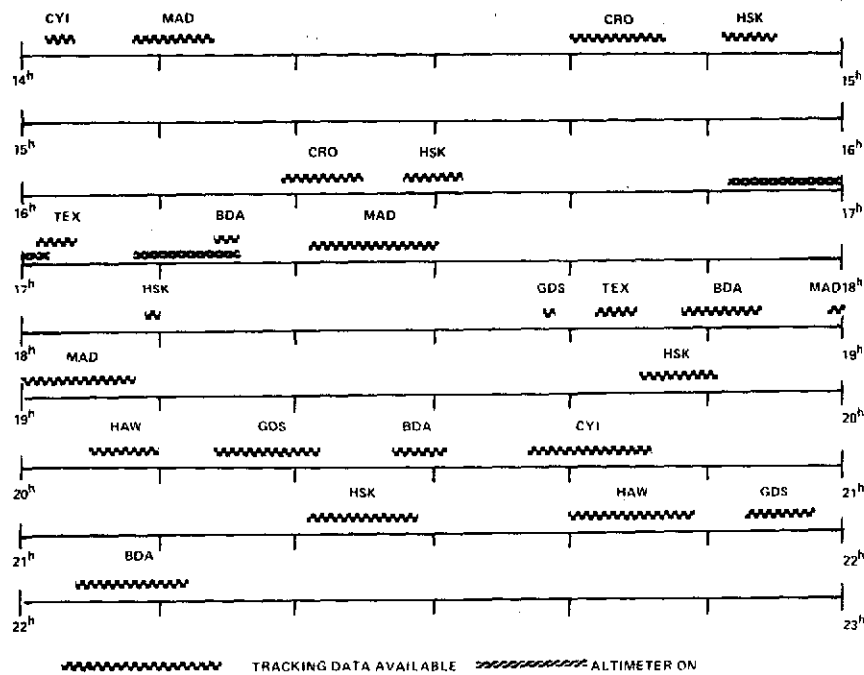
ORIGINAL PAGE IS
OF POOR QUALITY



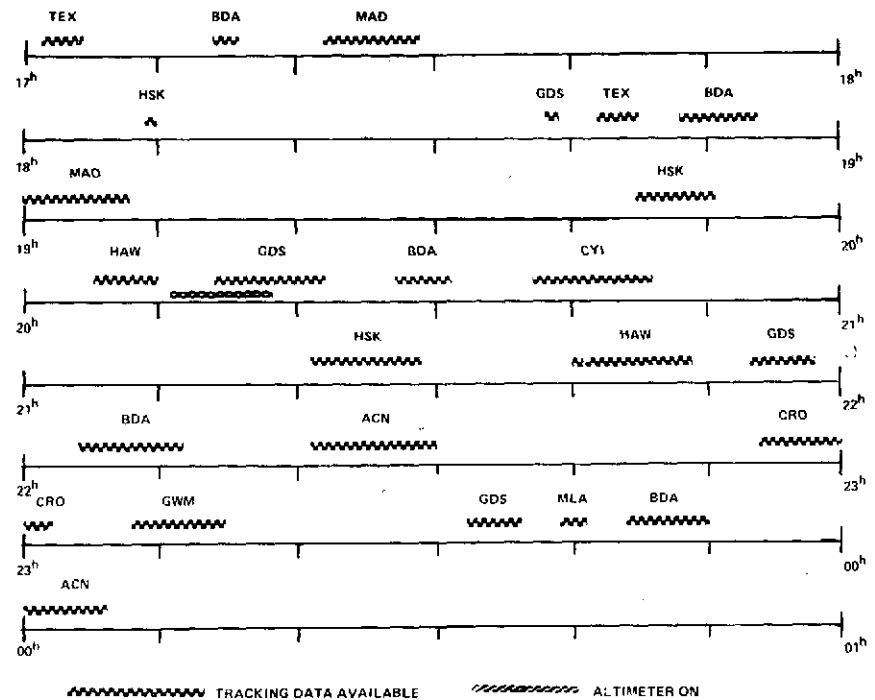
ARC LENGTH FOR ORBIT DETERMINATION 5h40m
TRACKING SCHEDULE AND ALTIMETER DATA TAKES
SL-3 PASS 23 11 SEPTEMBER 1973
MAP 57



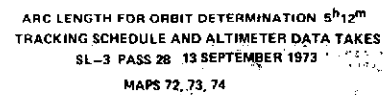
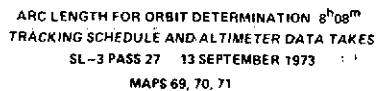
ARC LENGTH FOR ORBIT DETERMINATION 4h17m
TRACKING SCHEDULE AND ALTIMETER DATA TAKES
SL-3 PASS 24 12 SEPTEMBER 1973
MAPS 58, 59, 60

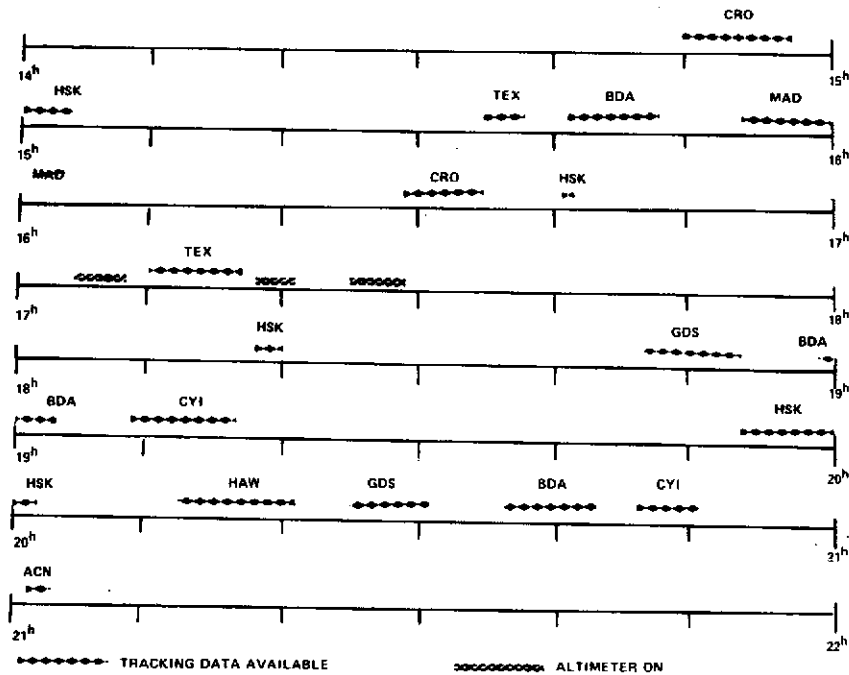


ARC LENGTH FOR ORBIT DETERMINATION 8^h10^m
 TRACKING SCHEDULE AND ALTIMETER DATA TAKES
 SL-3 PASS 25 12 SEPTEMBER 1973
 MAPS 61, 63, 64, 65

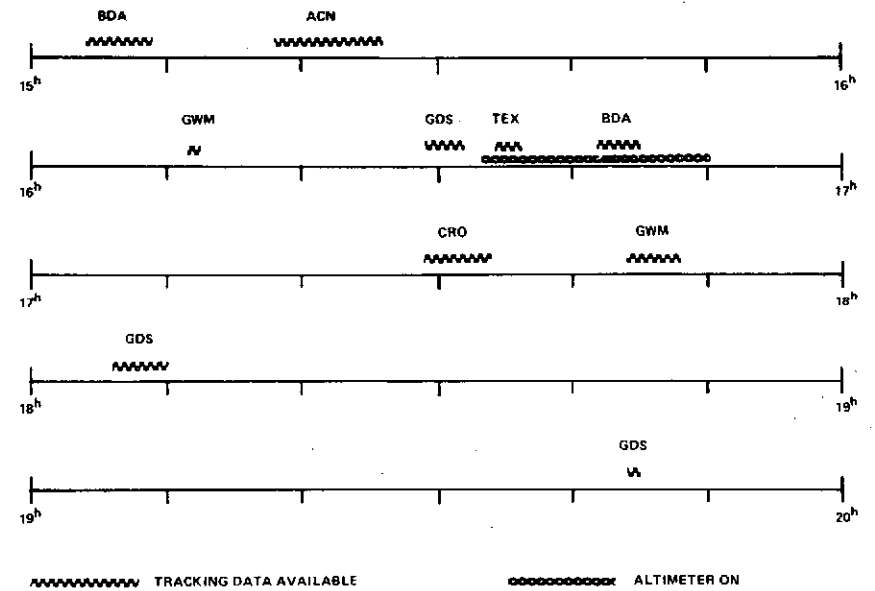


ARC LENGTH FOR ORBIT DETERMINATION 7^h05^m
 TRACKING SCHEDULE AND ALTIMETER DATA TAKES
 SL-3 PASS 26 12 SEPTEMBER 1973
 MAPS 66 AND 67





ARC LENGTH FOR ORBIT DETERMINATION 6^h13^m
 TRACKING SCHEDULE AND ALTIMETER DATA TAKES
 SL-3 PASS 29 14 SEPTEMBER 1973
 MAPS 75 AND 76



ARC LENGTH FOR ORBIT DETERMINATION 4^h41^m
 TRACKING SCHEDULE AND ALTIMETER DATA TAKES
 SL-4 PASS 64 11 NOV 1973
 MAPS 81, 83, 84

16h

CRO

17h

GWM TEX

17h

18h

18h

GDS TEX

19h

20h

HAW

20h

21h

21h

22h

HAW

22h

23h

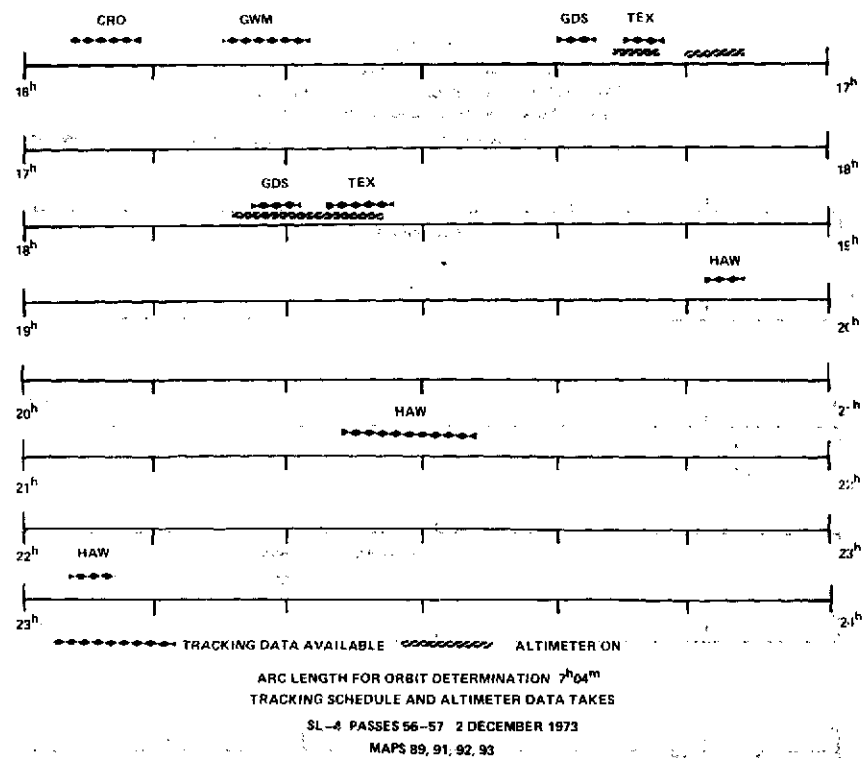
WAVY LINE TRACKING DATA AVAILABLE CIRCLES ALTIMETER ON

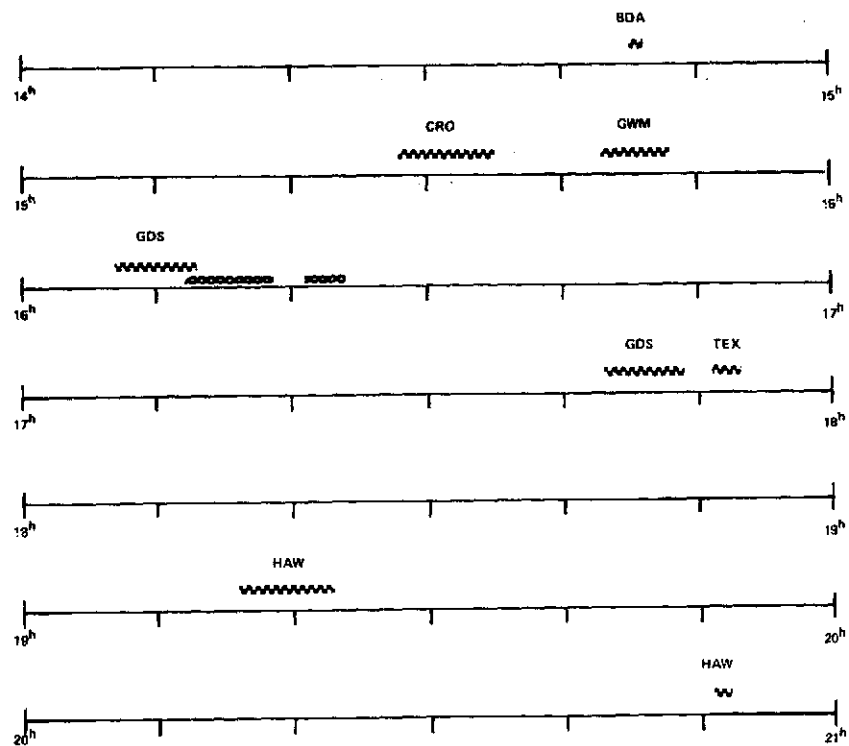
ARC LENGTH FOR ORBIT DETERMINATION 5°27'

TRACKING SCHEDULE AND ALTIMETER DATA TAKES

SL-4 PASS 55 01 DECEMBER 1973

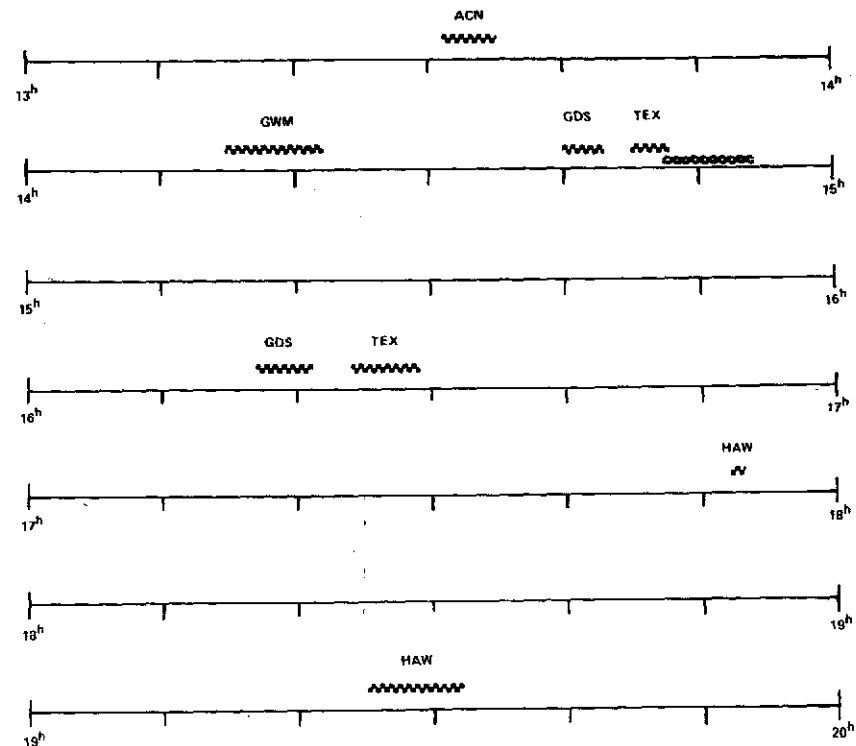
MAPS 85 AND 86





~~~~~ TRACKING DATA AVAILABLE      . . . . . ALTIMETER ON

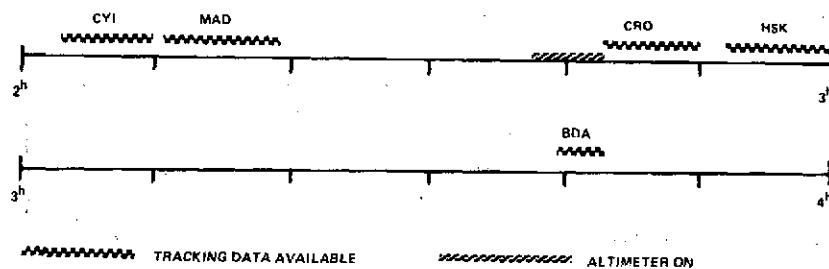
ARC LENGTH FOR ORBIT DETERMINATION  $6^{\circ}07^m$   
 TRACKING SCHEDULE AND ALTIMETER DATA TAKES  
 SL-4 PASS 61 5 DECEMBER 1973  
 MAPS 98 AND 99



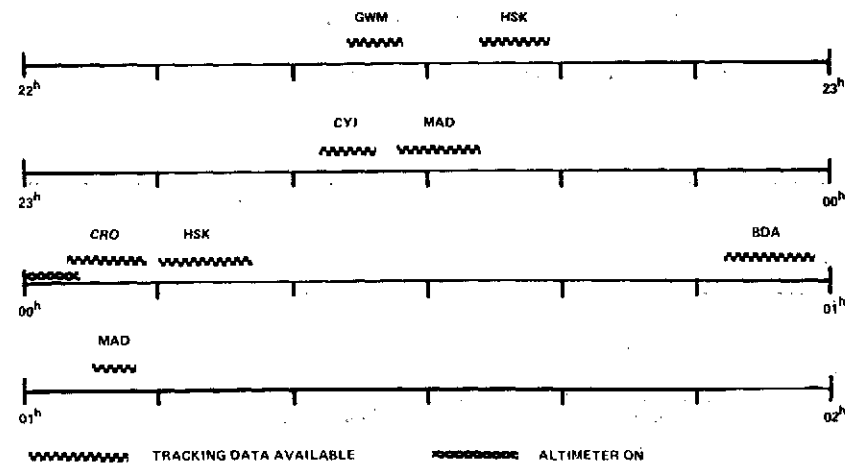
~~~~~ TRACKING DATA AVAILABLE      . . . . . ALTIMETER ON

ARC LENGTH FOR ORBIT DETERMINATION $6^{\circ}01^m$
 TRACKING SCHEDULE AND ALTIMETER DATA TAKES
 SL-4 PASS 62 7 DECEMBER 1973
 MAP 100

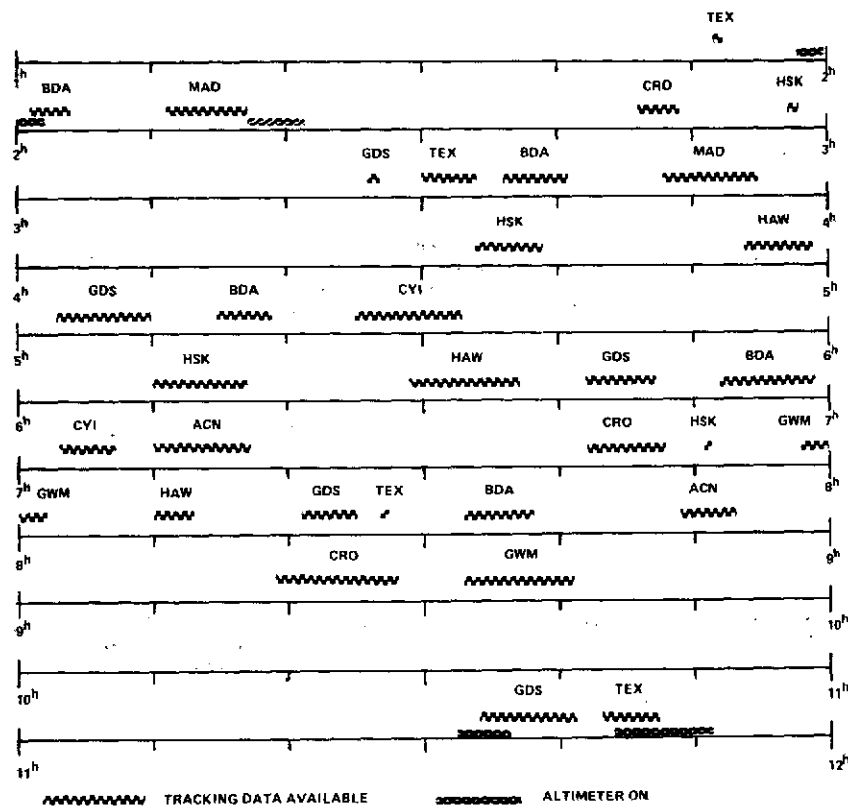
ORIGINAL PAGE IS
OF POOR QUALITY



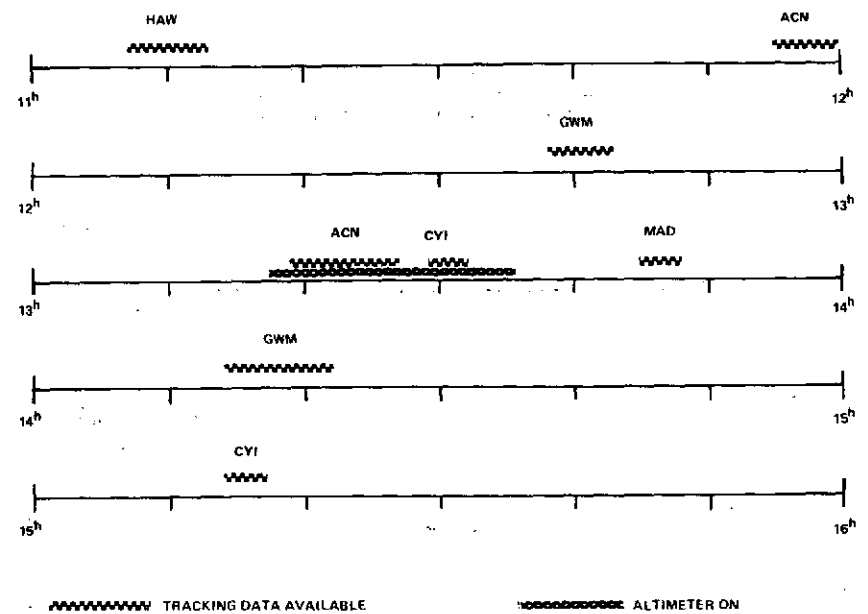
ARC LENGTH FOR ORBIT DETERMINATION $1^h 39^m$
TRACKING SCHEDULE AND ALTIMETER DATA TAKES
SL-4 PASS 64 9 DECEMBER 1973
MAPS 102, 103, 104



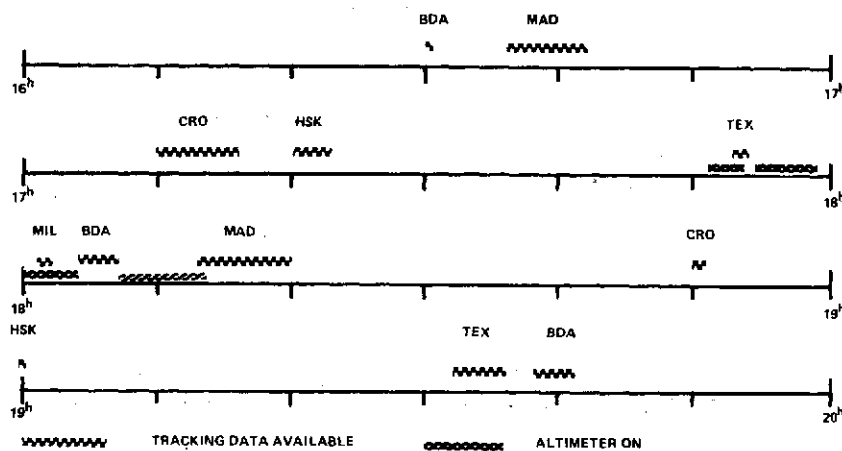
ARC LENGTH FOR ORBIT DETERMINATION $2^h 44^m$
TRACKING SCHEDULE AND ALTIMETER DATA TAKES
SL-4 PASS 65 15 DECEMBER 1973
MAP 105



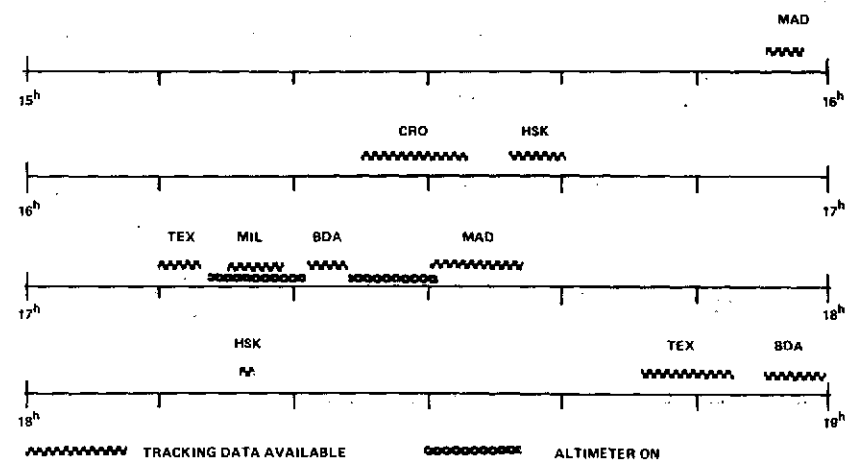
ARC LENGTH FOR ORBIT DETERMINATION $9^h 56^m$
 TRACKING SCHEDULE AND ALTIMETER DATA TAKES
 SL-4 PASSES 67-68 18 DECEMBER 1973
 MAPS 106, 108, 109, 110



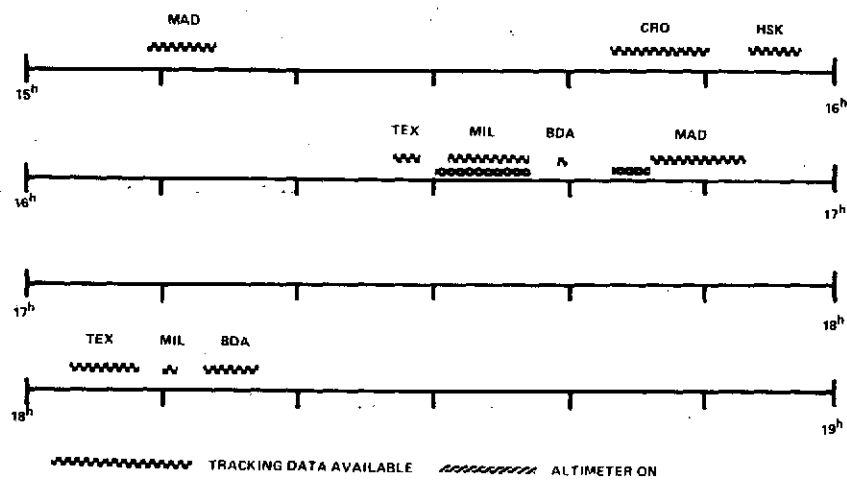
ARC LENGTH FOR ORBIT DETERMINATION $4^h 10^m$
 TRACKING SCHEDULE AND ALTIMETER DATA TAKES
 SL-4 PASS 71 01 JANUARY 1974
 MAPS 113, 114, 115



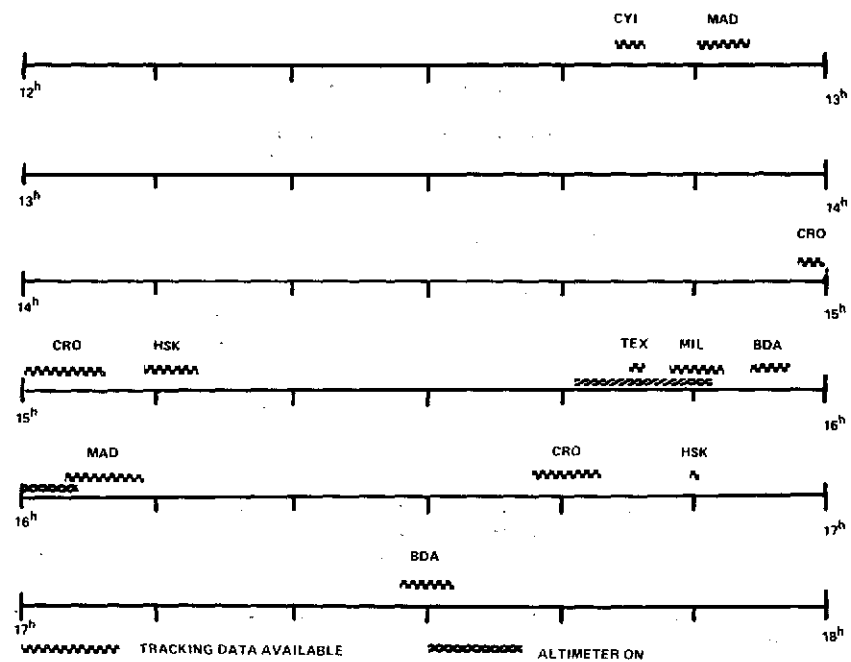
ARC LENGTH FOR ORBIT DETERMINATION 3^h11^m
 TRACKING SCHEDULE AND ALTIMETER DATA TAKES
 SL-4 PASS 74 06 JANUARY 1974
 MAPS 117, 118, 119, 120, 120A



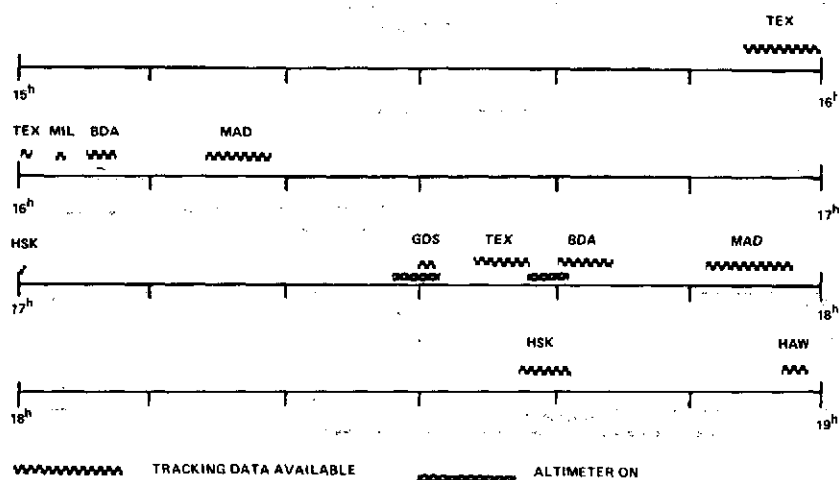
ARC LENGTH FOR ORBIT DETERMINATION 3^h05^m
 TRACKING SCHEDULE AND ALTIMETER DATA TAKES
 SL-4 PASS 76 07 JANUARY 1974
 MAPS 121, 122, 123, 124



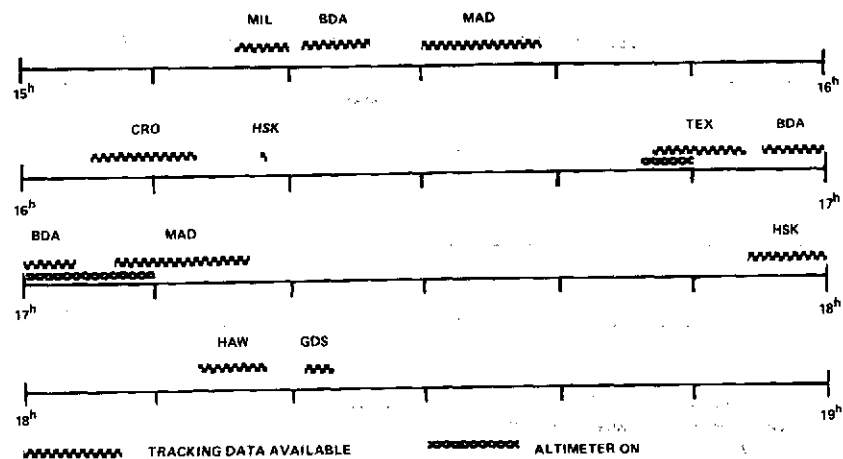
ARC LENGTH FOR ORBIT DETERMINATION 3^h08^m
 TRACKING SCHEDULE AND ALTIMETER DATA TAKES
 SL-4 PASS 78 08 JANUARY 1974
 MAPS 127, 128, 129



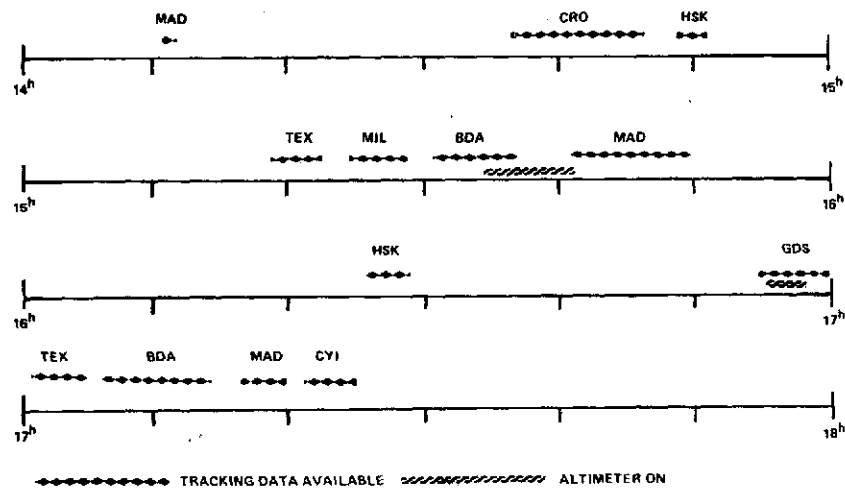
ARC LENGTH FOR ORBIT DETERMINATION 4^h48^m
 TRACKING SCHEDULE AND ALTIMETER DATA TAKES
 SL-4 PASS 79 09 JANUARY 1974
 MAPS 131, 132, 133, 134



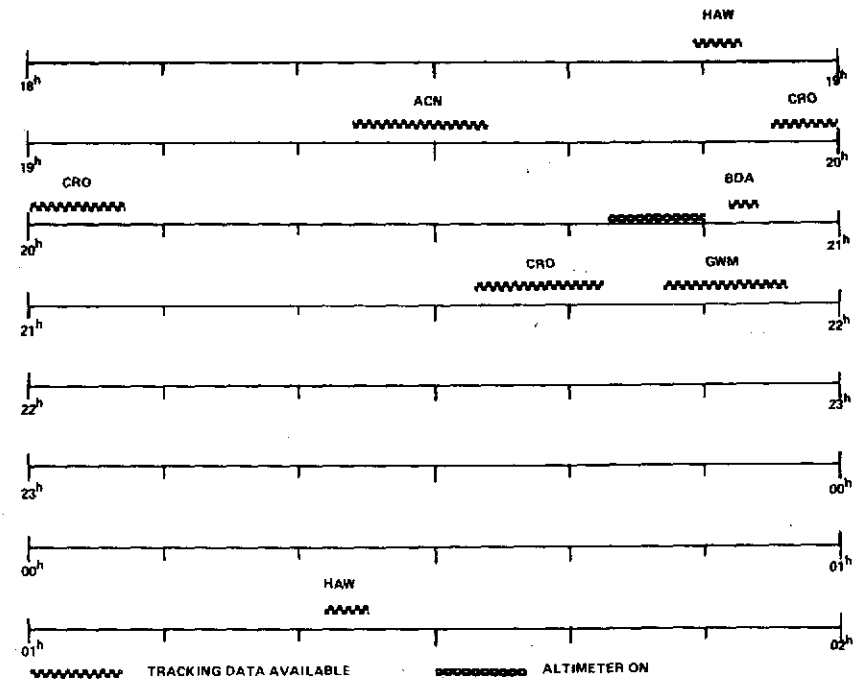
ARC LENGTH FOR ORBIT DETERMINATION 3^h05^m
 TRACKING SCHEDULE AND ALTIMETER DATA TAKES
 SL-4 PASS B1 11 JANUARY 1974
 MAP 135



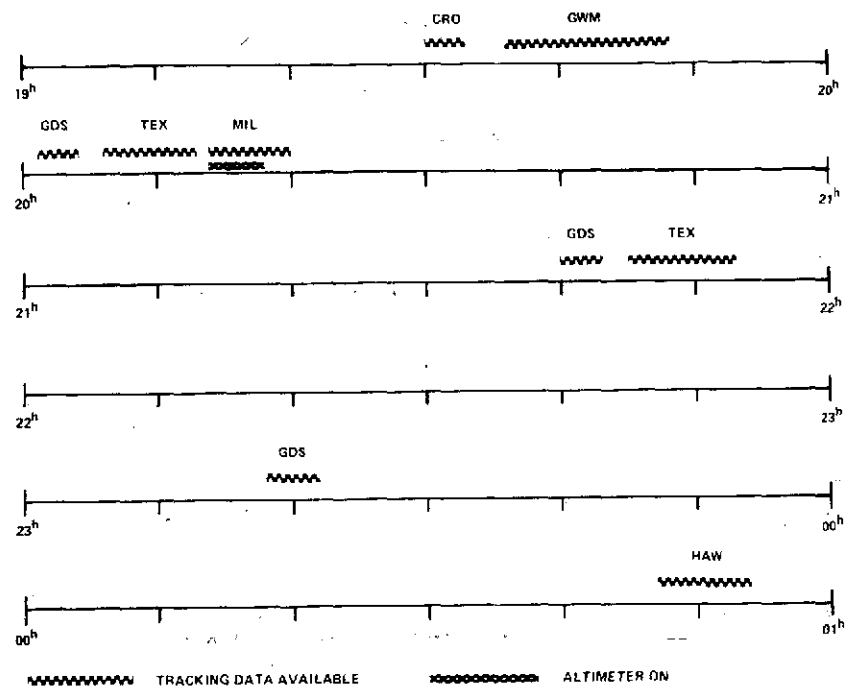
ARC LENGTH FOR ORBIT DETERMINATION 3^h07^m
 TRACKING SCHEDULE AND ALTIMETER DATA TAKES
 SL-4 PASS 82 12 JANUARY 1974
 MAP 139



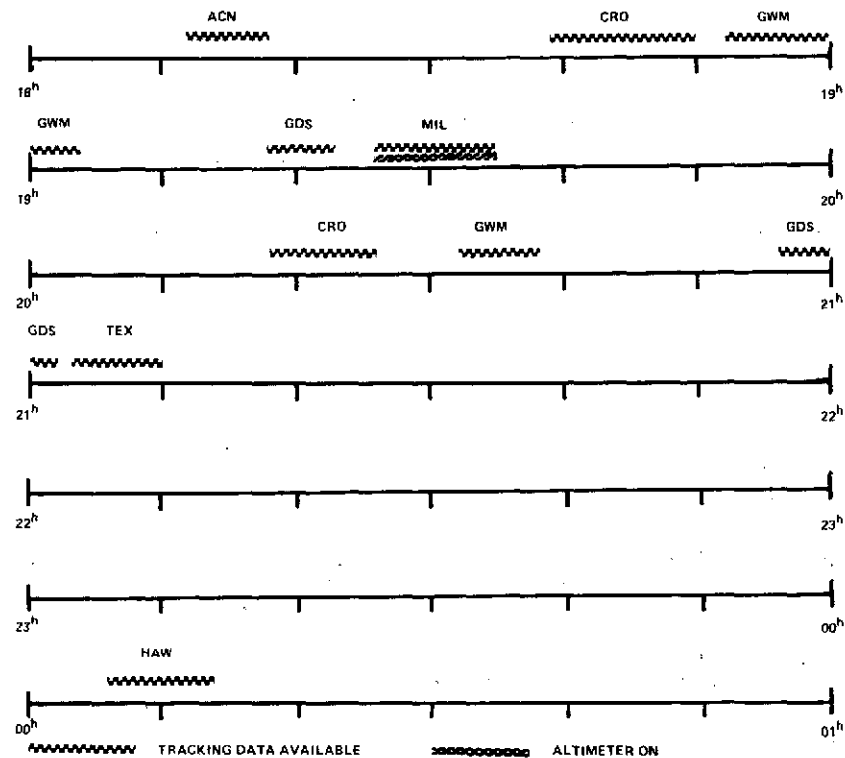
ARC LENGTH FOR ORBIT DETERMINATION 3^h14^m
 TRACKING SCHEDULE AND ALTIMETER DATA TAKES
 SL-4 PASS 83 14 JANUARY 1974
 MAPS 145, 147, 148



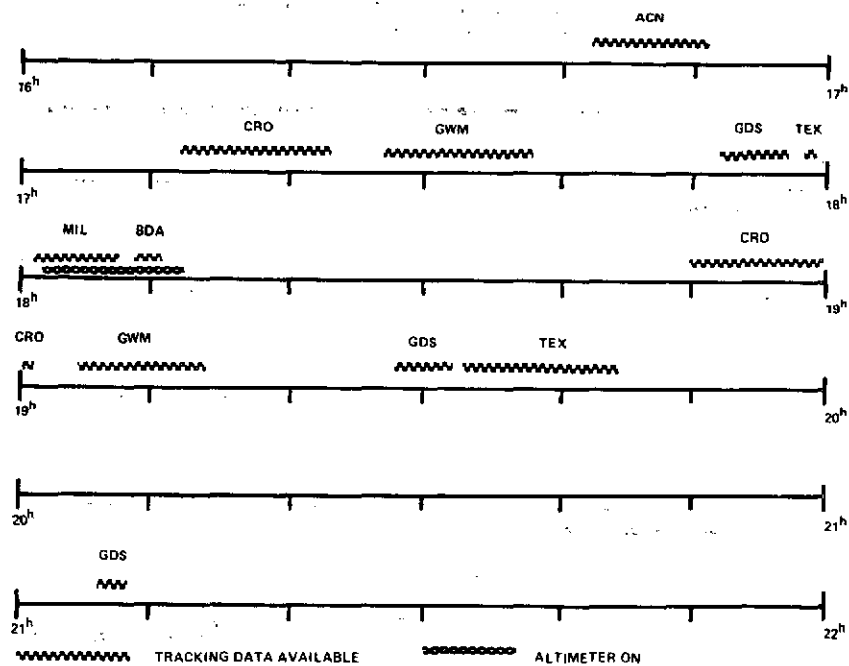
ARC LENGTH FOR ORBIT DETERMINATION 6^h36^m
 TRACKING SCHEDULE AND ALTIMETER DATA TAKES
 SL-4 PASS 85 18 JANUARY 1974
 MAP 151



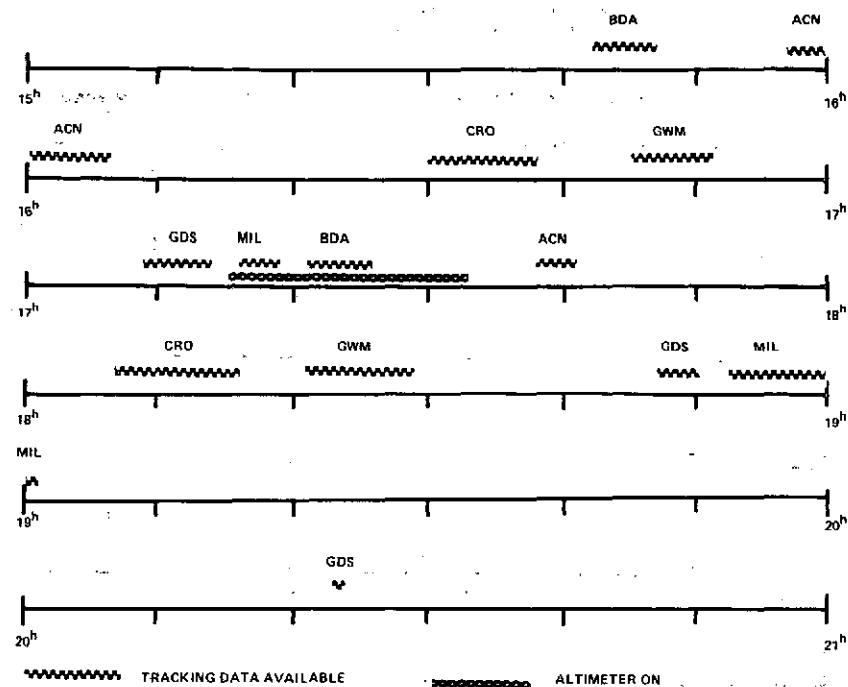
ARC LENGTH FOR ORBIT DETERMINATION 5^h24^m
 TRACKING SCHEDULE AND ALTIMETER DATA TAKES
 SL-4 PASS 87 21 JANUARY 1974
 MAP 152



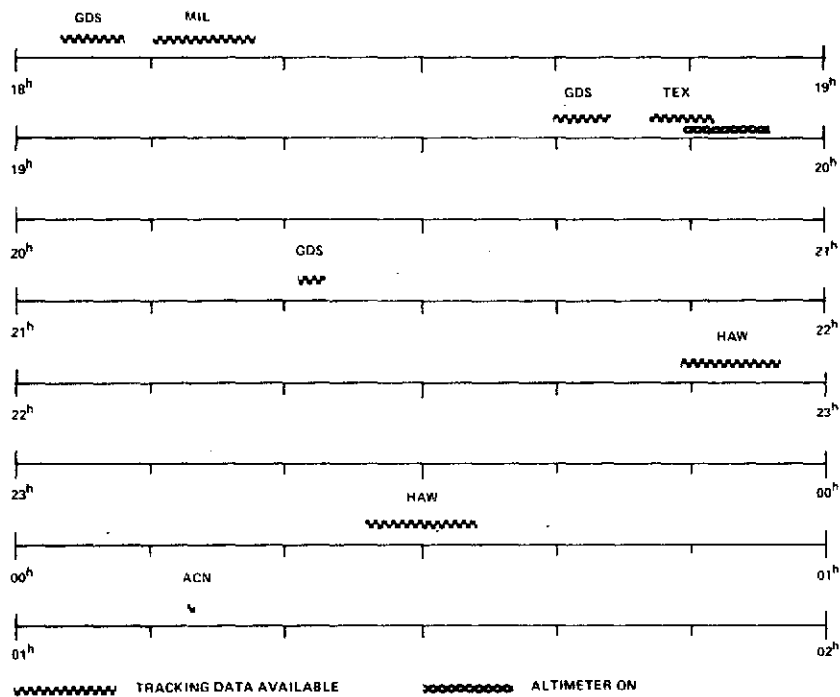
ARC LENGTH FOR ORBIT DETERMINATION 6^h02^m
 TRACKING SCHEDULE AND ALTIMETER DATA TAKES
 SL-4 PASS 88 22 JANUARY 1974
 MAPS 155 AND 156



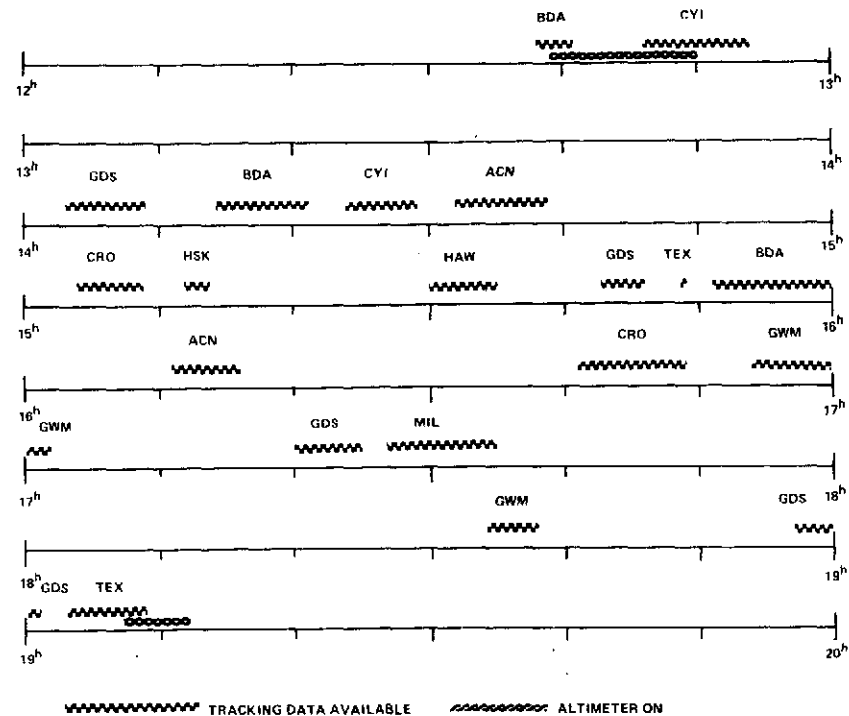
ARC LENGTH FOR ORBIT DETERMINATION 4^h26^m
 TRACKING SCHEDULE AND ALTIMETER DATA TAKES
 SL-4 PASS 89 24 JANUARY 1974
 MAPS 163 AND 164



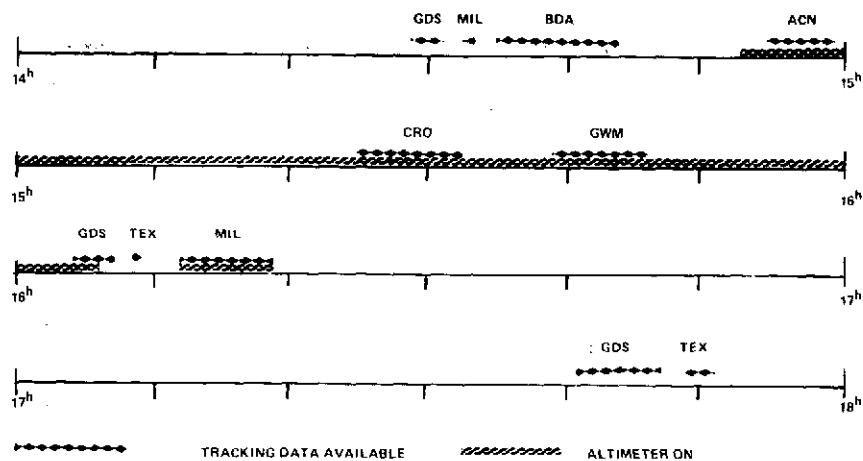
ARC LENGTH FOR ORBIT DETERMINATION 4^h42^m
 TRACKING SCHEDULE AND ALTIMETER DATA TAKES
 SL-4 PASS 90 25 JANUARY 1974
 MAPS 168 AND 169



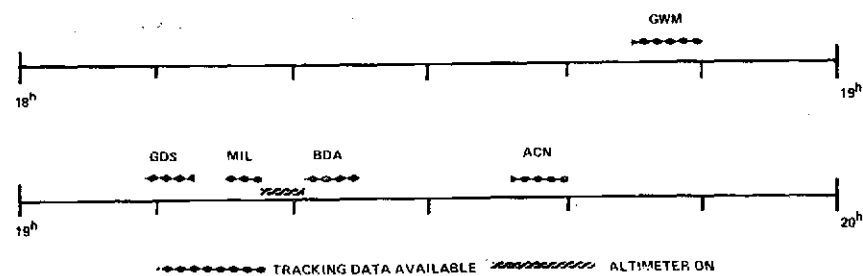
ARC LENGTH FOR ORBIT DETERMINATION 7^h10^m
 TRACKING SCHEDULE AND ALTIMETER DATA TAKES
 SL-4 PASS 91 26-27 JANUARY 1974
 MAP 175



ARC LENGTH FOR ORBIT DETERMINATION 6^h31^m
 TRACKING SCHEDULE AND ALTIMETER DATA TAKES
 SL-4 PASSES 92-93 27 JANUARY 1974
 MAPS 182 AND 185



ARC LENGTH FOR ORBIT DETERMINATION 3^h22^m
 TRACKING SCHEDULE AND ALTIMETER DATA TAKES
 SL-4 PASS 97 31 JANUARY 1974
 MAPS 201-218, 222, 223, 225, 226



ARC LENGTH FOR ORBIT DETERMINATION 1^h55^m
 TRACKING SCHEDULE AND ALTIMETER DATA TAKES
 SL-4 PASS 86 20 JANUARY 1974
 MAP 233

POINTING DETERMINATION

Analysis of Waveform Trailing Edge

The antenna beamwidth, pulse width (100 ns Modes) and altitude of the S-193 altimeter give rise to essentially a beamwidth limited system. For such a system, the peak average received power is a very sensitive function of pointing angle with respect to nadir. For example, a 0.75° pointing error can result in an altitude bias of 2 meters and a 4 dB reduction in received power. If these errors are neglected, σ_0 measurements will be erroneous and geoid measurements will be compromised. This pointing error problem was further complicated by spacecraft attitude drift (due to a Command Module Gimble (CMG) problem) during all three missions. Thus, it became necessary to devise a method for determining pointing angle which did not depend on the spacecraft as a reference. In the course of comparing measured average return waveforms with theoretical waveforms, it was found that pointing angle could be determined from the shape of the trailing edge of the average return waveform [5]. This observation follows from the convolutional or linear scattering model in which the antenna pattern and the pointing angle are dominant effects in the trailing edge region of the average return, as shown in Figure 5.

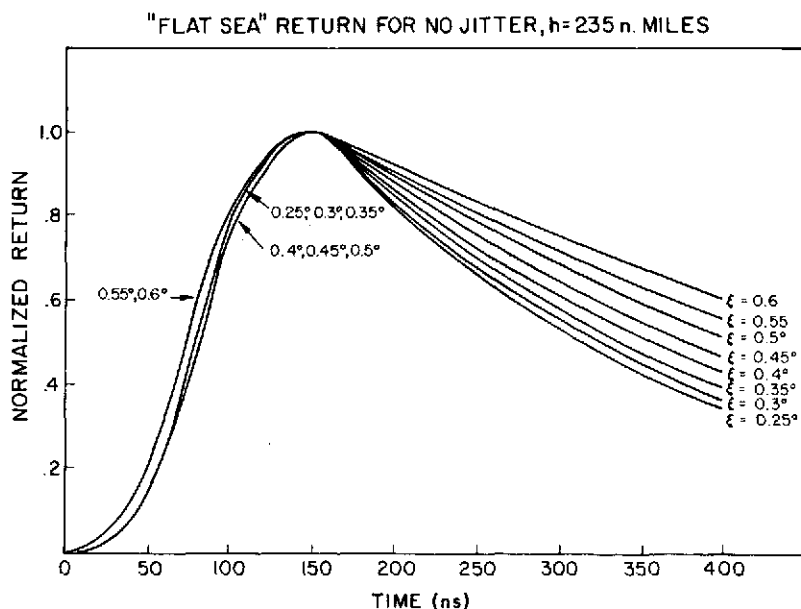


Figure 5

This method applies only over oceans or large water bodies when off-nadir angles are from 0.25° to about 1.2° , and the accuracy of determining pointing angle depends primarily upon the number of individual waveforms averaged and the signal-to-noise ratio. This can be seen in the sample waveforms of Figures 6 and 7. Note the low variance on the trailing edge of the pulses. The results indicate the possibility that properly designed altimeters can also be employed as very accurate attitude sensors with angular accuracies $\leq \pm 0.05^\circ$. A multi-variable χ^2 (chi squared) minimization program has been adapted by Dr. G. S. Hayne for estimating, from the waveforms, pointing error and other parameters of interest. It is important to note that without a pointing angle determination capability, much of the data from the altimeter would have been questionable because pointing is very critical.

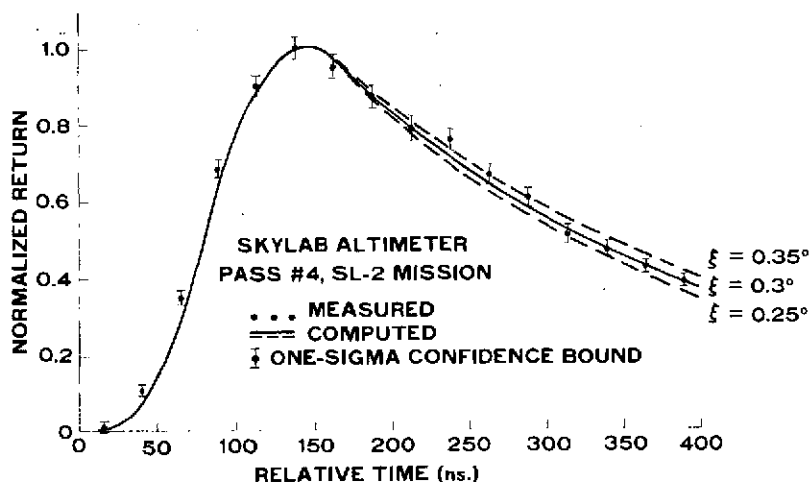


Figure 6 Comparison of Measured and Theoretical Mean Return Waveforms for a 100 ns Transmitted Pulse Width. Pointing $.3^\circ$ Off Nadir.

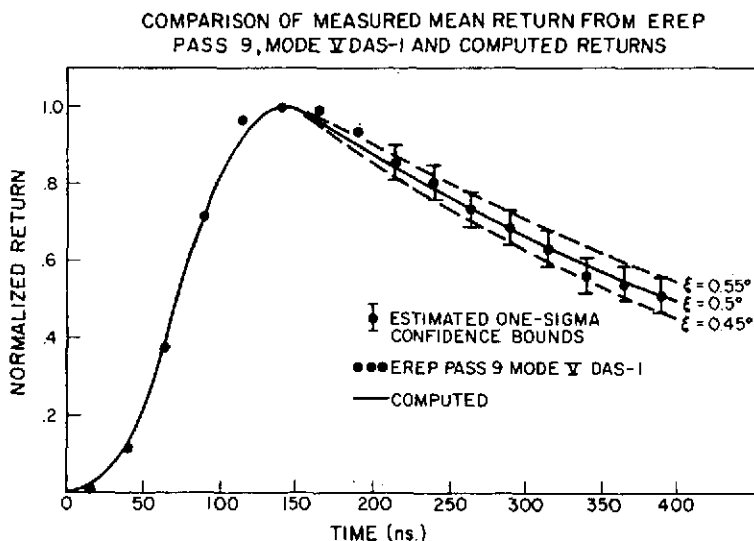


Figure 7 Comparison of Measured Mean Return and Theoretical Return for a 100 ns Transmitted Pulse Width. Pointing $.5^\circ$ Off Nadir.

Analysis of Tracker Response and AGC

By analyzing the altitude tracker response and automatic gain control (AGC) another method is obtained for determining satellite pointing. This technique is not as accurate but is somewhat complimentary to the above method since it appears to be practical with pointing errors from $.75^\circ$ through 1.7° . The accuracy is only a few tenths of a degree. This technique also can be utilized only over broad ocean or large water body areas where uniform reflectance is available.

As was illustrated in the previous section in Figure 5, the leading edge of the pulse does not show much change with pointing for at least the first $.75^\circ$ of error. However, as the pointing moves further off-nadir, both leading edge distortion and signal level drop-off rapidly occur. Figure 8 shows an artist's concept of how pointing might typically affect selected waveforms.

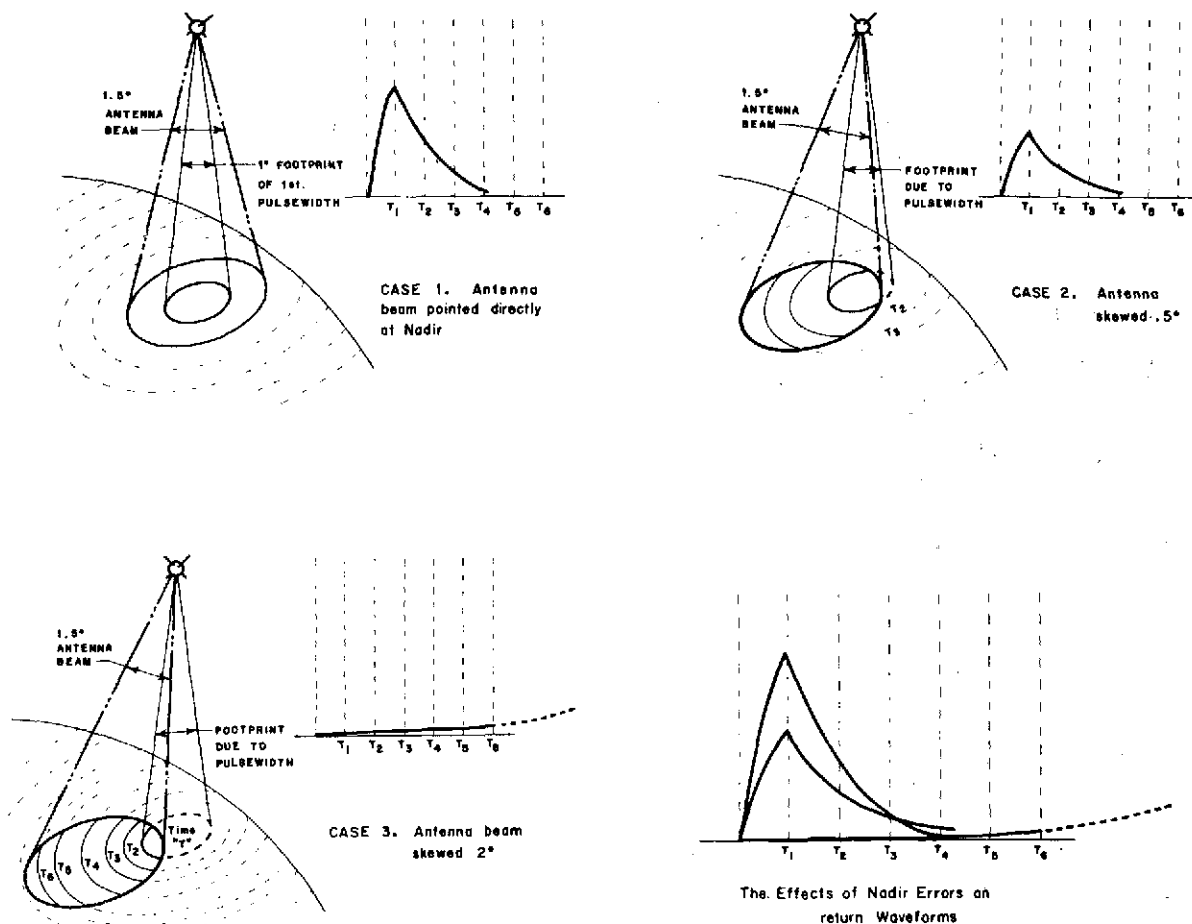


Figure 8

Since the S-193 altitude tracker is a split gate error detector as illustrated in Figure 9 (from [6]), it can be visualized that these more extreme distortions associated with large pointing errors can cause large biases in altitude measurements. In addition, since the rise time of the returns tends to be extended and the amplitude drops, it is then necessary for the AGC to increase the gain in the system to provide a more constant discriminator curve. With this increased gain, the noise is also amplified and the tracker jitter therefore increases (see Figure 10). Since AGC can't completely compensate for the rise-time change, the altitude servo system gets more sluggish (loses frequency response).

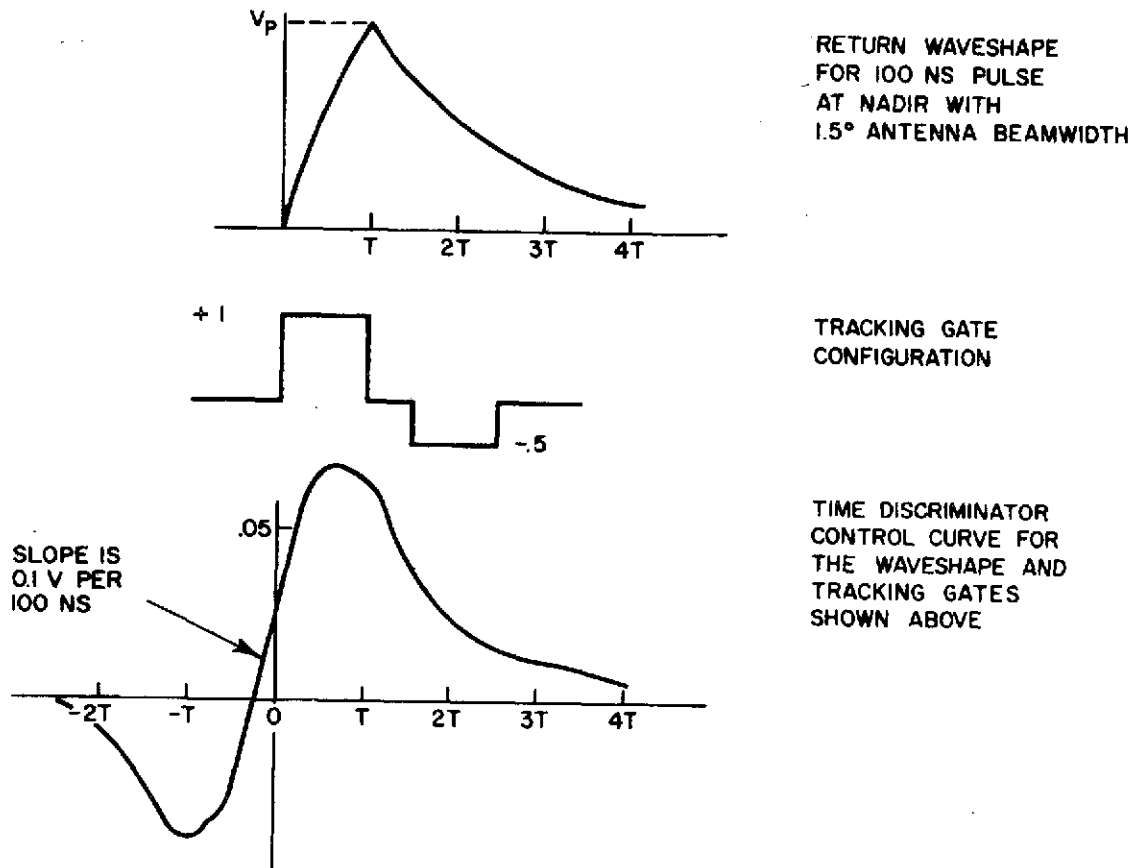
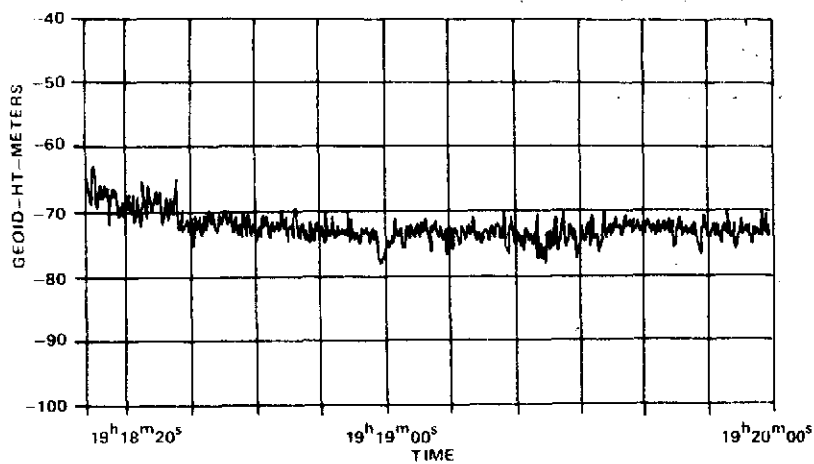
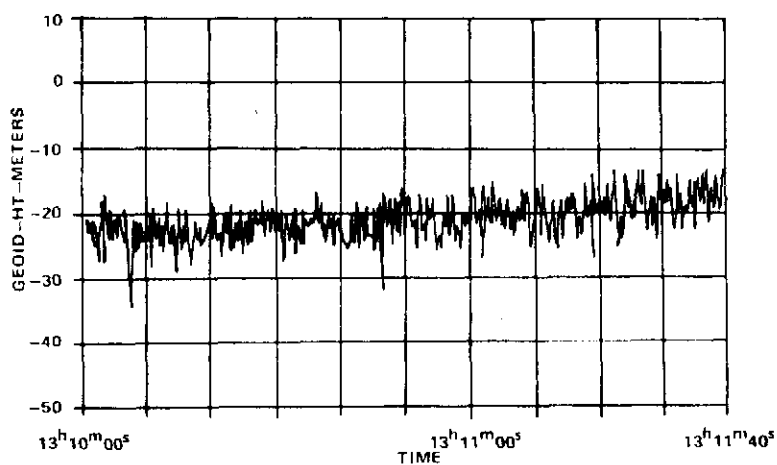
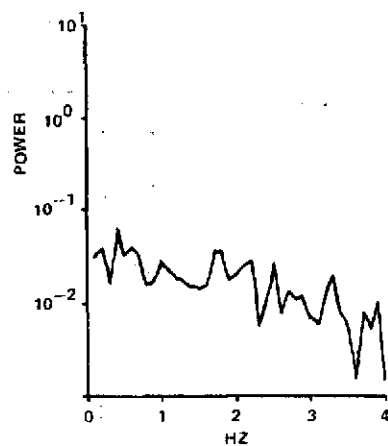


Figure 9 Illustration of Split Gate Error Detector

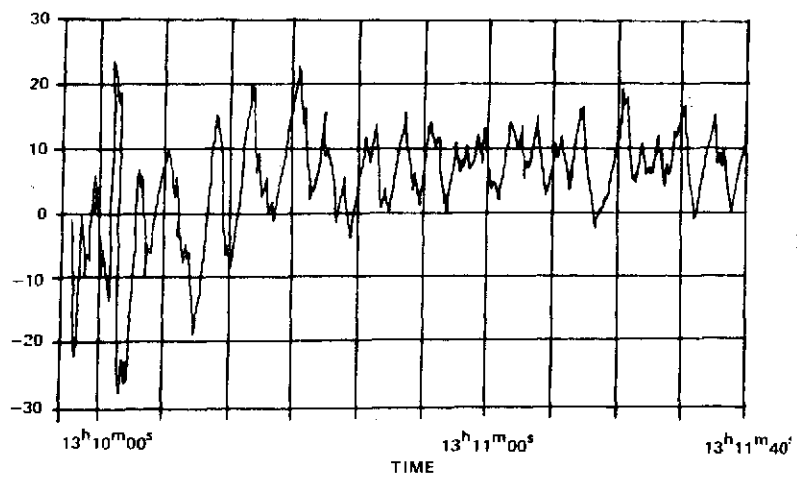
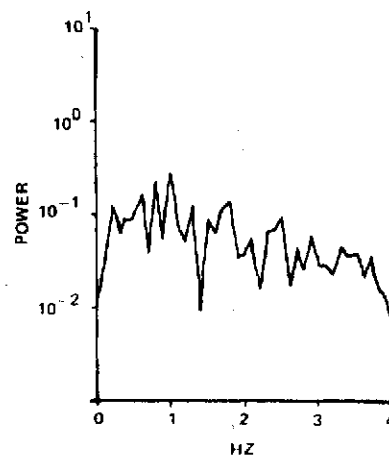
By modeling the various waveforms and predicting the bias for different pointing conditions, it is possible to produce a correction curve as shown in Figure 11. To utilize this curve for correcting the SKYLAB data, a calibration is needed to relate a particular jitter, servo bandwidth and/or AGC level to a bias condition. By carefully selecting SKYLAB data in regions where the geoid and orbit are well known, some data can be obtained to provide the calibration. It is important to note that the SL-4 mission required an independent calibration, for the antenna feed failure on that mission reduced the gain by 23 db and changed the pattern.



SL-4 PASS 38/86 POINTING = .6°



SL-2 PASS 9 POINTING = 1.1°



SL-3 PASS 21/32 POINTING = 1.4°

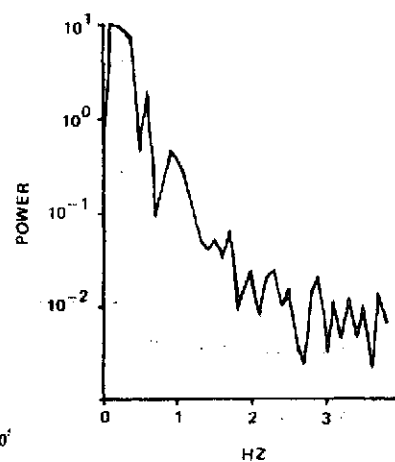


FIGURE 10. OFF NADIR POINTING EFFECTS

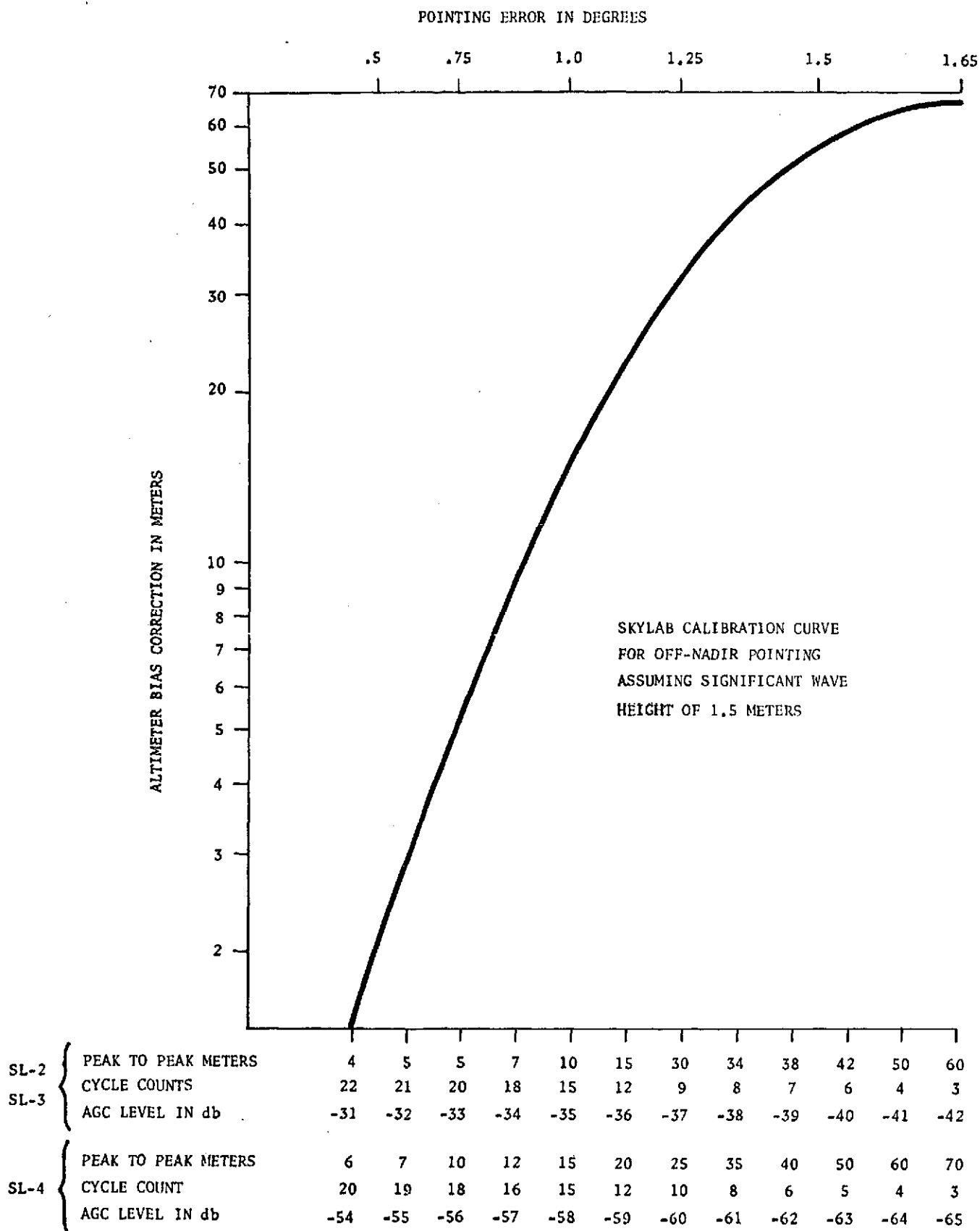


FIGURE 11

Pointing Data Summary

Using both of the methods discussed, the pointing for all three SKYLAB missions are summarized in Table 5. In the Table, the waveform determined pointing is only partially complete, for that method requires much more time-consuming detailed analysis. Since the pointing has largely been obtained by analysis of the tracker performance, where the technique is largely dependent on empirical data, the accuracy is felt to be only about 5 meters. Therefore, in determining the altitude corrections from the pointing errors, the corrections have been rounded off to the nearest 5 meters to prevent the user for over-estimating the accuracy.

Similiarly, the bias with respect to the existing GEM-6 geoid is also rounded off to the nearest 5 meters. These biases were extracted from the residual plots manually, and are not, therefore, highly accurate. If more accuracy is required, both the pointing and the geoid biases could be refined to under one meter. However, if one reviews the whole SKYLAB altimeter error budget discussed in the Accuracy Section, then it becomes evident that further removal of these errors will not improve the overall accuracy.

The Summary Table contains an orbit quality indicator where the numbers represent the estimated meters of uncertainty in the orbit determination. In addition, the AGC level peak cycle counts (a parameter used to estimate the frequency of direction changes in the altitude servo) and peak-to-peak altitude noise in meters are both put in the Table, for they are the parameters on which the tracker pointing determination is based (see Figure 11). Finally, the table contains the new bias that the data pass would have with respect to the GEM-6 geoid if the pointing bias correction is applied.

| MAP
NO. | PASS
NO. | ORBIT
QUALITY | HEIGHT
RATE
M/SEC | AGC
LEVEL | PEAK
CYCLE
COUNTS | PEAK
TO
PEAK | BIAS
FROM
GEM-6 | TRACKER
DETERMINED
POINTING | WAVEFORM
DETERMINED
POINTING | | RECOMMENDED
BIAS
CORRECTION | NEW
BIAS |
|------------|-------------|------------------|-------------------------|--------------|-------------------------|--------------------|-----------------------|-----------------------------------|------------------------------------|------|-----------------------------------|-------------|
| | | | | | | | | | MIN | MAX | | |
| 1 | 1 | 5 | - 2.9 | -36 | 14 | 7 | -30 | 1.10 | | .6° | +20 | -10 |
| 2 | 2 | 13 | - 2.9 | -36.5 | 23 | 5 | 0 | .6° | | | 0 | 0 |
| 3 | 4 | 16 | - 3.5 | -32.5 | 22 | 4 | -20 | .6° | 0.25° | .47° | 0 | -20 |
| 4 | 4 | 18 | - 1.8 | -32.5 | 22 | 4 | -20 | .6° | | .15° | 0 | -20 |
| 5 | 6 | 16 | 1.1 | -33.5 | 17 | 6 | -35 | .8° | .43° | .55° | 5 | -30 |
| 6 | 7 | 79 | - .5 | -37 | 12 | 22 | -55 | 1.2° | 1.15° | 1.2° | +25 | -30 |
| 7 | 7 | 100 | 1.3 | -37 | NA | 30 | -60 | 1.25° | | | +30 | -30 |
| 8 | 7 | 120 | -20.6 | -39 | 8 | 50+ | -80 | 1.45° | | 1.2° | +50 | -30 |
| 10 | 8 | 11 | 3.6 | -33.5 | 20 | 6 | +40 | .75° | | .3° | +5 | +45 |
| 11 | 9 | 5 | .4 | -33 | 21 | 4 | +10 | .6° | .3° | .43° | 0 | +10 |
| 12 | 9 | 5 | 4.5 | -35.6 | 15 | 12 | +20 | 1.1° | | .65° | +22 | +42 |
| 13 | 9 | 6 | 16.5 | -35.5 | 11 | 18 | 0 | 1.1° | | .9° | +20 | +20 |
| 14 | 10 | 11 | 3.3 | -33 | 19 | 8 | -25 | .8° | | .5° | +5 | -20 |
| 15 | 10 | 14 | 5.6 | -33 | 18 | 8 | -5 | .8° | | | +5 | 0 |
| 18 | 11 | 200 | 8.4 | -32 | 15 | 8 | .50 | .7° | | .62° | 5 | +55 |
| 20 | 11 | 200 | 13.9 | -62 | 12 | 15 | 115 | 1.1° | | | +20 | 135 |
| 22 | 12 | 9 | -15.9 | -34 | 20 | 6 | +20 | .8° | .55° | .95° | 5 | +25 |
| 23 | 12 | 25 | - 8.8 | -34 | 18 | 10 | +30 | .85° | | .8° | +10 | +40 |
| 26 | 14 | 11 | -16.2 | -35 | 16 | 8 | +25 | 1.0° | .55° | .8° | +15 | +40 |
| 28 | 17 | 4 | -14.8 | -36 | 7 | 30 | +5 | 1.3° | .9° | 1.0° | +35 | +40 |
| 29 | 17 | 5 | -13.9 | -35 | 15 | 12 | +10 | 1.0° | | .82° | +15 | +25 |
| 30 | 17 | 5 | - 3.4 | -30 | 18 | 9 | +20 | <.5° | .65° | .67° | 0 | +20 |

TABLE 5. SKYLAB POINTING CORRECTION SUMMARY

| MAP
NO. | PASS
NO. | ORBIT
QUALITY | HEIGHT
RATE
M/SEC | AGC
LEVEL | PEAK
CYCLE
COUNTS | PEAK
TO
PEAK | BIAS
FROM
GEM-6 | TRACKER
DETERMINED
POINTING | WAVEFORM
DETERMINED
POINTING | | RECOMMENDED
BIAS
CORRECTION | NEW
BIAS |
|------------|-------------|------------------|-------------------------|--------------|-------------------------|--------------------|-----------------------|-----------------------------------|------------------------------------|--------|-----------------------------------|-------------|
| | | | | | | | | | MIN | MAX | | |
| 32 | 18 | 5 | -7.7 | -31 | 20 | 4 | +25 | <.5° | .2° | .35° | +0 | +25 |
| 33 | 19 | 10 | 8.9 | -36 | 18 | 12 | +35 | 1.05° | .8° | 1.15° | +15 | +50 |
| 34 | 19 | 19 | -3.2 | -35 | 9 | 20 | +20 | 1.1° | | | +20 | +40 |
| 34A | 20 | 14 | -6.3 | -33 | 14 | 20 | +25 | 1.1° | | .5° | +20 | +45 |
| 35 | 21 | 5 | -14.9 | -32 | 20 | 4 | 0 | <.6° | | 0° | 0 | +0 |
| 36 | 21 | 10 | -6.7 | -31.1 | 20 | 4 | +15 | <.5° | | .1° | 0 | +15 |
| 37 | 21 | 13 | -1.1 | -29.8 | 18 | 5 | +25 | .75° | | .25° | 0 | +25 |
| 38 | 22 | 17 | -22.3 | -32.2 | 21 | 5 | -20 | <.6° | .3° | .35° | +0 | -20 |
| 39 | 22 | 18 | -22.9 | -32 | 18 | 4 | -20 | <.6° | .2° | .32° | +0 | -20 |
| 40 | 22 | 18 | -19.3 | -31 | 18 | 5 | -5 | <.5° | .1° | .35° | +0 | -5 |
| 41 | 22 | 18 | -12.4 | -30 | 18 | 5 | +5 | <.5° | .0° | .45° | +0 | +5 |
| 42 | 22 | 18 | -5.9 | -31.2 | 18 | 5 | +20 | <.5° | .0° | .55° | +0 | +20 |
| 43 | 24 | 7 | -5.0 | -33 | 18 | 5 | +30 | .8° | | 0° | +5 | +35 |
| 44 | 24 | 10 | 3.7 | -33.5 | 18 | 5 | +50 | .8° | | .15° | +5 | +55 |
| 45 | 24 | 12 | 11.6 | -32.5 | 18 | 5 | +45 | <.6° | | .35° | +5 | +50 |
| 46 | 25 | 11 | -8.2 | -32 | 20 | 4 | +15 | <.6° | | 0 | +0 | +15 |
| 47 | 25 | 15 | -7 | -30.5 | 20 | 4 | +20 | <.5° | | .15° | +0 | +20 |
| 48 | 27 | 8 | 6.5 | -32.3 | 18 | 5 | +60 | <.6° | | .3° | +0 | +60 |
| 50 | 28 | 3 | 3.9 | -32.2 | 18 | 4 | +50 | <.6° | | .15° | +0 | +50 |
| 54 | 32 | 3 | 5.1 | -39 | 5 | 35 | -35 | 1.6° | | 1.2° | +50 | +15 |
| 55 | 32 | 4 | 8.6 | -35 | 7 | 35 | -40 | 1.4° | | > 1.3° | +40 | 0 |
| 58 | | 14 | 6.7 | -39 | 5 | 12 | -30 | 1.4° | | ≥ 1.3° | +40 | +10 |

TABLE 5. SKYLAB POINTING CORRECTION SUMMARY (Continued)

| MAP
NO. | PASS
NO. | ORBIT
QUALITY | HEIGHT
RATE
M/SEC | AGC
LEVEL | PEAK
CYCLE
COUNTS | PEAK
TO
PEAK | BIAS
FROM
GEM-6 | TRACKER
DETERMINED
POINTING | WAVEFORM
DETERMINED
POINTING | | RECOMMENDED
BIAS
CORRECTION | NEW
BIAS |
|------------|-------------|------------------|-------------------------|--------------|-------------------------|--------------------|-----------------------|-----------------------------------|------------------------------------|-------------------|-----------------------------------|-------------|
| | | | | | | | | | MIN | MAX | | |
| 61 | 36 | 6 | -16.4 | -37.7 | 9 | 12 | -30 | 1.25 ⁰ | | 1.35 ⁰ | +30 | 0 |
| 62 | 36 | 6 | -15.2 | -37.1 | 5 | 15 | -45 | 1.3 ⁰ | | | +35 | -10 |
| 63 | 36 | 7 | -2.3 | -38.4 | 6 | 30 | -35 | 1.4 ⁰ | | 1.3 ⁰ | +40 | 5 |
| 65 | 36 | 3 | 9.1 | -36 | 7 | 20 | -40 | 1.3 ⁰ | | 1.3 ⁰ | +35 | -5 |
| 66 | 37 | 10 | 5.4 | -37.4 | 5 | 30 | -45 | 1.3 ⁰ | | | +35 | -10 |
| 67 | 37 | 11 | 7.7 | -39 | 6 | 35 | -40 | 1.4 ⁰ | | 1.4 ⁰ | +45 | +5 |
| 70 | 38 | 6 | 6.4 | -42 | 3 | 60 | -70 | 1.65 ⁰ | | | +65 | -5 |
| 71 | 38 | 8 | 4.1 | -39.9 | 3 | 30 | -75 | 1.55 ⁰ | | 1.35 ⁰ | +65 | -20 |
| 73 | 39 | 15 | 2.2 | -32 | 18 | 7 | +40 | .85 ⁰ | .6 ⁰ | .65 ⁰ | +10 | +50 |
| 74 | 39 | 15 | .5 | -36 | 18 | 7 | +45 | .85 ⁰ | .68 ⁰ | .75 ⁰ | +10 | +55 |
| 75 | 40 | 3 | -6.9 | -37 | 15 | 12 | -10 | 1.0 ⁰ | | 1.2 ⁰ | +15 | +5 |
| 76 | 40 | 4 | 2.3 | -36 | 12 | 15 | 10 | 1.1 ⁰ | | | +20 | 30 |
| 83 | 54 | 8 | 2.7 | -55 | 17 | 7 | +5 | .75 ⁰ | | | +5 | +10 |
| 84 | 54 | 7 | 5.6 | -56 | 17 | 10 | +20 | .75 | | | 5 | +25 |
| 85 | 55 | 4 | 2.8 | -54 | 20 | 7 | -20 | < .5 ⁰ | | | 0 | -0 |
| 86 | 55 | 4 | 4.6 | -53.5 | 19 | 7 | +5 | < .5 ⁰ | | | 0 | +5 |
| 89 | 57 | 4 | 3.5 | -54 | 19 | 8 | -5 | < .5 ⁰ | | | 0 | -5 |
| 91 | 57 | 3 | 3.7 | -54 | 16 | 8 | +10 | < .5 ⁰ | | | +0 | +10 |
| 92 | 57 | 4 | 4.9 | -54 | 19 | 5 | -15 | < .5 | | | +0 | -15 |

TABLE 5. SKYLAB POINTING CORRECTION SUMMARY (Continued)

| MAP
NO. | PASS
NO. | ORBIT
QUALITY | HEIGHT
RATE
M/SEC | AGC
LEVEL | PEAK
CYCLE
COUNTS | PEAK
TO
PEAK | BIAS
FROM
GEM-6 | TRACKER
DETERMINED
POINTING | WAVEFORM
DETERMINED
POINTING | | RECOMMENDED
BIAS
CORRECTION | NEW
BIAS |
|------------|-------------|------------------|-------------------------|--------------|-------------------------|--------------------|-----------------------|-----------------------------------|------------------------------------|-----|-----------------------------------|-------------|
| | | | | | | | | | MIN | MAX | | |
| 93 | 57 | 4 | 6.4 | -56 | 16 | 10 | -10 | < .5 | | | +5 | -5 |
| 98 | 61 | 5 | 4.2 | -56 | 12 | 13 | -20 | .85 ⁰ | | | +10 | -10 |
| 99 | 61 | 5 | 8.9 | -57.5 | 11 | 25 | -15 | 1.1 ⁰ | | | +20 | +5 |
| 100 | 62 | 6 | 5.1 | -59.5 | 9 | 40 | -15 | 1.3 ⁰ | | | +35 | +20 |
| 102 | 64 | 12 | -2.7 | -51 | 10 | 8 | +5 | < .5 ⁰ | | | 0 | +5 |
| 103 | 64 | 12 | -24.8 | -58 | 17 | 12 | +15 | .75 ⁰ | | | +5 | +19 |
| 105 | 65 | 15 | 20.7 | -54 | 18 | 12 | +35 | .75 ⁰ | | | +10 | +45 |
| 106 | 67 | 3 | 2.9 | -58 | 19 | 9 | +5 | .75 | | | +5 | +10 |
| 108 | 68 | 6 | .7 | -58.8 | 15 | 12 | -30 | 1.0 ⁰ | | | +15 | -15 |
| 109 | 68 | 4 | 11.1 | -55.2 | 16 | 8 | -5 | .75 ⁰ | | | +5 | 0 |
| 110 | 68 | 3 | 17.7 | -55.4 | 16 | 8 | +0 | .75 ⁰ | | | +5 | +5 |
| 113 | 71 | 7 | -17.6 | -55.2 | 16 | 6 | -40 | .75 ⁰ | | | +5 | -35 |
| 114 | 71 | 8 | -17.5 | -55 | 17 | 8 | -30 | .75 ⁰ | | | +5 | -25 |
| 115 | 71 | 8 | -15.1 | -54.5 | 19 | 5 | -25 | < .5 ⁰ | | | 0 | -25 |
| 117 | 74 | 6 | -4.3 | -55.5 | 19 | 5 | -5 | < .5 ⁰ | | | 0 | -5 |
| 118 | 74 | 7 | -5.0 | -55.5 | 16 | 7 | -5 | .75 ⁰ | | | +5 | 0 |
| 119 | 74 | 5 | -11.1 | -59.6 | 15 | 12 | +5 | 1.0 ⁰ | | | +15 | +20 |
| 120 | 74 | 6 | -13.4 | -59.6 | 17 | 10 | -15 | 1.0 ⁰ | | | +15 | 0 |
| 121 | 76 | 7 | -3.6 | -57 | 15 | 10 | -10 | .9 ⁰ | | | +10 | 0 |
| 122 | 76 | 5 | -3.8 | -58.6 | 14 | 15 | -15 | 1.0 ⁰ | | | +15 | 0 |
| 123 | 76 | 5 | -4.7 | -57.6 | 9 | 25 | -25 | 1.2 ⁰ | | | +30 | +5 |
| 124 | 76 | 4 | -9.3 | -59 | 12 | 25 | -25 | | | | +25 | +0 |

TABLE 5. SKYLAB POINTING CORRECTION SUMMARY (Continued)

| MAP NO. | PASS NO. | ORBIT QUALITY | HEIGHT RATE M/SEC | AGC LEVEL | PEAK CYCLE COUNTS | PEAK TO PEAK | BIAS FROM GEM-6 | TRACKER DETERMINED POINTING | WAVEFORM DETERMINED POINTING | | RECOMMENDED BIAS CORRECTION | NEW BIAS |
|---------|----------|---------------|-------------------|-----------|-------------------|--------------|-----------------|-----------------------------|------------------------------|------|-----------------------------|----------|
| | | | | | | | | | MIN | MAX | | |
| 127 | 78 | 7 | -2.8 | -53.7 | 16 | 7 | +5 | <.5° | | | +0 | +15 |
| 128 | 78 | 6 | -3.2 | -57 | 16 | 6 | -5 | .65° | | .57° | 5 | 0 |
| 129 | 78 | 15 | -11.7 | -57.5 | 15 | 9 | -20 | .75° | | .57° | 5 | -15 |
| 131 | 79 | 4 | -2.6 | -56.5 | 18 | 7 | 0 | .75° | | | +5 | +5 |
| 132 | 79 | 3 | -2.1 | -54.8 | 17 | 6 | -5 | .5° | | .60° | +0 | -5 |
| 133 | 79 | 4 | -2.8 | -55.2 | 20 | 5 | +0 | .5° | | .60° | +5 | +5 |
| 134 | 79 | 12 | -11.4 | -58.5 | 14 | 10 | -15 | 1.0° | | | +15 | 0 |
| 135 | 81 | 3 | -.7 | -59 | 16 | 10 | +5 | 1.0° | | | +15 | +20 |
| 139 | 82 | 4 | -15.3 | -54/-59 | 7 | 40 | -45 | 1.3° | | | +40 | -5 |
| 145 | 83 | 5 | -9.8 | -58 | 16 | 11 | -10 | .75° | | | +5 | -5 |
| 145A | 83 | 5 | -12.4 | -60 | 18 | 10 | -10 | .75° | | | +5 | -5 |
| 146 | 83 | 5 | -7.1 | -60 | 17 | 10 | -20 | .75° | | | +5 | -15 |
| 147 | 83 | 3 | -18.6 | -58 | 18 | 8 | -20 | .70° | | .48° | +5 | -15 |
| 148 | 83 | 7 | 1.9 | -57.5 | 14 | 16 | -10 | 1.0° | | | +15 | +5 |
| 151 | 85 | 13 | -15.6 | -56 | 17 | 8 | -25 | .75° | | | +5 | -20 |
| 152 | 87 | 9 | -14.8 | -57 | 16 | 7 | -0 | <.5° | | | +0 | -0 |
| 155 | 88 | 4 | -17.5 | -57.5 | 10 | 26 | -25 | 1.25° | | | +30 | +5 |
| 156 | 88 | 5 | 23.7 | -58 | 15 | 15 | +20 | 1.0° | | | +15 | +35 |
| 163 | 89 | 4 | -15.3 | -58.0 | 15 | 12 | -15 | .85° | | | +15 | 0 |
| 164 | 89 | 4 | -13.5 | -58 | 9 | 15 | -15 | 1.1° | | | +20 | +5 |
| 168 | 90 | 4 | -19.8 | -58 | 7 | 20 | -40 | 1.3° | | | +35 | -5 |
| 169 | 90 | 5 | -18.3 | -58 | 6 | 25 | -40 | 1.35° | | | +40 | +0 |

TABLE 5. SKYLAB POINTING CORRECTION SUMMARY (Continued)

| MAP NO. | PASS NO. | ORBIT QUALITY | HEIGHT RATE M/SEC | AGC LEVEL | PEAK CYCLE COUNTS | PEAK TO PEAK | BIAS FROM GEM-6 | TRACKER DETERMINED POINTING | WAVEFORM DETERMINED POINTING MIN MAX | RECOMMENDED BIAS CORRECTION | NEW BIAS |
|---------|----------|---------------|-------------------|-----------|-------------------|--------------|------------------|-----------------------------|--------------------------------------|-----------------------------|----------|
| 175 | 91 | 4 | -8.4 | -58 | 8 | 18 | -25 | 1.25 ⁰ | | +30 | +5 |
| 182 | 92 | 13 | -12.8 | -49 | 18 | 6 | -20 | .75 ⁰ | | +5 | -15 |
| 185 | 93 | 6 | -10.6 | -55.8 | 15 | 8 | -20 | .85 ⁰ | | +10 | -10 |
| 201 | 97 | 3 | 3.8 | -57 | 15 | | +5 | .75 ⁰ | | 5 | 10 |
| 202 | 97 | 3 | 7.2 | -54 | 17 | | +10 | .75 ⁰ | | 5 | 15 |
| 203 | 97 | 3 | 6.5 | -55 | 18 | | +15 | .75 ⁰ | | 5 | 20 |
| 204 | 97 | 3 | 3.3 | -57 | 16 | | +10 | .75 ⁰ | | 5 | 15 |
| 205 | 97 | 3 | -.5 | -57 | 17 | | -5 | .75 ⁰ | | 5 | 0 |
| 206 | 97 | 3 | -4.8 | -56 | 15 | | 0 | .75 ⁰ | | 5 | 5 |
| 207 | 97 | 3 | -7.7 | -57 | 16 | | -5 | .75 ⁰ | | 5 | 0 |
| 208 | 97 | 3 | -5.9 | -56 | 18 | | -10 | .75 ⁰ | | +5 | -5 |
| 209 | 97 | 3 | -1.4 | -55 | 17 | | -5 | .75 ⁰ | | 5 | 0 |
| 210 | 97 | 4 | 4.2 | -54 | 16 | | 5 | .75 ⁰ | | 5 | 10 |
| 211 | 97 | 3 | 10.4 | -54 | 18 | | 5 | .75 ⁰ | | 5 | 10 |
| 212 | 97 | 3 | 15.1 | -56 | 16 | | 15 | .75 ⁰ | | 5 | 20 |
| 213 | 97 | 4 | 17.0 | -55 | 17 | | 10 | .75 ⁰ | | 5 | 15 |
| 214 | 97 | 5 | 18.7 | -55.8 | 19 | +5 | .75 ⁰ | | | 5 | 10 |
| 215 | 97 | 4 | 10.7 | -57.7 | 18 | 10 | +10 | .75 ⁰ | | +5 | 15 |
| 216 | 97 | 3 | 4.7 | -57 | 18 | 8 | -0 | .75 ⁰ | | +5 | 5 |
| 217 | 97 | 3 | -1.9 | -54 | 14 | 10 | -10 | .85 ⁰ | | +10 | 0 |
| 218 | 17 | 3 | -6.8 | -57 | 18 | 8 | -10 | .75 ⁰ | | +5 | -5 |
| 222 | 97 | 3 | -16.6 | -49 | 16 | 7 | -20 | .75 ⁰ | | +5 | -15 |

TABLE 5. SKYLAB POINTING CORRECTION SUMMARY (Continued)

| MAP
NO. | PASS
NO. | ORBIT
QUALITY | HEIGHT
RATE
M/SEC | AGC
LEVEL | PEAK
CYCLE
COUNTS | PEAK
TO
PEAK | BIAS
FROM
GEM-6 | TRACKER
DETERMINED
POINTING | WAVEFORM
DETERMINED
POINTING | | RECOMMENDED
BIAS
CORRECTION | NEW
BIAS |
|------------|-------------|------------------|-------------------------|--------------|-------------------------|--------------------|-----------------------|-----------------------------------|------------------------------------|------|-----------------------------------|-------------|
| | | | | | | | | | MIN | MAX | | |
| 223 | 97 | 3 | -16.2 | -55 | 16 | 10 | -15 | .75° | | | +5 | -10 |
| 225 | 97 | 4 | -14.5 | -55.9 | 19 | 6 | -5 | .6° | | | +5 | 0 |
| 226 | 97 | 4 | -12.9 | -57 | 19 | 8 | -5 | .75° | | | +5 | 0 |
| 233 | 86 | 4 | -23.2 | 19 | 6 | -5 | .6° | | | .60° | +5 | -20 |

TABLE 5. SKYLAB POINTING CORRECTION SUMMARY (Continued)

ERROR BUDGET

Instrument Errors

Instrument Bias - One of the largest instrument errors is bias. The removal of this error is extremely important to anyone wishing to use the absolute accuracy of the altitude measurements. Since this error is comparatively large with respect to other errors (see Table 6), and is difficult to remove, it often determines the system accuracy.

One of the bias errors is the zero set error (initial alignment) which is a fixed bias for the duration of the satellite life. Internal instrument delay caused by processing transmission methods such as path delays are included in this bias. Field calibration efforts are usually focused on minimizing this error.

These bias errors also change if operating parameters are changed. For example, the changing of a pulsewidth or bandwidth in the altimeter will cause a jump in altitude. These are easy to recognize in SKYLAB data since the altimeter was constrained to a fixed routine, and mode changes had to occur at certain times. The magnitude of these jumps are not necessarily consistent from one pass to the next, for the satellite pointing can change the operating conditions (signal-to-noise, pulseshape, etc.) significantly.

System drift can cause the zero set error to slowly change. In mode 1 calibration, step CDS 3, the altimeter locks on and tracks its own transmitted pulse. This test was instrumented to measure any drift present in the system. SKYLAB results have shown that this error has been only a few centimeters over the whole satellite life.

When the overall SKYLAB mission errors are reviewed, the instrument bias error is found to be under 10 meters. This is a conservative estimate, for the 10 meter error measured includes more than the instrument bias. (See System Accuracy Discussion.)

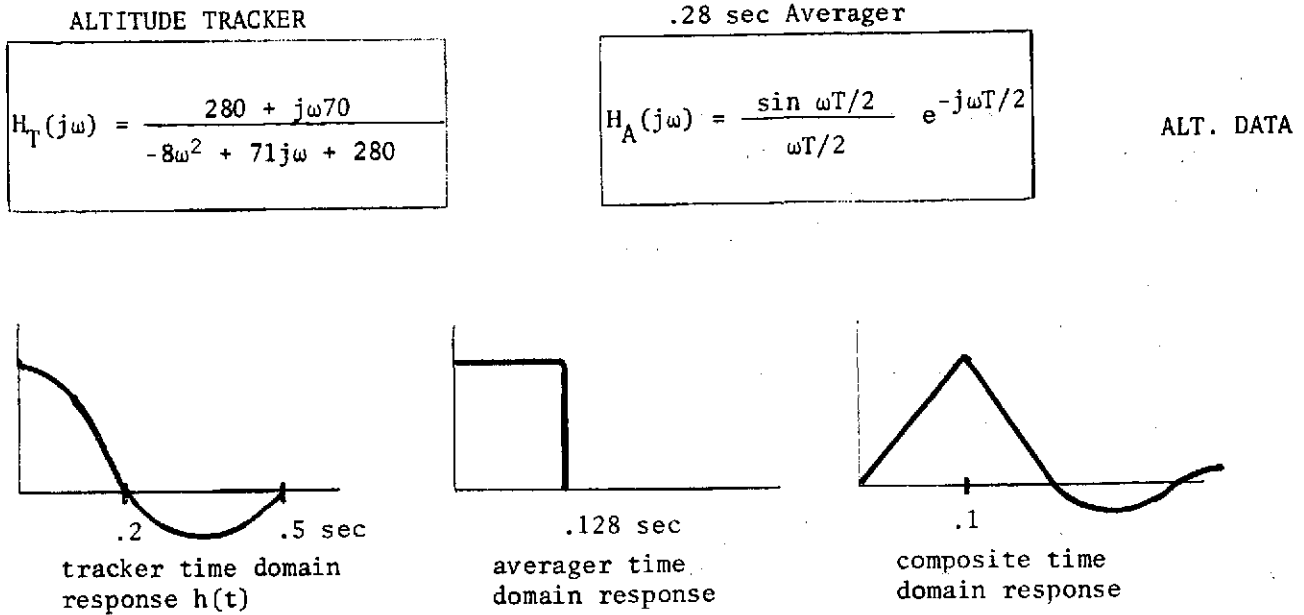
Timing Bias - The two primary sources of timing bias errors are time tag vs true Greenwich Mean Time (GMT) and the altimeter processor time delay. The time tag error is the bias between the satellite timing system and the GMT time. This error is usually small (approximately 100 microseconds) and can be ignored. However, in a few isolated instances some large timing errors (approximately one second) were found when data processed by Kennedy Space Center was compared with that processed at Johnson Space Center. While there have been extremely careful attempts to locate and remove such errors, the user should be aware that a few passes might still contain errors of this magnitude.

SYSTEM ERROR MODEL AND RESIDUALS

| | UNCORRECTED
MAGNITUDE | ERROR SOURCE | CORRECT
RESIDUALS (THEORETICAL) |
|------------------------------------|--------------------------|--|---|
| 1. INSTRUMENT ERRORS
Systematic | Up to 50 meters | Zero set error, discriminator drift, servo unbalance, operating parameter changes | < 10 m
(Correcting for operating parameters only) |
| | Up to 1.5 meters | Timing Errors | < 1 m Normally
(No correction applied) |
| | ≈ 10 cm peak | Transit Time Error | < 1 cm Normally
(No correction applied) |
| | Up to 35 cm | Dynamic Lag Error
K_v = Servo Acceleration Constant (276 per sec)
K_a = Servo Velocity Constant (35 per sec ²) | < 10 m Normally
(No correction applied) |
| Random | Up to 80 cm | σ_{h_t} = Height Thermal Noise | < 1 m for 1 sec average
≈ 30 cm
(where features permit more averaging can be applied) |
| | Approx. 15 cm | σ_{h_q} = Quantizing Error | |
| 2. POINTING | Up to 60 meters | Off Nadir Pointing | < 5 m
(Primarily using the tracker response as a pointing indicator) |
| 3. SEA SURFACE | Up to .70 m | Electromagnetic MSL vs MSL | Up to 70 cm
(No correction applied) |
| 4. ATMOSPHERE | Up to 3 meters | Atmospheric refraction path delay | < 50 cm
(Using mean atmospheric correction) |
| 5. ORBIT | < 10 meters | Uncertainty in orbit height | < 10 m
(No correction available) |
| SYSTEM ACCURACY | < 20 meters | RMS of all errors | < 10 m |

TABLE 6

The altimeter processor time delay correction is largely due to the delay characteristics of the on-board averaging operation. The S-193 altitude measurement process is shown in block diagram form below, along with the frequency domain (Fourier) transfer functions $H(j\omega)$ and impulse response



functions $h(t)$. As shown in these sketches, a particular altitude value represents contributions from a large number of past values, i.e. a given value is not centrally weighted since the tracker cannot be anticipative. As will be discussed, if desired, the non-anticipatory restriction can be removed in computer (non-real time) data processing. A fixed-value time correction is developed in the following paragraphs, which is considered adequate for most altimeter data applications.

The altitude tracker transfer function can be expressed in polar form as

$$H_T(j\omega) = |H_T(j\omega)| \exp \left(-j \tan^{-1} \frac{\omega + 2\omega^3}{280 + 9.75\omega^2} \right)$$

Similarly,

$$H_A(j\omega) = |H_A(j\omega)| e^{-j\omega T/2}$$

where the averaging period T is .128 sec. Since an idealized linear phase-shift device will have a transfer function of the form,

$$H(j\omega) = |H(j\omega)| e^{-j t_o \omega}$$

by analogy, a frequency range can be established over which the altitude data may be considered to be derived from a fixed-time delay system. Using this analogy, the time delay t_o is given by

$$t_o = \frac{1}{\omega} \tan^{-1} \left[\frac{\omega + 2\omega^3}{280 + 9.75\omega^2} \right] + \frac{T}{2}$$

This expression is evaluated in Table 1 with frequency in Hz, ω (omega) in radian/sec., wavelength in km (assuming a ground track velocity of 7.4 km/sec), and time delay t_o in milliseconds. Analysis shows that

- 1) the S-193 altimeter behaves essentially as a fixed time delay system for surface wavelengths equal to or greater than ~50 km, with a time delay of ~68 milliseconds, and
- 2) the time delay of the on-board averaging operation is the dominant effect for the long wavelength case (its time delay alone accounts for 64 ns and the residual delay is essentially the tracker lag error).

For detailed studies of short wavelength geoid and ocean-topographic features, a fixed-value time correction is not recommended. In these cases the altitude time-series can be more accurately corrected by convolving the data with a symmetrical impulse response function (i.e. $h(t) = h(-t)$)*. Such a centrally weighted response may be obtained by convolving the S-193 data with a time-reversed replica of the composite system response.

Under the most extreme conditions (height rates of 20 m/sec) an error of 1.5 meters would be possible. Under normal conditions, the typical error is under 1 meter.

For both of the above errors no correction has been applied. However, if one wishes to make a correction, the following equation can be utilized:

$$h_t = \Delta_t \dot{h} + (\Delta_t)^2 \ddot{h} + \dots$$

Δ_t = timing bias

\dot{h}_t = height error

\dot{h} = height rates

\ddot{h} = height acceleration

The satellite height dynamics for various SKYLAB passes are summarized in Table 5.

*In such cases the "spot size" spatial filter characteristics should also be considered.

Transit Time Correction - The measurement time tags can be corrected to the time the altimeter pulse arrived at the earth's surface by the relationship:

$$T_c = T_o - h/C$$

where

T_c = corrected observation time (seconds)

T_o = sampled time at radar

C = velocity of light = 299,792.5 km/sec

h = height of satellite over the surface

The error caused by not considering the transit time is dependent on the height dynamics and has the following form:

$$h_{tt} = \frac{1}{C} \dot{h} h + \frac{1}{C} h^2 \ddot{h} \dots$$

where \dot{h} and \ddot{h} are the height rate and height acceleration respectively. Using a maximum \dot{h} of 50 m/sec and \ddot{h} of 5 m/sec² and a nominal satellite height of 500 km an approximate 10 cm error results. Since this error is so insignificant in the total error budget, no transit time correction was applied.

Dynamic Lag Error - The error of the height tracker in following relative motion of the ocean surface undulations and the satellite height variations is defined as the Dynamic Lag Error. These servo lag errors can better be expressed as follows:

$$h_{dL} = \frac{\dot{h}}{K_v} + \frac{\ddot{h}}{K_a} + \dots$$

h_{dL} = total dynamic lag error

K_v = altitude tracker servo velocity constant

K_a = altitude tracker servo acceleration constant

\dot{h} = height velocity encountered

\ddot{h} = height acceleration encountered

Using 50 meter/sec velocity and 5 meters/sec acceleration, which are conservative values, the dynamic lag error is under 35 centimeters. In the SKYLAB mission, 20 meter/sec velocity caused by the orbit and 1 meter/sec² acceleration caused by an ocean feature were the largest dynamics experienced.

No correction has been applied to the data for this error.

Random Error - The total random error is primarily made up of a quantizing error and the thermal noise of the height tracker. These errors are combined as follows:

$$\sigma_h = \sqrt{\sigma_{h_t}^2 + \sigma_{h_q}^2}$$

where

σ_{h_t} = thermal noise

σ_{h_q} = quantizing error

The quantizing error is expressed as:

$$\sigma_{h_q} = \sqrt{\sigma_{h_{q1}}^2 + \sigma_{h_{q2}}^2}$$

where

$\sigma_{h_{q1}}$ = start of digital delay generator

$\sigma_{h_{q2}}$ = stop of digital delay generator

The typical error for each term is computed as follows:

$$\sigma_{h_q} = \frac{\text{Bit Weight}}{\sqrt{12}}$$

The bit weight is 2.5 n seconds which results in a σ_{h_q} of approximately 15 cm.

The σ_{h_t} is computed as follows:

$$\sigma_{h_t} = \frac{T \sqrt{7/6 + \frac{6}{S/N} + \frac{8}{(S/N)^2}}}{\sqrt{\frac{\text{prf}}{\pi b}}} \times \frac{C}{2}$$

where

T = pulsewidth (100 n sec)

S/N = signal to noise (100:1)

prf = 250

b = servo bandwidth (1.3 Hz)

C = 299792.5 Km/sec (speed of light)

Since the above equation yields the noise for each independent sample of the servo, the noise is further divided by the $\sqrt{8}$ to get the one second noise level, providing all 8 samples are independent.

Pointing

As was stated in the Pointing Section of this report, pointing errors cannot only cause an altitude bias but also can cause the altitude tracker to become sluggish. Slight pointing errors (less than $.75^\circ$) mainly affect the altitude bias and can very accurately be removed by waveform analysis down to a residual of a few centimeters. Larger pointing errors, where the tracker peak jitter increases and the stracker servo becomes sluggish, are not as straightforward to correct. The waveform techniques for determining pointing errors can't be used, and the less accurate tracker performance modeling technique must be utilized. This technique can remove large biases (60 meters or so) and leave the residuals under 5 meters but cannot overcome the lack of response of the servo to higher frequency topographic features. The increased jitter level associated with these large pointing errors also cannot be overcome. However, if the geoid or topographic features being recovered are sufficiently known that the analyst is sure that their wavelength is longer than the wavelength of the frequency response of the tracker, then an appropriate filter can be applied to the data. This filtering can reduce the effects of the jitter and will therefore aid in the recovery of the feature of interest.

Sea Surface

Sea surface error is a bias caused by the difference between the true mean sea level and the mean point that the radar tracks. This error is further complicated by the fact that it probably changes as sea state changes.

By modeling the change of rise time as sea state increases and by considering that the SKYLAB altimeter tracker gate was fixed, it can be seen that the error will increase linearly with significant wave height (SWH). However, real data to confirm the nature of this bias is very sparse. By using some data obtained by Yaplee, et al, (NRL) which indicated approximately 14 cm bias for a 2 meter SWH [5], an extrapolation was made to 70 cm for a 10 meter SWH, but this is felt to be pessimistic. Since the model is somewhat questionable and knowledge of the SWH is very limited, no attempt to correct for this error has been made.

Atmosphere

Without corrections for atmospheric delay, the error would not exceed 3 meters. However, it was decided that a mean correction would be used, which left residual errors of approximately 50 cm.

The refraction model being used to correct the altitude data for tropospheric effects has been defined in the Data Processing Section of the report. The error in this model is about 10% of the total correction assuming no error exists in the pointing or in the surface N unit measurement. However, the value of the surface refractivity used

in the refraction model was fixed at 340 N units. This value was obtained by calculating the average annual value of the surface refractivity over water independent of geographical position. Since instantaneous values of surface refractivity could depart from the mean value used by as much as 40-50 N units, a 15% error in using the average value N unit could result in evaluating the refraction correction equation. These two errors could result in a total error of about 20% in the tropospheric refraction correction applied to all altitude data. Also, no correction was made for ionospheric effects since these were felt to be only a few centimeters. (Reference [7].)

Orbit Error

Not only is orbit error one of the larger sources of error, but also since the orbit is the reference for altimeter measurements, these errors project directly into geoid error.

For each SKYLAB pass, both the bias and the shape error of the orbit can affect the overall system accuracy. The shape error over the duration of an operation (approximately 3 minutes) is generally felt not to exceed 1 meter. This can be confirmed by looking at passes that overlap (see Figures 12 and 13). This error could be larger if insufficient tracking data were available for forming the orbit. The orbit quality indicator on the pointing charts is one attempt to provide the user with an estimate of the uncertainty in the orbit. A higher uncertainty can mean that the data might be both more biased and more trended. However, these computed uncertainties are based on the geometrical strength of the stations in the orbit solution, and do not consider unexpected tracking station errors. Therefore, the user must apply these with caution.

The average orbit bias error based on the overall accuracy histogram of the altimeter system is estimated to be under 10 meters (see Figure 14).

System Accuracy

To establish the overall system accuracy, the altimeter data was compared with the GEM-6 [8] geoid. The differences between the GEM-6 geoid and the altimeter measurements were plotted in the histogram of Figure 14. In the same figure, a histogram of the pointing error corrections was convolved with an assumed 10 meter normal distribution of other errors. It should be noted that the resulting error difference distribution favorably compared with the geoid histogram. Therefore, it can be concluded that the combination of orbit error, uncertainty in the GEM-6 geoid and altimeter bias is under ± 10 meters rms.

It is not possible to break down further these three main errors, but the orbit and geoid errors will probably supply the largest contribution to the data spread. The altimeter instrument bias has an uncertainty of 10 meters since it can not presently be calibrated below this level. However, the instrument is probably consistent within a meter.

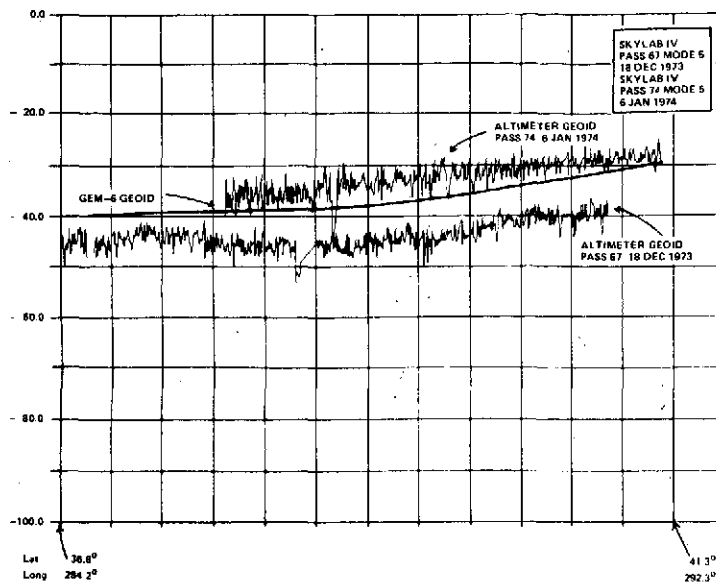


Figure 12 Comparison of Altimeter Geoid With GEM-6 Geoid For 2 Passes over the Same Area

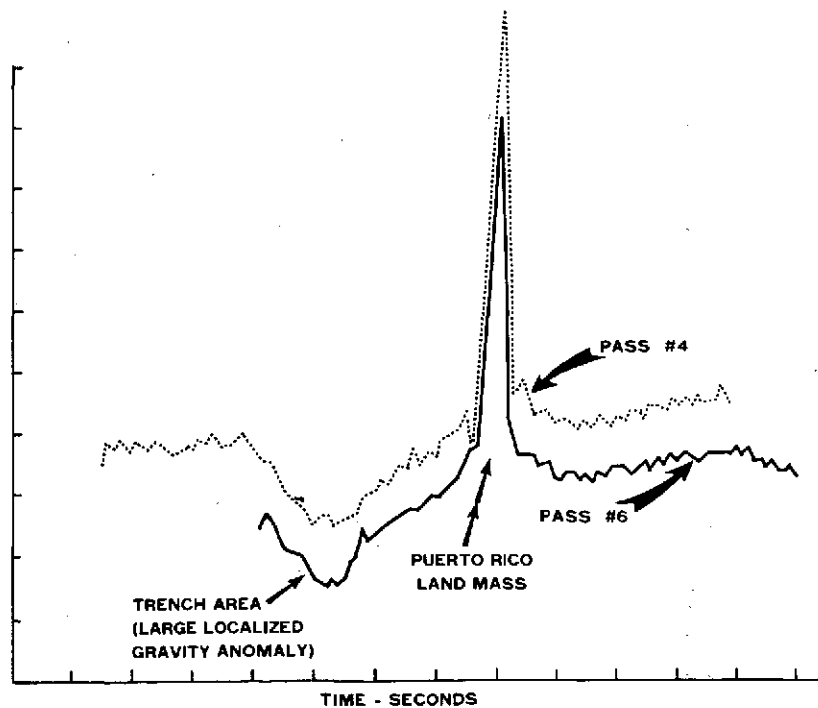


Figure 13 SKYLAB Passes over Puerto Rico Area

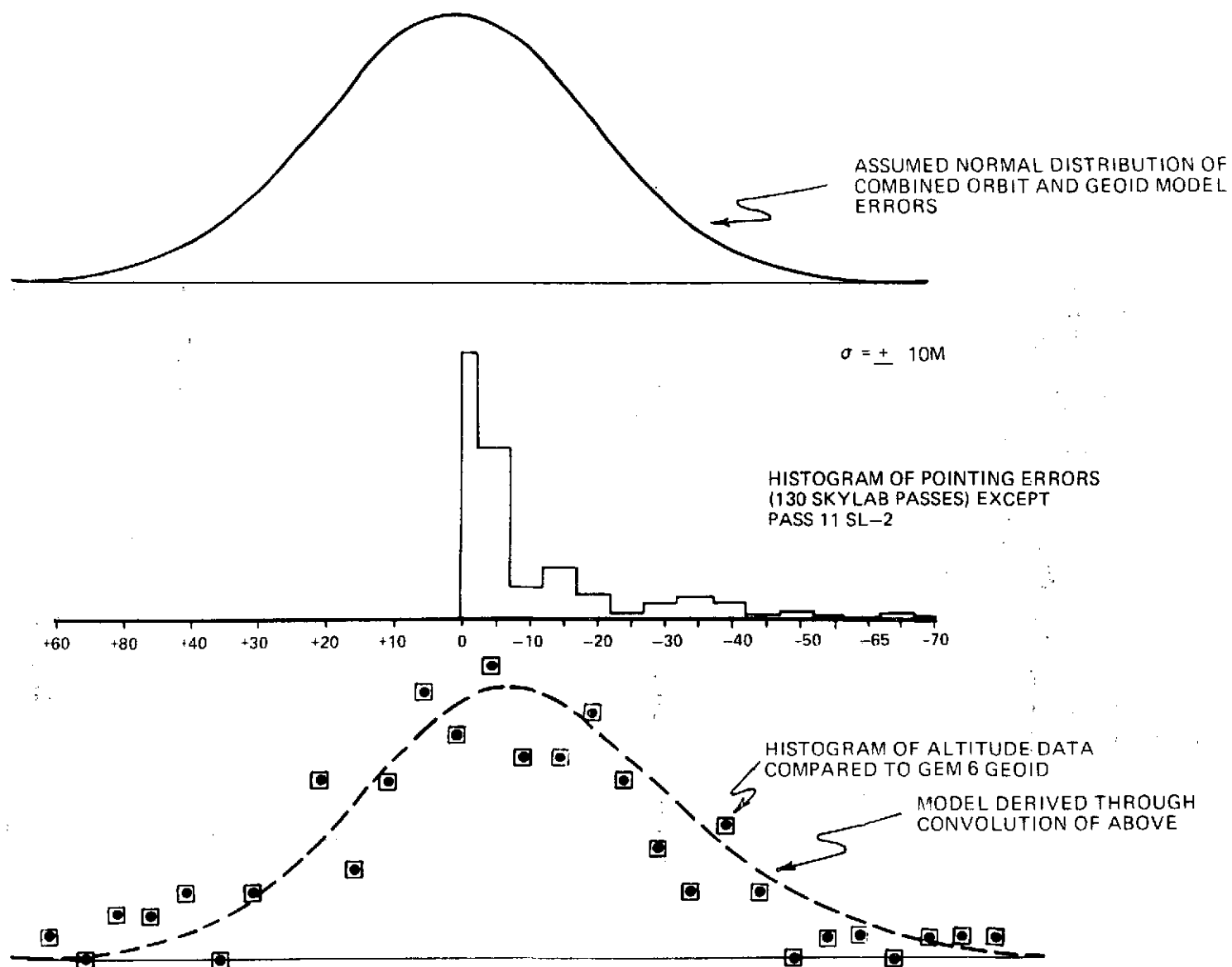


FIGURE 14. DIFFERENCES BETWEEN THE GEM-6 GEOID AND THE ALTIMETER MEASUREMENTS

DATA SUMMARY

Table 7 in this section tabulates the altimeter data passes according to SKYLAB pass number, time, and ground track latitude and longitude. In addition, map numbers are assigned which can be cross-referenced to the ground track plots which immediately follow in this section. The ground tracks are laid out on National Geographic Ocean floor maps so that the data can be compared with ocean floor topographic features.

ORIGINAL PAGE IS
OF POOR QUALITY

| DOY | DATE | PASS | MODE | MAP | TIME | | START | | STOP | |
|-----|---------------|------|------|-----|----------|----------|-------|-------|-------|-------|
| | | | | | START | STOP | LAT | LONG | LAT | LONG |
| 150 | May 30, 1973 | 1 | 1 | 1 | 20 37 55 | 20 38 10 | 43.6 | 235.2 | 43.3 | 235.9 |
| 153 | June 2, 1973 | 2 | 1 | 2 | 20 05 40 | 20 07 10 | 40.6 | 232.2 | 36.8 | 238.8 |
| 155 | June 4, 1973 | 4 | 1 | 3 | 17 11 10 | 17 14 15 | 31.1 | 279.8 | 23.1 | 287.9 |
| 155 | June 4, 1973 | 4 | 5 | 4 | 17 15 15 | 17 16 30 | 19.8 | 291.4 | 16.0 | 294.7 |
| 159 | June 9, 1973 | 6 | 5 | 5 | 15 15 30 | 15 18 20 | 21.2 | 290.2 | 13.6 | 297.5 |
| 160 | June 10, 1973 | 7 | 1 | 6 | 14 28 15 | 14 31 00 | 33.6 | 281.3 | 26.1 | 290.0 |
| 160 | June 10, 1973 | 7 | 5 | 7 | 14 32 10 | 14 34 50 | 23.5 | 292.7 | 15.7 | 299.7 |
| 160 | June 10, 1973 | 7 | 3 | 8 | 14 36 30 | 14 38 50 | 11.0 | 303.4 | 4.2 | 308.2 |
| 161 | June 11, 1973 | 8 | 1 | 9 | 15 19 50 | 15 20 10 | 31.6 | 265.0 | 30.5 | 266.4 |
| 161 | June 11, 1973 | 8 | 3 | 10 | 15 25 10 | 15 27 15 | 16.8 | 279.8 | 10.5 | 284.9 |
| 162 | June 12, 1973 | 9 | 5 | 11 | 13 01 35 | 13 04 25 | 37.5 | 285.1 | 30.5 | 294.7 |
| 162 | June 12, 1973 | 9 | 3 | 12 | 13 10 00 | 13 12 20 | 15.3 | 309.5 | 8.0 | 315.5 |
| 162 | June 12, 1973 | 9 | 3 | 13 | 13 15 35 | 13 18 00 | -0.9 | 322.0 | -8.3 | 327.6 |
| 163 | June 13, 1973 | 10 | 1 | 14 | 13 58 50 | 14 01 00 | 20.5 | 286.0 | 17.2 | 289.0 |
| 163 | June 13, 1973 | 10 | 1 | 15 | 14 01 50 | 14 02 30 | 11.9 | 293.2 | 9.7 | 295.1 |
| 164 | June 14, 1973 | 11 | 5 | 18 | 14 54 00 | 14 55 35 | 7.2 | 278.1 | 2.7 | 281.4 |
| 164 | June 14, 1973 | 11 | 3 | 19 | 15 02 15 | 15 02 55 | 297.1 | -52.6 | 298.0 | -61.5 |
| 164 | June 14, 1973 | 11 | 5 | 20 | 15 07 05 | 15 07 50 | -29.7 | 304.2 | -31.9 | 311.8 |

TABLE 7. SKYLAB DATA SUMMARY

| DOY | DATE | PASS | MODE | MAP | TIME | | START | | STOP | |
|-----|-------------------|-----------|------|-----|----------|----------|-------|-------|-------|-------|
| | | | | | START | STOP | LAT | LONG | LAT | LONG |
| 215 | August 3, 1973 | 12/SL3/1 | 1 | 22 | 18 06 35 | 18 09 00 | 29.1 | 264.0 | 23.2 | 270.1 |
| 215 | August 3, 1973 | 12/SL3/1 | 1 | 23 | 18 12 35 | 18 13 50 | 12.2 | 279.7 | 8.8 | 282.4 |
| 217 | August 5, 1973 | 14/SL3/3 | 1 | 26 | 15 04 00 | 15 06 30 | 39.1 | 283.3 | 33.2 | 292.2 |
| 221 | August 9, 1973 | 17/SL3/6 | 1 | 28 | 13 47 20 | 13 49 50 | 36.4 | 283.2 | 31.0 | 290.4 |
| 221 | August 9, 1973 | 17/SL3/6 | 3 | 29 | 13 51 10 | 13 53 30 | 27.1 | 294.9 | 20.7 | 301.2 |
| 221 | August 9, 1973 | 17/SL3/6 | 5 | 30 | 13 58 30 | 14 01 20 | 6.1 | 313.1 | - 2.3 | 319.5 |
| 223 | August 11, 1973 | 18/SL3/7 | 1 | 31 | 15 29 30 | 15 32 20 | 33.6 | 249.3 | 26.7 | 257.5 |
| 223 | August 11, 1973 | 18/SL3/7 | 5 | 32 | 15 36 50 | 15 39 40 | 13.1 | 269.9 | 5.2 | 276.0 |
| 224 | August 12, 1973 | 19/SL3/8 | 1 | 33 | 02 35 00 | 02 38 10 | - 4.6 | 117.6 | -13.4 | 124.5 |
| 224 | August 12, 1973 | 19/SL3/8 | 5 | 34 | 02 46 50 | 02 49 30 | -37.5 | 150.5 | -42.4 | 159.7 |
| 224 | August 12, 1973 | 20/SL3/9 | 1 | 34A | 14 54 40 | 14 57 30 | 11.9 | 275.6 | 3.5 | 282.1 |
| 244 | September 1, 1973 | 21/SL3/10 | 5 | 35 | 15 22 45 | 15 25 40 | -16.5 | 322.9 | - 8.7 | 329.2 |
| 244 | September 1, 1973 | 21/SL3/10 | 5 | 36 | 15 26 35 | 15 29 30 | - 5.2 | 332.2 | 2.0 | 337.8 |
| 244 | September 1, 1973 | 21/SL3/10 | 5 | 37 | 15 30 30 | 15 31 30 | 5.7 | 340.0 | 9.2 | 342.7 |
| 245 | September 2, 1973 | 22/SL3/11 | 1 | 38 | 14 29 55 | 14 32 45 | -41.9 | 296.1 | -30.1 | 306.4 |
| 245 | September 2, 1973 | 22/SL3/11 | 1 | 39 | 14 33 40 | 14 36 35 | -33.7 | 309.8 | -26.4 | 318.5 |
| 245 | September 2, 1973 | 22/SL3/11 | 1 | 40 | 14 37 20 | 14 40 15 | -24.1 | 320.8 | -16.1 | 328.1 |
| 245 | September 2, 1973 | 22/SL3/11 | 1 | 41 | 14 41 20 | 14 44 00 | -12.7 | 330.9 | - 5.3 | 336.6 |
| 245 | September 2, 1973 | 22/SL3/11 | 1 | 42 | 14 44 45 | 14 47 35 | - 2.3 | 338.8 | 5.7 | 334.8 |
| 246 | September 3, 1973 | 24/SL3/13 | 3 | 43 | 15 35 40 | 15 38 00 | - .7 | 321.1 | 6.7 | 326.7 |
| 246 | September 3, 1973 | 24/SL3/13 | 3 | 44 | 15 40 05 | 15 42 30 | 12.6 | 331.4 | 19.4 | 337.1 |
| 246 | September 3, 1973 | 24/SL3/13 | 3 | 45 | 15 44 40 | 15 47 05 | 26.4 | 343.8 | 31.7 | 349.8 |
| 247 | September 4, 1973 | 25/SL3/14 | 5 | 46 | 14 51 35 | 14 54 30 | -4.2 | 323.3 | 4.2 | 329.7 |
| 247 | September 4, 1973 | 25/SL3/14 | 5 | 47 | 14 55 10 | 14 58 00 | 5.7 | 330.8 | 14.6 | 337.7 |

TABLE 7. SKYLAB DATA SUMMARY (Continued)

| DOY | DATE | PASS | MODE | MAP | TIME | | START | | STOP | |
|-----|--------------------|-----------|------|-----|----------|----------|-------|-------|-------|-------|
| | | | | | | | LAT | LONG | LAT | LONG |
| 249 | September 6, 1973 | 27/SL3/16 | 5 | 48 | 21 19 45 | 21 22 25 | 19.8 | 233.4 | 27.6 | 241.6 |
| 249 | September 6, 1973 | 27/SL3/16 | 1 | 49 | 21 24 00 | 21 26 30 | 31.1 | 245.2 | 37.6 | 254.3 |
| 250 | September 7, 1973 | 28/SL3/17 | 5 | 50 | 20 35 15 | 20 38 05 | 15.1 | 234.2 | 23.1 | 241.4 |
| 250 | September 7, 1973 | 28/SL3/17 | 1 | 51 | 20 45 40 | 20 48 45 | 41.6 | 266.4 | 46.8 | 280.3 |
| 252 | September 9, 1973 | 29/SL3/18 | 1 | 52 | 19 15 10 | 19 18 40 | 30.5 | 258.9 | 38.2 | 269.7 |
| 254 | September 11, 1973 | 32/SL3/21 | 5 | 54 | 13 06 15 | 13 09 00 | 20.6 | 329.4 | 28.0 | 336.7 |
| 254 | September 11, 1973 | 32/SL3/21 | 5 | 55 | 13 09 45 | 13 12 30 | 30.2 | 339.2 | 37.2 | 348.7 |
| 254 | September 11, 1973 | 32/SL3/21 | 5 | 56 | 13 13 10 | 13 15 20 | 38.7 | 351.1 | 43.1 | 0.0 |
| 254 | September 11, 1973 | 34/SL3/23 | 1 | 57 | 21 02 25 | 21 05 20 | -23.7 | 23.7 | -31.7 | 28.6 |
| 255 | September 12, 1973 | 35/SL3/24 | 5 | 58 | 12 25 30 | 12 28 20 | 24.9 | 338.2 | 32.4 | 346.6 |
| 255 | September 12, 1973 | 35/SL3/24 | 5 | 59 | 12 28 45 | 12 29 50 | 33.6 | 348.3 | 36.0 | 351.7 |
| 255 | September 12, 1973 | 35/SL3/24 | 1 | 60 | 12 30 10 | 12 31 35 | 37.2 | 353.4 | 39.8 | 357.8 |
| 255 | September 12, 1973 | 36/SL3/25 | 5 | 61 | 16 52 10 | 16 55 00 | -10.5 | 238.7 | -2.1 | 245.2 |
| 255 | September 12, 1973 | 36/SL3/25 | 5 | 63 | 16 59 20 | 17 01 40 | 10.4 | 254.6 | 17.2 | 260.1 |
| 255 | September 12, 1973 | 36/SL3/25 | 1 | 64 | 17 09 35 | 17 11 50 | 38.2 | 284.2 | 42.4 | |
| 255 | September 12, 1973 | 36/SL3/25 | 5 | 65 | 17 12 30 | 17 15 20 | 44.0 | 295.9 | 48.1 | 309.9 |
| 255 | September 12, 1973 | 37/SL3/26 | 5 | 66 | 20 10 35 | 20 13 30 | 25.8 | 220.8 | 32.4 | 228.3 |
| 255 | September 12, 1973 | 37/SL3/26 | 1 | 67 | 20 14 45 | 20 16 00 | 35.7 | 232.8 | 38.4 | 237.0 |
| 256 | September 13, 1973 | 38/SL3/27 | 1 | 69 | 18 02 00 | 18 03 40 | 42.6 | 273.8 | 45.5 | 281.4 |
| 256 | September 13, 1973 | 38/SL3/27 | 5 | 70 | 18 06 25 | 18 09 30 | 49.0 | 296.0 | 50.2 | 312.1 |
| 256 | September 13, 1973 | 38/SL3/27 | 5 | 71 | 18 09 50 | 18 12 35 | 50.2 | 315.0 | 48.6 | 330.0 |
| 256 | September 13, 1973 | 39/SL3/28 | 1 | 72 | 19 34 10 | 19 34 40 | 40.7 | 246.0 | 41.7 | 248.1 |
| 256 | September 13, 1973 | 39/SL3/28 | 5 | 73 | 19 45 50 | 19 48 25 | 48.5 | 307.4 | 45.1 | 320.0 |
| 256 | September 13, 1973 | 39/SL3/28 | 5 | 74 | 19 49 25 | 19 52 15 | 43.4 | 324.6 | 37.5 | 336.0 |
| 257 | September 14, 1973 | 40/SL3/29 | 3 | 75 | 17 05 15 | 17 07 40 | 6.4 | 237.5 | 12.8 | 242.5 |
| 257 | September 14, 1973 | 40/SL3/29 | 1 | 76 | 17 11 10 | 17 11 40 | 23.3 | 251.7 | 24.7 | 253.1 |

TABLE 7. SKYLAB DATA SUMMARY (Continued)

| DOY | DATE | PASS | MODE | MAP | TIME | | START | | STOP | |
|-----|-------------------|-----------|-------|-----|----------|----------|-------|-------|-------|-------|
| | | | | | START | STOP | LAT | LONG | LAT | LONG |
| 334 | November 30, 1973 | 54/SL4 04 | RESET | 80 | | | | | | |
| 334 | November 30, 1973 | 54/SL4 04 | 1 | 81 | 16 35 40 | 16 36 00 | 38.8 | 269.7 | 38.1 | 271.0 |
| 334 | November 30, 1973 | 54/SL4 04 | 1 | 82 | | | | | | |
| 334 | November 30, 1973 | 54/SL4 04 | 1 | 83 | 16 42 45 | 16 43 35 | 20.2 | 292.2 | 18.3 | 293.8 |
| 334 | November 30, 1973 | 54/SL4 04 | 1 | 84 | 16 46 45 | 16 48 00 | 8.6 | 301.8 | 5.2 | 304.4 |
| 335 | December 1, 1973 | 55/SL4 05 | 1 | 85 | 17 30 20 | 17 33 05 | 28.6 | 264.9 | 21.8 | 271.8 |
| 335 | December 1, 1973 | 55/SL4 05 | 1 | 86 | 17 34 00 | 17 36 50 | 18.7 | 274.6 | 11.0 | 281.4 |
| 336 | December 2, 1973 | 56/SL4 06 | 1 | 87 | | | | | | |
| 336 | December 2, 1973 | 56/SL4 06 | 5 | 88 | | | | | | |
| 336 | December 2, 1973 | 57/SL4 07 | 3 | 89 | 18 17 10 | 18 17 50 | 38.3 | 232.8 | 36.8 | 235.2 |
| 336 | December 2, 1973 | 57/SL4 07 | 1 | 90 | | | | | | |
| 336 | December 2, 1973 | 57/SL4 07 | 1 | 91 | 18 22 30 | 18 23 45 | 24.9 | 249.9 | 21.6 | 253.0 |
| 336 | December 2, 1973 | 57/SL4 07 | 5 | 92 | 18 24 20 | 18 26 20 | 19.8 | 254.7 | 14.0 | 259.6 |
| 336 | December 2, 1973 | 57/SL4 07 | 5 | 93 | 18 27 05 | 18 27 30 | 11.6 | 261.6 | 10.6 | 262.3 |
| 337 | December 3, 1973 | 58/SL4 08 | 1 | 94 | | | | | | |
| 337 | December 3, 1973 | 58/SL4 08 | 2 | 95 | | | | | | |
| 337 | December 3, 1973 | 59/SL4 09 | 1 | 96 | | | | | | |
| 339 | December 5, 1973 | 61/SL4 11 | 1 | 97 | | | | | | |
| 339 | December 5, 1973 | 61/SL4 11 | 3 | 98 | 16 15 30 | 16 16 10 | 22.6 | 266.3 | 20.8 | 268.0 |
| 339 | December 5, 1973 | 61/SL4 11 | 5 | 99 | 16 21 05 | 16 22 20 | 6.6 | 279.6 | 2.7 | 282.6 |
| 341 | December 7, 1973 | 62/SL4 12 | 1 | 100 | 14 48 10 | 14 48 55 | 29.0 | 269.3 | 26.7 | 271.7 |
| 341 | December 7, 1973 | 62/SL4 12 | 5 | 101 | | | | | | |
| 342 | December 9, 1973 | 64/SL4 14 | 5 | 102 | 02 37 05 | 02 38 45 | 11.3 | 100.9 | 6.3 | 104.7 |
| 342 | December 9, 1973 | 64/SL4 14 | 1 | 103 | 02 43 10 | 02 46 05 | -7.1 | 114.7 | -15.3 | 121.3 |
| 342 | December 9, 1973 | 64/SL4 14 | 1 | 104 | 02 46 55 | 02 47 45 | -17.7 | 123.3 | -20.1 | 125.4 |
| 349 | December 15, 1973 | 65/SL4 15 | 5 | 105 | 00 01 00 | 00 01 50 | -5.8 | 118.5 | -8.7 | 120.8 |

TABLE 7. SKYLAB DATA SUMMARY (Continued)

| DOY | DATE | PASS | MODE | MAP | TIME | | START | | STOP | |
|-----|-------------------|-----------|------|------|----------|----------|-------|-------|-------|-------|
| | | | | | START | STOP | LAT | LONG | LAT | LONG |
| 352 | December 18, 1973 | 67/SL4 16 | 5 | 106 | 02 00 20 | 02 01 50 | 41.9 | 293.6 | 44.7 | 300.0 |
| 352 | December 18, 1973 | 67/SL4 16 | 2 | 107 | | | | | | |
| 352 | December 18, 1973 | 68/SL4 17 | 1 | 108 | 11 33 20 | 11 35 20 | 44.0 | 225.7 | 40.9 | 232.9 |
| 352 | December 18, 1973 | 68/SL4 17 | 5 | 109 | 11 44 50 | 11 46 50 | 15.2 | 263.2 | 10.3 | 267.1 |
| 352 | December 18, 1973 | 68/SL4 17 | 5 | 110 | 11 48 10 | 11 50 10 | 5.8 | 270.8 | - 0.1 | 275.3 |
| 1 | January 1, 1974 | 71/SL4 18 | 1 | 111 | | | | | | |
| 1 | January 1, 1974 | 71/SL4 18 | 5 | 112 | | | | | | |
| 1 | January 1, 1974 | 71/SL4 18 | 5 | 113 | 13 25 20 | 13 27 15 | -26.0 | 322.0 | -20.5 | 327.3 |
| 1 | January 1, 1974 | 71/SL4 18 | 5 | 114 | 13 29 00 | 13 31 00 | 15.3 | 331.9 | - 9.5 | 336.6 |
| 1 | January 1, 1974 | 71/SL4 18 | 5 | 115 | 13 32 35 | 13 34 35 | -5.0 | 340.0 | + .9 | 344.4 |
| 6 | January 6, 1974 | 74/SL4 21 | 3 | 116 | | | | | | |
| 6 | January 6, 1974 | 74/SL4 21 | 5 | 117 | 17 55 40 | 17 57 25 | 23.7 | 268.4 | 28.2 | 273.0 |
| 6 | January 6, 1974 | 74/SL4 21 | 5 | 118 | 18 00 50 | 18 02 40 | 36.8 | 284.2 | 40.8 | 291.2 |
| 6 | January 6, 1974 | 74/SL4 21 | 5 | 119 | 18 09 00 | 18 09 10 | 49.7 | 322.3 | 49.8 | 323.2 |
| 6 | January 6, 1974 | 74/SL4 21 | 5 | 120 | 18 11 20 | 18 11 40 | 50.2 | 335.2 | 50.1 | 338.1 |
| 6 | January 6, 1974 | 74/SL4 21 | 5 | 120A | 18 14 25 | 18 15 00 | 48.1 | 353.9 | 47.8 | 355.1 |
| 7 | January 7, 1974 | 76/SL4 22 | 1 | 121 | 17 13 30 | 17 14 30 | 24.5 | 273.9 | 27.7 | 277.2 |
| 7 | January 7, 1974 | 76/SL4 22 | 5 | 122 | 17 17 20 | 17 17 35 | 34.6 | 285.7 | 35.0 | 286.3 |
| 7 | January 7, 1974 | 76/SL4 22 | 5 | 123 | 17 18 40 | 17 20 30 | 37.8 | 290.5 | 41.4 | 297.0 |
| 7 | January 7, 1974 | 76/SL4 22 | 5 | 124 | 17 24 40 | 17 25 00 | 48.1 | 317.2 | 48.5 | 318.9 |
| 7 | January 7, 1974 | 76/SL4 22 | 5 | 125 | | | | | | |
| 7 | January 7, 1974 | 76/SL4 22 | 5 | 126 | | | | | | |
| 8 | January 8, 1974 | 78/SL4 23 | 1 | 127 | 16 31 30 | 16 33 40 | 26.0 | | 31.3 | 286.1 |
| 8 | January 8, 1974 | 78/SL4 23 | 5 | 128 | 16 34 05 | 16 36 00 | 32.7 | 287.9 | 37.1 | 294.2 |
| 8 | January 8, 1974 | 78/SL4 23 | 5 | 129 | 16 44 30 | 16 46 25 | 49.9 | 334.9 | 50.1 | 346.4 |
| 9 | January 9, 1974 | 79/SL4 24 | 3 | 130 | | | | | | |
| 9 | January 9, 1974 | 79/SL4 24 | 5 | 131 | 15 45 55 | 15 47 25 | 17.5 | 276.9 | 21.7 | 280.7 |
| 9 | January 9, 1974 | 79/SL4 24 | 5 | 132 | 15 49 45 | 15 50 40 | 28.1 | 287.2 | 33.3 | 293.4 |
| 9 | January 9, 1974 | 79/SL4 24 | 5 | 133 | 15 52 50 | 15 53 05 | 35.8 | 297.0 | 36.4 | 297.9 |
| 9 | January 9, 1974 | 79/SL4 24 | 5 | 134 | 16 00 45 | 16 02 40 | 49.2 | 332.8 | 50.2 | 344.1 |

TABLE 7. SKYLAB DATA SUMMARY (Continued)

| DOY | DATE | PASS | MODE | MAP | TIME | | START | | STOP | |
|-----|------------------|-----------|------|------|----------|----------|-------|-------|------|-------|
| | | | | | START | STOP | LAT | LONG | LAT | LONG |
| 11 | January 11, 1974 | 81/SL4 26 | 3 | 135 | 17 29 10 | 17 29 50 | 23.1 | 244.1 | 24.9 | 245.9 |
| 11 | January 11, 1974 | 81/SL4 26 | 1 | 136 | | | | | | |
| 12 | January 12, 1974 | 82/SL4 27 | 3 | 137 | | | | | | |
| 12 | January 12, 1974 | 82/SL4 27 | 3 | 138 | | | | | | |
| 12 | January 12, 1974 | 82/SL4 27 | 5 | 139 | 17 00 30 | 17 00 50 | 49.8 | 305.4 | 50.0 | 307.3 |
| 12 | January 12, 1974 | 82/SL4 27 | 5 | 140 | | | | | | |
| 12 | January 12, 1974 | 82/SL4 27 | 5 | 141 | | | | | | |
| 12 | January 12, 1974 | 82/SL4 27 | 5 | 142 | | | | | | |
| 12 | January 12, 1974 | 82/SL4 27 | 3 | 143 | | | | | | |
| 12 | January 12, 1974 | 82/SL4 27 | 3 | 144 | | | | | | |
| 14 | January 14, 1974 | 83/SL4 29 | 5 | 145 | 15 34 35 | 15 35 15 | 49.4 | 310.8 | 49.8 | 314.5 |
| 14 | January 14, 1974 | 83/SL4 29 | 5 | 145A | 15 36 15 | 15 37 00 | 50.1 | 320.2 | 50.2 | 324.1 |
| 14 | January 14, 1974 | 83/SL4 29 | 5 | 146 | 15 38 25 | 15 40 20 | 49.9 | 332.4 | 48.5 | 342.5 |
| 14 | January 14, 1974 | 83/SL4 29 | 5 | 147 | 15 41 20 | 15 41 50 | 47.2 | 348.3 | 46.8 | 350.0 |
| 14 | January 14, 1974 | 83/SL4 29 | 5 | 148 | 16 56 00 | 16 57 50 | 26.6 | 238.2 | 31.5 | 243.7 |
| 18 | January 18, 1974 | 85/SL4 30 | 1 | 149 | | | | | | |
| 18 | January 18, 1974 | 85/SL4 30 | 1 | 150 | | | | | | |
| 18 | January 18, 1974 | 85/SL4 30 | 5 | 151 | 20 48 35 | 20 49 30 | 20.9 | 291.6 | 18.5 | 293.7 |
| 21 | January 21, 1974 | 87/SL4 35 | 1 | 152 | 20 14 40 | 20 16 45 | 19.4 | 283.5 | 13.2 | 288.8 |
| 22 | January 22, 1974 | 88/SL4 37 | 5 | 153 | | | | | | |
| 22 | January 22, 1974 | 88/SL4 37 | 5 | 154 | | | | | | |
| 22 | January 22, 1974 | 88/SL4 37 | 5 | 155 | 19 31 30 | 19 31 45 | 21.4 | 286.4 | 20.5 | 287.2 |
| 22 | January 22, 1974 | 88/SL4 37 | 5 | 156 | 19 33 00 | 19 33 25 | 16.9 | 290.4 | 16.0 | 291.2 |
| 24 | January 24, 1974 | 89/SL4 40 | 1 | 157 | | | | | | |
| 24 | January 24, 1974 | 89/SL4 40 | 1 | 158 | | | | | | |
| 24 | January 24, 1974 | 89/SL4 40 | 1 | 159 | | | | | | |
| 24 | January 24, 1974 | 89/SL4 40 | 1 | 160 | | | | | | |
| 24 | January 24, 1974 | 89/SL4 40 | 1 | 161 | | | | | | |
| 24 | January 24, 1974 | 89/SL4 40 | 1 | 162 | | | | | | |
| 24 | January 24, 1974 | 89/SL4 40 | 1 | 163 | 18 08 00 | 18 08 50 | 17.4 | 299.4 | 15.0 | 301.5 |
| 24 | January 24, 1974 | 89/SL4 40 | 5 | 164 | 18 09 10 | 18 11 10 | 13.6 | 302.6 | 8.2 | 306.8 |

TABLE 7. SKYLAB DATA SUMMARY (Continued)

| DOY | DATE | PASS | MODE | MAP | TIME | | START | | STOP | |
|-----|------------------|-----------|-------|-----|----------|----------|-------|-------|------|-------|
| | | | | | START | STOP | LAT | LONG | LAT | LONG |
| 25 | January 25, 1974 | 90/SL4 41 | 1 | 165 | | | | | | |
| 25 | January 25, 1974 | 90/SL4 41 | 1 | 166 | | | | | | |
| 25 | January 25, 1974 | 90/SL4 41 | 3 | 167 | | | | | | |
| 25 | January 25, 1974 | 90/SL4 41 | 5 | 168 | 17 19 10 | 17 21 05 | 37.1 | 282.2 | 32.5 | 288.6 |
| 25 | January 25, 1974 | 90/SL4 41 | 5 | 169 | 17 22 30 | 17 24 20 | 25.9 | 296.2 | 20.8 | 301.1 |
| 25 | January 25, 1974 | 90/SL4 41 | 5 | 170 | | | | | | |
| 25 | January 25, 1974 | 90/SL4 41 | 5 | 171 | | | | | | |
| 25 | January 25, 1974 | 90/SL4 41 | 5 | 172 | | | | | | |
| 26 | January 26, 1974 | 91/SL4 42 | 3 | 173 | | | | | | |
| 26 | January 26, 1974 | 91/SL4 42 | 3 | 174 | | | | | | |
| 26 | January 26, 1974 | 91/SL4 42 | 5 | 175 | 19 53 50 | 19 54 10 | 4.4 | 271.8 | 3.4 | 272.6 |
| 27 | January 27, 1974 | 92/SL4 44 | 5 | 176 | | | | | | |
| 27 | January 27, 1974 | 92/SL4 44 | 5 | 177 | | | | | | |
| 27 | January 27, 1974 | 92/SL4 44 | 5 | 178 | | | | | | |
| 27 | January 27, 1974 | 92/SL4 44 | 5 | 179 | | | | | | |
| 27 | January 27, 1974 | 92/SL4 44 | 5 | 180 | | | | | | |
| 27 | January 27, 1974 | 92/SL4 44 | 5 | 181 | | | | | | |
| 27 | January 27, 1974 | 92/SL4 44 | 5 | 182 | 12 48 45 | 12 49 05 | 32.2 | 345.8 | 31.4 | 346.9 |
| 27 | January 27, 1974 | 92/SL4 44 | 5 | 183 | | | | | | |
| 27 | January 27, 1974 | 92/SL4 44 | 3 | 184 | | | | | | |
| 27 | January 27, 1974 | 93/SL4 44 | 5 | 185 | 19 09 20 | 19 11 15 | 10.3 | 272.0 | 4.4 | 276.6 |
| 28 | January 28, 1974 | 94/SL4 46 | 5 | 186 | | | | | | |
| 28 | January 28, 1974 | 94/SL4 46 | 5 | 187 | | | | | | |
| 28 | January 28, 1974 | 94/SL4 46 | 5 | 188 | | | | | | |
| 28 | January 28, 1974 | 94/SL4 46 | 2 | 189 | | | | | | |
| 28 | January 28, 1974 | 94/SL4 46 | 2 | 190 | | | | | | |
| 28 | January 28, 1974 | 94/SL4 46 | 2 | 191 | | | | | | |
| 29 | January 29, 1974 | 95/SL4 47 | NAL | 192 | | | | | | |
| 29 | January 29, 1974 | 95/SL4 47 | 5 | 193 | | | | | | |
| 29 | January 29, 1974 | 95/SL4 47 | 5 | 194 | | | | | | |
| 29 | January 29, 1974 | 95/SL4 47 | 5 | 195 | | | | | | |
| 29 | January 29, 1974 | 95/SL4 47 | RESET | 196 | | | | | | |

TABLE 7. SKYLAB DATA SUMMARY (Continued)

| DOY | DATE | PASS | MODE | MAP | TIME | | START | | STOP | |
|-----|------------------|-----------|------|-----|----------|----------|-------|-------|-------|-------|
| | | | | | START | STOP | LAT | LONG | LAT | LONG |
| 30 | January 30, 1974 | 96/SL4 48 | 5 | 197 | | | | | | |
| 30 | January 30, 1974 | 96/SL4 48 | 5 | 198 | | | | | | |
| 30 | January 30, 1974 | 96/SL4 48 | 5 | 199 | | | | | | |
| 31 | January 31, 1974 | 97/SL4 49 | 1 | 200 | | | | | | |
| 31 | January 31, 1974 | 97/SL4 49 | 1 | 201 | 14 55 25 | 14 58 15 | -16.8 | 335.6 | -24.8 | 343.0 |
| 31 | January 31, 1974 | 97/SL4 49 | 1 | 202 | 15 00 25 | 15 03 20 | -30.7 | 349.3 | -38.0 | 359.5 |
| 31 | January 31, 1974 | 97/SL4 49 | 1 | 203 | 15 04 20 | 15 07 15 | -39.5 | 2.9 | -45.2 | 15.2 |
| 31 | January 31, 1974 | 97/SL4 49 | 1 | 204 | 15 08 05 | 15 11 10 | -46.7 | 19.8 | -49.5 | 34.9 |
| 31 | January 31, 1974 | 97/SL4 49 | 1 | 205 | 15 11 55 | 15 14 15 | -50.1 | 41.0 | -49.9 | 54.5 |
| 31 | January 31, 1974 | 97/SL4 49 | 1 | 206 | 15 15 40 | 15 18 35 | -49.1 | 61.9 | -45.7 | 76.6 |
| 31 | January 31, 1974 | 97/SL4 49 | 1 | 207 | 15 22 10 | 15 25 00 | -38.5 | 92.7 | -31.7 | 102.5 |
| 31 | January 31, 1974 | 97/SL4 49 | 1 | 208 | 15 25 50 | 15 28 45 | -29.3 | 105.3 | -21.1 | 113.7 |
| 31 | January 31, 1974 | 97/SL4 49 | 1 | 209 | 15 29 45 | 15 32 30 | -18.1 | 116.4 | -11.3 | 122.0 |
| 31 | January 31, 1974 | 97/SL4 49 | 1 | 210 | 15 33 20 | 15 36 10 | - 8.1 | 124.5 | - 0.2 | 130.5 |
| 31 | January 31, 1974 | 97/SL4 49 | 1 | 211 | 15 37 10 | 15 40 05 | 3.3 | 133.1 | 11.2 | 139.2 |
| 31 | January 31, 1974 | 97/SL4 49 | 1 | 212 | 15 41 00 | 15 44 00 | 14.4 | 141.7 | 22.5 | 148.8 |
| 31 | January 31, 1974 | 97/SL4 49 | 1 | 213 | 15 44 40 | 15 47 30 | 24.5 | 150.8 | 32.0 | 159.2 |
| 31 | January 31, 1974 | 97/SL4 49 | 1 | 214 | 15 48 30 | 15 51 25 | 34.7 | 162.8 | 41.1 | 173.3 |
| 31 | January 31, 1974 | 97/SL4 49 | 5 | 215 | 15 52 35 | 15 55 30 | 43.4 | 178.5 | 47.7 | 192.1 |
| 31 | January 31, 1974 | 97/SL4 49 | 5 | 216 | 15 56 25 | 15 58 25 | 48.8 | 197.3 | 50.0 | 208.5 |
| 31 | January 31, 1974 | 97/SL4 49 | 5 | 217 | 15 59 40 | 16 01 40 | 50.2 | 216.4 | 49.5 | 226.8 |
| 31 | January 31, 1974 | 97/SL4 49 | 1 | 218 | 16 02 55 | 16 03 15 | 48.5 | 233.7 | 48.1 | 235.4 |
| 31 | January 31, 1974 | 97/SL4 49 | 1 | 219 | | | | | | |
| 31 | January 31, 1974 | 97/SL4 49 | 1 | 220 | | | | | | |
| 31 | January 31, 1974 | 97/SL4 49 | 1 | 221 | | | | | | |
| 31 | January 31, 1974 | 97/SL4 49 | 5 | 222 | 16 12 25 | 16 13 40 | 29.4 | 273.3 | 25.4 | 277.7 |
| 31 | January 31, 1974 | 97/SL4 49 | 1 | 223 | 16 14 15 | 16 14 50 | 24.9 | 278.1 | 23.6 | 279.5 |
| 31 | January 31, 1974 | 97/SL4 49 | 1 | 224 | | | | | | |
| 31 | January 31, 1974 | 97/SL4 49 | 1 | 225 | 16 16 25 | 16 17 30 | 18.9 | 283.8 | 16.0 | 286.3 |
| 31 | January 31, 1974 | 97/SL4 49 | 1 | 226 | 16 18 00 | 16 19 00 | 14.4 | 287.7 | 11.4 | 290.0 |
| 32 | February 1, 1974 | 98/SL4 50 | 1 | 227 | | | | | | |
| 32 | February 1, 1974 | 98/SL4 49 | 1 | 228 | | | | | | |
| 32 | February 1, 1974 | 98/SL4 50 | 5 | 229 | | | | | | |
| 32 | February 1, 1974 | 98/SL4 49 | 2 | 230 | | | | | | |

TABLE 7. SKYLAB DATA SUMMARY (Continued)

| DOY | DATE | PASS | MODE | MAP | TIME | | START | | STOP | |
|-----|------------------|-----------|------|-----|----------|----------|-------|-------|------|-------|
| | | | | | START | STOP | LAT | LONG | LAT | LONG |
| 20 | January 20, 1974 | 86/SL4 32 | 5 | 233 | 19 18 15 | 19 20 10 | 34.7 | 285.7 | 30.0 | 291.7 |

TABLE 7. SKYLAB DATA SUMMARY (Continued)



ORIGINAL PAGE IS
OF POOR QUALITY

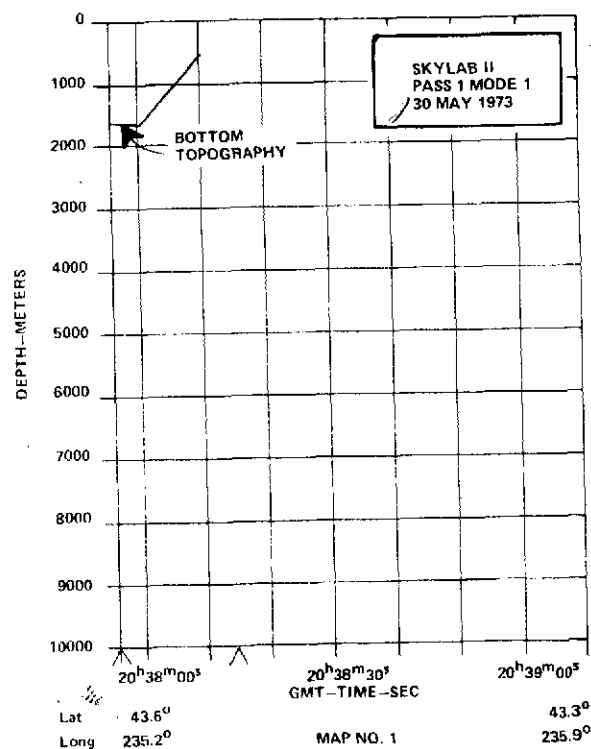
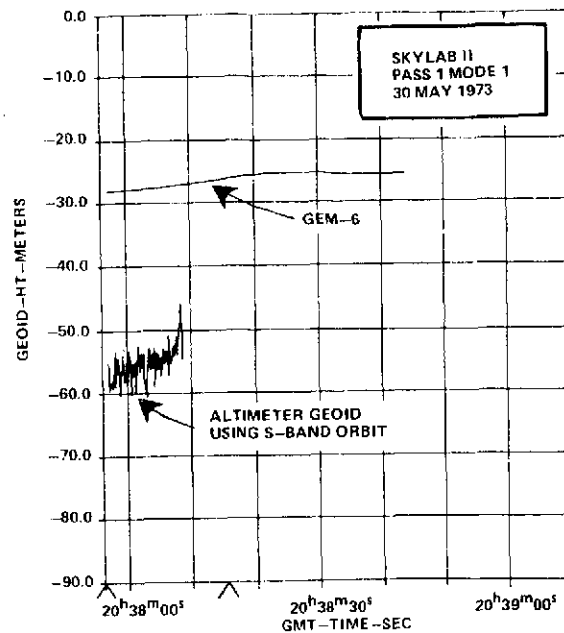


ORIGINAL PAGE IS
OF POOR QUALITY

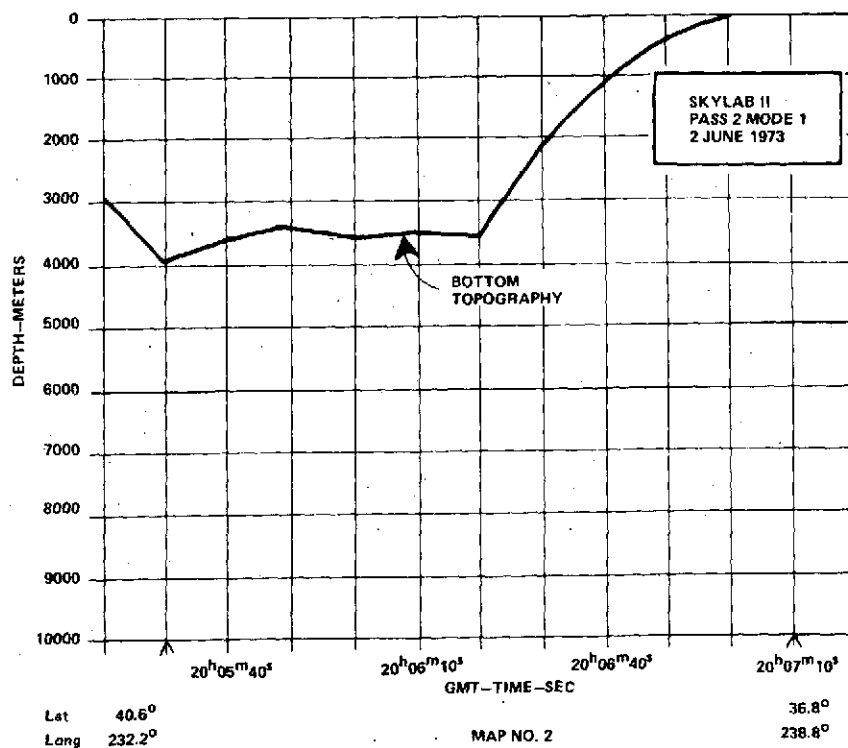
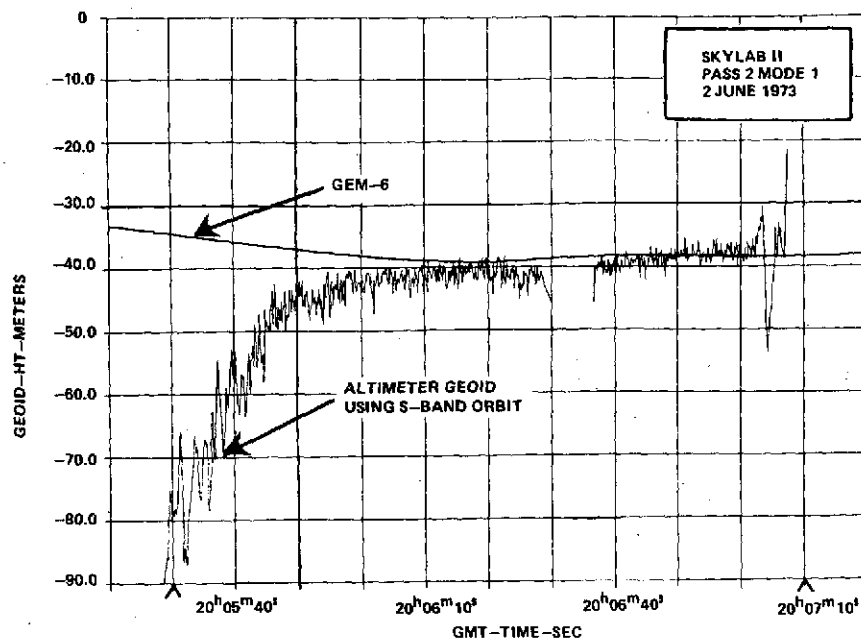
RESIDUALS AND BOTTOM TOPOGRAPHY

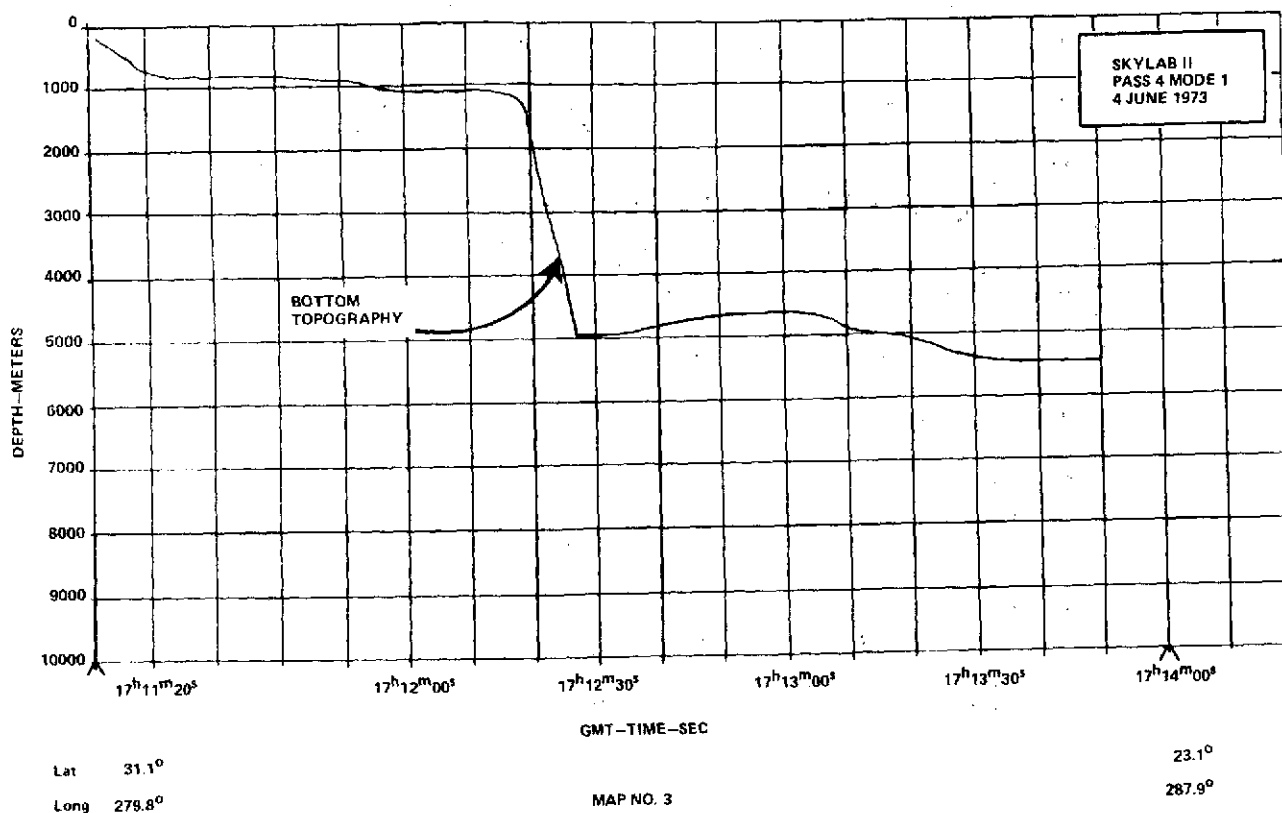
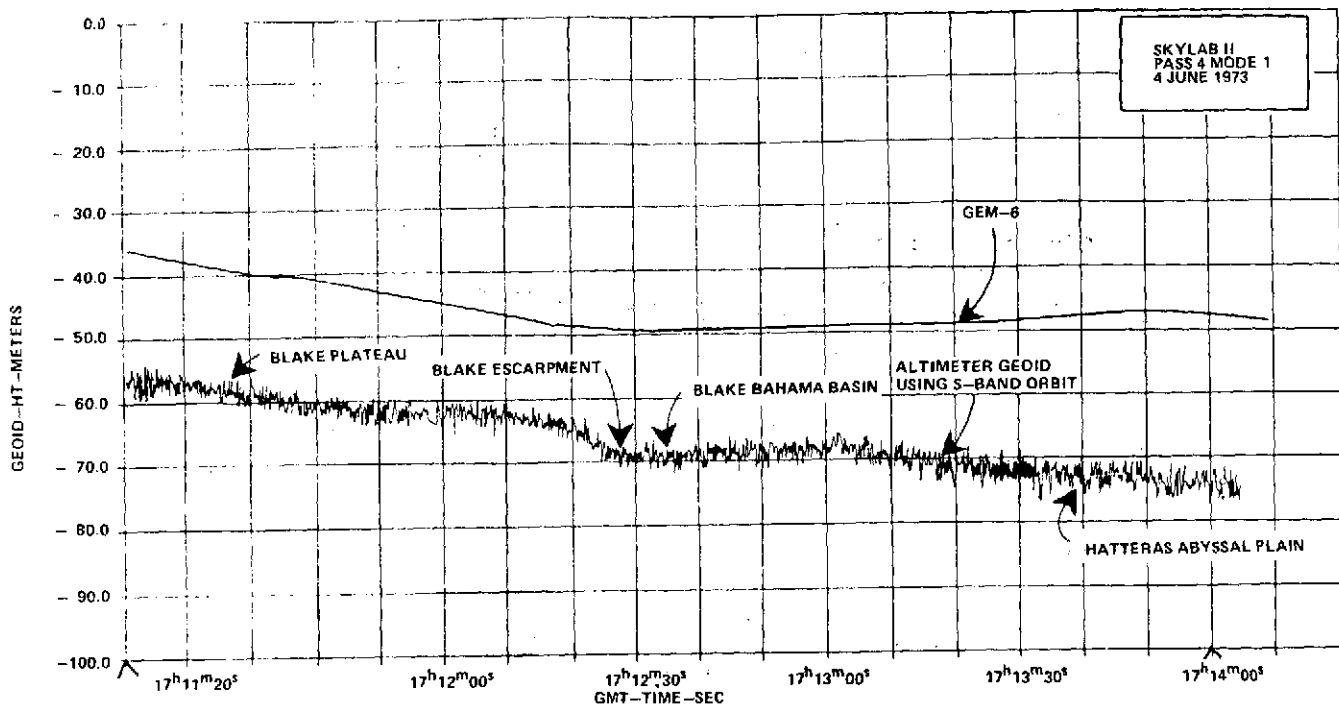
This section contains plots of the residuals (altimeter derived geoid which is computed minus observed height above the referenced ellipsoid) for each SKYLAB pass reduced. These plots represent raw data at the 8 sample per second rate. Also, on the same plot for passes over water, the GEM-6 [8] geoid is supplied for comparison. Finally, a plot of the ocean bottom topography profile is displayed so that one might compare the correlation between the topographic features and the high frequency geoid undulations. The plots were digitized from unclassified ocean bottom contour maps obtained from the Defense Mapping Agency, the Naval Oceanographic Office, and the National Science Foundation. The contours were sampled approximately every 15 km along the subsatellite trace. Where no bottom topography is given one can assume that these are land passes or that ocean bottom contour maps were not available. In the over land cases, the heights are given above mean sea level and are not geoid heights.

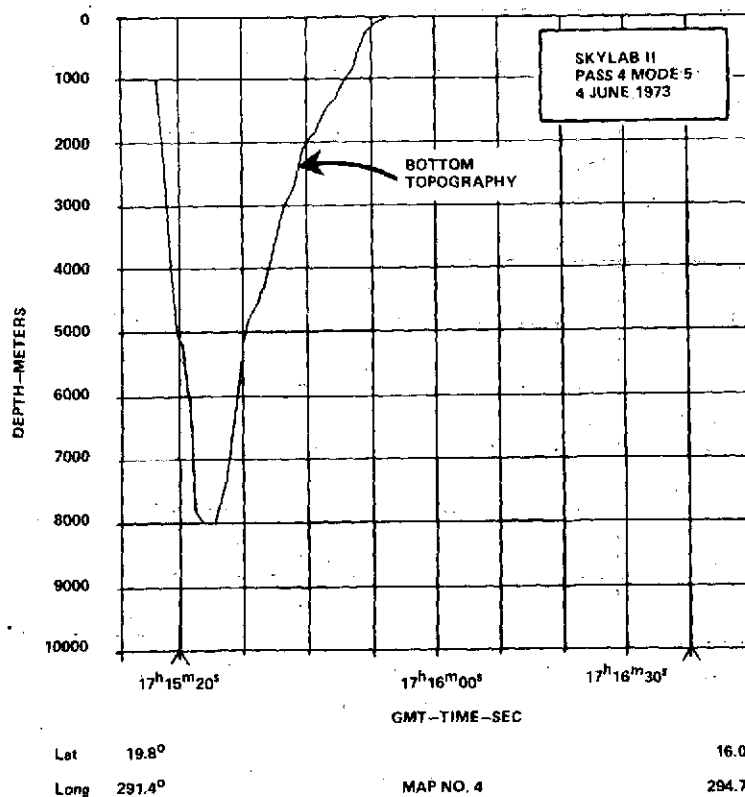
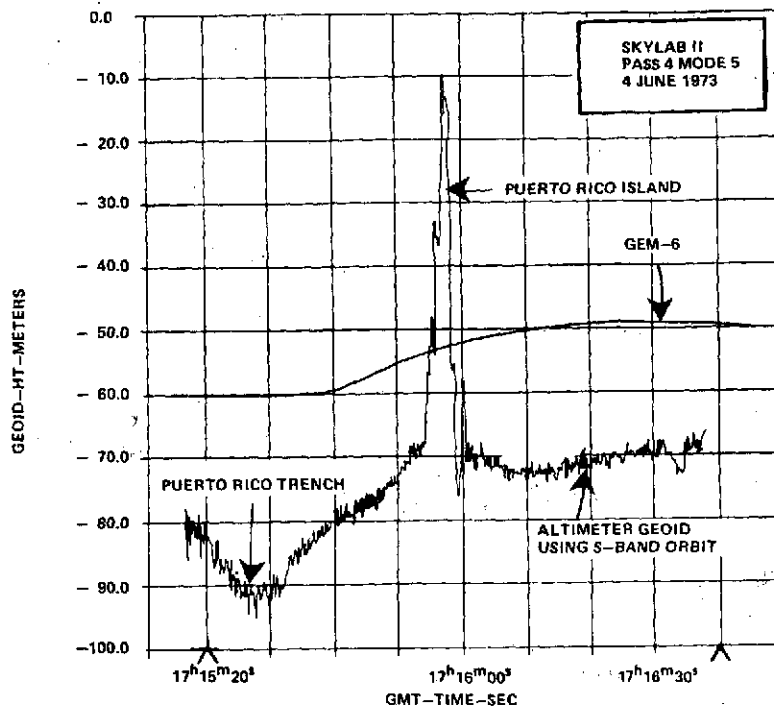
It should be noted that latitudes and longitudes are labeled for two specific times on each residual plot. These are denoted with an arrow (A) immediately above the time of interest. In reviewing these plots, an occasional drop-out of the altitude residuals will be noted. These are due to loss of track, and on SL-2 and SL-3 usually occur over land areas. During SL-4, these losses were common even over the open ocean for an antenna problem caused the operating signal to noise to be marginal. In addition, when the altitude jitter increases, one should be aware that a pointing problem is the likely cause and therefore the absolute bias and even the trends in these passes will be questionable.

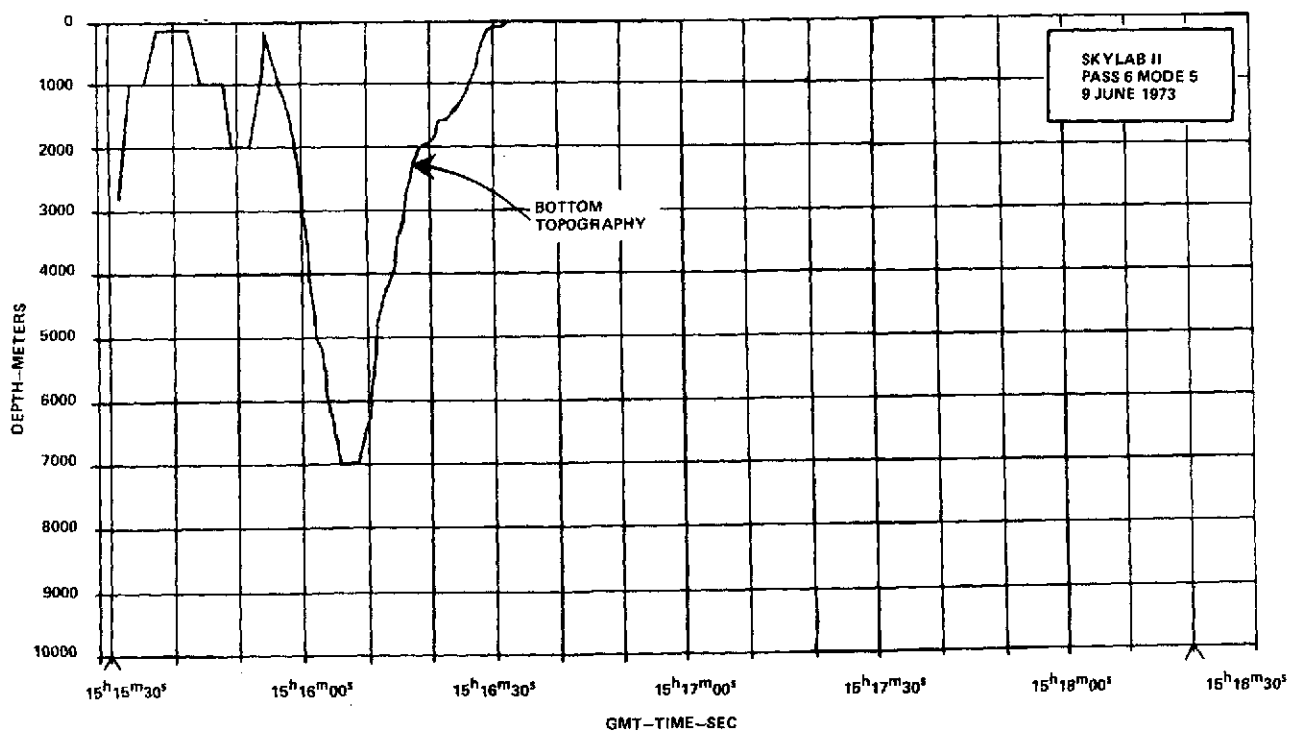
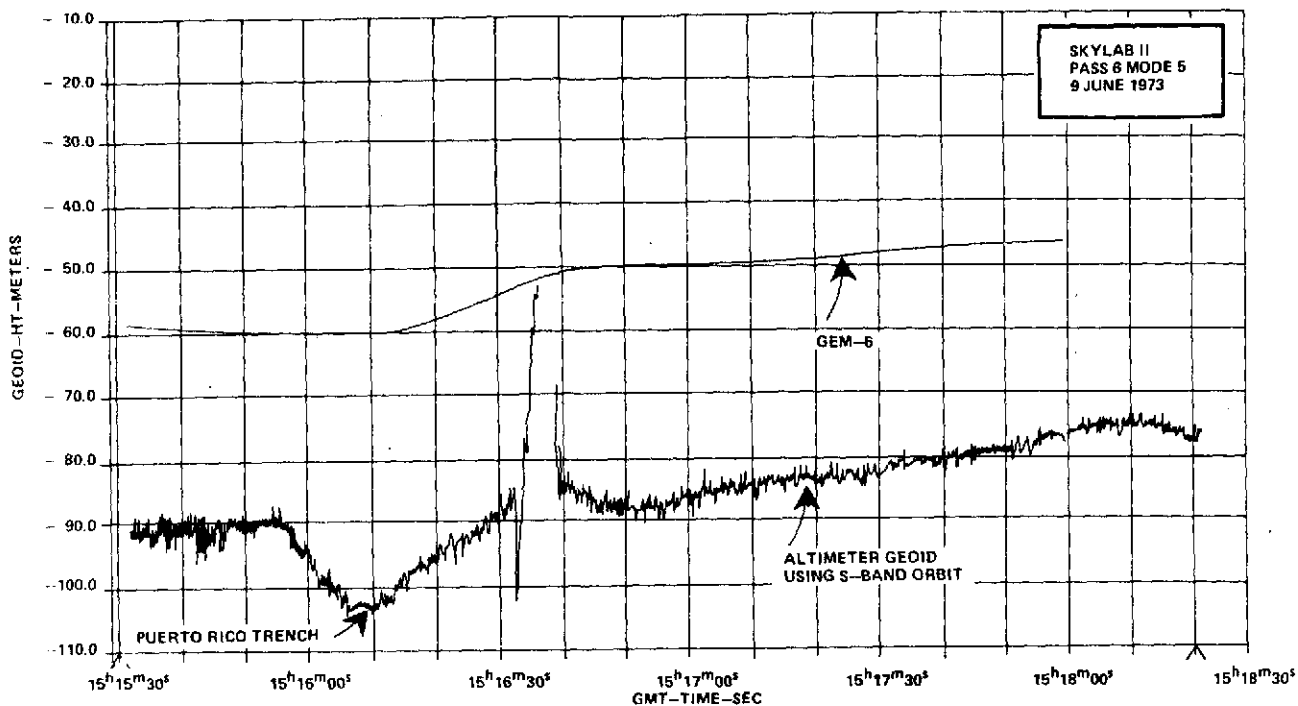


ORIGINAL PAGE IS
OF POOR QUALITY





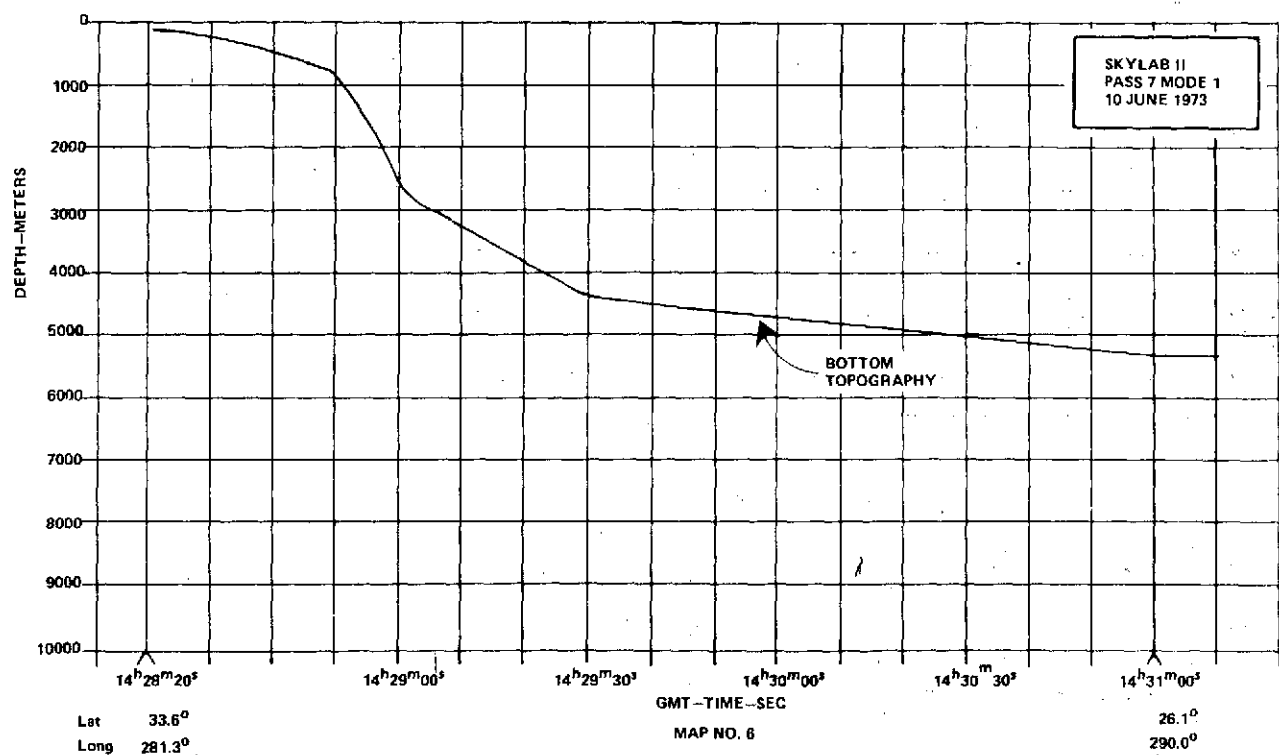
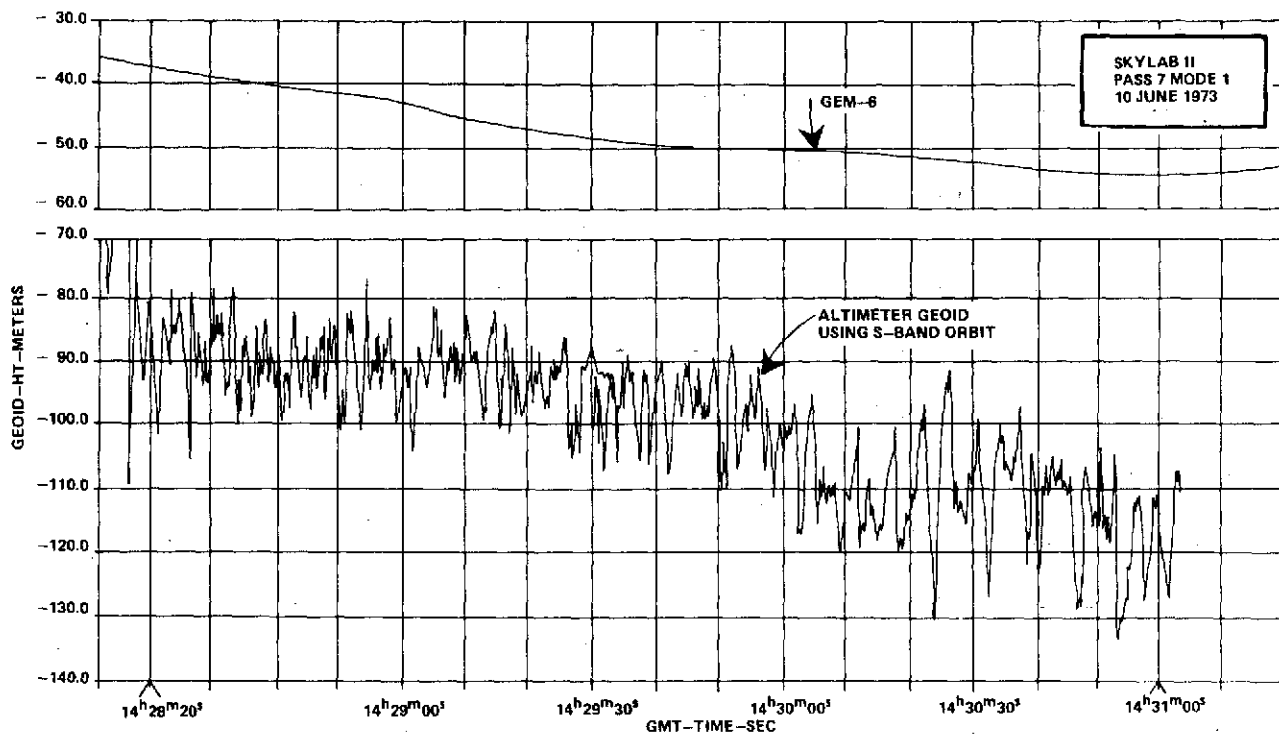


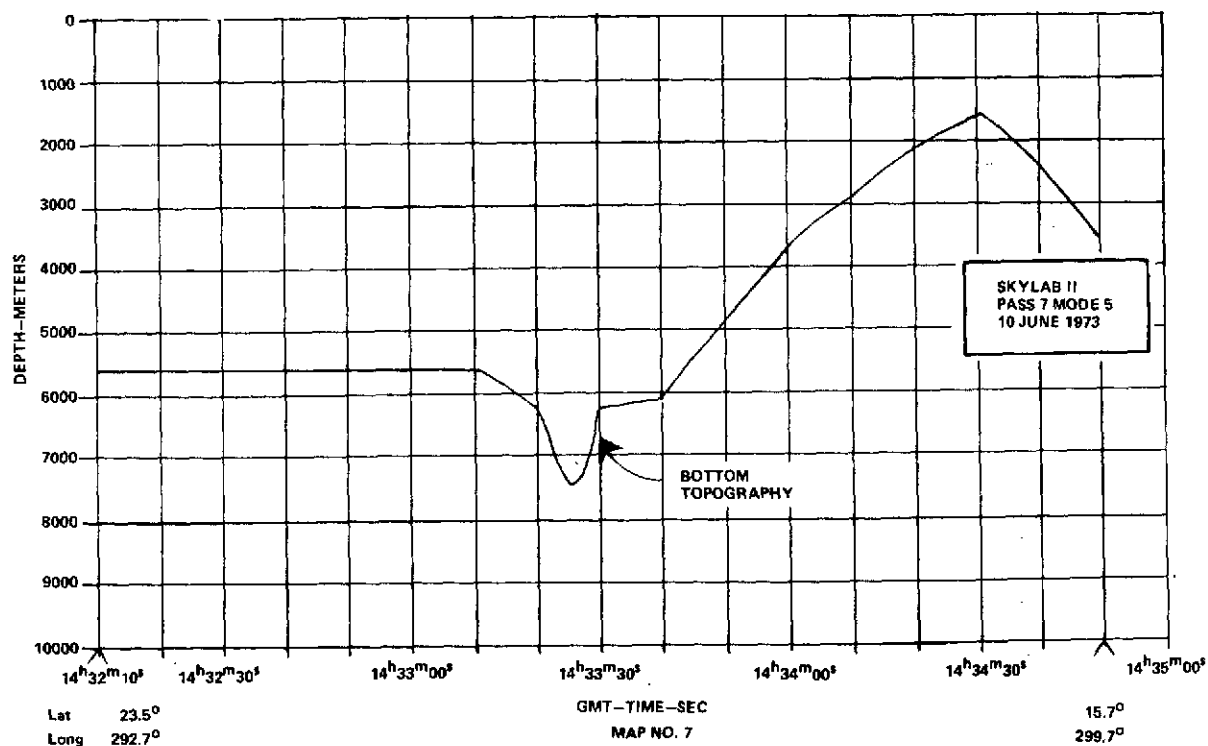
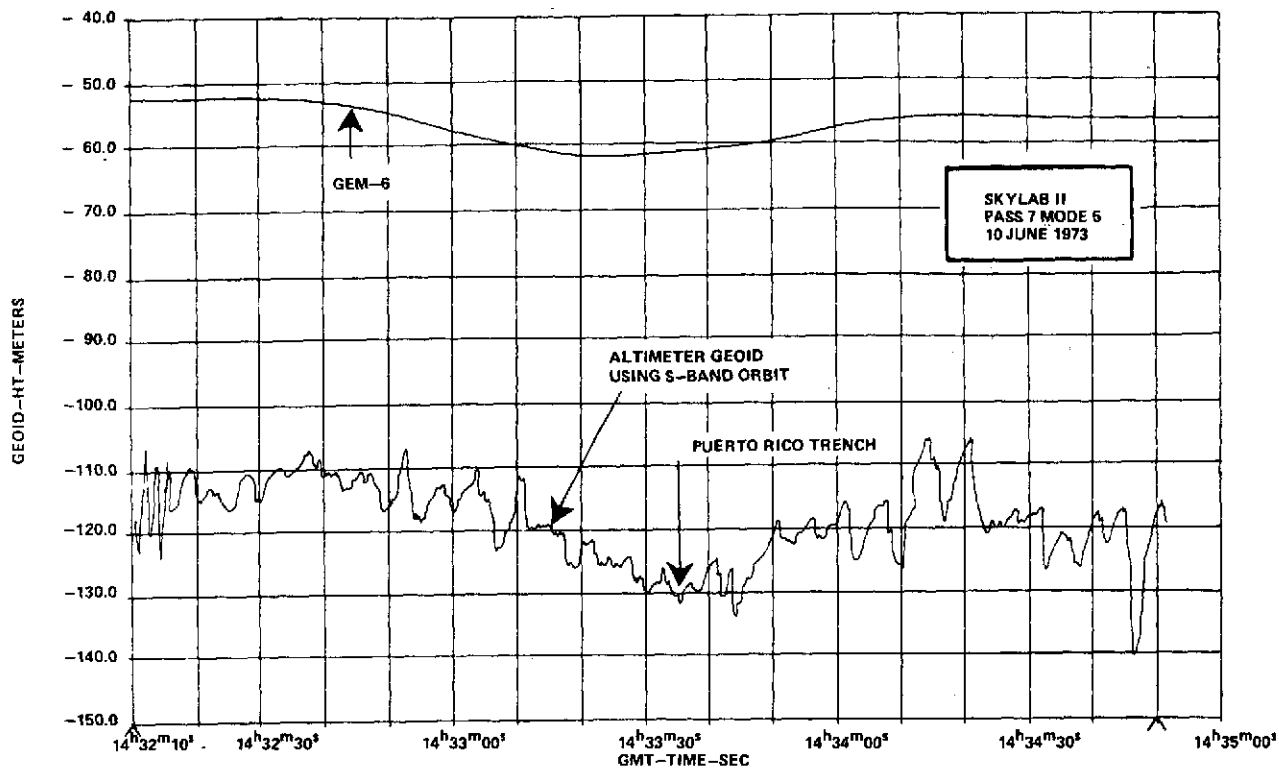


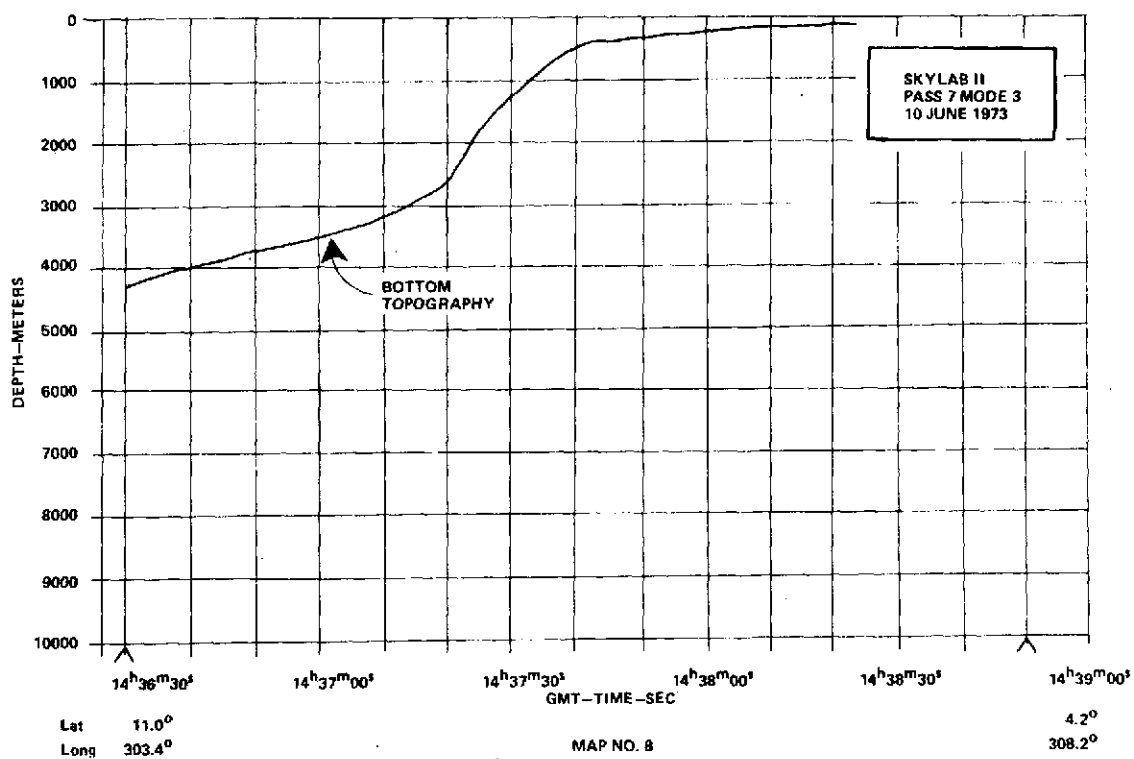
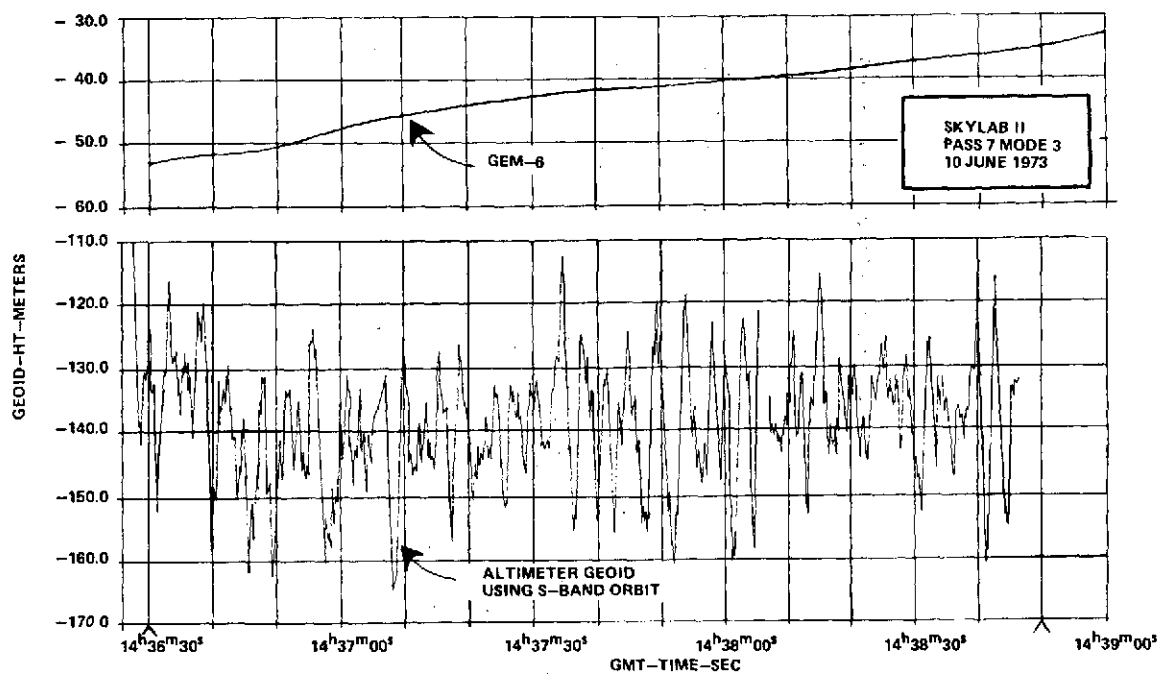
Lat 21.2°
Long 290.2°

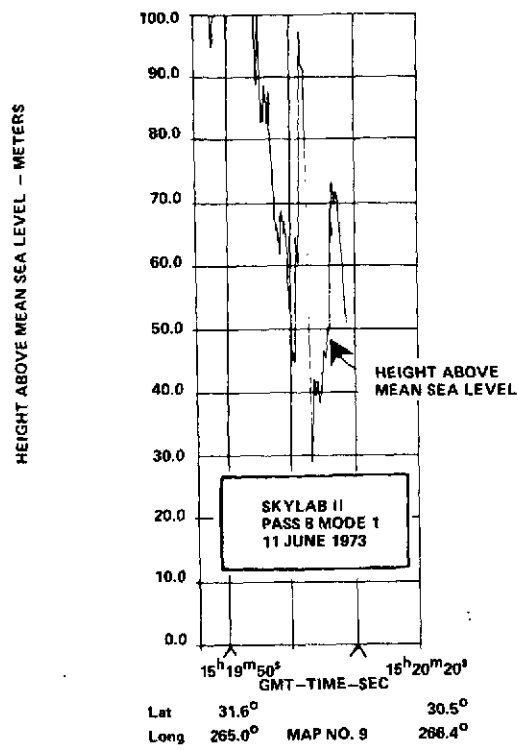
MAP NO. 5

13.6°
297.5°

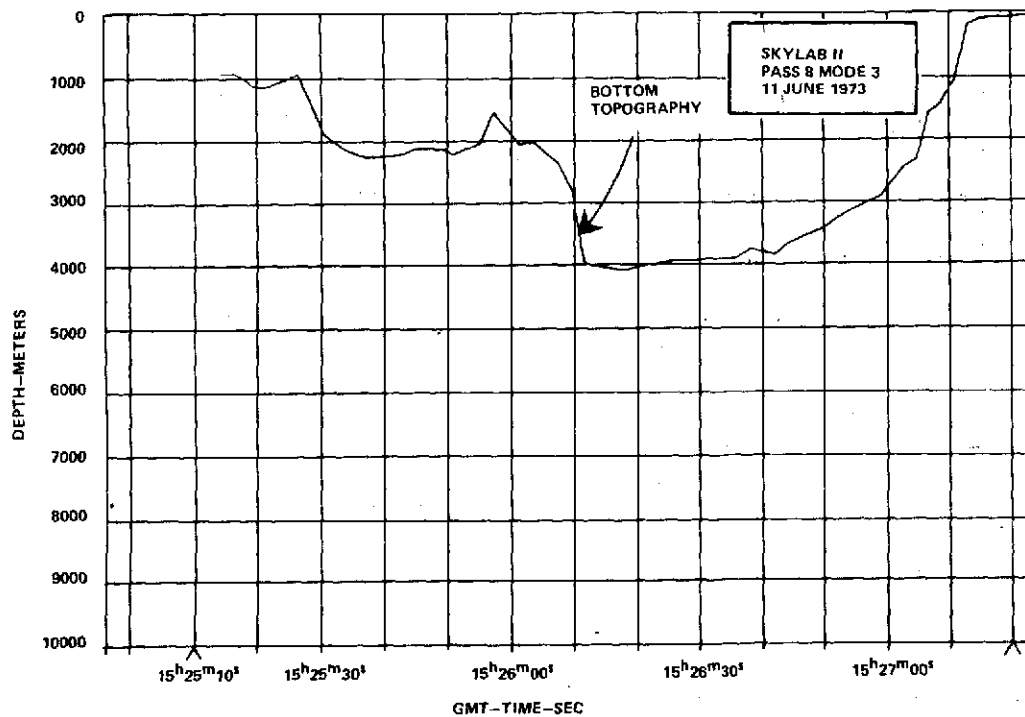
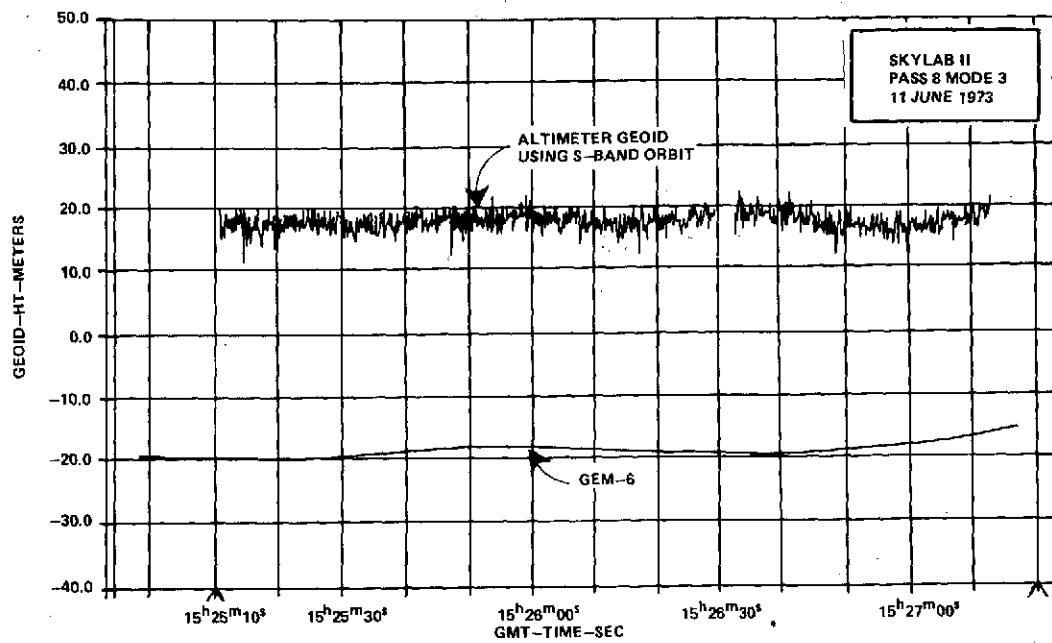








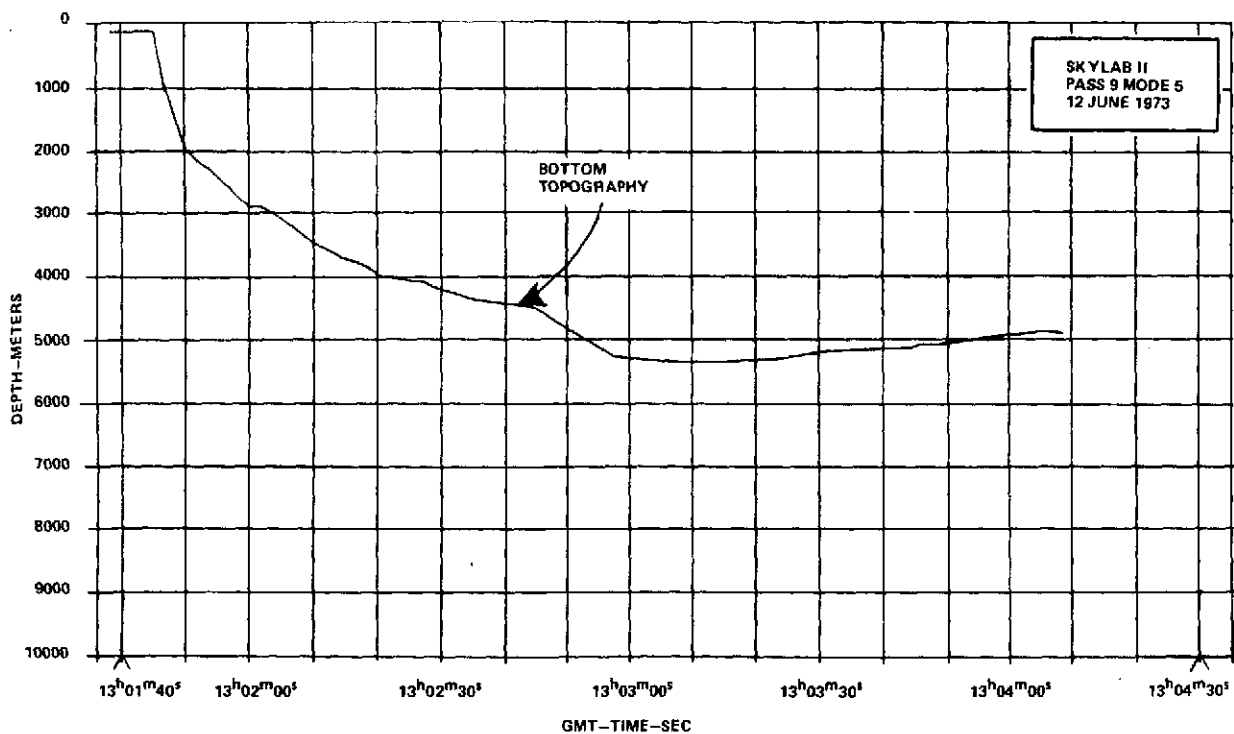
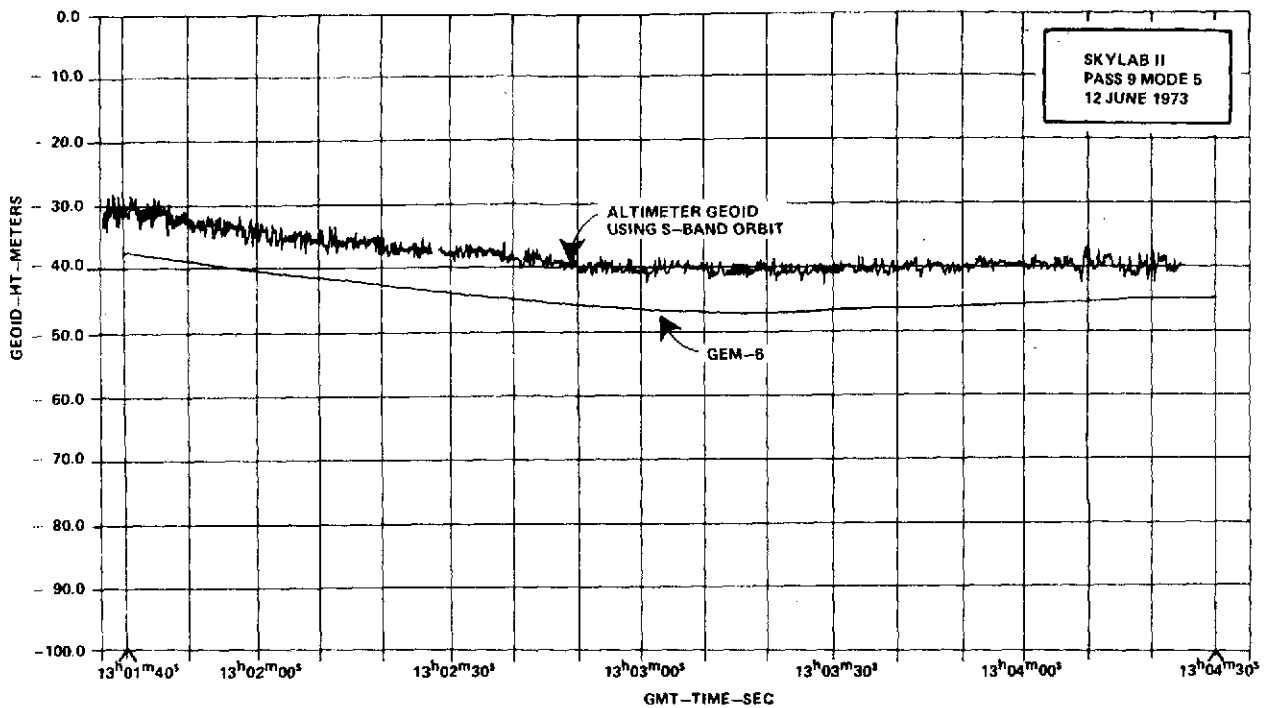
ORIGINAL PAGE
FOR POOR QUALITY



Lat 16.8°
Long 279.8°

MAP NO. 10

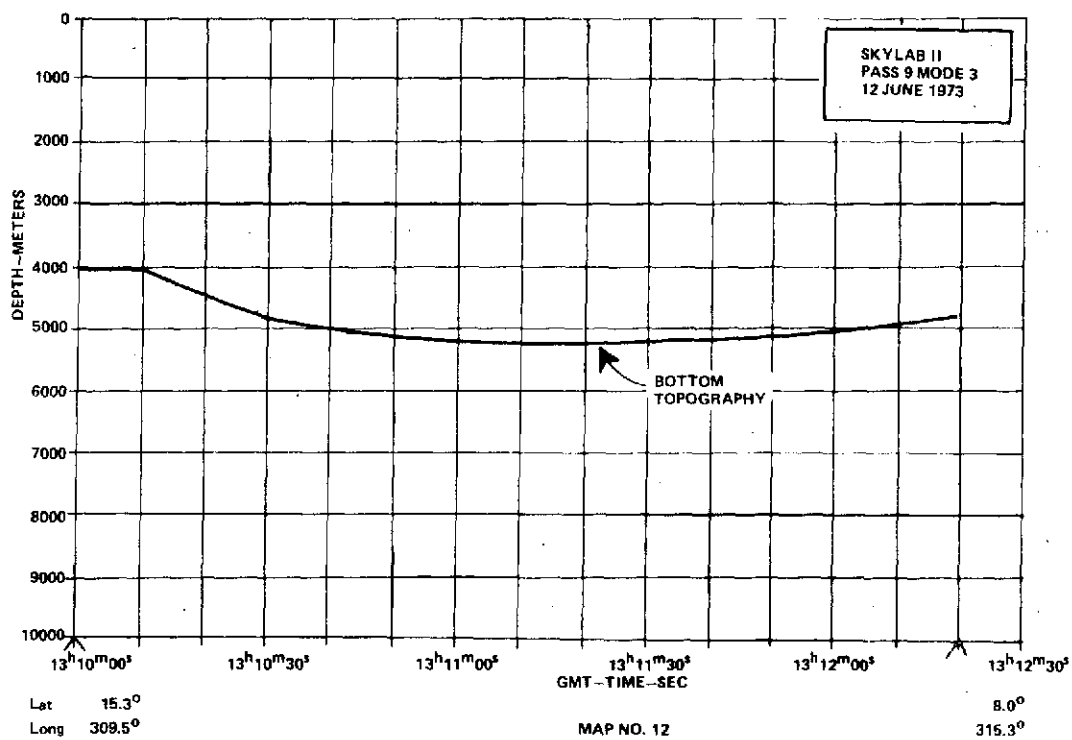
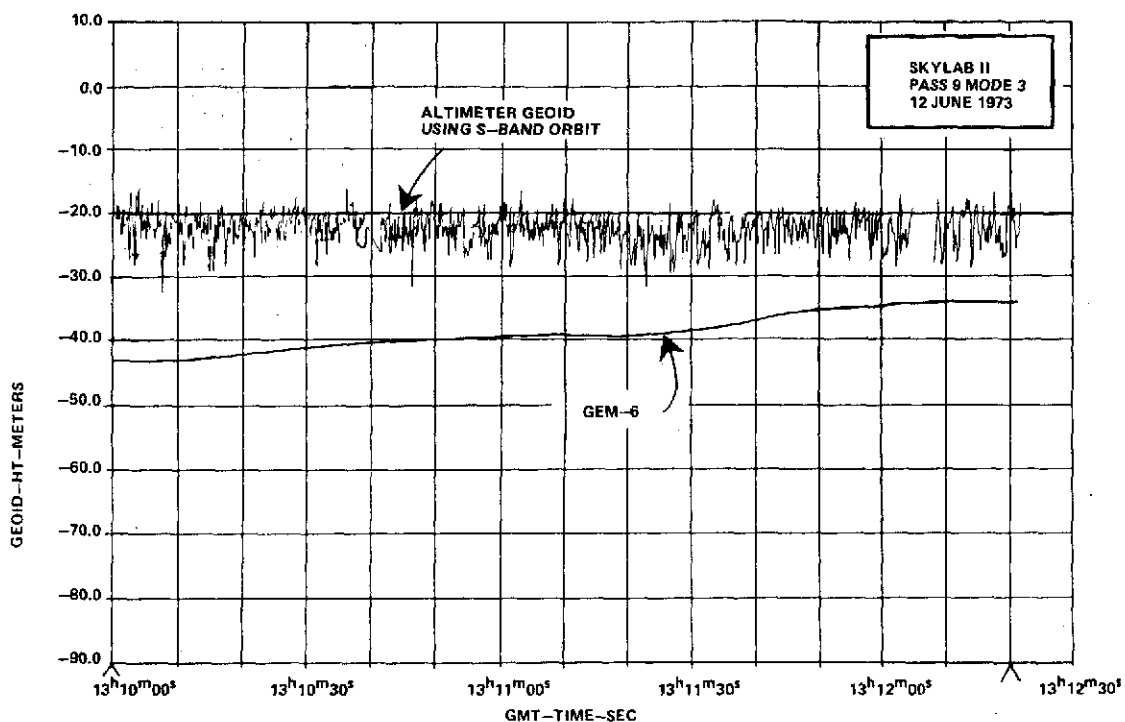
10.5°
284.9°

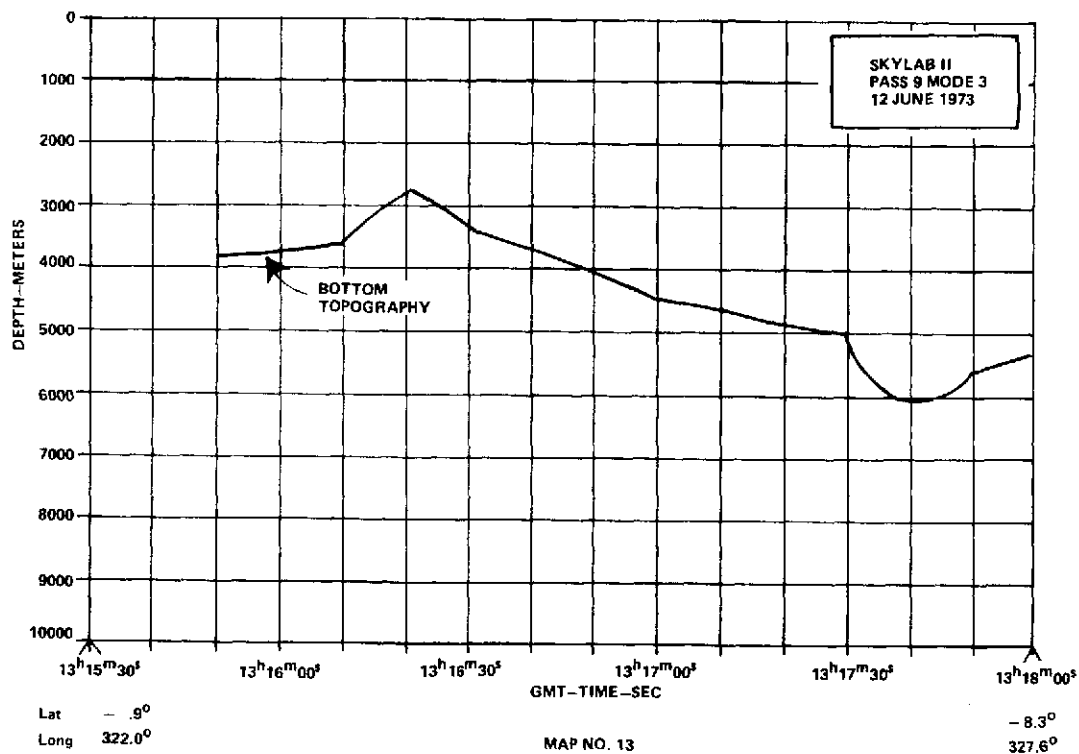
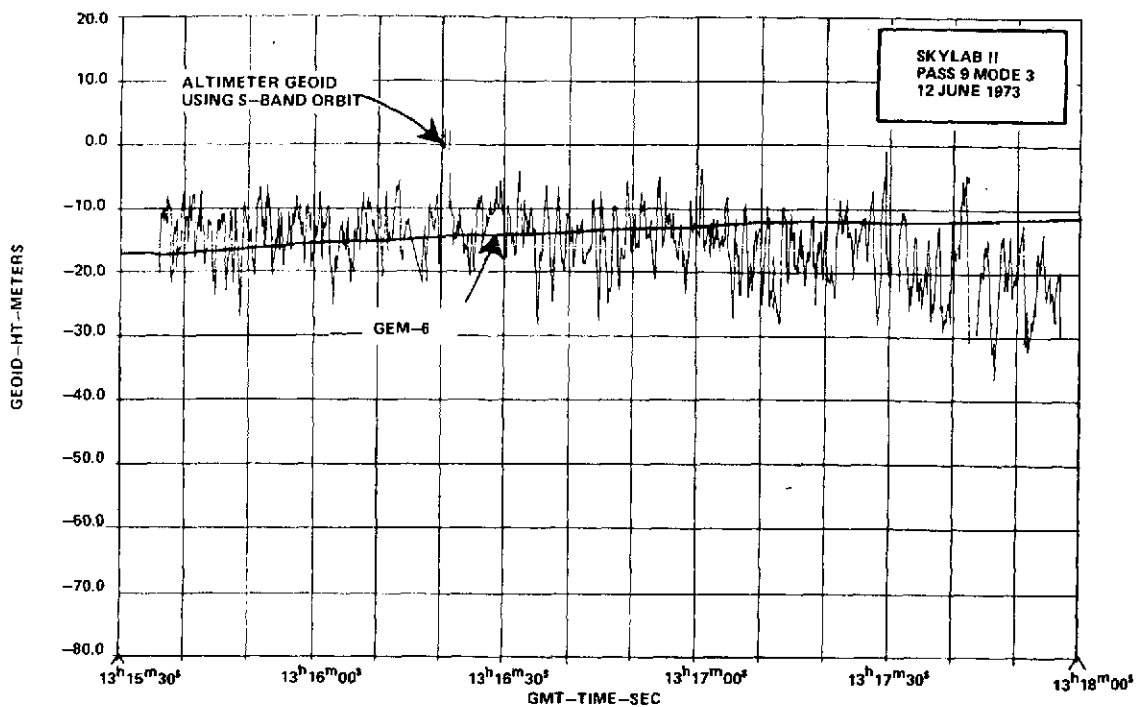


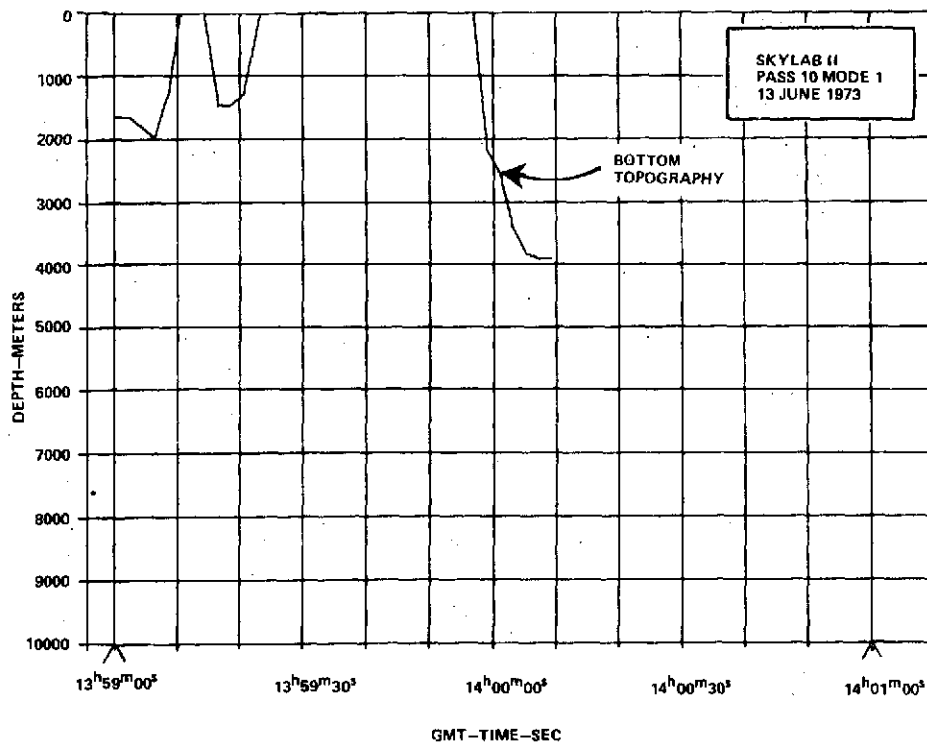
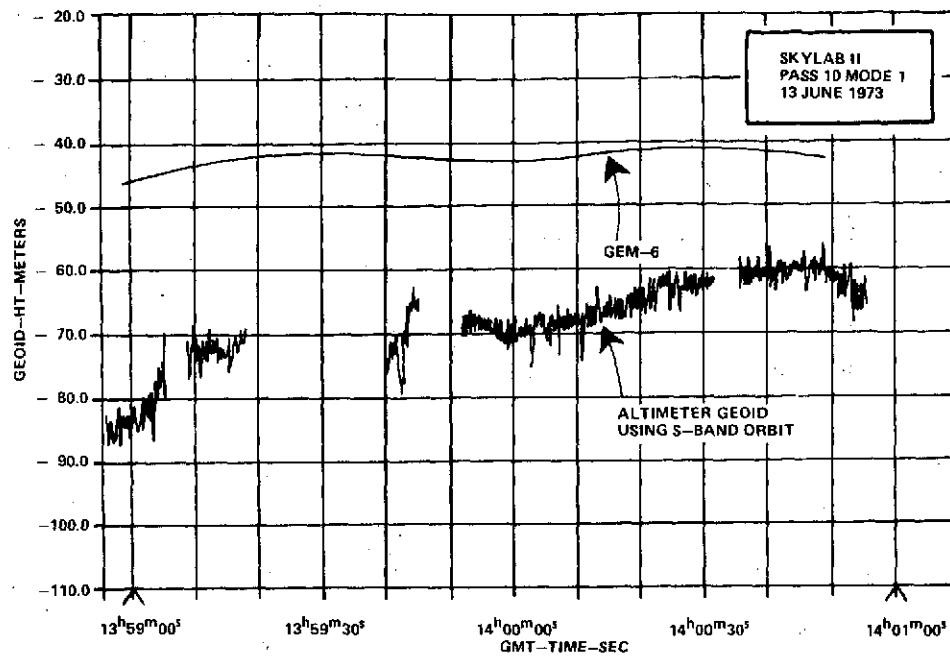
Lat 37.5°
Long 285.1°

MAP NO. 11

30.5°
294.7°



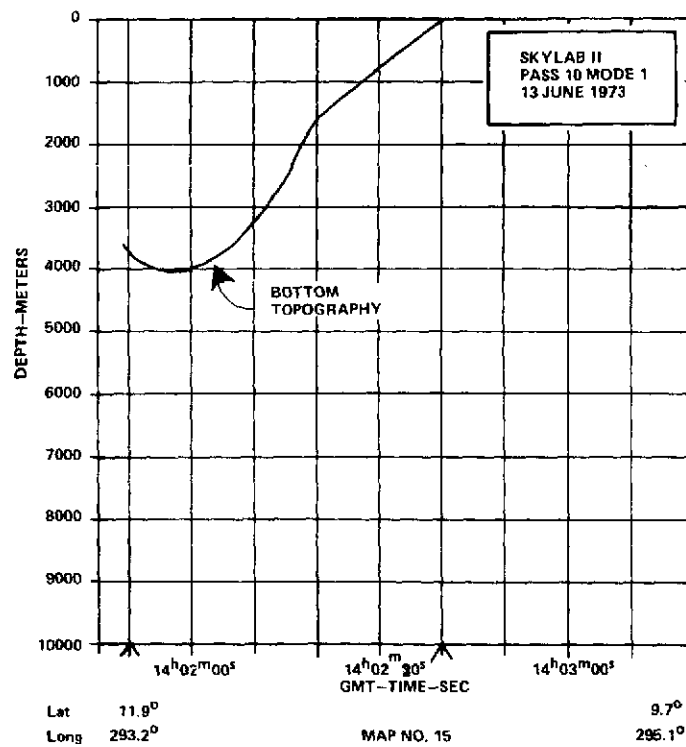
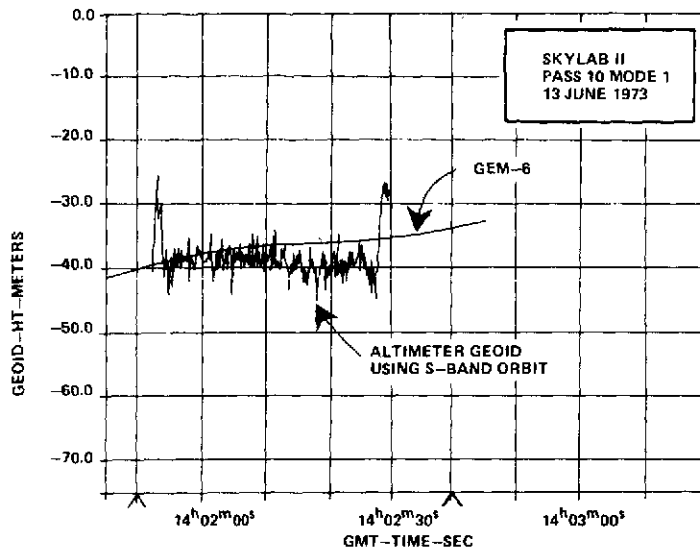


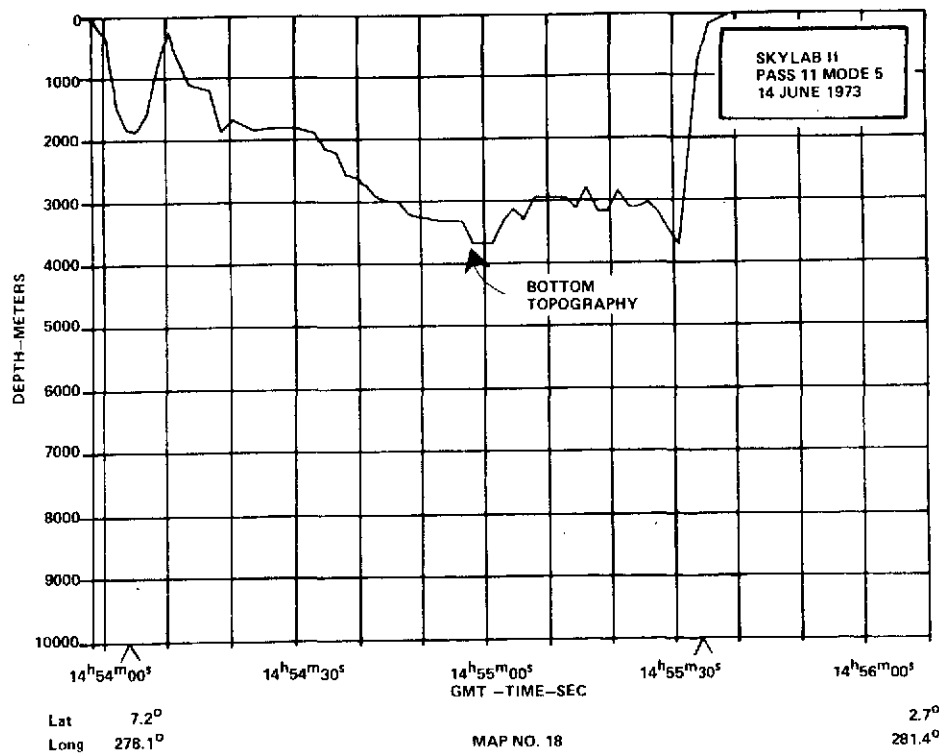
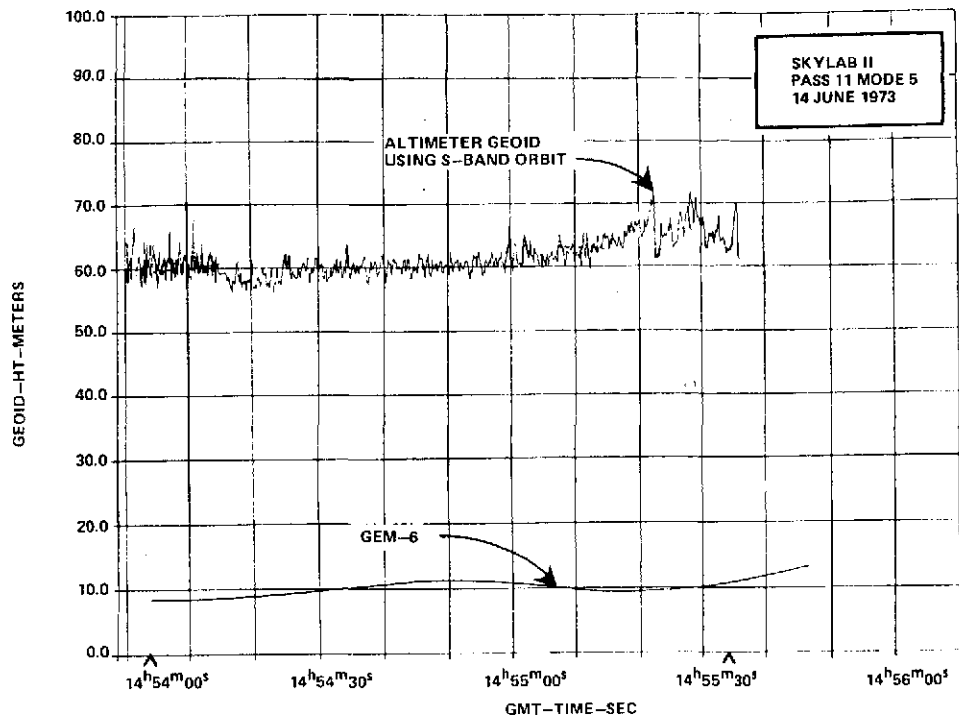


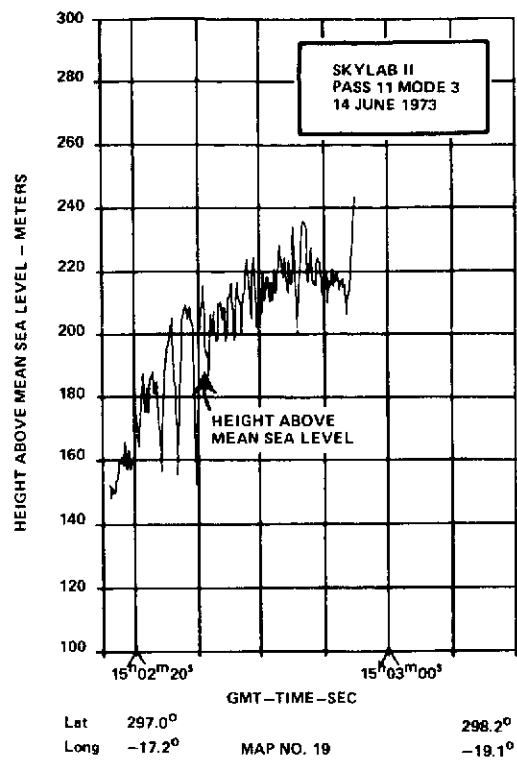
Lat 20.3°
Long 286.3°

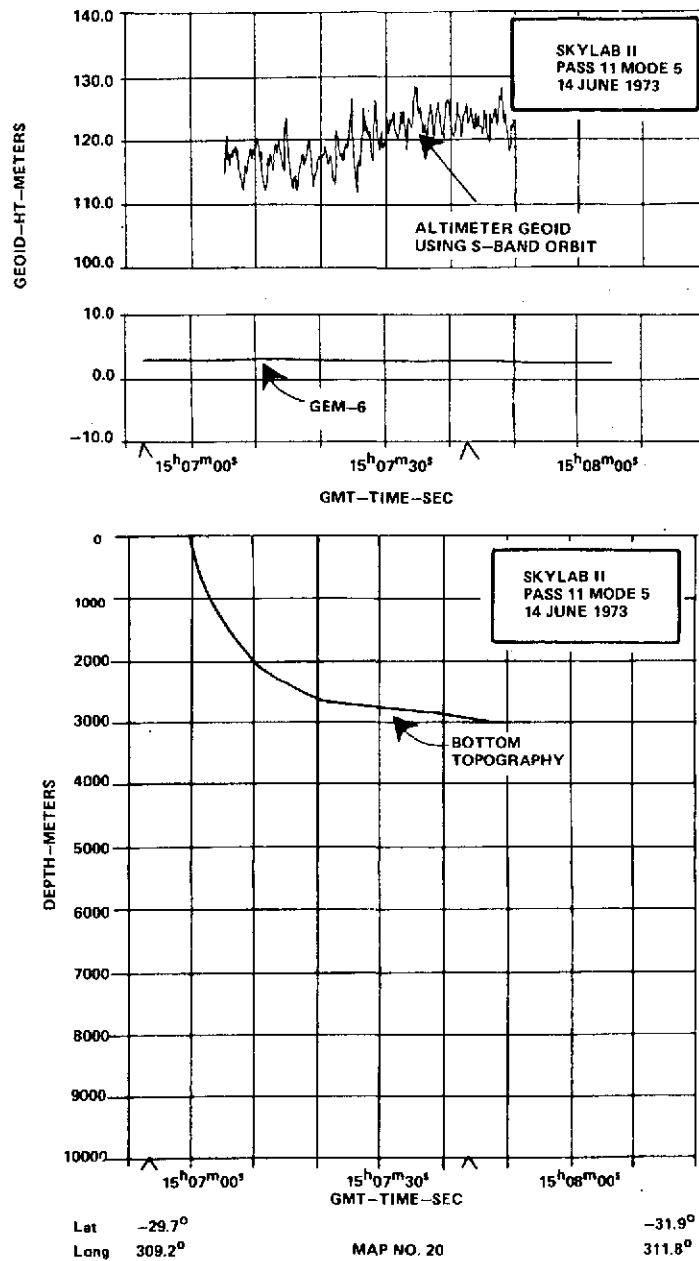
MAP NO. 14

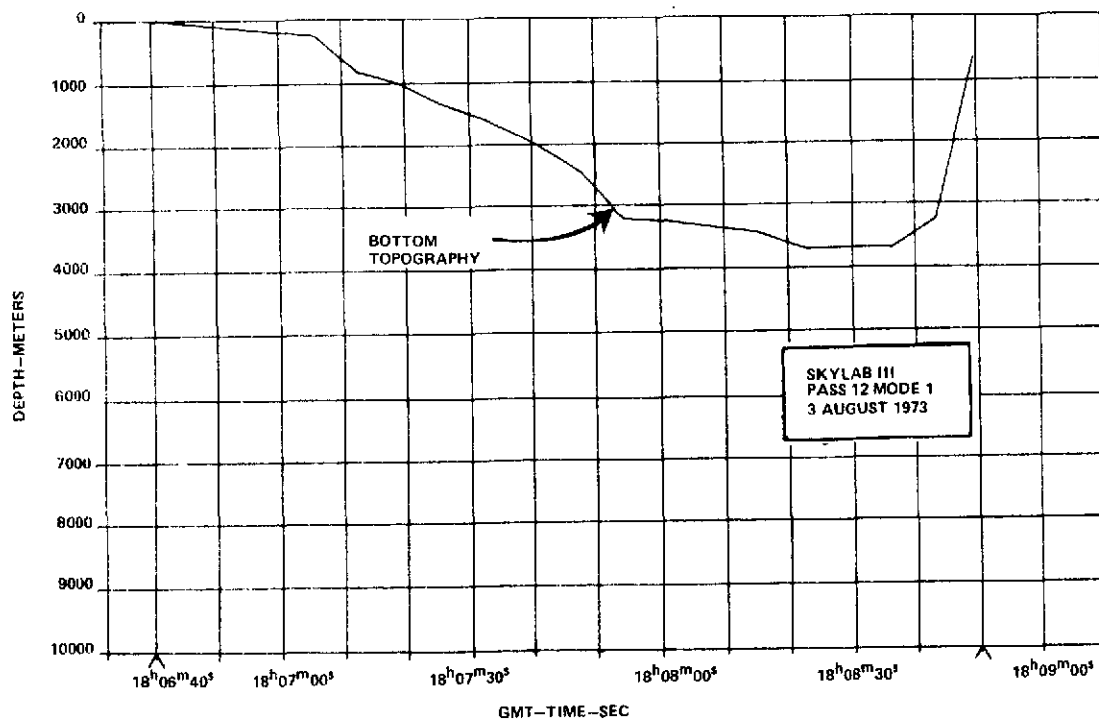
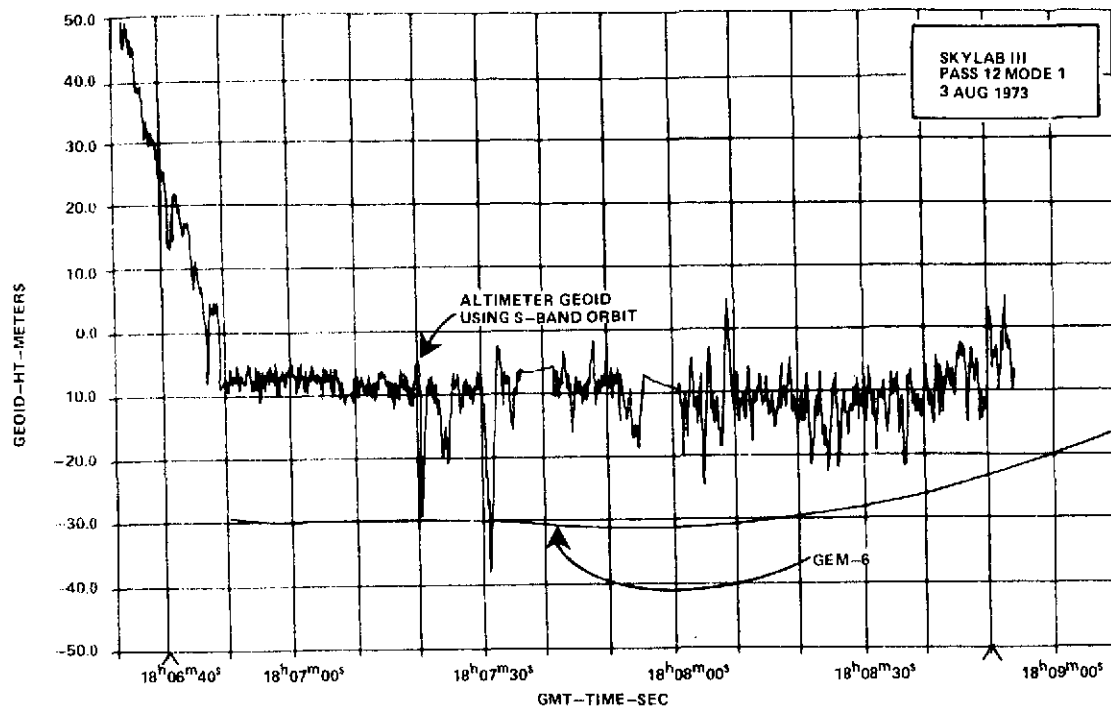
17.2°
291.2°







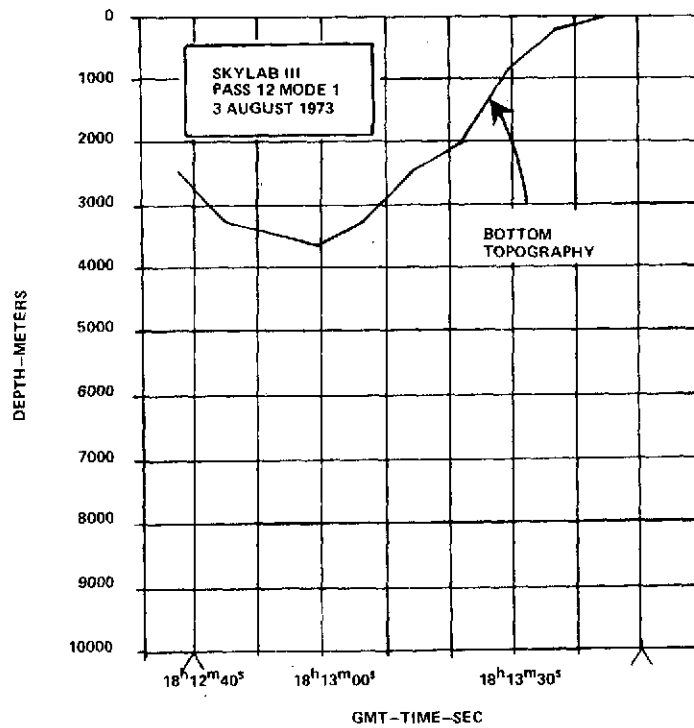
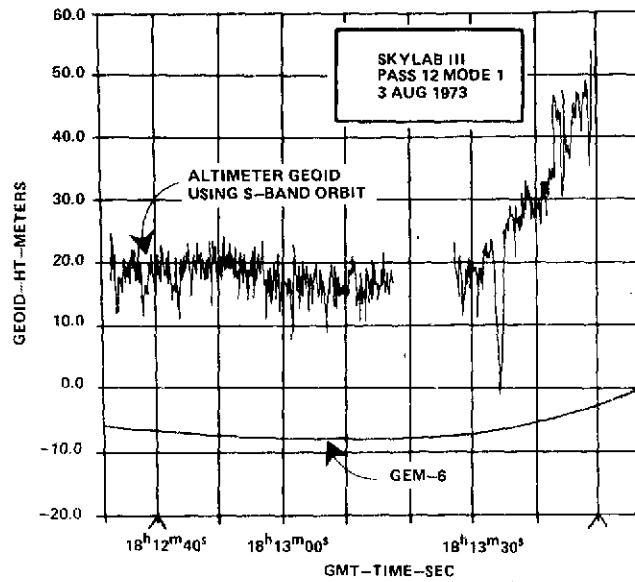




Lat 29.1°
Long 264.0°

MAP NO. 22

23.2°
270.1°



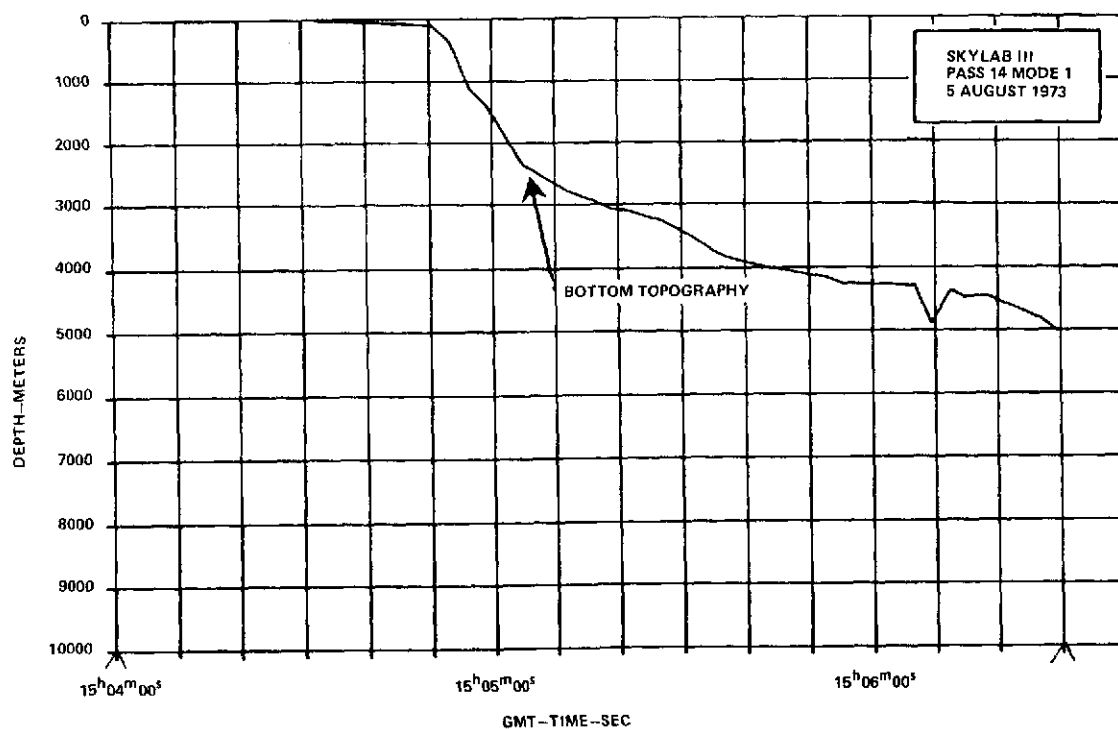
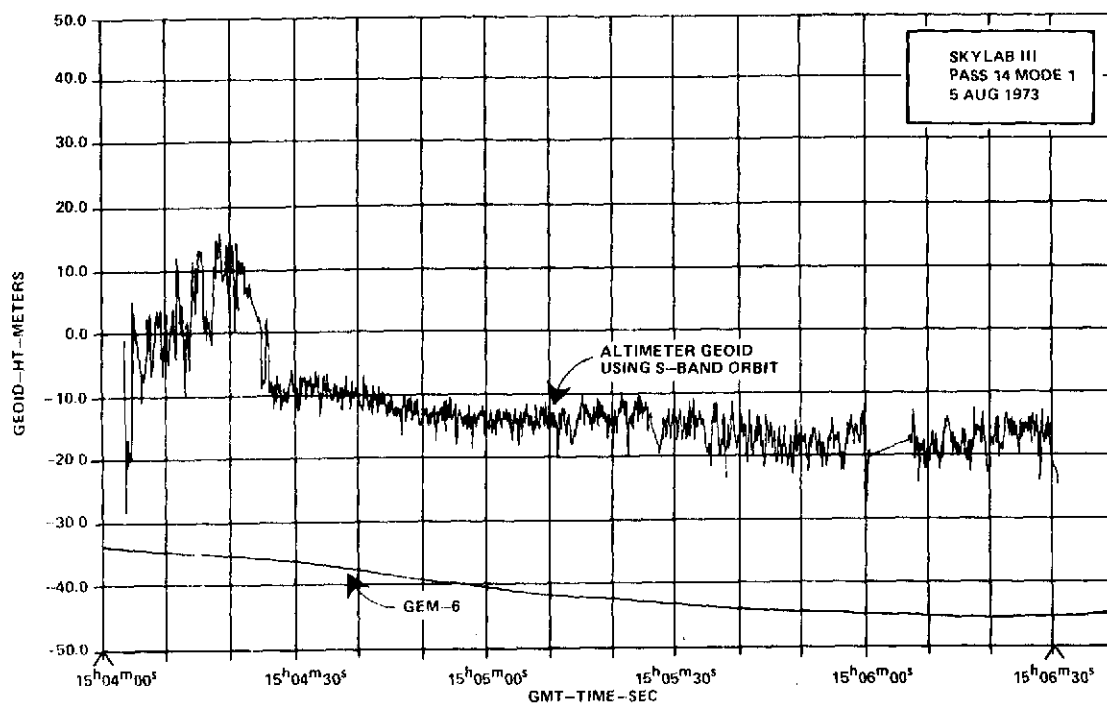
Lat 12.2°

Long 279.7°

MAP NO. 23

8.8°

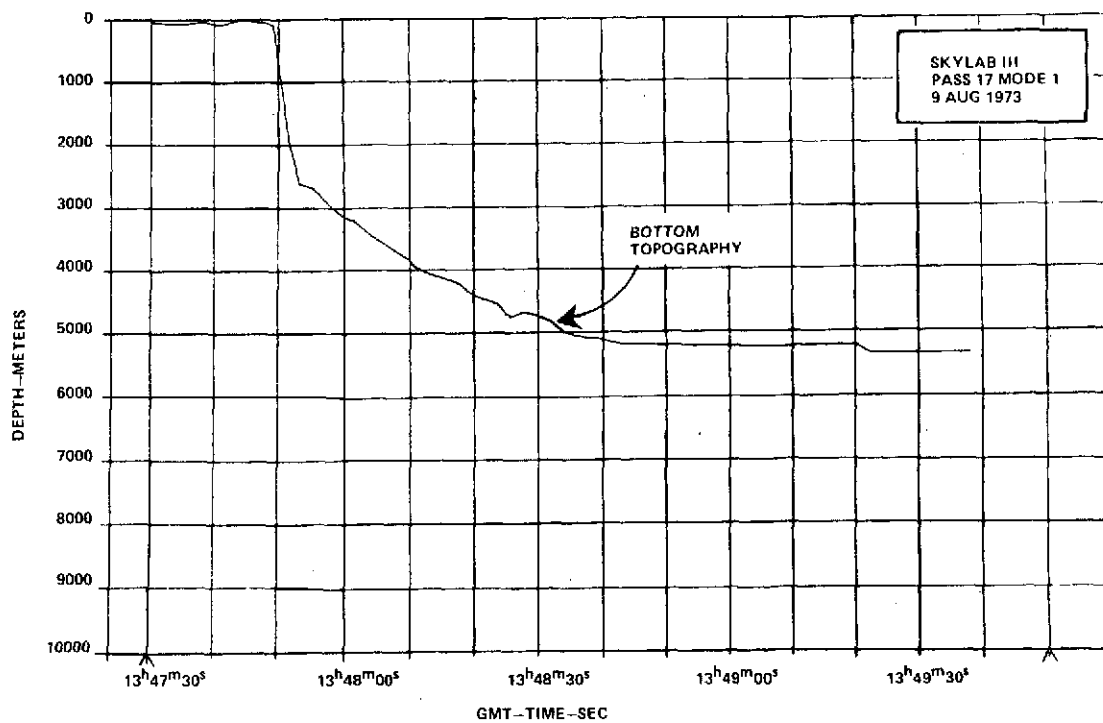
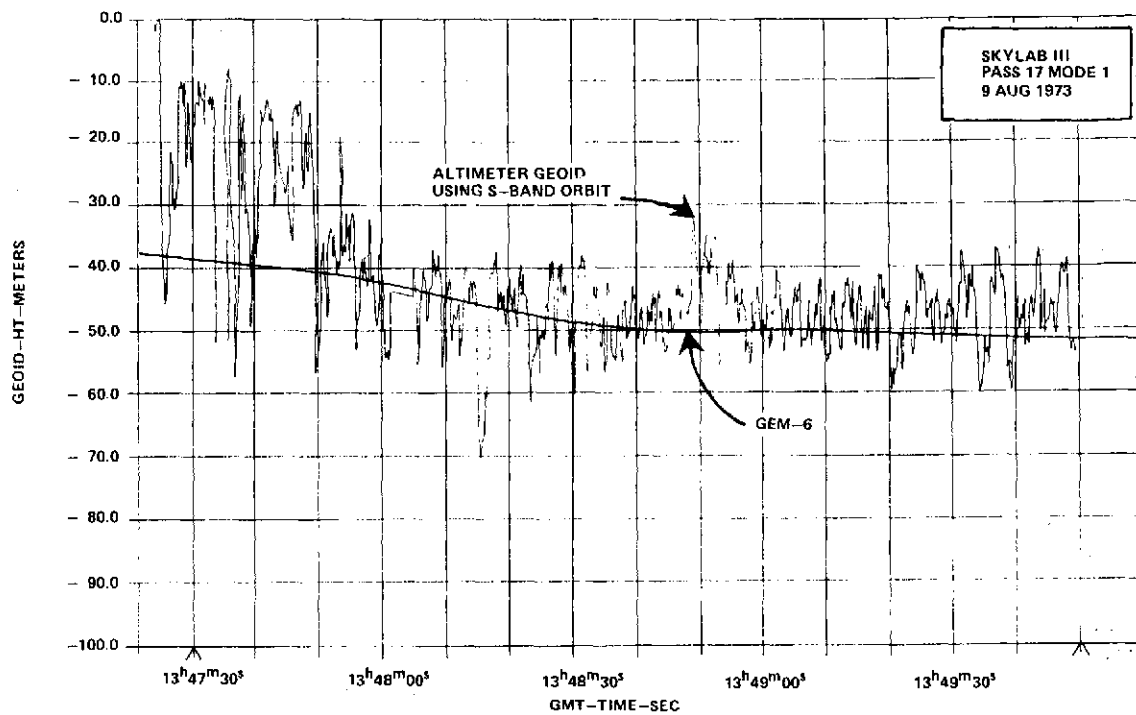
282.4°



Lat 39.1°
Long 283.3°

MAP NO. 26

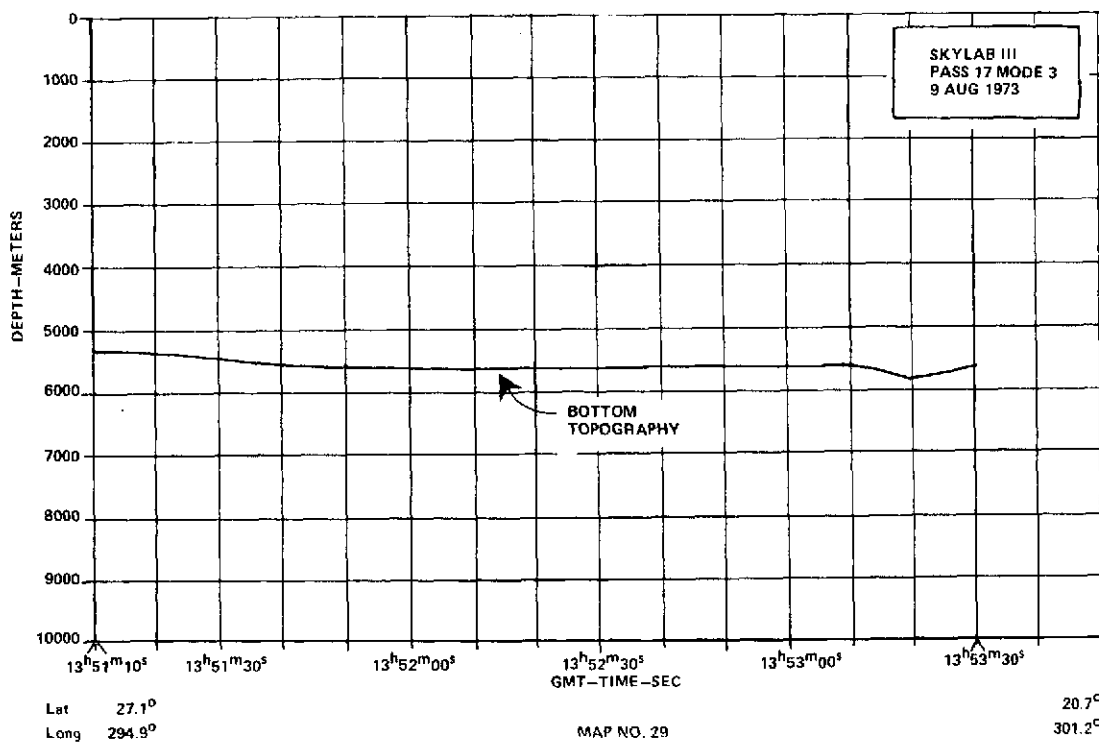
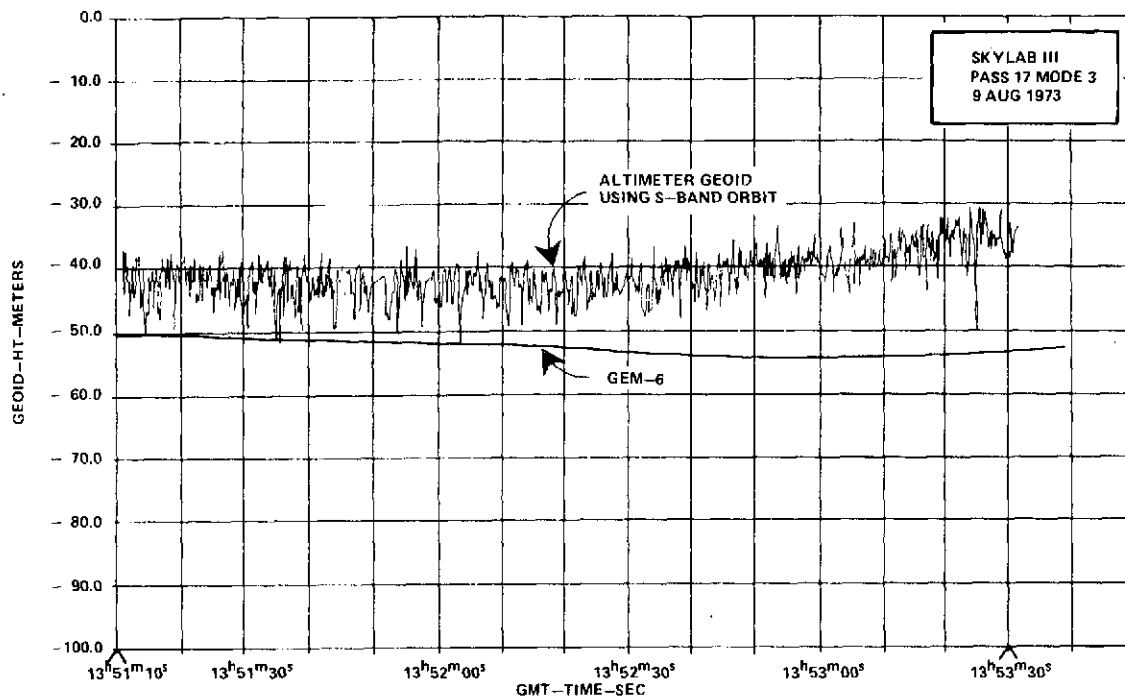
33.2°
292.2°

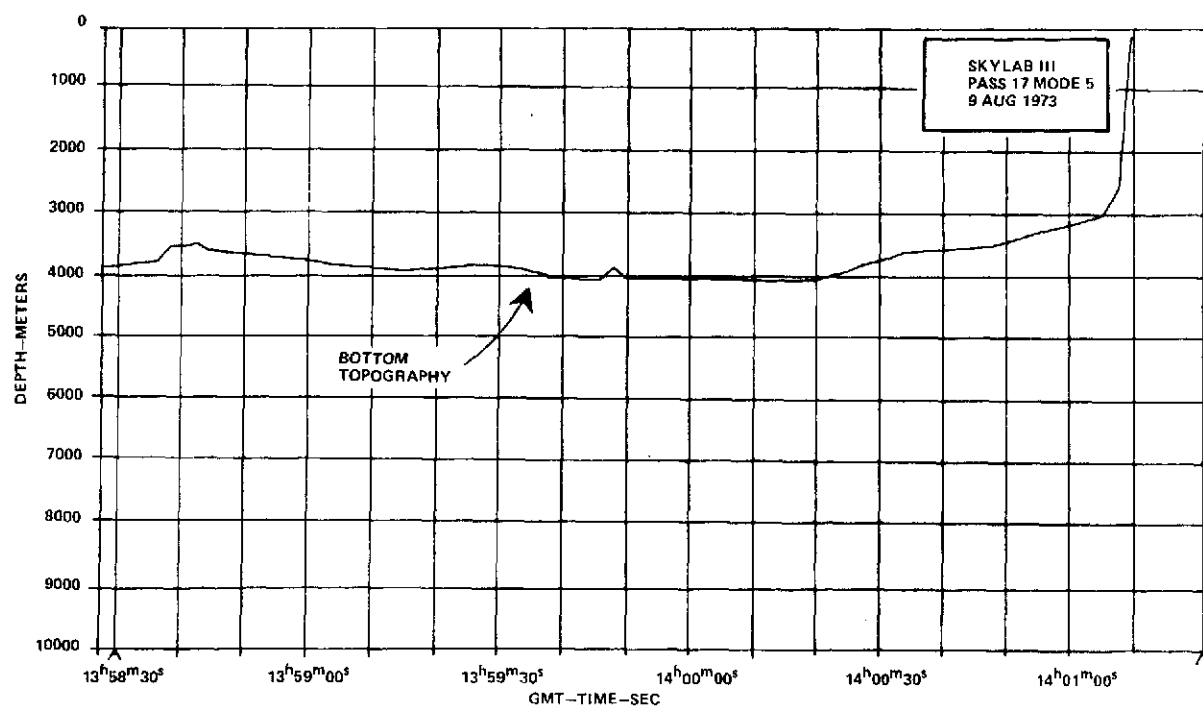
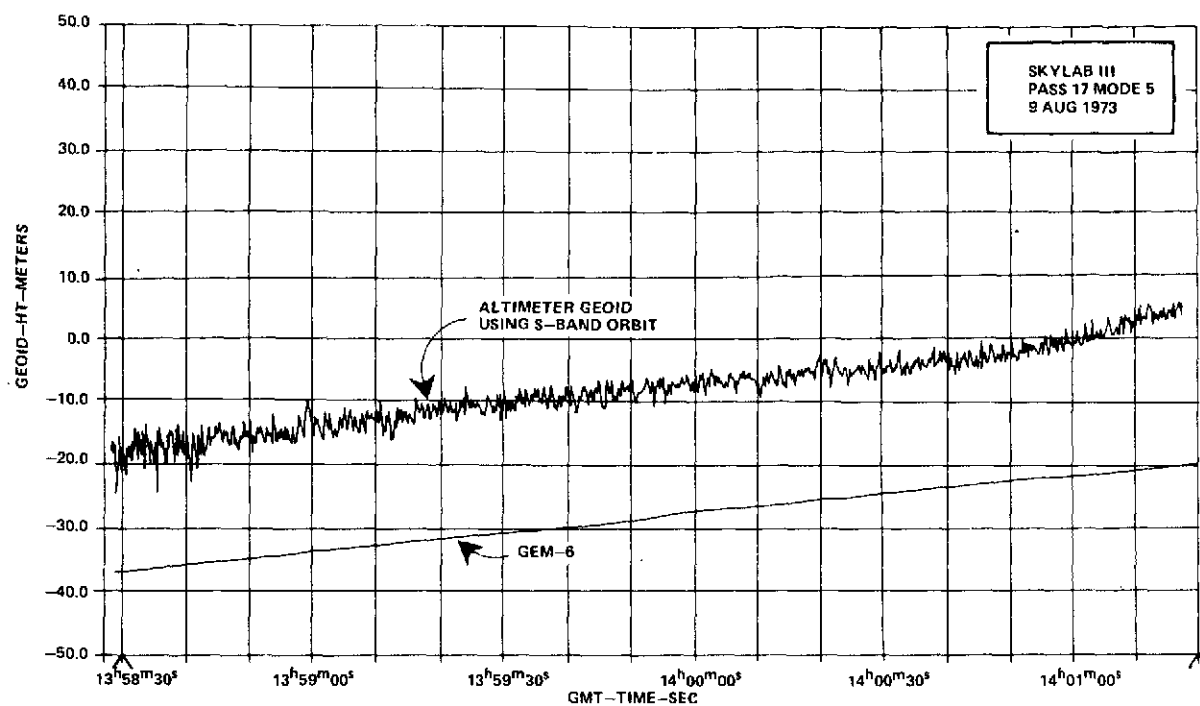


Lat 35.4°
Long 283.2°

MAP NO. 28 -

31.0°
290.4°

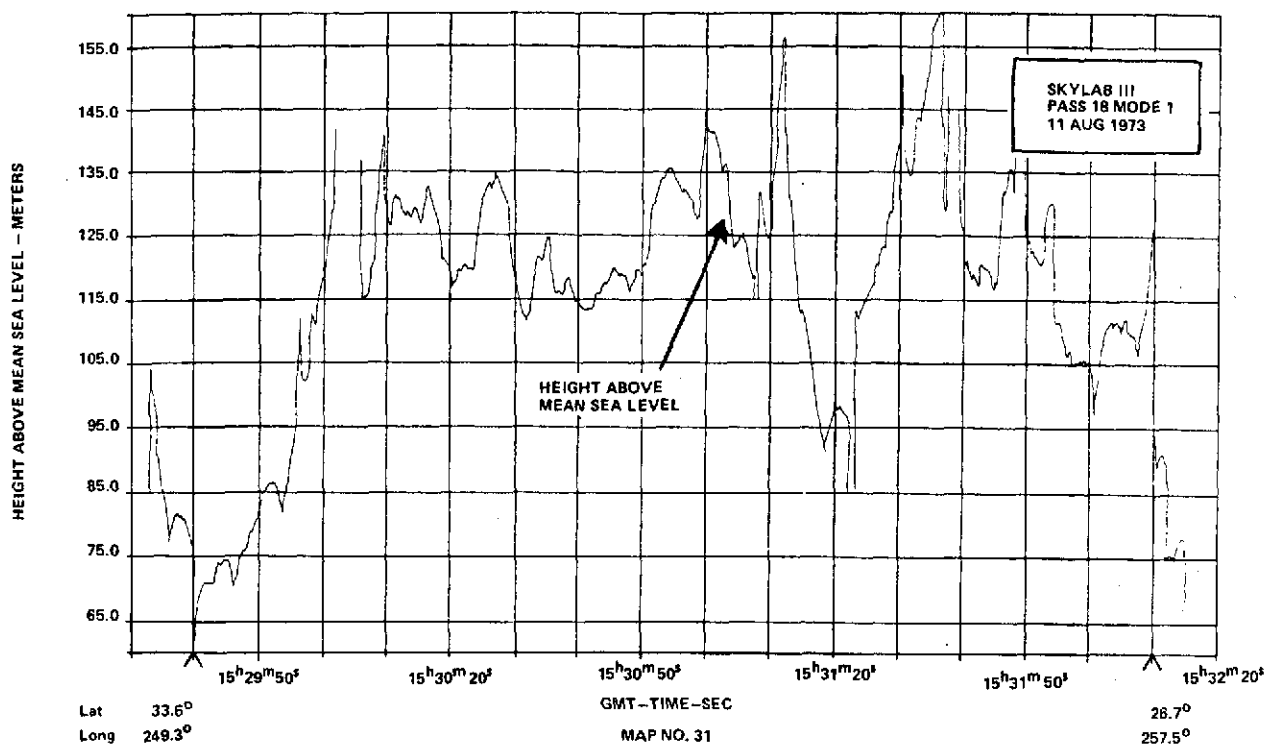


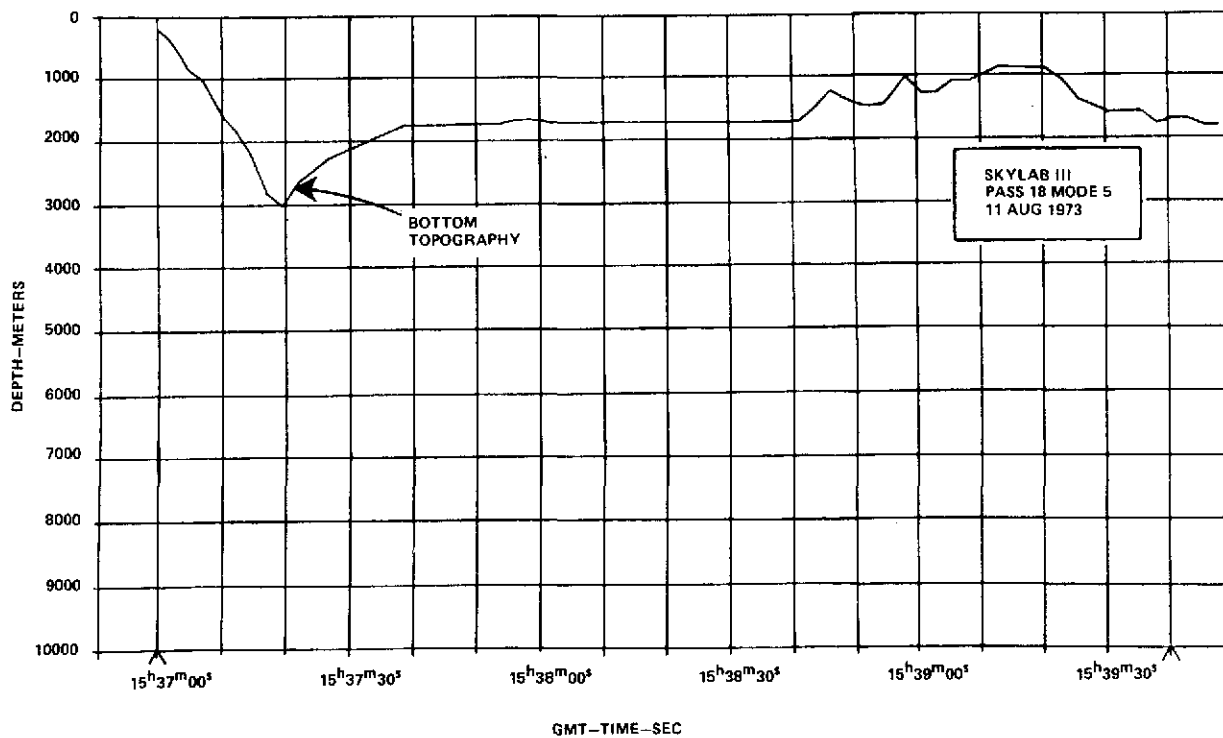
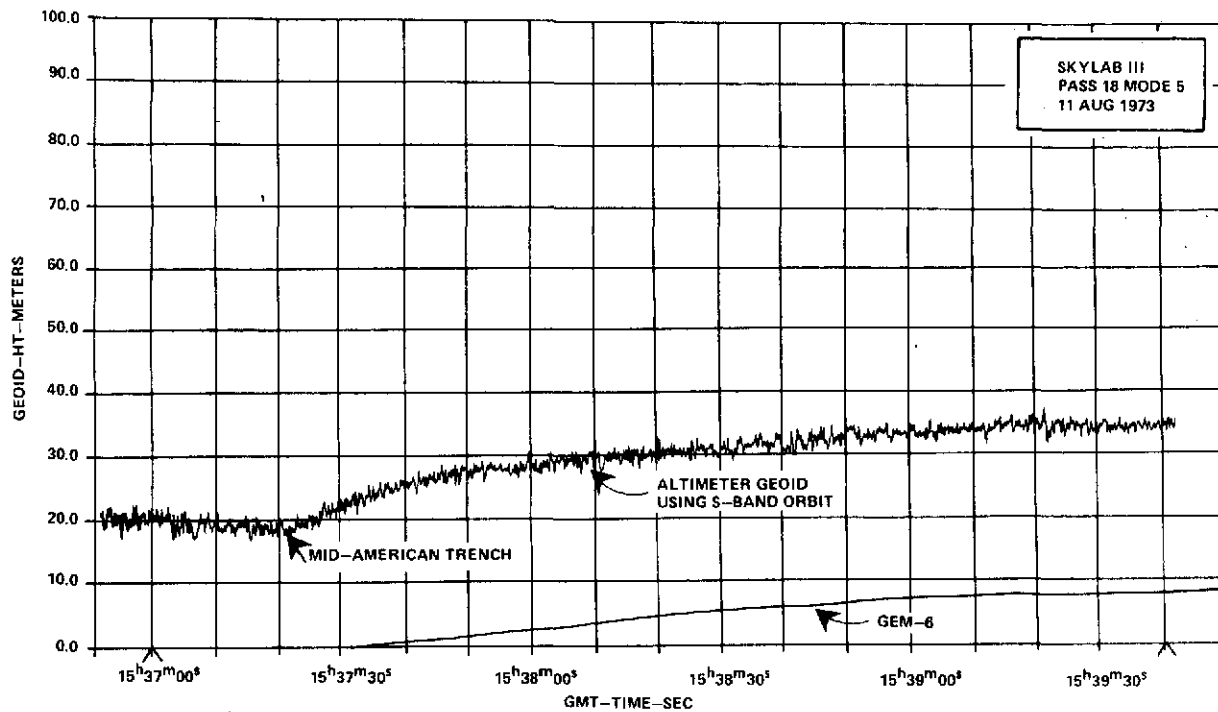


Lat 6.1°
Long 313.1°

MAP NO. 30

-2.3°
319.5°

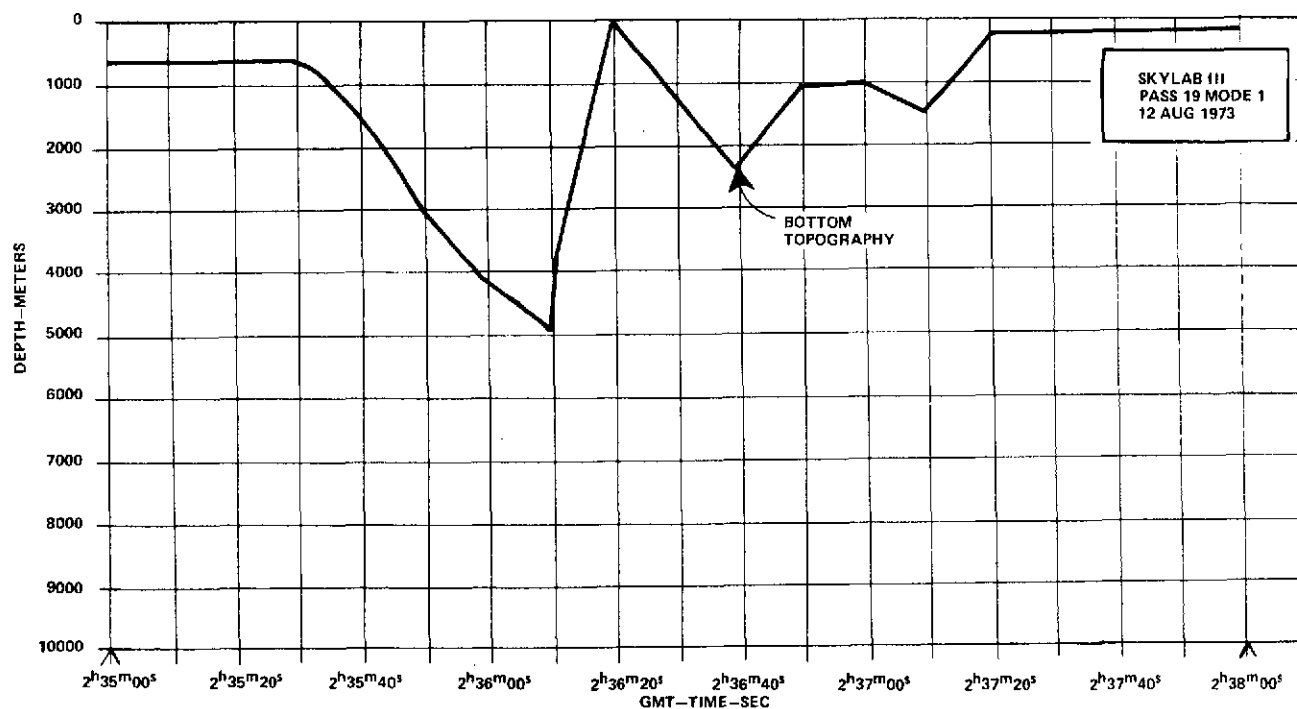
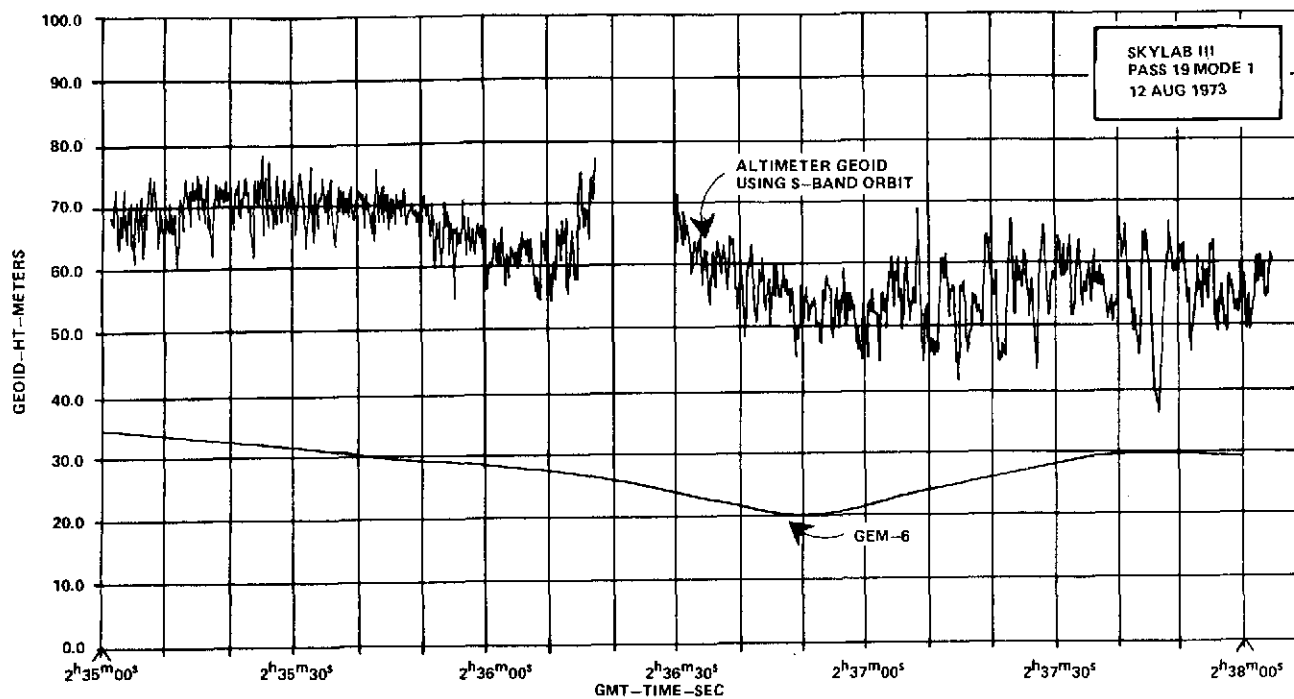




Lat 13.1°
Long 269.9°

MAP NO. 32

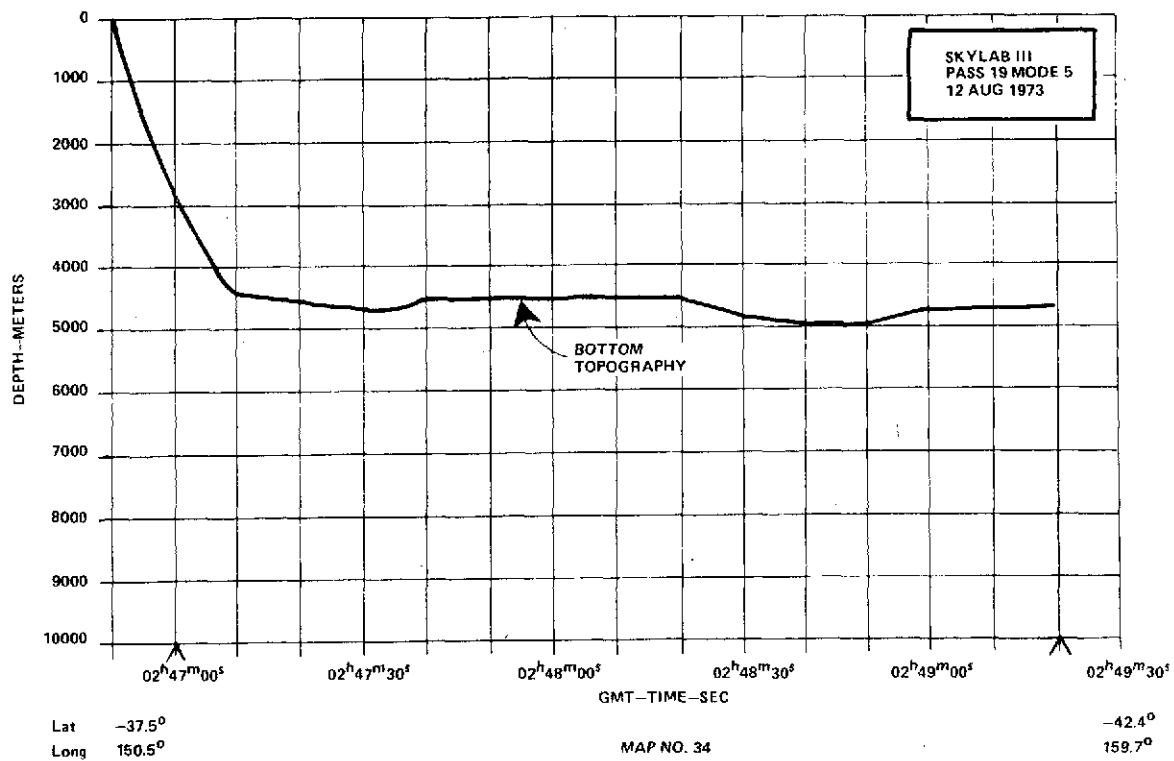
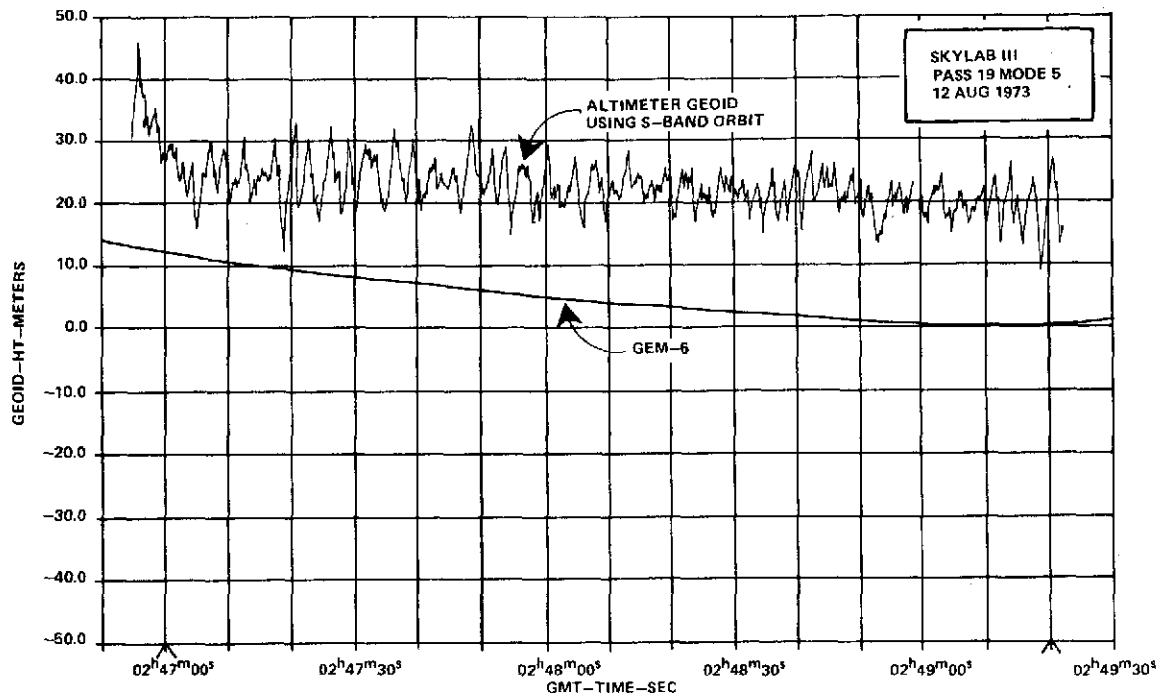
5.2°
276.0°

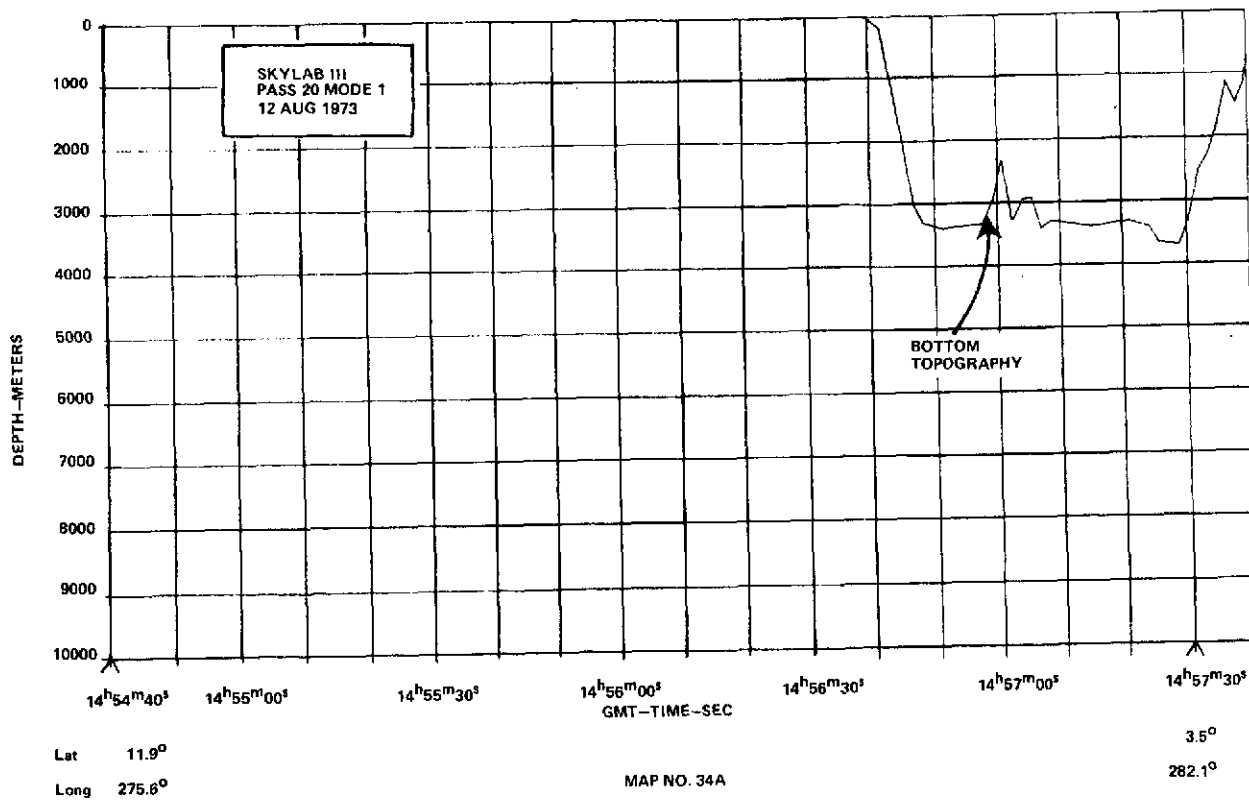
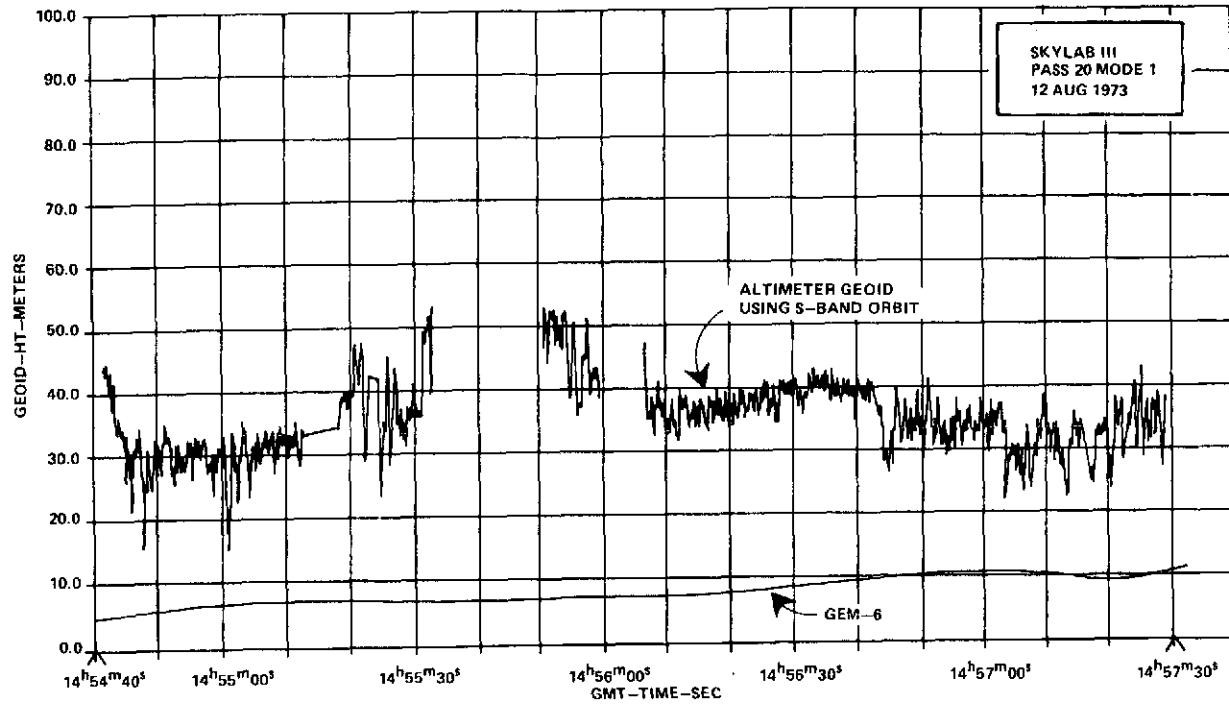


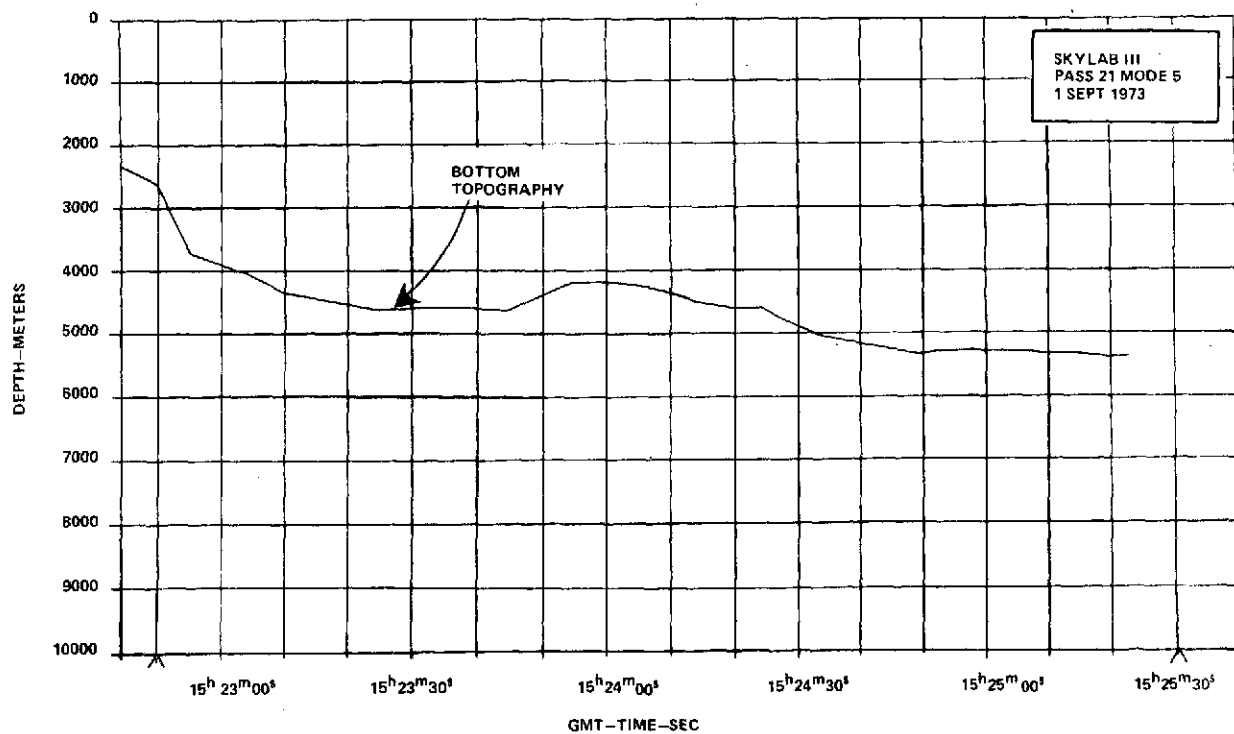
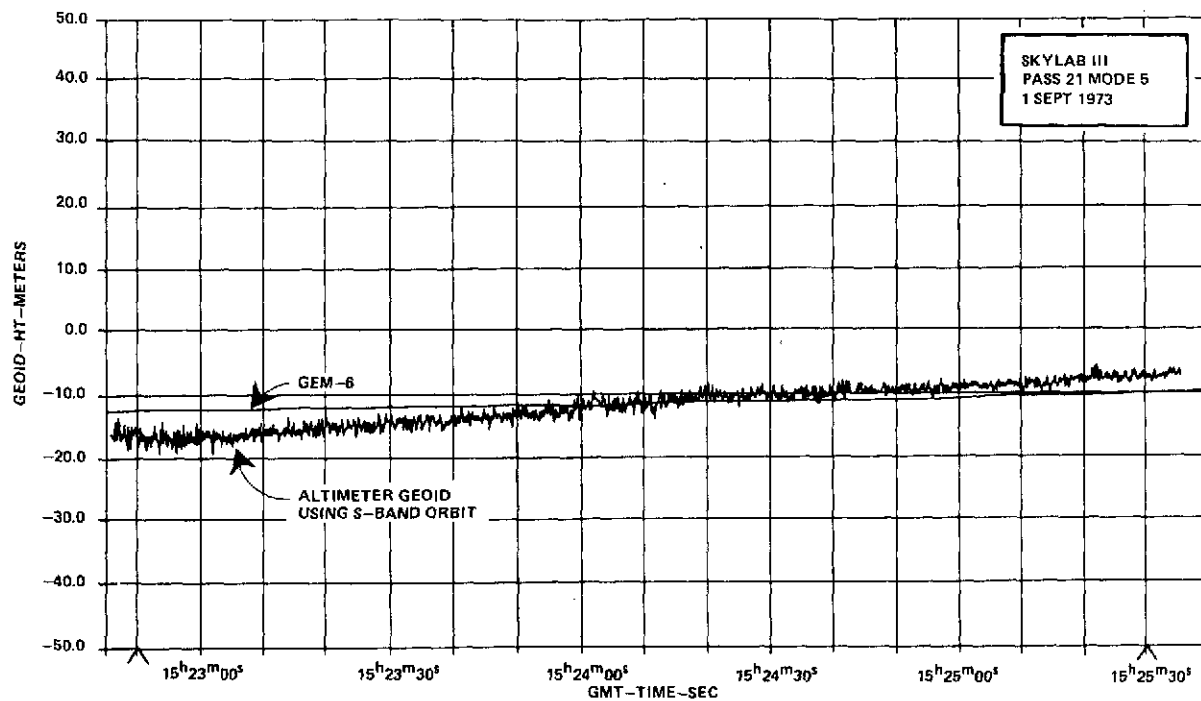
Lat -4.6°
Long 117.6°

MAP NO. 33

-13.4°
124.5°



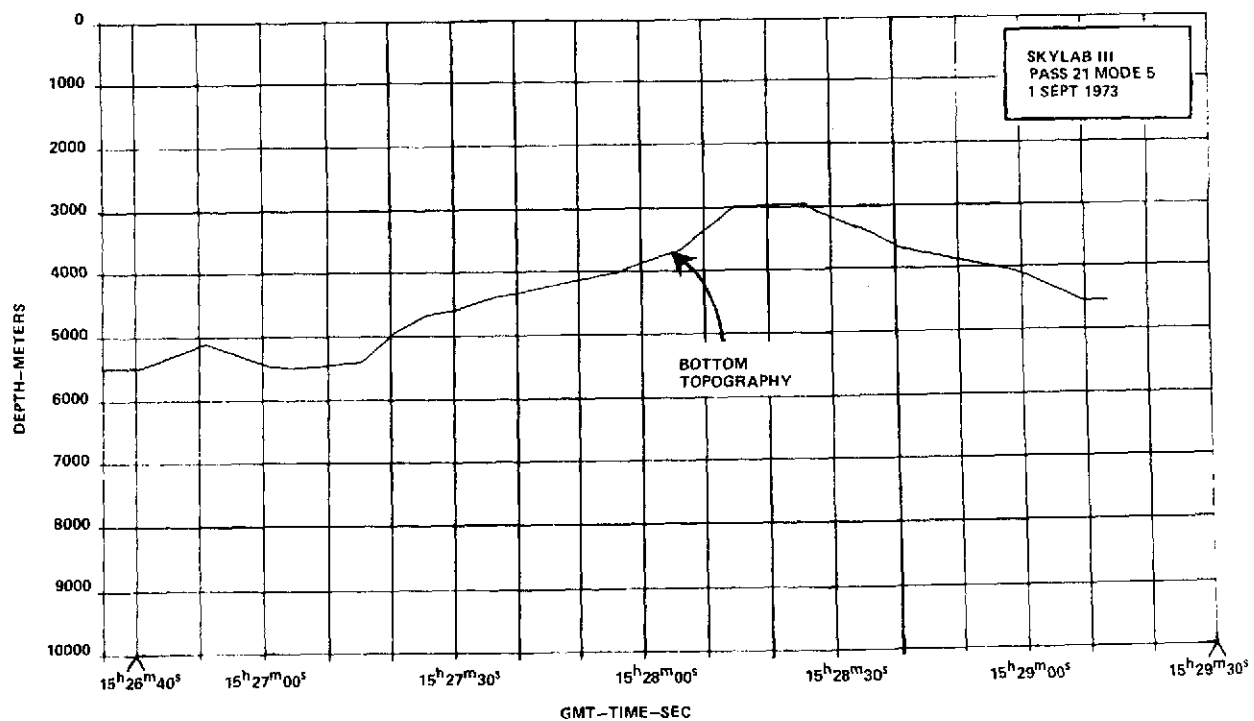
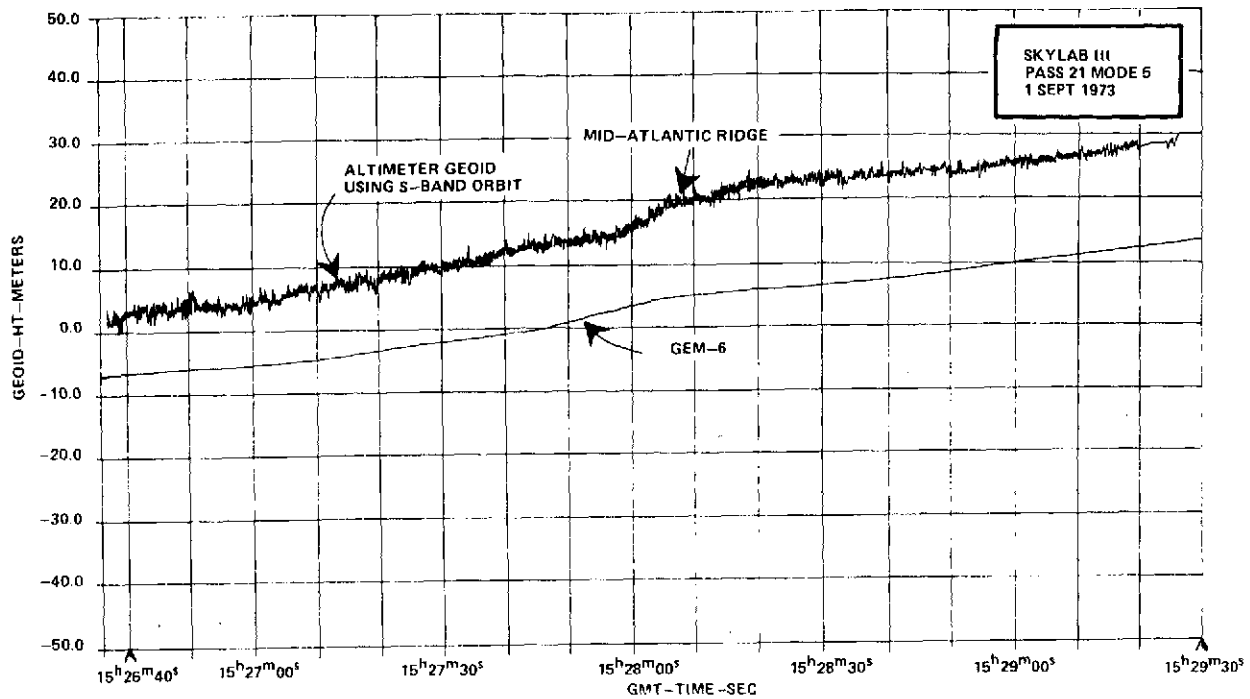




Lat -16.5°
Long 322.9°

MAP NO. 35

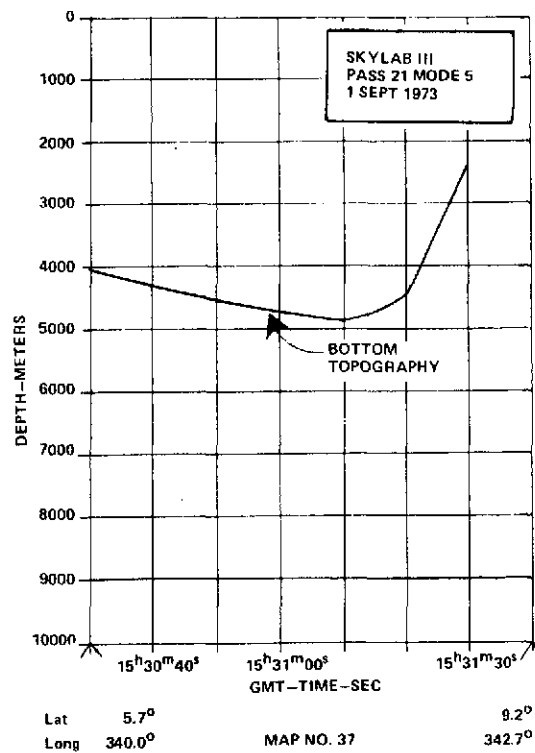
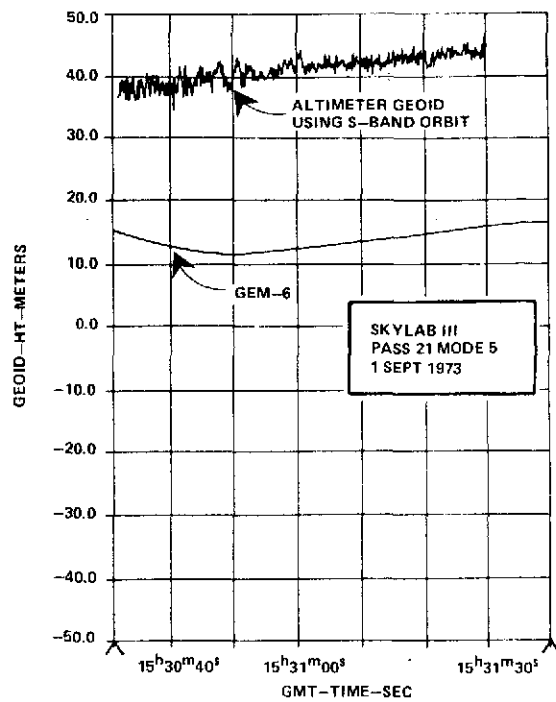
-8.7°
329.2°

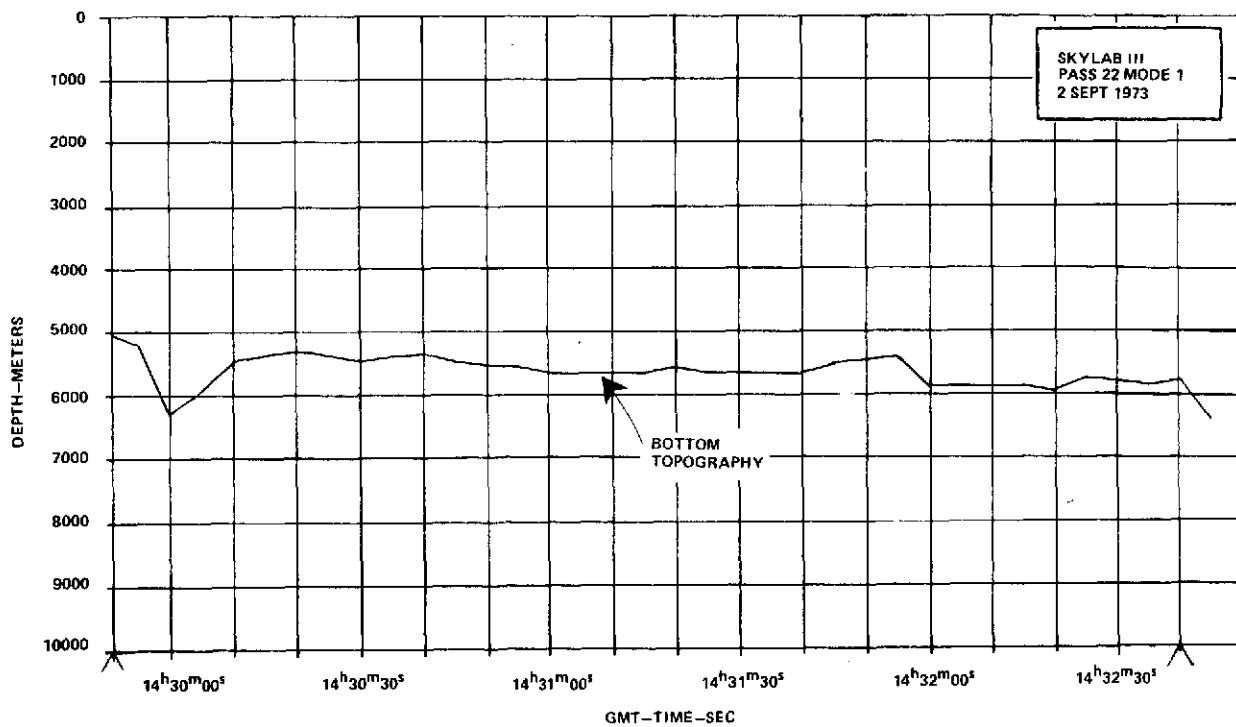
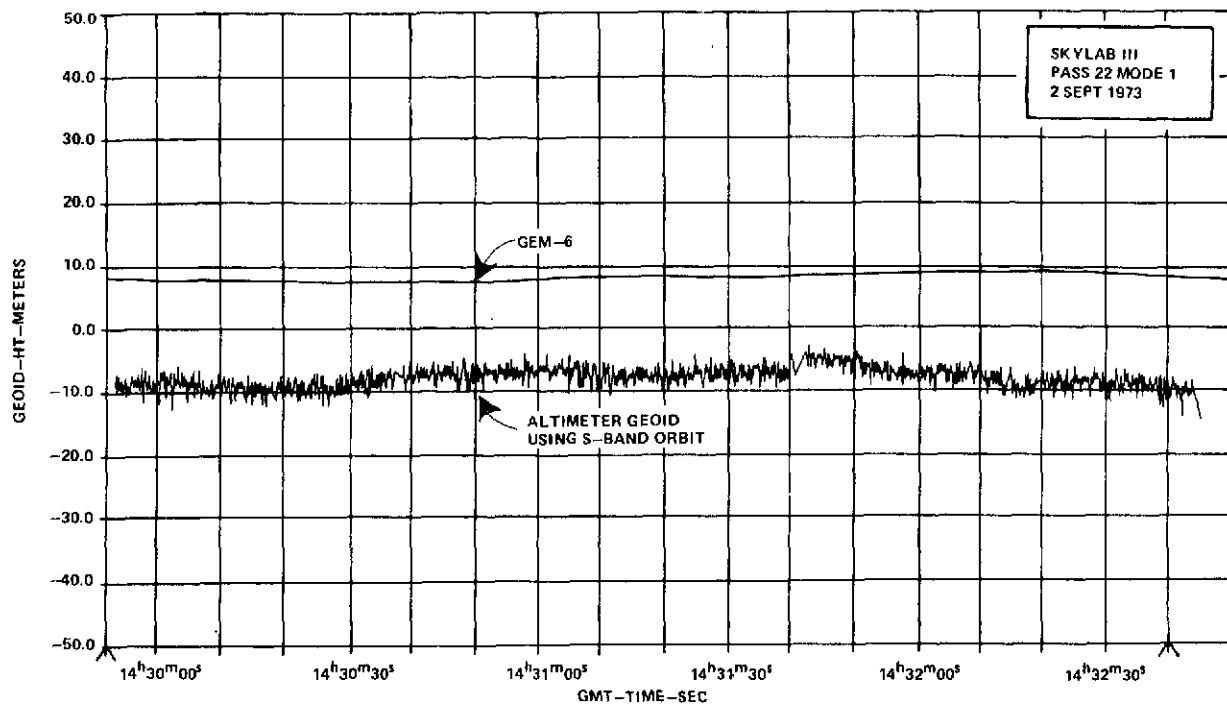


Lat - 5.2°
Long 332.2°

MAP NO. 36

2.8°
337.8°

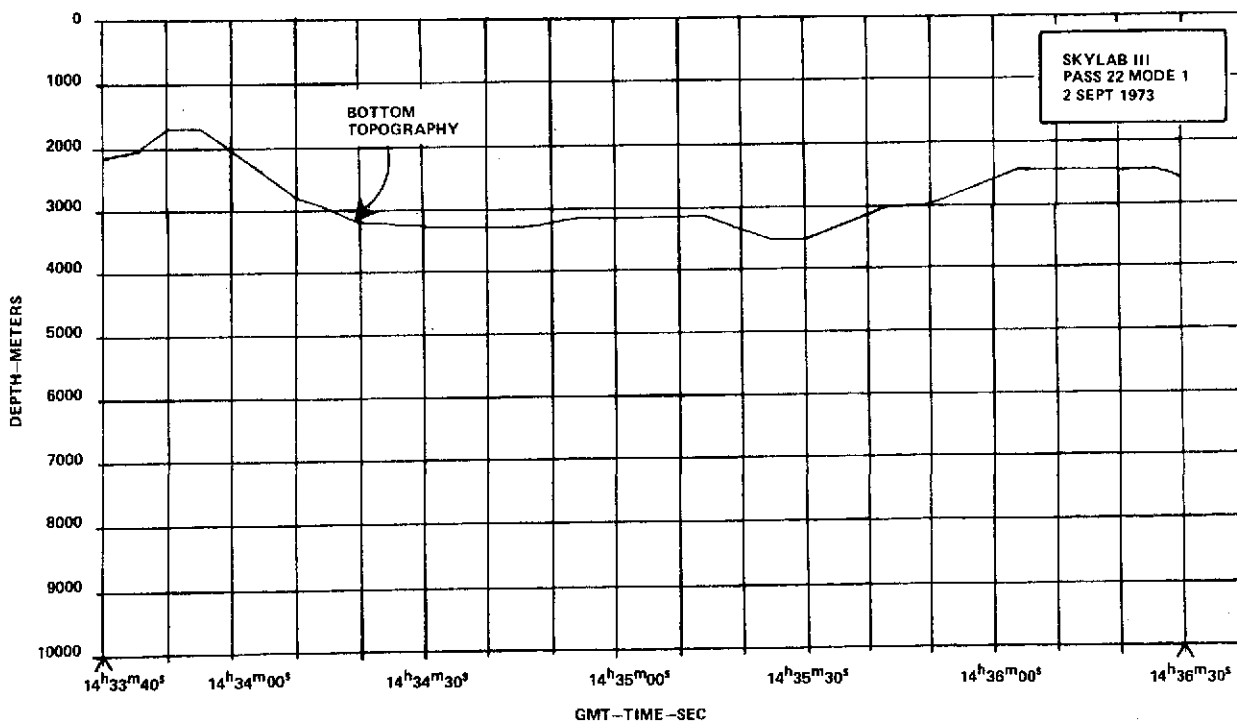
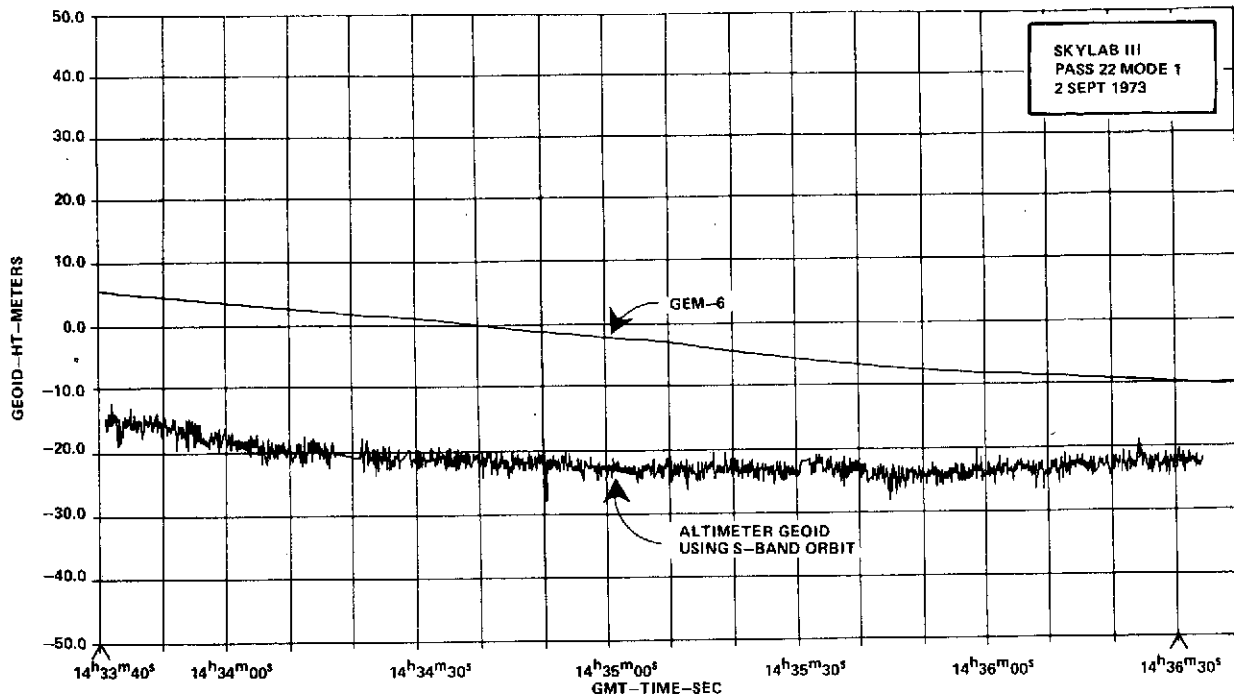




Lat -41.9°
Long 298.1°

MAP NO. 38

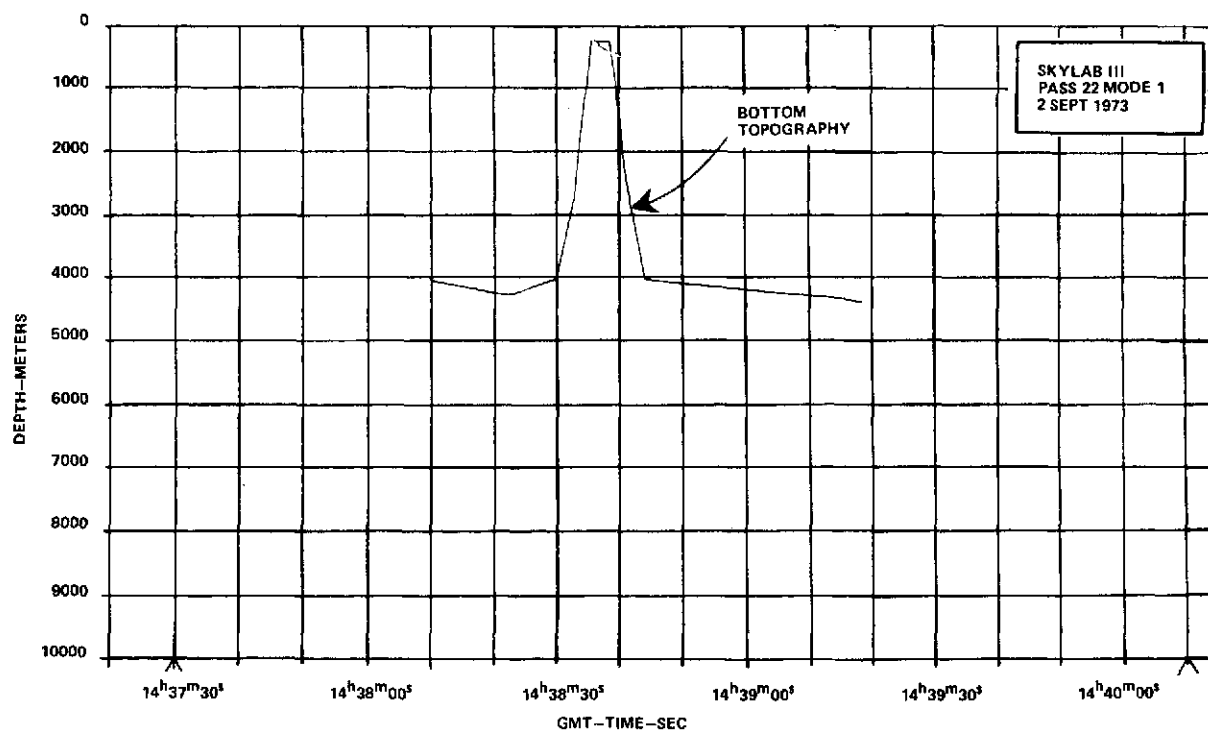
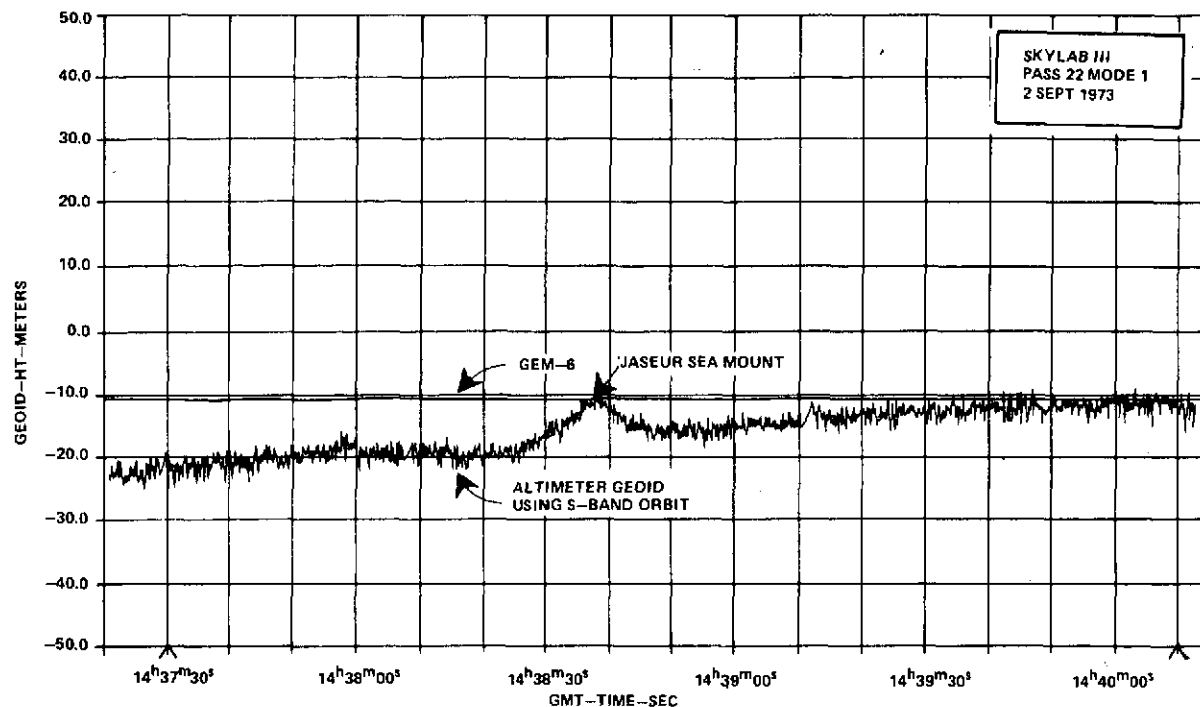
-36.1°
306.4°



Lat -33.7°
Long 309.8°

MAP NO. 39

-26.4°
 318.5°



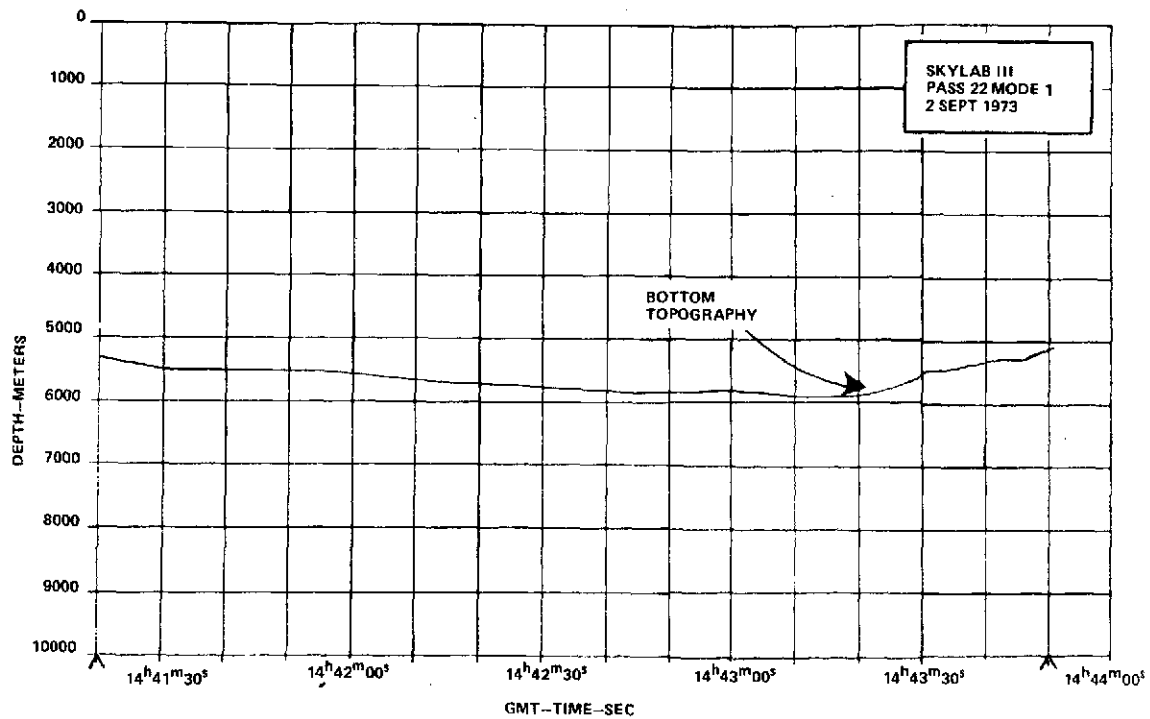
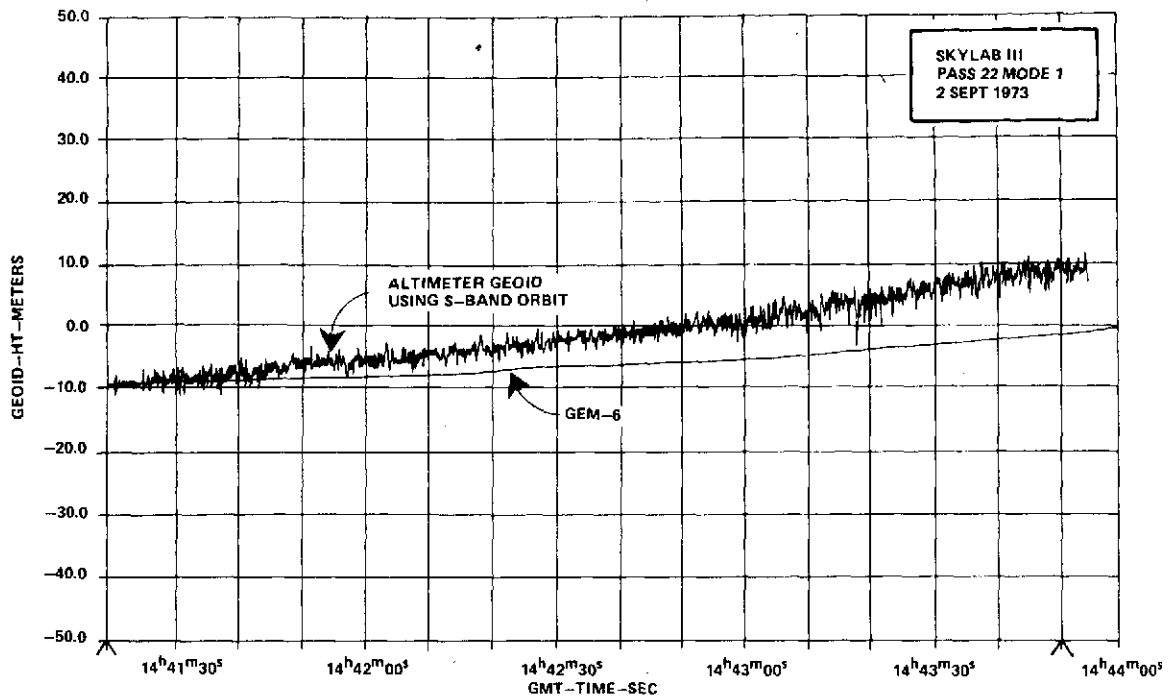
Lat -24.1°

Long 320.8°

MAP NO. 40

-16.1°

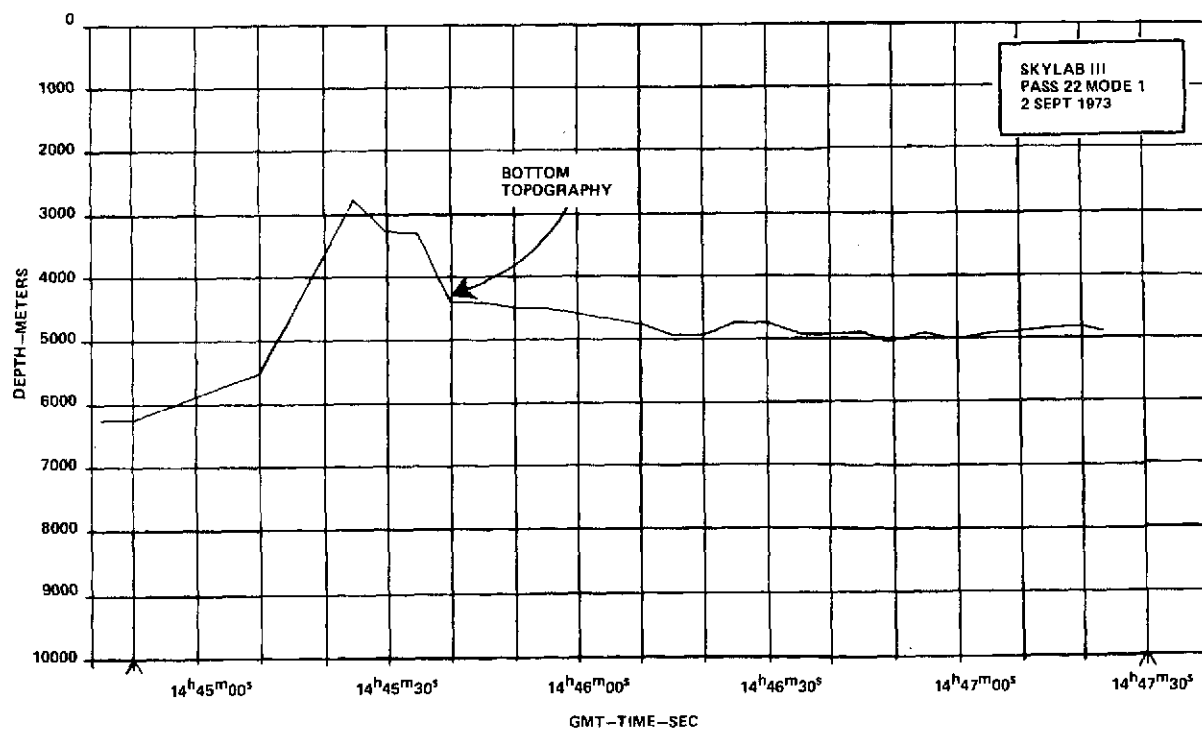
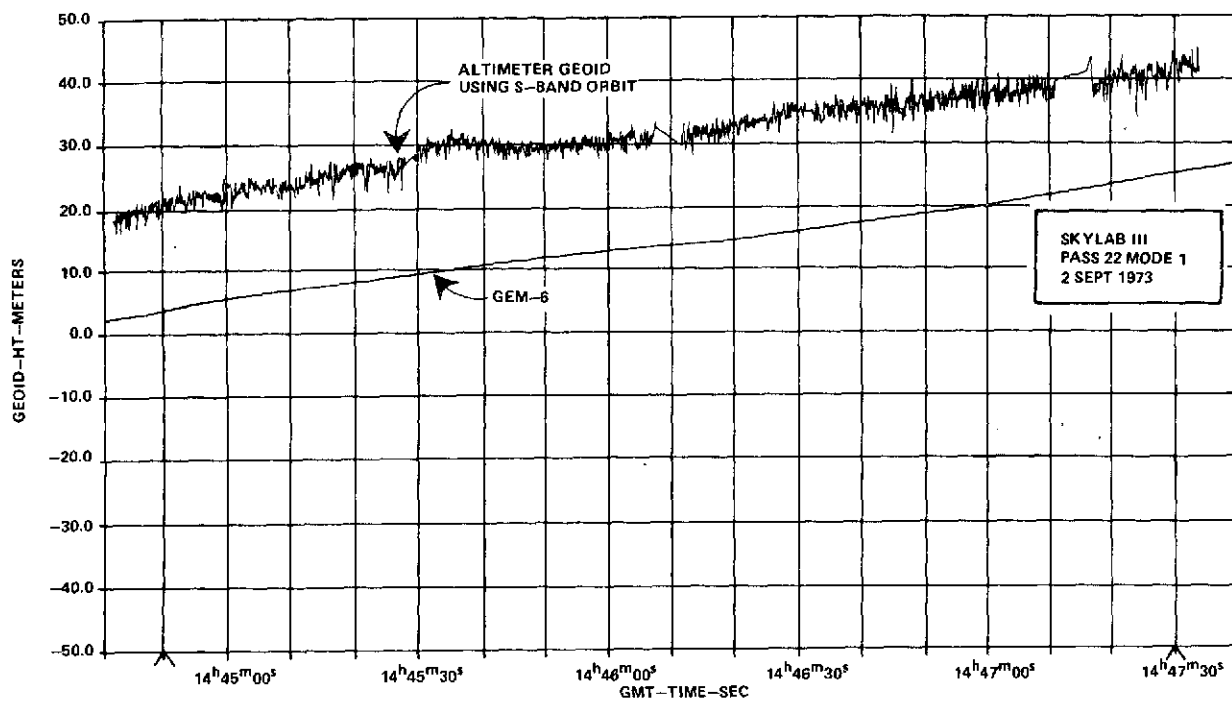
328.1°



Lat -12.7°
Long 330.9°

MAP NO. 41

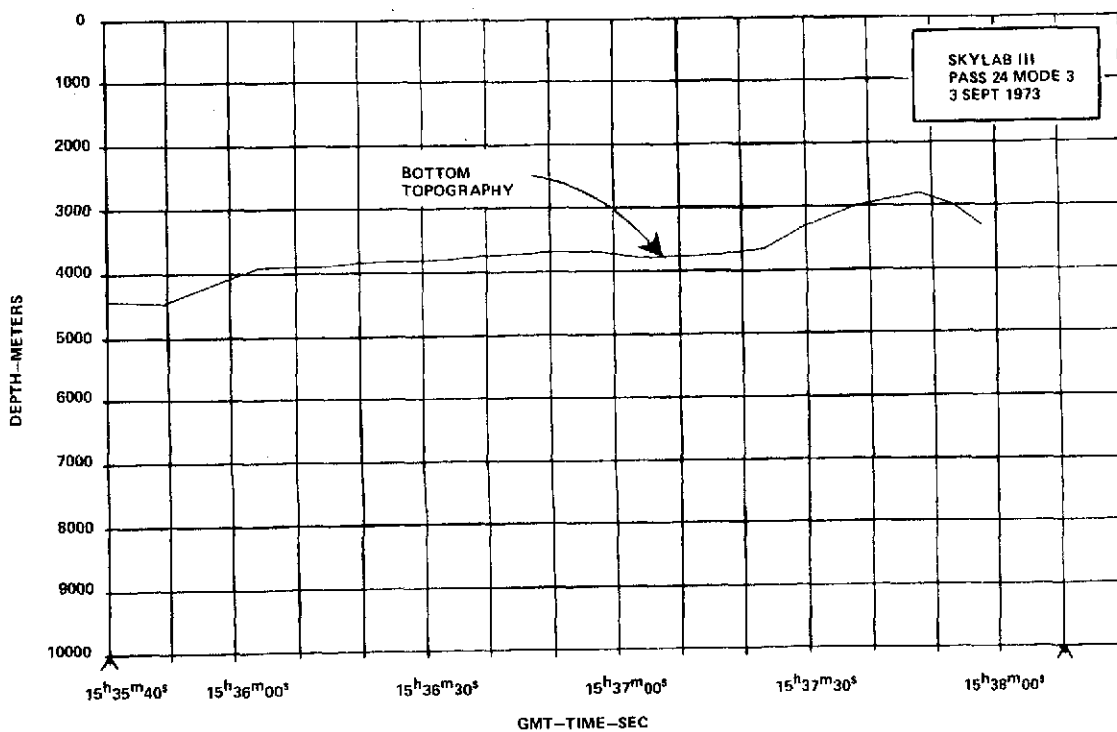
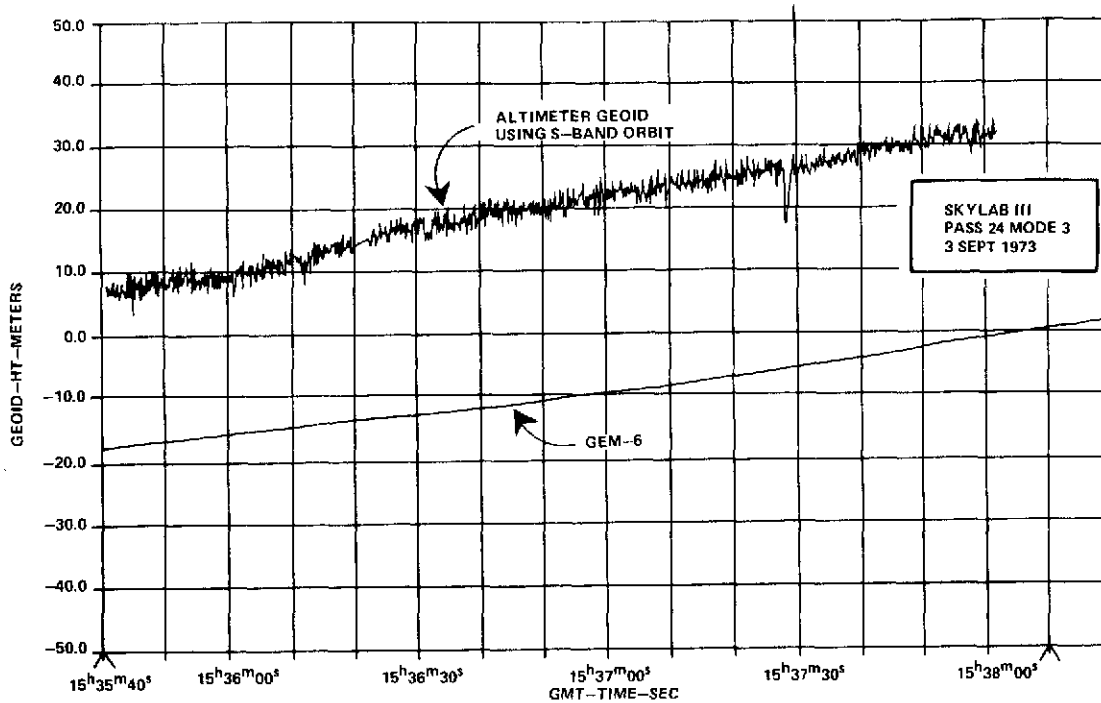
-5.3°
338.6°



Lat -2.3°
Long 338.8°

MAP NO. 42

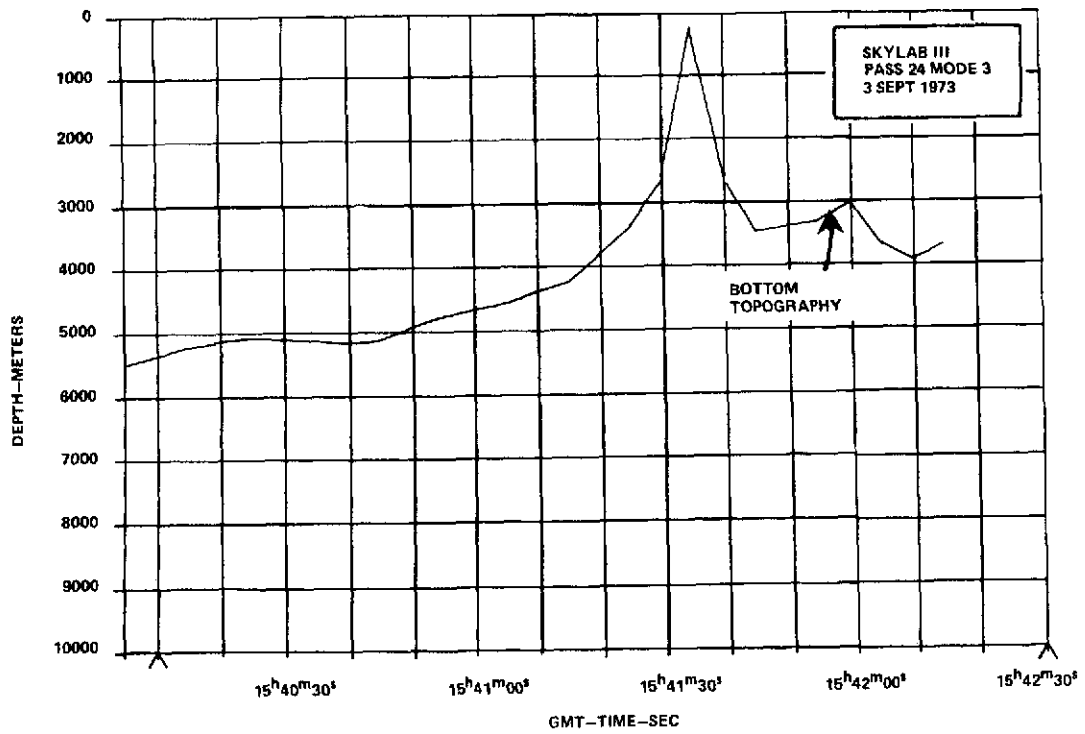
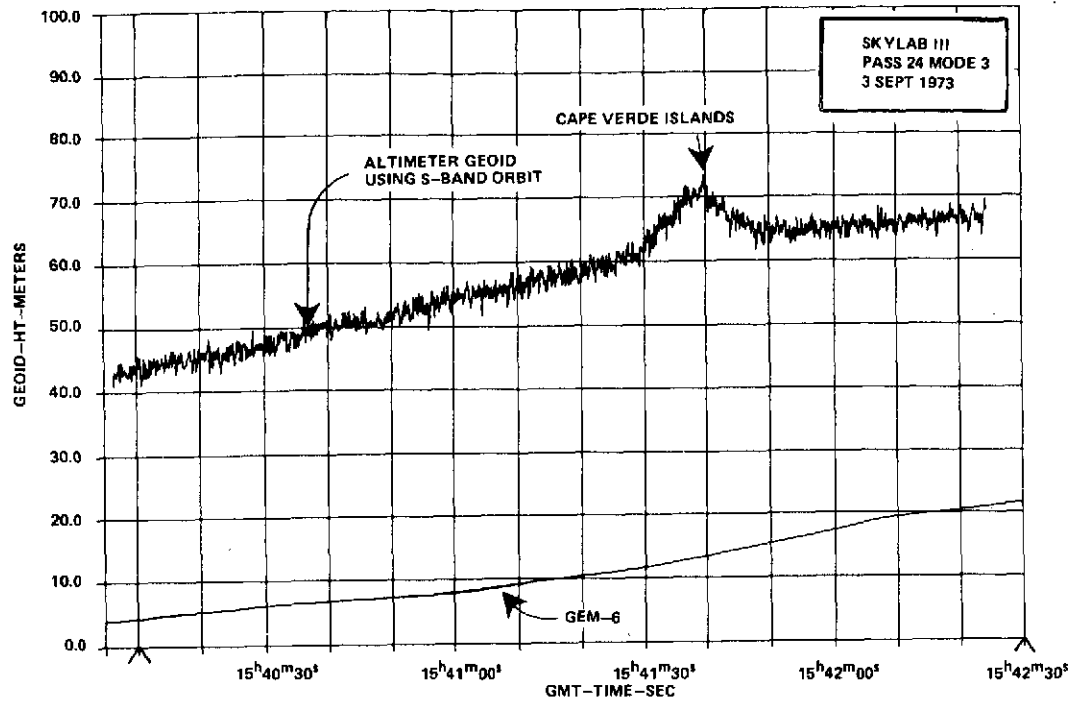
5.7°
 334.8°



Lat - 0.7°
Long 321.4°

MAP NO. 43

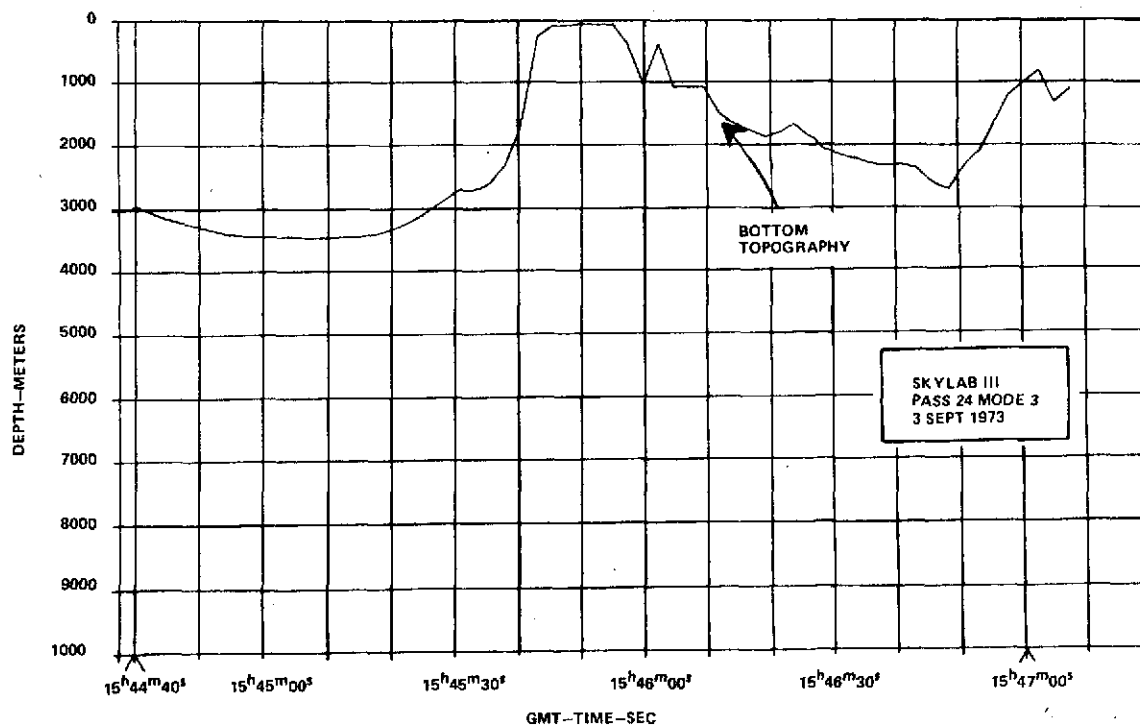
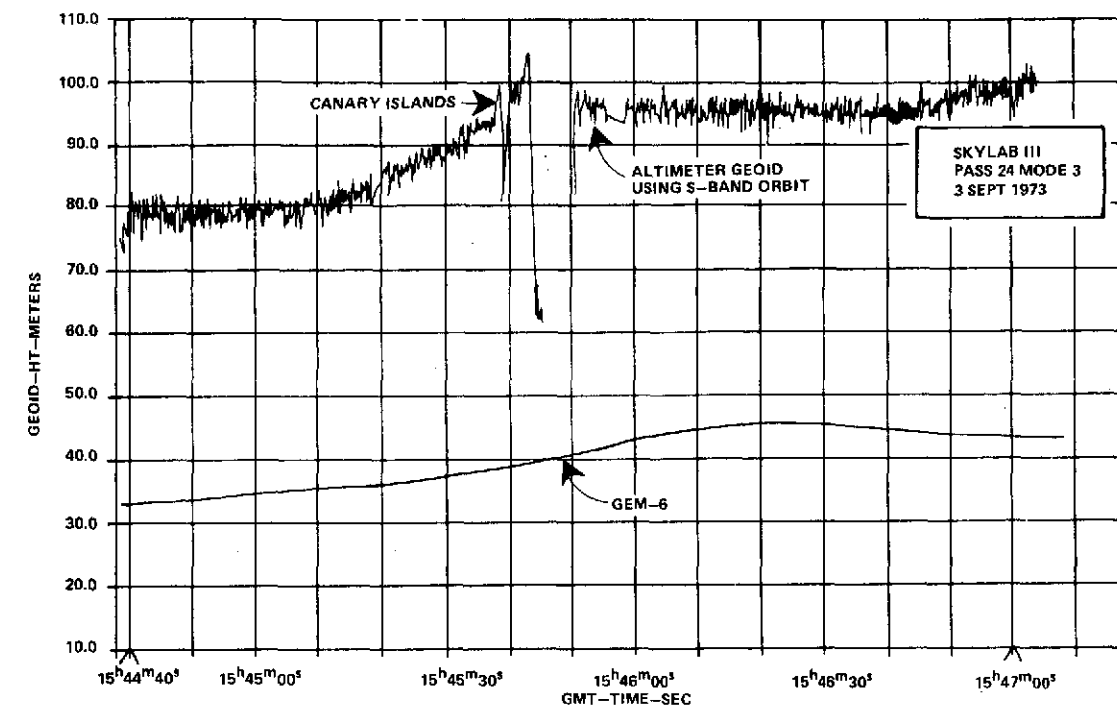
6.7°
326.7°



Lat 12.6°
Long 331.4°

MAP NO. 44

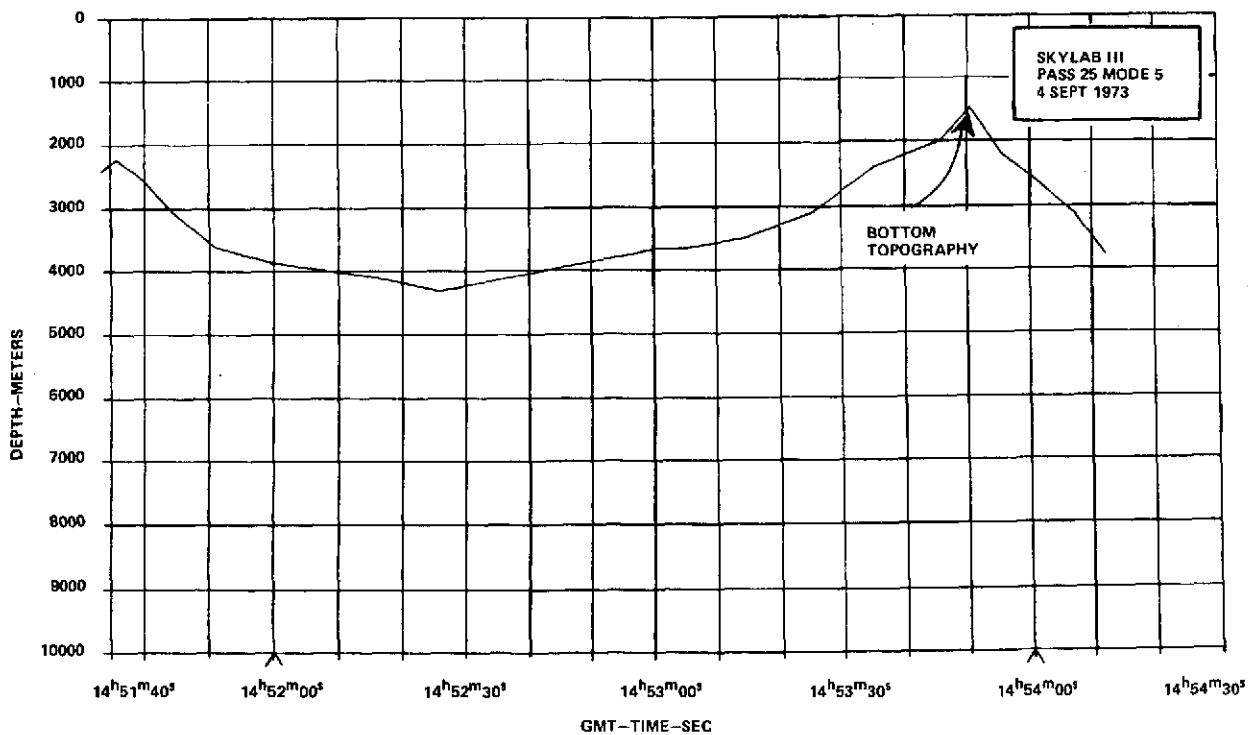
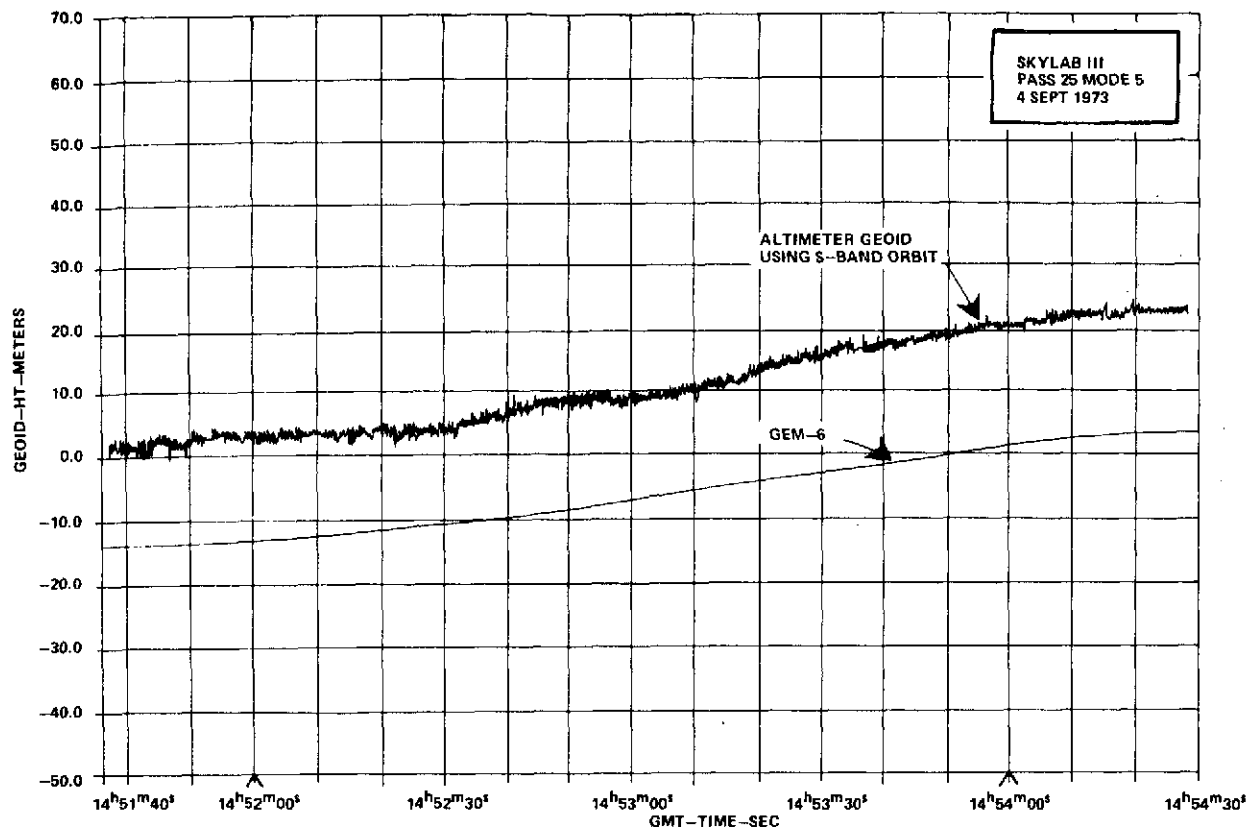
19.4°
337.1°



Lat 26.4°
Long 343.8°

MAP NO. 45

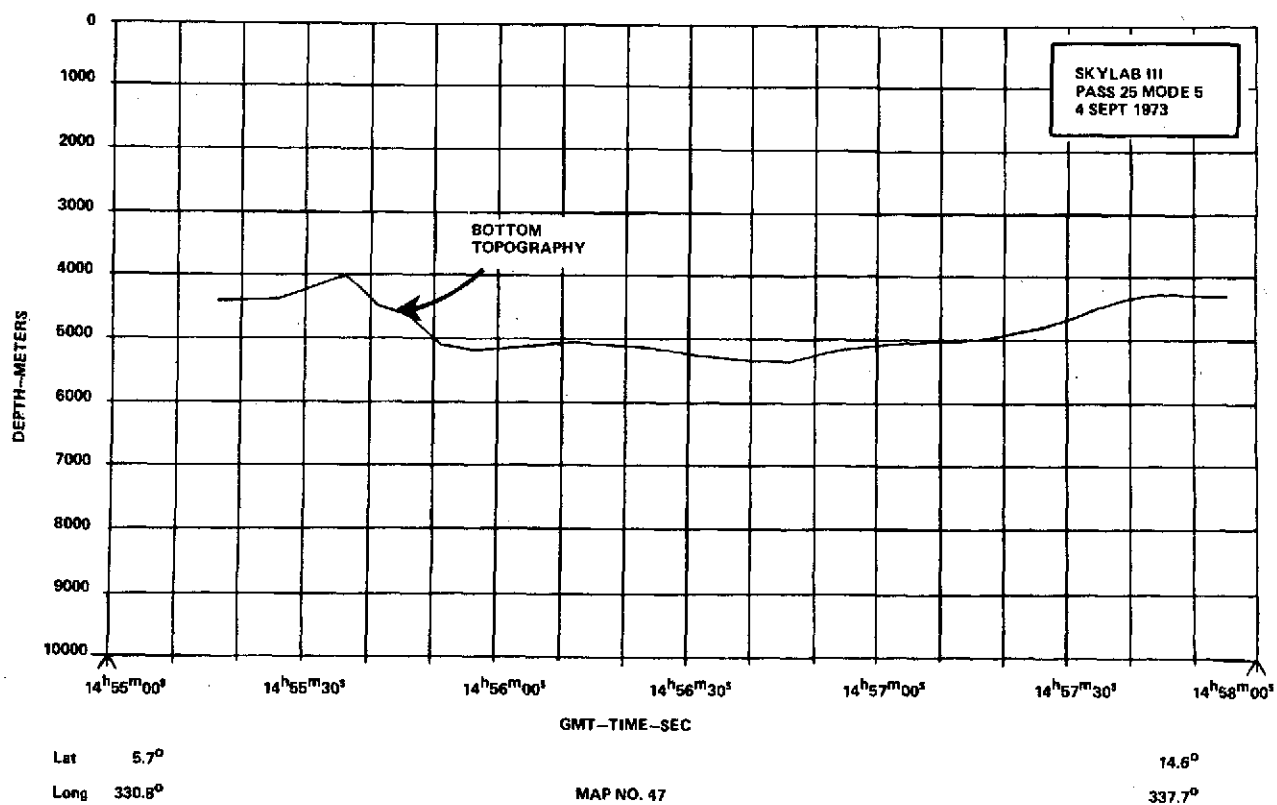
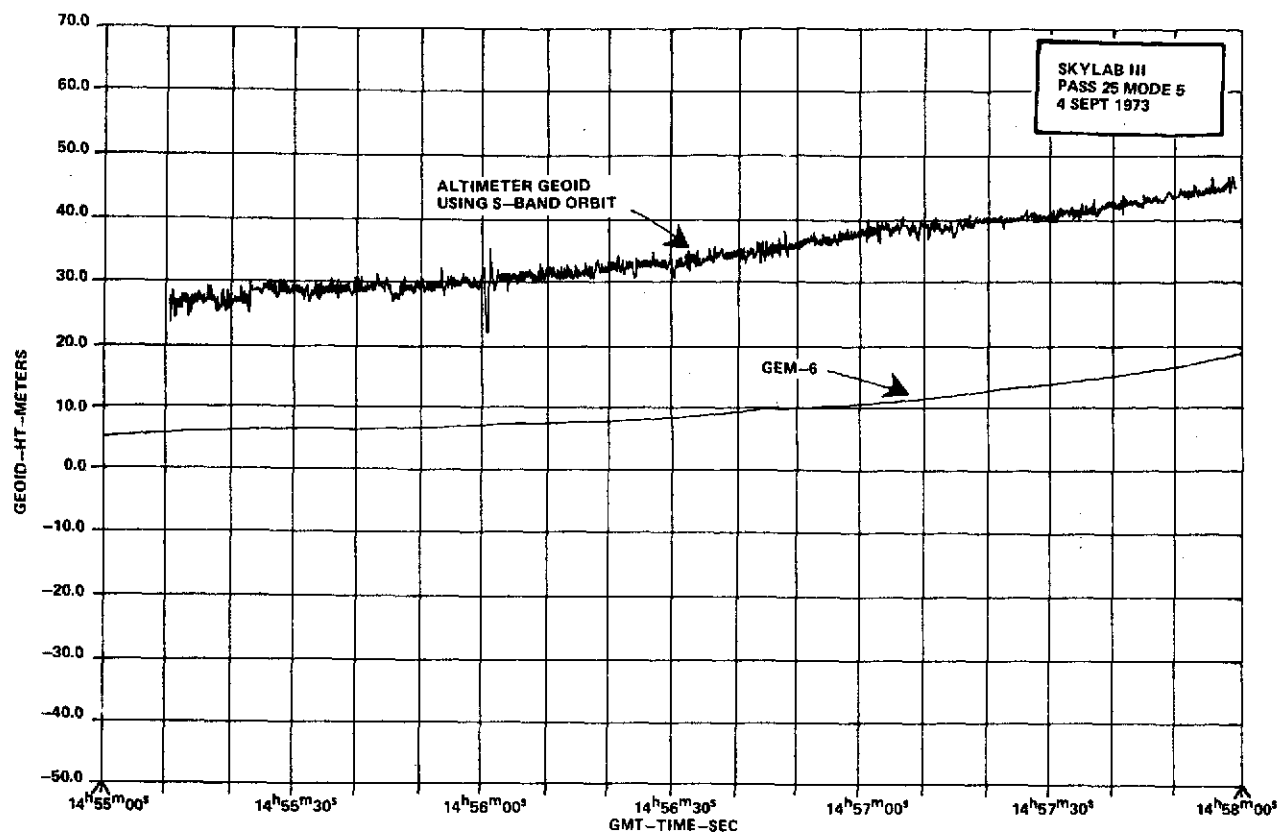
31.7°
349.8°

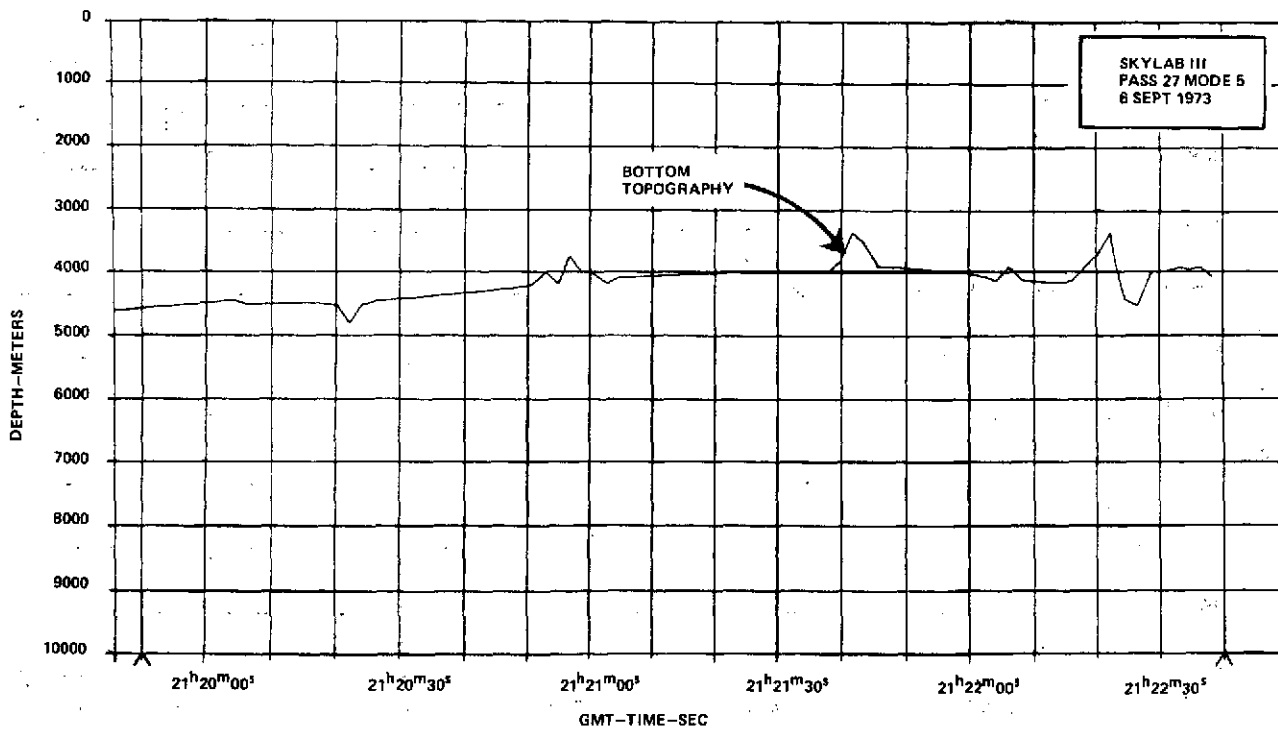
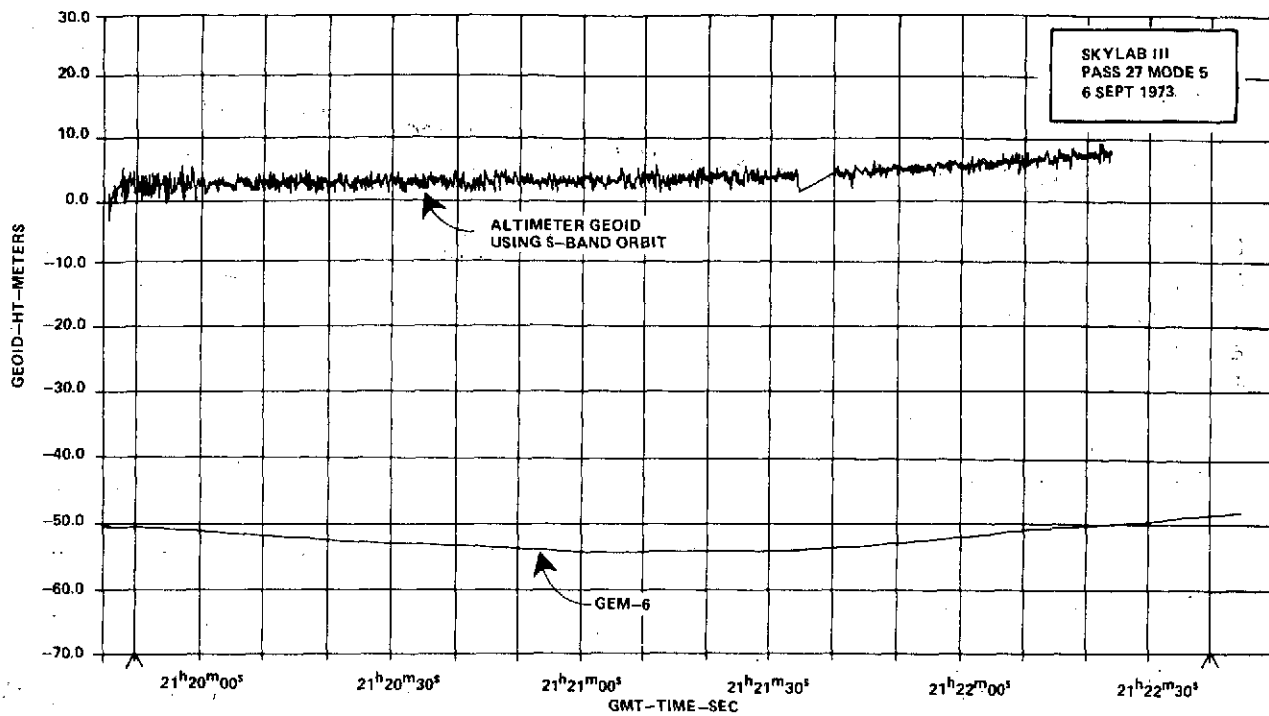


Lat - 4.2°
Long 323.3°

MAP NO. 48

4.2°
329.7°

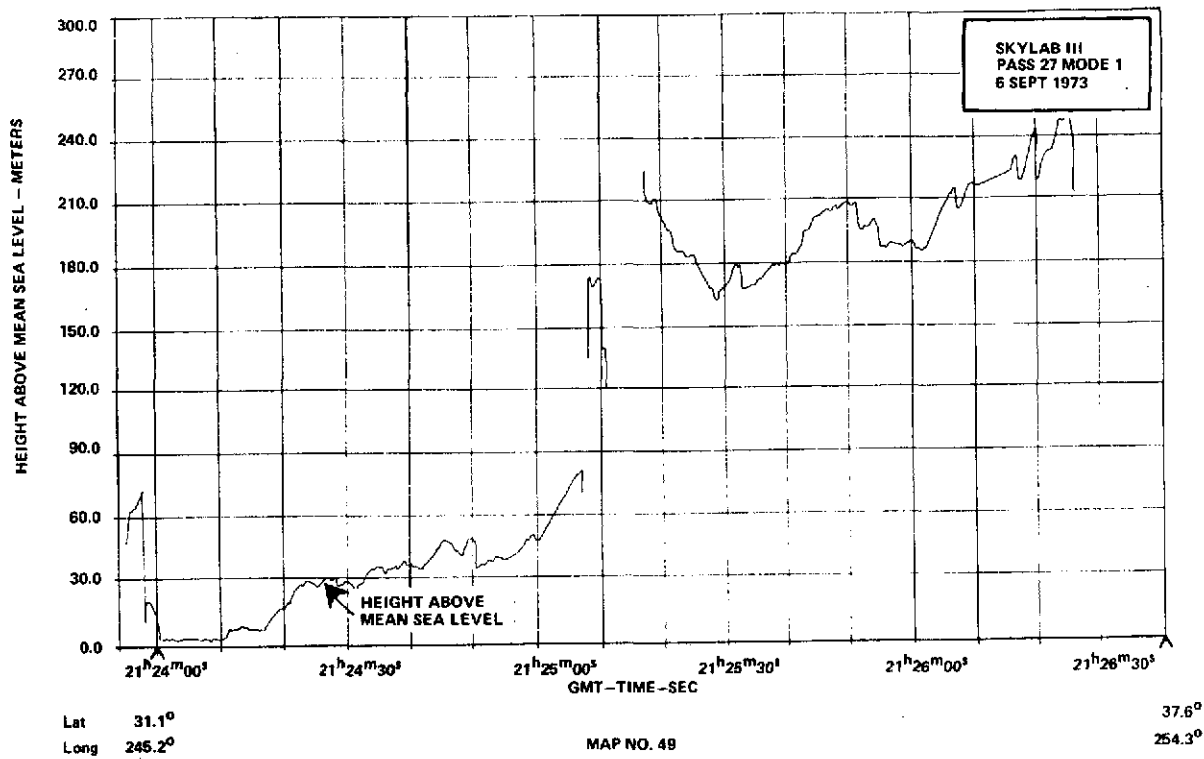


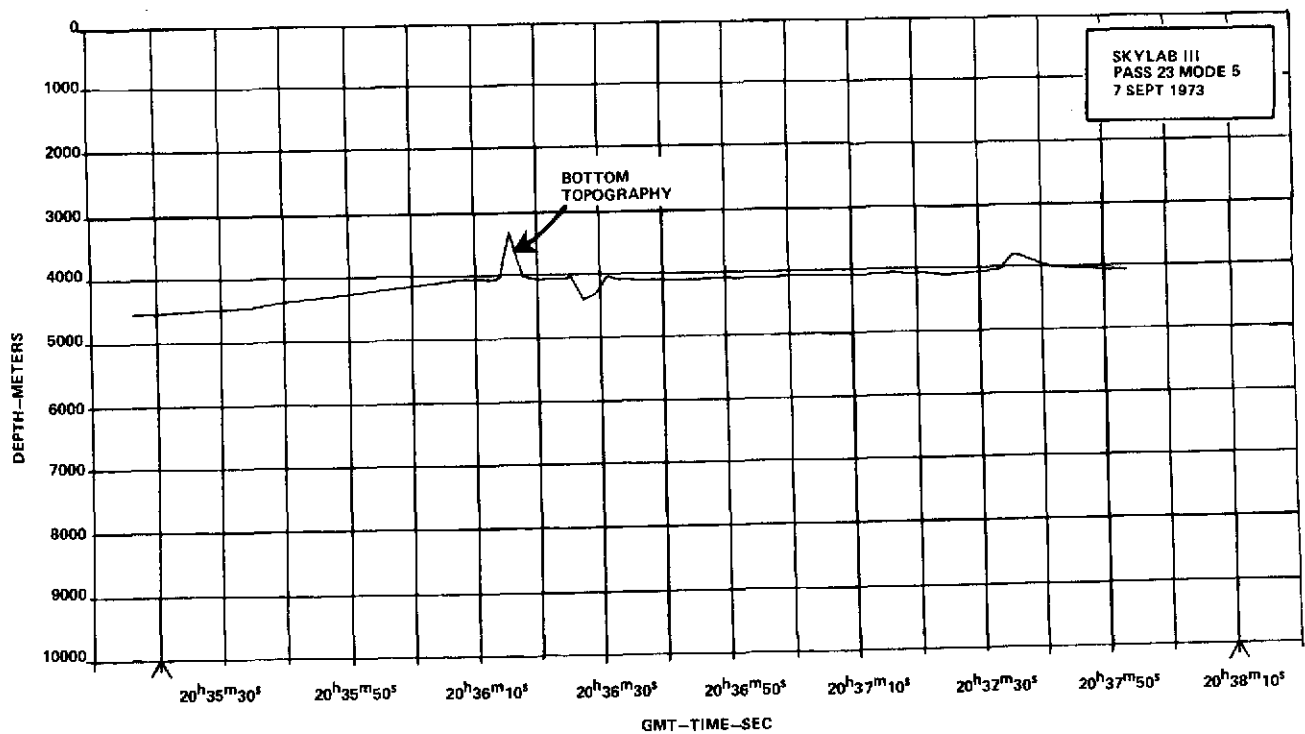
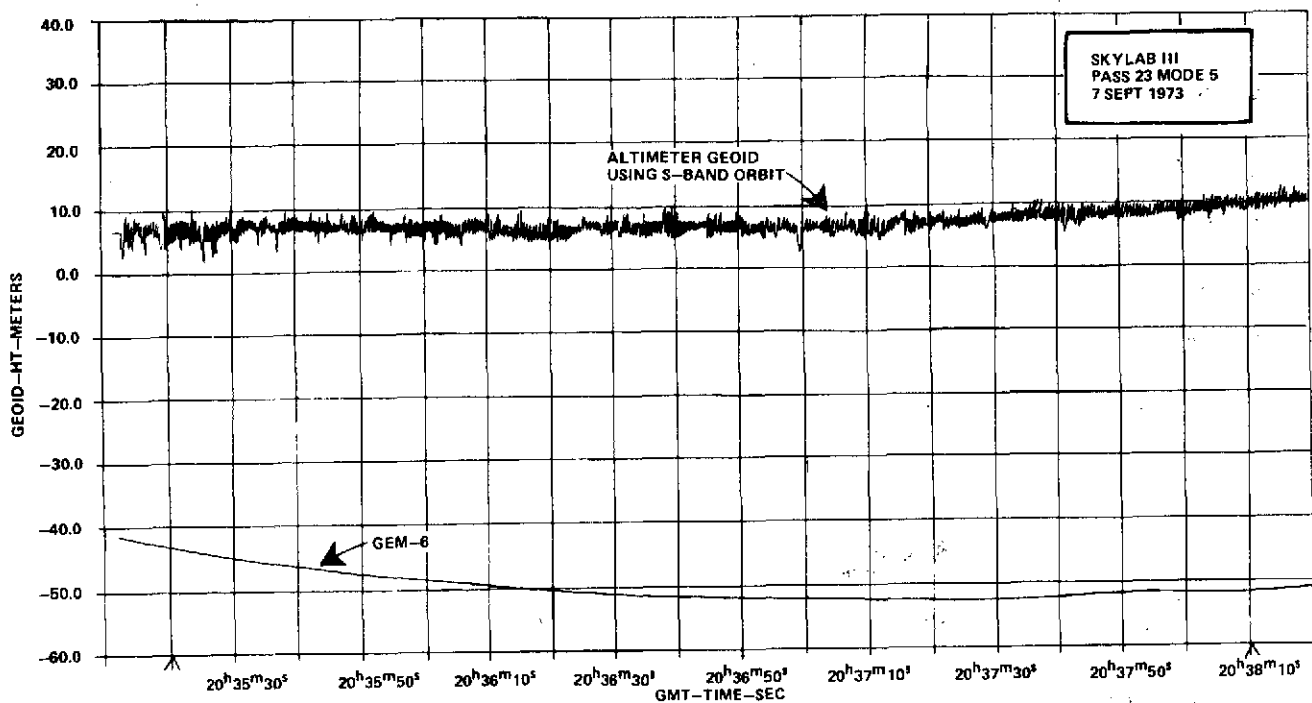


Lat 19.8°
Long 233.4°

MAP NO. 48

27.6°
241.6°

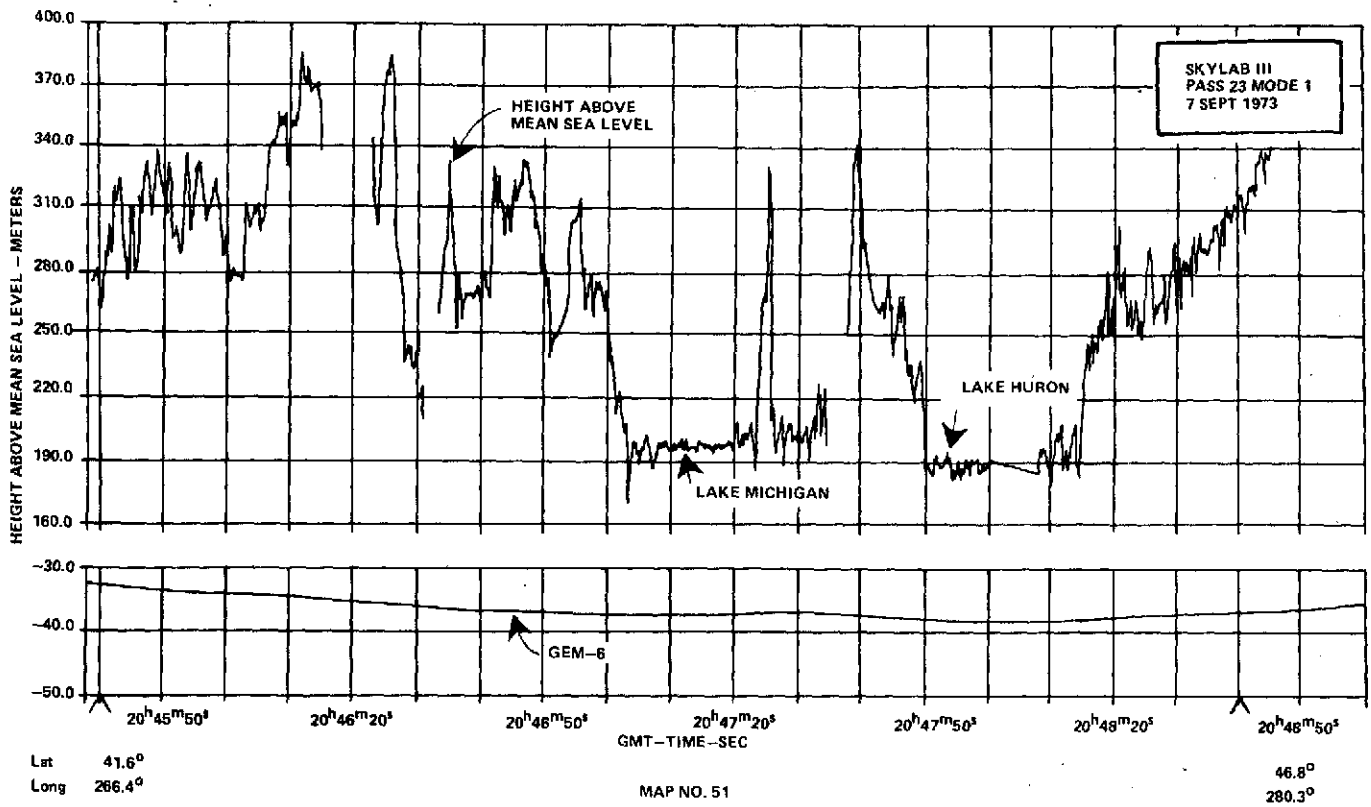




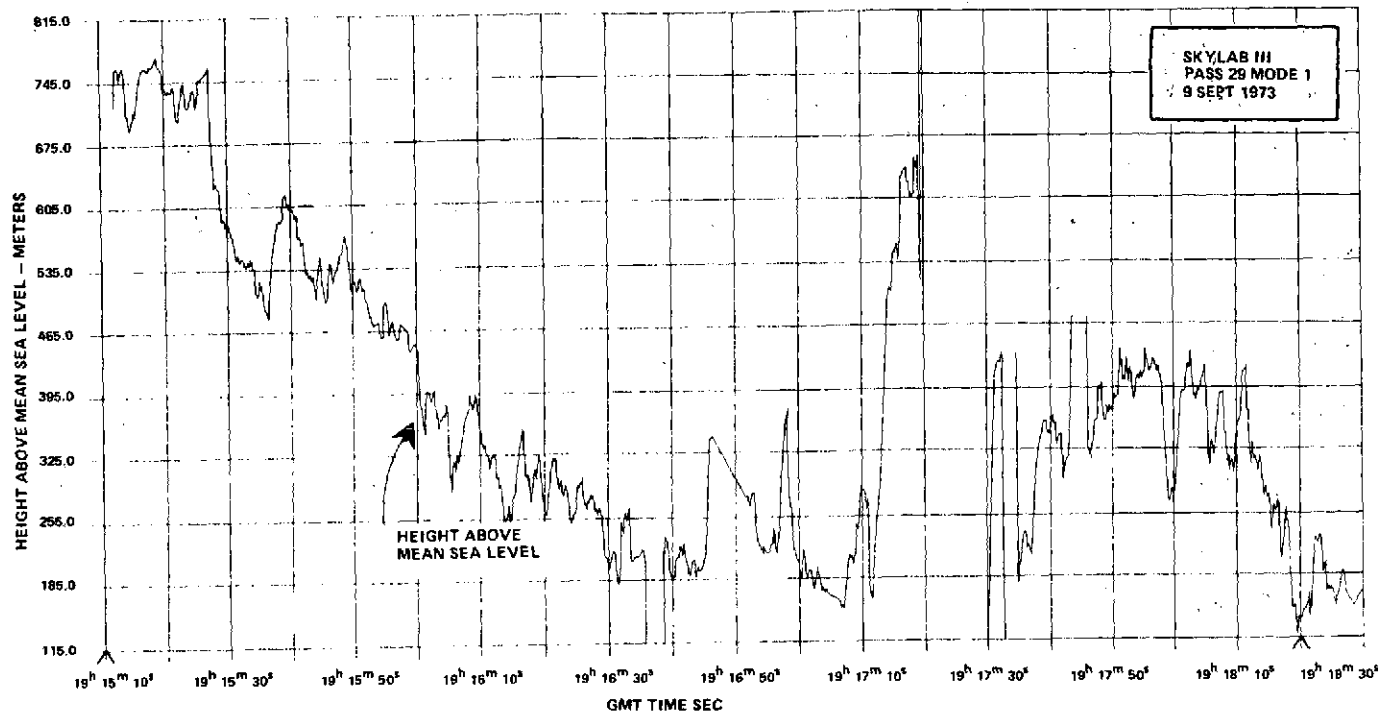
Lat 15.1°
Long 234.2°

MAP NO. 50

23.1°
241.4°



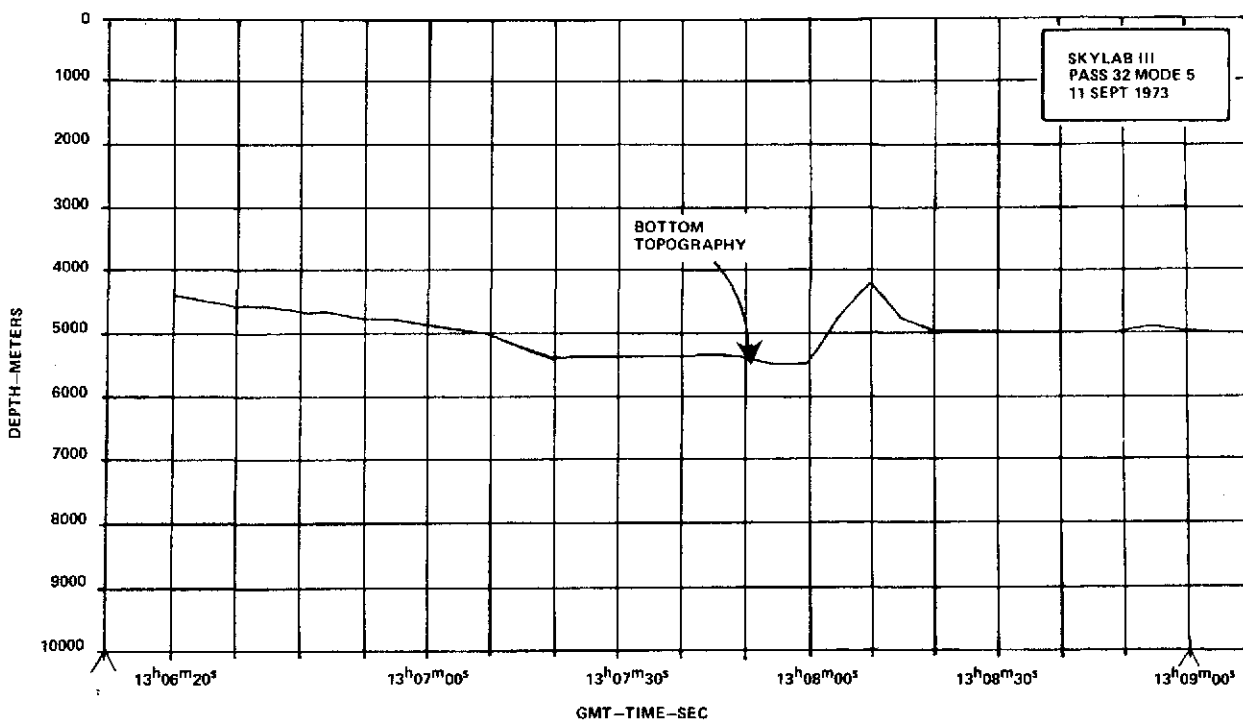
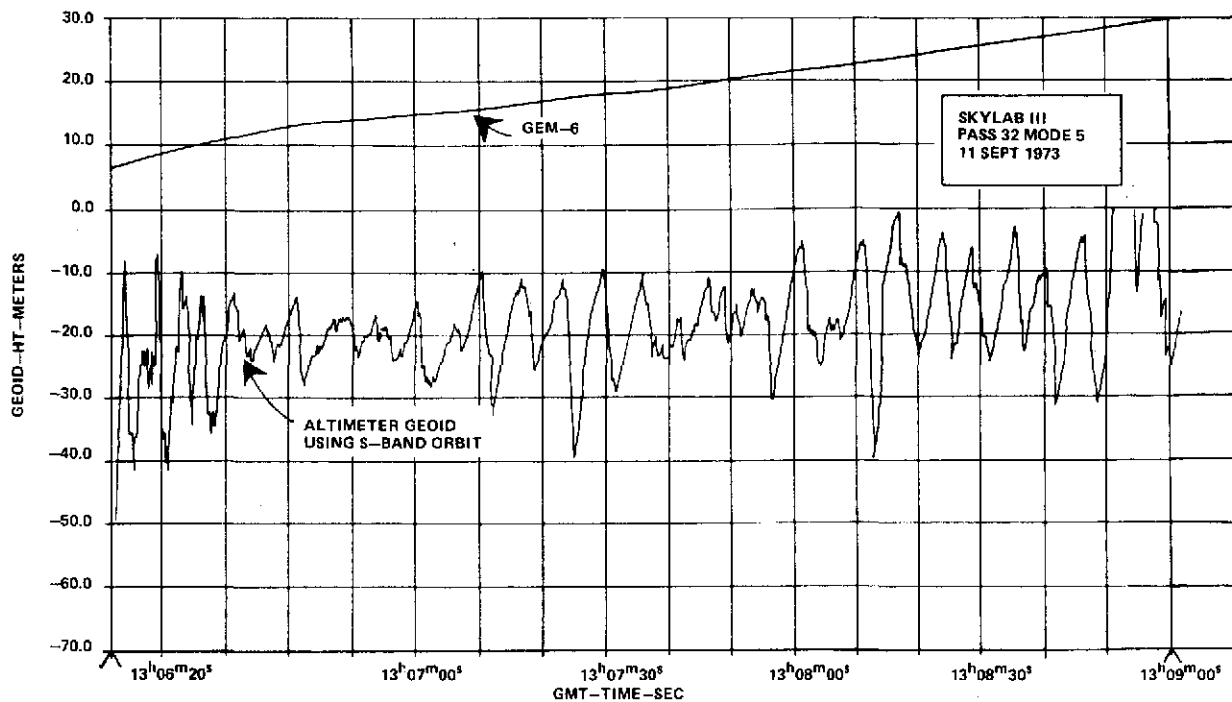
DIFFERENCE IN HEIGHT DETERMINED FOR LAKE HURON AND LAKE MICHIGAN IS DUE TO MODE CHANGE DURING DATA TAKE



Lat 30.5°
Long 258.9°

MAP NO. 52

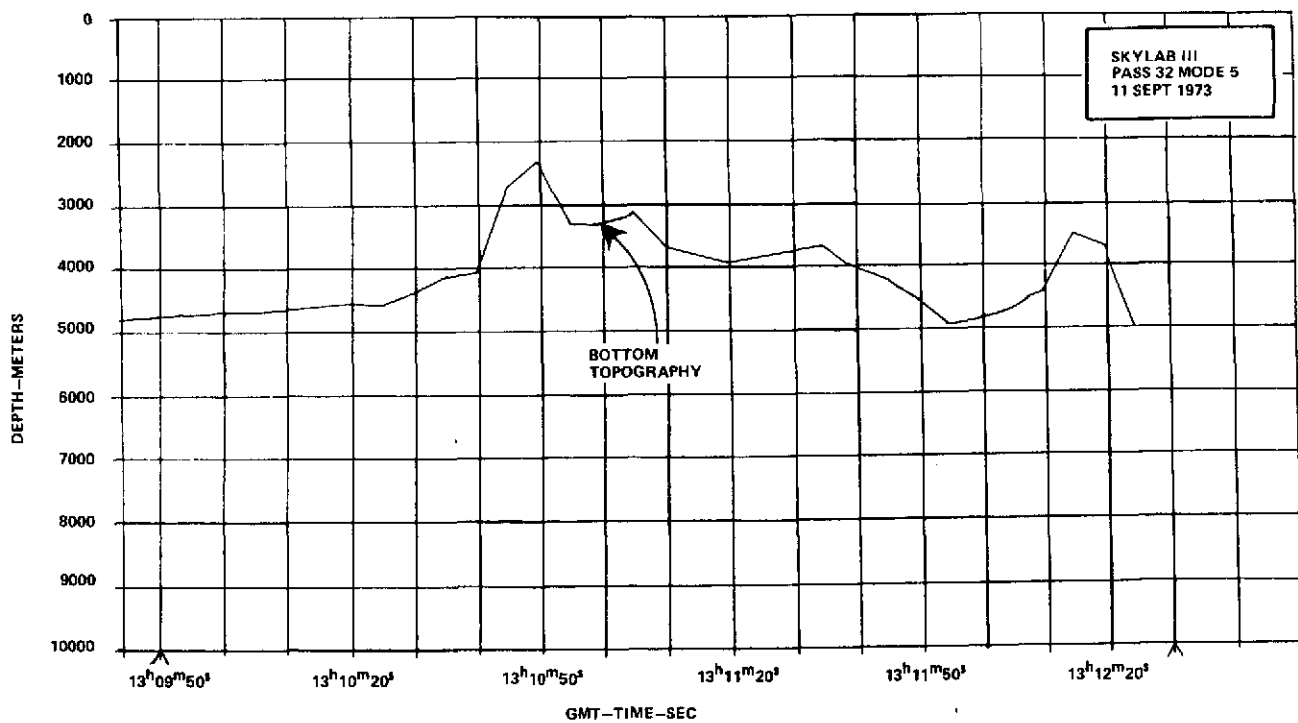
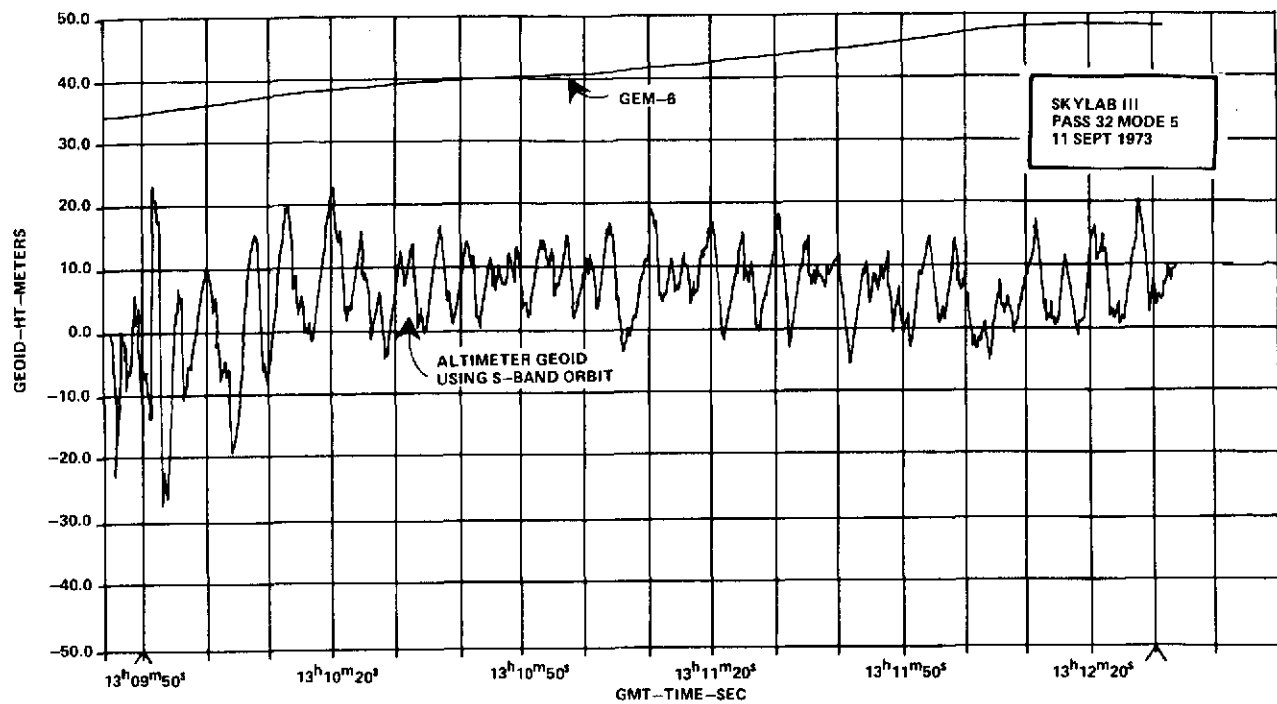
38.2°
269.7°



Lat 20.6°
Long 329.4°

MAP NO. 54

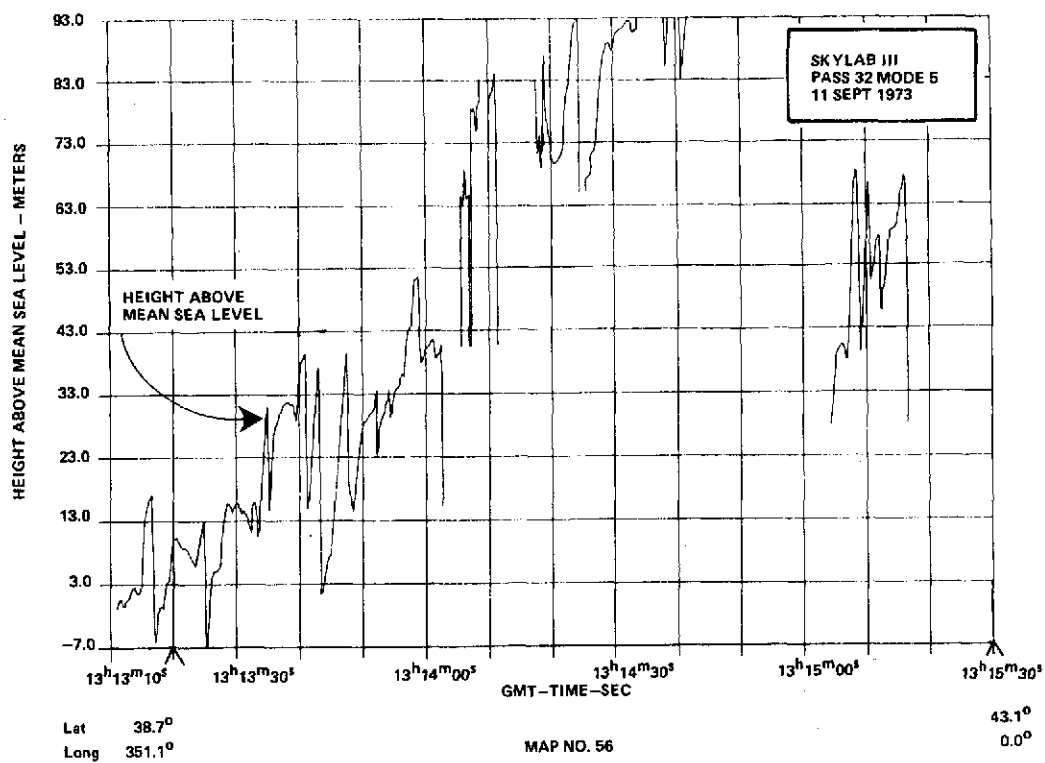
28.0°
336.7°

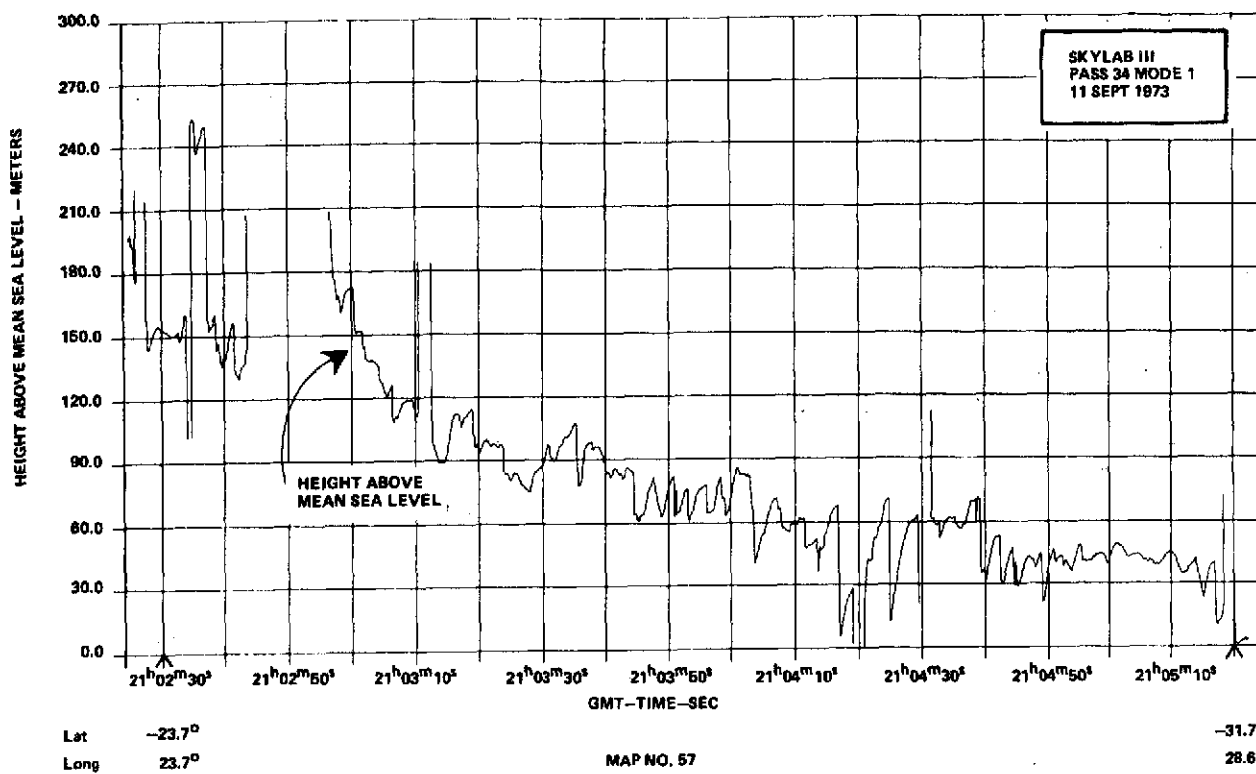


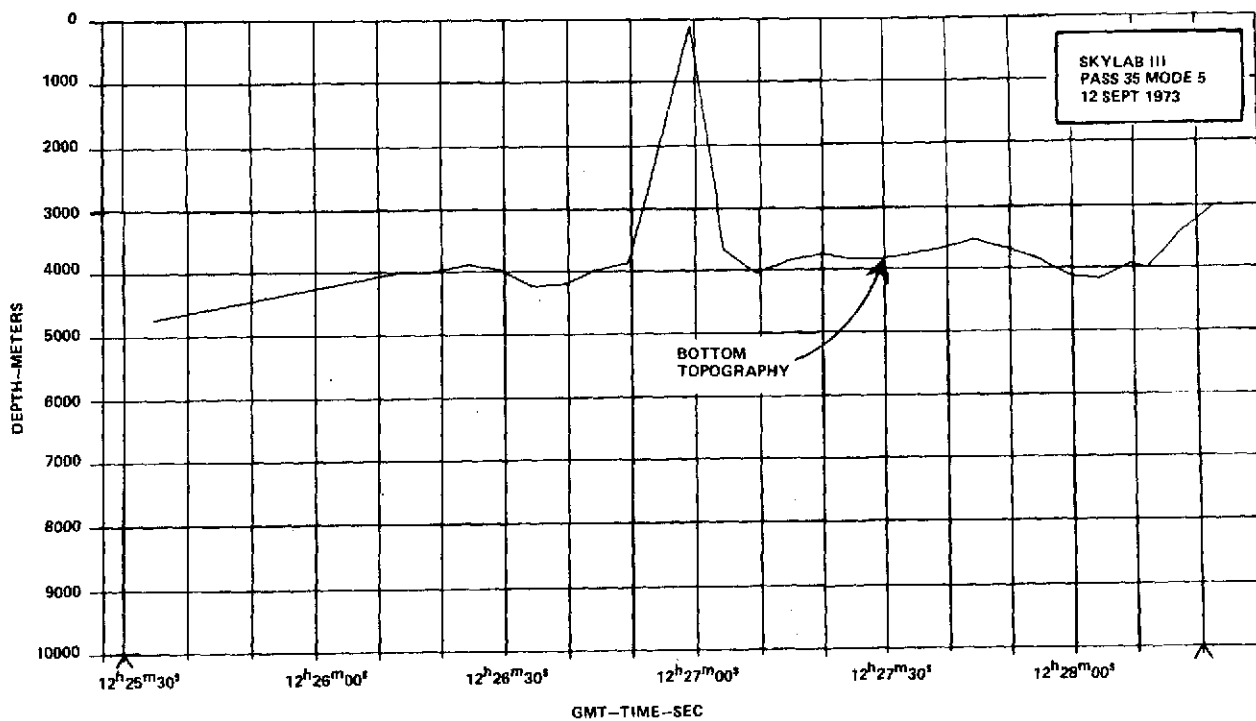
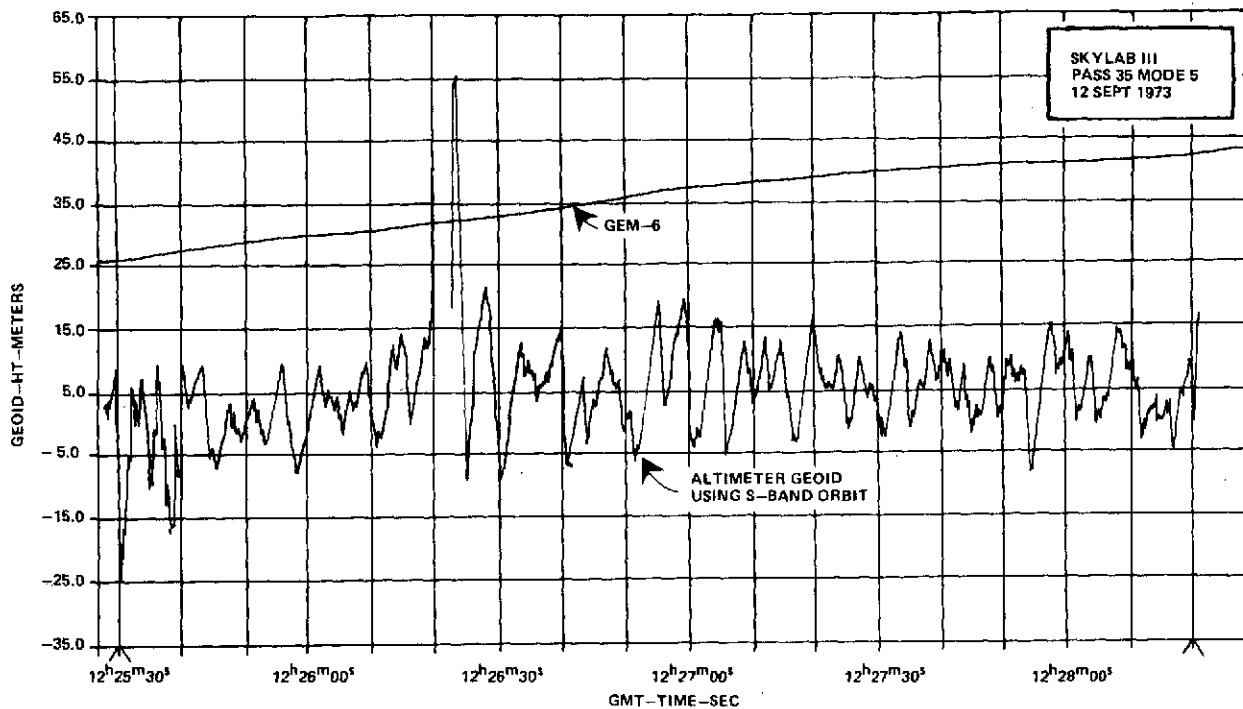
Lat 30.2°
Long 339.2°

MAP NO. 55

37.2°
348.7°



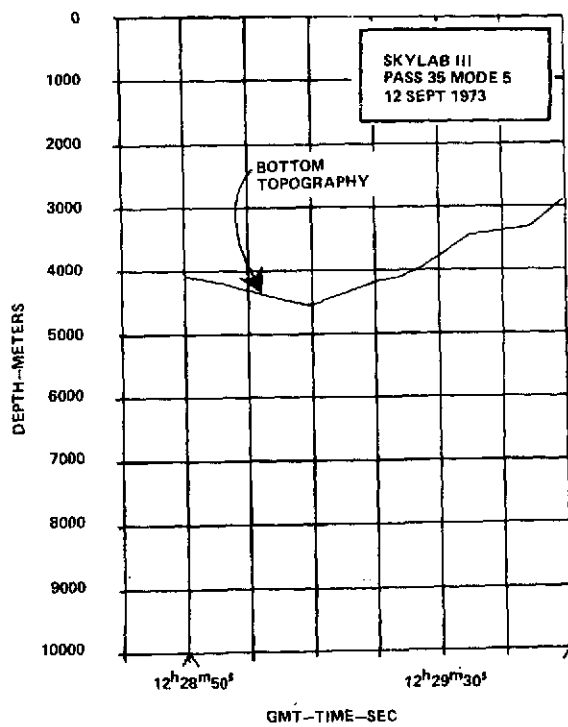
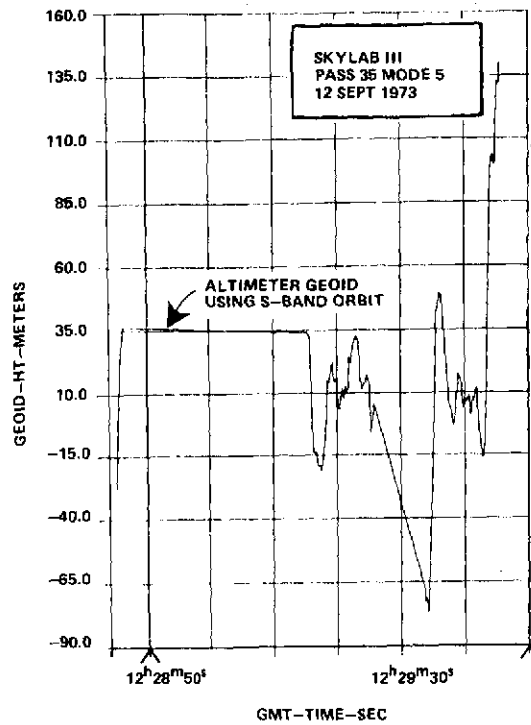




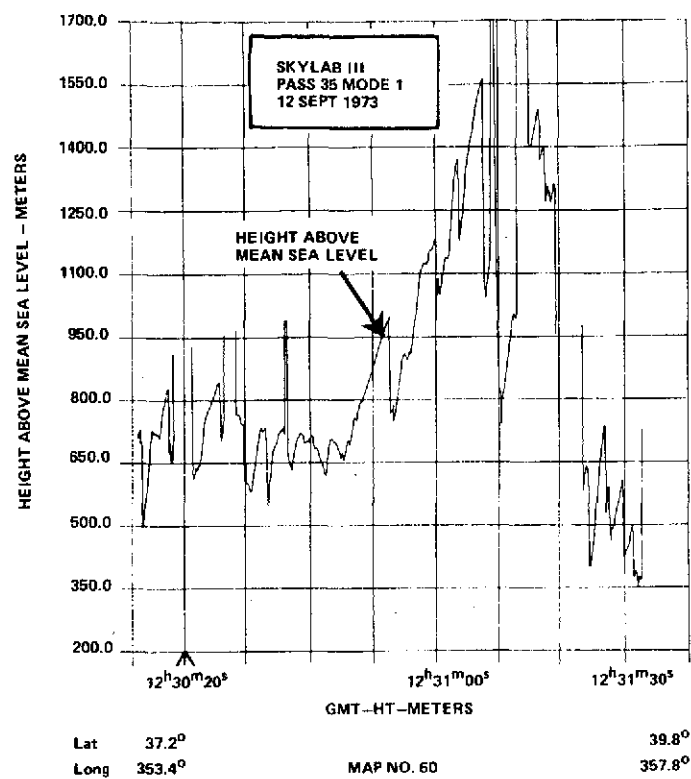
Lat 24.9°
Long 338.2°

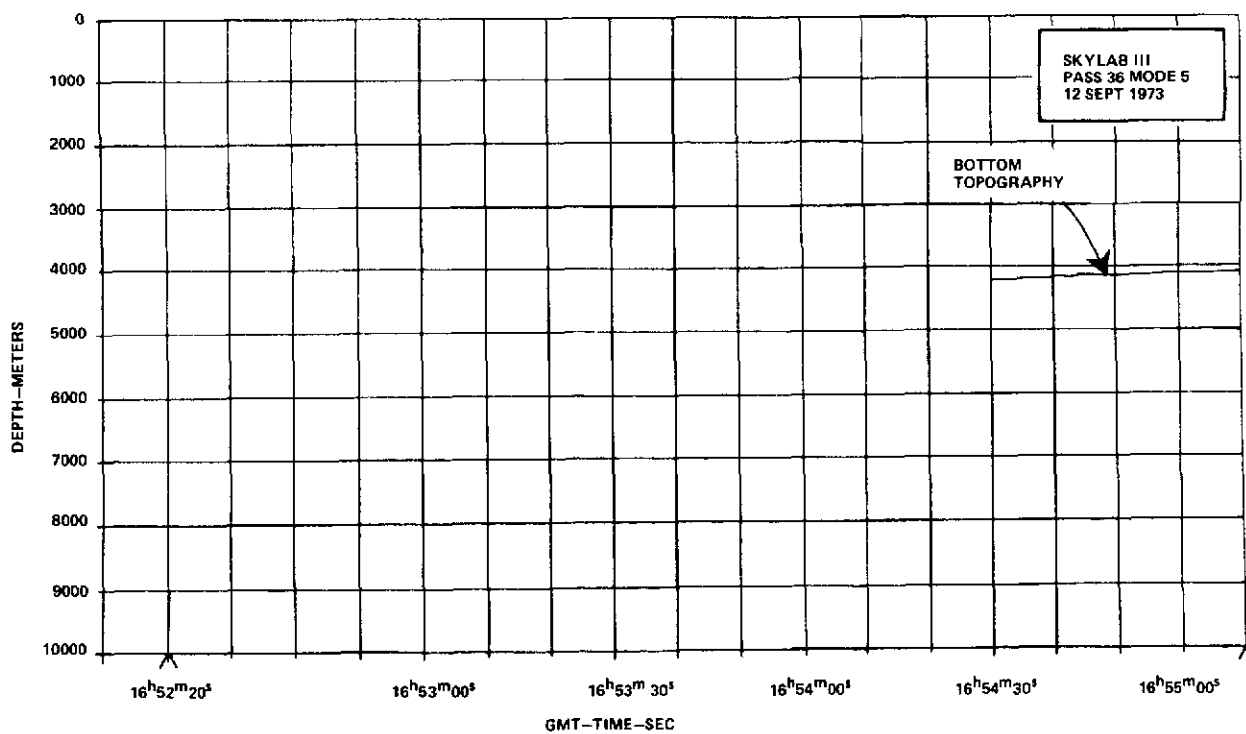
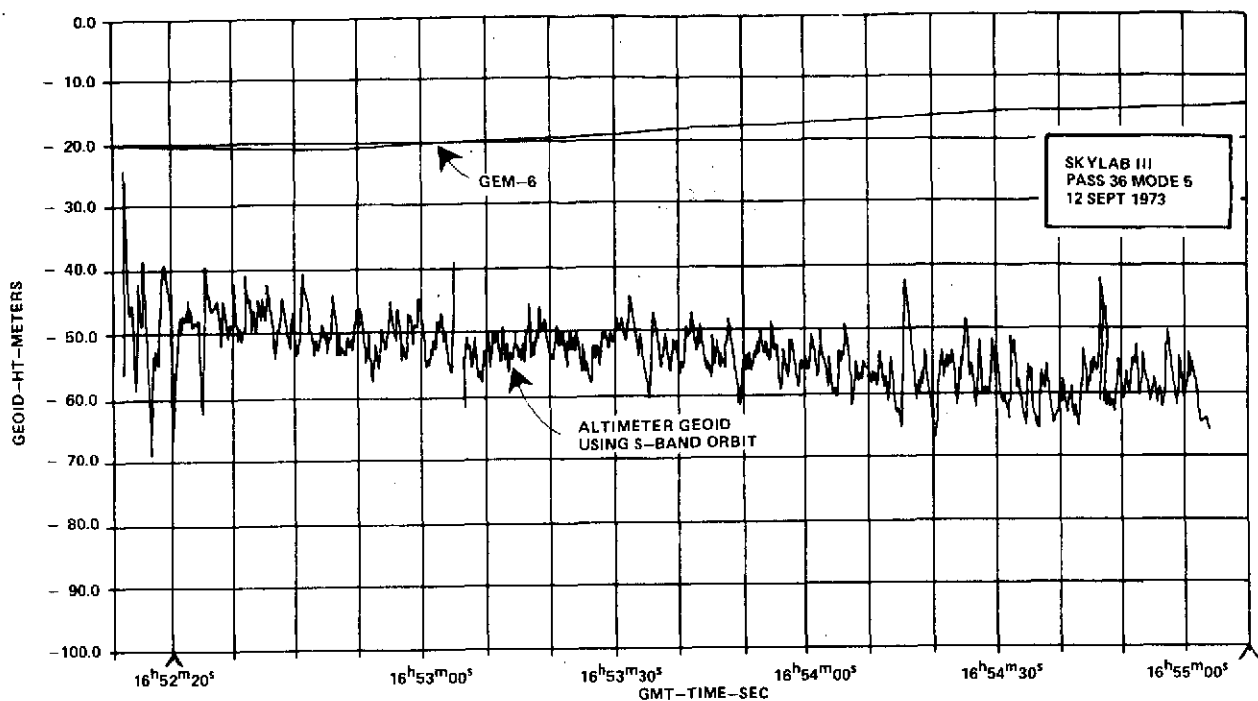
MAP NO. 58

32.4°
346.6°



| | | | |
|------|--------|------------|--------|
| Lat | 33.6° | | 36.0° |
| Long | 348.3° | MAP NO. 59 | 351.7° |

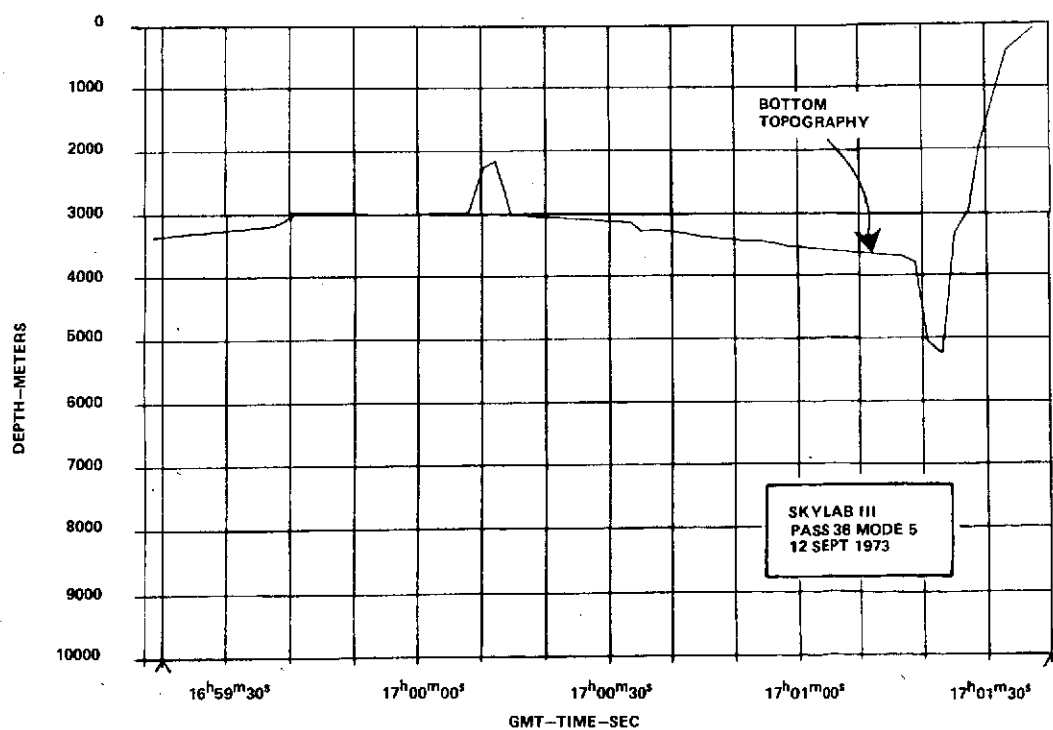
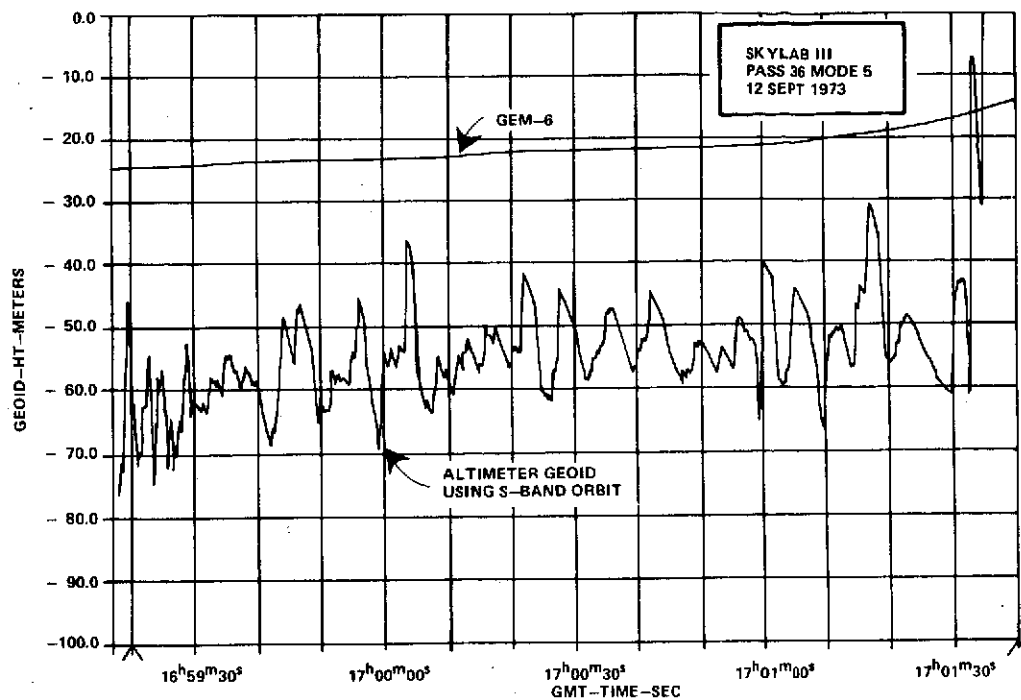




Lat -10.5°
Long 238.7°

MAP NO. 61

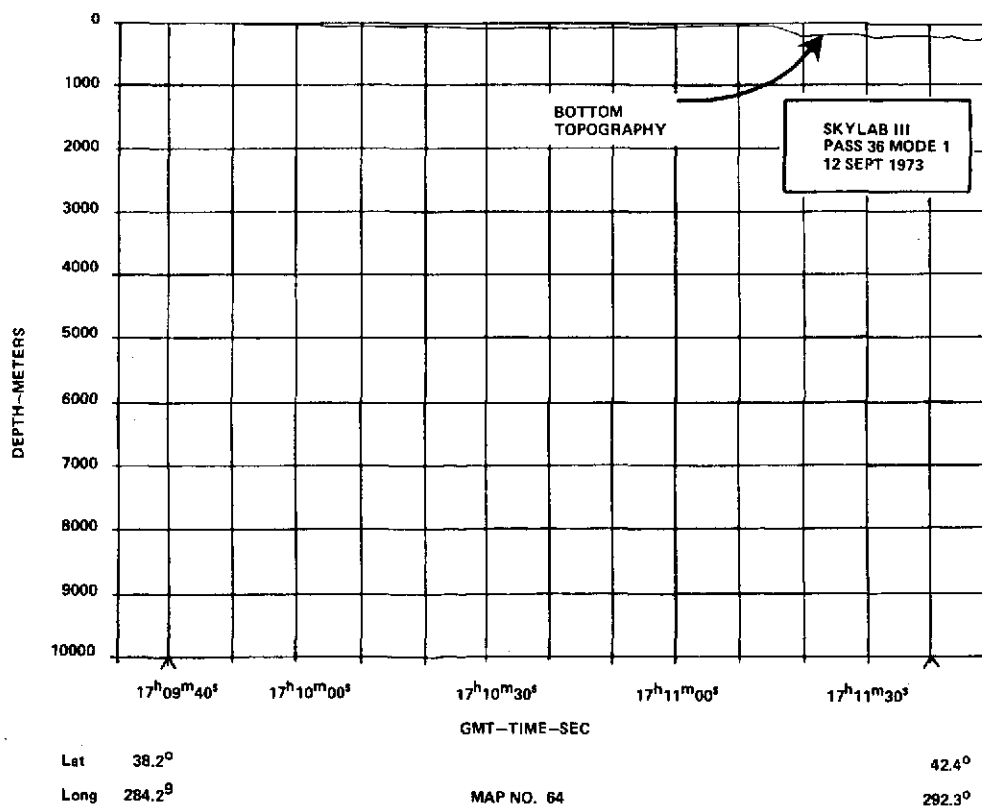
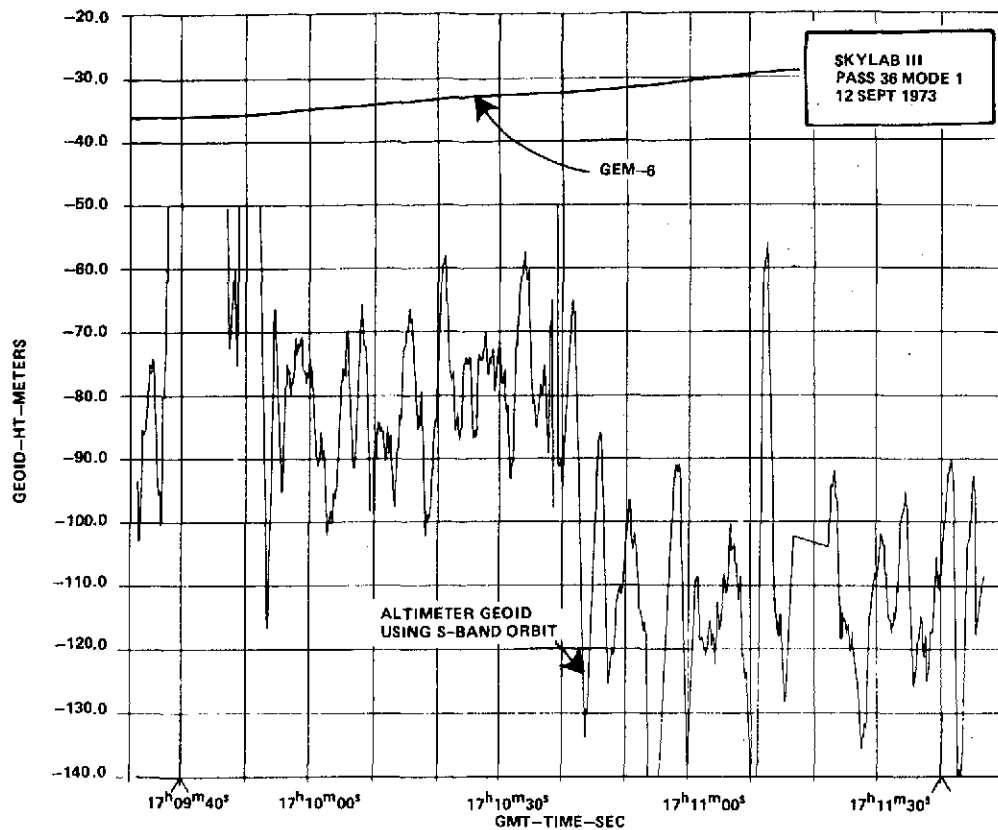
- 2.1°
245.2°

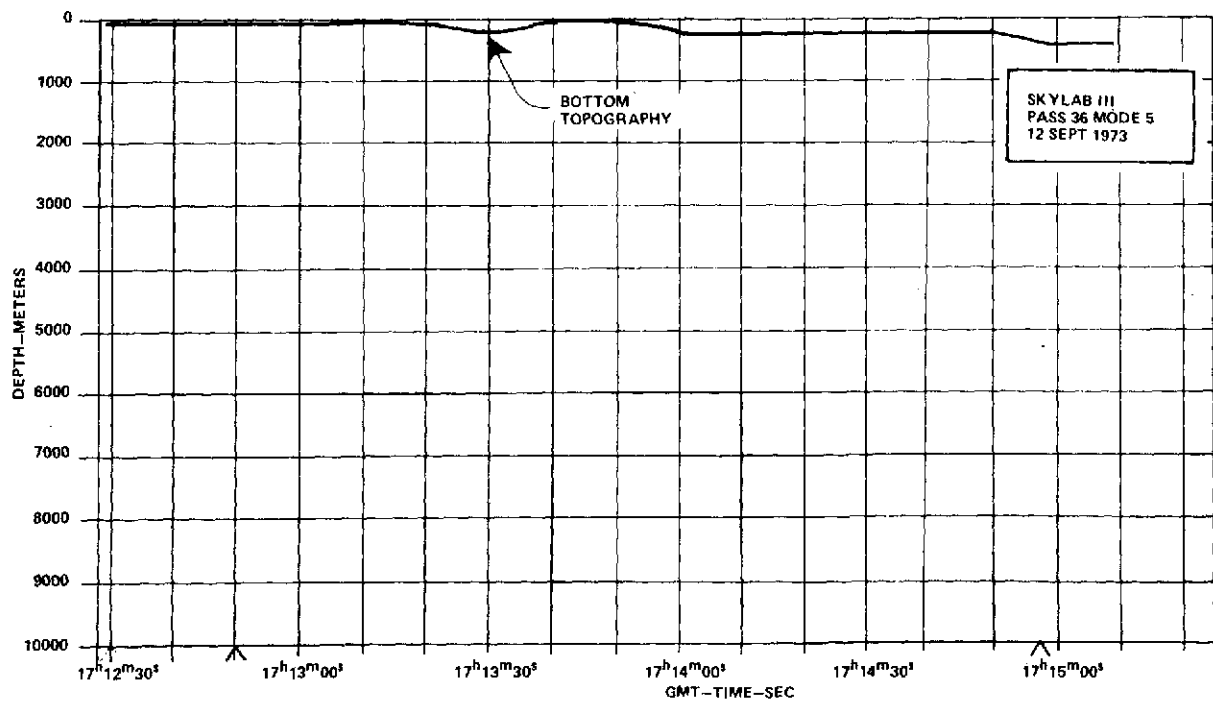
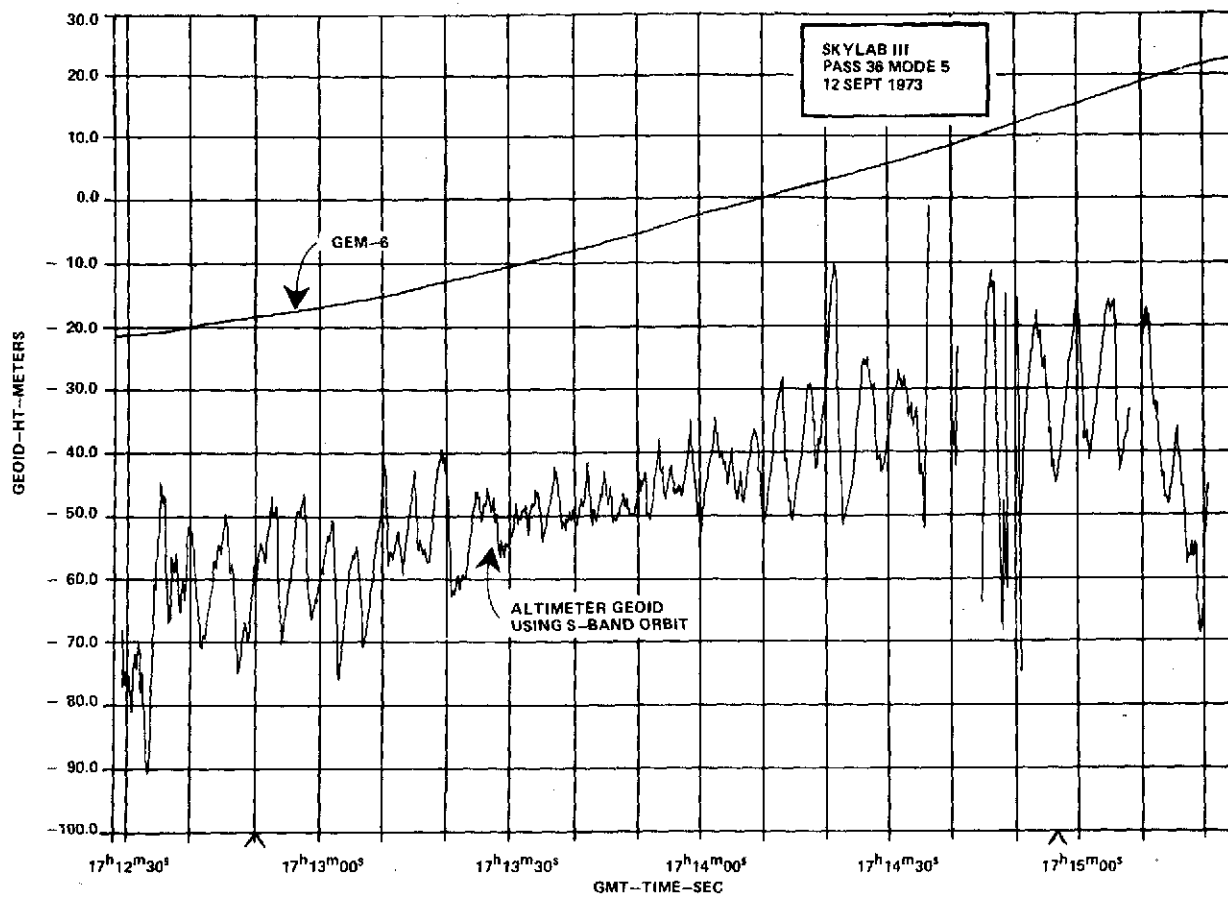


Lat 10.4°
Long 264.6°

MAP NO. 63

17.2°
260.1°

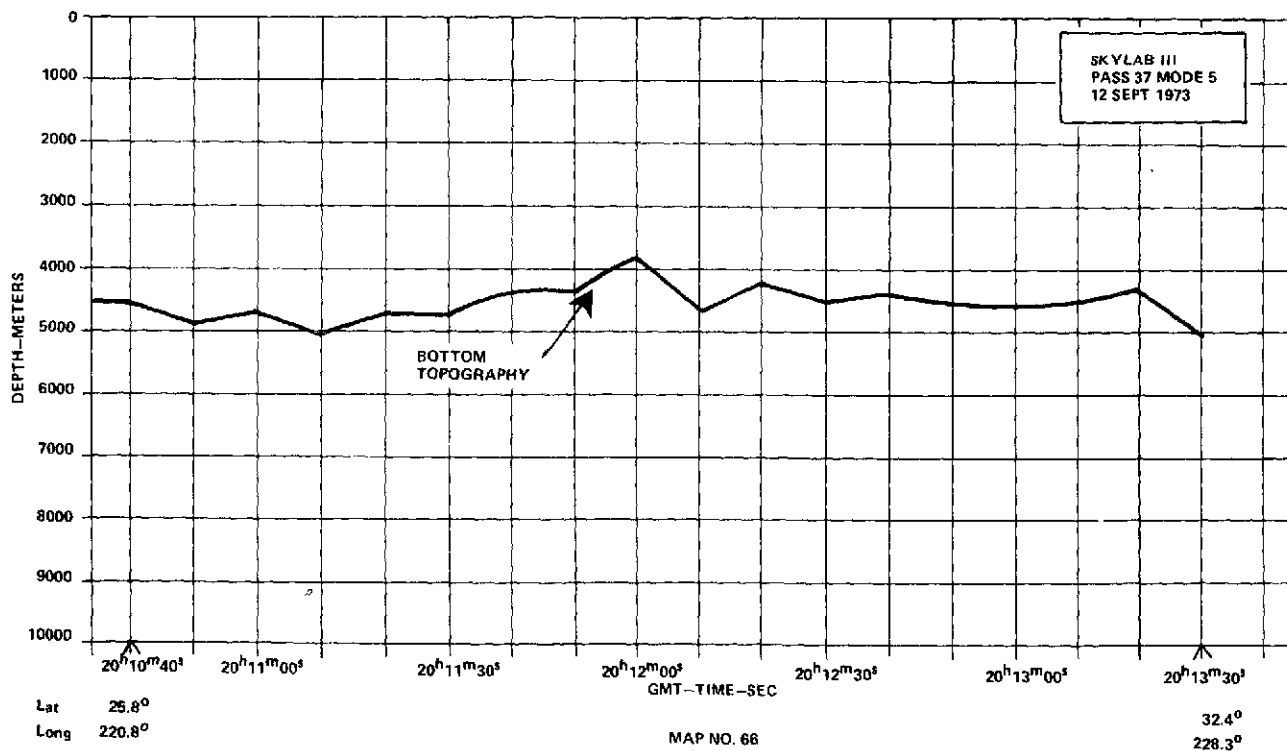
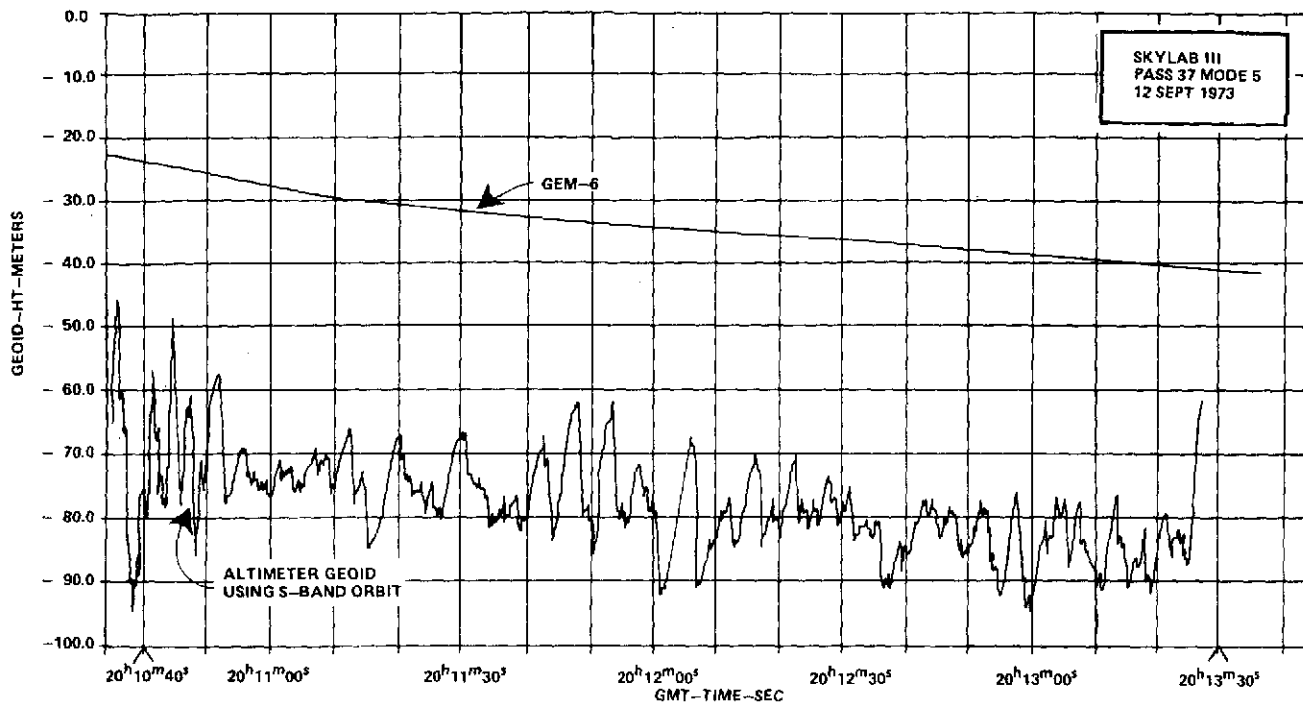


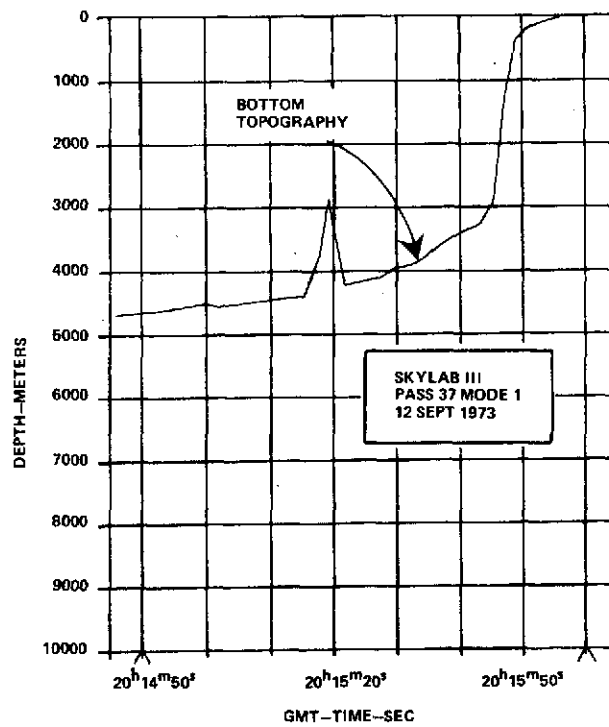
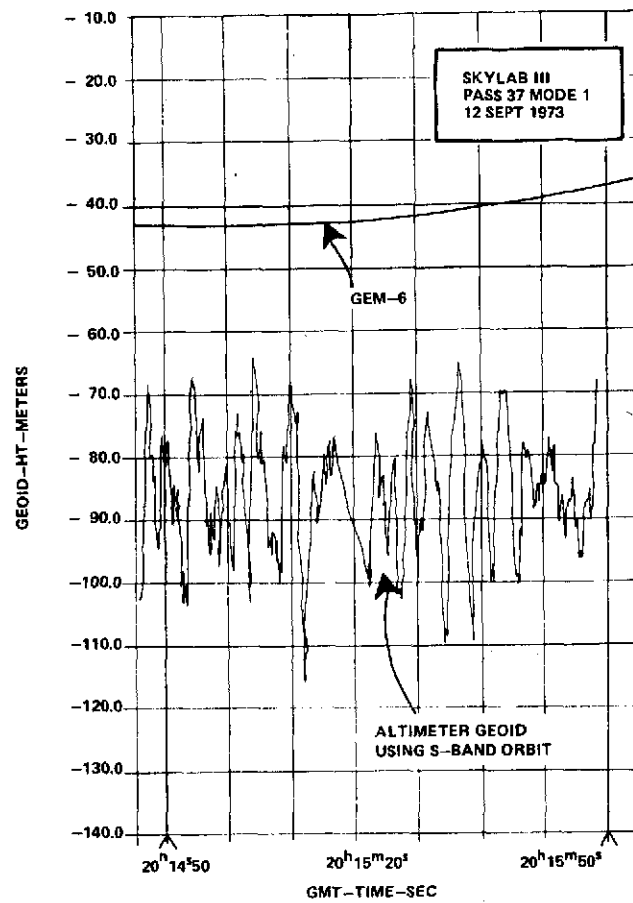


Lat 44.0°
Long 295.9°

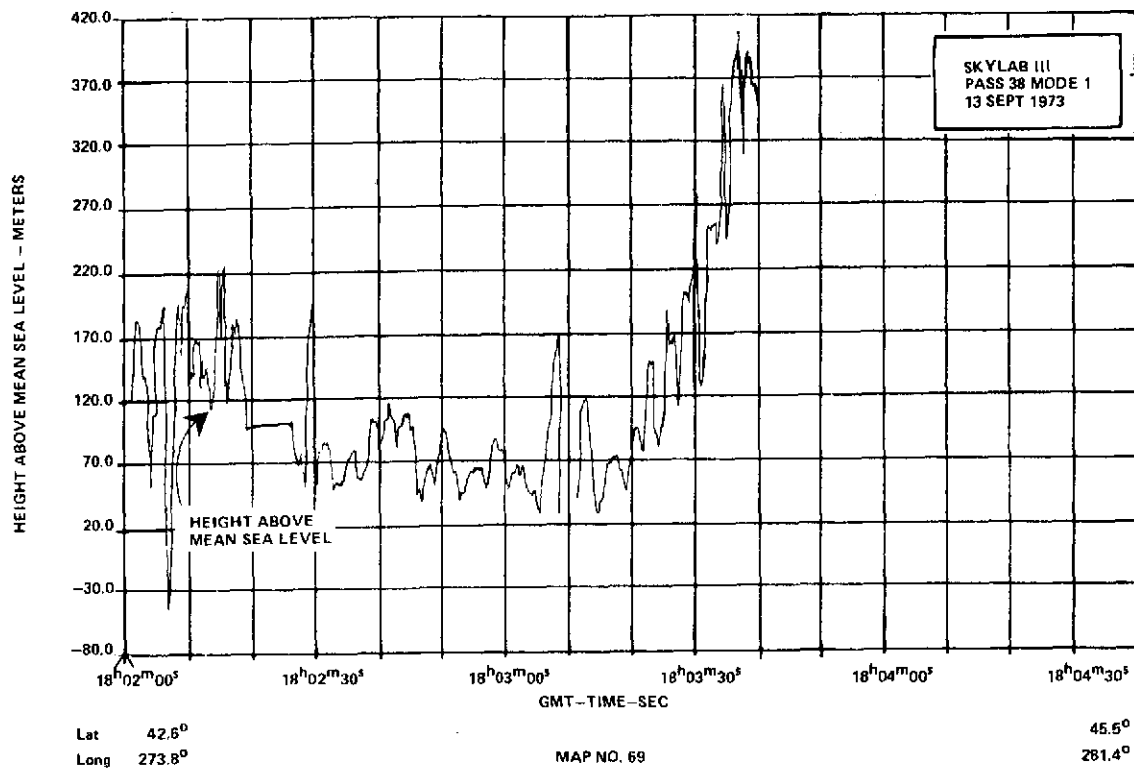
MAP NO. 65

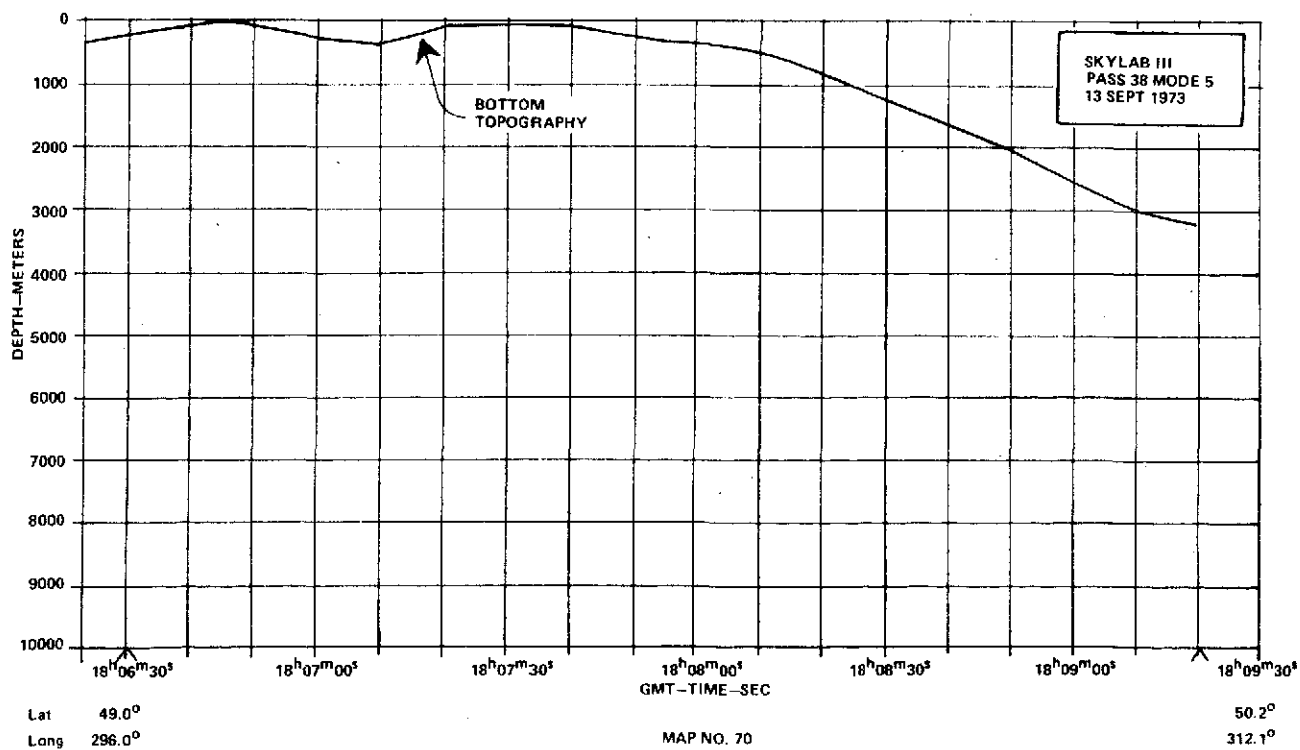
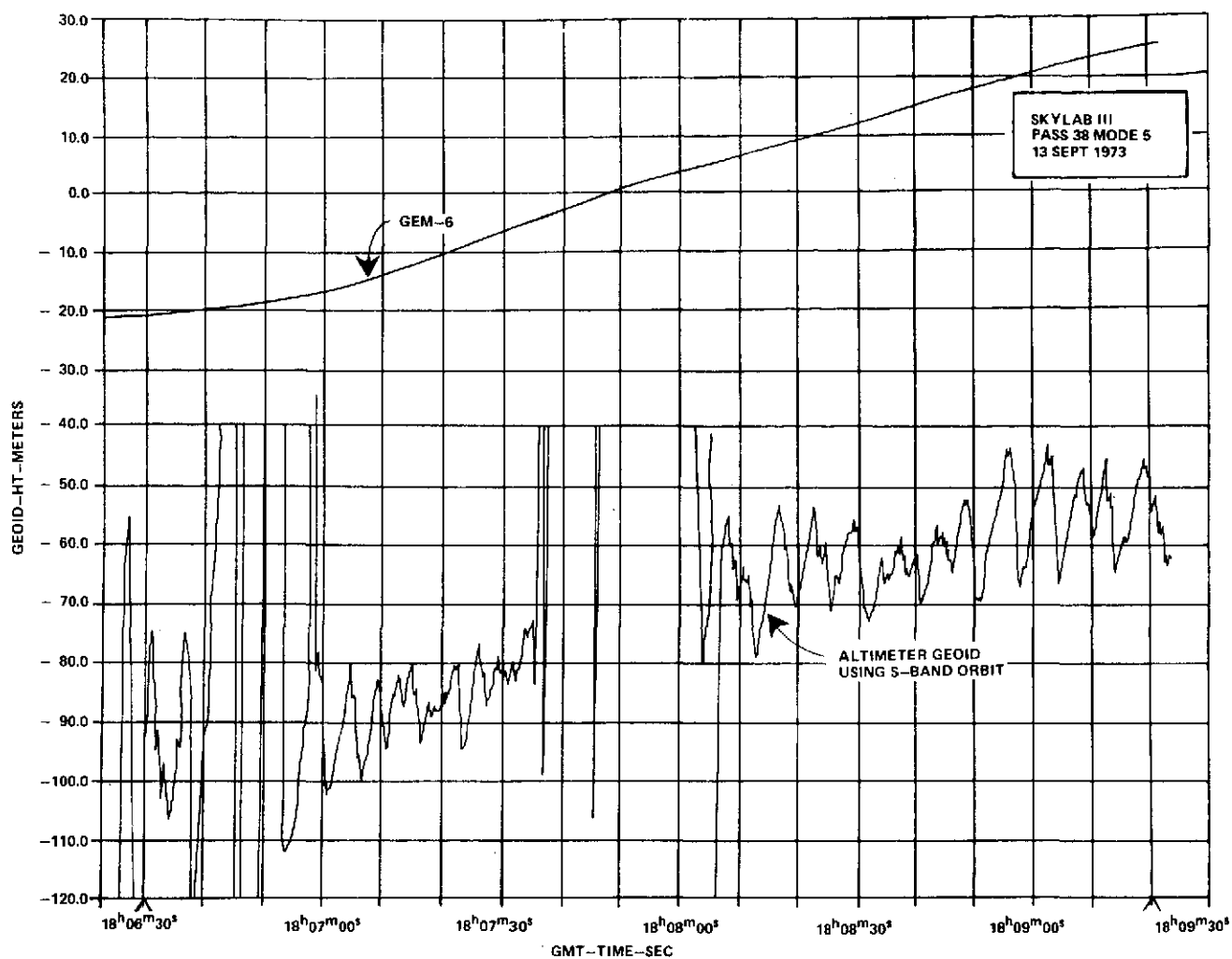
48.1°
309.9°

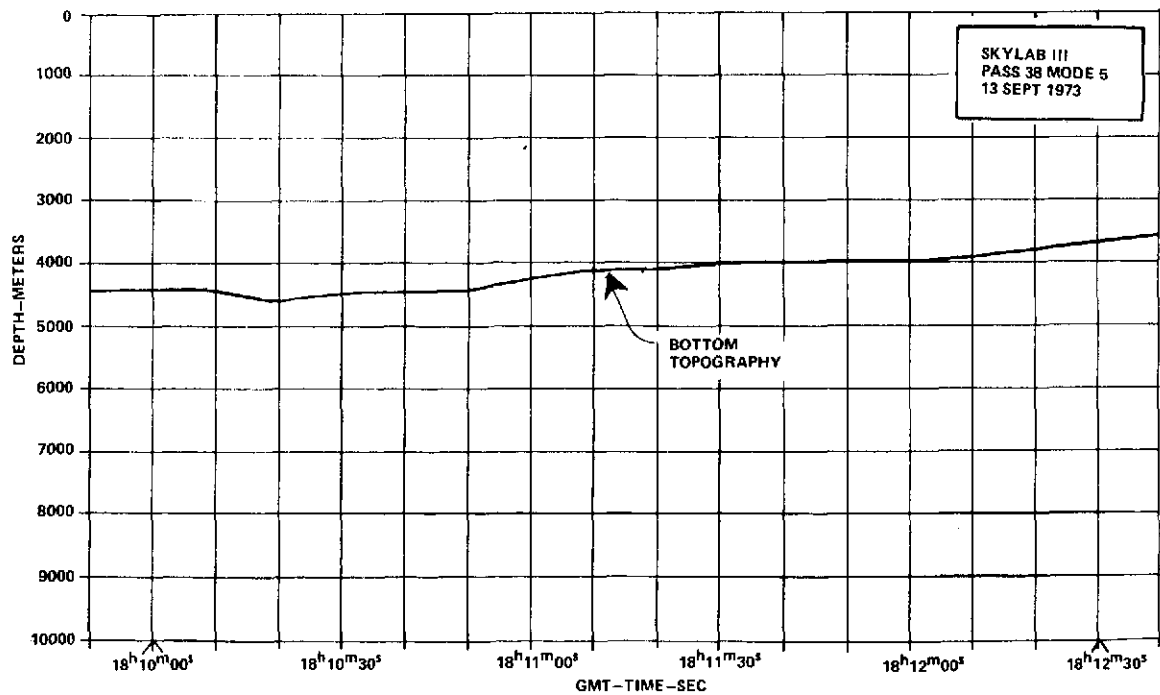
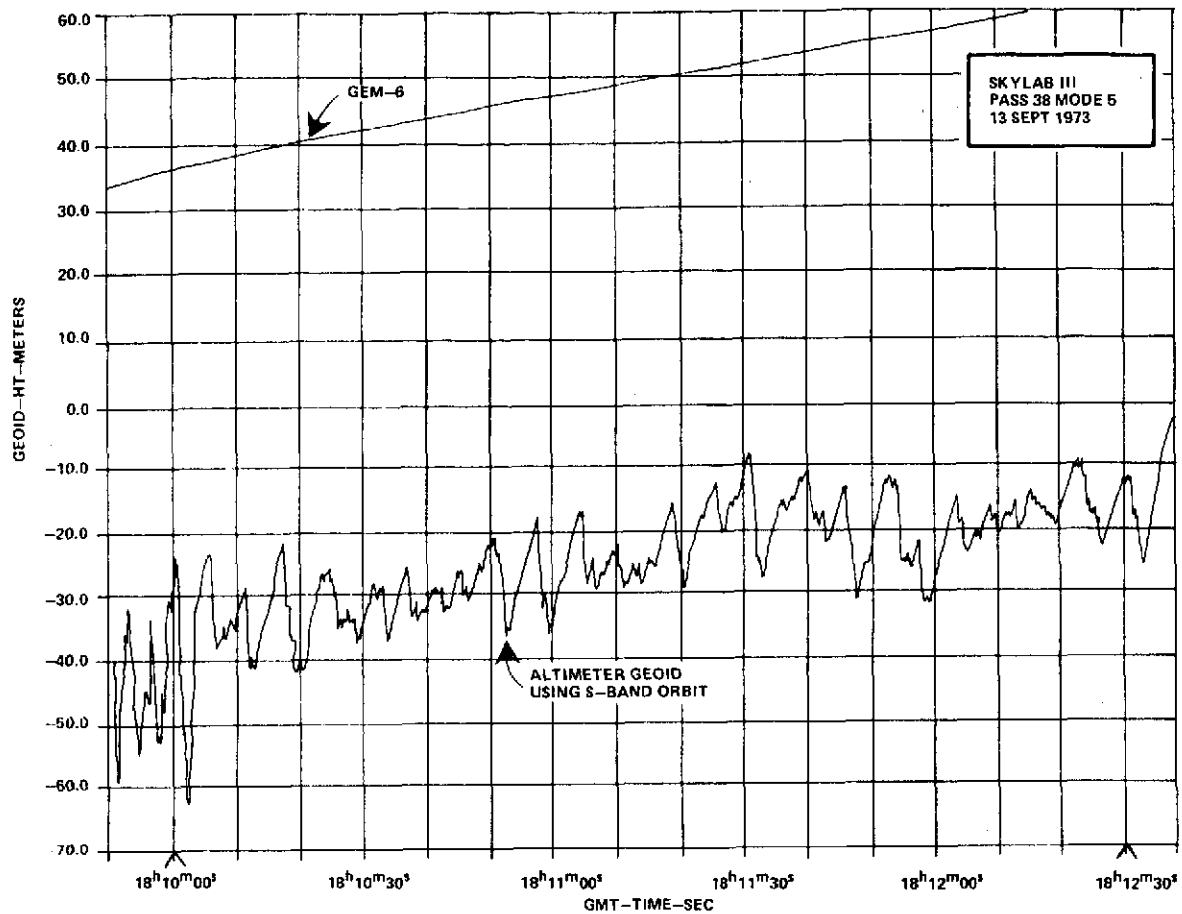




| | | | |
|------|--------|------------|--------|
| Lat | 35.7° | | 38.4° |
| Long | 232.8° | MAP NO. 67 | 237.0° |



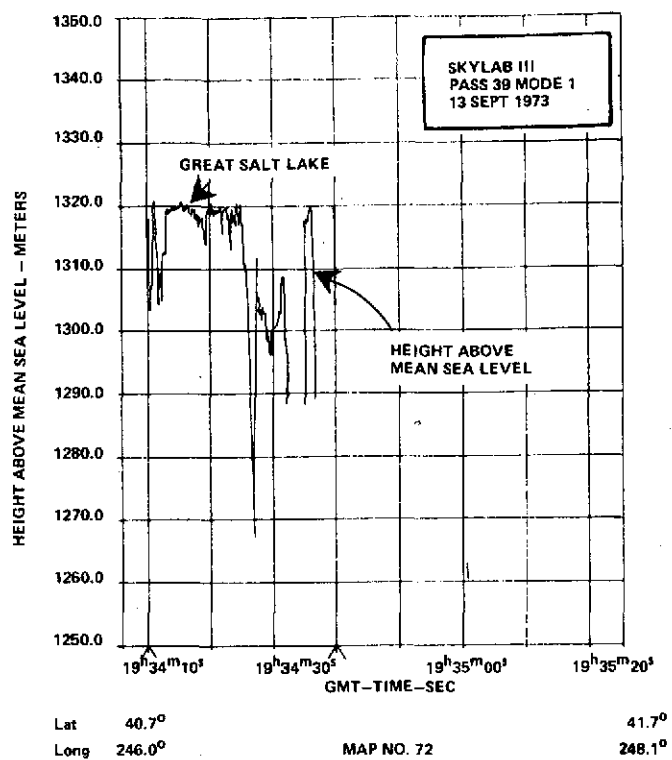


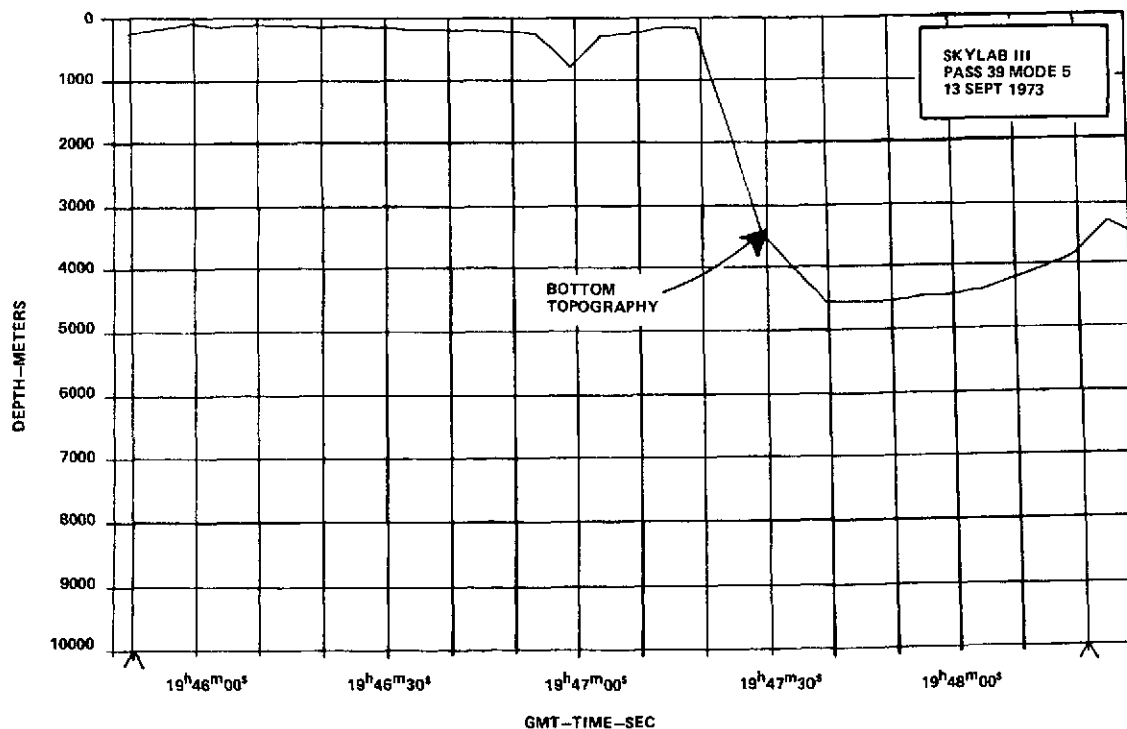
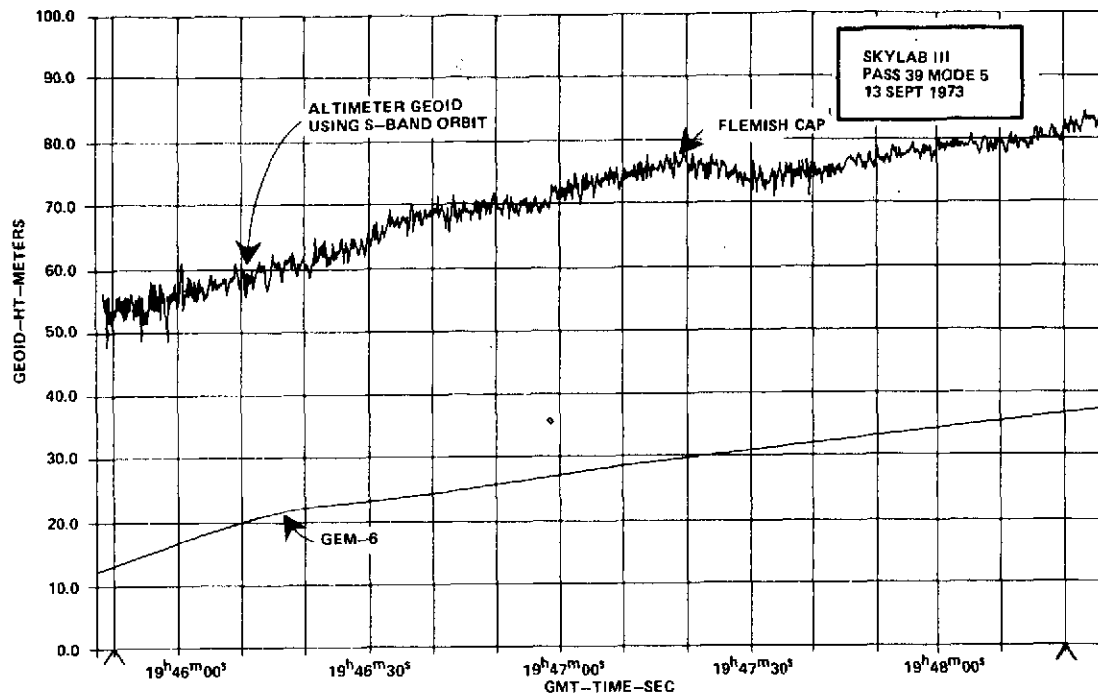


Lat 50.2°
Long 315.0°

MAP NO. 71

48.6°
330.0°

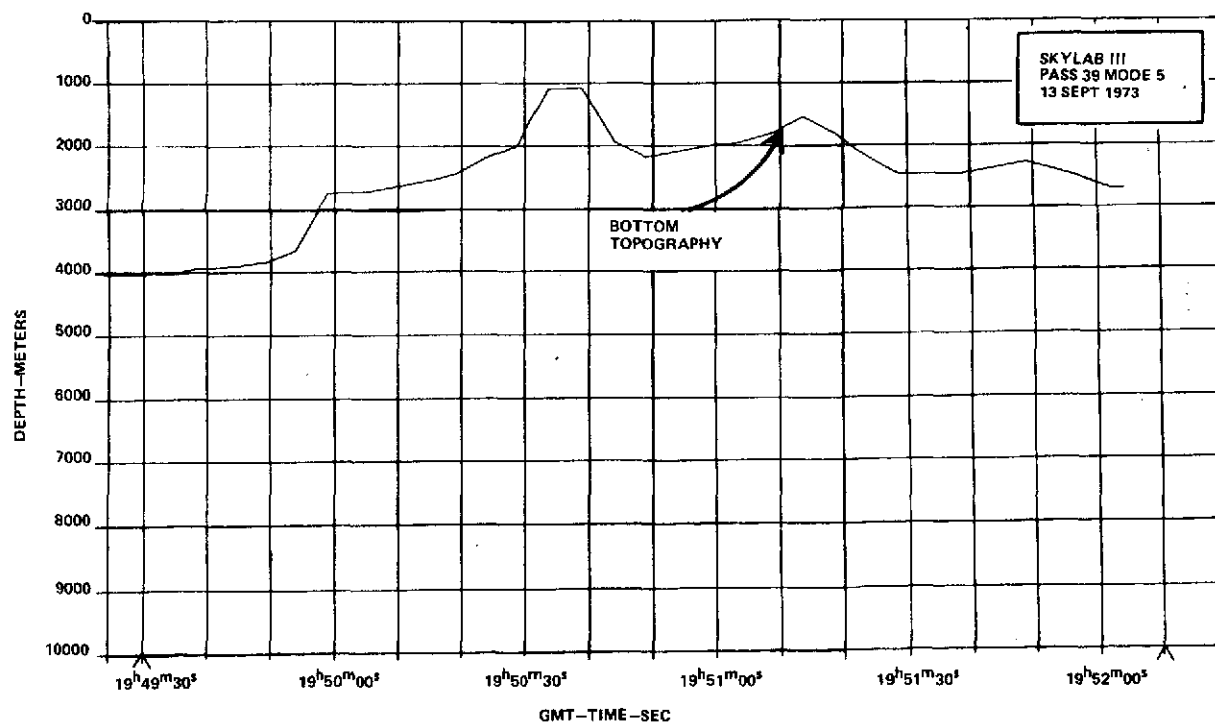
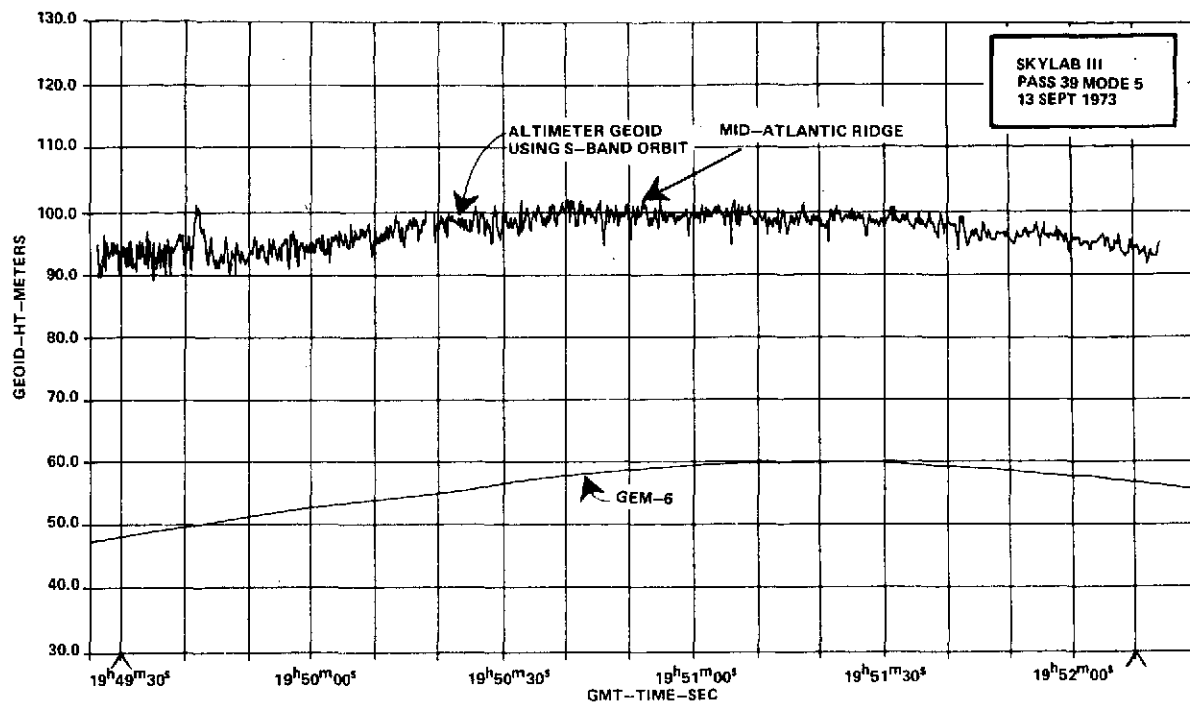




Lat 48.5°
Long 307.4°

MAP NO. 73

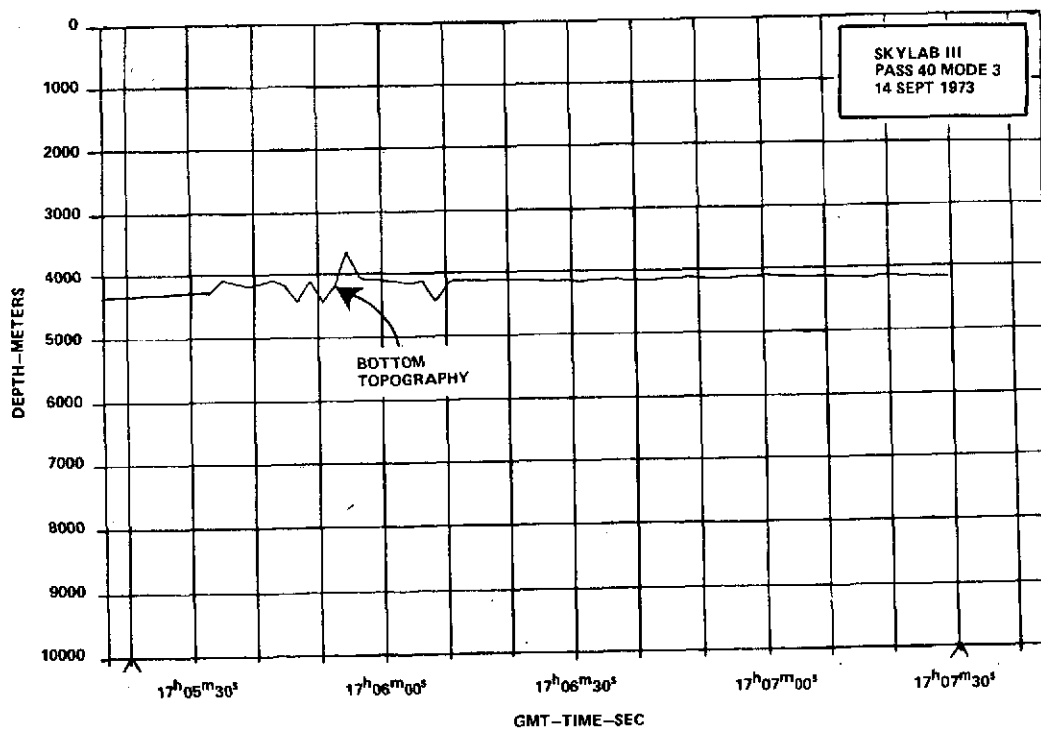
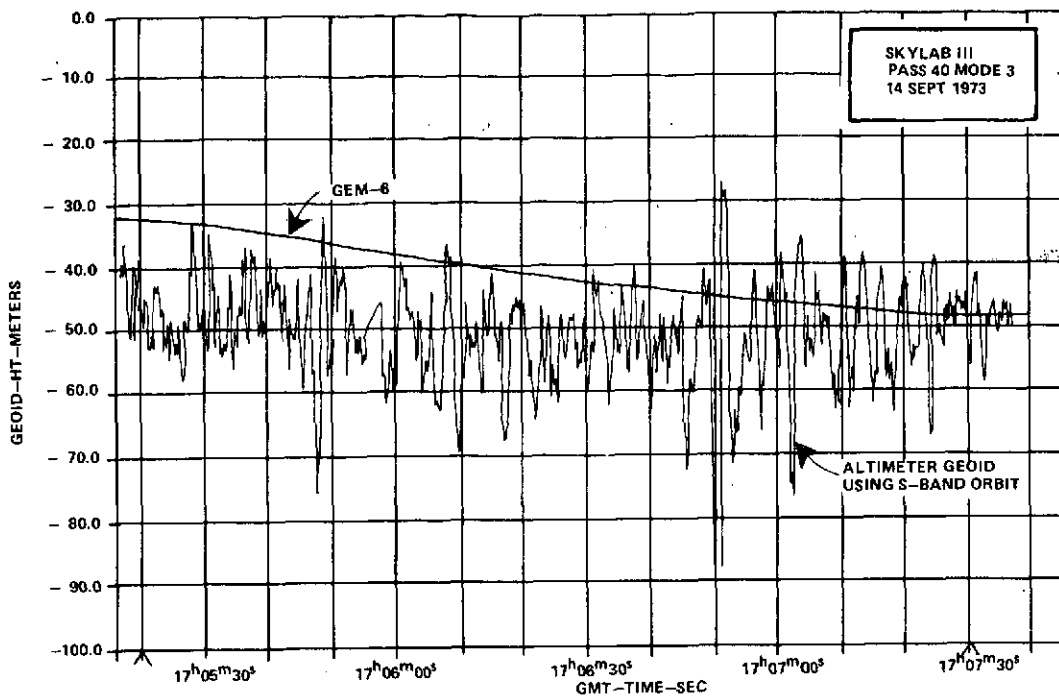
45.1°
320.0°



Lat 43.4°
Long 324.6°

MAP NO. 74

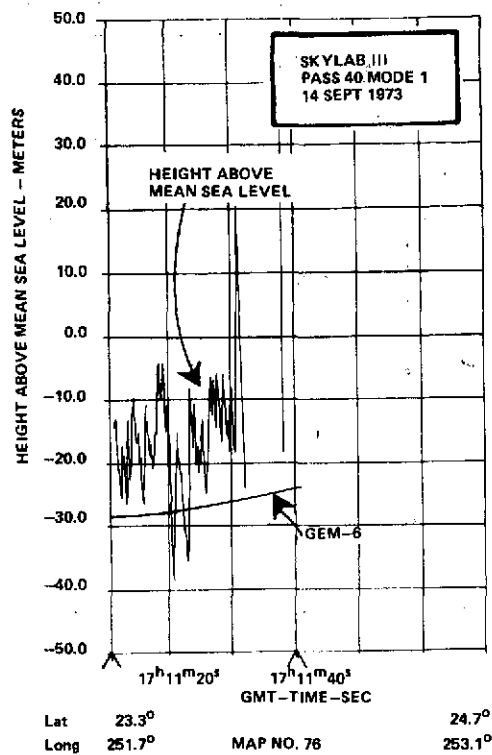
37.5°
336.0°



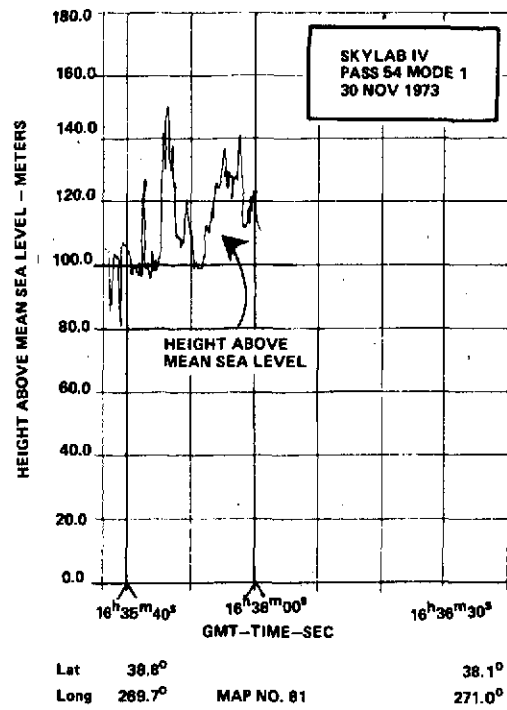
Lat 6.4°
Long 237.5°

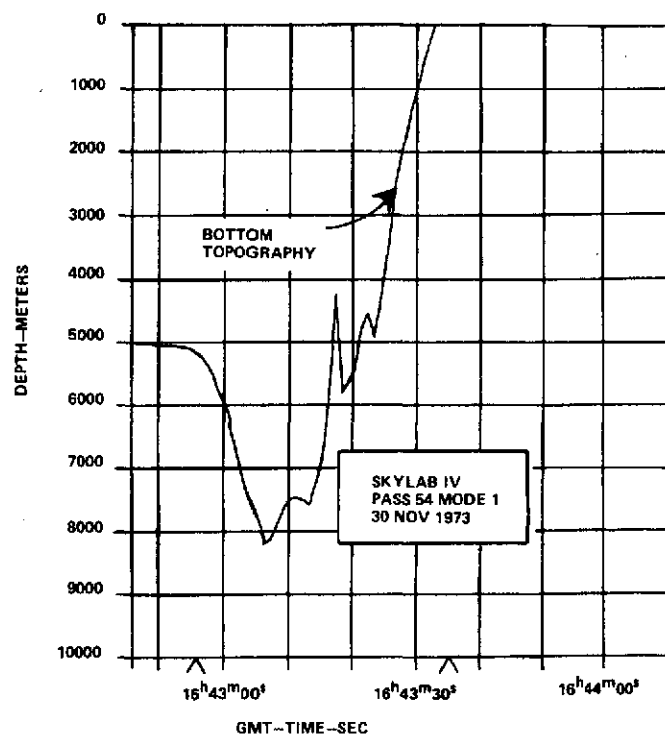
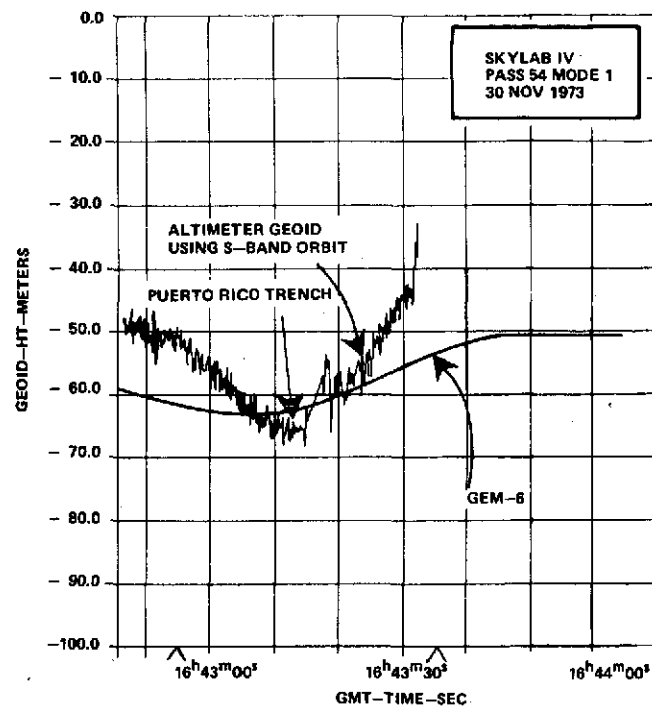
MAP NO. 75

12.8°
242.5°

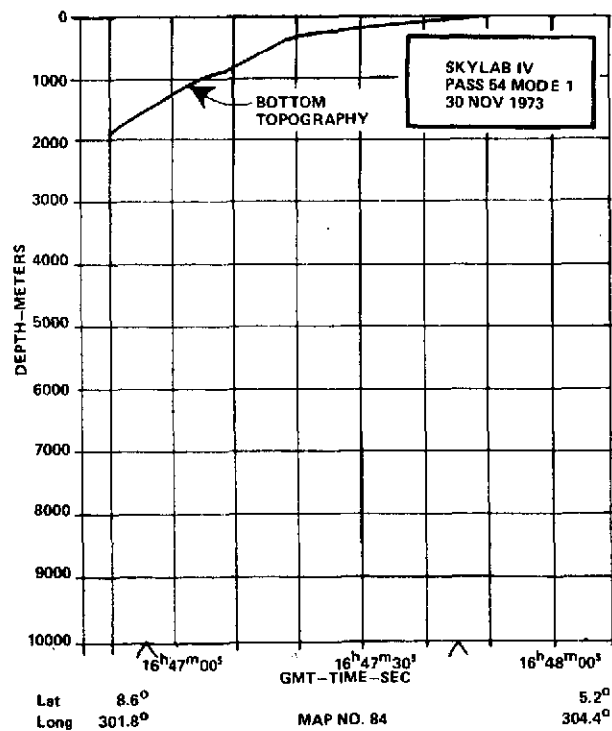
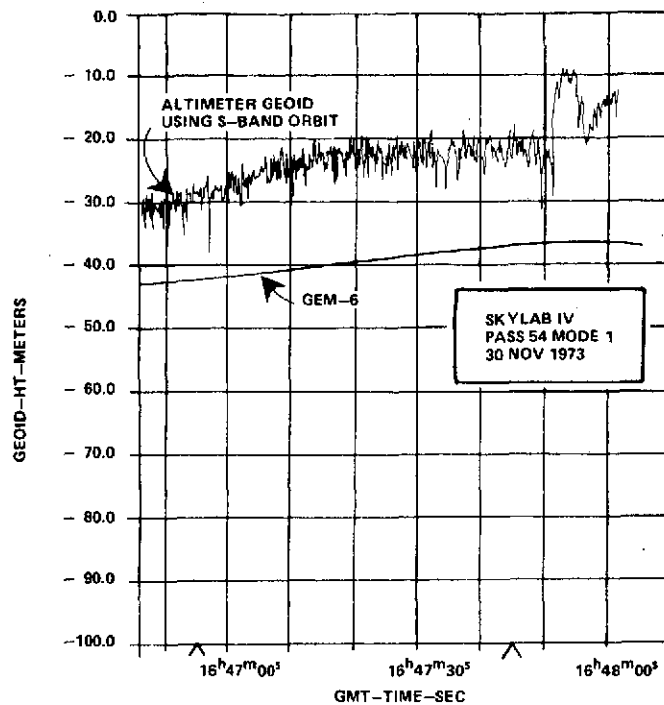


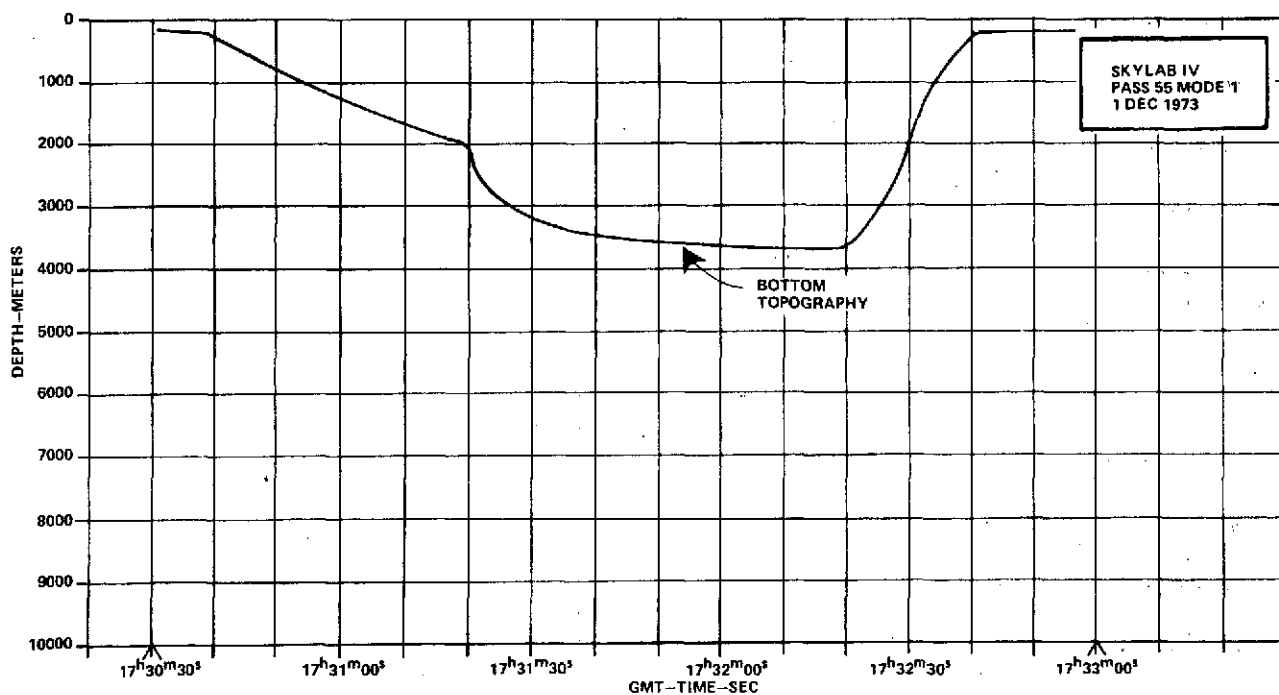
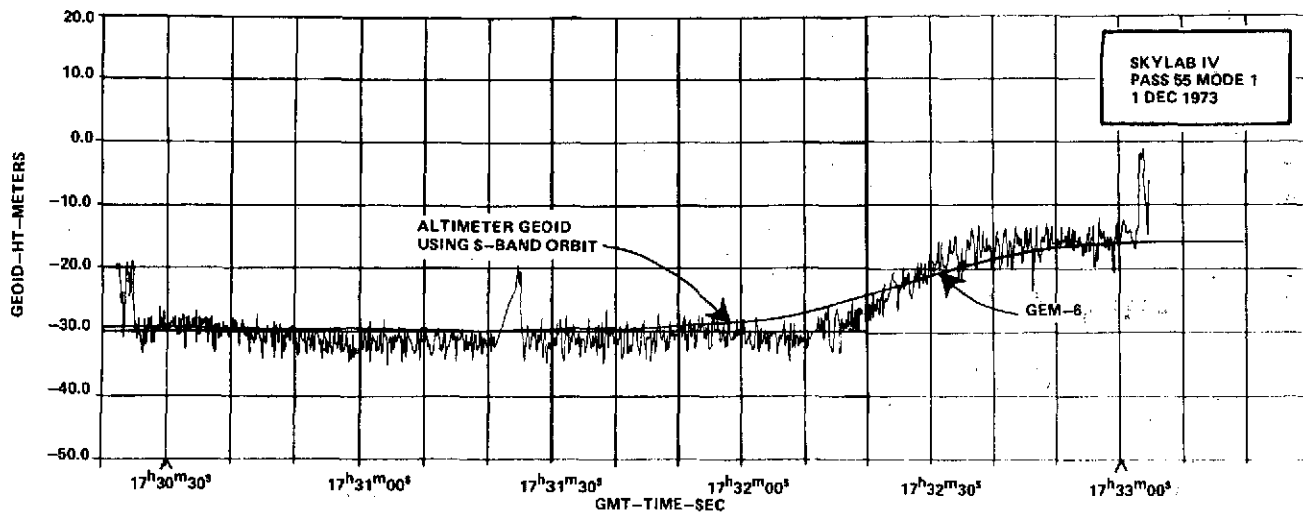
ORIGINAL PAGE IS
OF POOR QUALITY





Lat 20.2° 18.3°
Long 292.2° 293.8°
MAP NO. 83

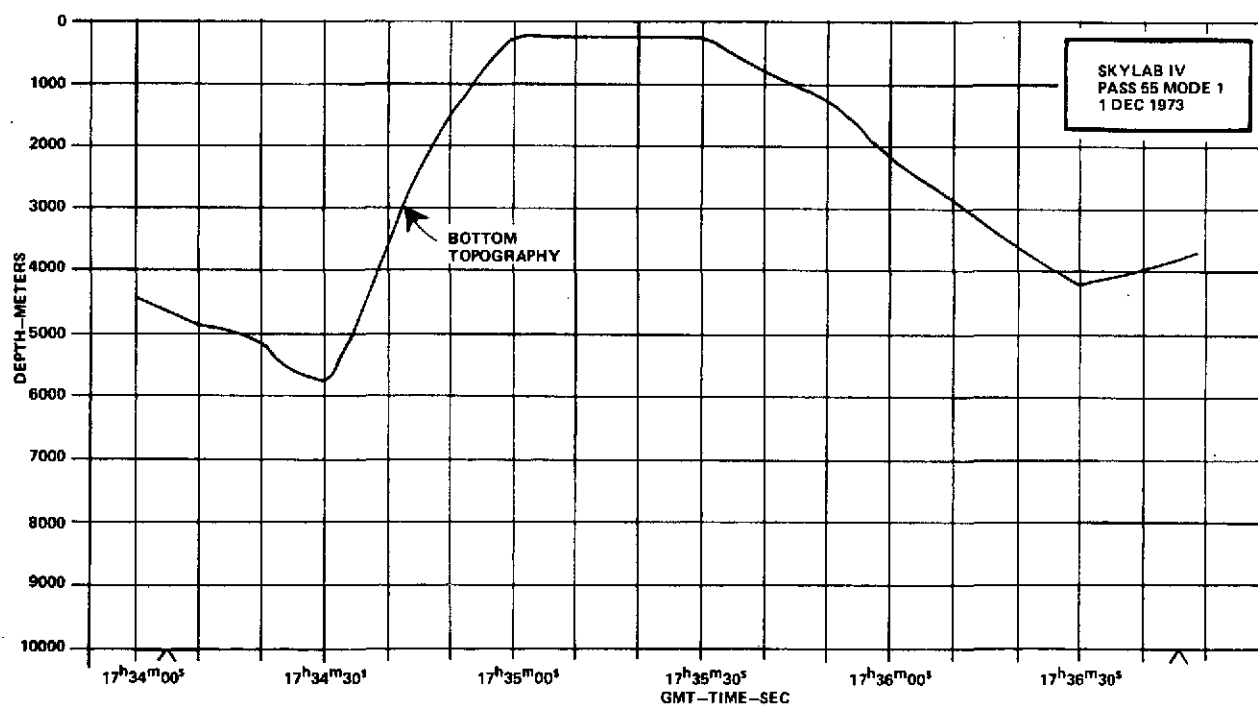
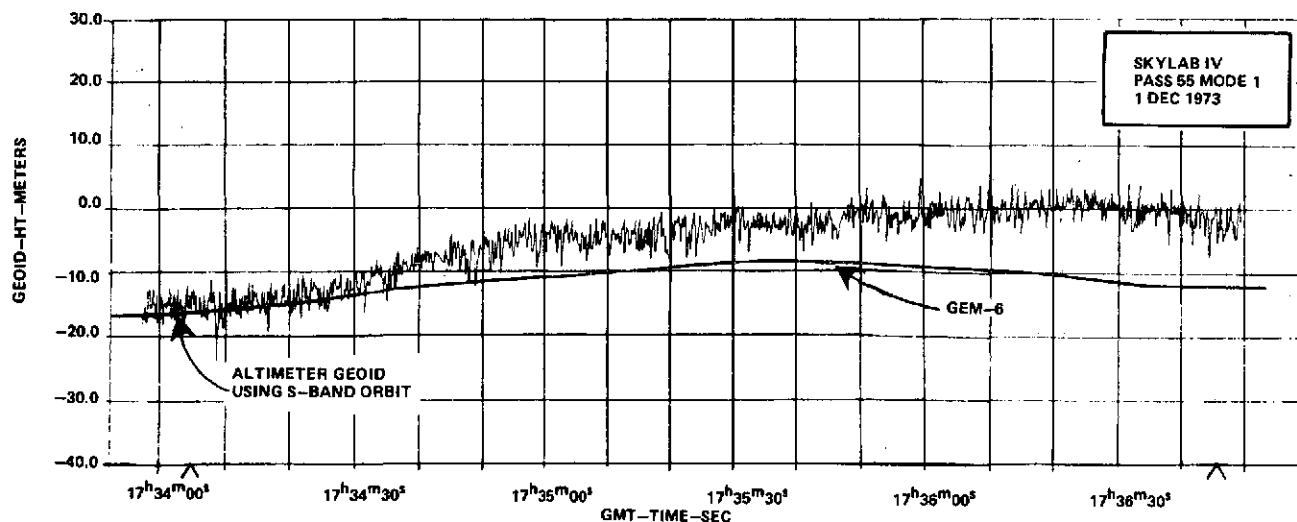




Lat 28.6°
Long 264.9°

MAP NO. 85

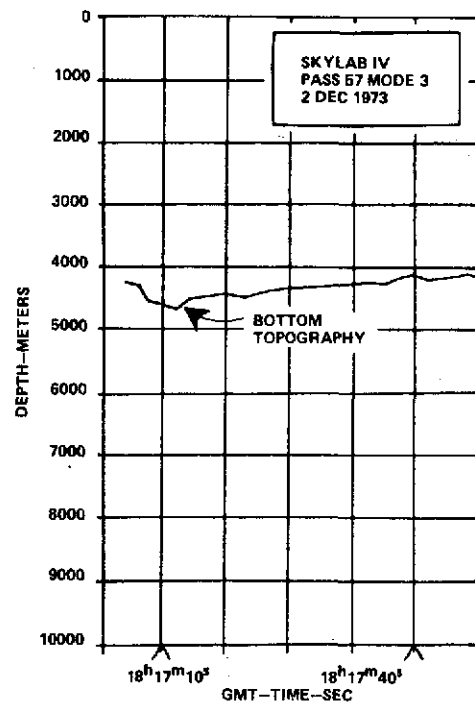
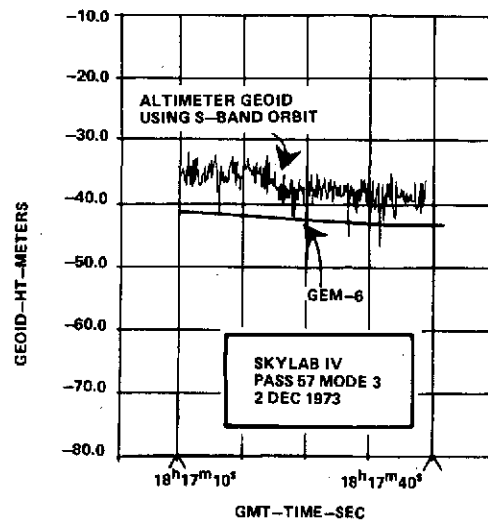
21.8°
271.8°



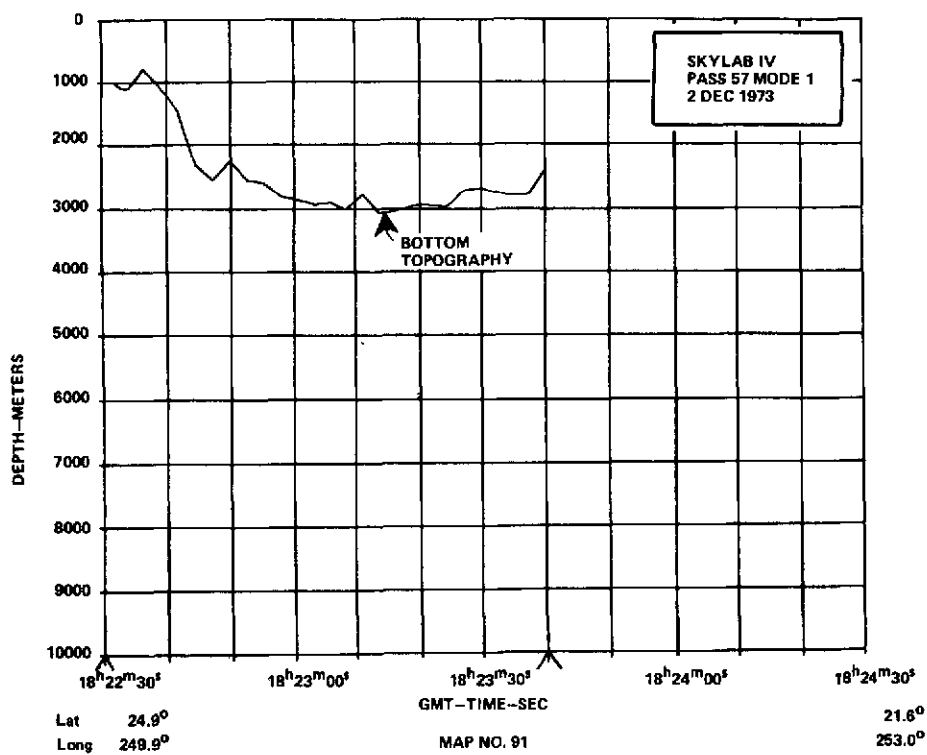
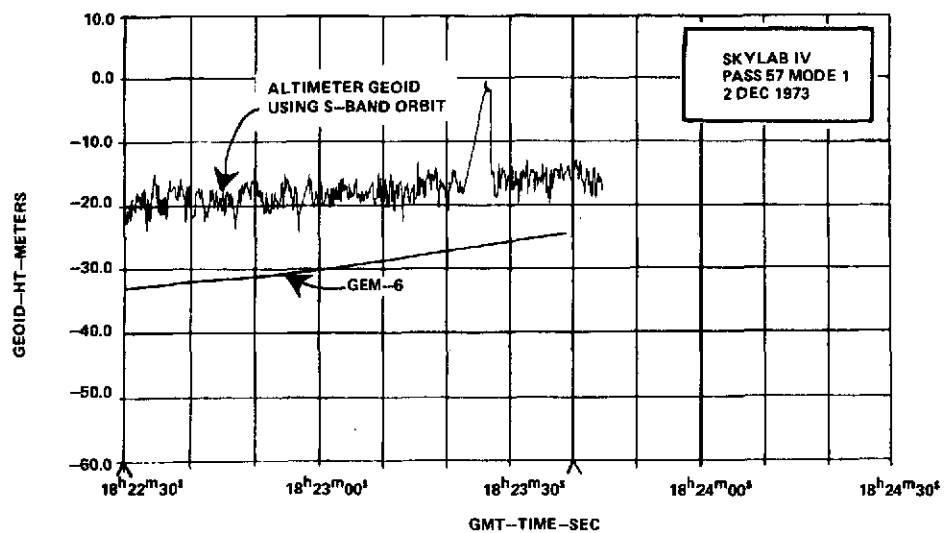
Lat 18.7°
Long 274.6°

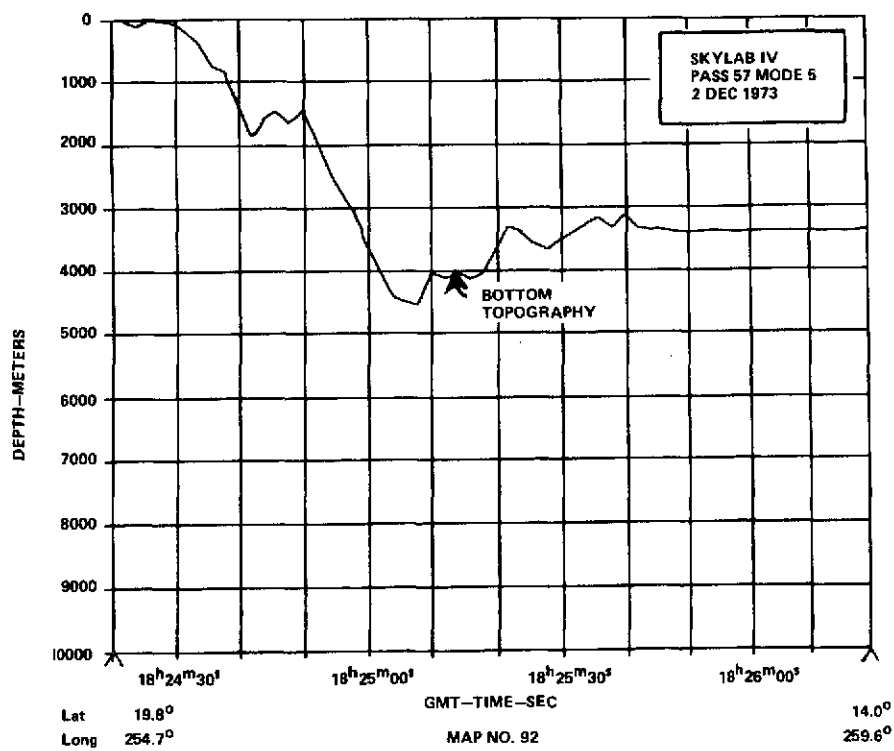
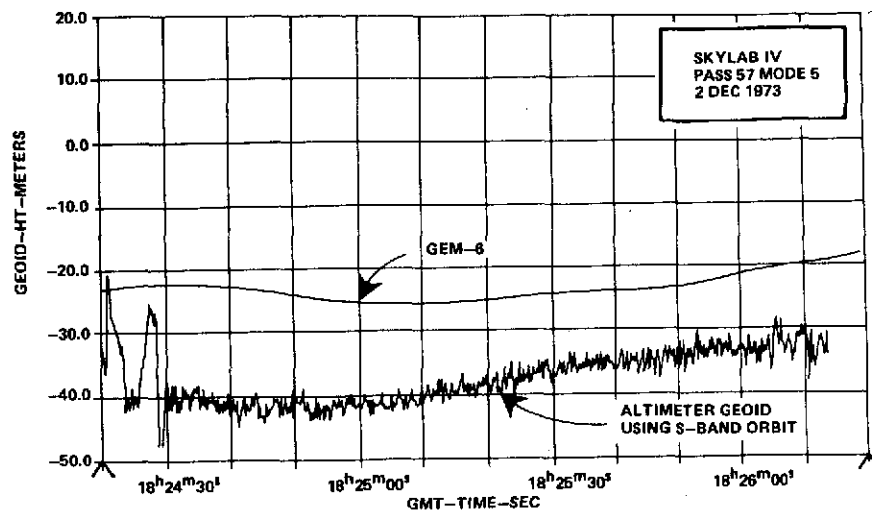
MAP NO. 86

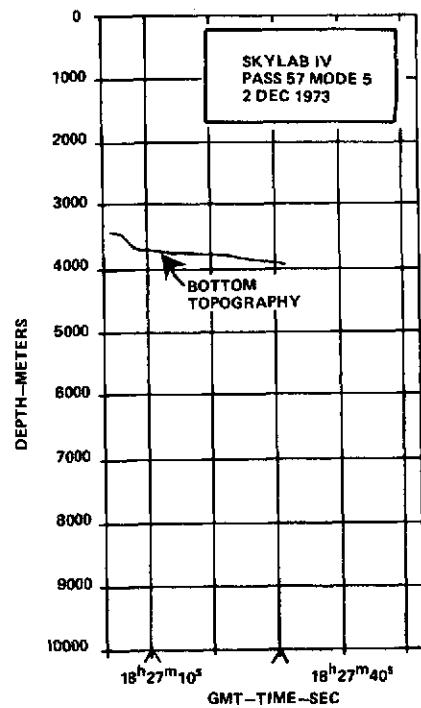
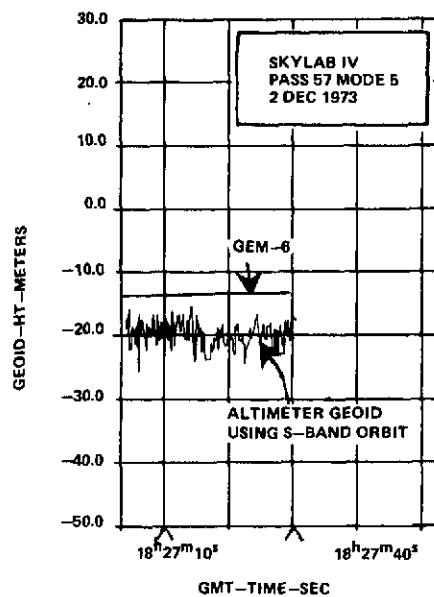
11.0°
281.4°



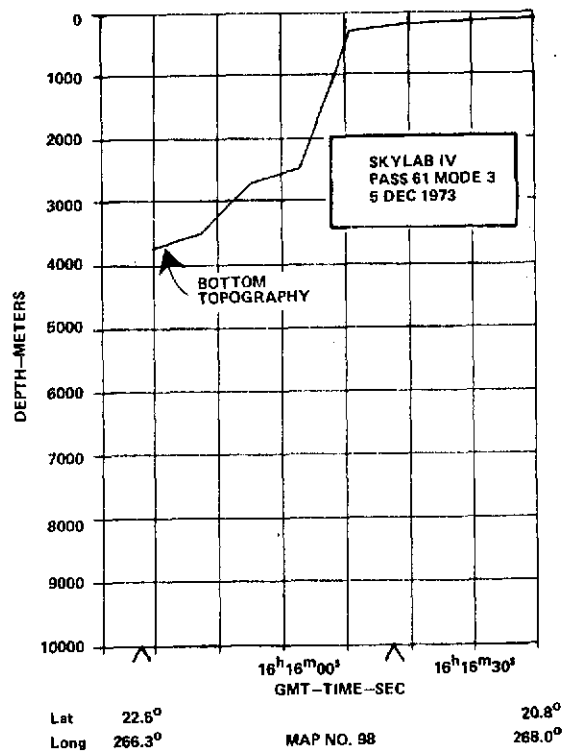
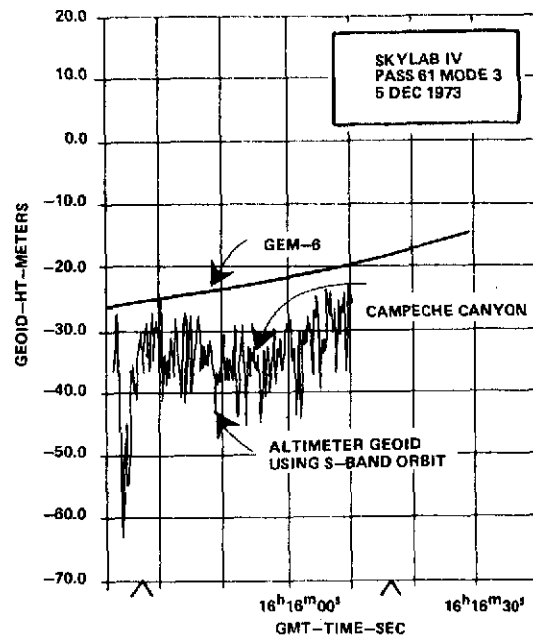
Lat 38.3° 38.8°
Long 232.8° MAP NO. 89 235.2°

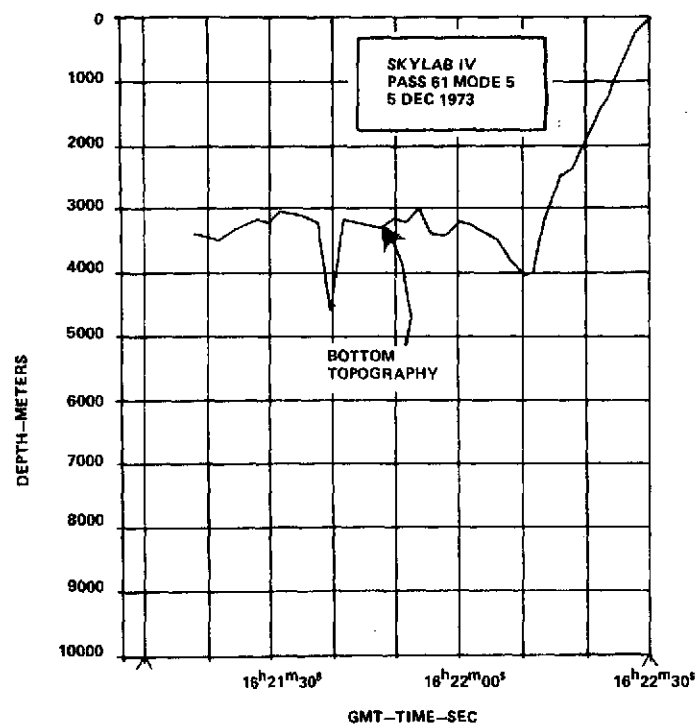
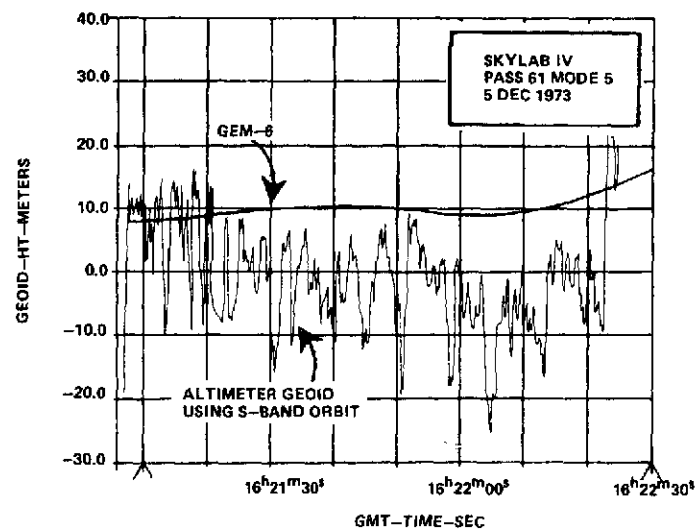




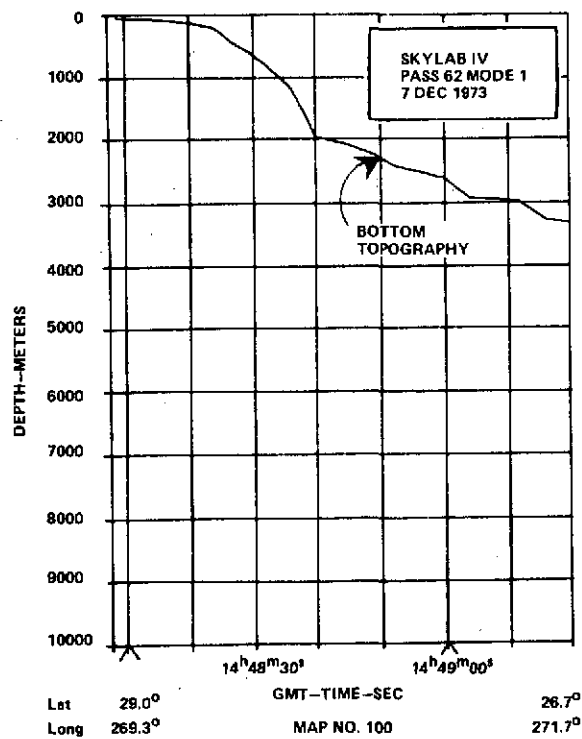
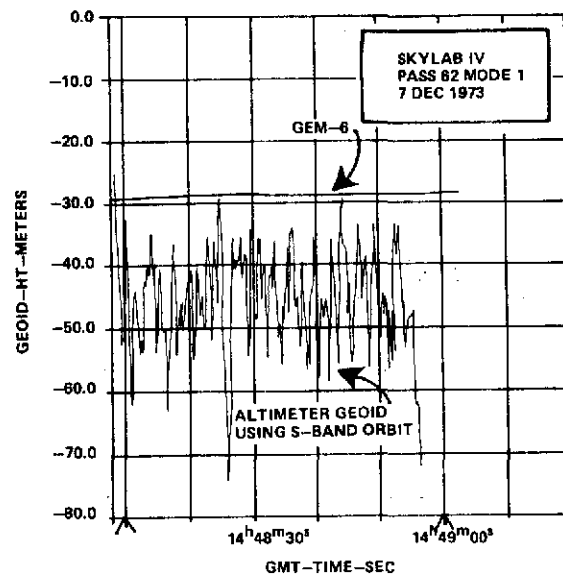


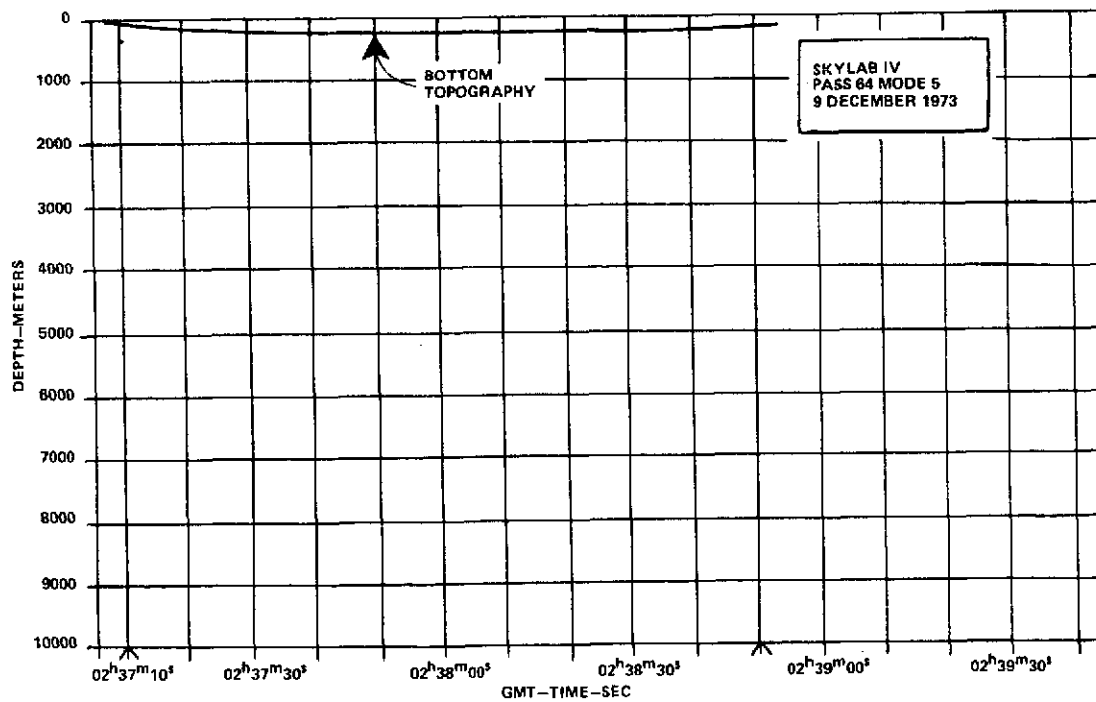
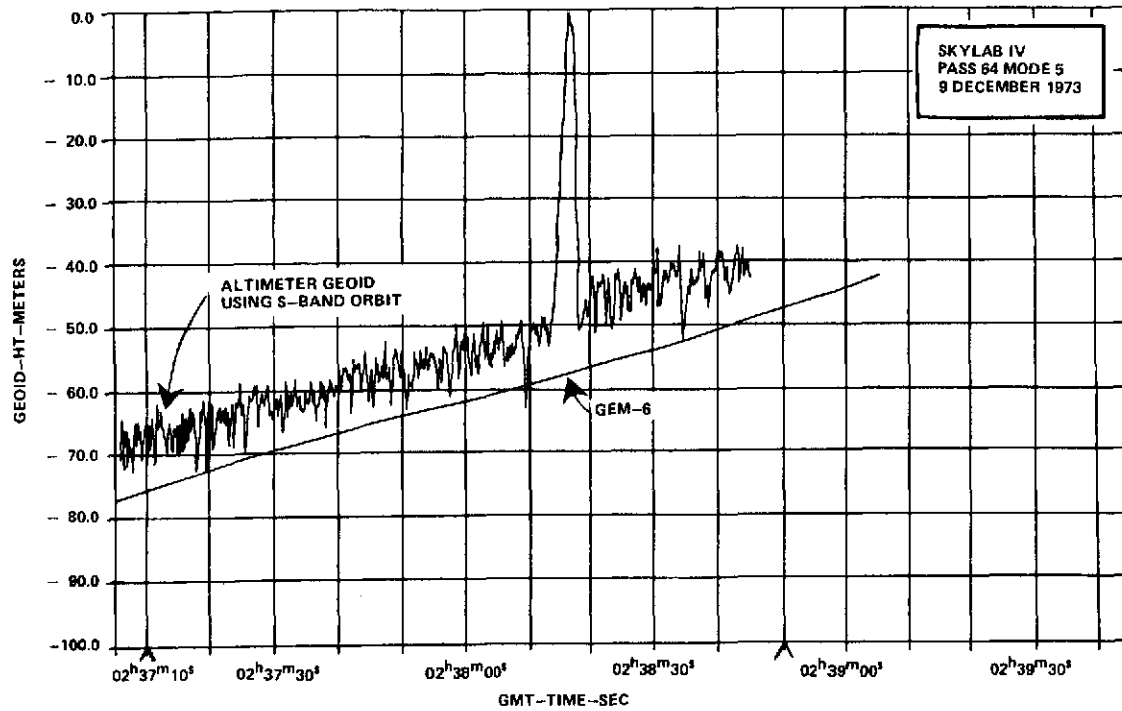
Lat 11.6° 10.6°
Long 261.6° MAP NO. 93 262.3°





| | | |
|------|------------|--------|
| Lat | 8.6° | 2.7° |
| Long | 279.5° | 282.6° |
| | MAP NO. 99 | |

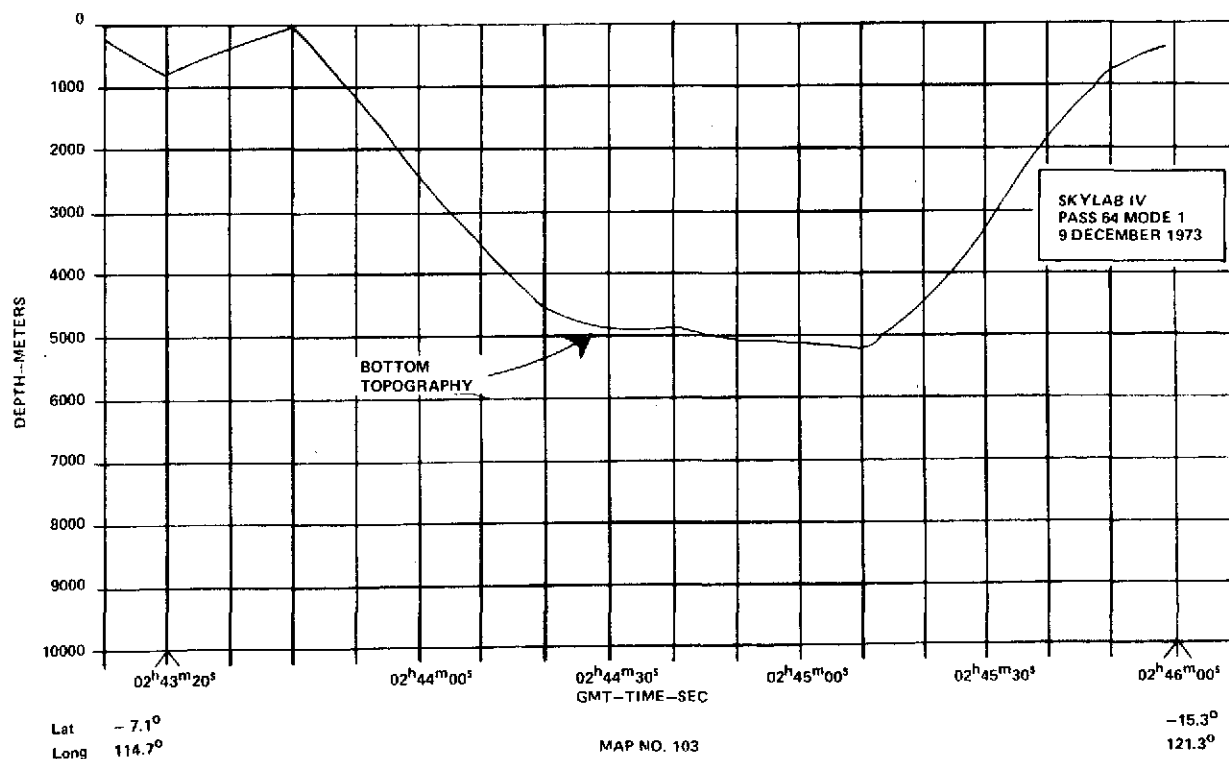
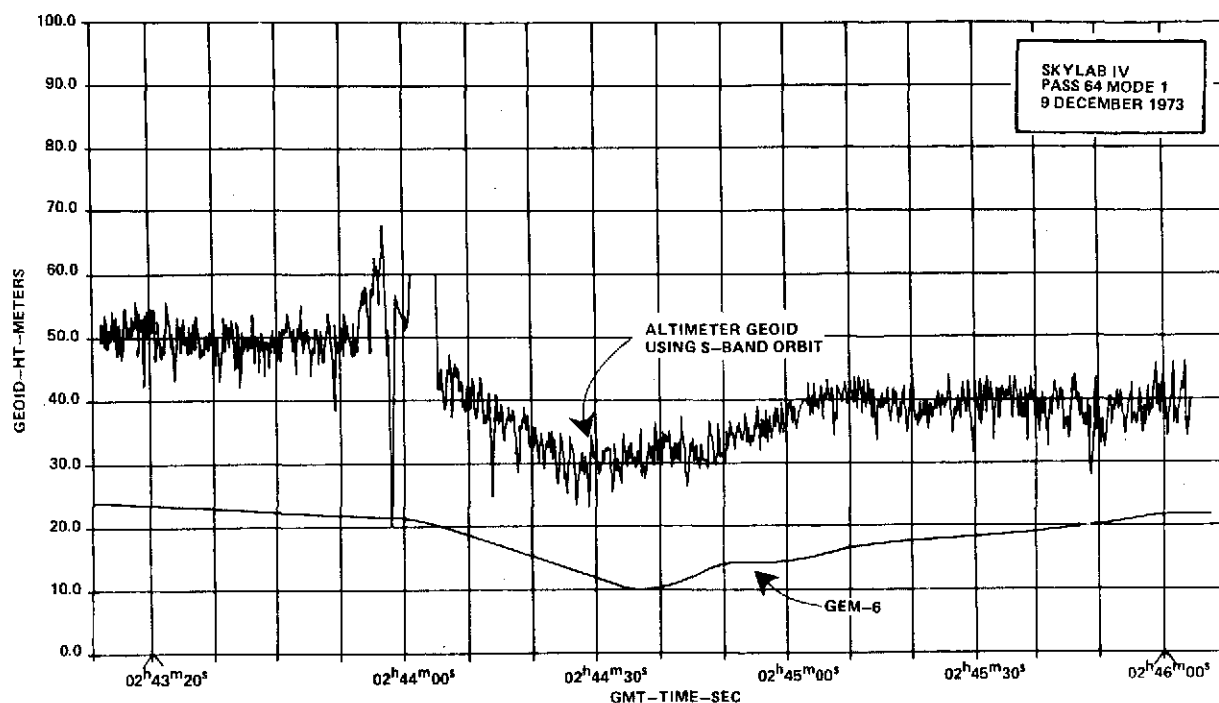


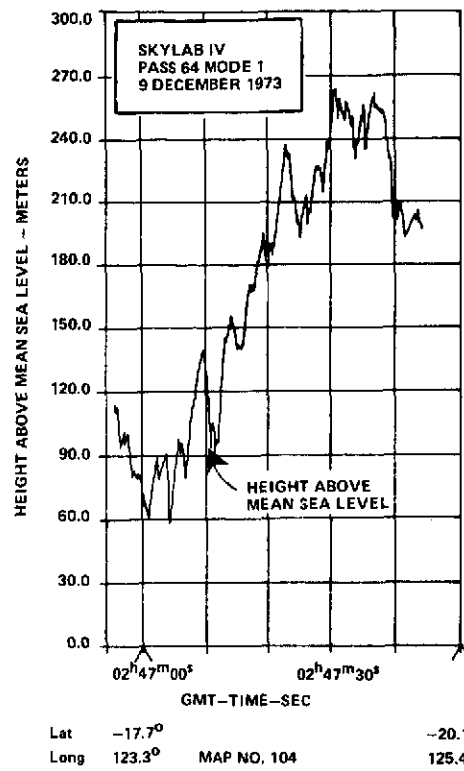


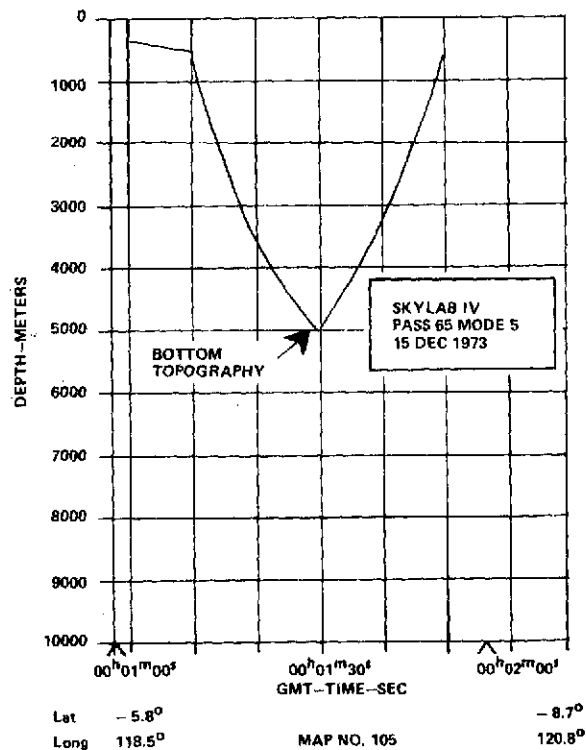
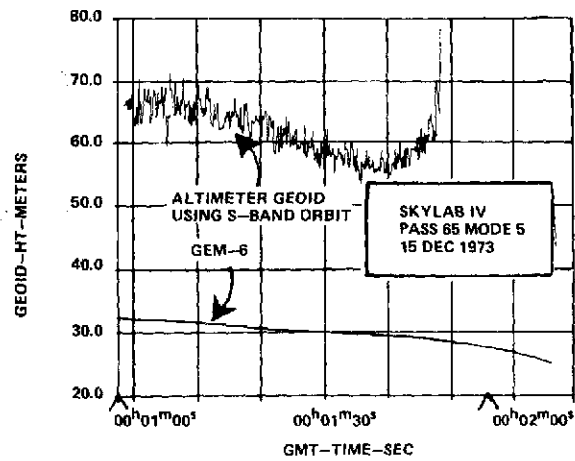
Lat 11.3°
Long 100.9°

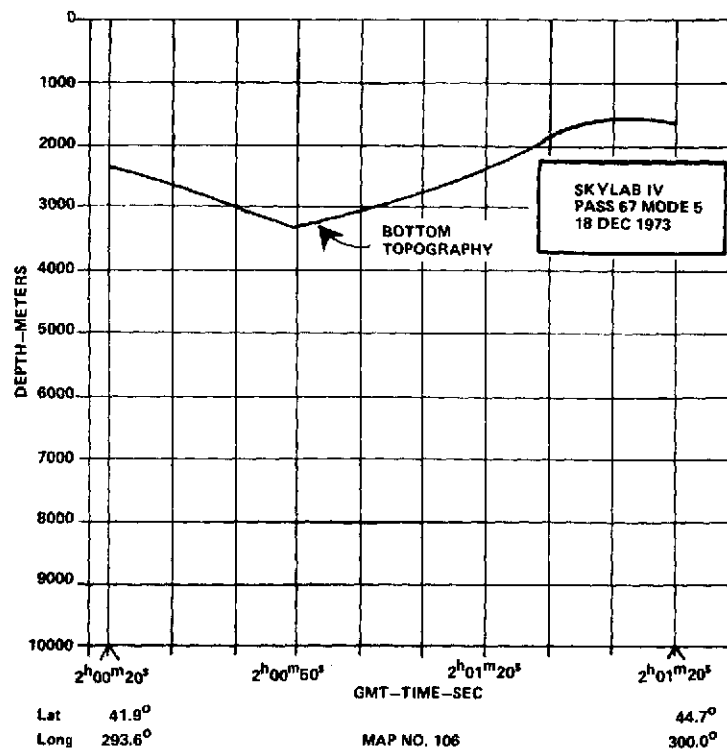
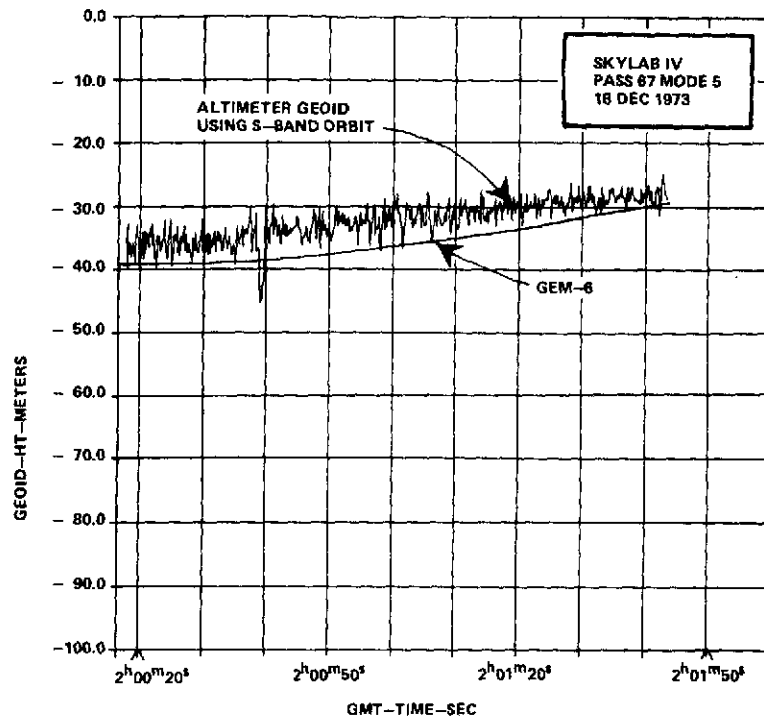
MAP NO. 102

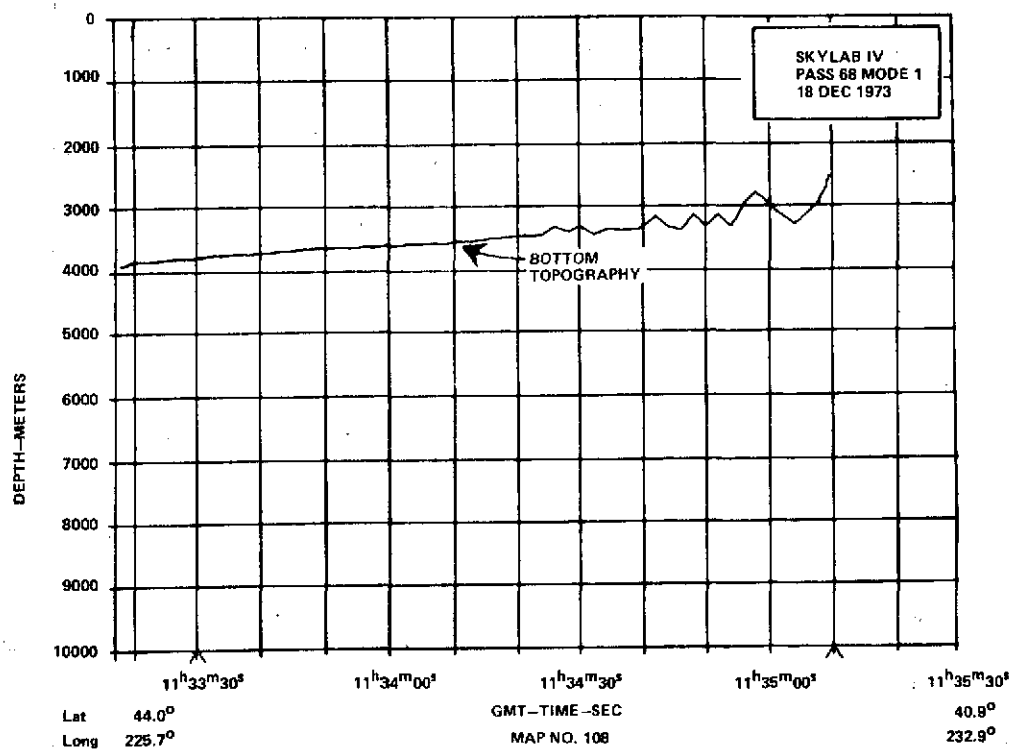
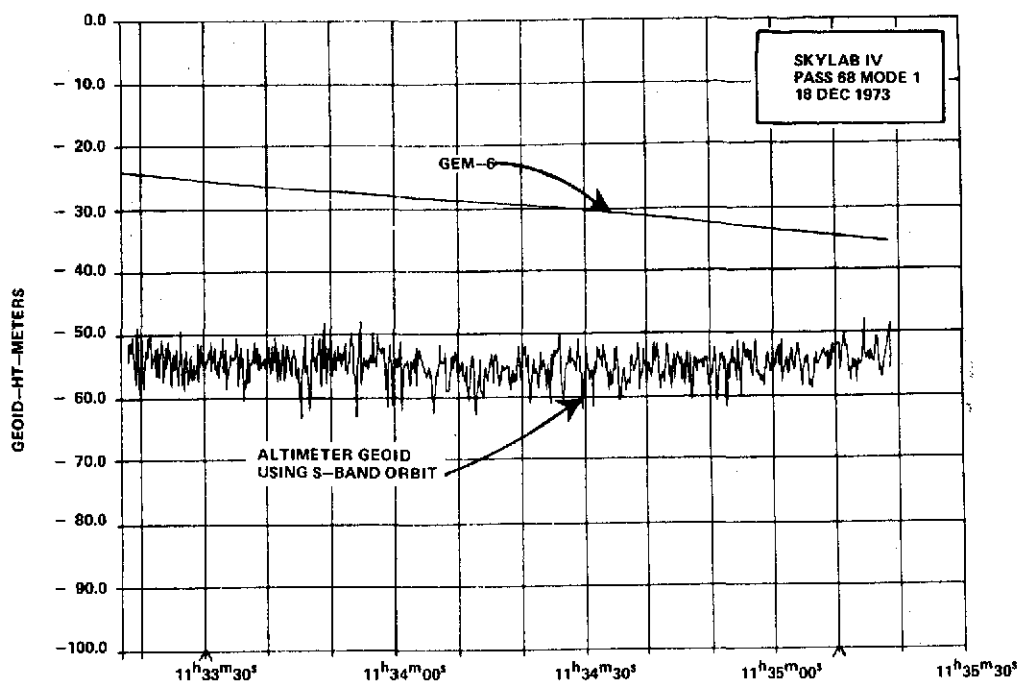
6.3°
104.7°

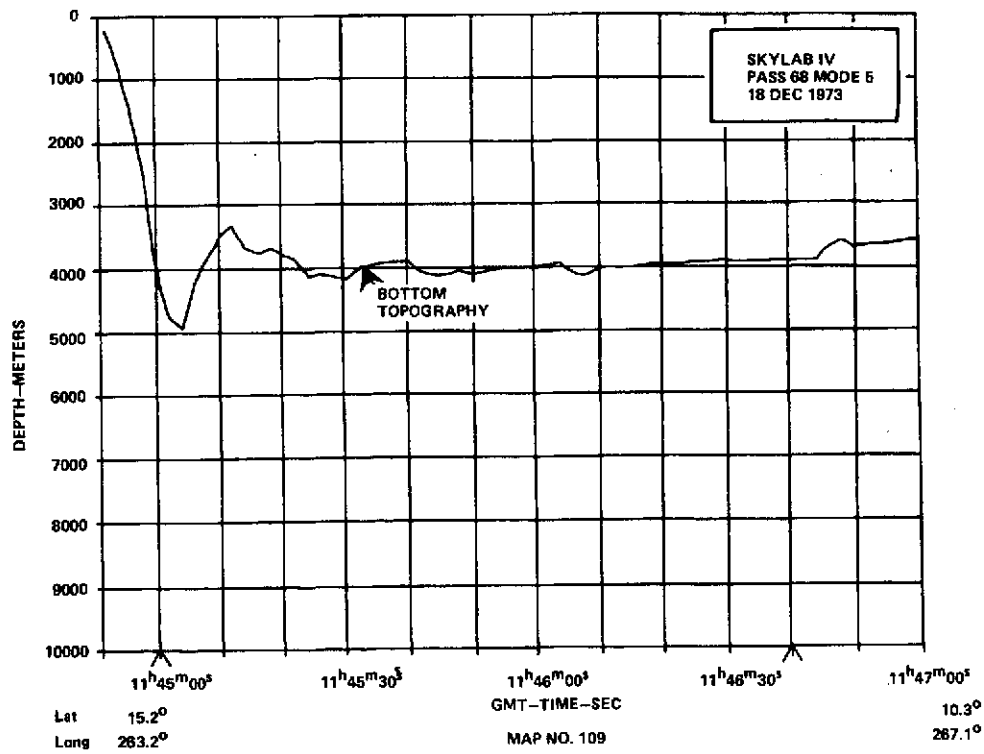
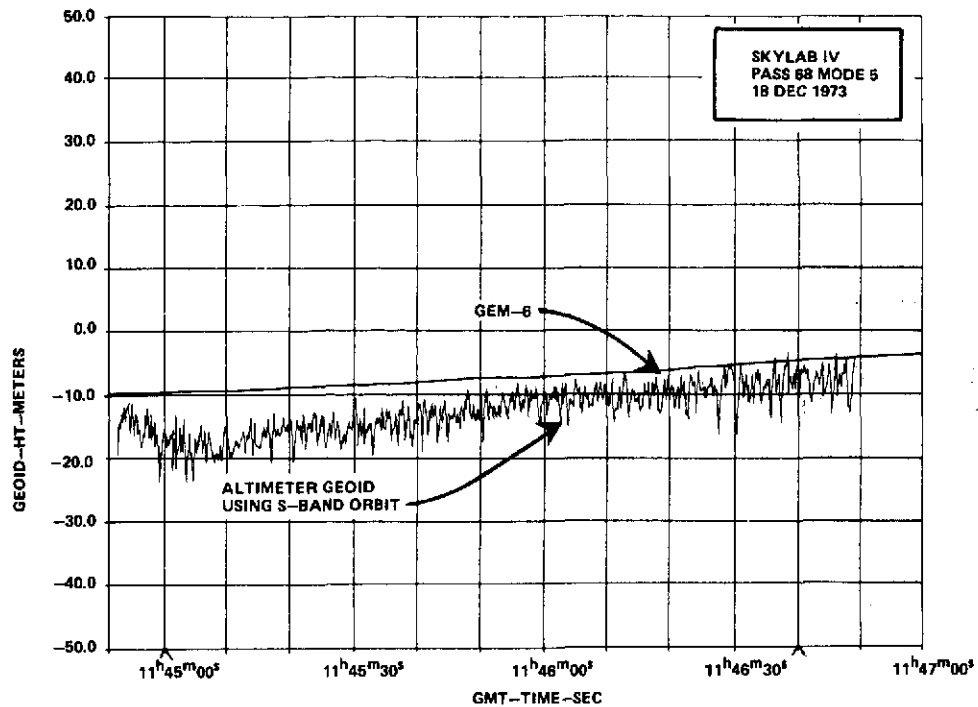


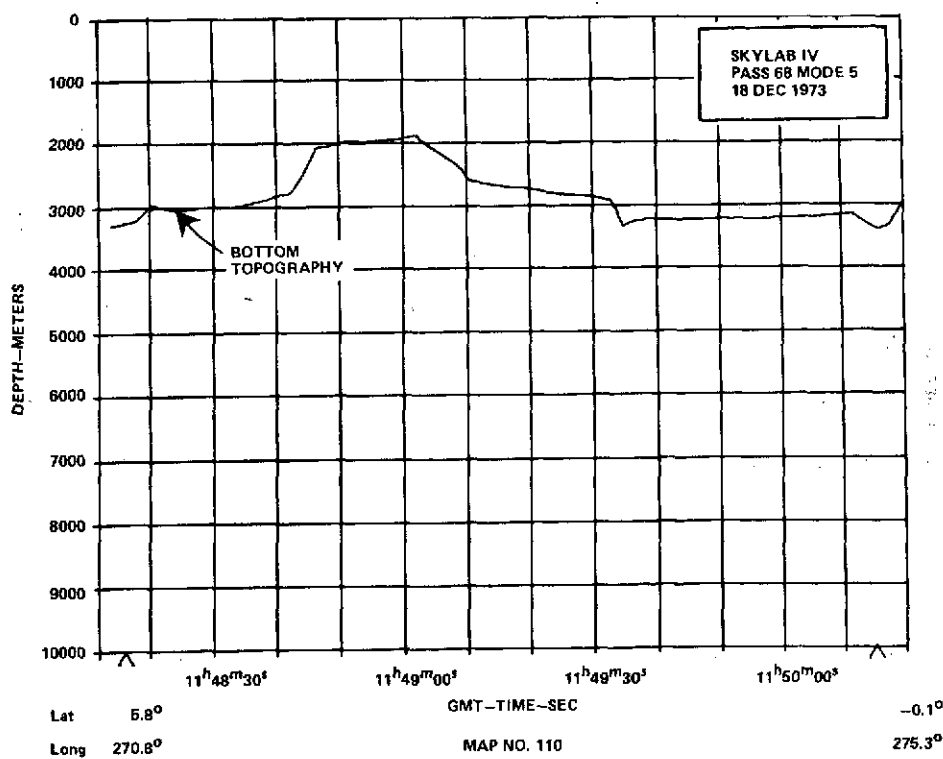
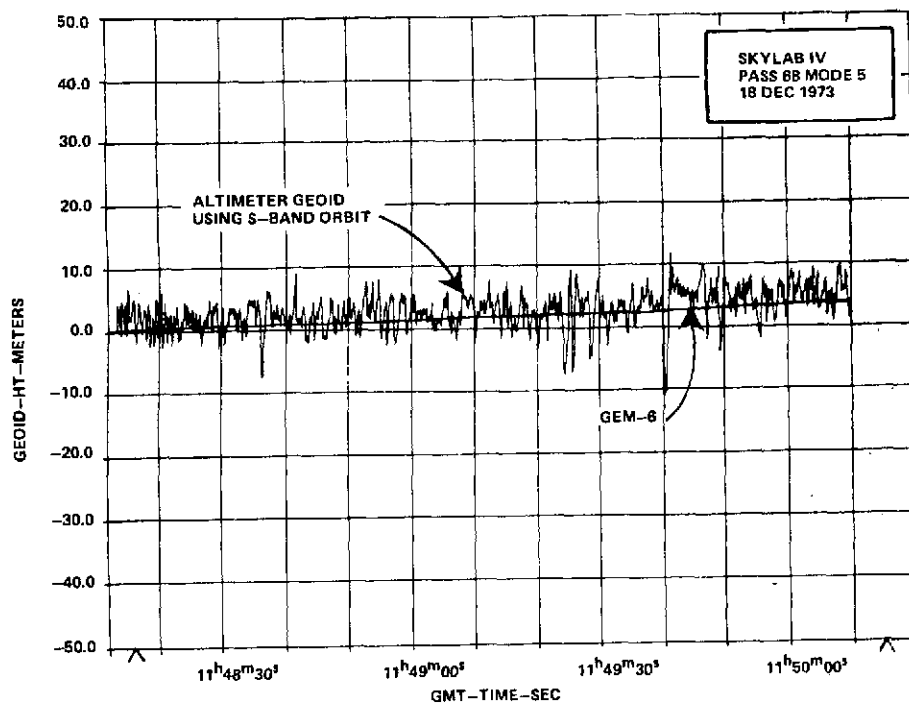


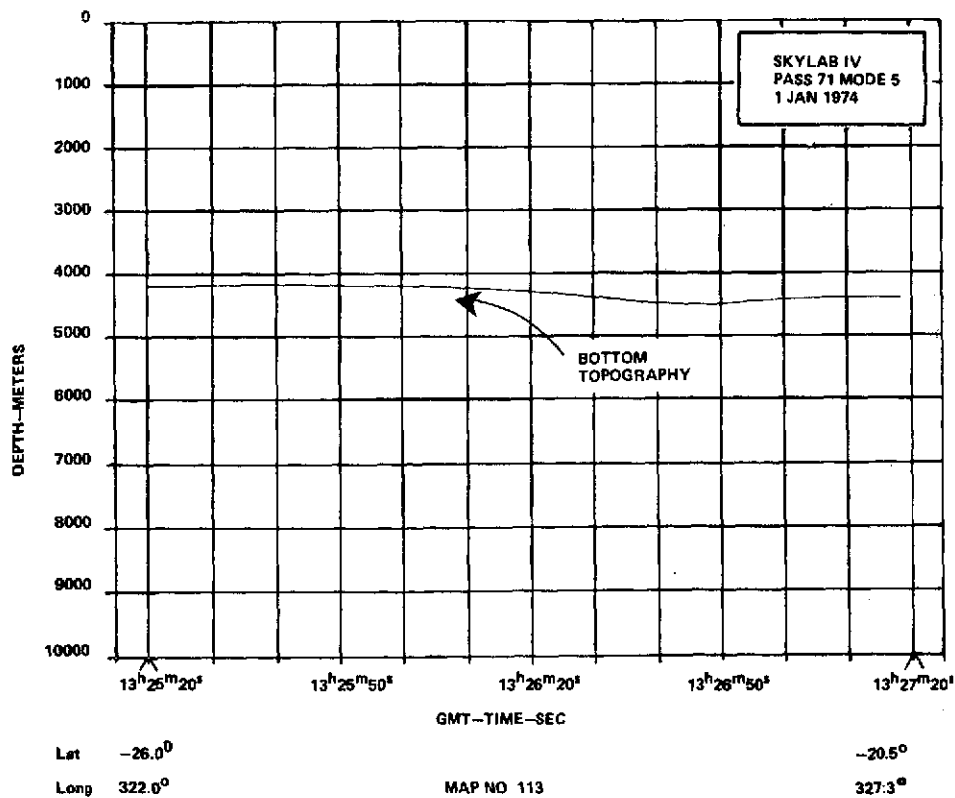
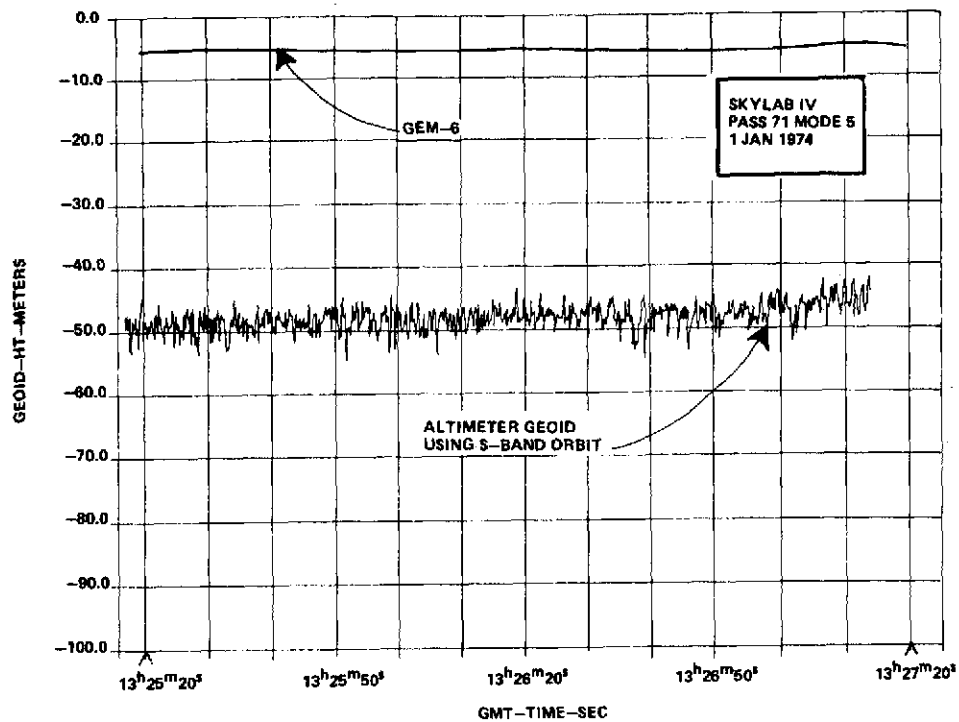


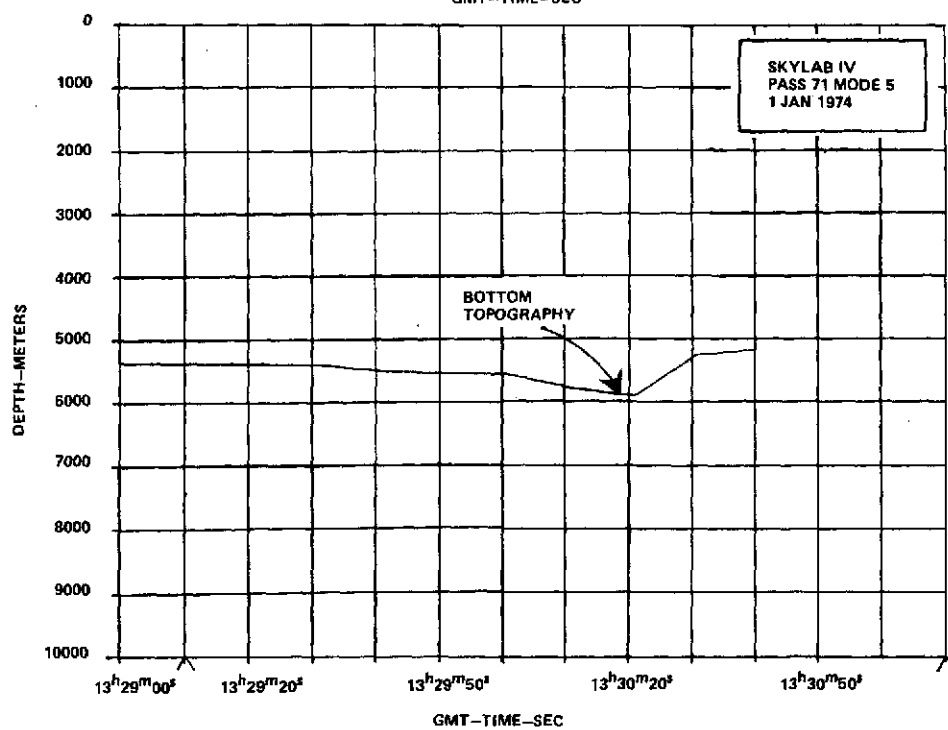
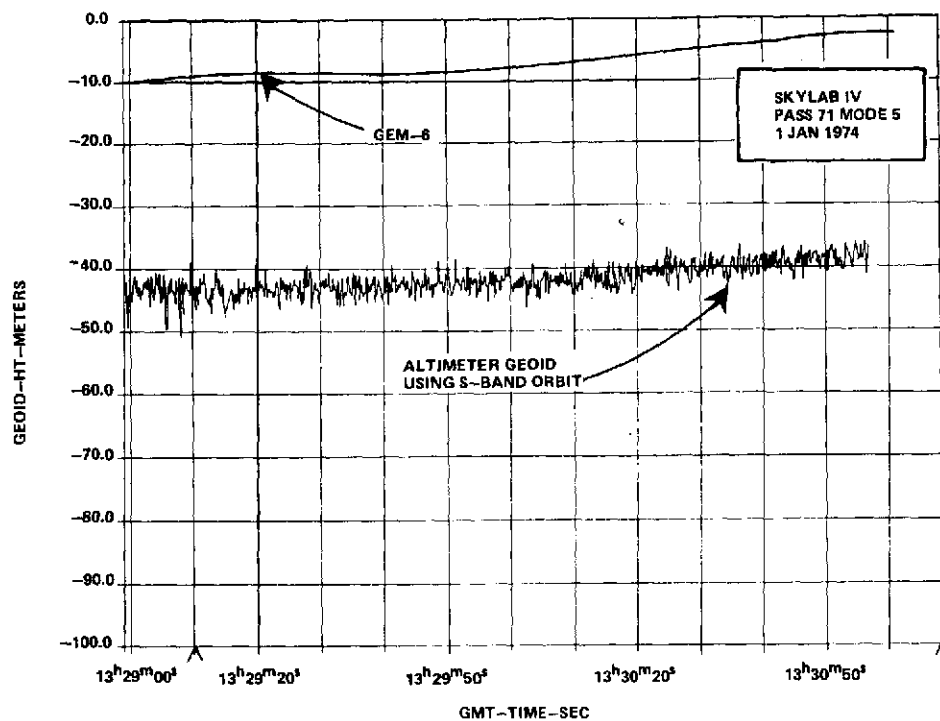








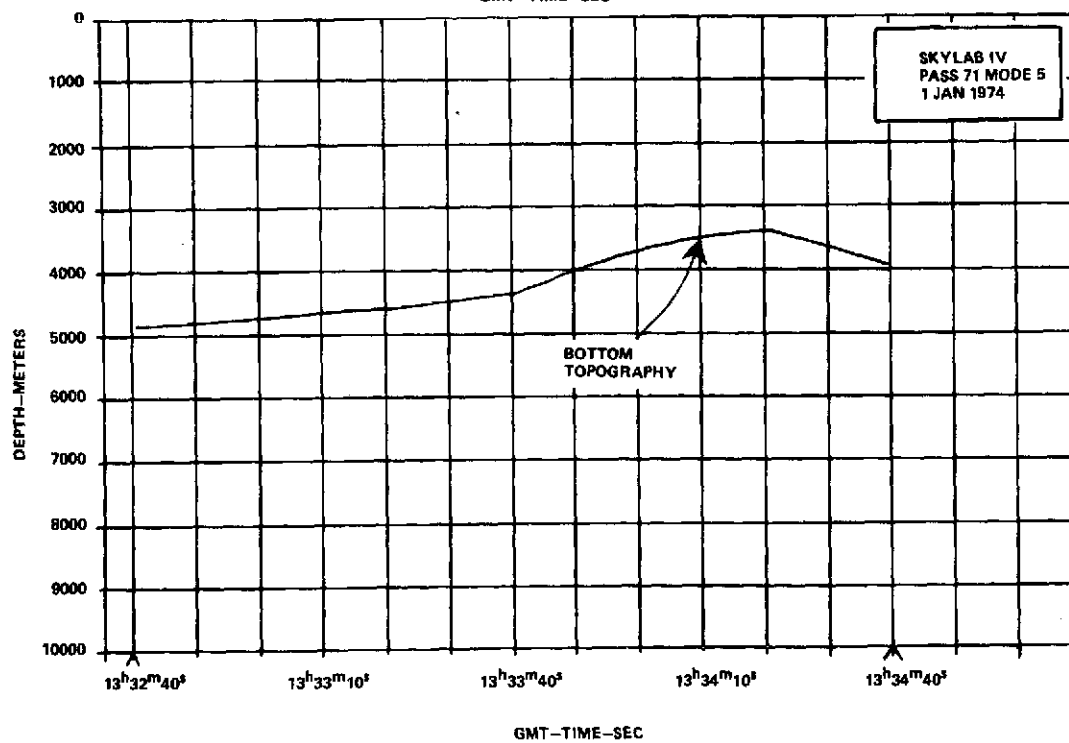
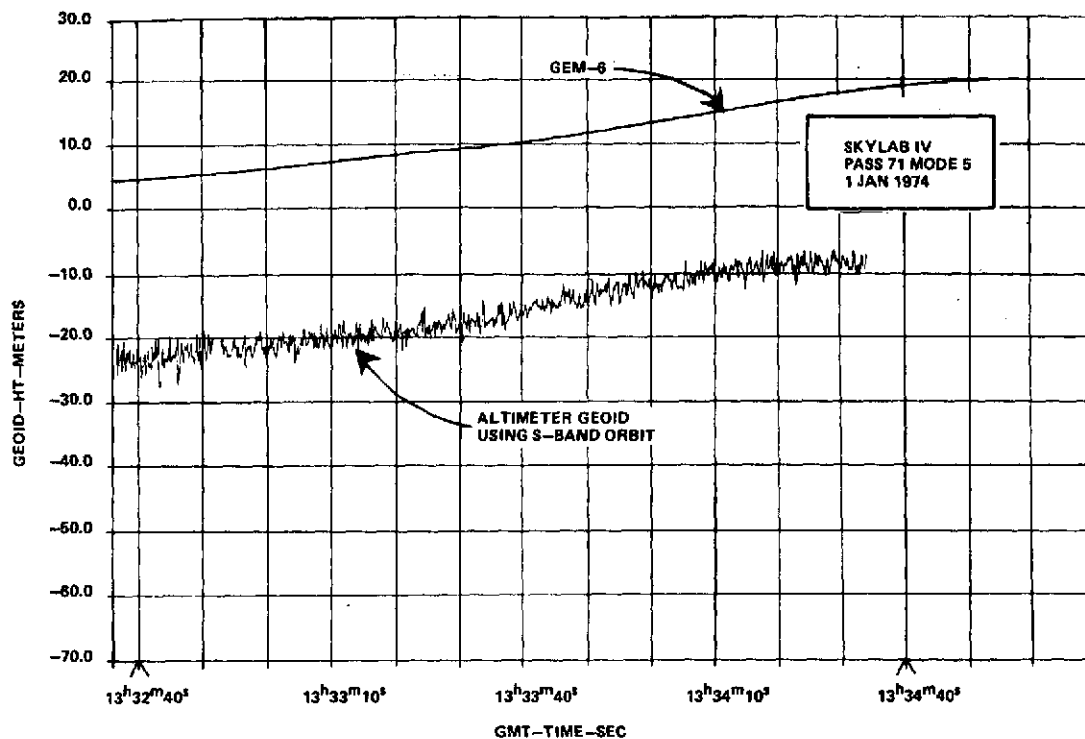




Lat -15.3°
Long 331.9°

MAP NO. 114

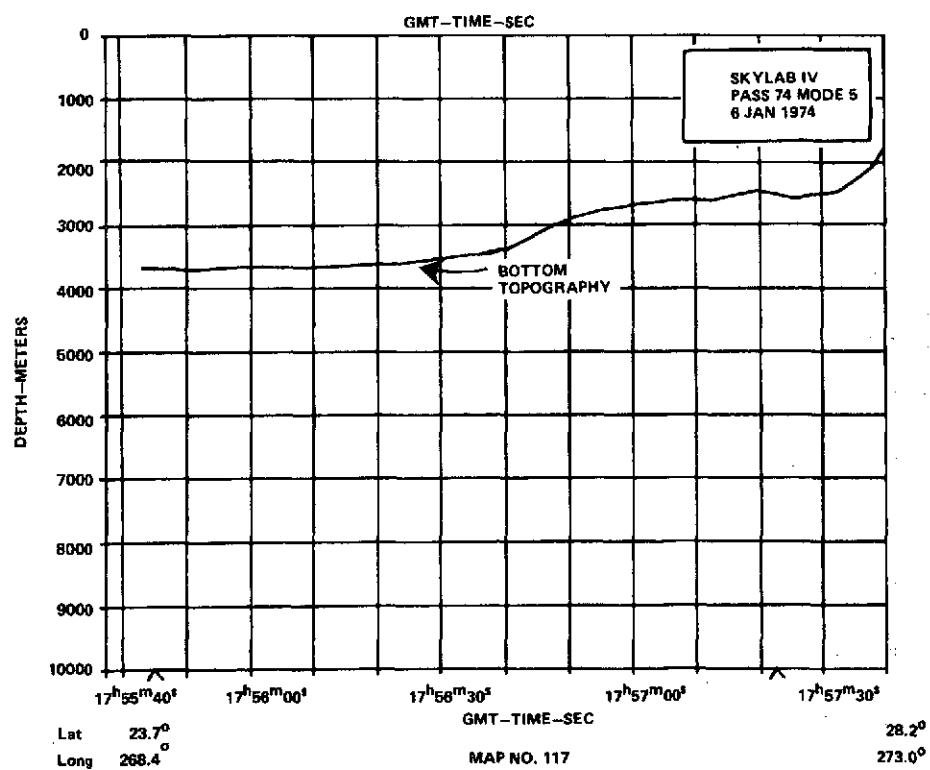
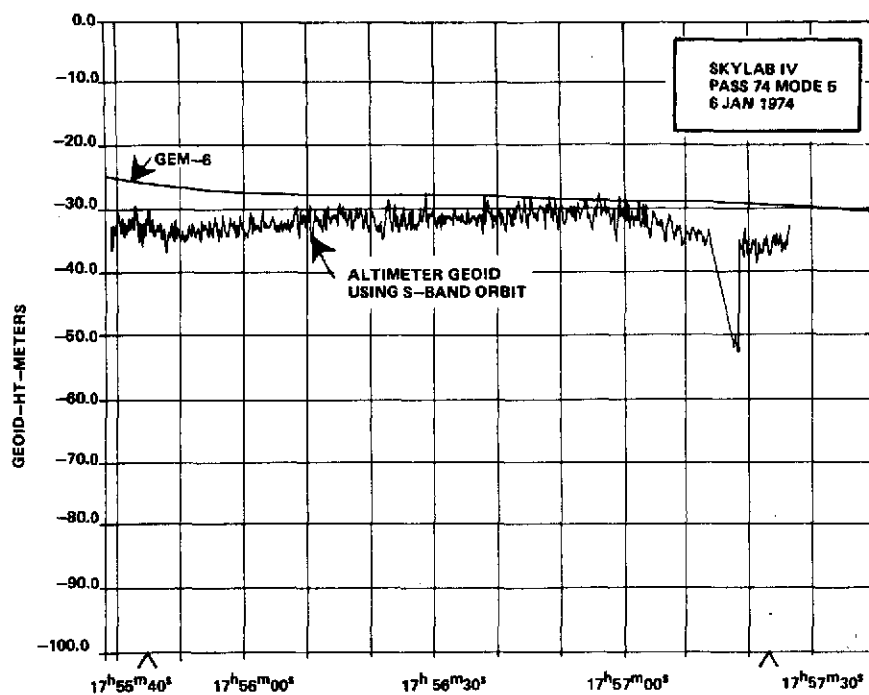
- 9.5°
336.6°

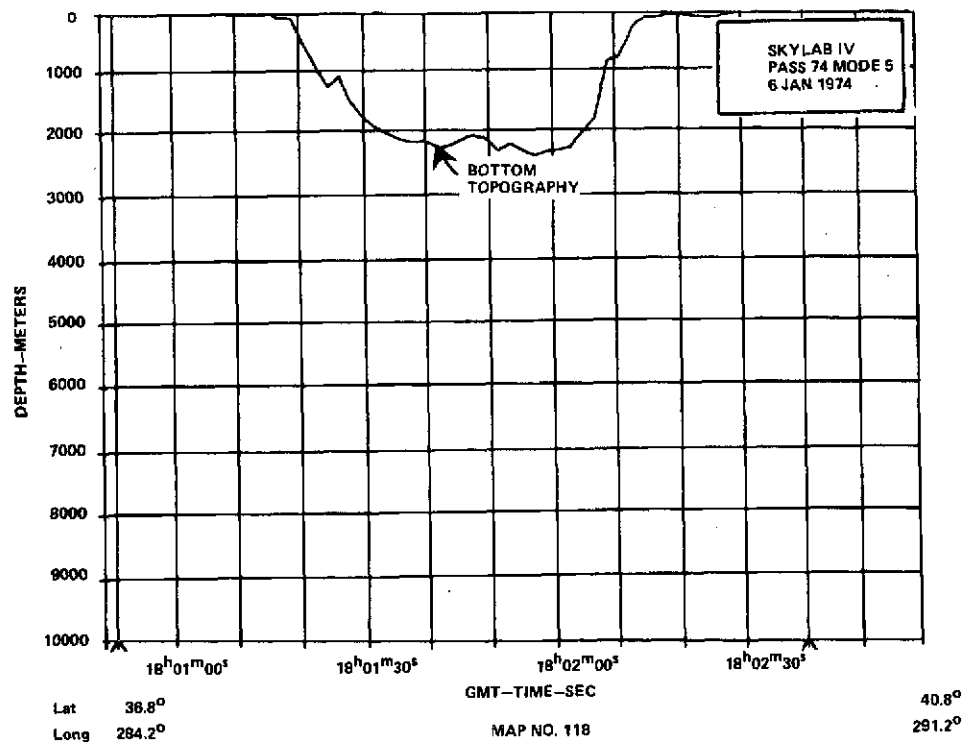
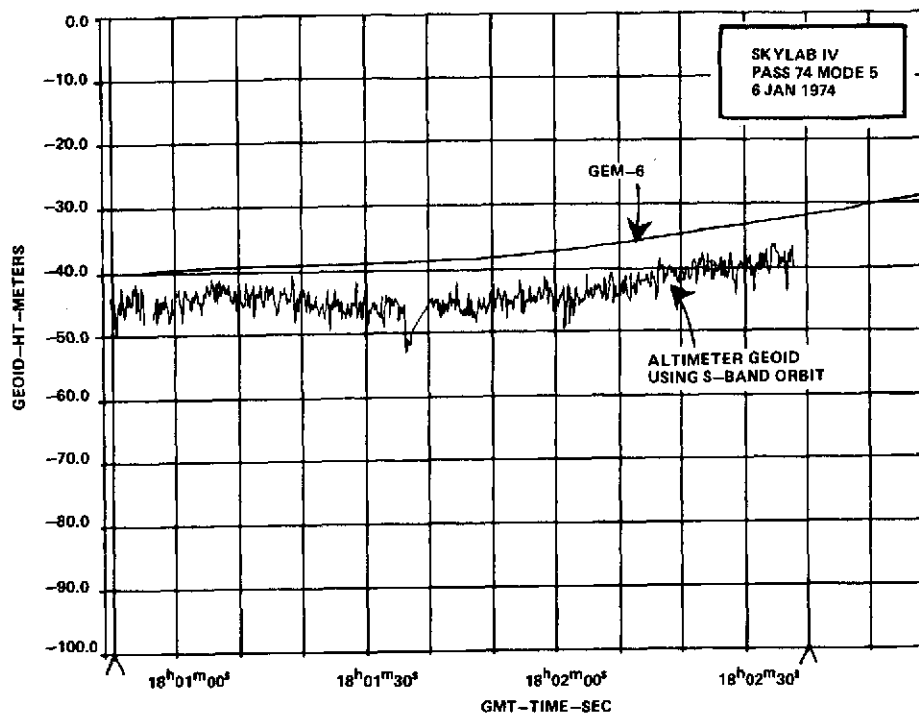


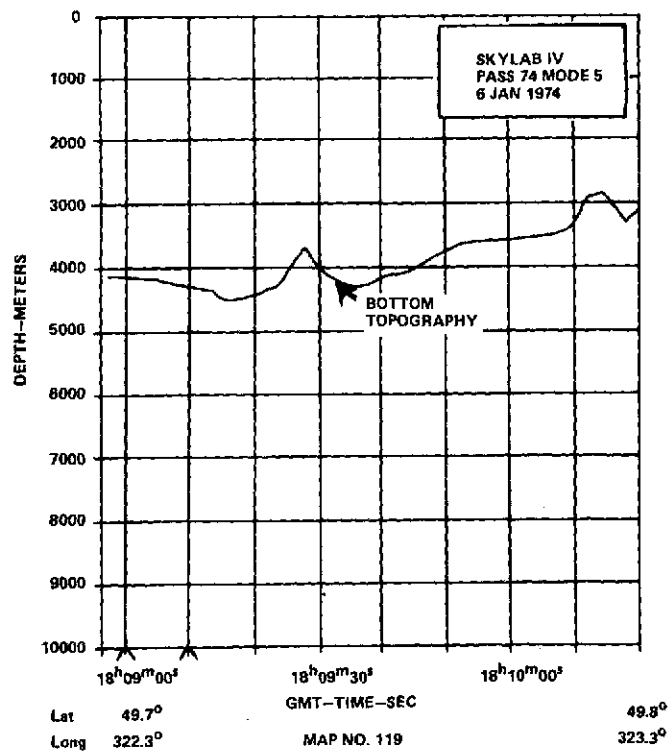
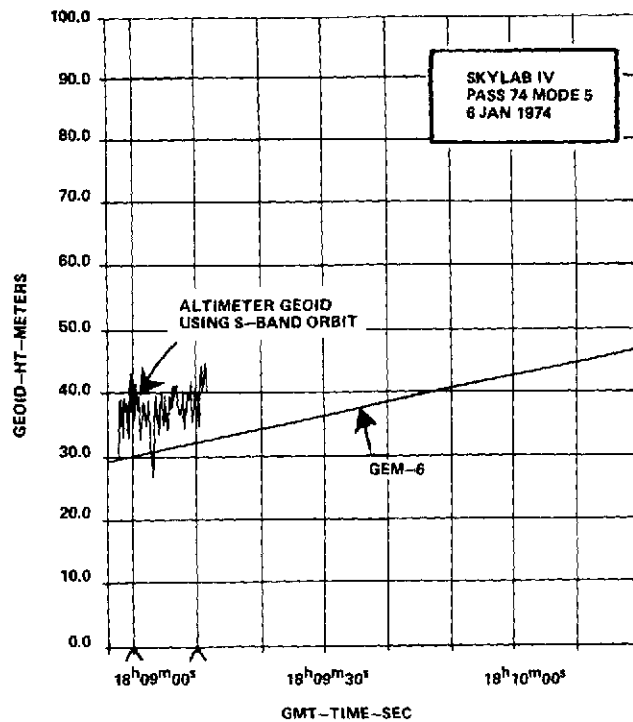
Lat -5.0
Long 340.0°

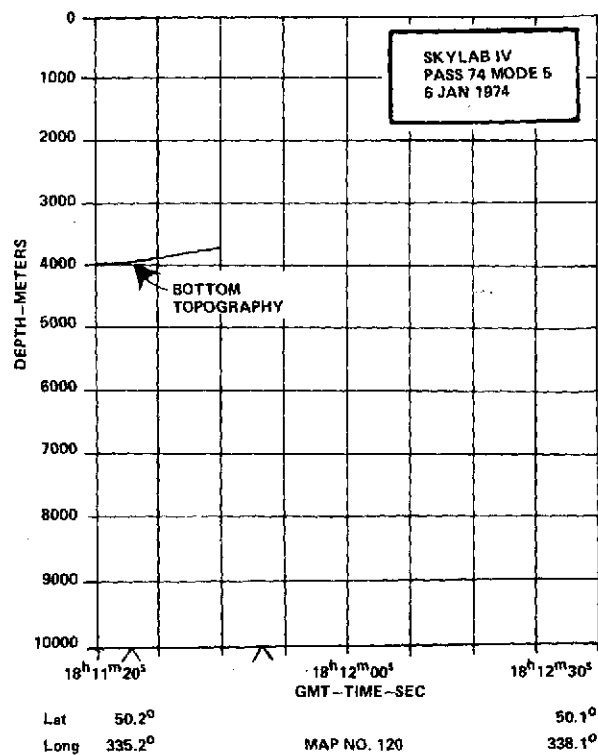
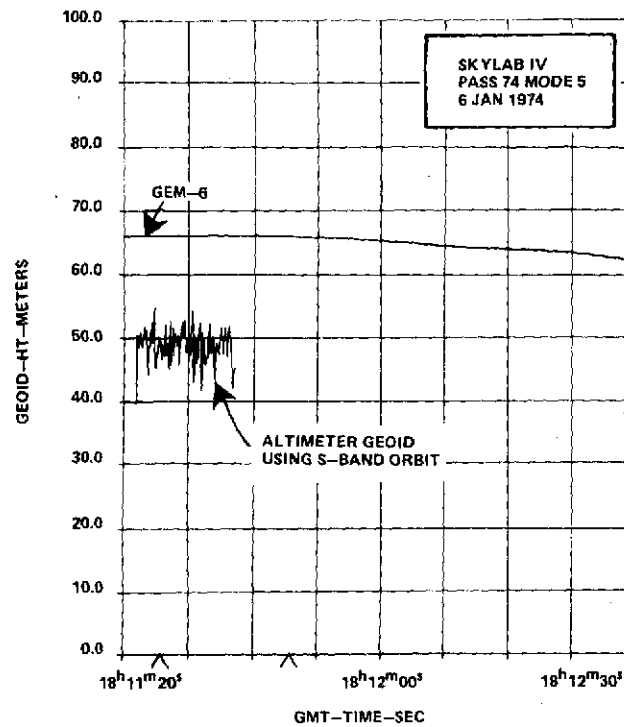
MAP NO. 115

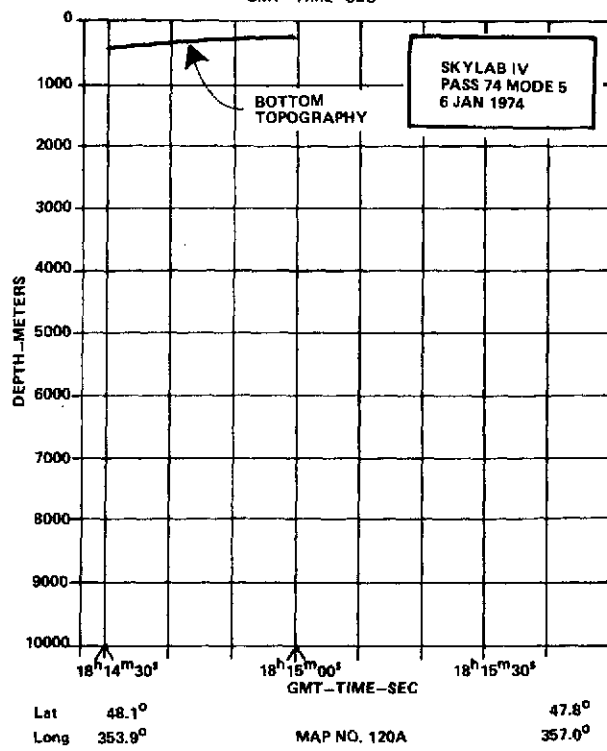
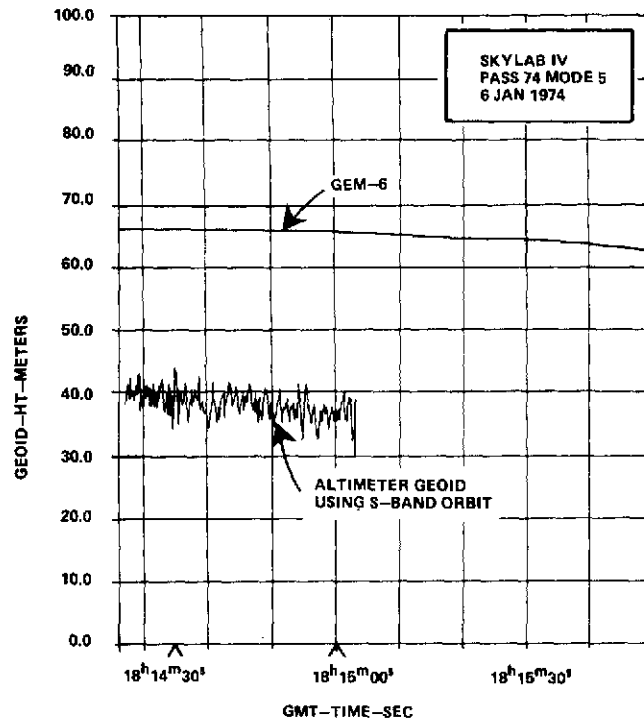
0.9°
344.4°

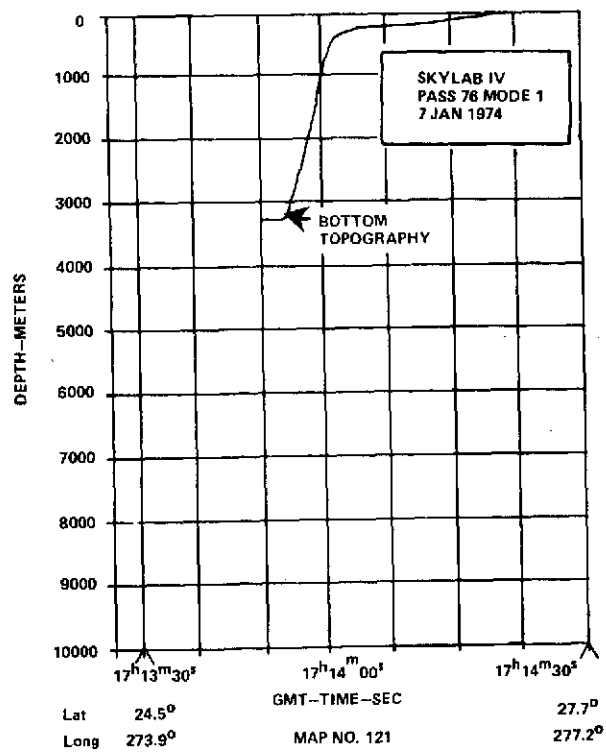
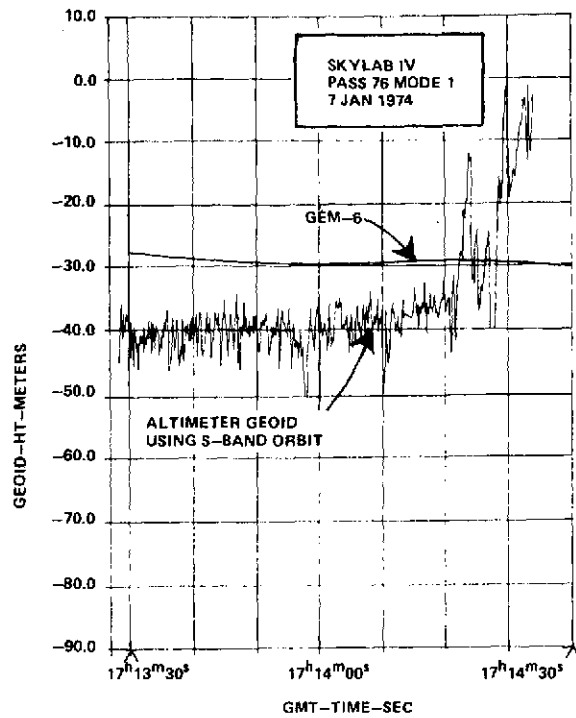


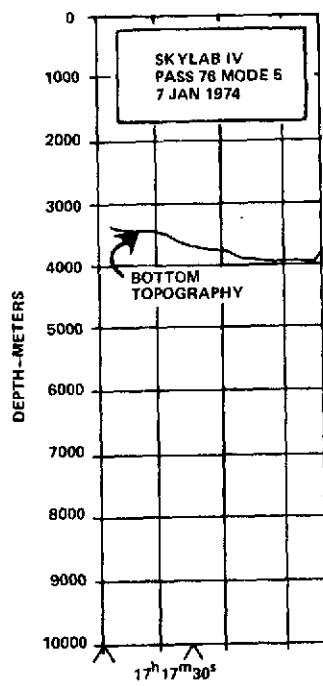
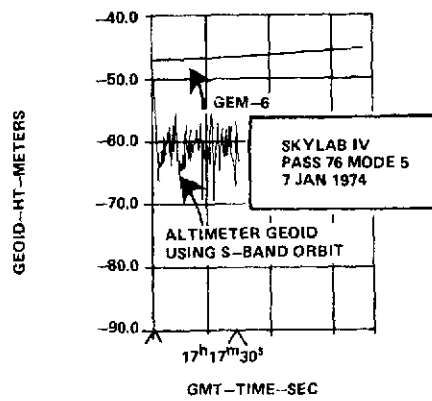




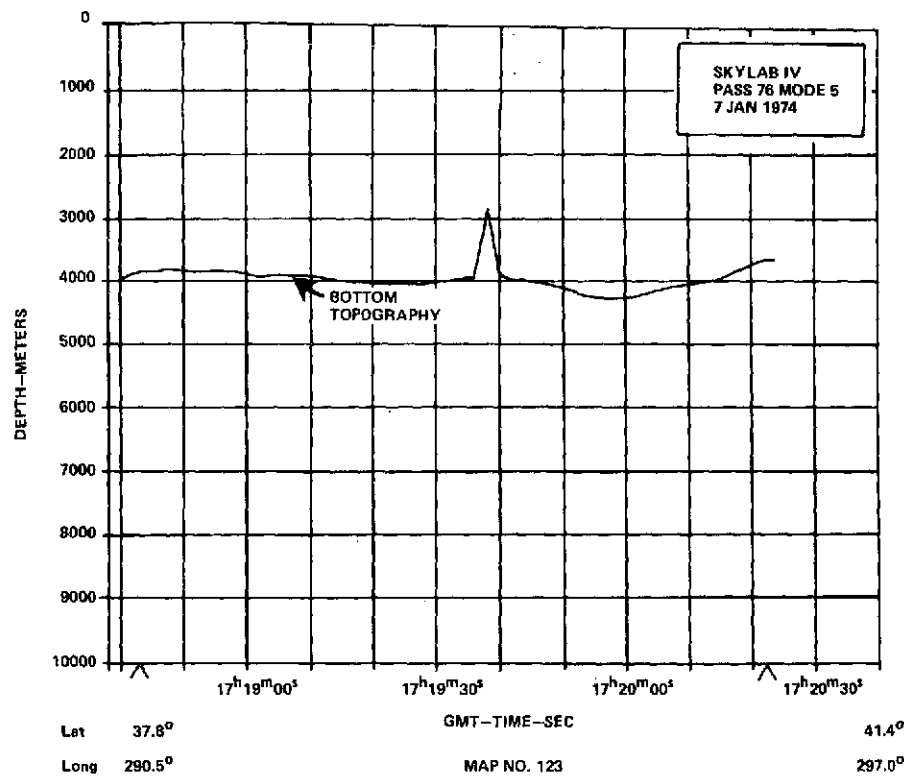
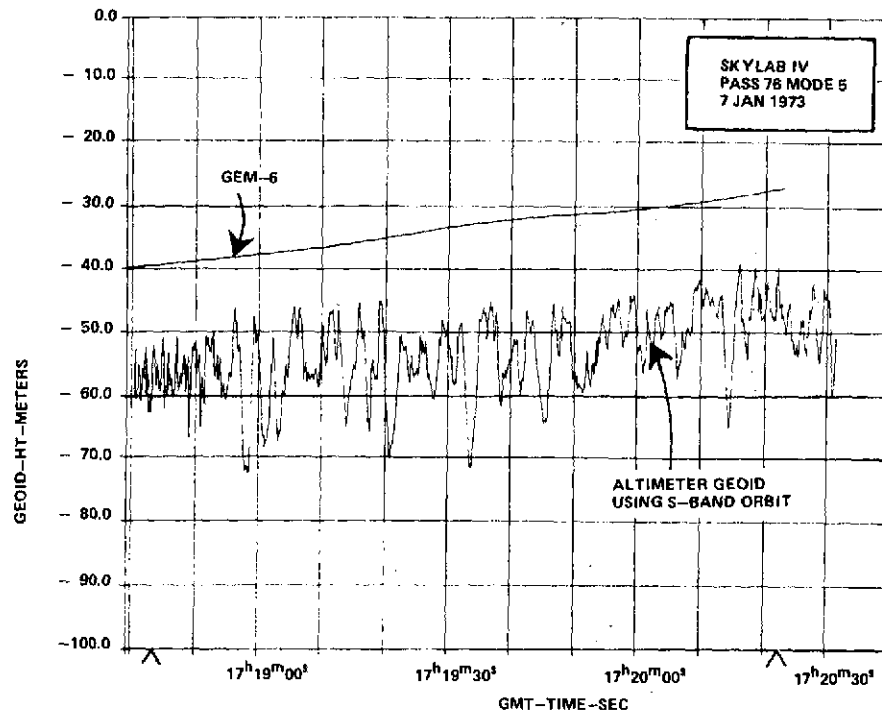


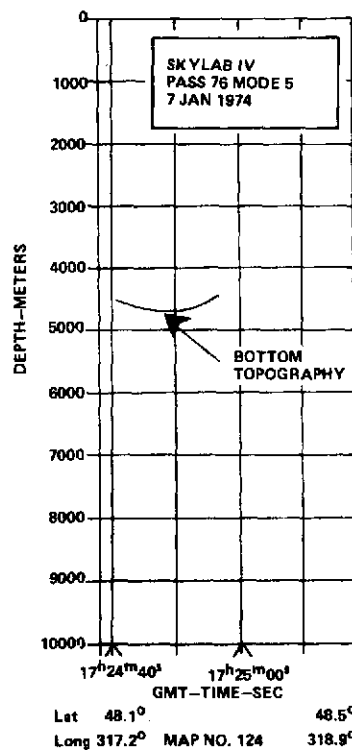
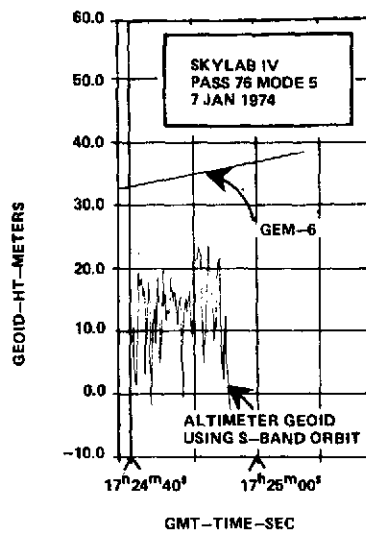


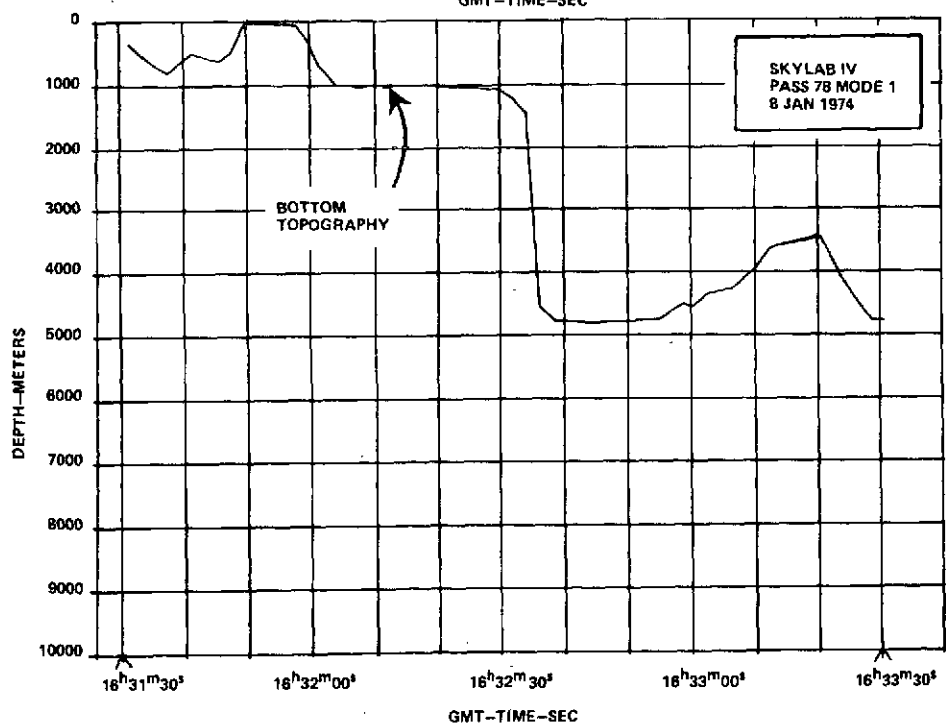
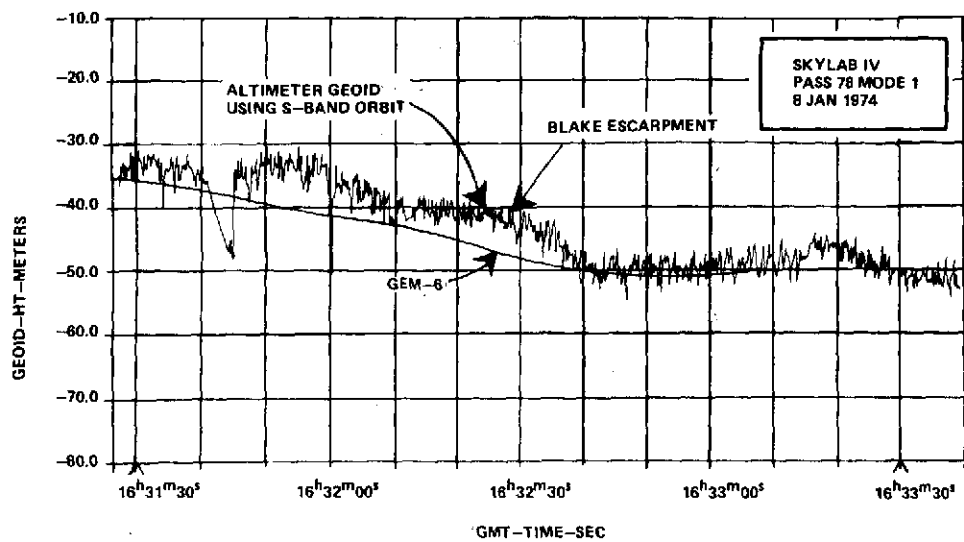




| | | | |
|------|--------|---------------|--------|
| Lat | 34.6° | GMT-TIME--SEC | 35.0° |
| Long | 285.7° | MAP NO. 122 | 286.3° |



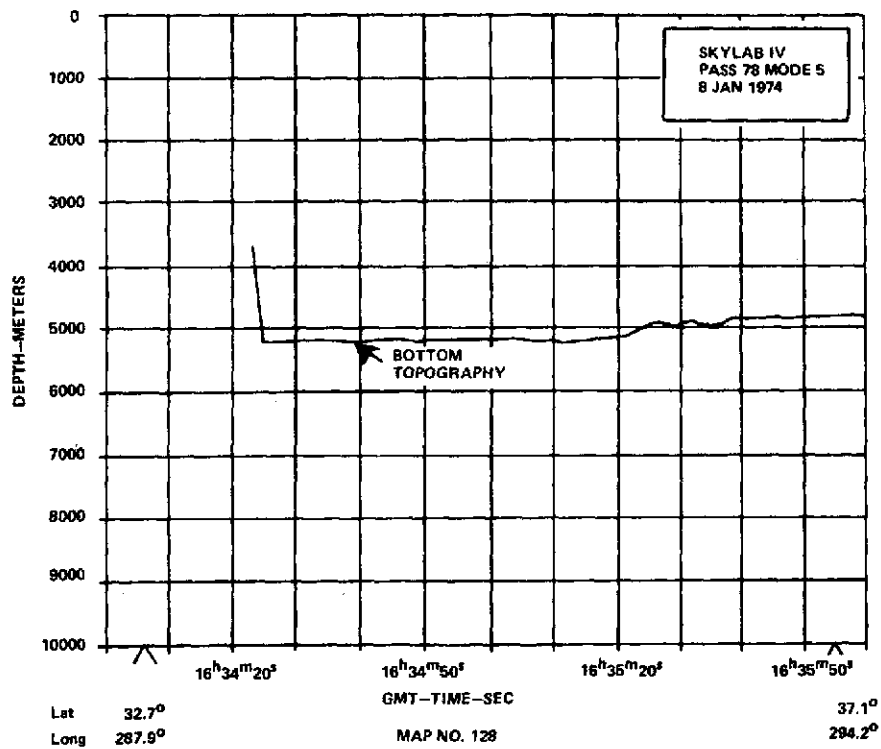
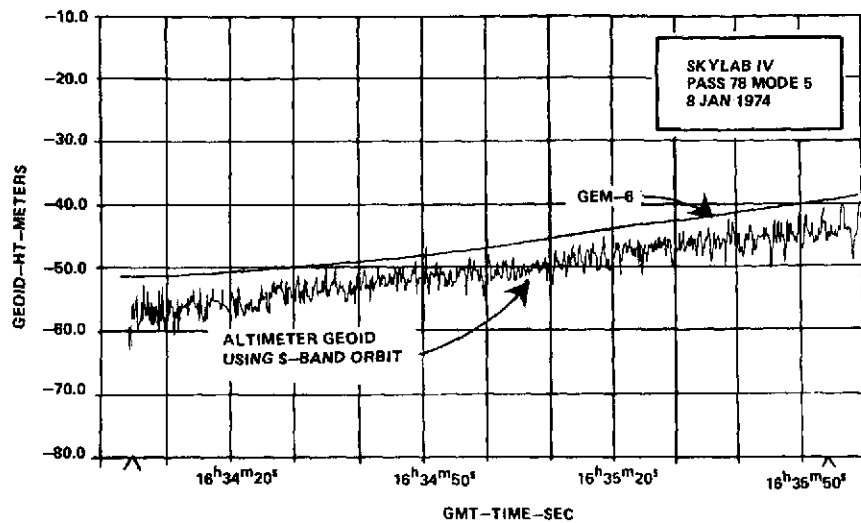


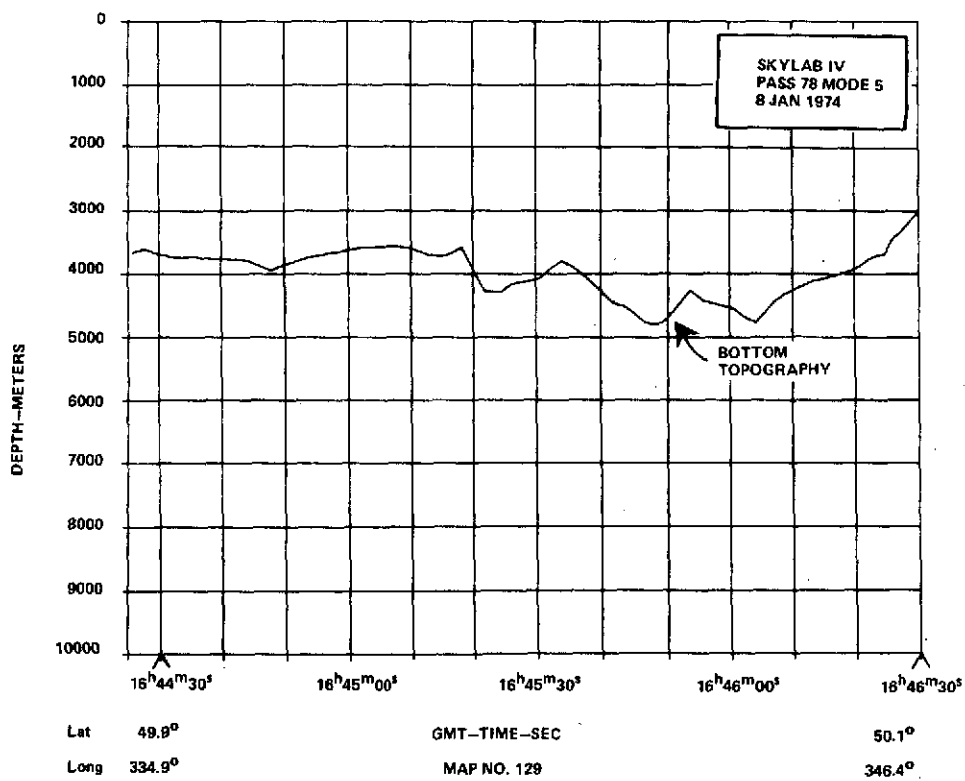
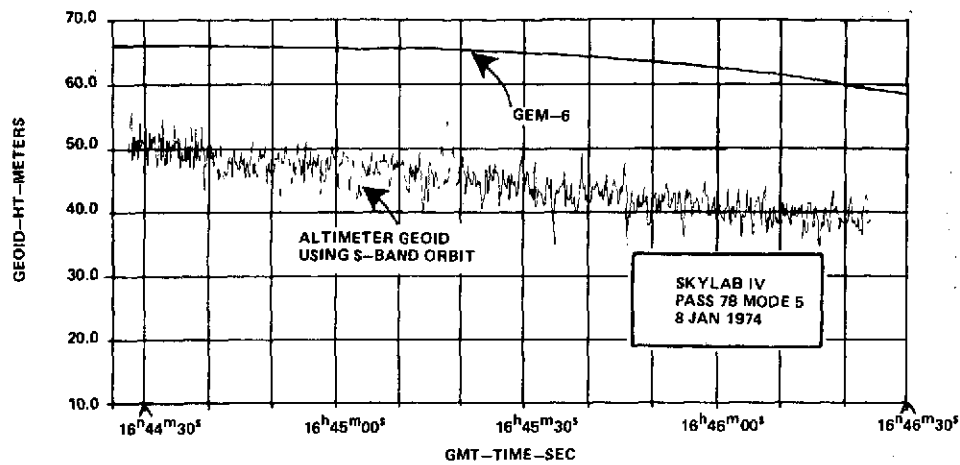


Lat 26.0°
Long 280.1°

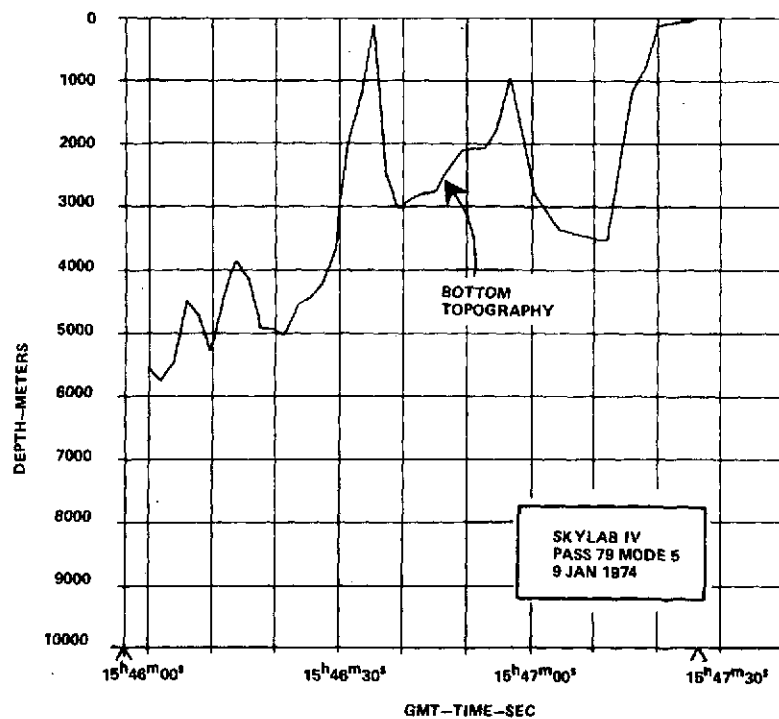
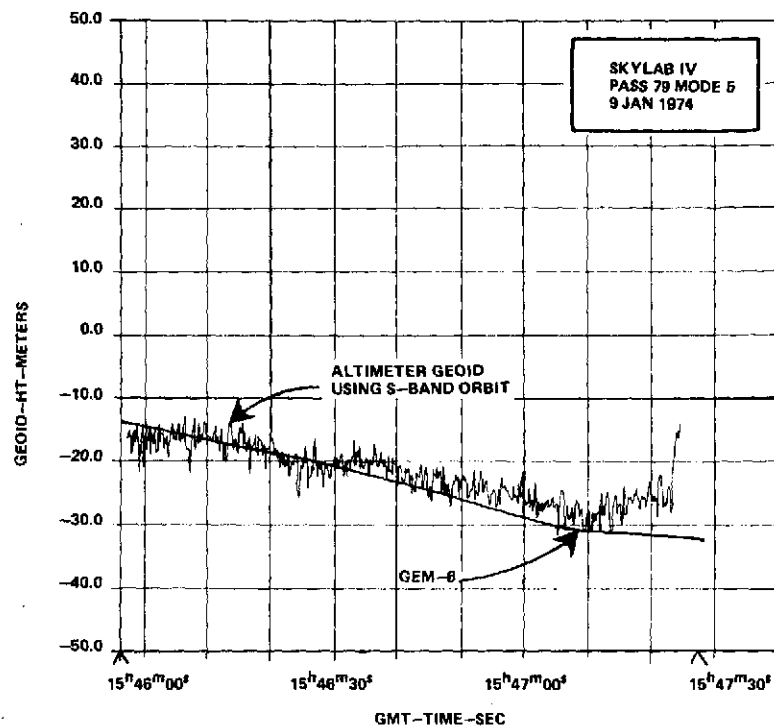
MAP NO. 127

31.3°
286.1°





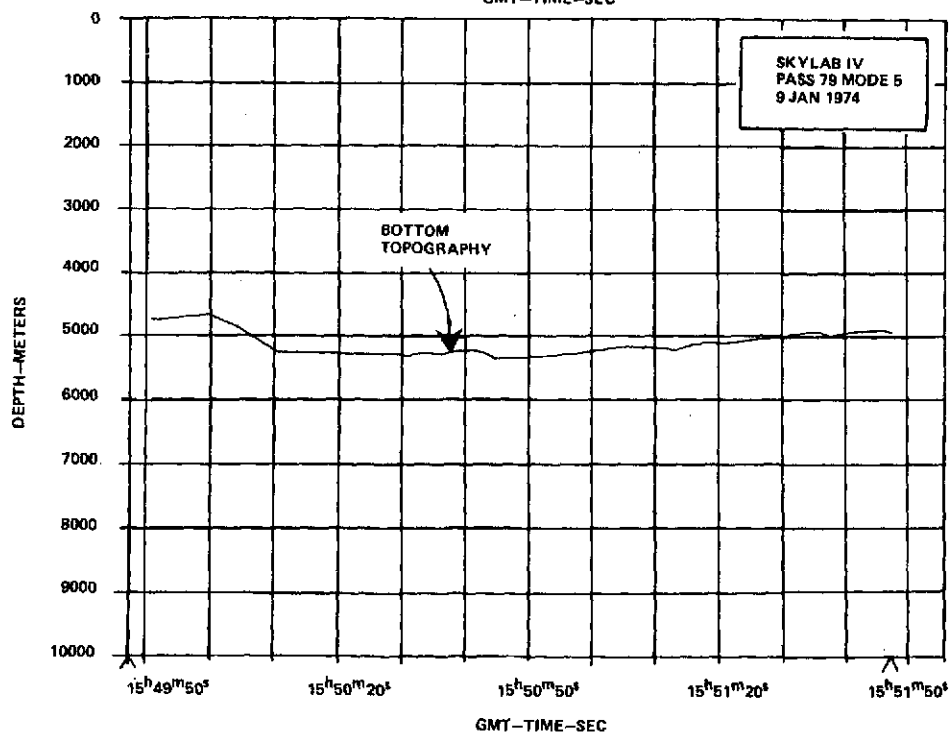
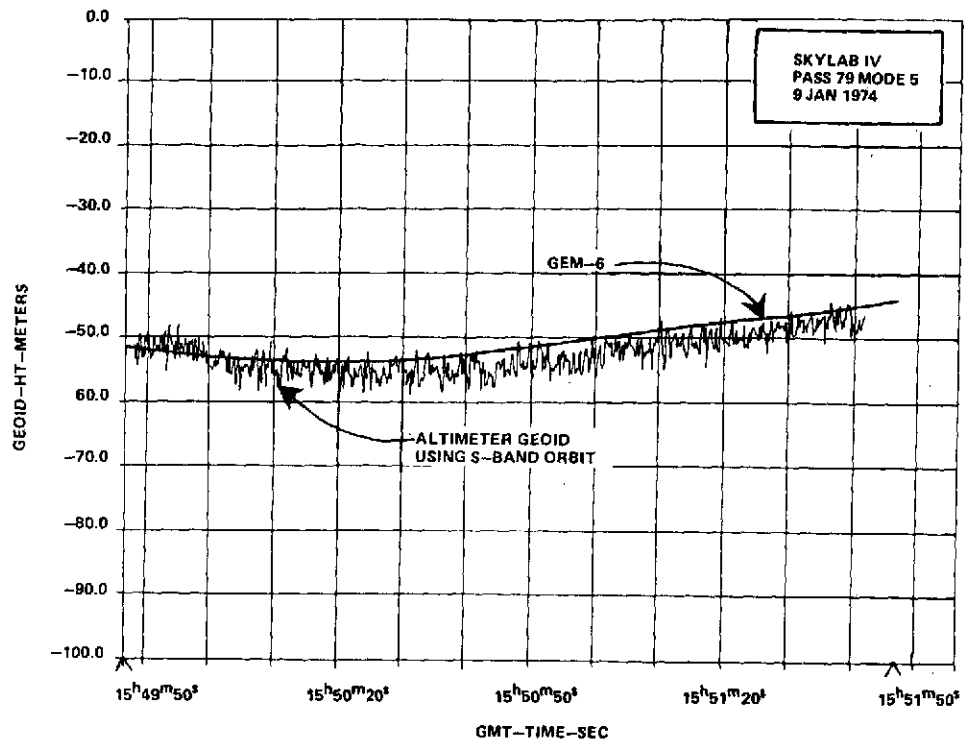
| | | | |
|------|--------|--------------|--------|
| Lat | 49.9° | GMT-TIME-SEC | 50.1° |
| Long | 334.9° | MAP NO. 129 | 346.4° |



Lat 17.5°
Long 276.9°

MAP NO. 131

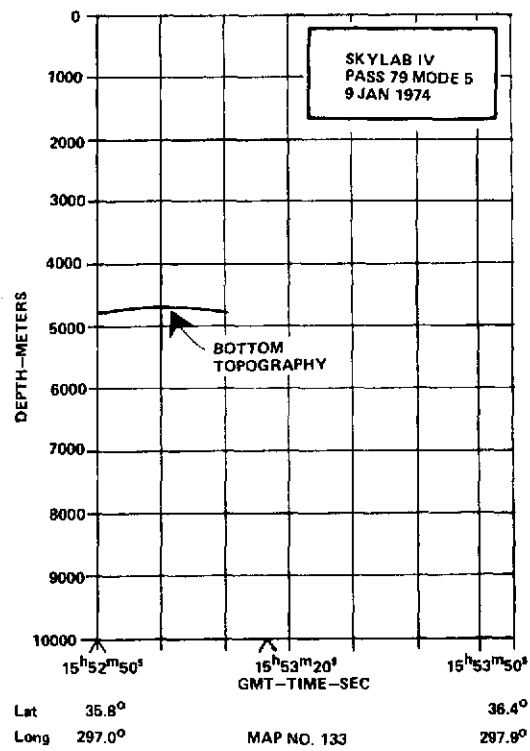
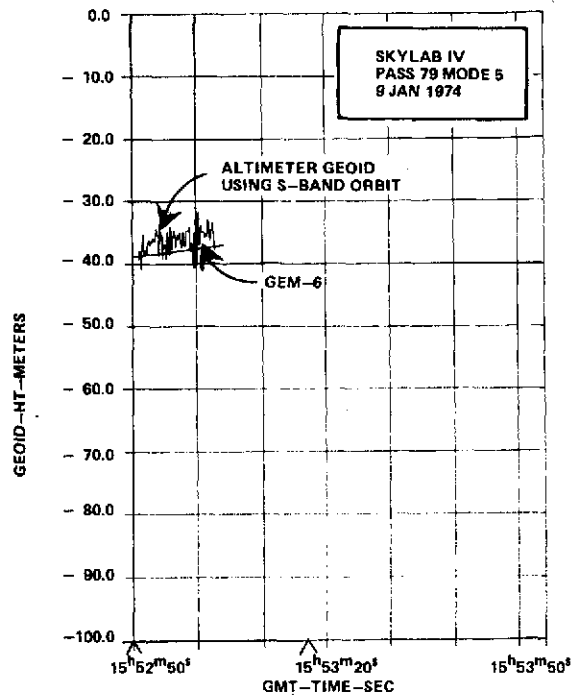
21.7°
280.7°

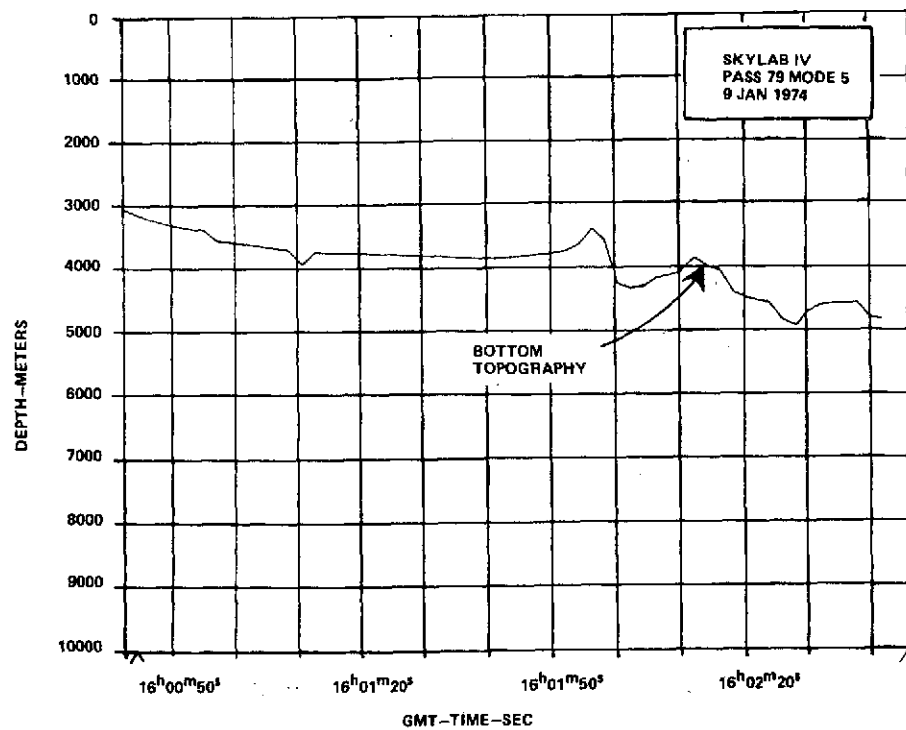
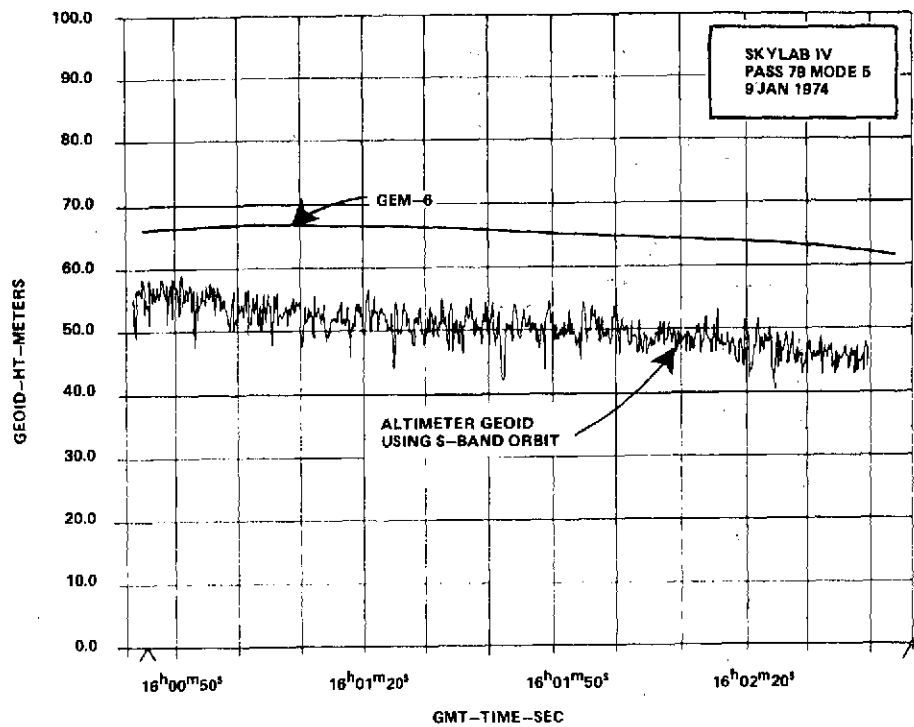


Lat 28.1°
Long 287.2°

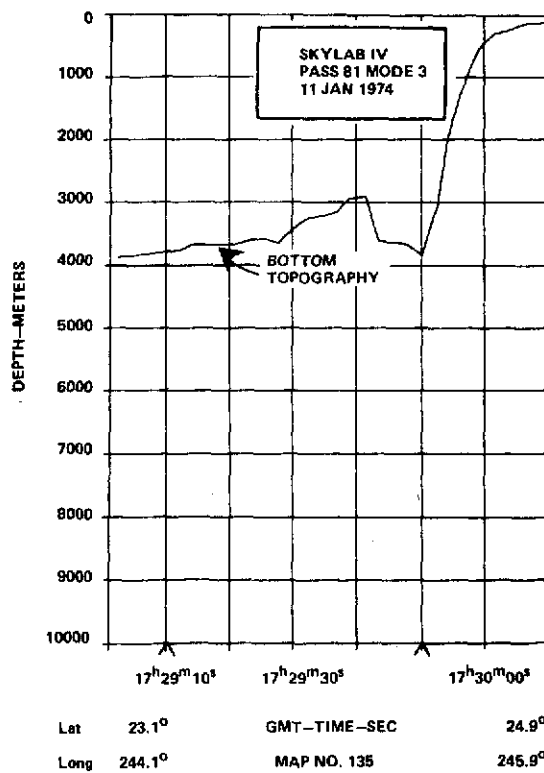
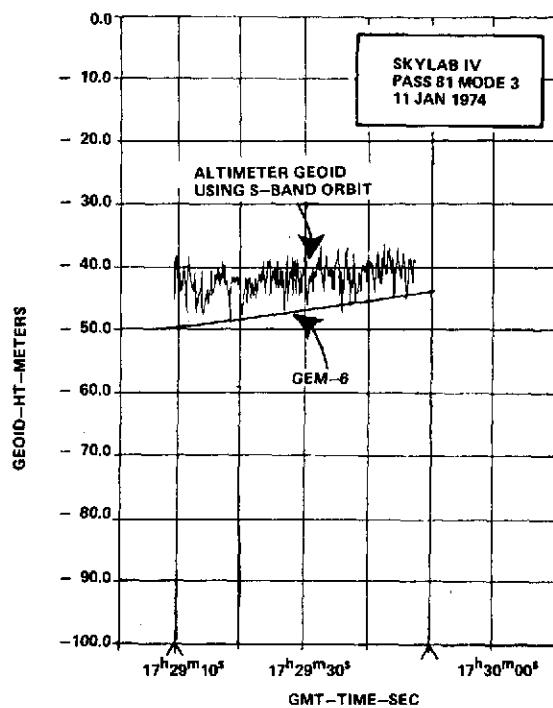
MAP NO. 132

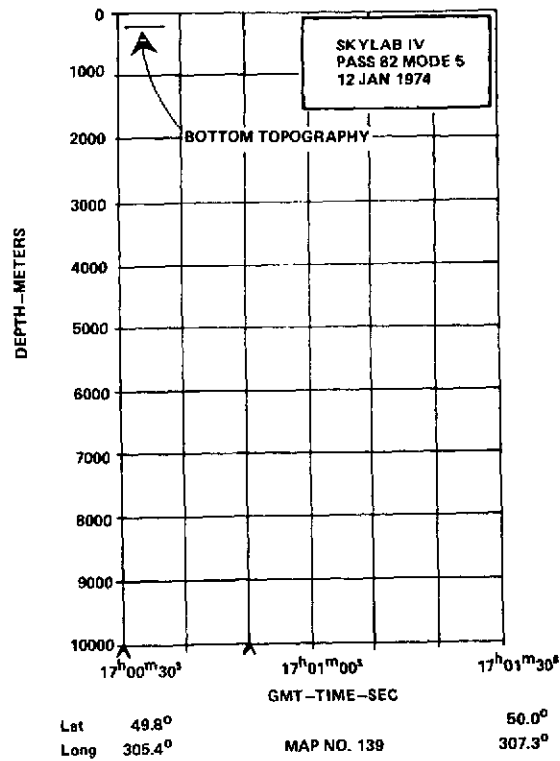
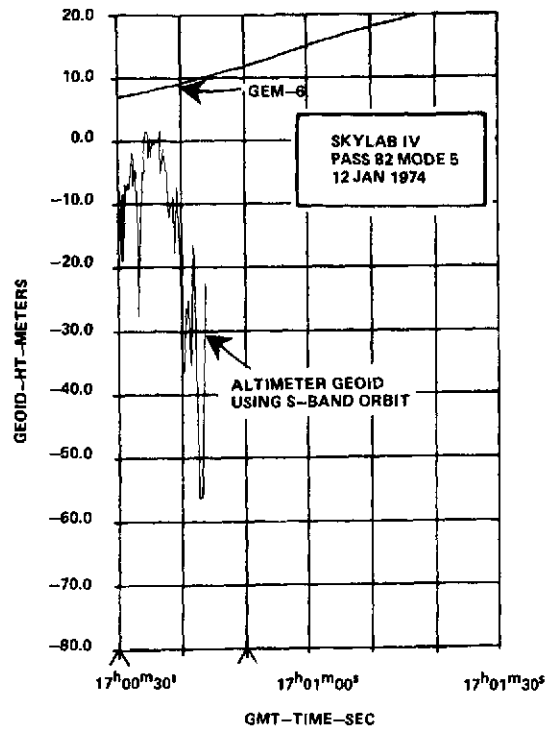
33.3°
293.4°

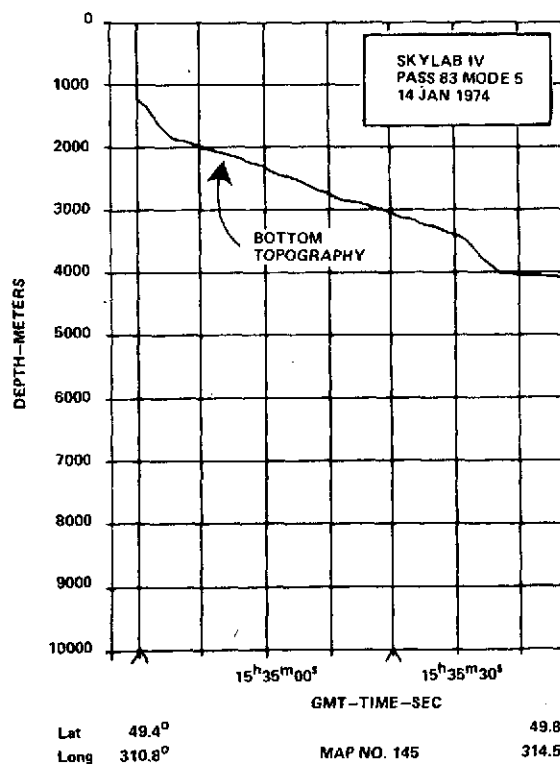
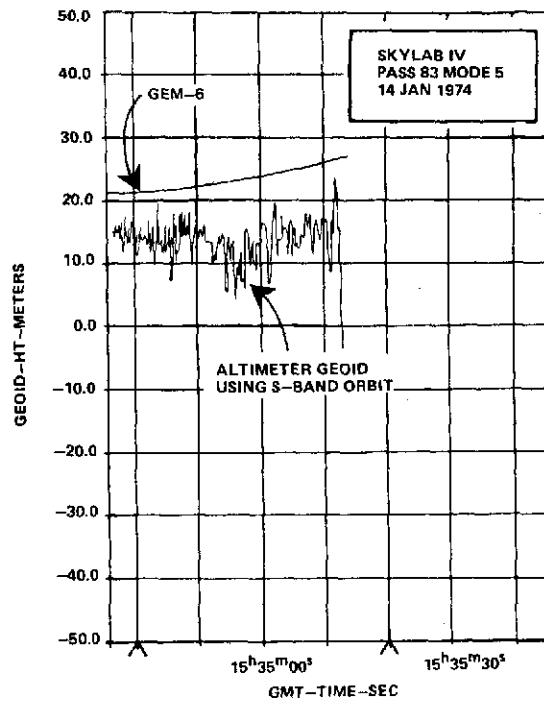




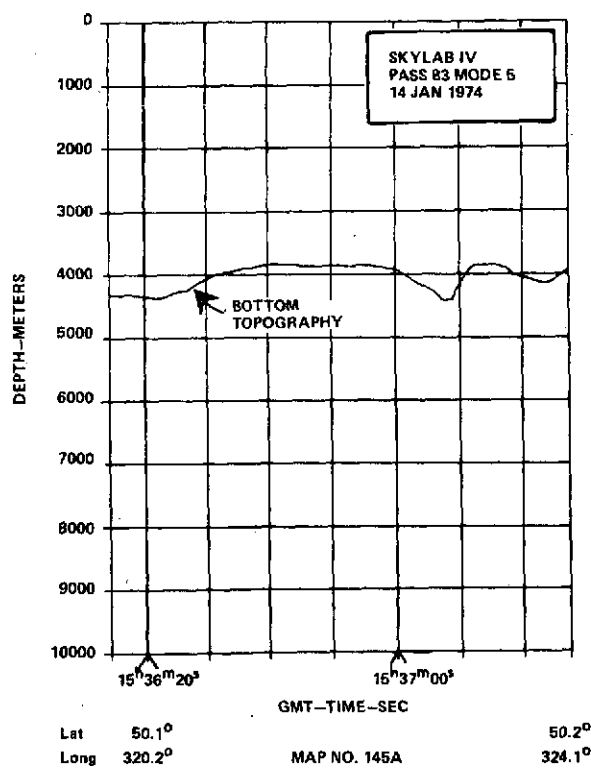
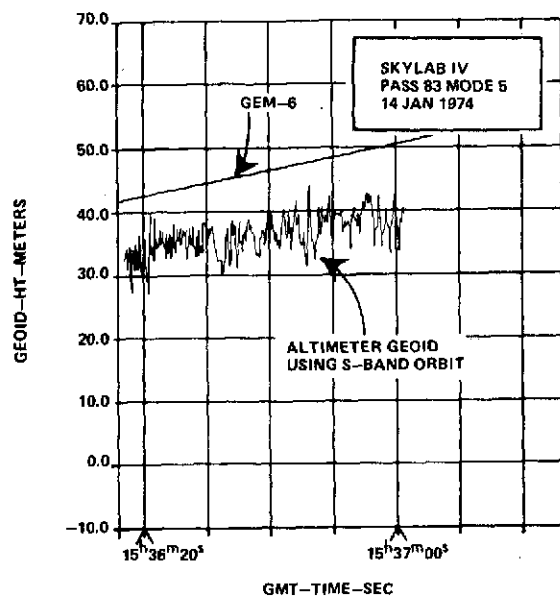
| | | | |
|------|--------|-------------|--------|
| Lat | 49.2° | | 50.2° |
| Long | 332.8° | MAP NO. 134 | 344.1° |

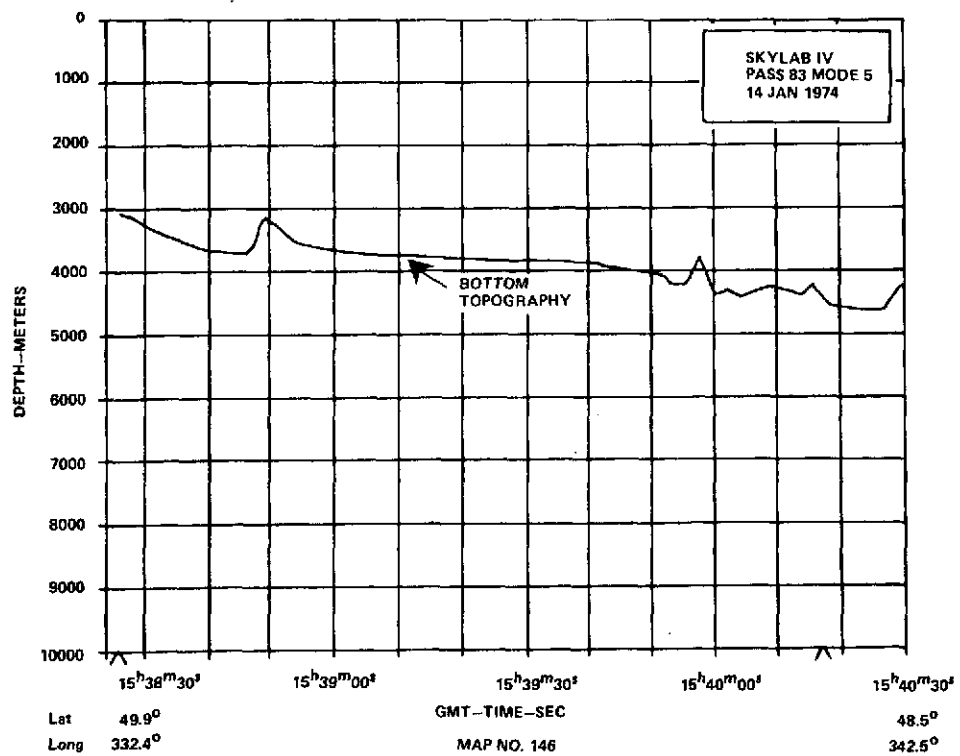
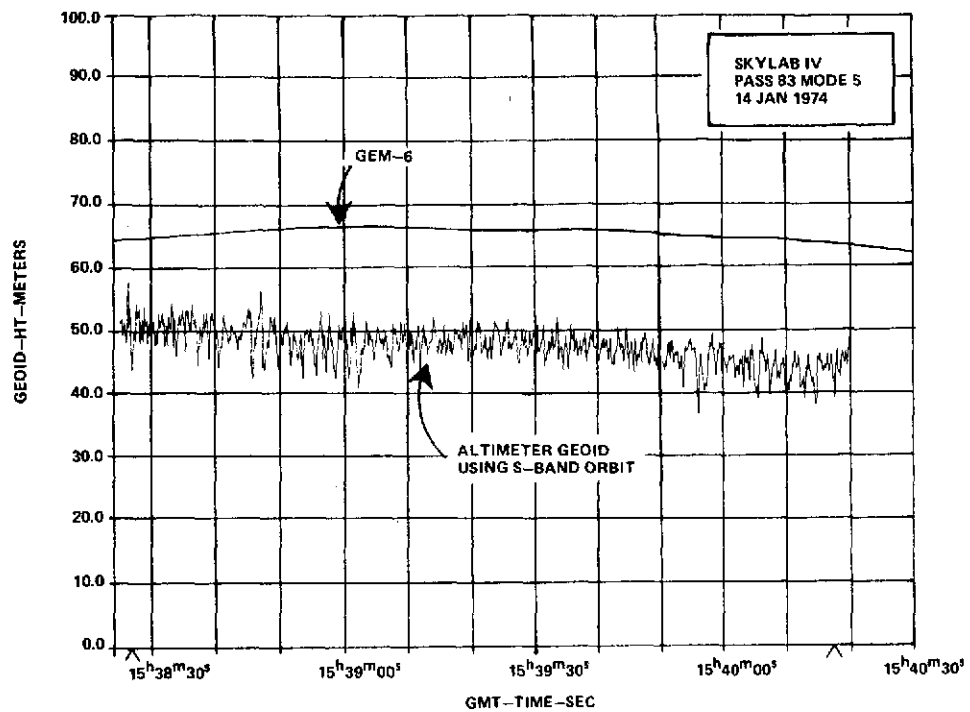


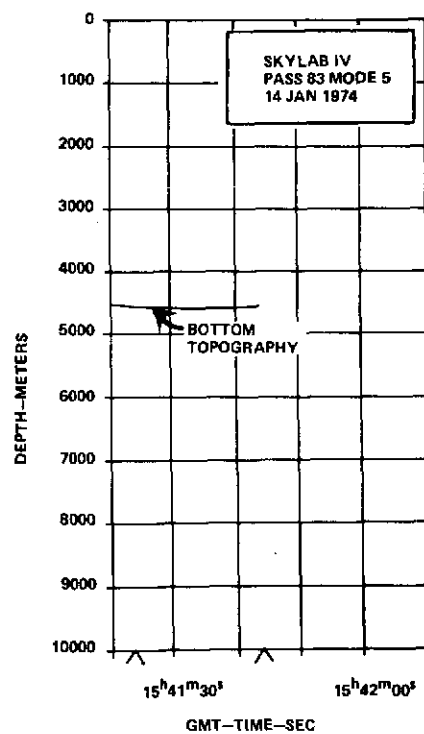
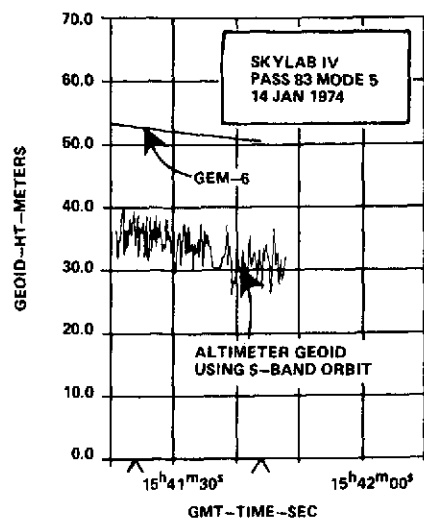




C-3

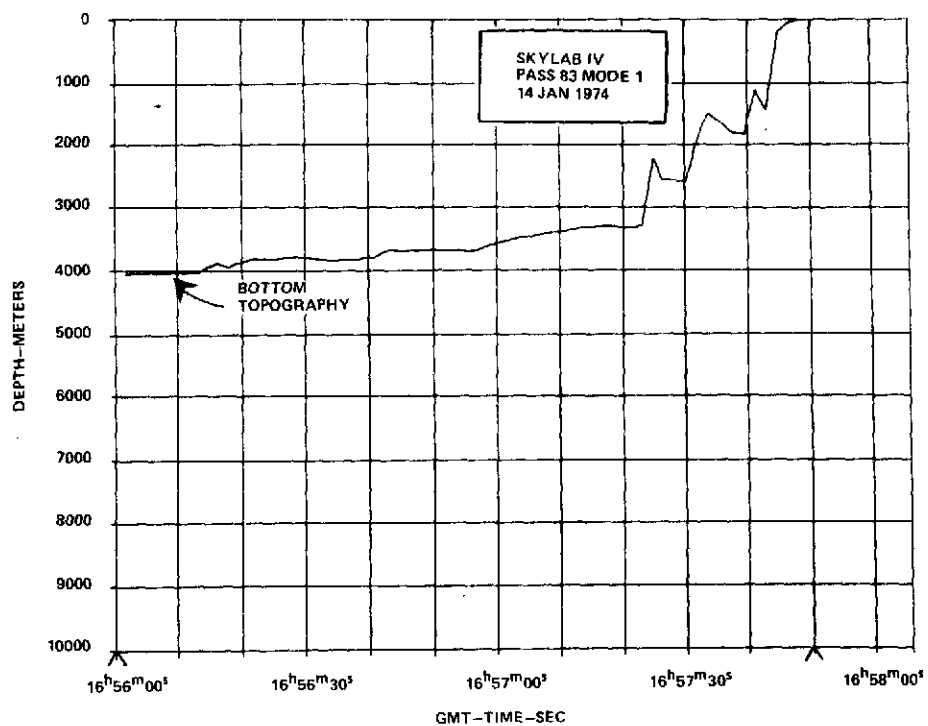
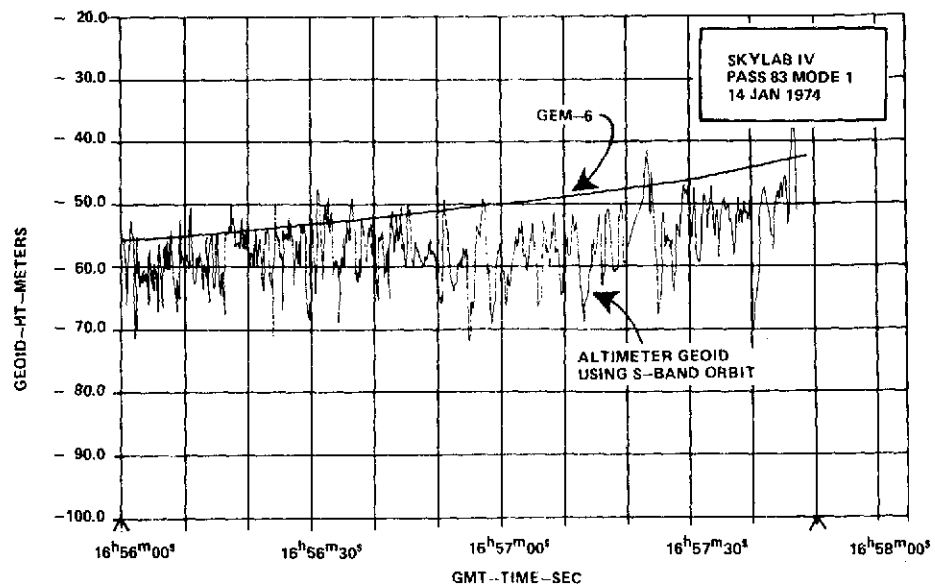






| | | |
|------|--------|--------|
| Lat | 47.2° | 46.8° |
| Long | 348.3° | 350.0° |

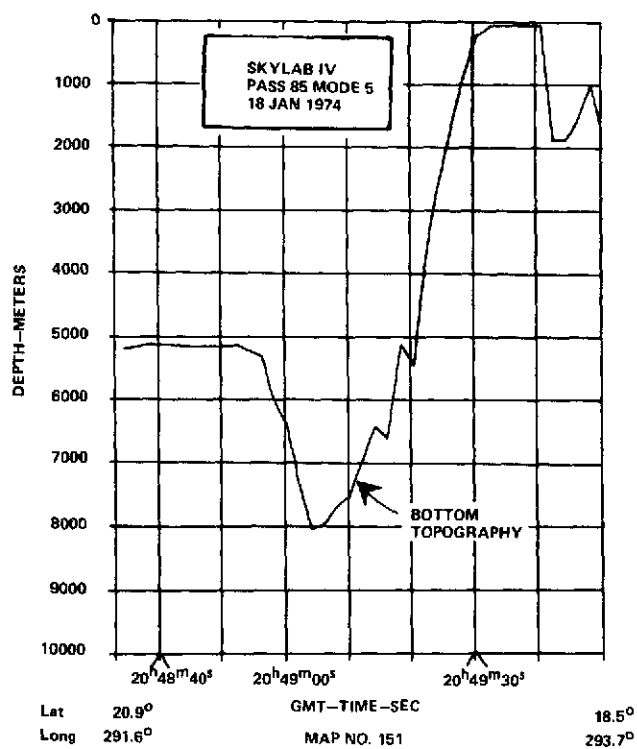
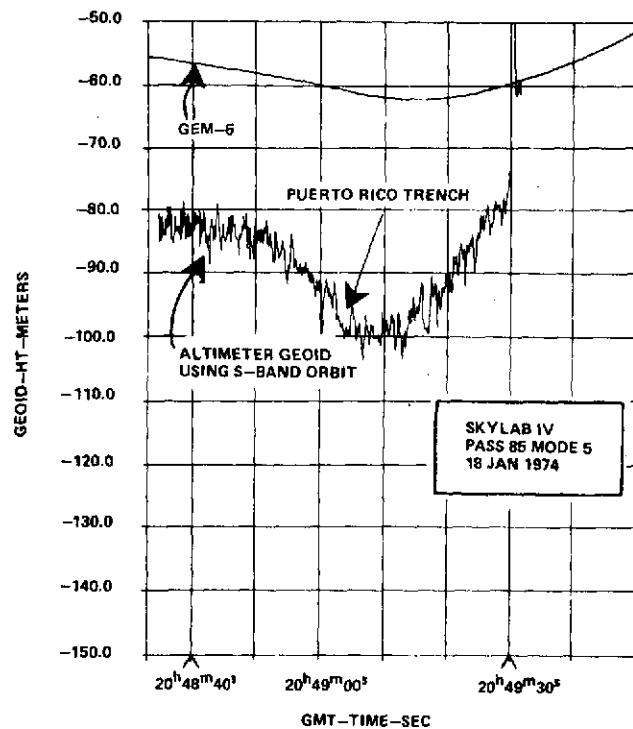
MAP NO. 147

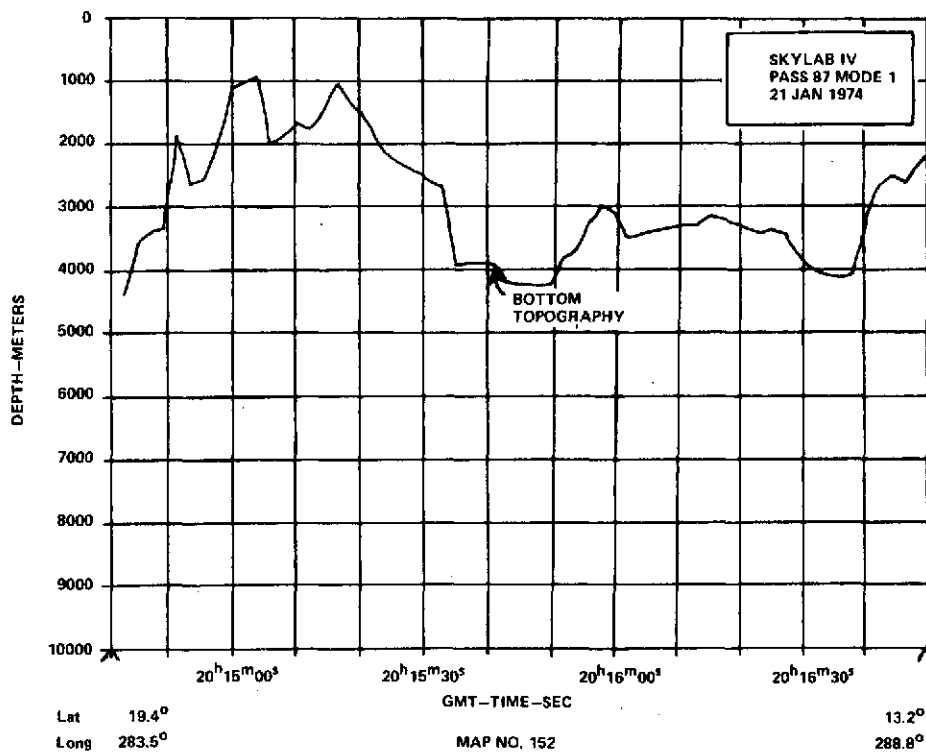
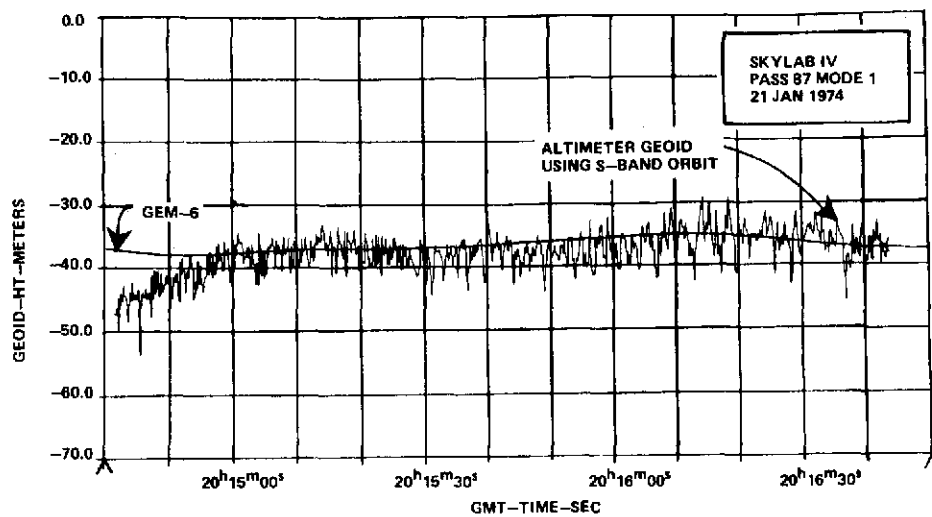


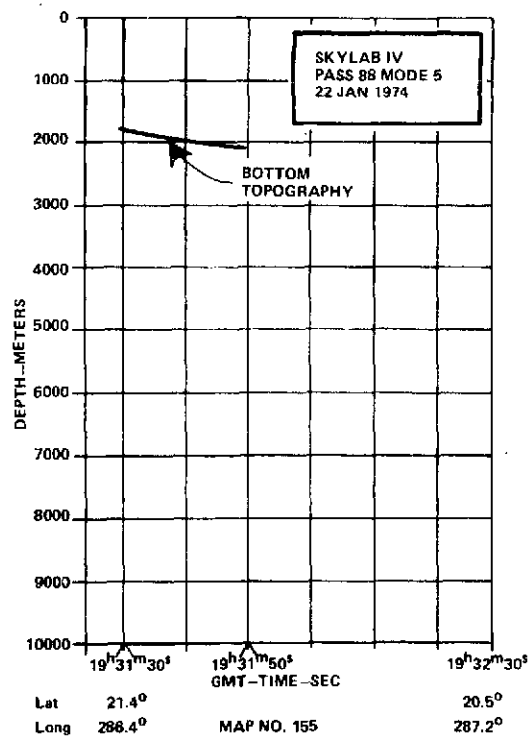
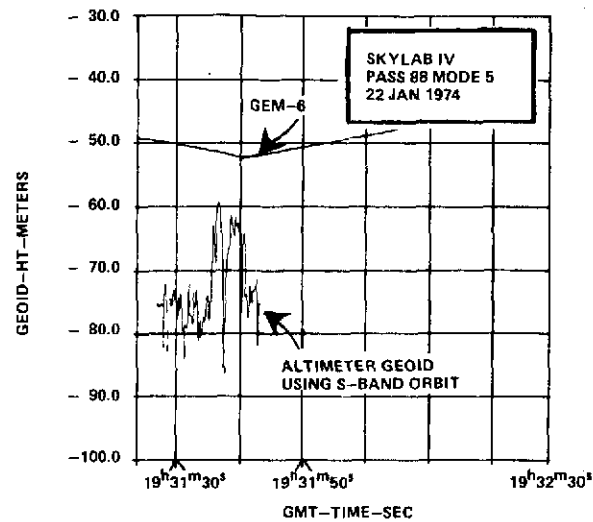
Lat 26.6°
Long 238.2

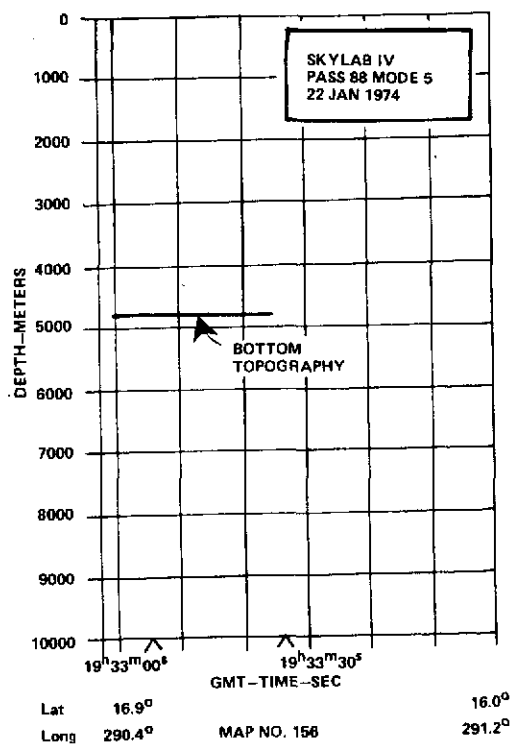
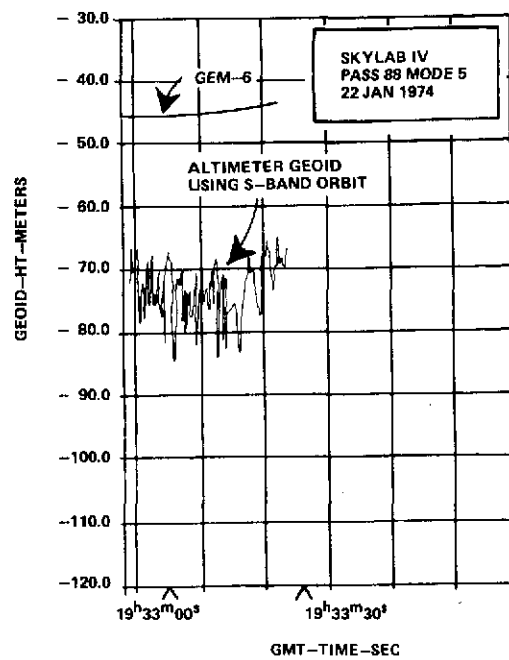
MAP NO. 148

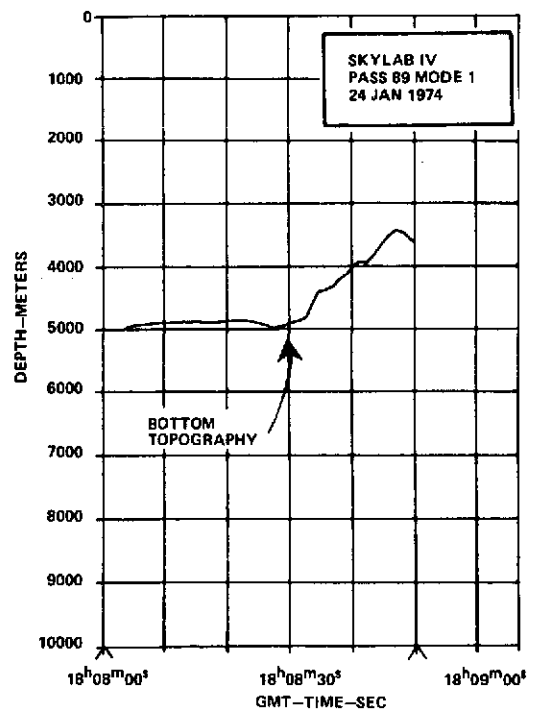
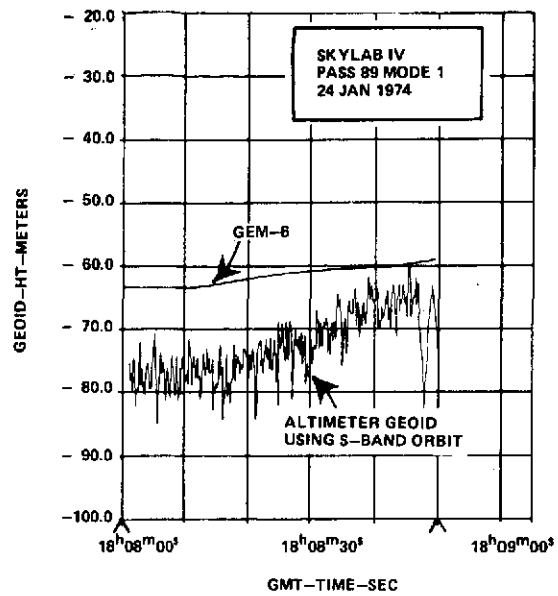
31.5°
243.7°



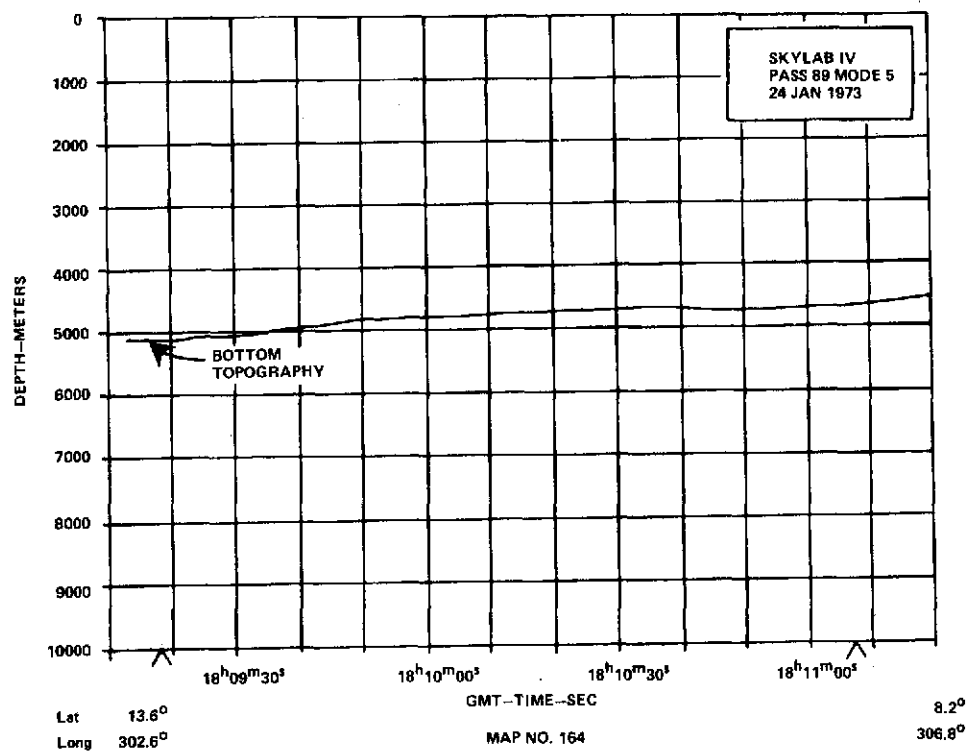
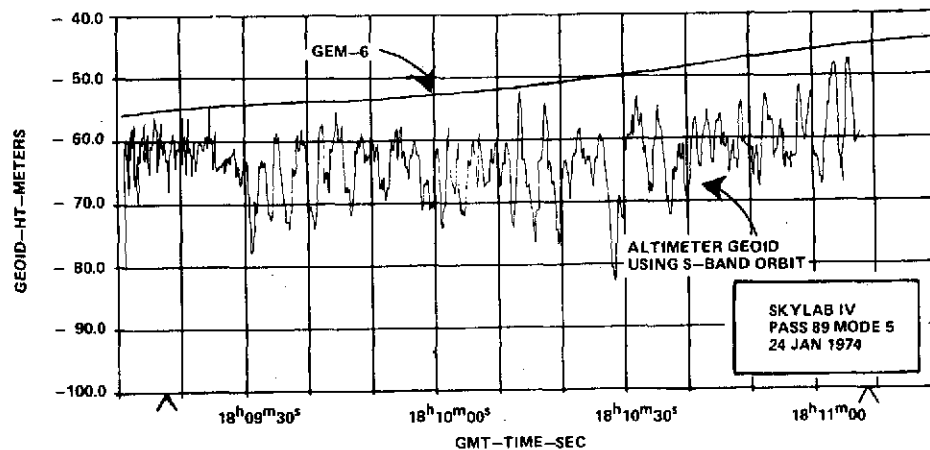


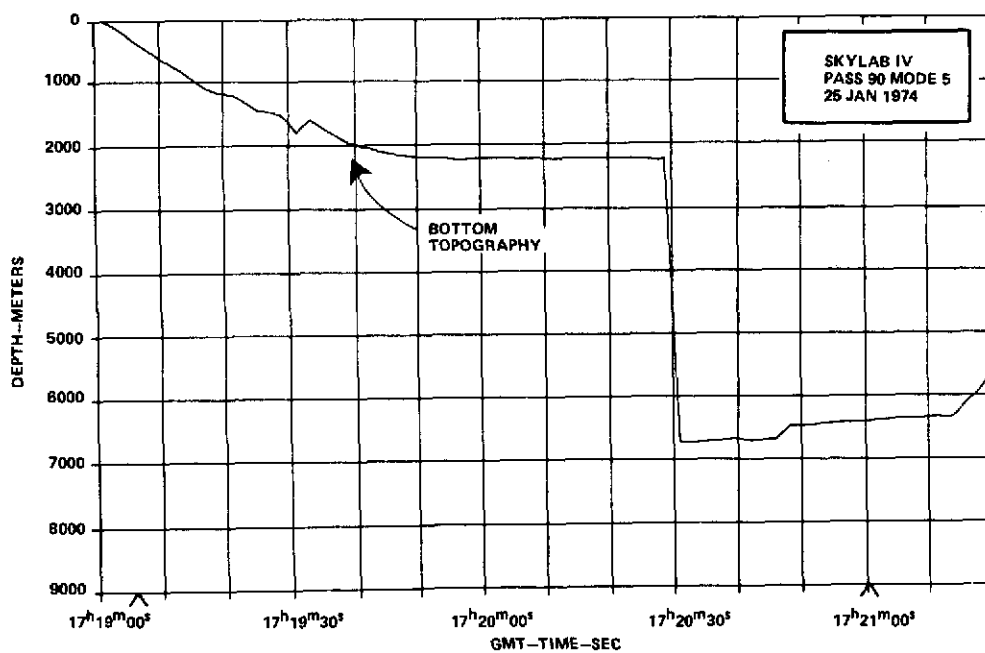
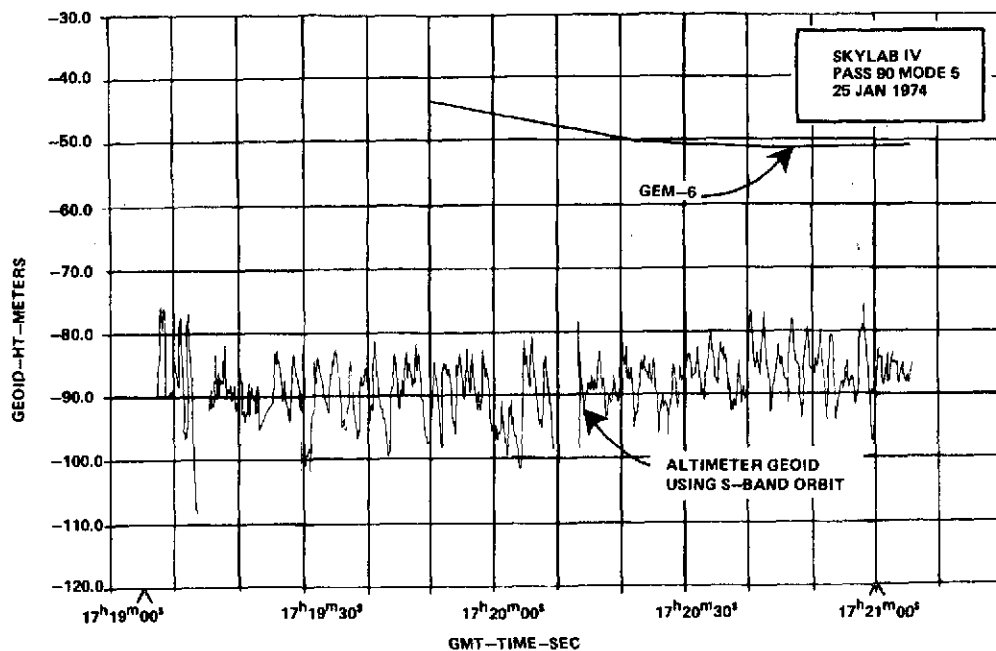






Lat 17.4° 15.0°
Long 299.4° 301.5°
MAP NO. 163

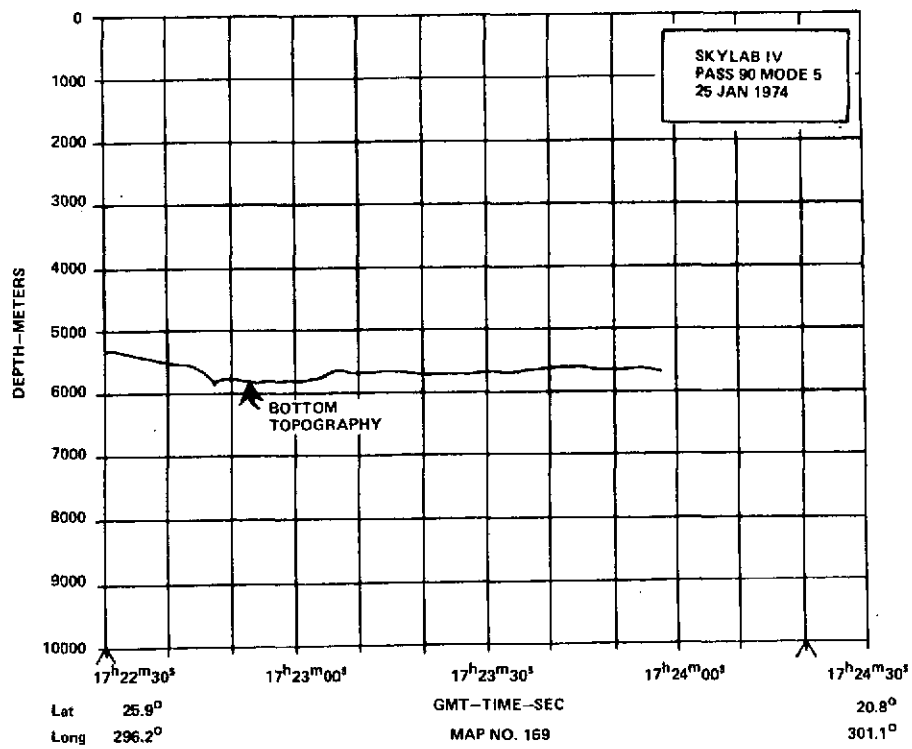
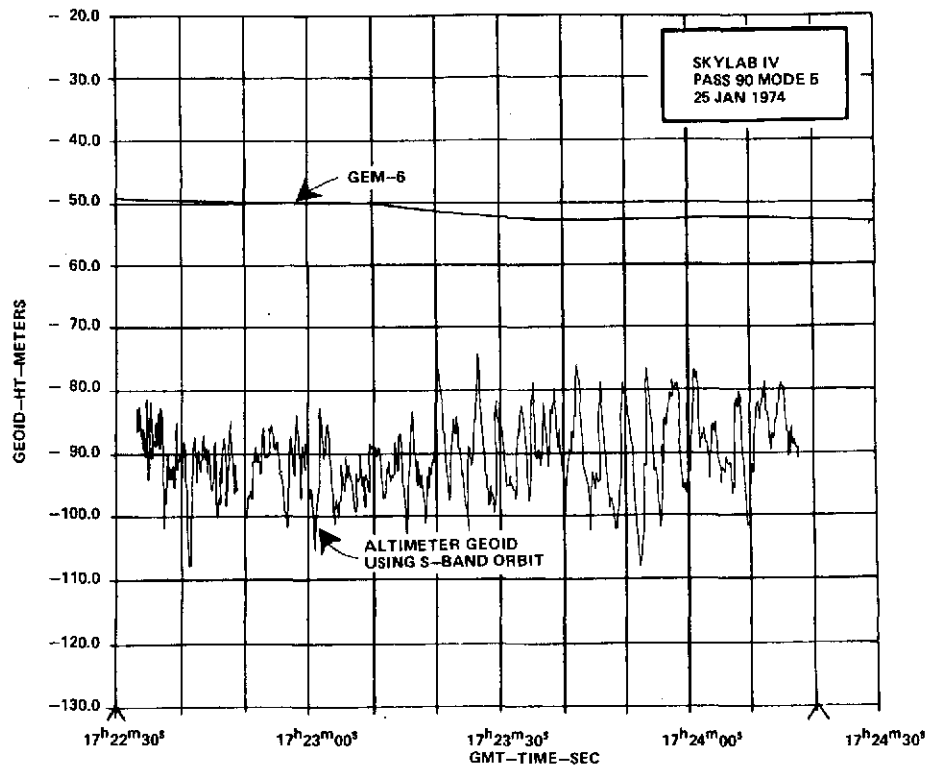


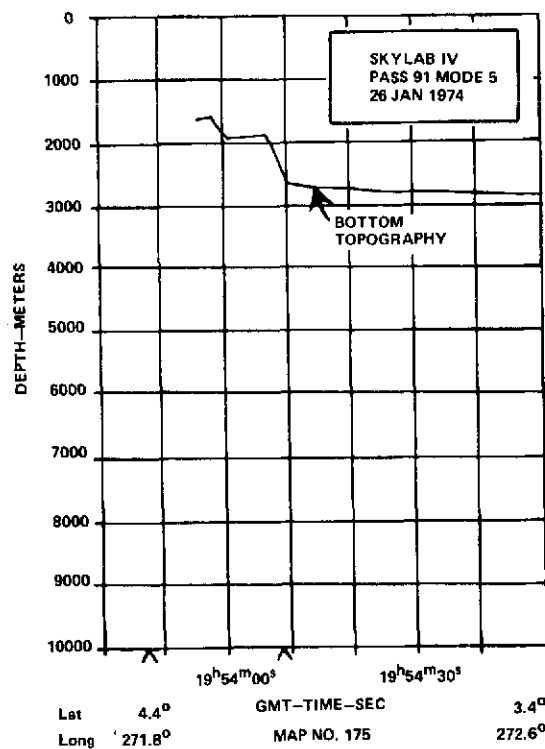
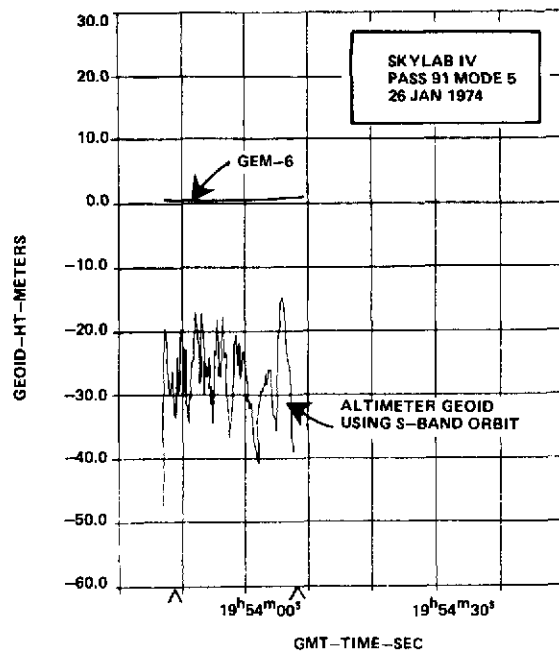


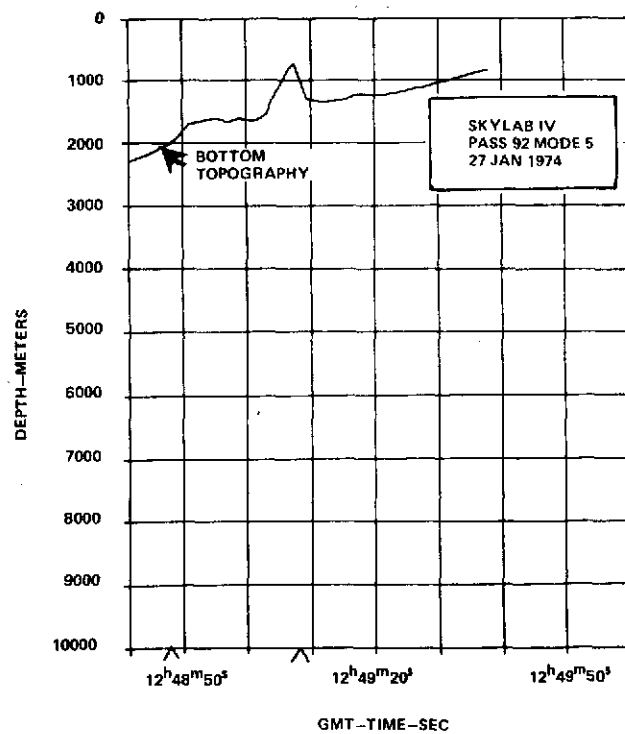
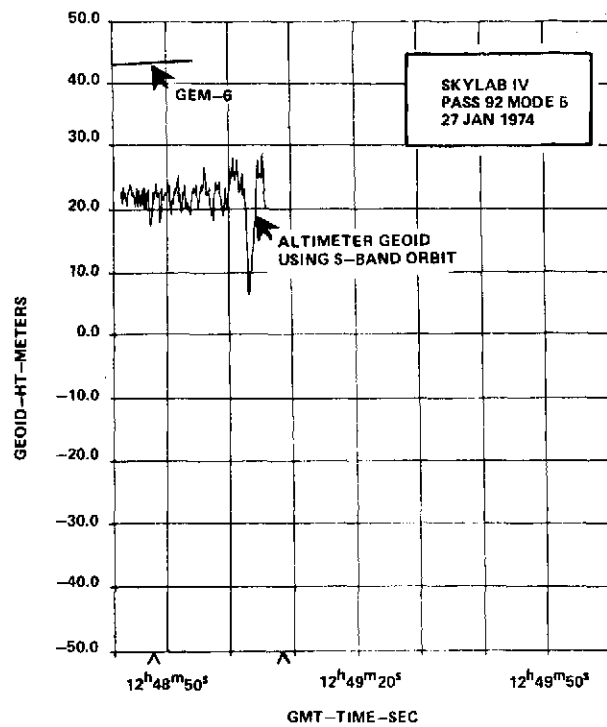
Lat 37.1°
Long 282.2°

MAP NO. 168

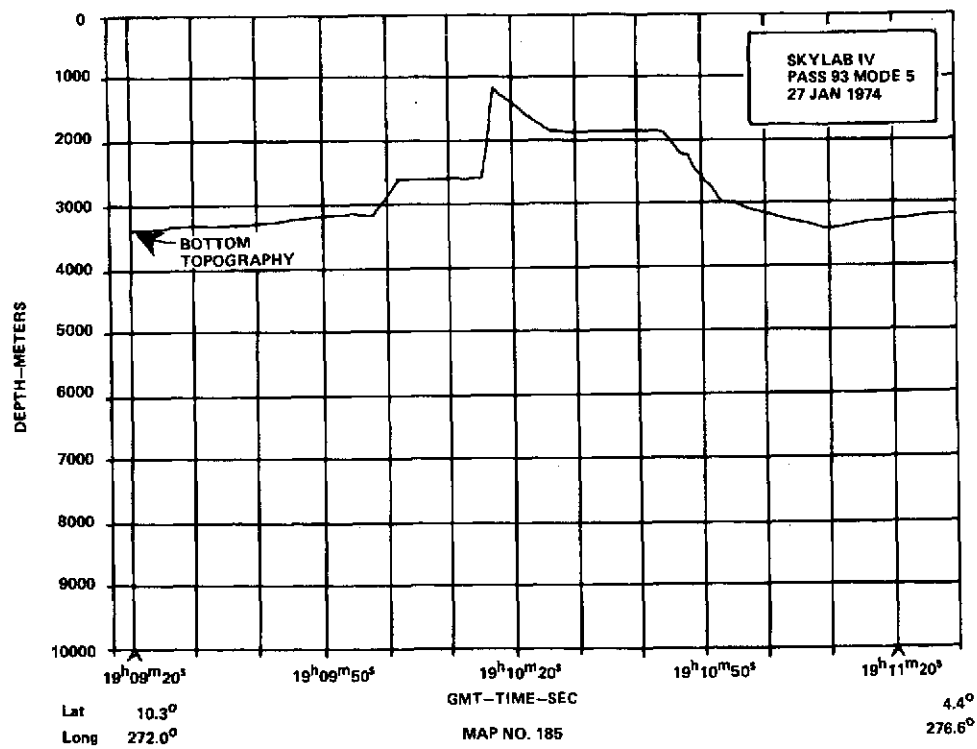
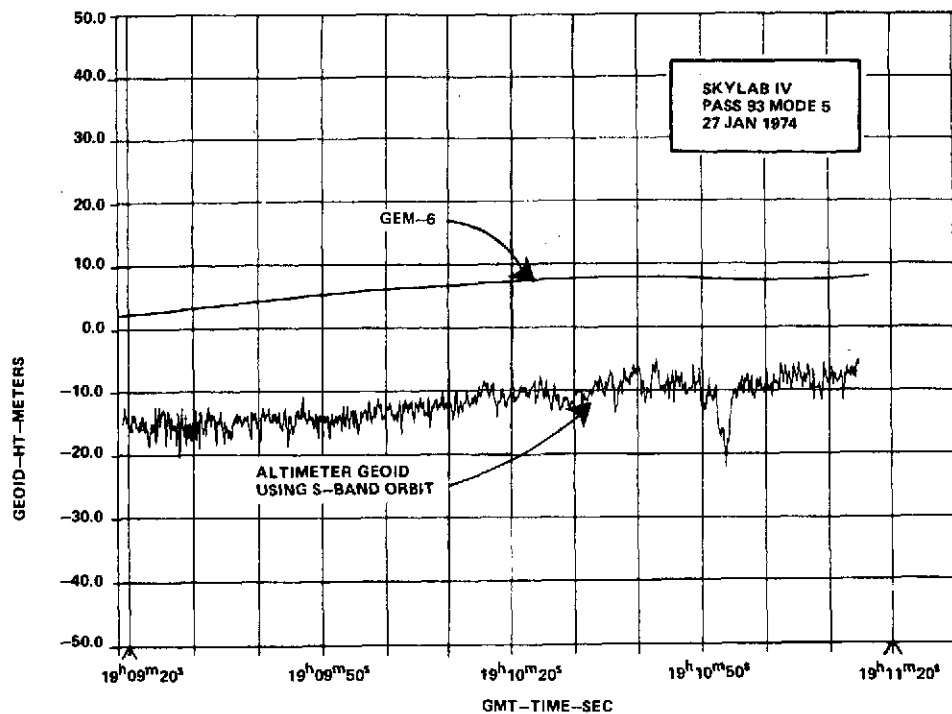
28.9°
291.8°

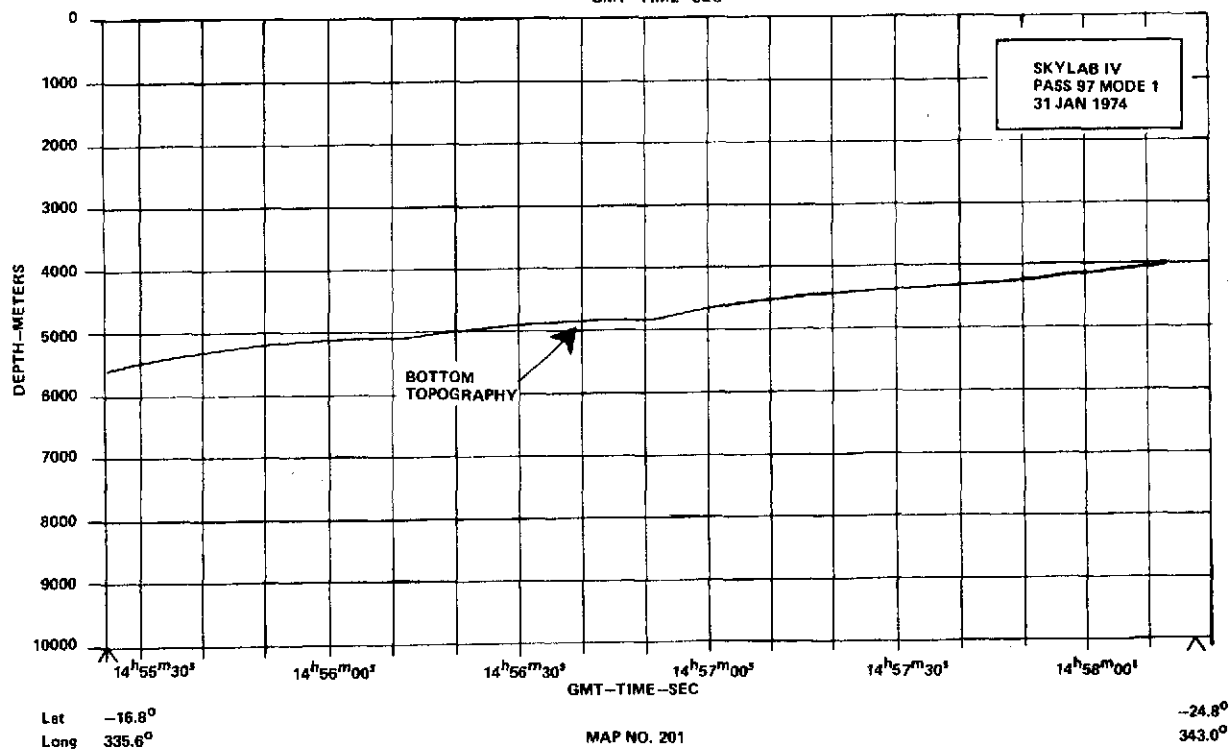
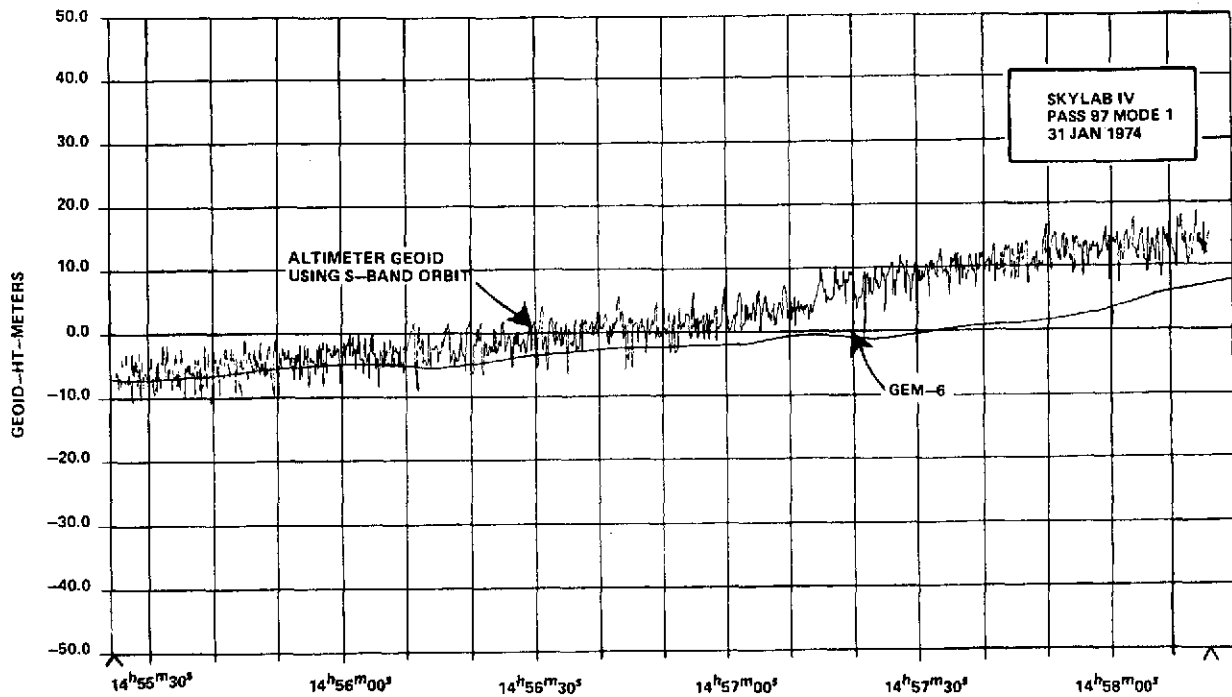


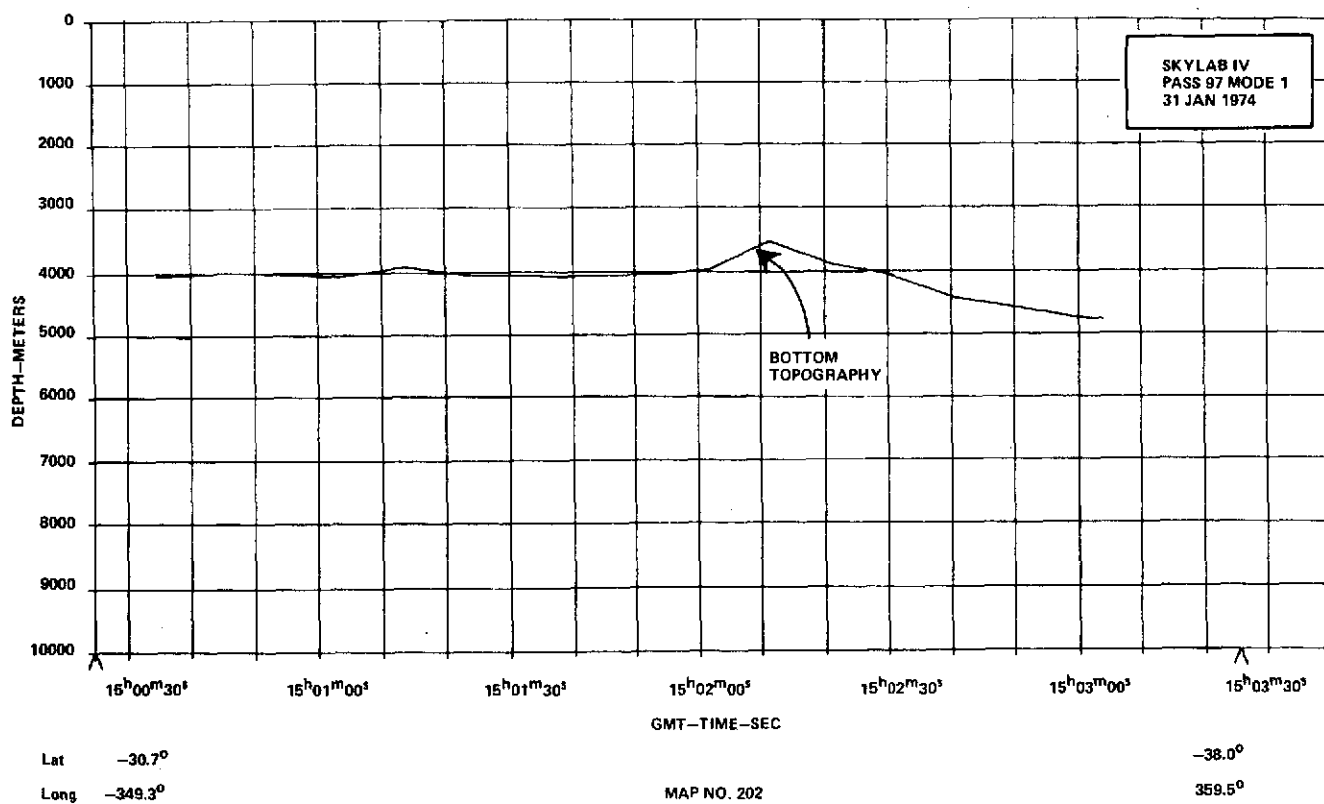
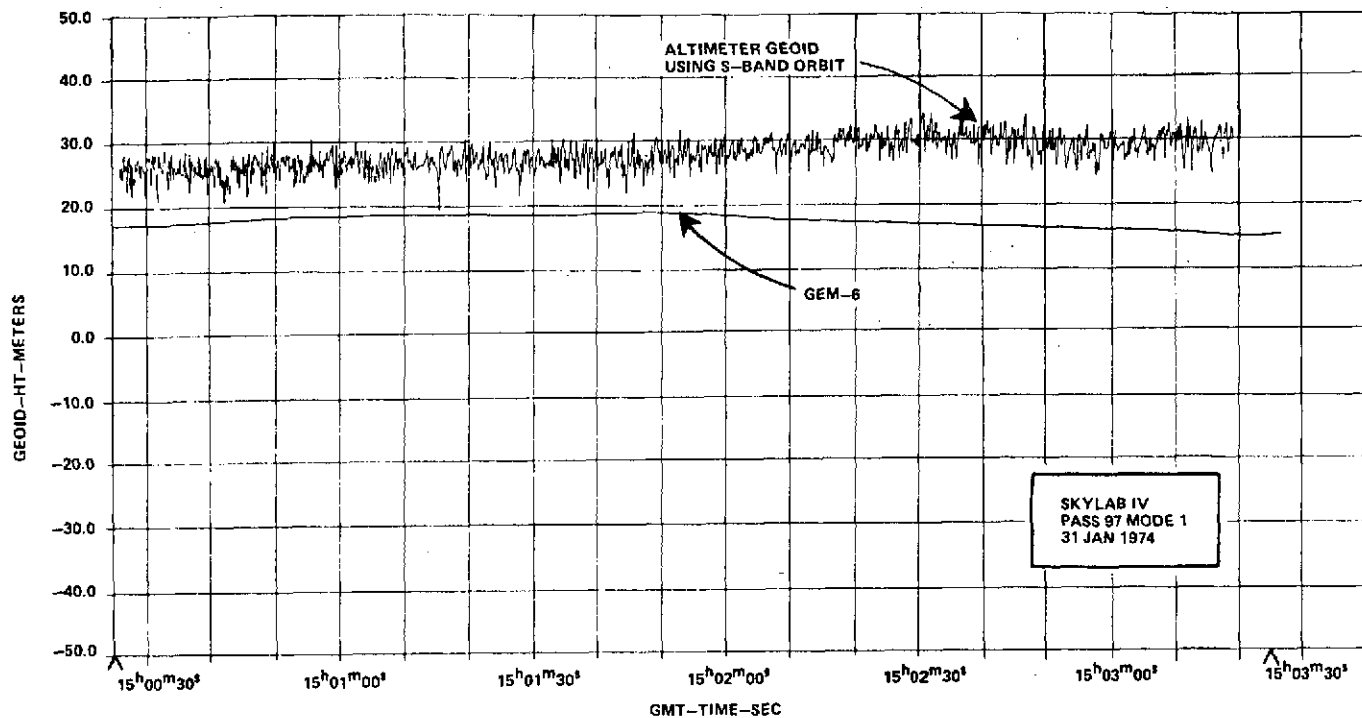




| | | | |
|------|--------|-------------|--------|
| Lat | 32.2° | | 31.4° |
| Long | 345.8° | MAP NO. 182 | 346.9° |



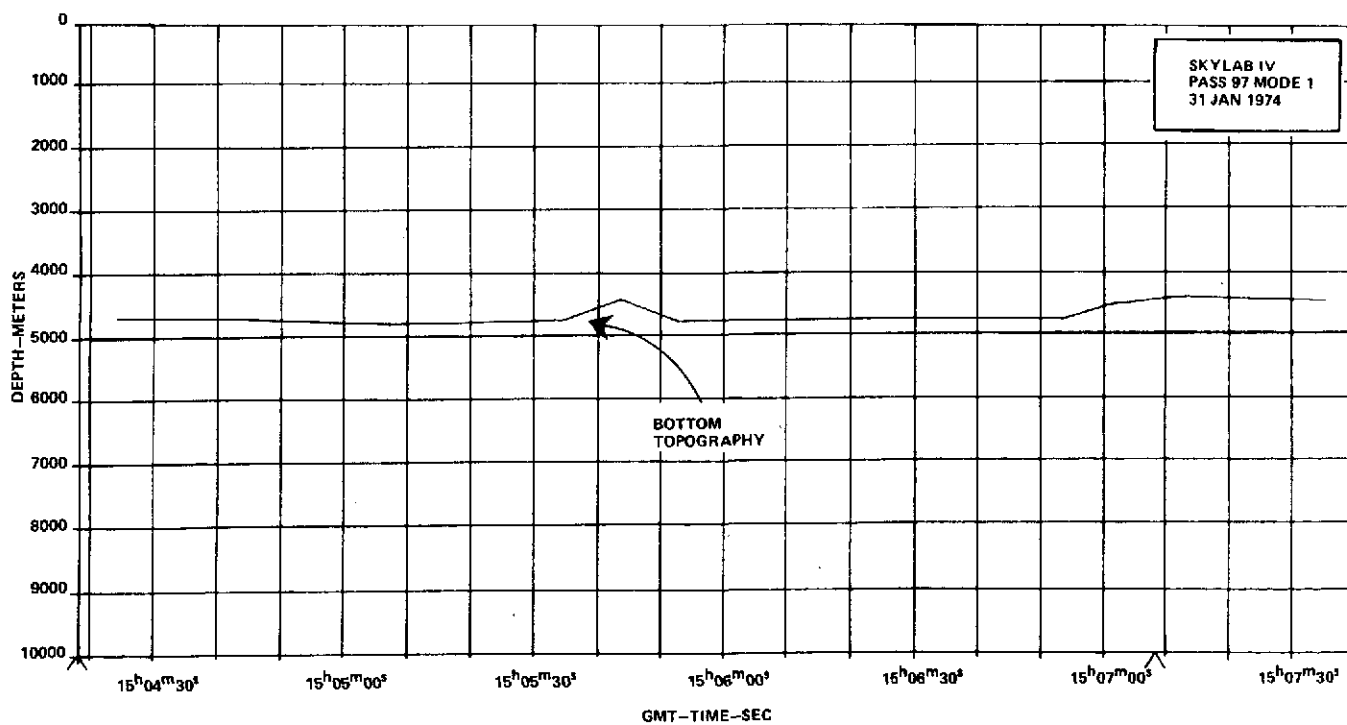
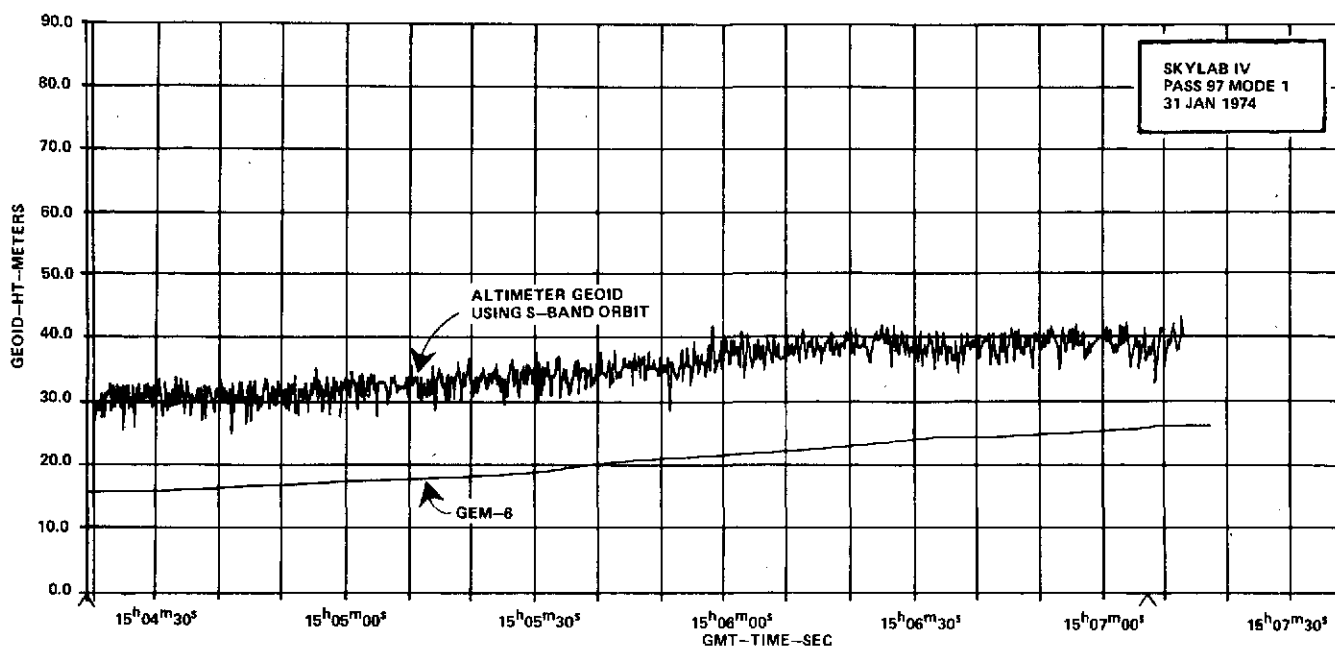




Lat -30.7°
Long -349.3°

MAP NO. 202

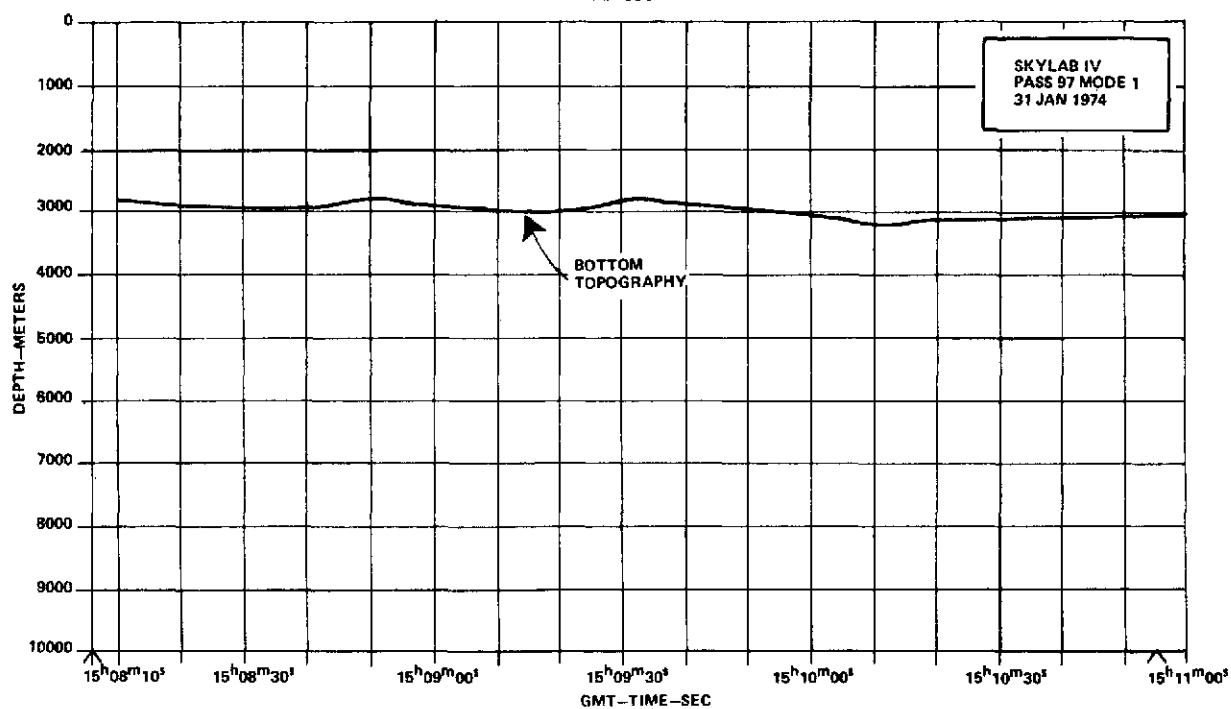
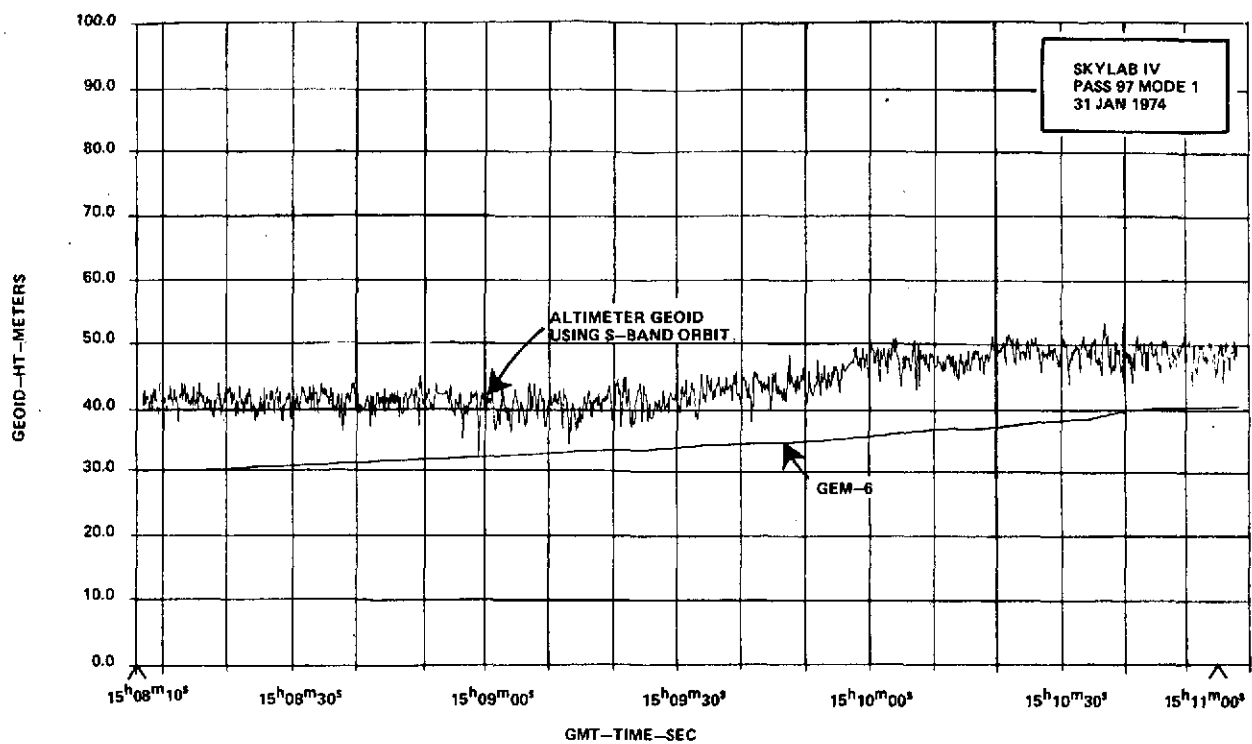
-38.0°
359.5°



Lat -39.9°
Long 2.9°

MAP NO. 203

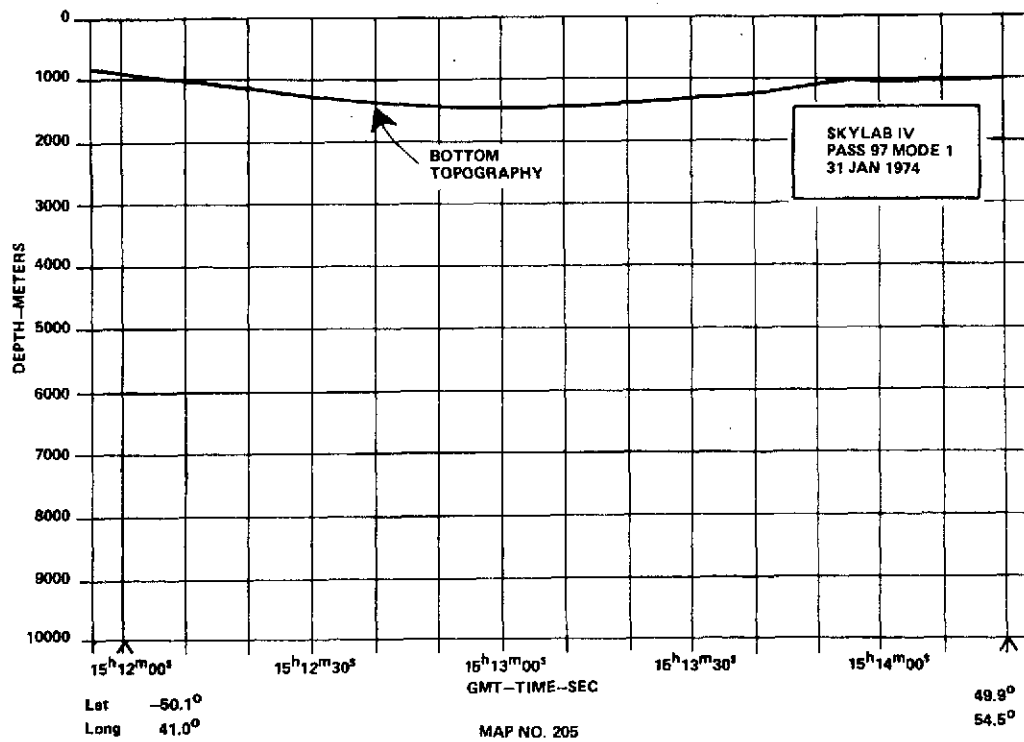
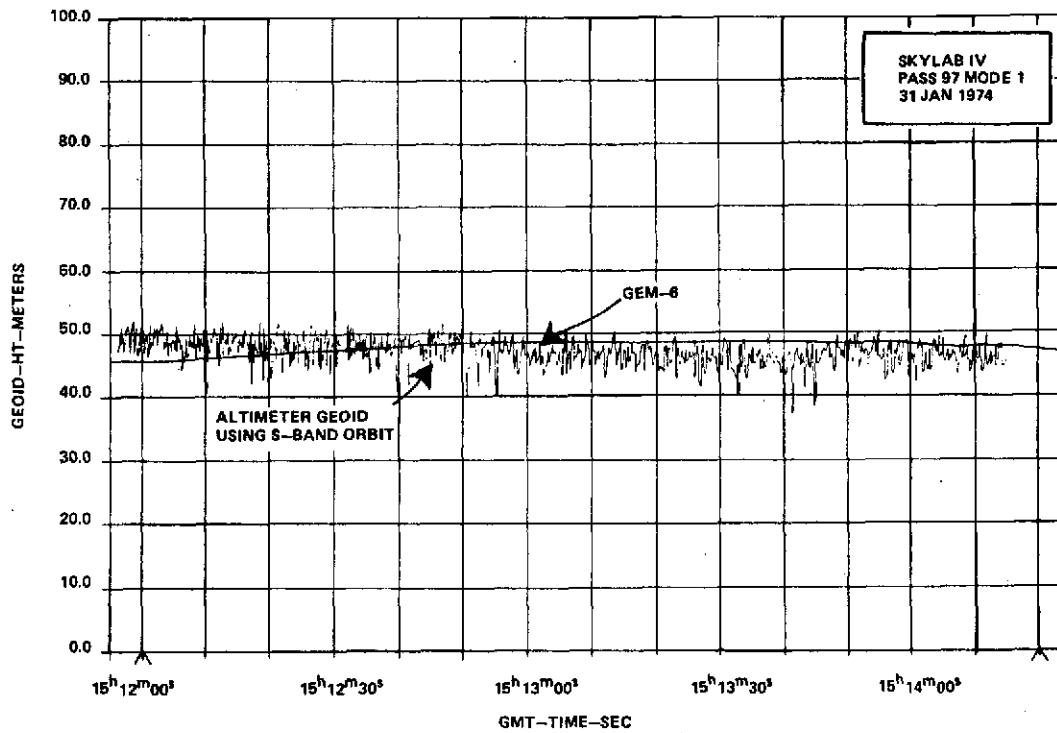
-45.2°
15.2°

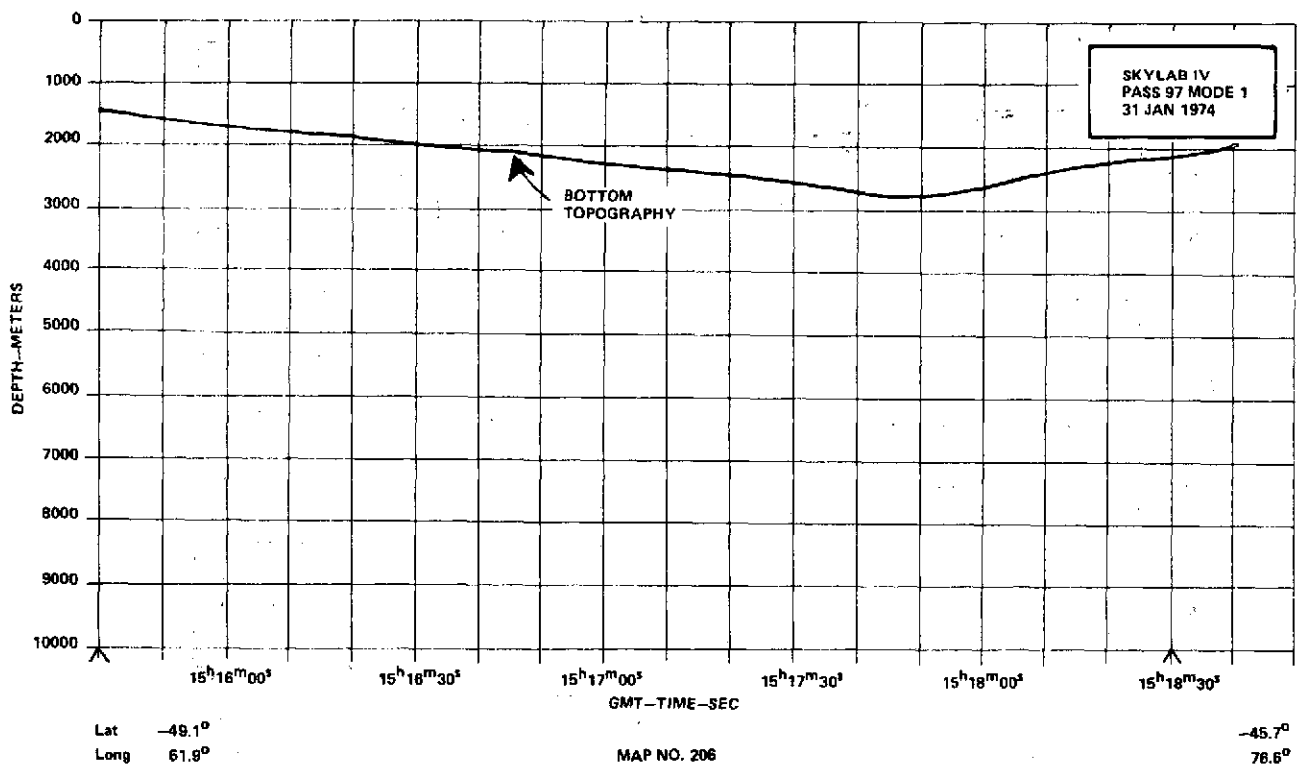
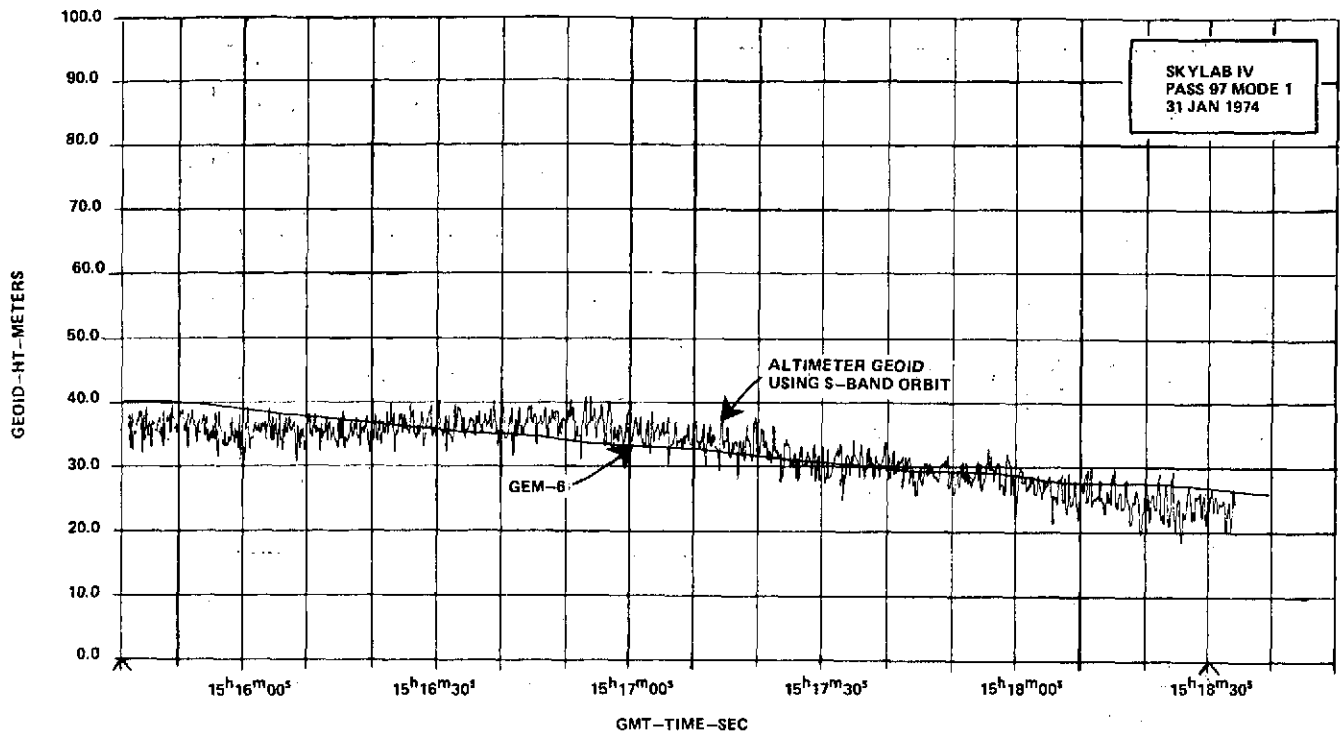


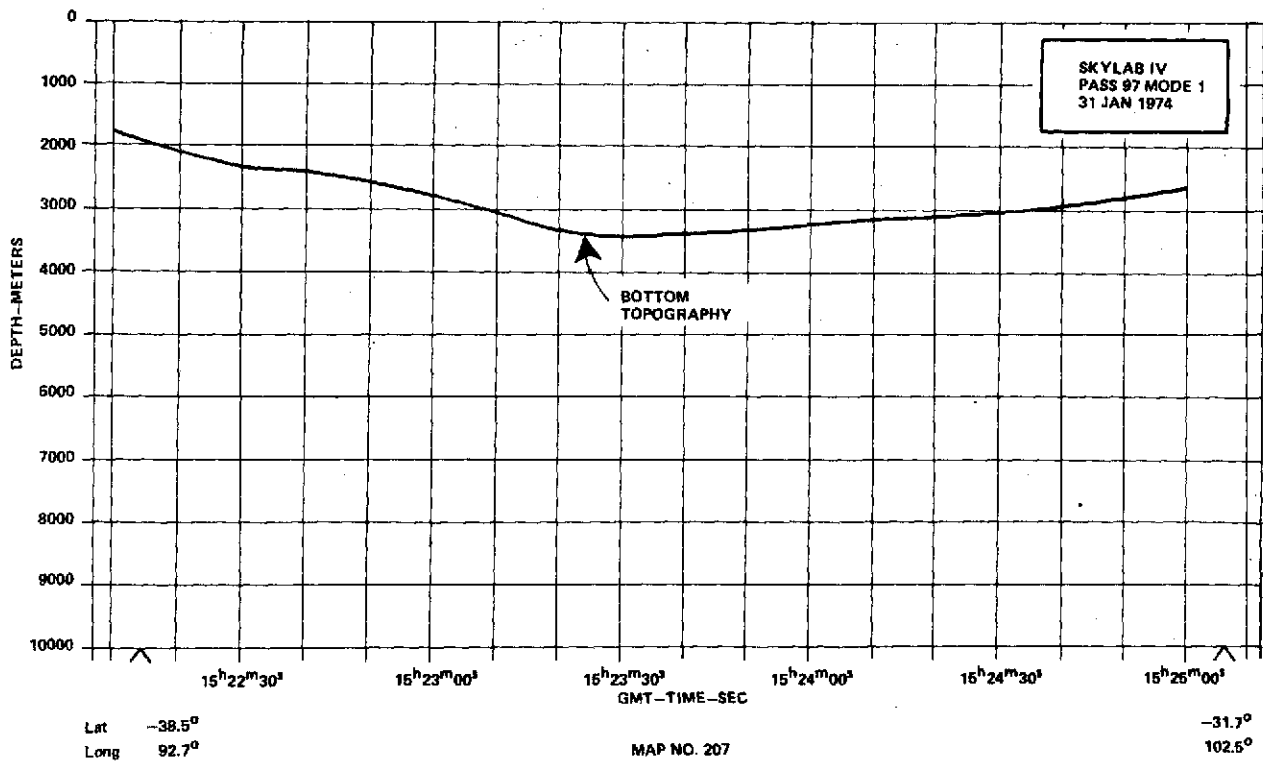
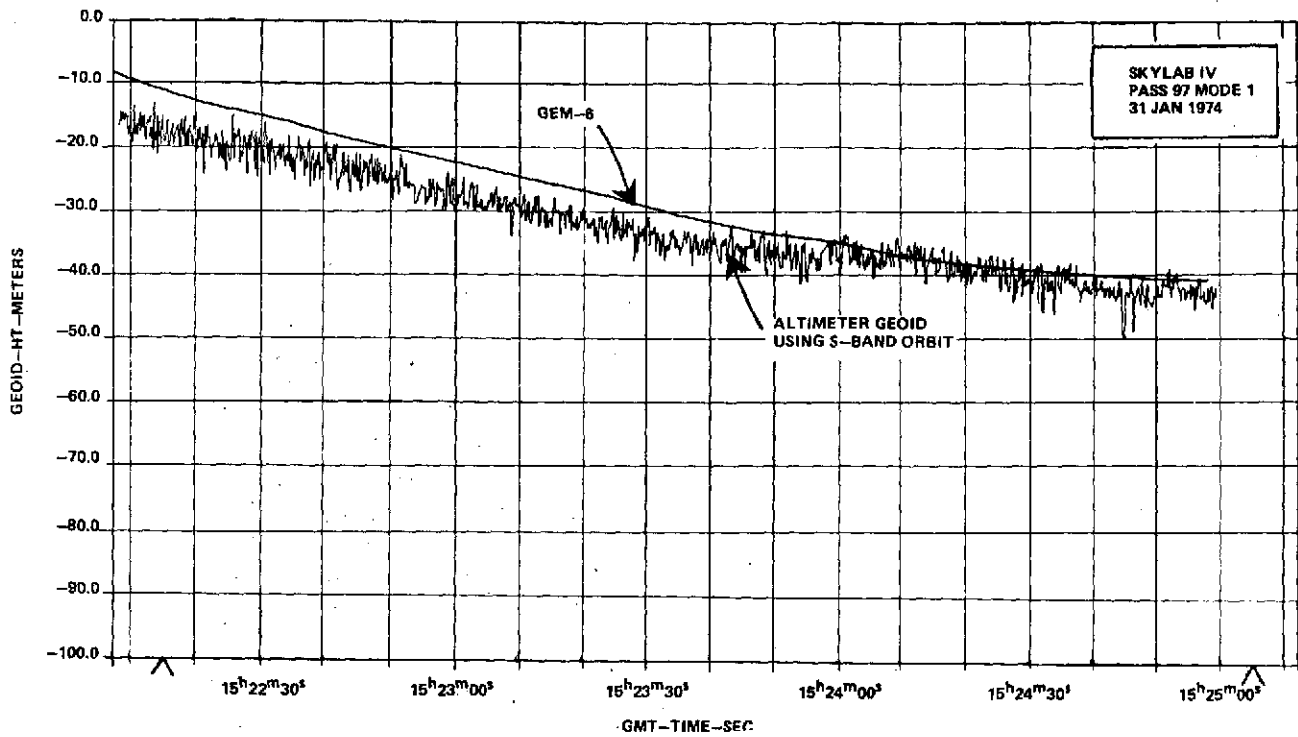
Lat -46.7°
Long 19.8°

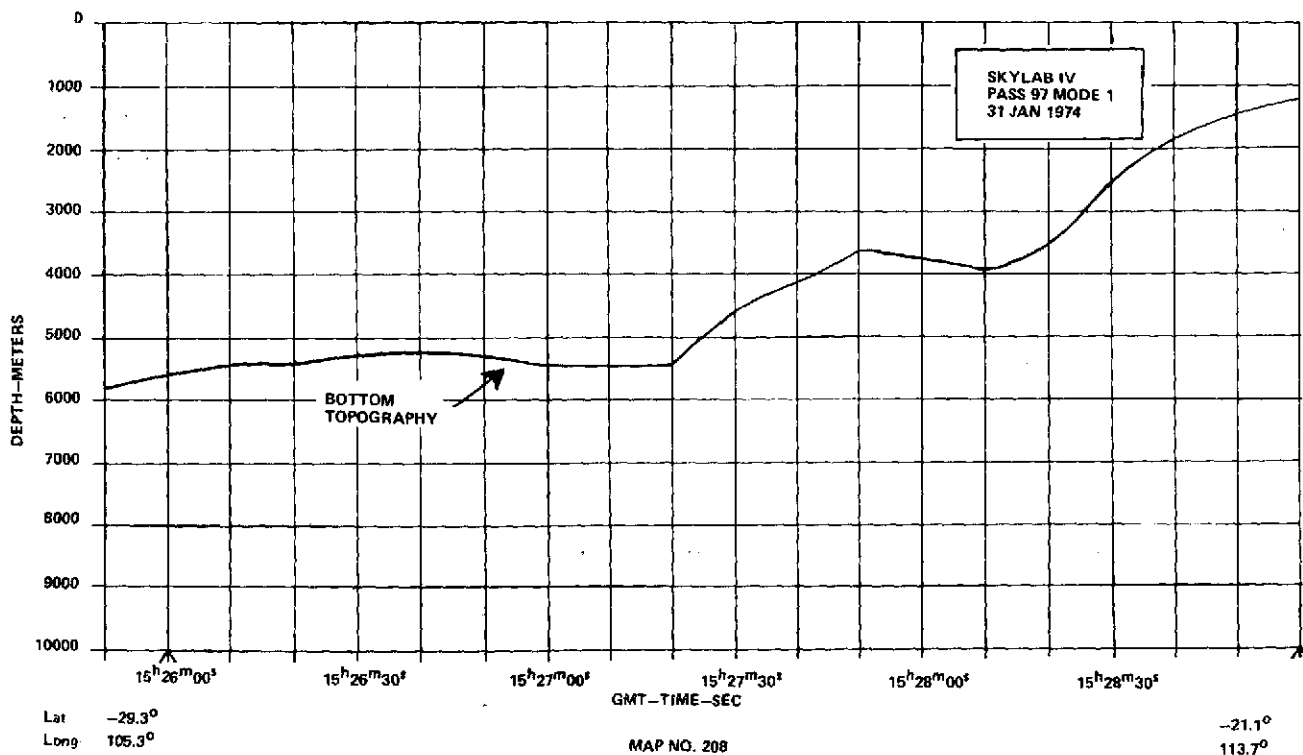
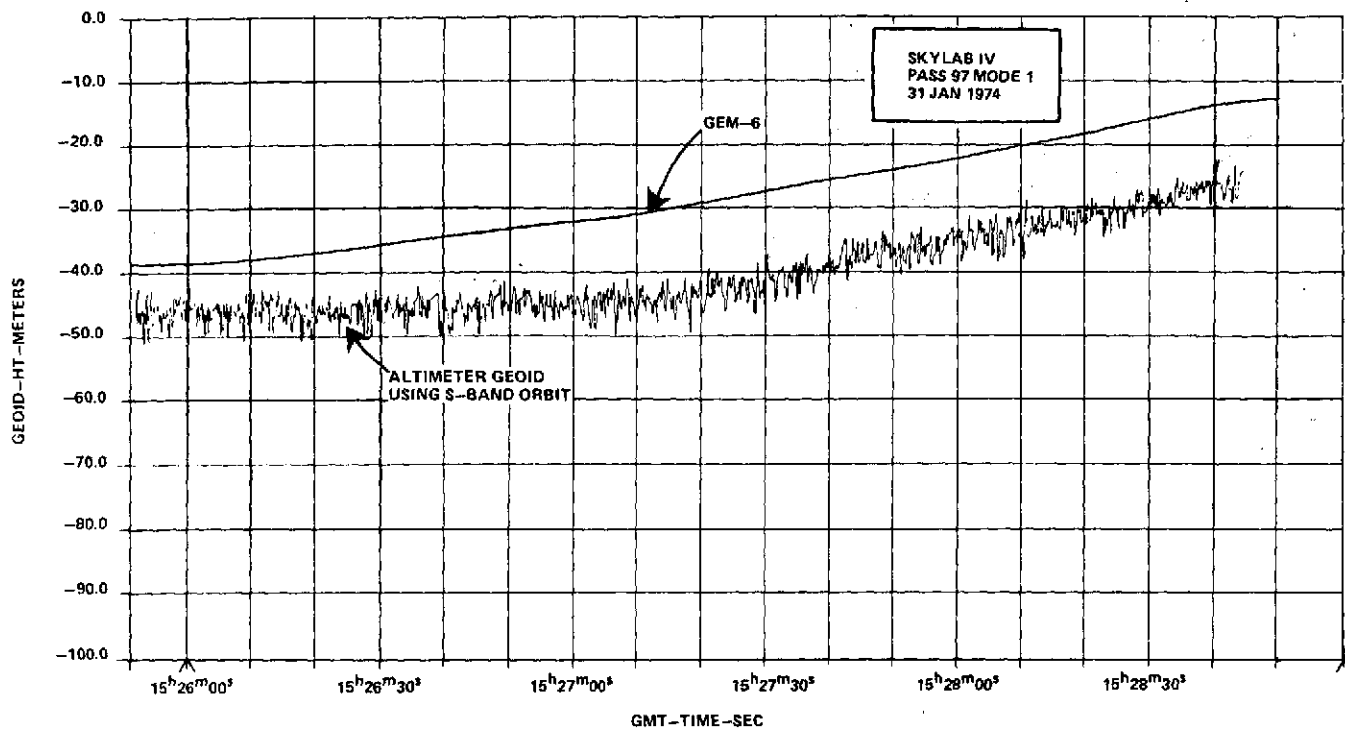
MAP NO. 204

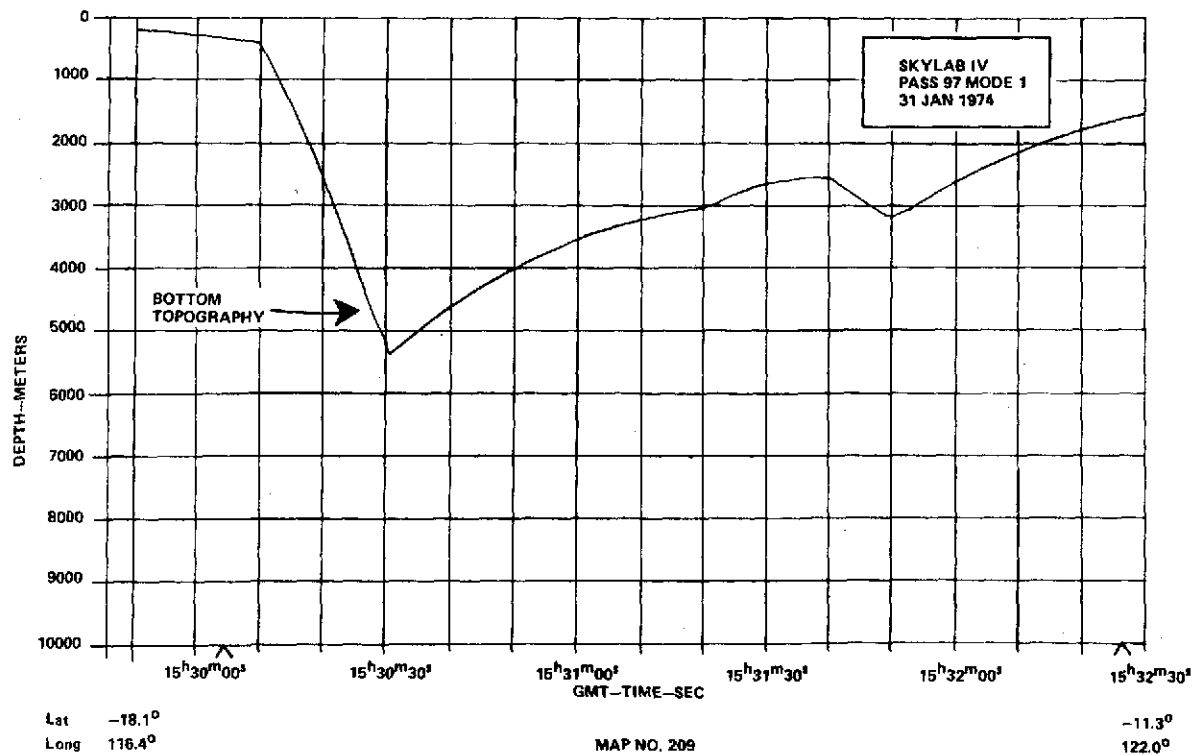
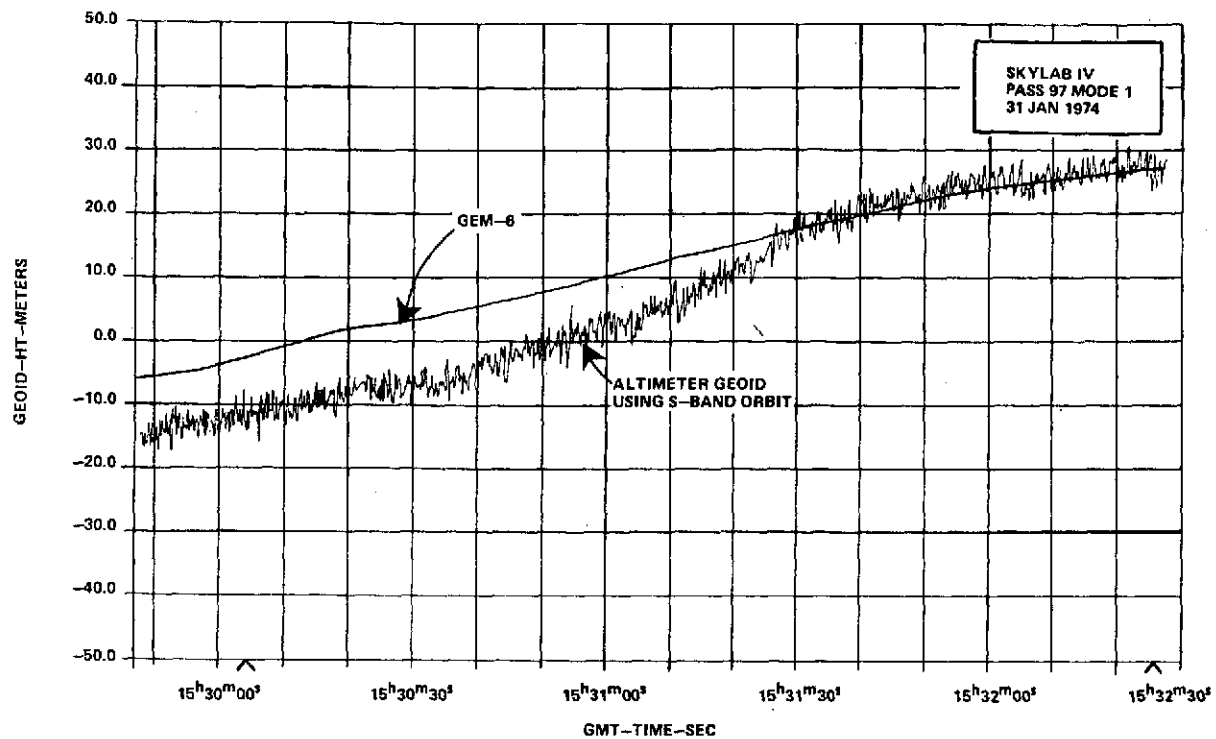
49.5°
 34.9°

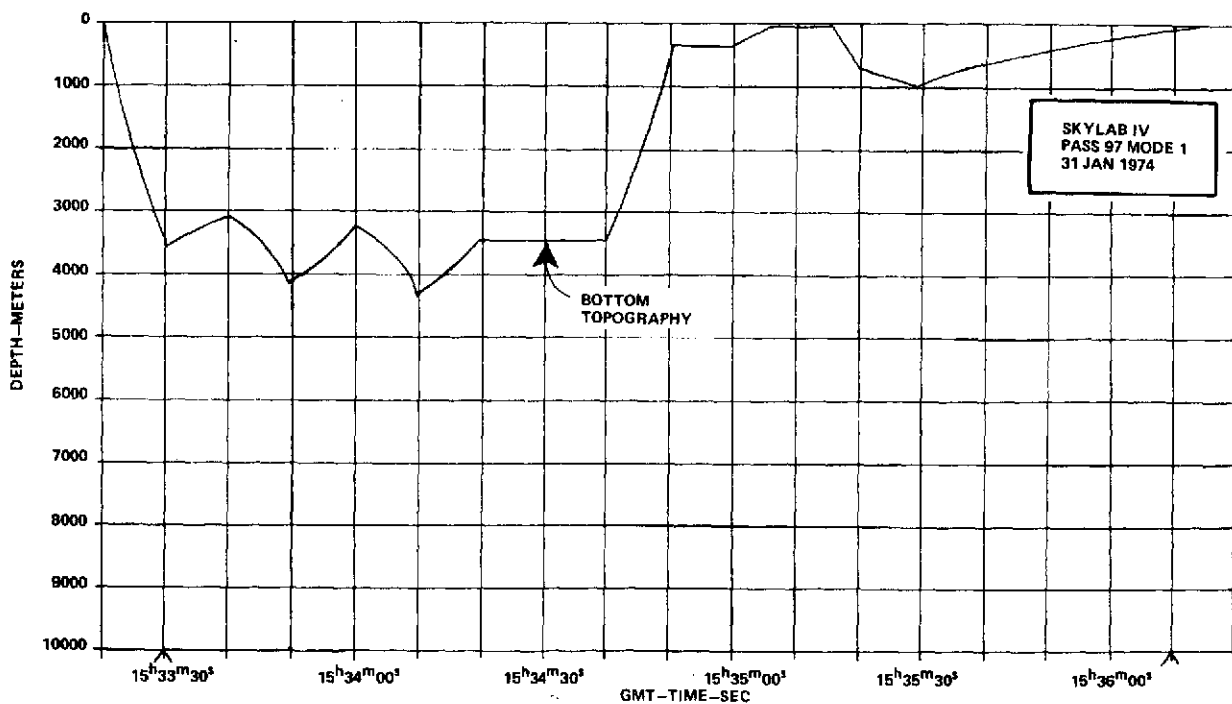
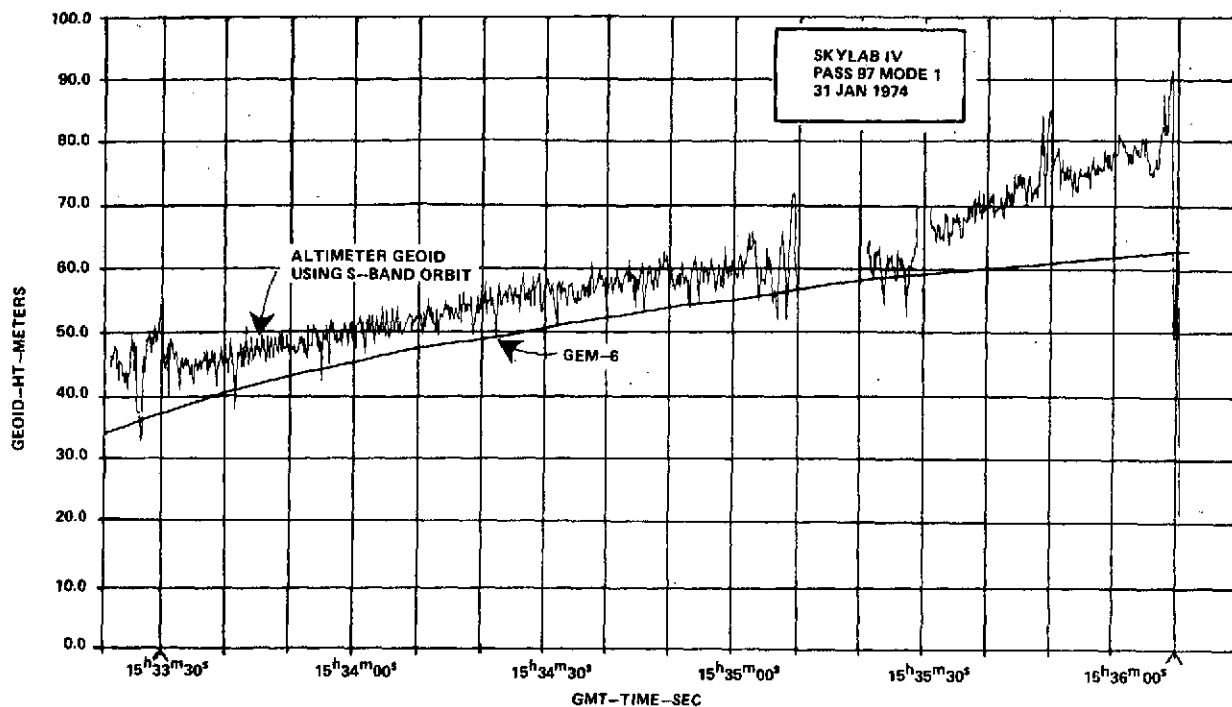








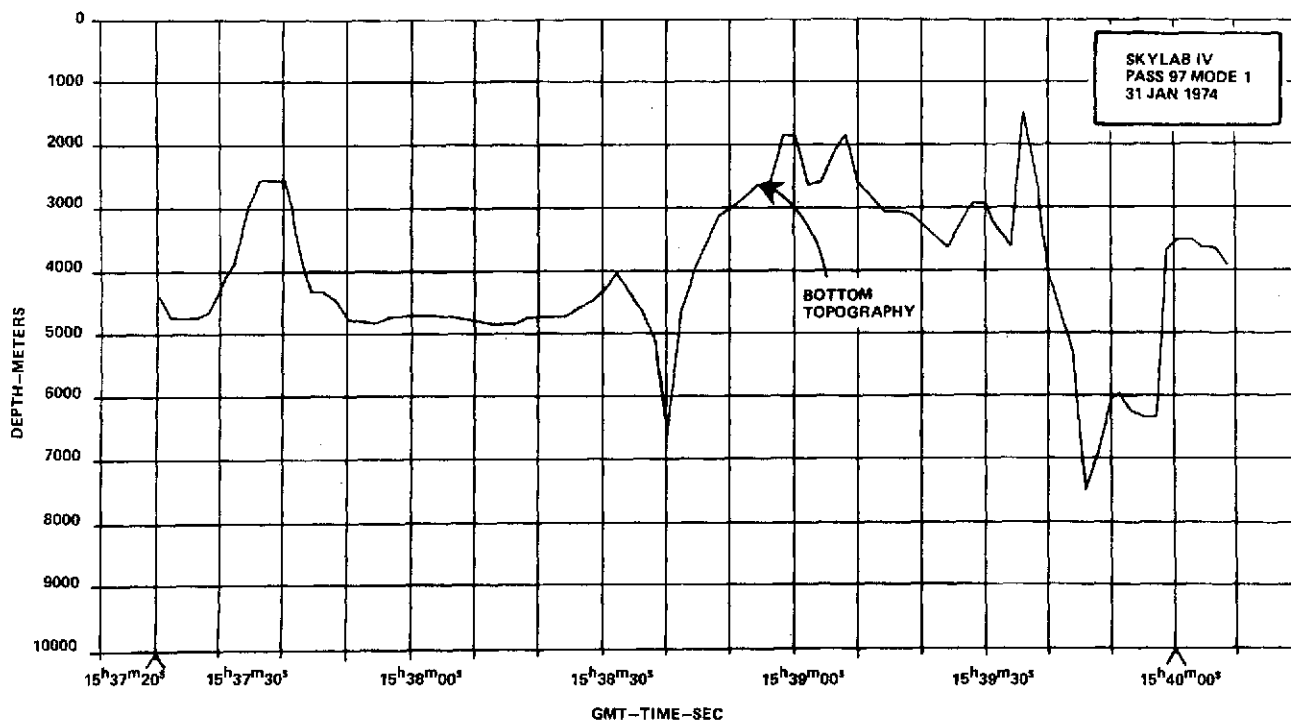
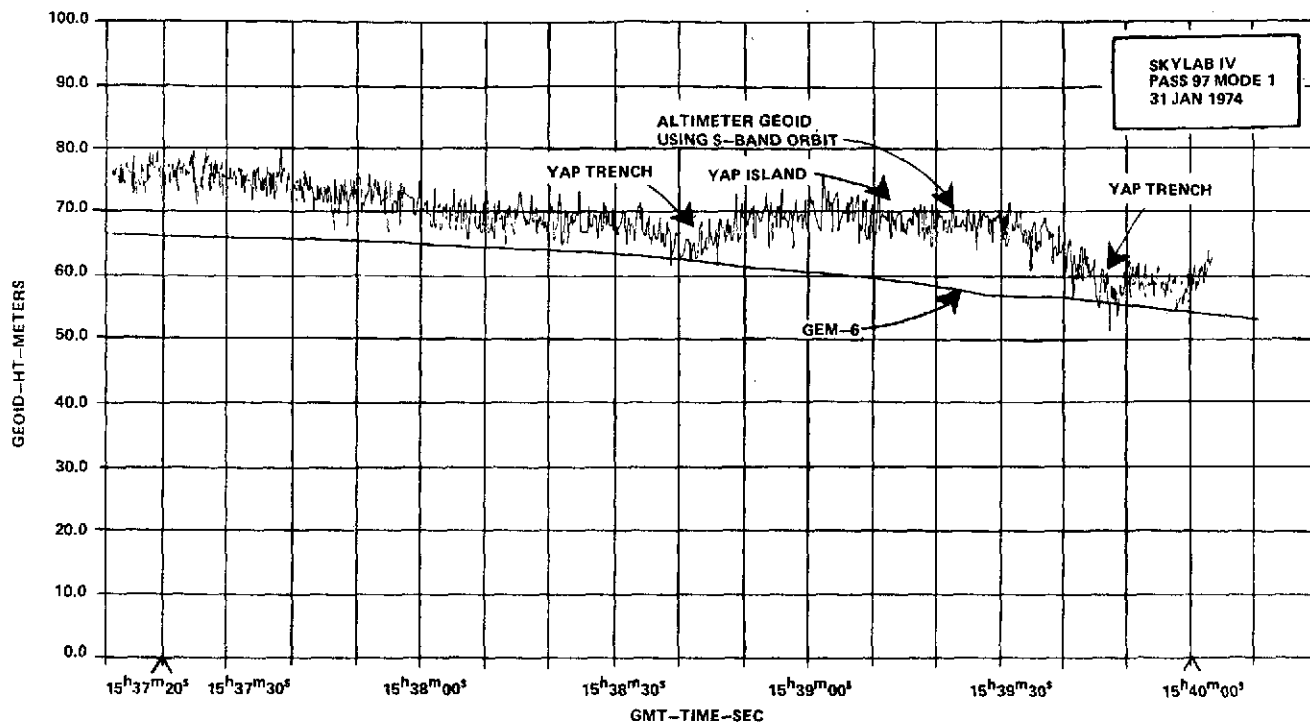




Lat - 8.1°
Long 124.5°

MAP NO. 210

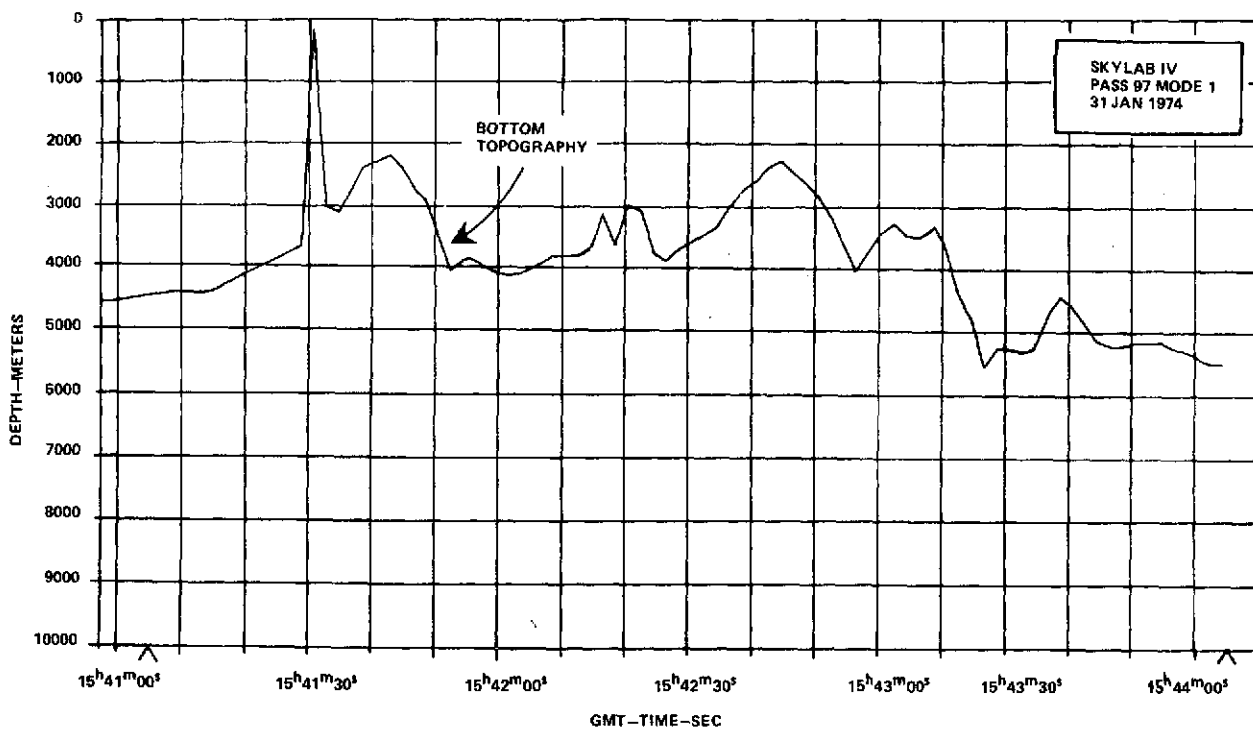
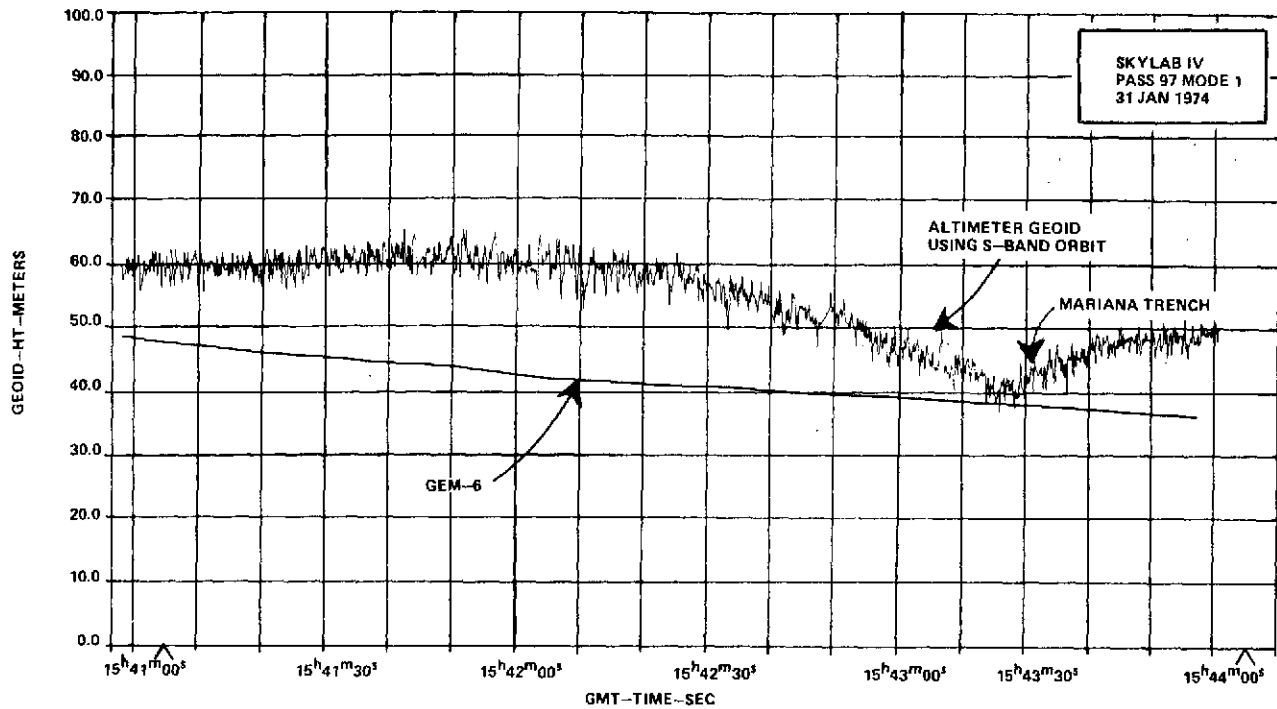
- 0.2°
130.5°



Lat 3.3°
Long 133.1°

MAP NO. 211

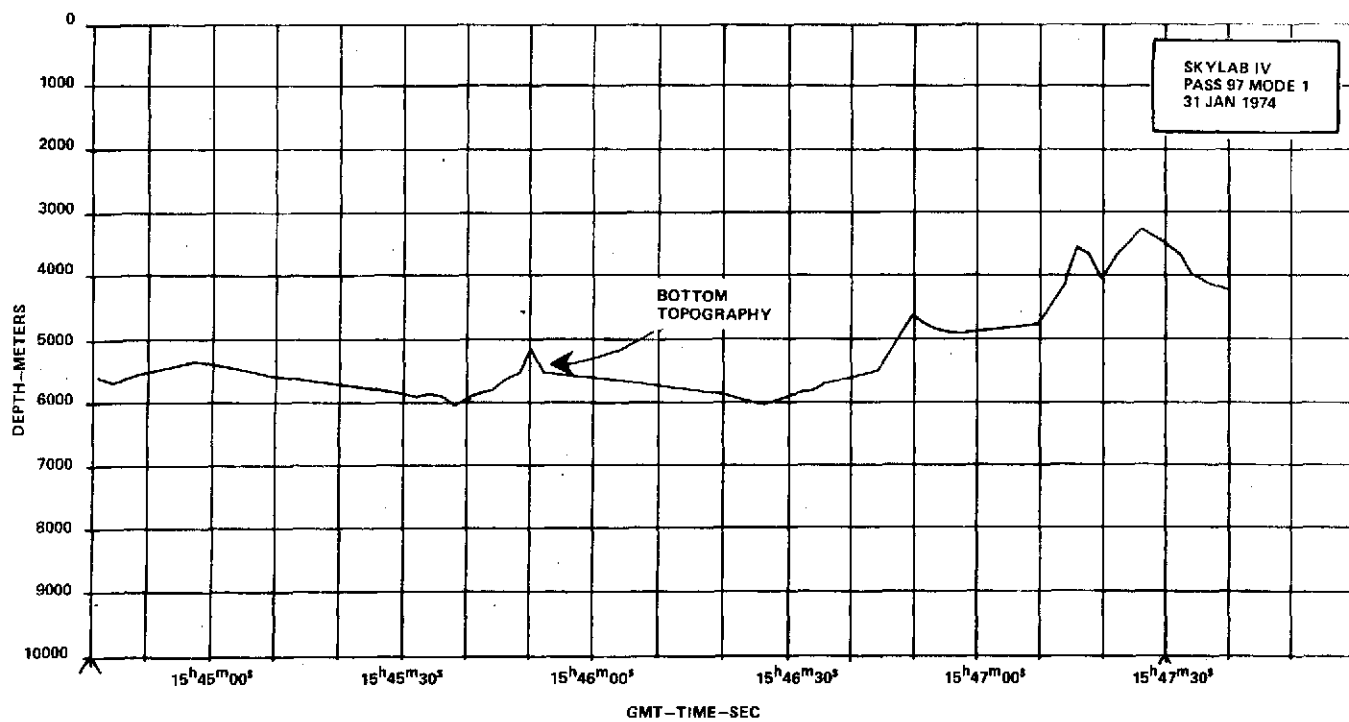
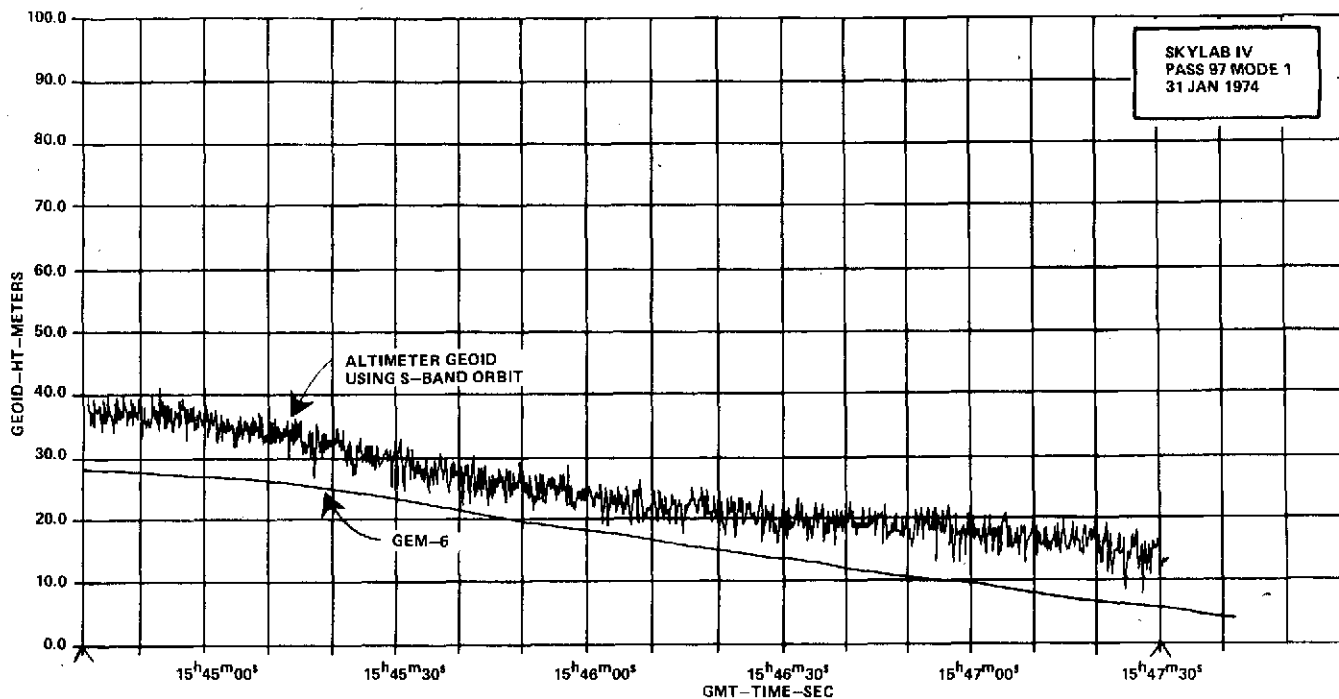
11.2°
139.2°



Lat 14.4°
Long 141.7°

MAP NO. 212

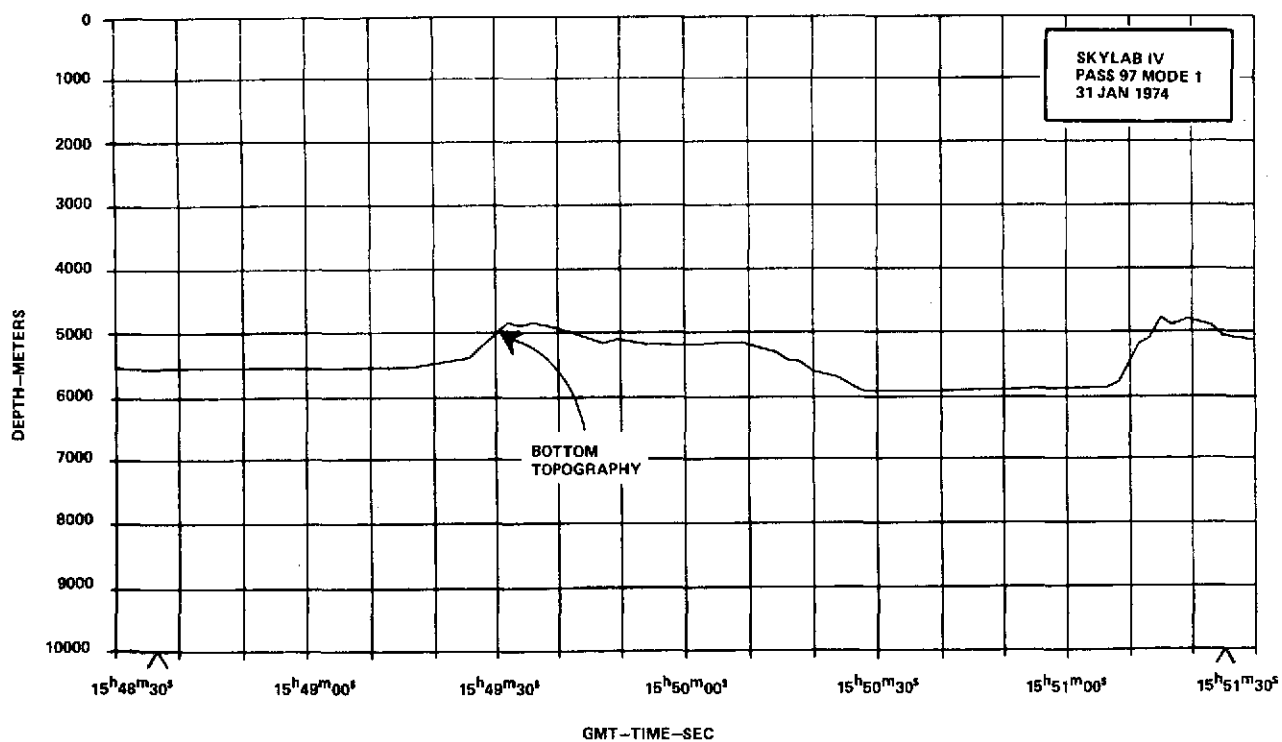
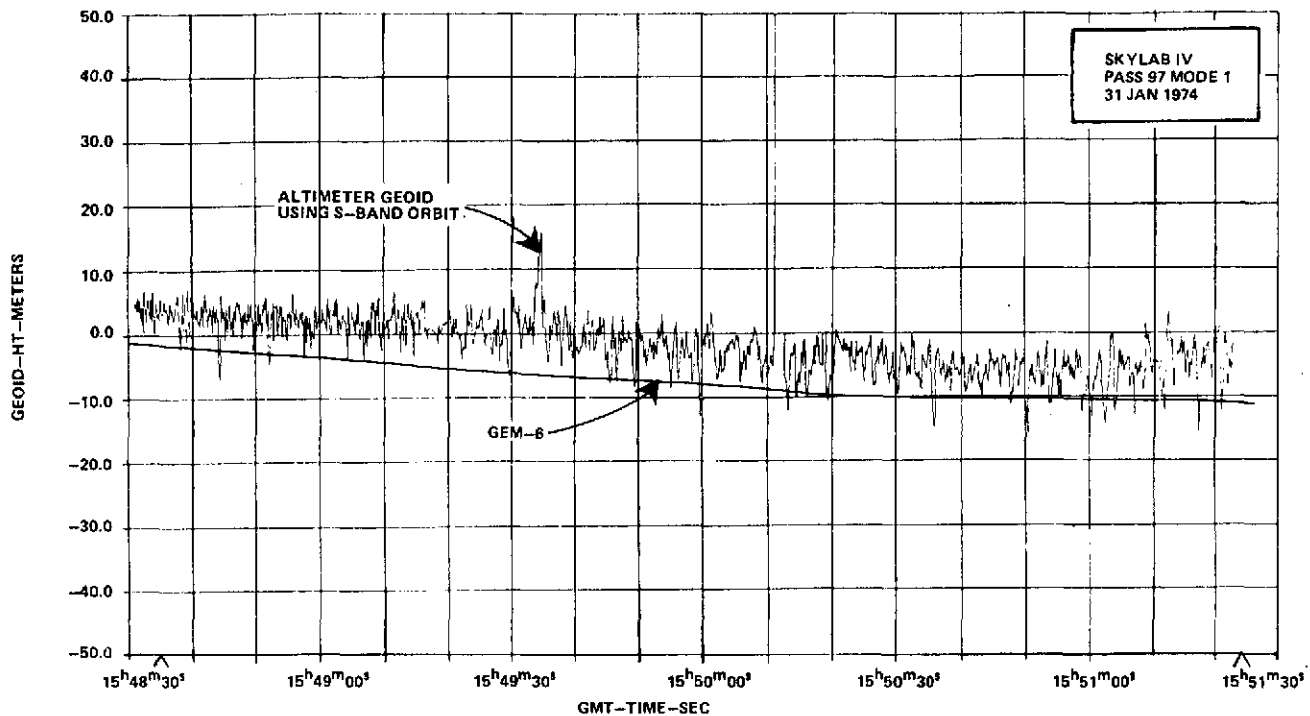
22.5°
148.8°



Lat Lat 34.5°
Long 150.8°

MAP NO. 213

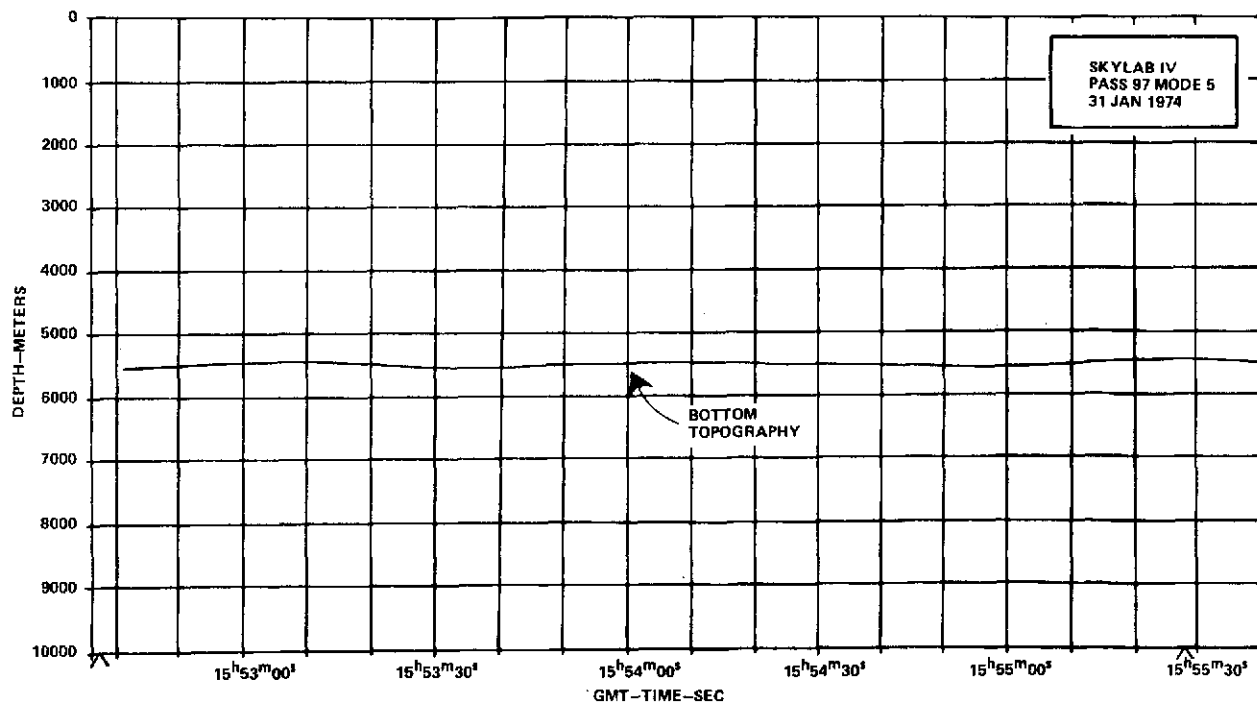
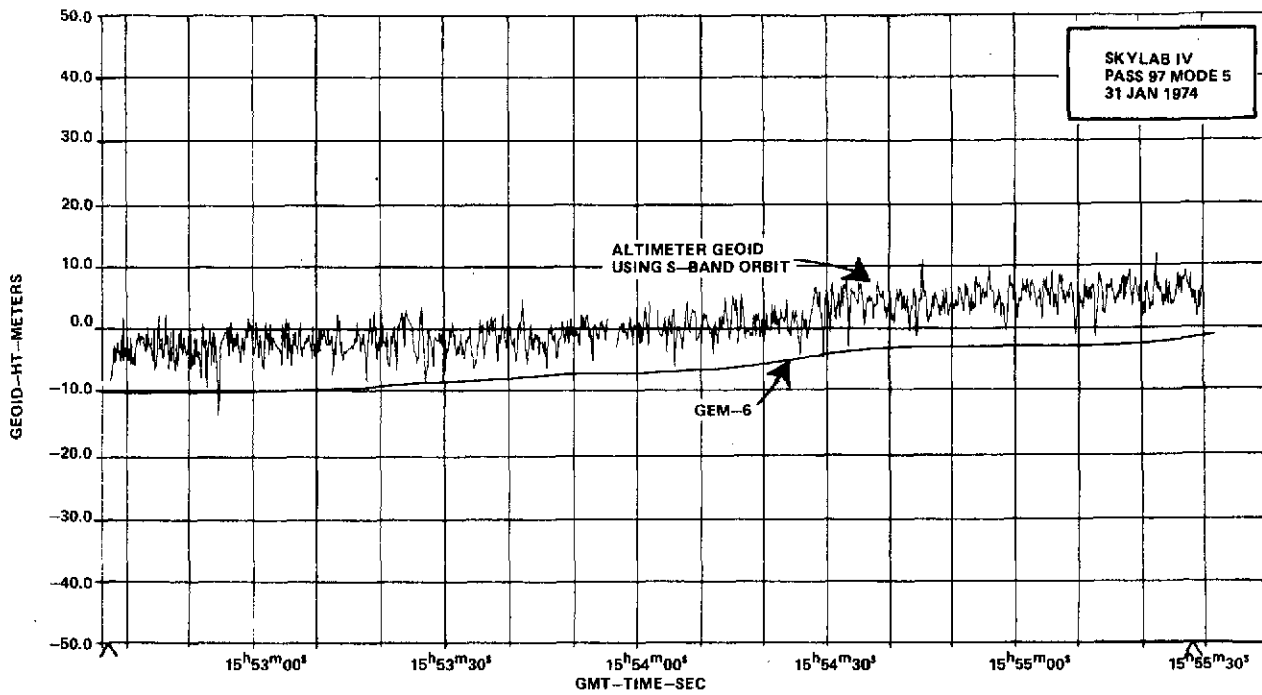
32.0°
159.2°



Lat 34.7°
Long 162.8°

MAP NO. 214

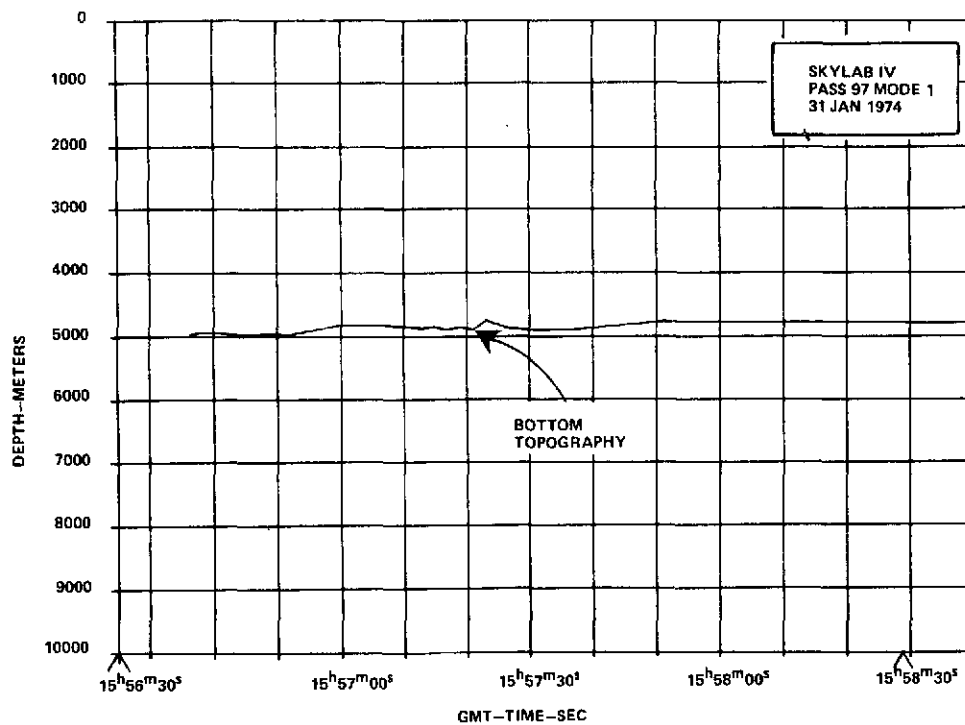
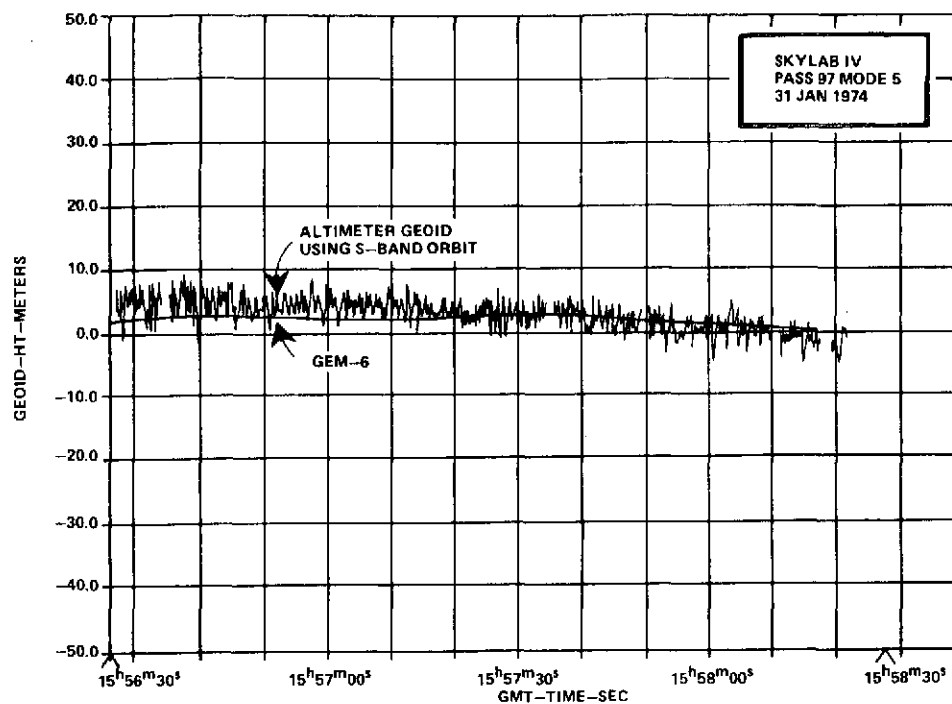
41.1°
173.3°



Lat 43.4°
Long 178.5°

MAP NO. 215

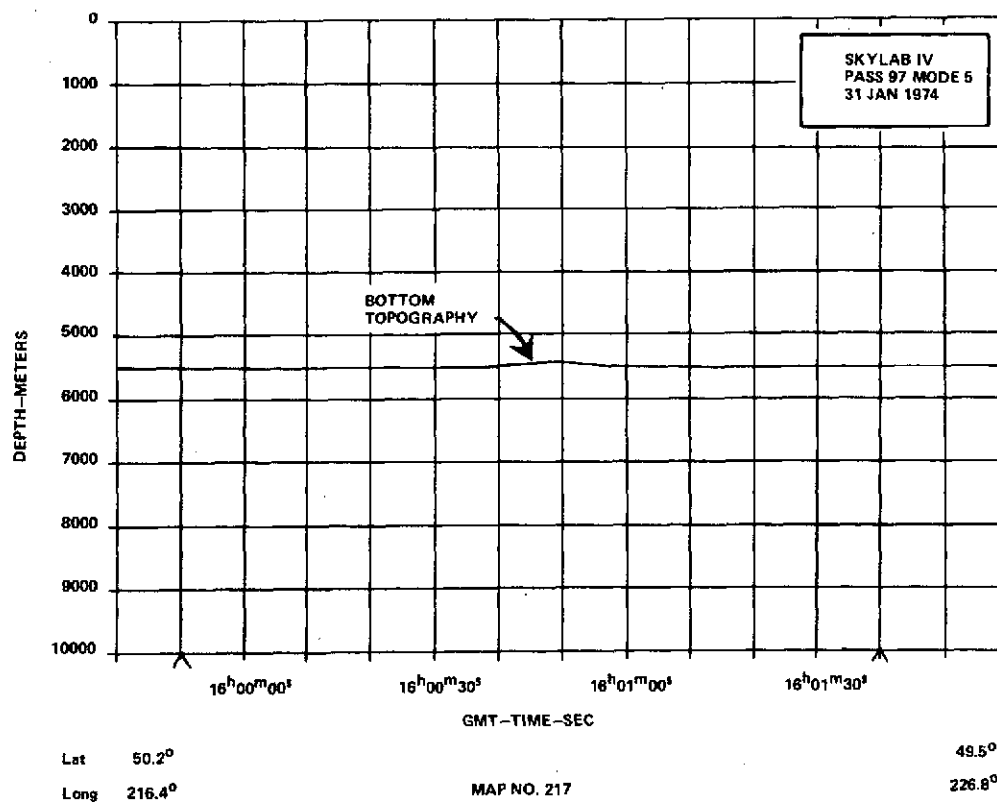
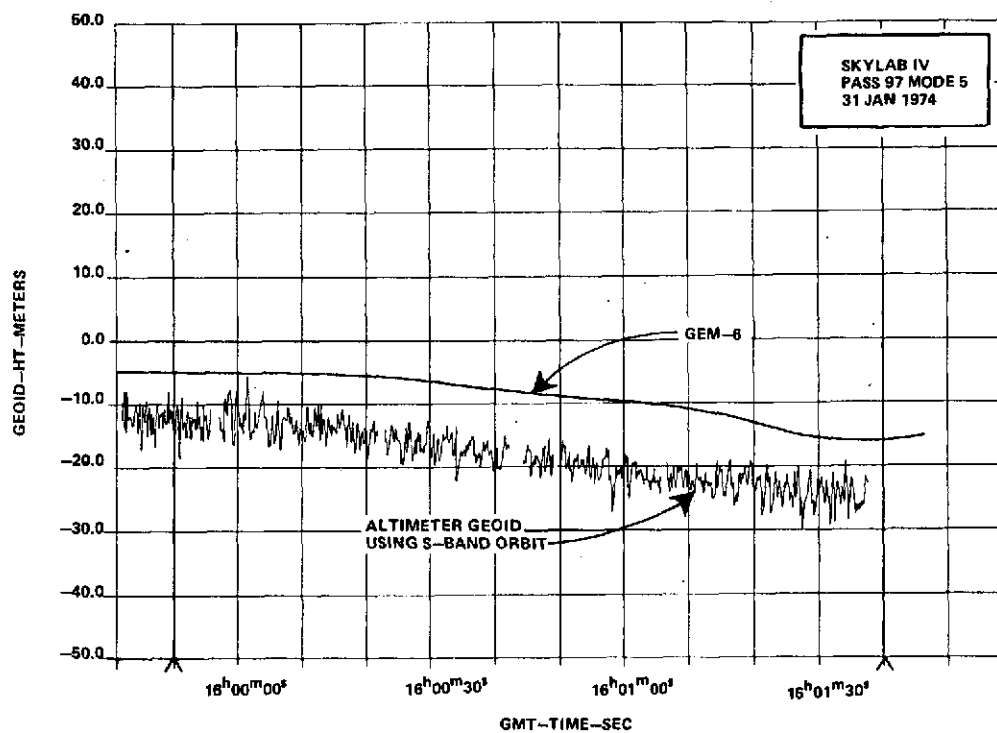
47.7°
192.1°

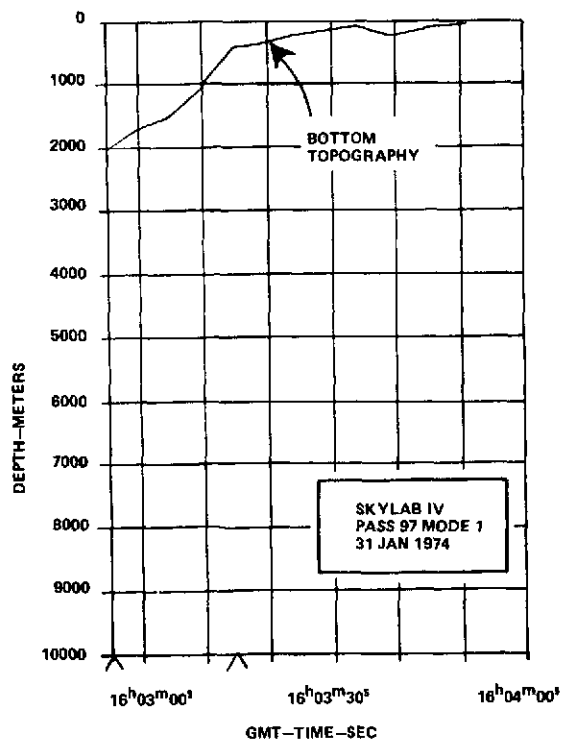
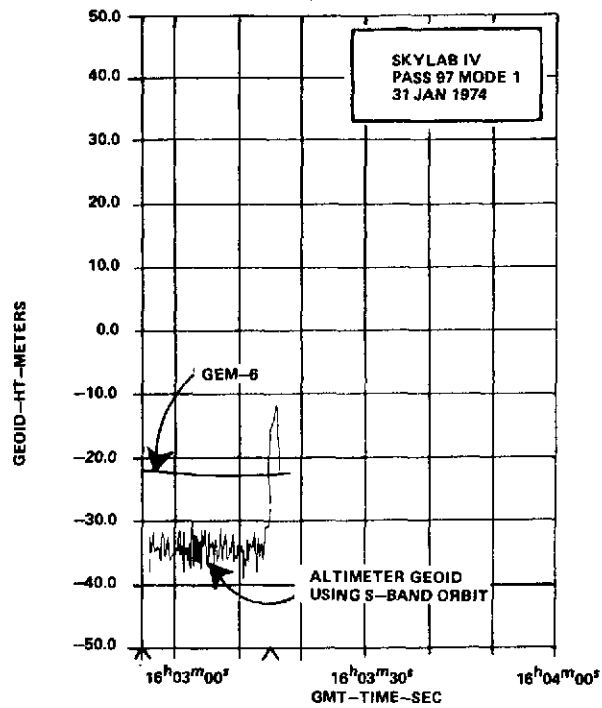


Lat 48.8°
Long 197.3°

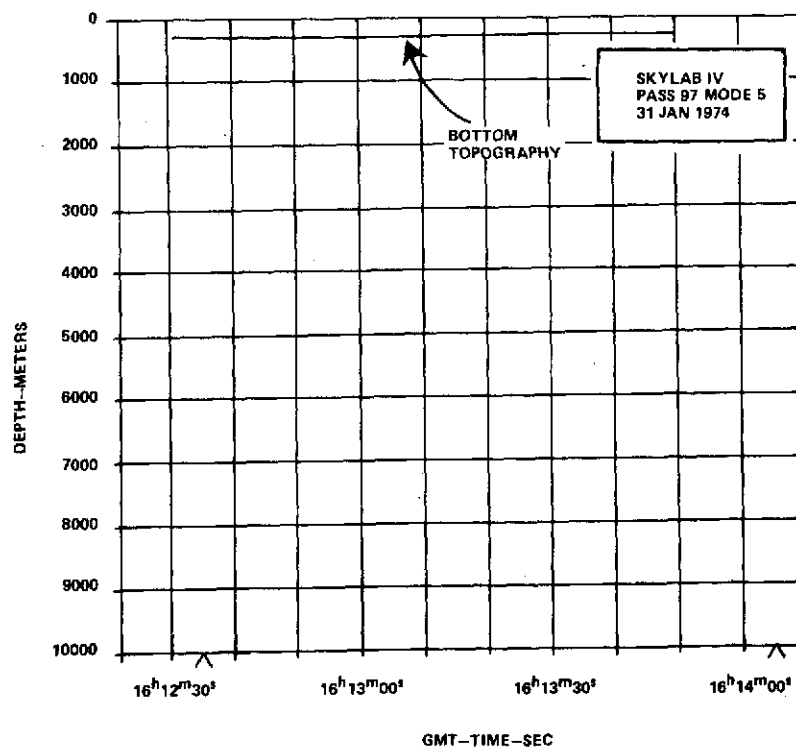
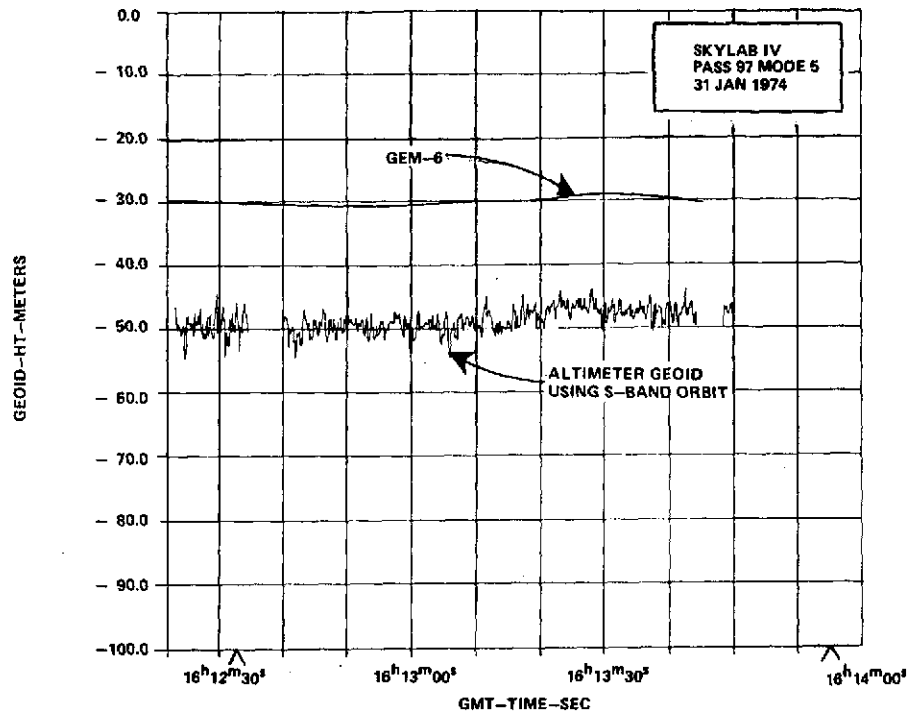
MAP NO. 216

50.0°
208.5°





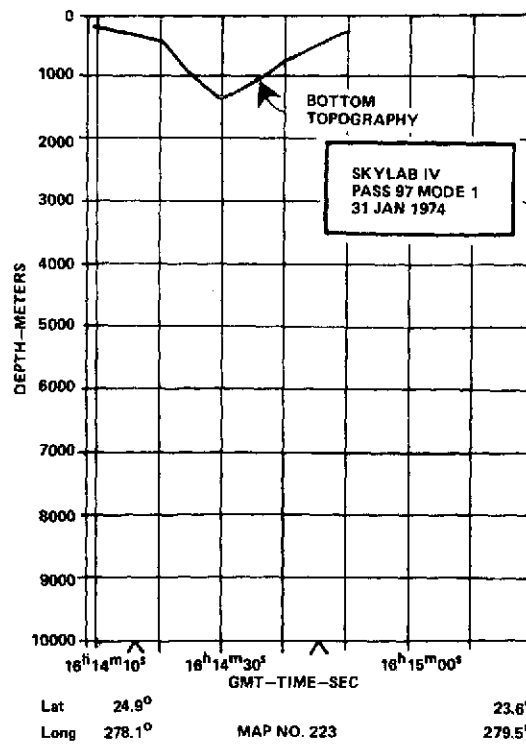
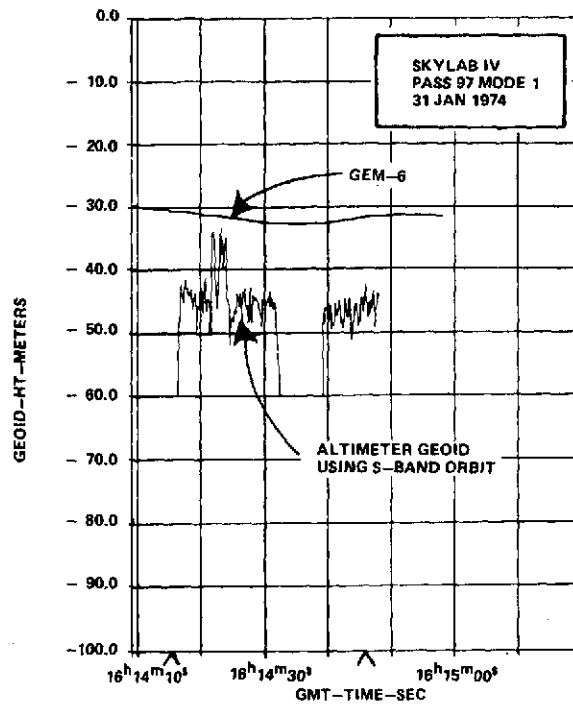
| | | | |
|------|--------|-------------|--------|
| Lat | 48.5° | | 48.1° |
| Long | 233.7° | MAP NO. 218 | 235.4° |

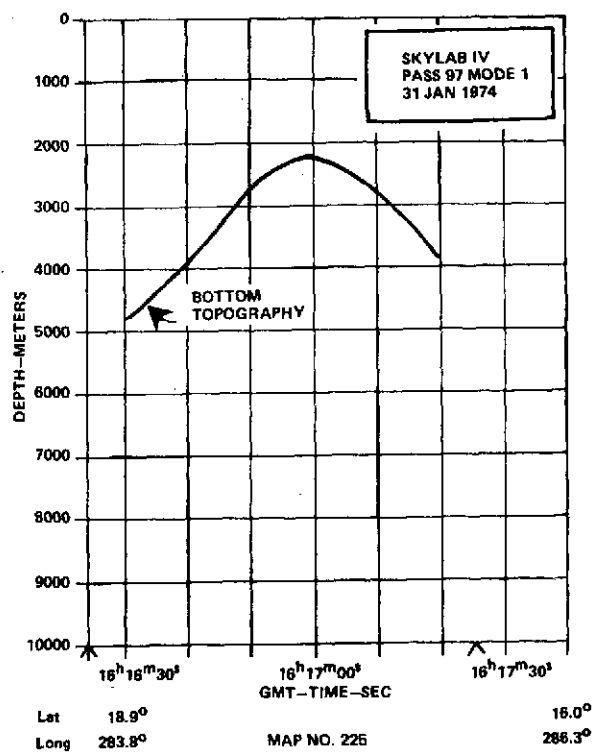
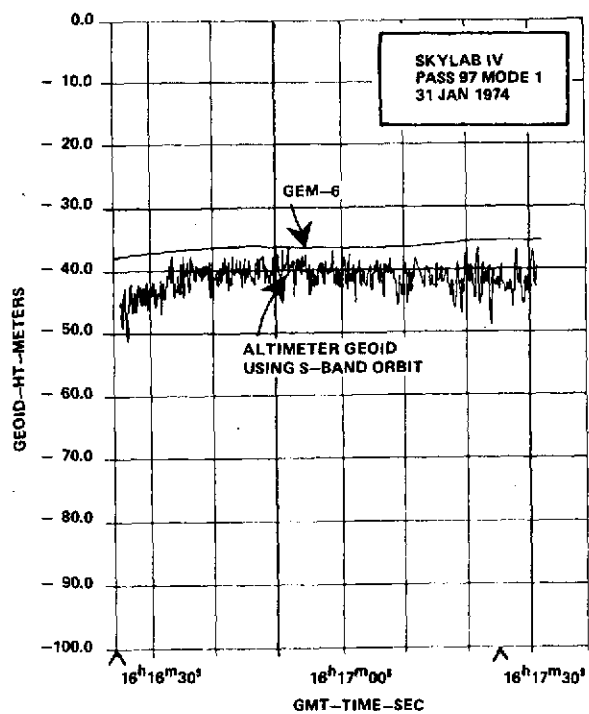


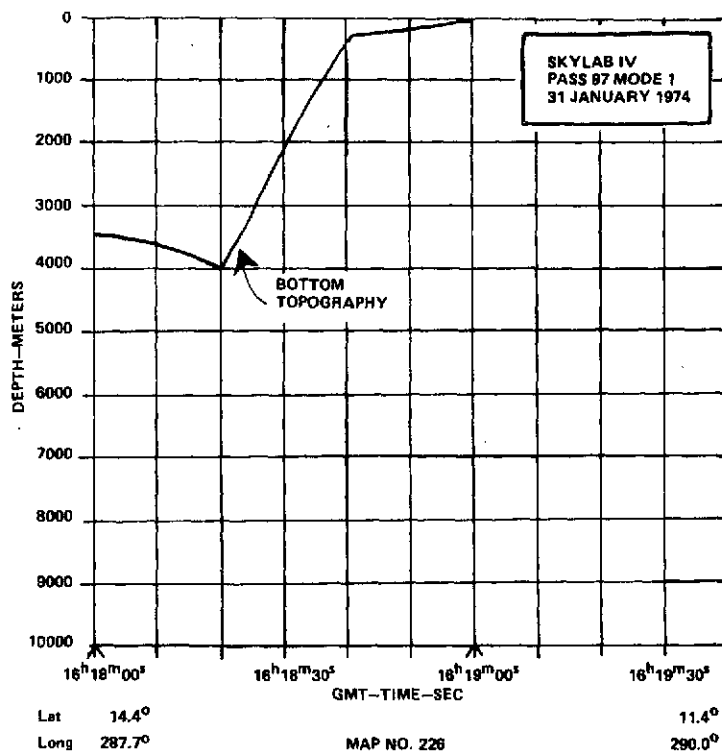
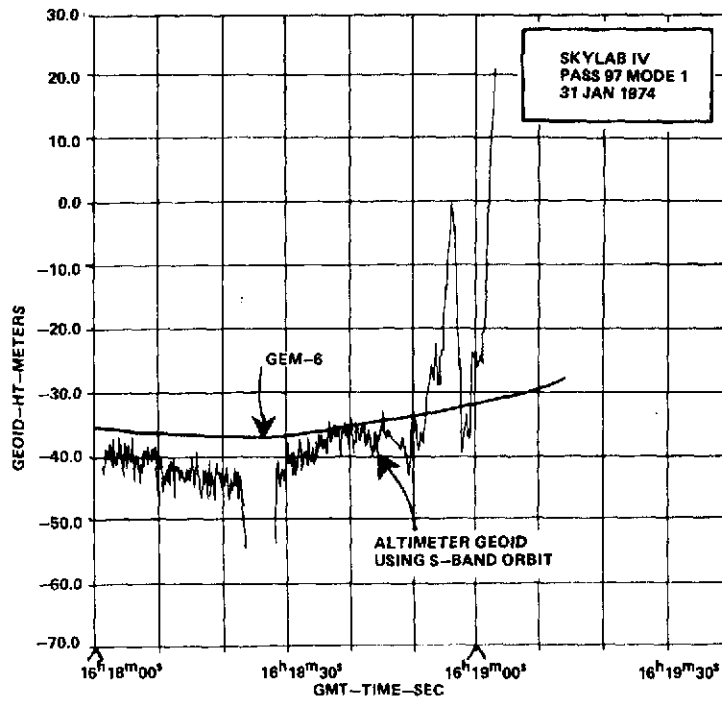
Lat 29.4°
Long 273.3°

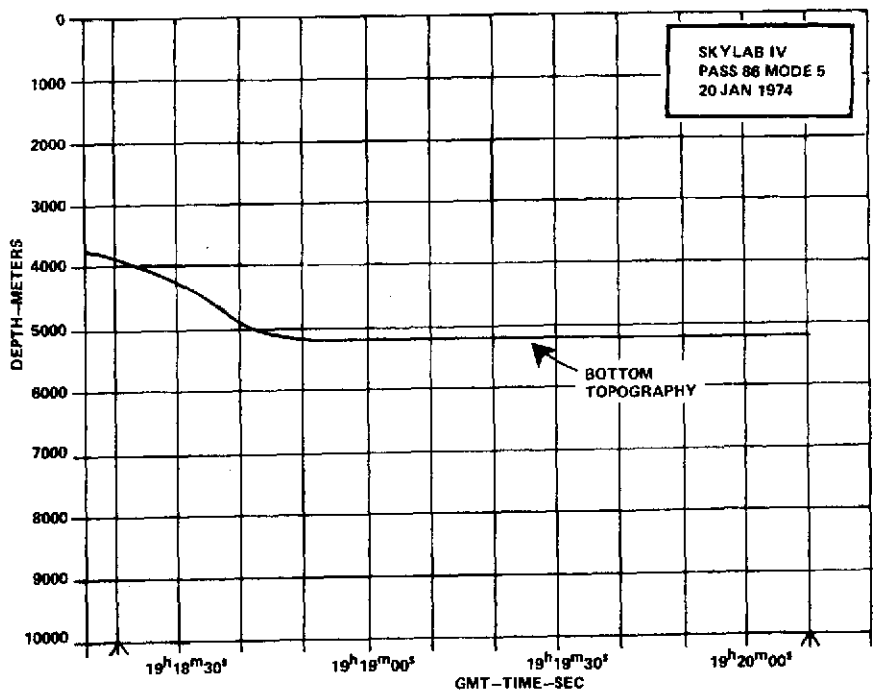
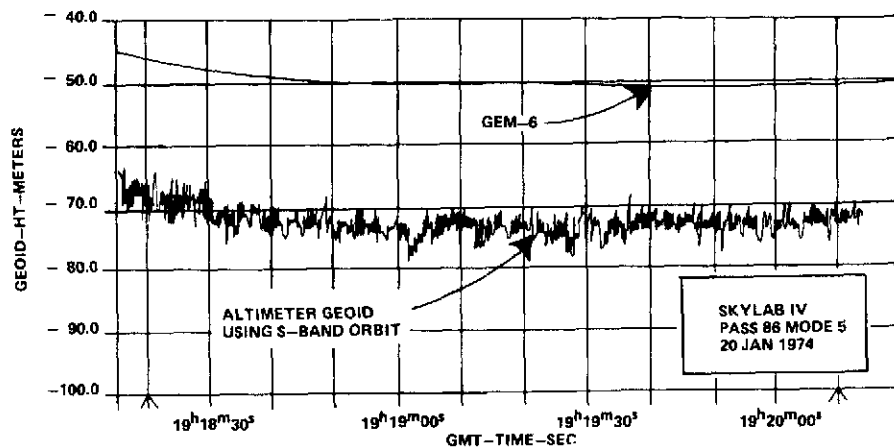
MAP NO. 222

25.4°
277.7°









Lat 34.7°
Long 285.7°

MAP NO. 233

30.0°
291.7°

AUTOMATIC GAIN CONTROL

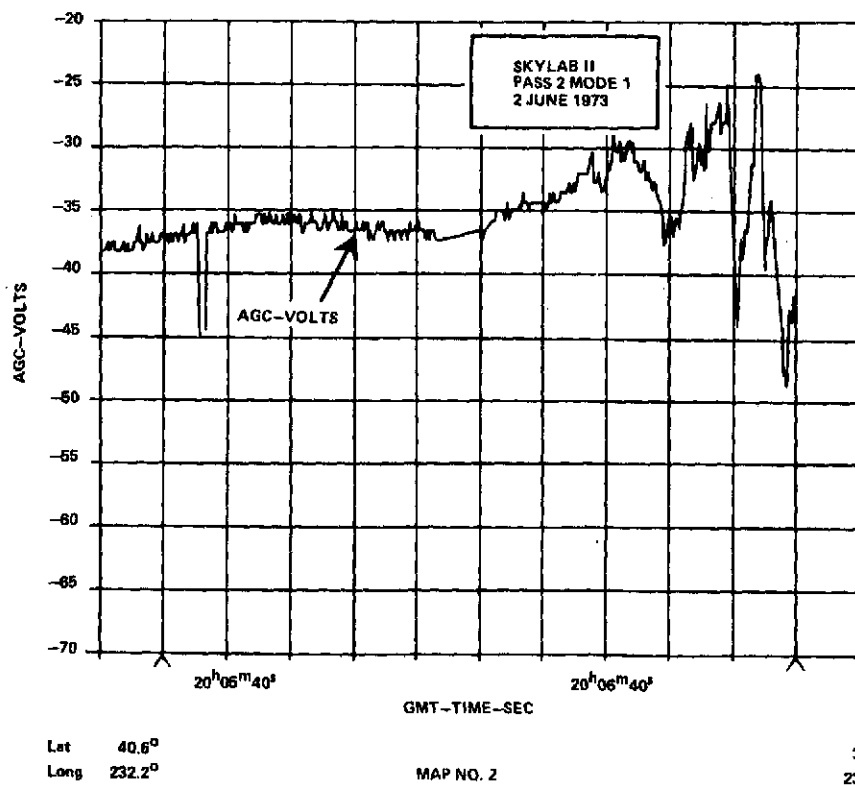
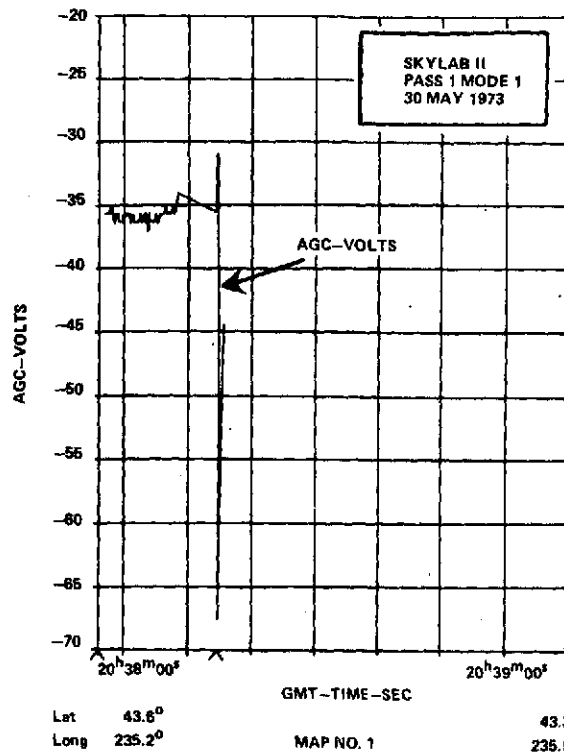
The Automatic Gain Control (AGC) of the altimeter is a good indicator of the relative signal strength of the return signals. Unfortunately, in the conversion of counts to volts that can be related to signal level, the wrong calibration curve was mistakenly utilized in the ground processing. The effort required to reprocess the AGC to correct this error was not felt to be justified, for the relative values of signal strength would still be significant even if the absolute calibration was lost. In addition, it was thought that those whose interest centered on the use of the altitude measurements for topography or geoid studies would primarily use AGC as a relative signal quality indicator.

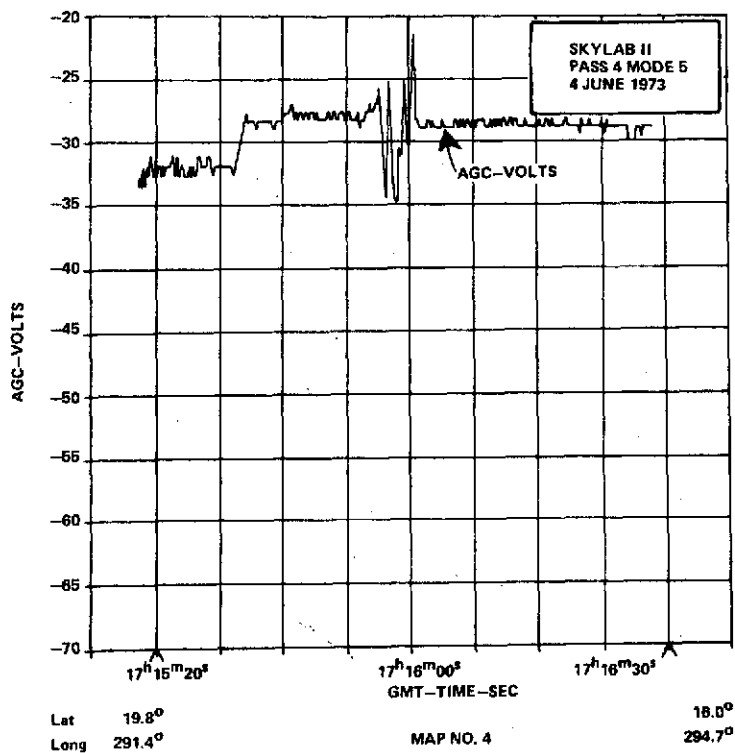
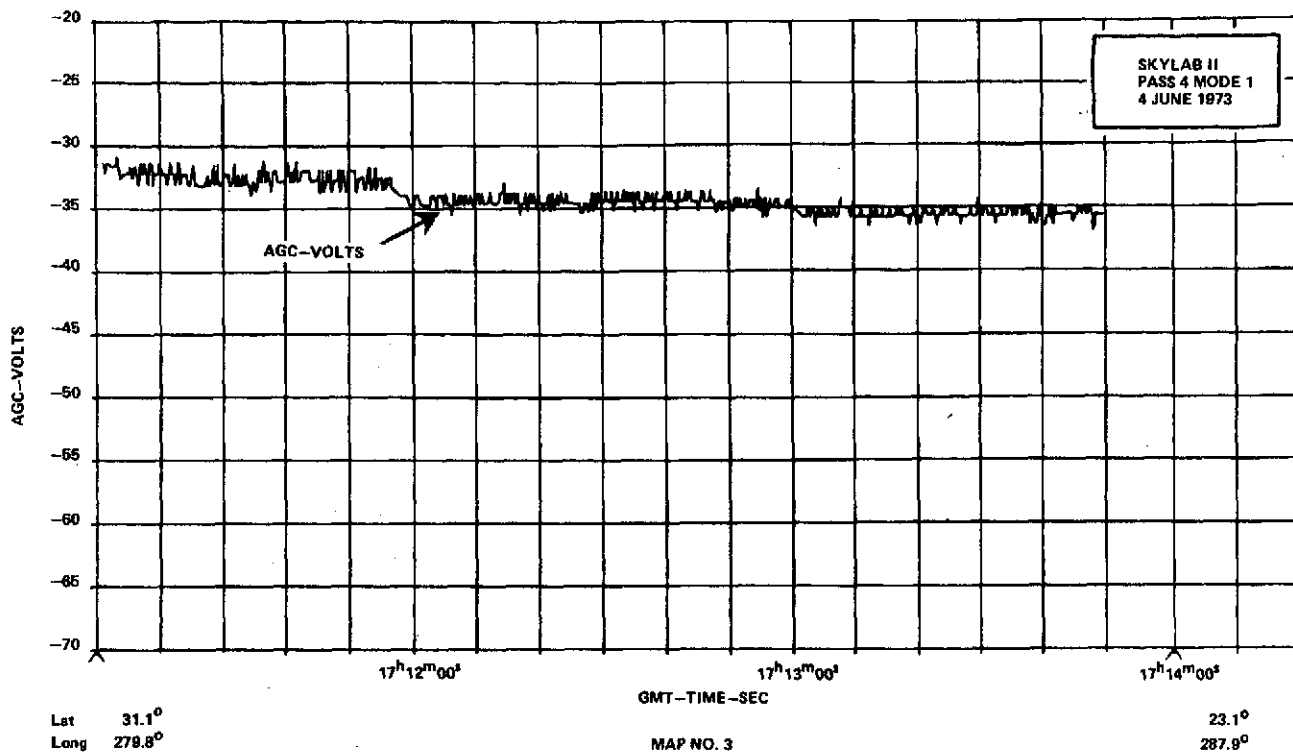
In using the plots supplied in this document, it should be remembered that a -30 db AGC level, when operating with the 100 ns pulsewidth and 10 MHz bandwidth, is the strongest expected signal. If the returns get stronger, chances are the surface has become specular. At this -30 db level the system is operating with a signal-to-noise of approximately 30 db. As operating parameters are changed, the signal level will change in discrete steps; therefore, these steps can help establish exact times of sub-mode changes. By comparing signal levels of good pointing passes to those where pointing was not good, the direct effects of pointing on AGC can be appreciated.

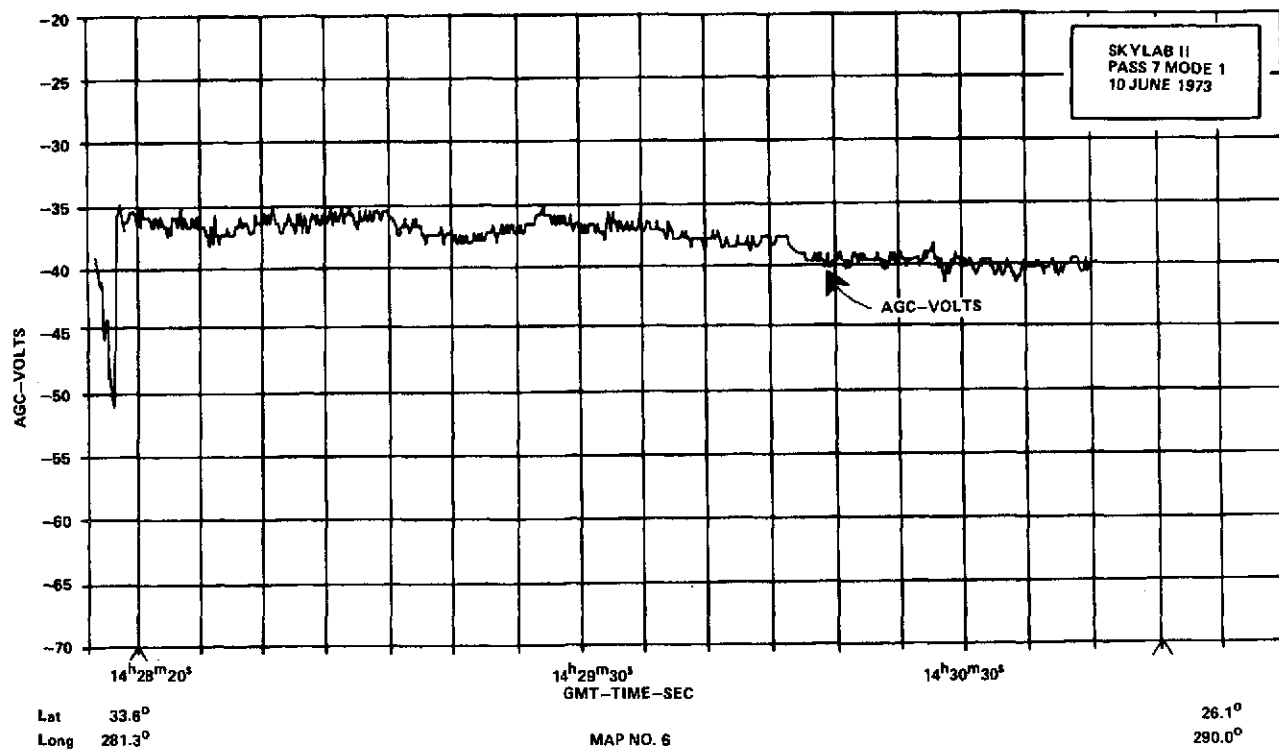
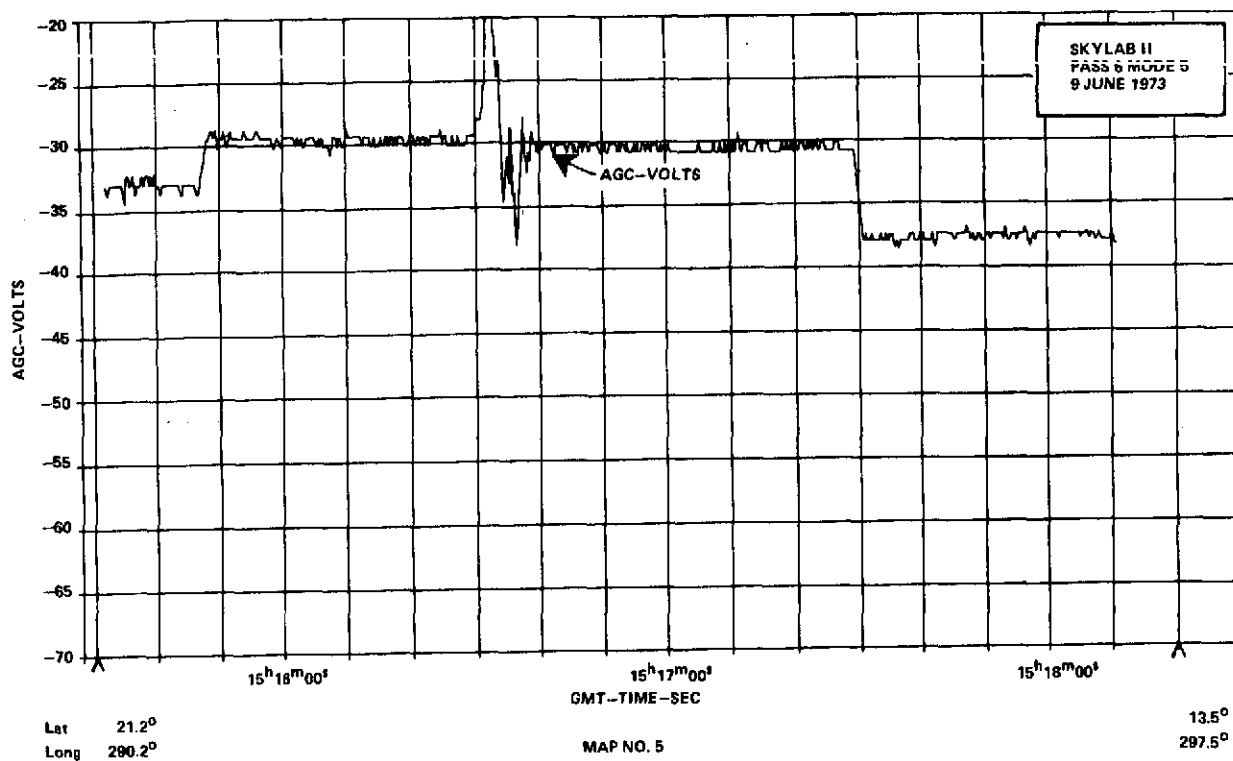
Sharp spikes (less than 10 sec in duration) in the altitude residuals can often be related to the AGC plots as sudden loss of signal (deep fades) or sudden increases in signal (specular returns). These can cause the altitude tracker momentarily to lose track which in turn creates both the positive and negative sharp spikes seen.

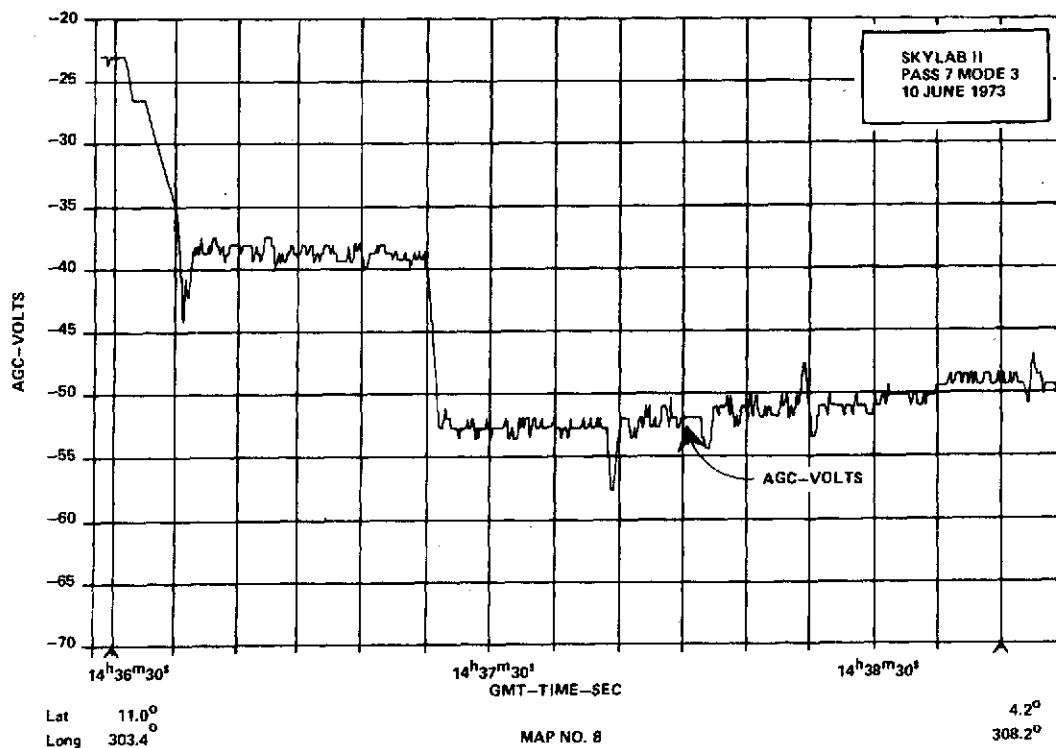
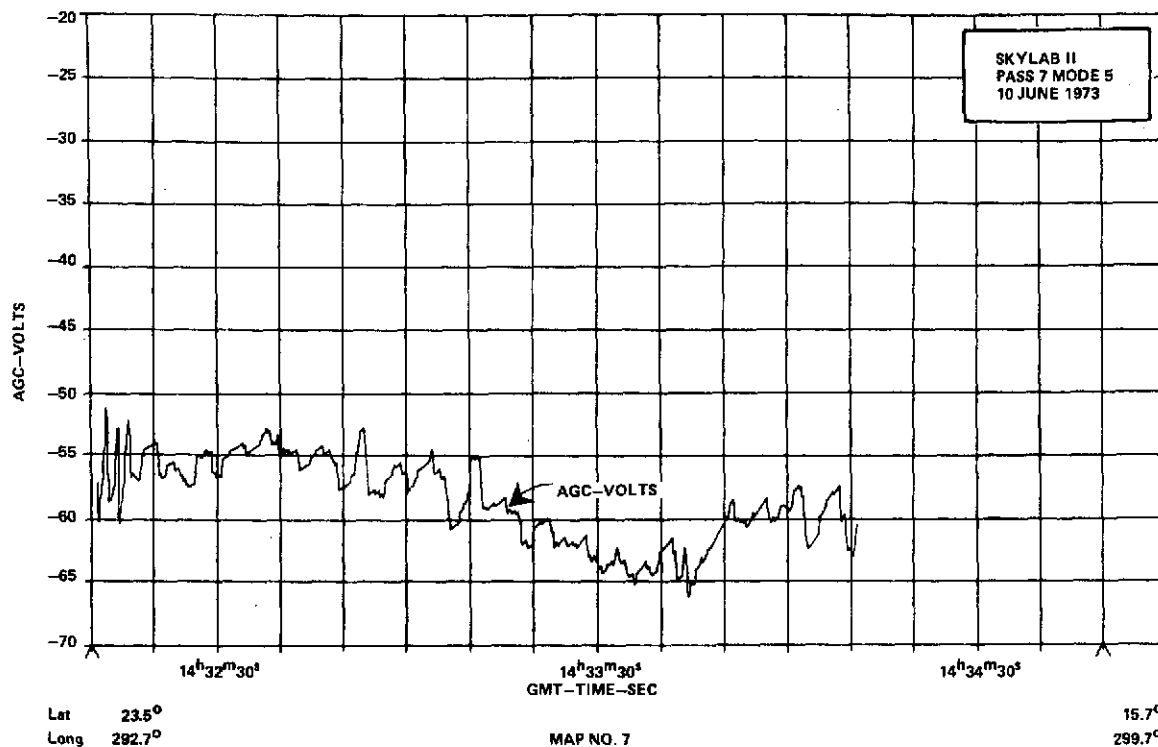
Changes in AGC are primarily due to the changes in the ocean surface roughness. Therefore, the subsurface topography, currents, surface winds, etc. are parameters being sensed by the altimeter AGC. In addition, rain may attenuate the signal causing the AGC to show a loss of signal up to 5 db.

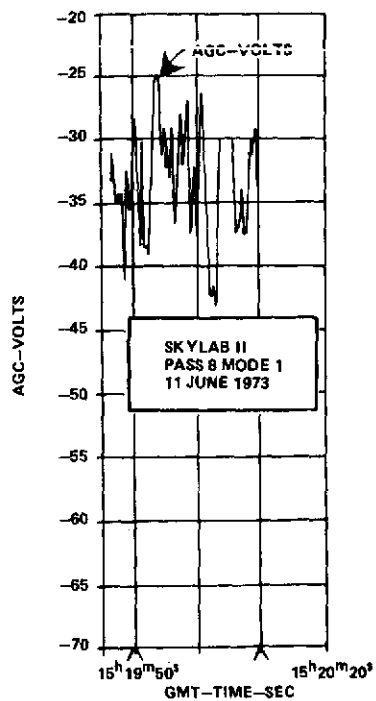
PRECEDING PAGE BLANK NOT FILMED



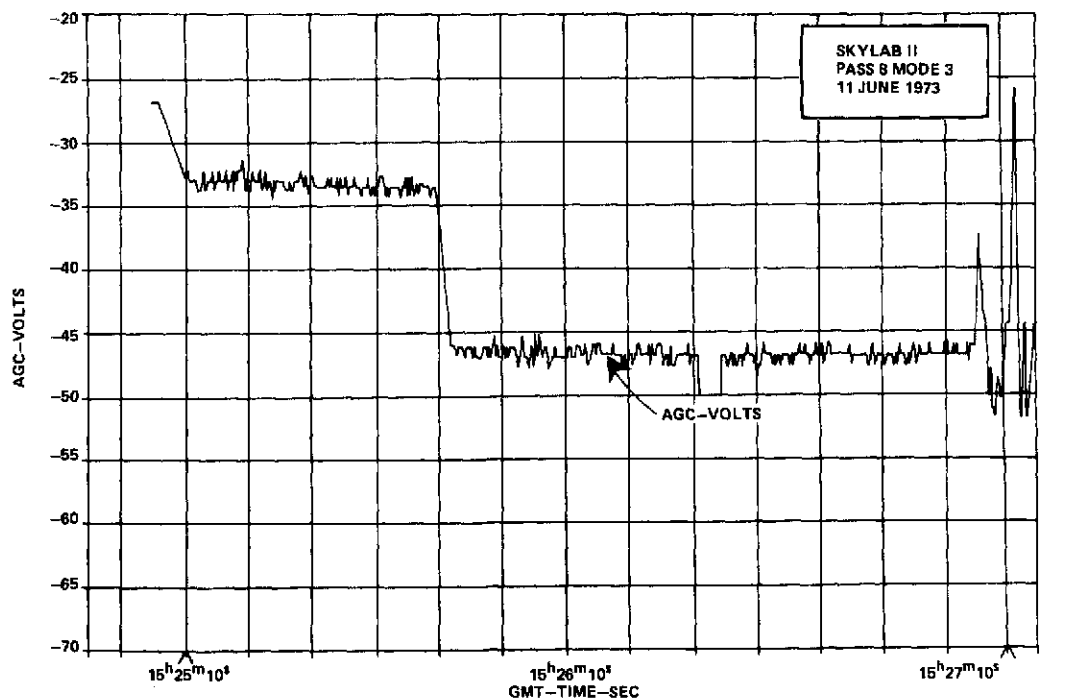




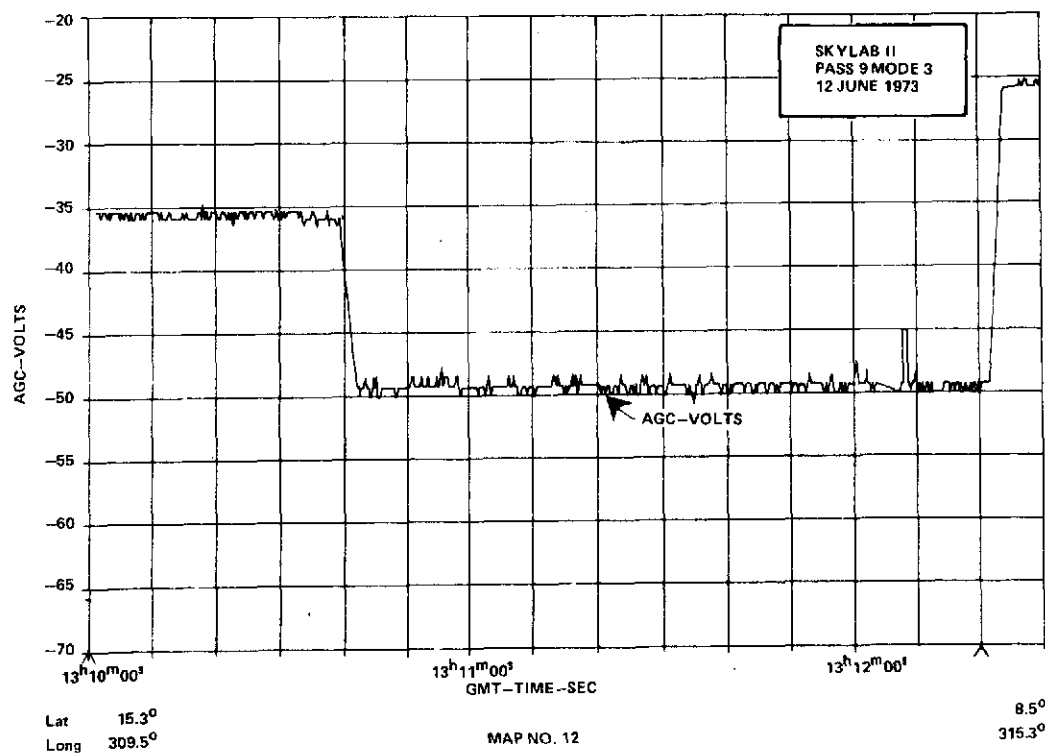
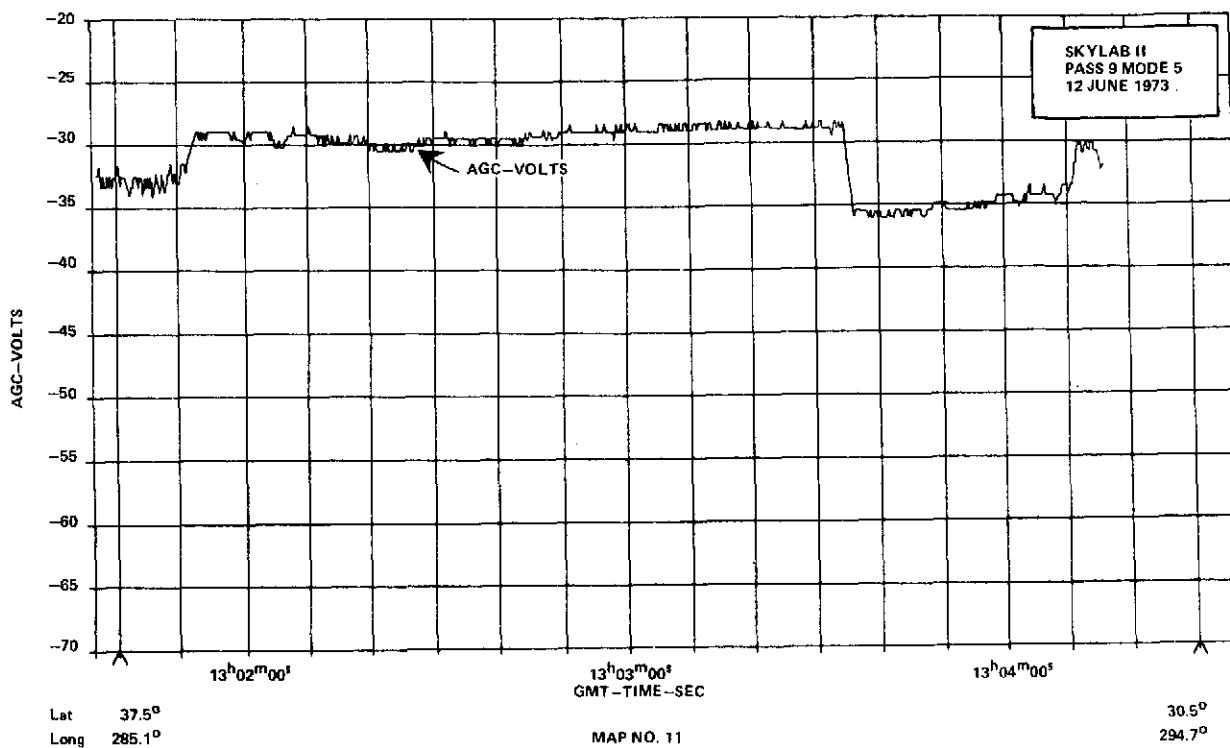


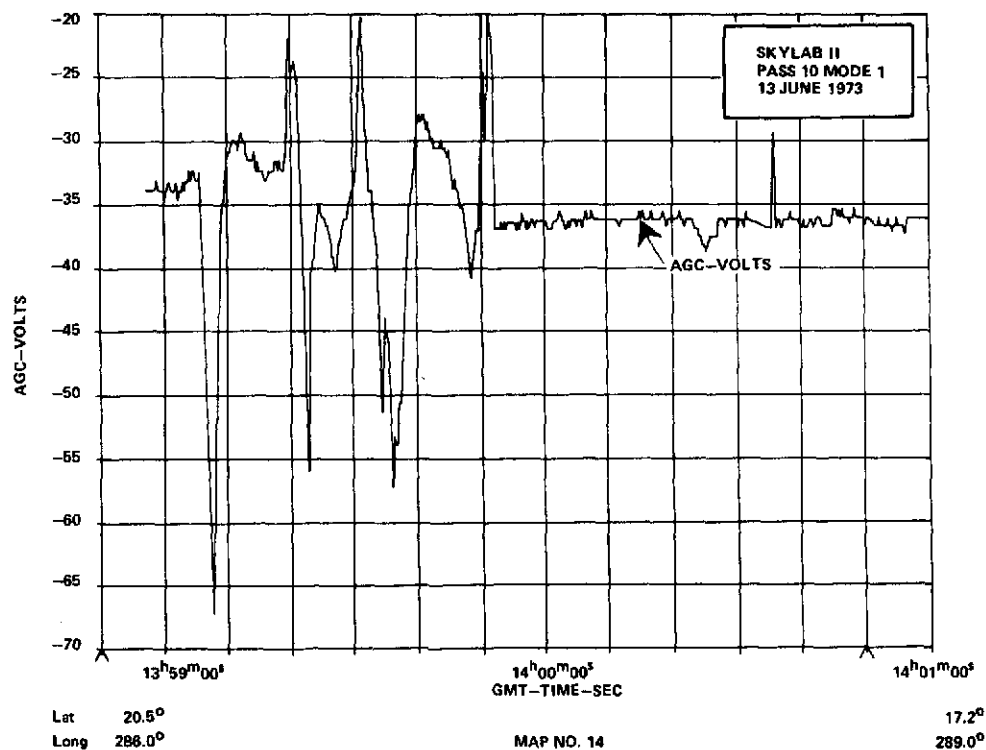
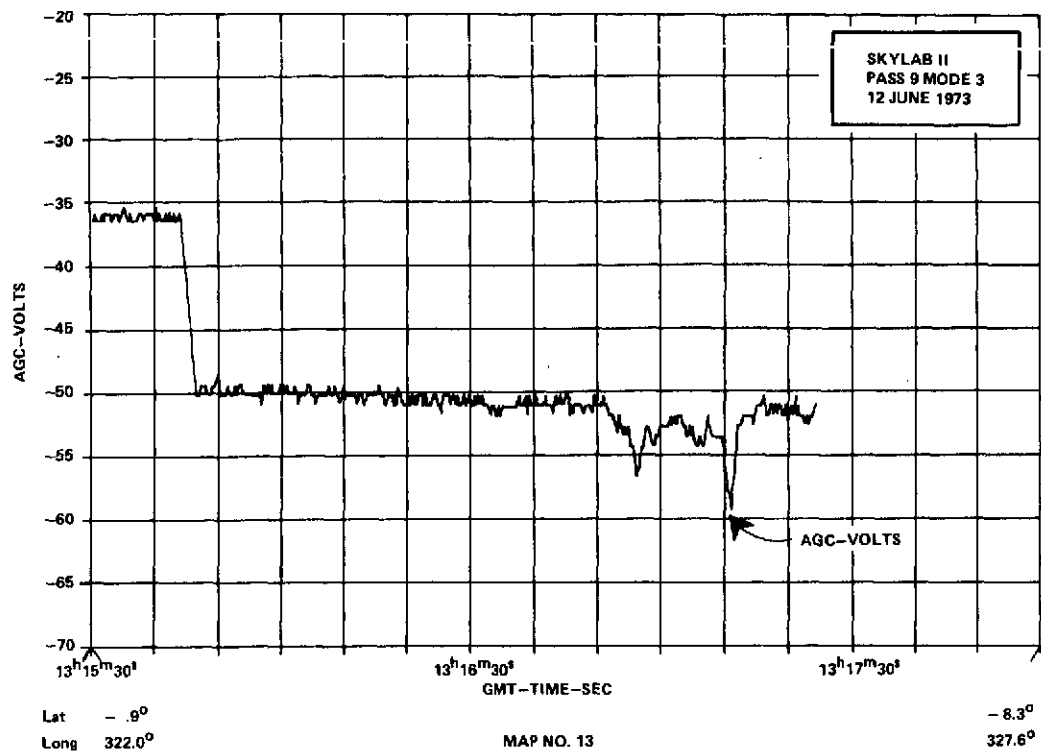


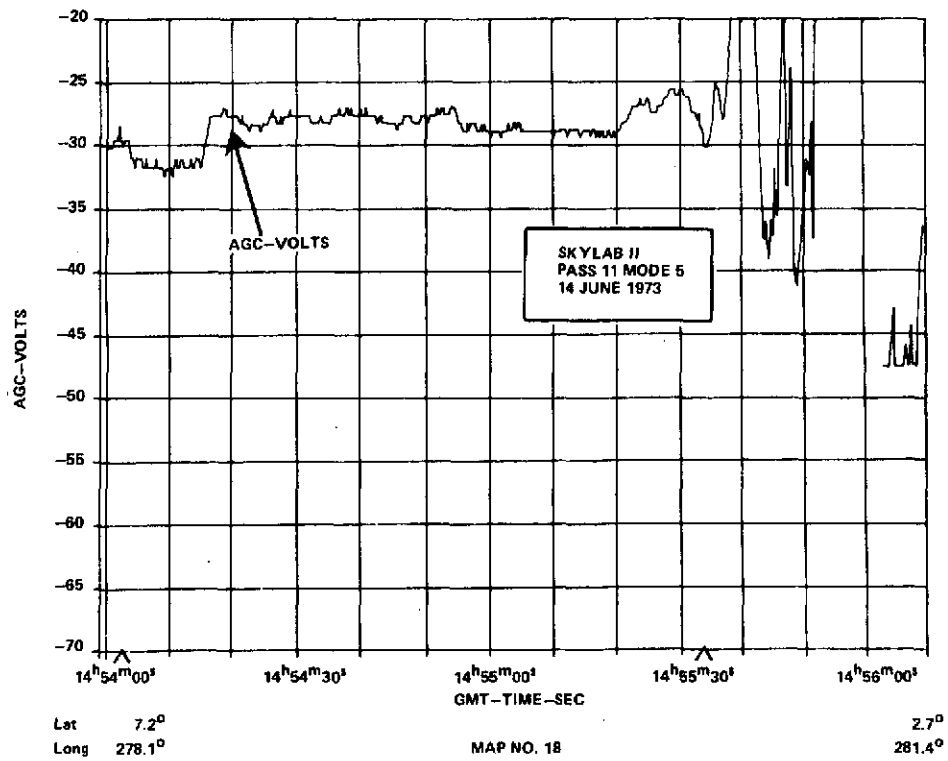
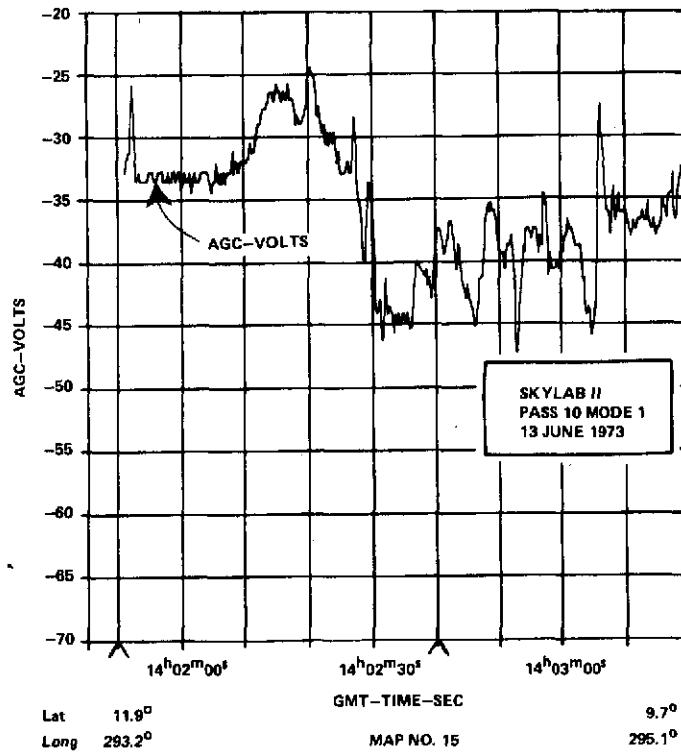
Lat 31.6° 30.5°
Long 285.0° MAP NO. 9 288.4°

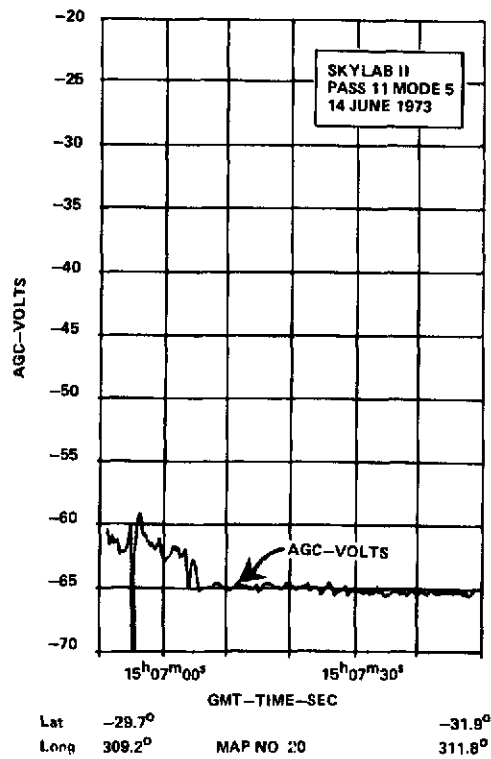
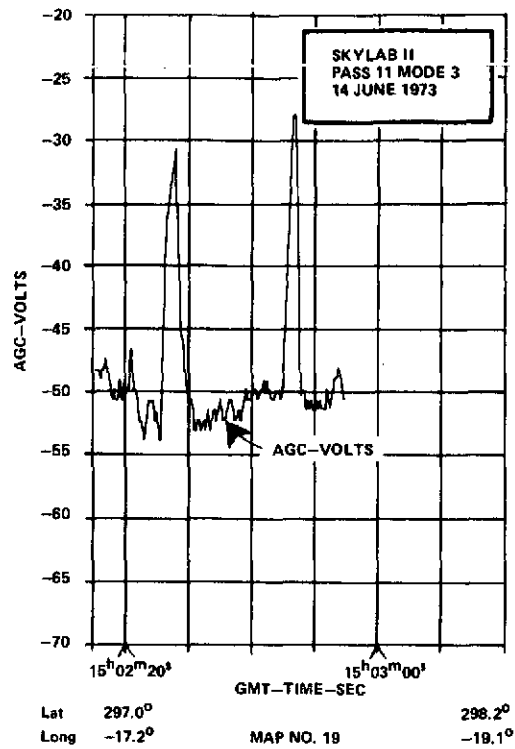


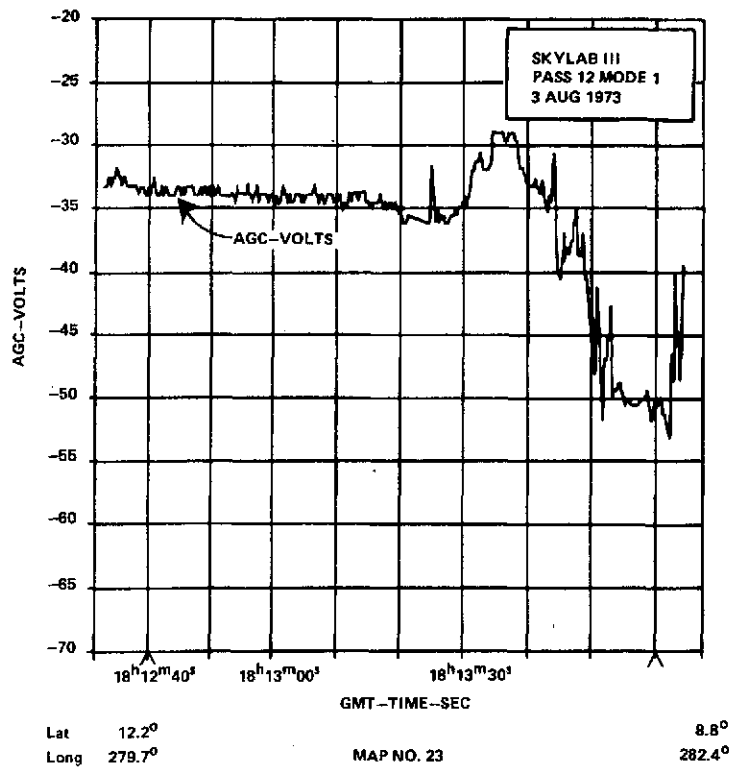
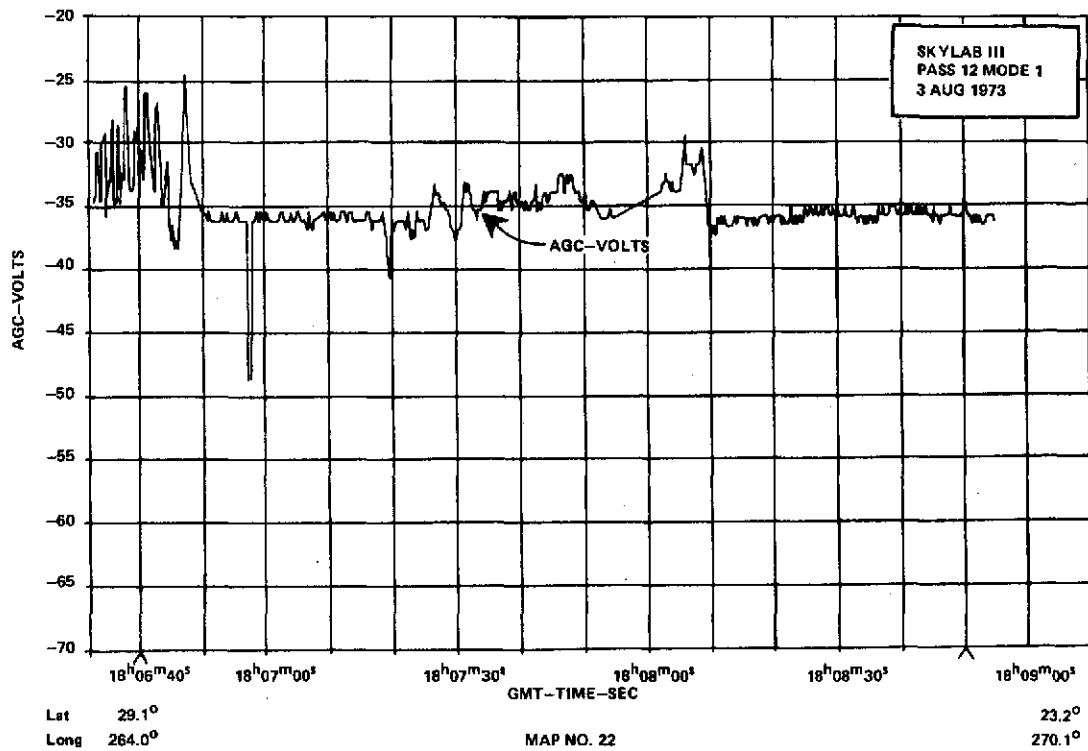
Lat 16.8° 10.5°
Long 279.8° MAP NO. 10 284.9°

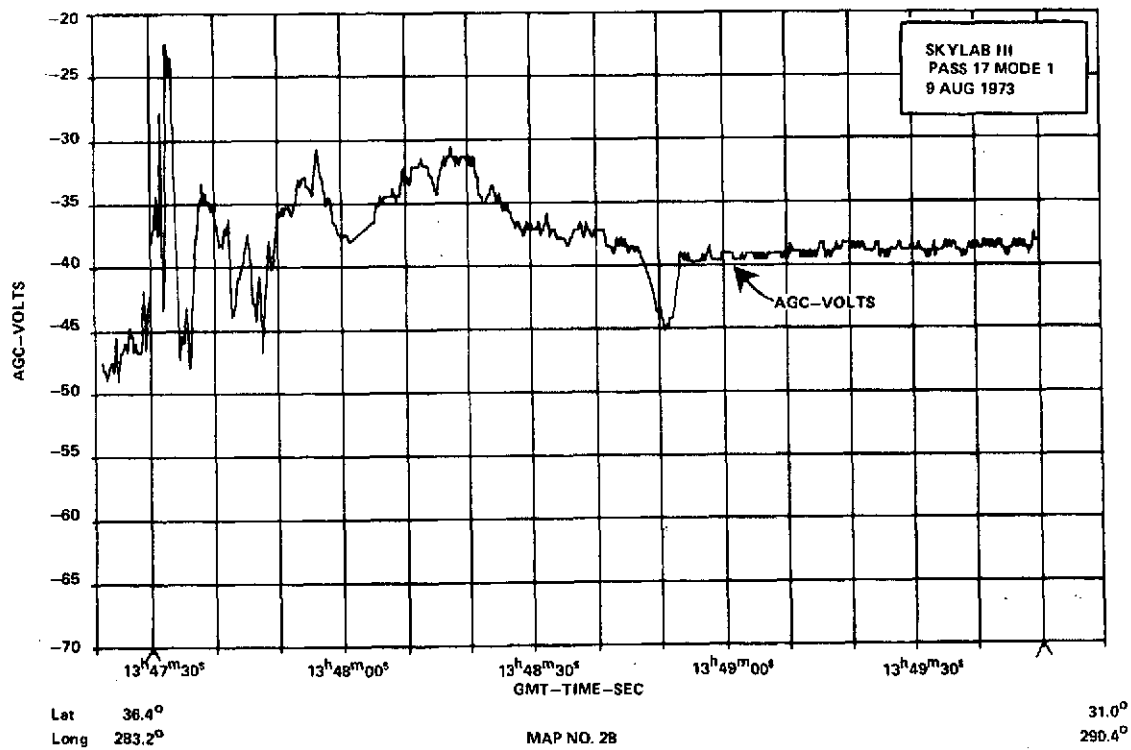
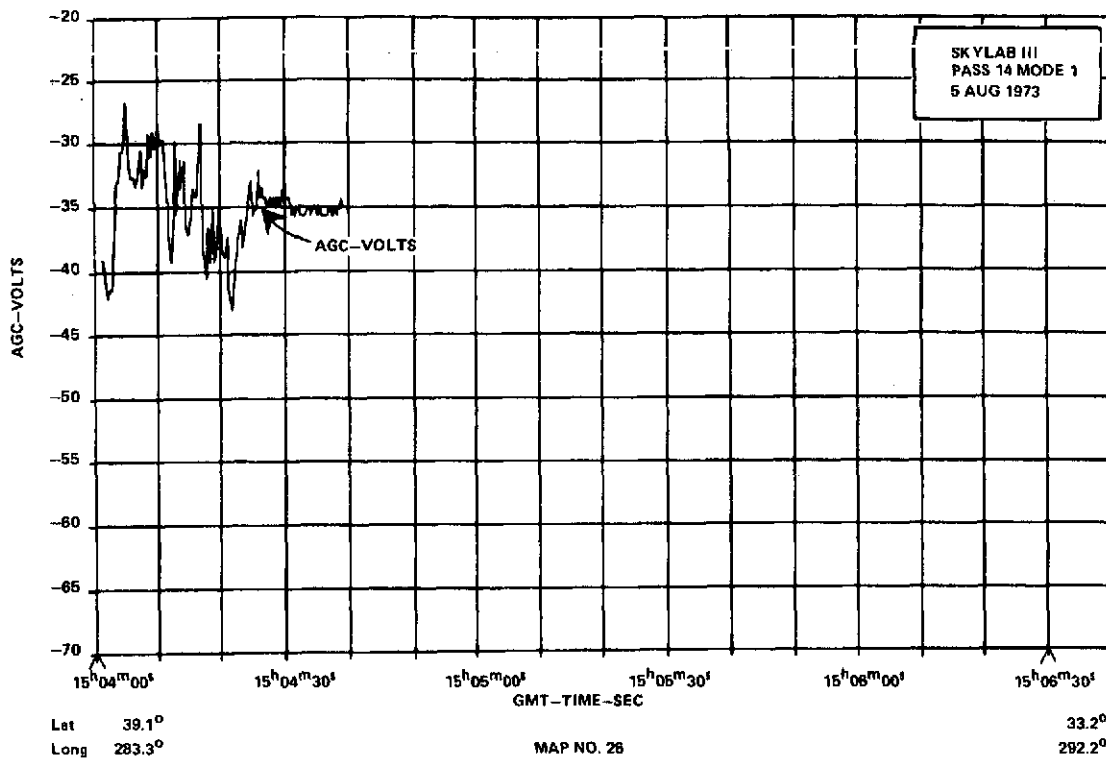


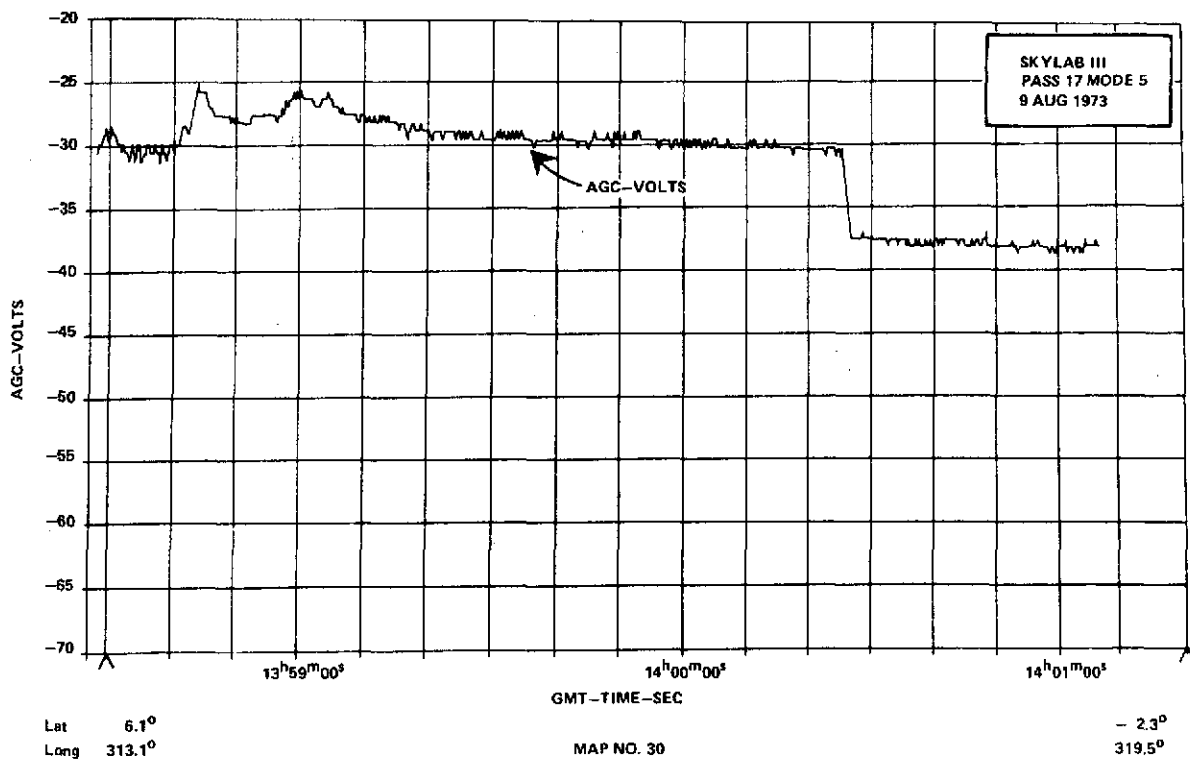
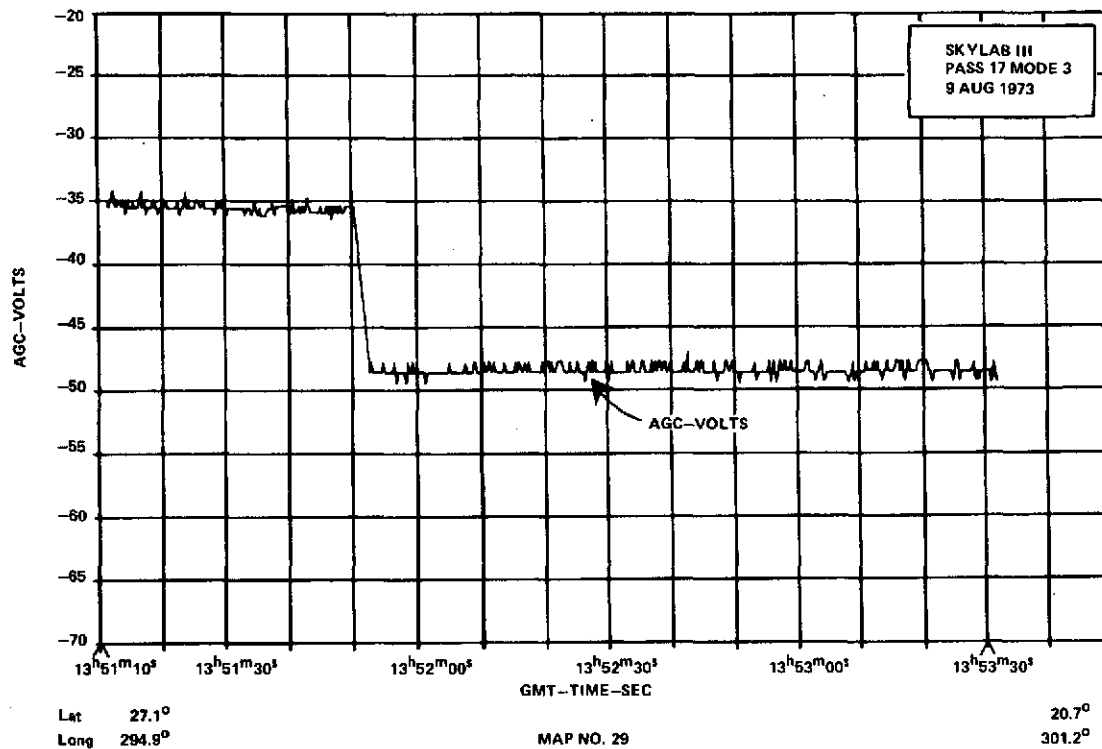


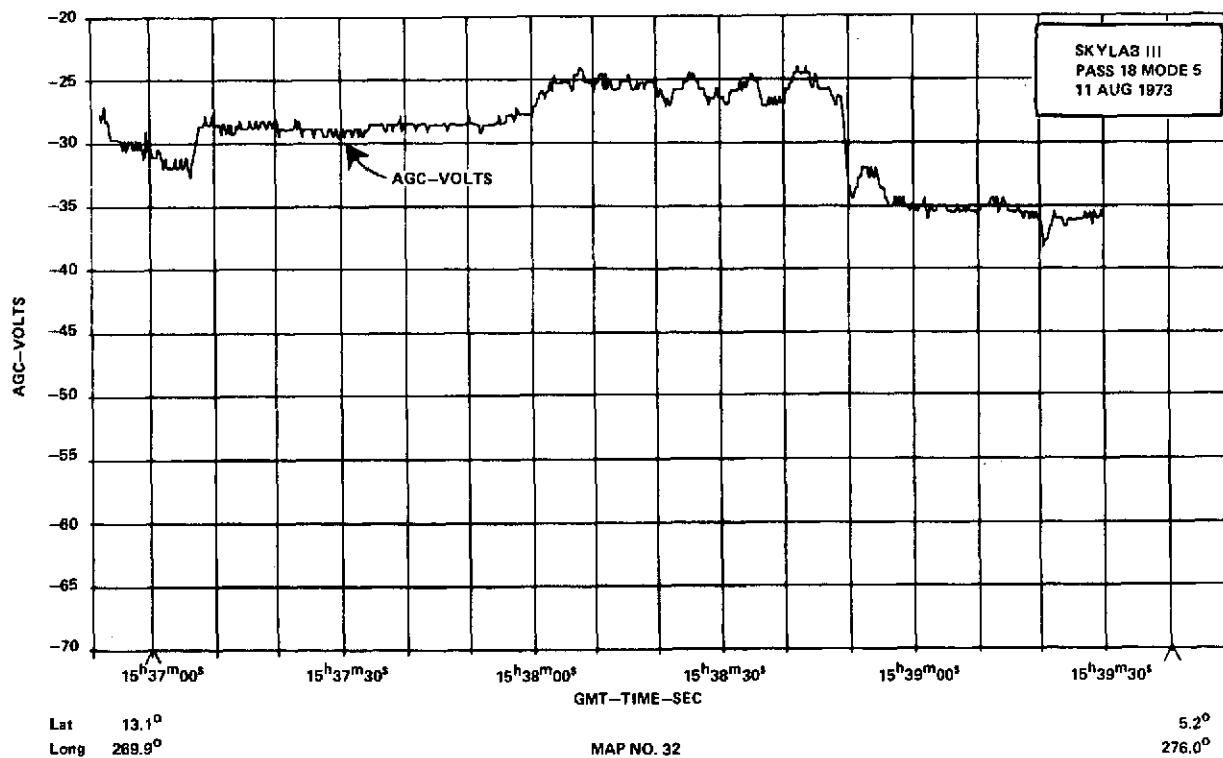
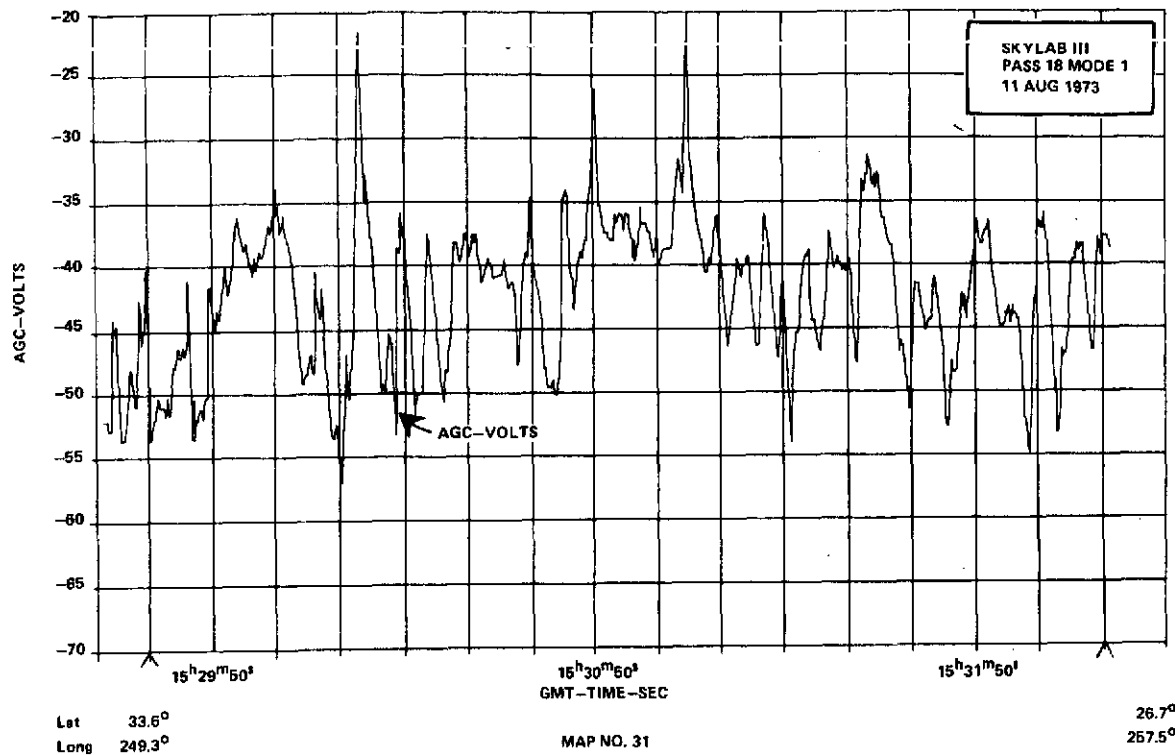


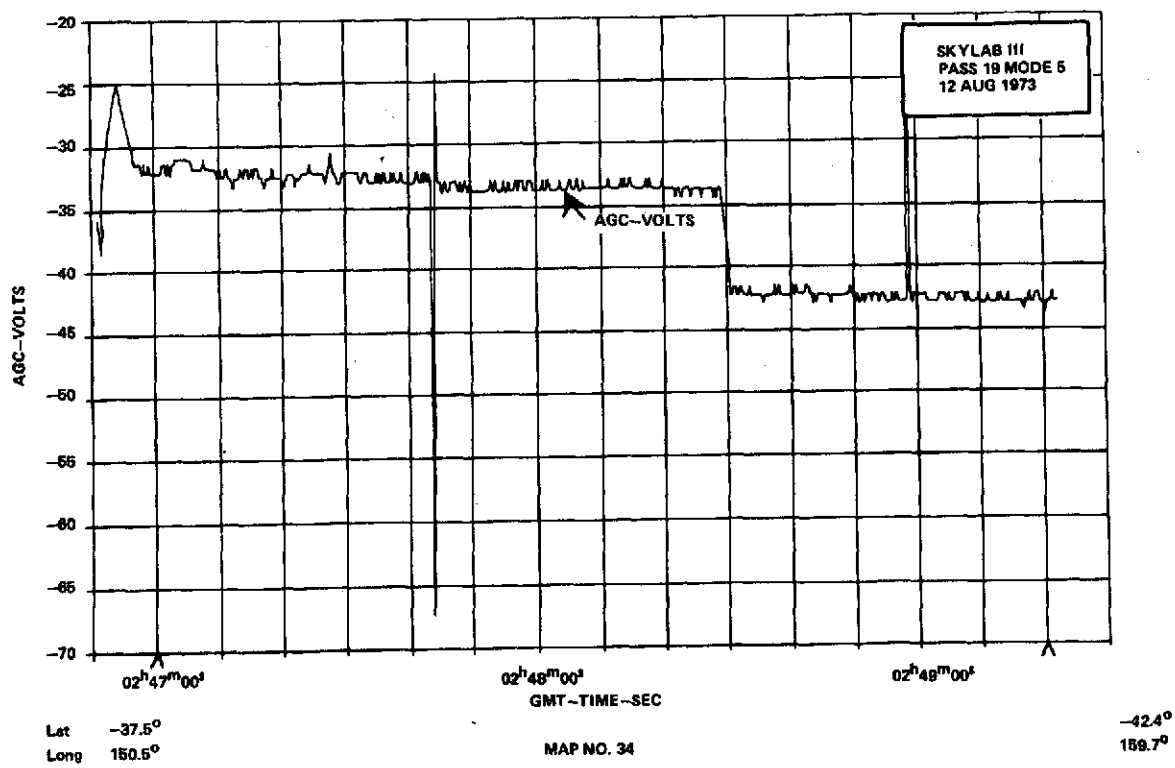
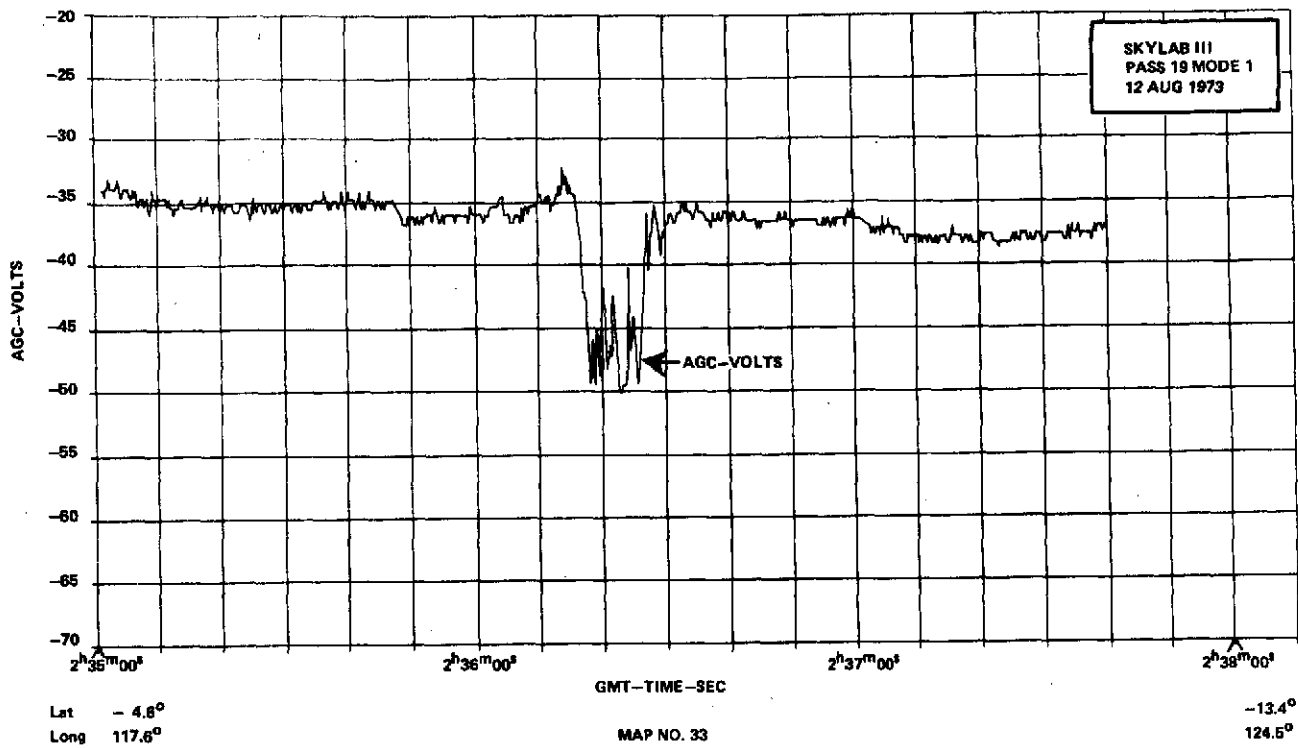


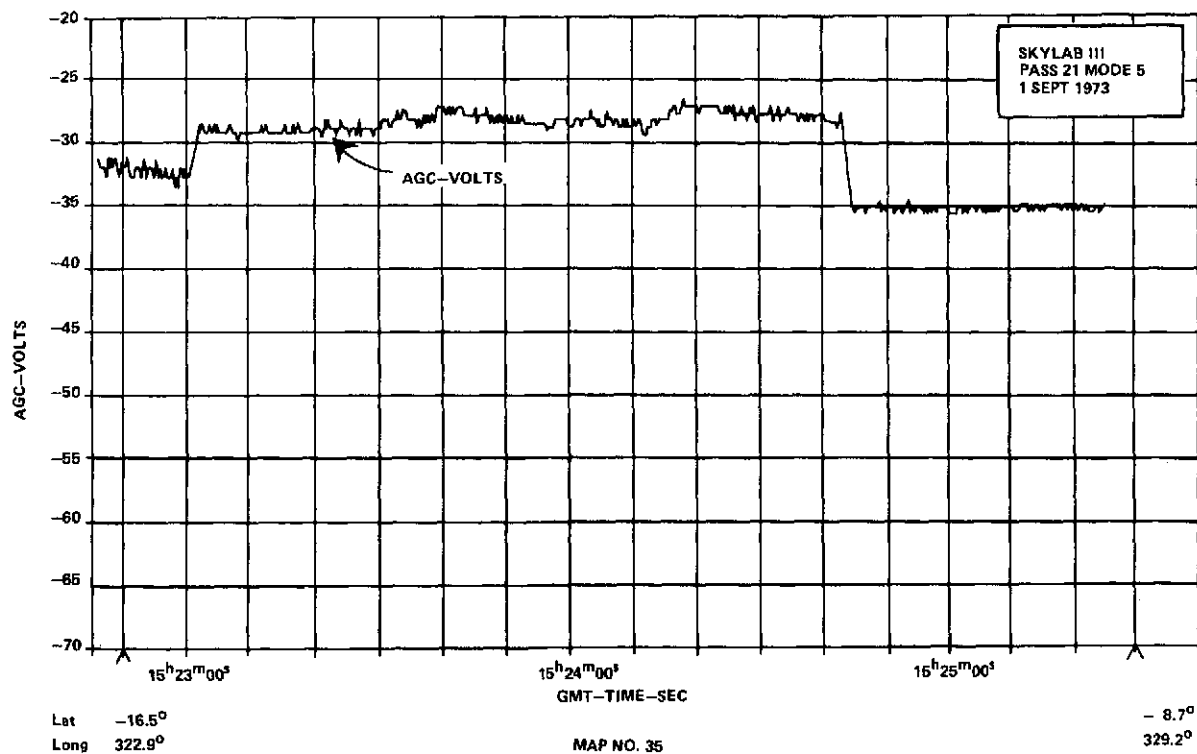
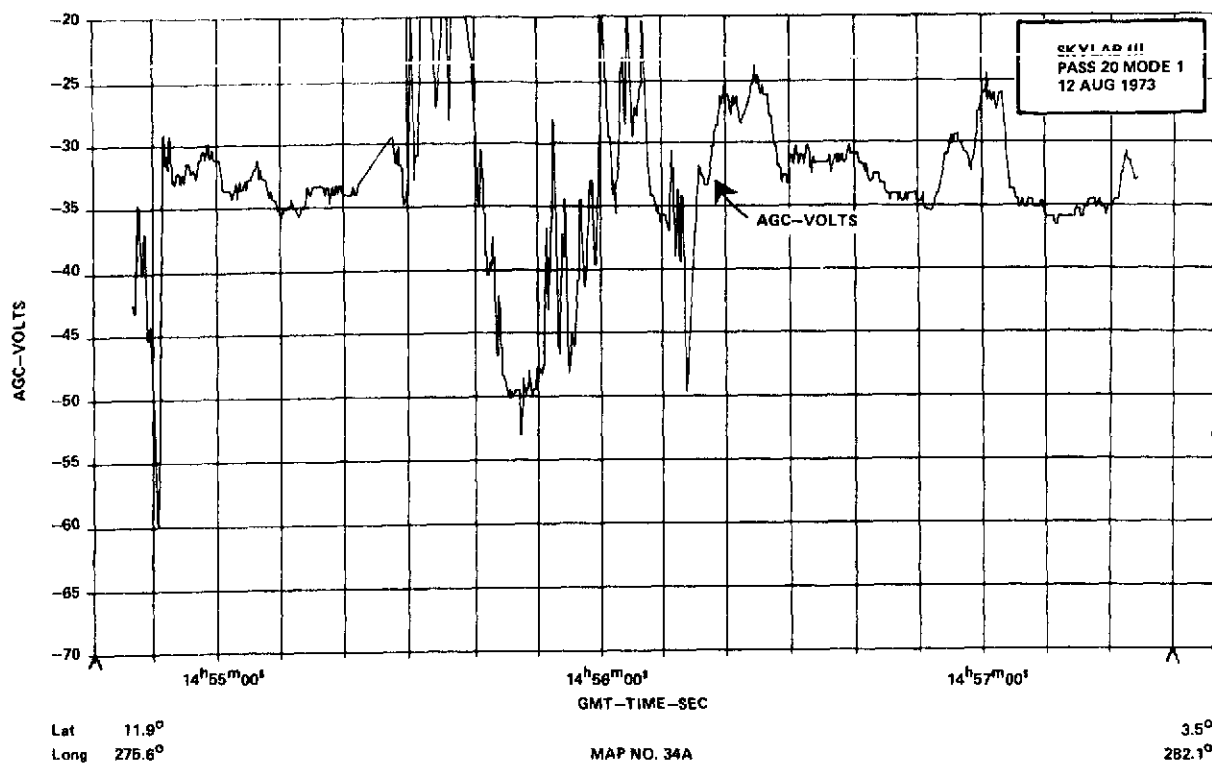


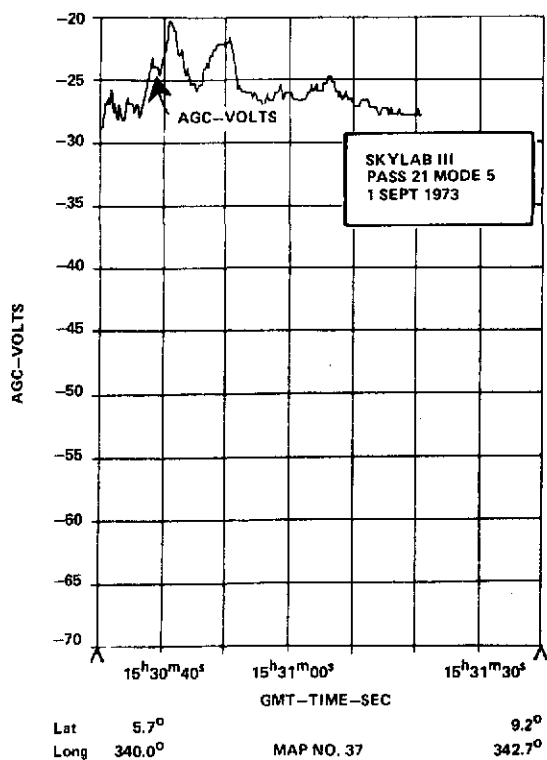
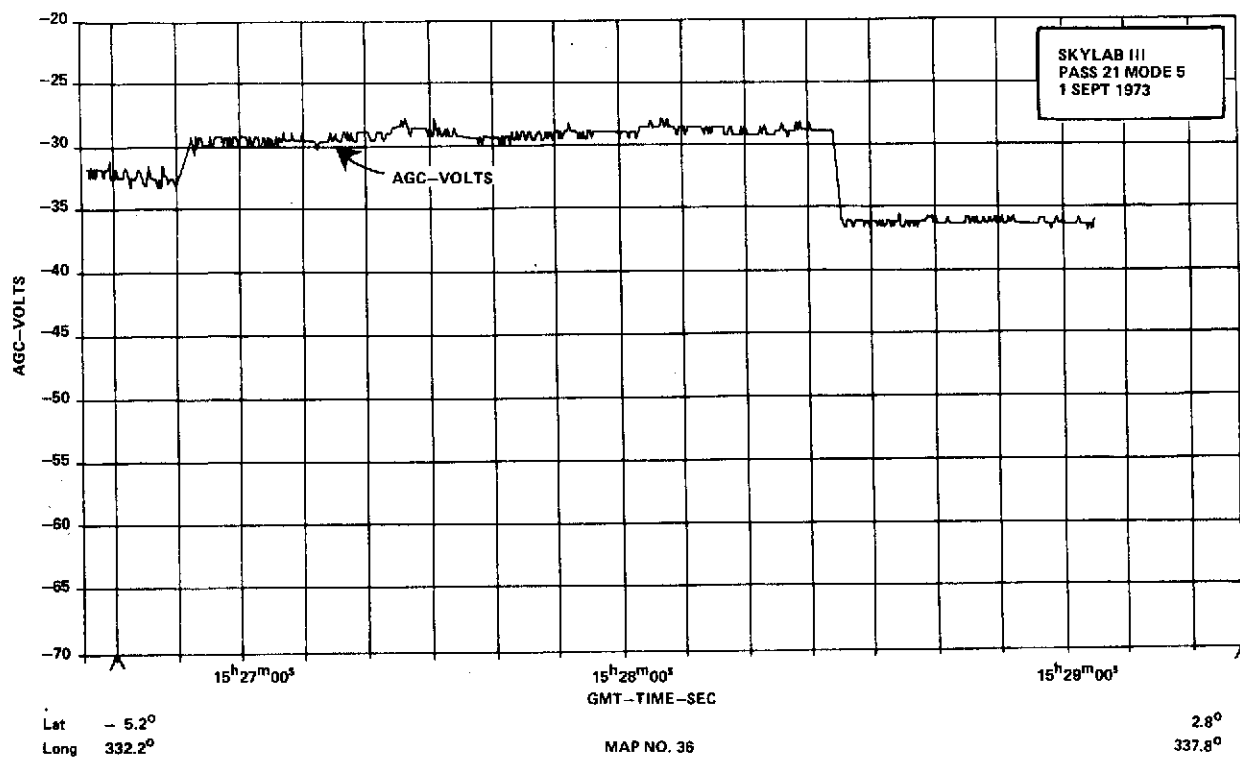


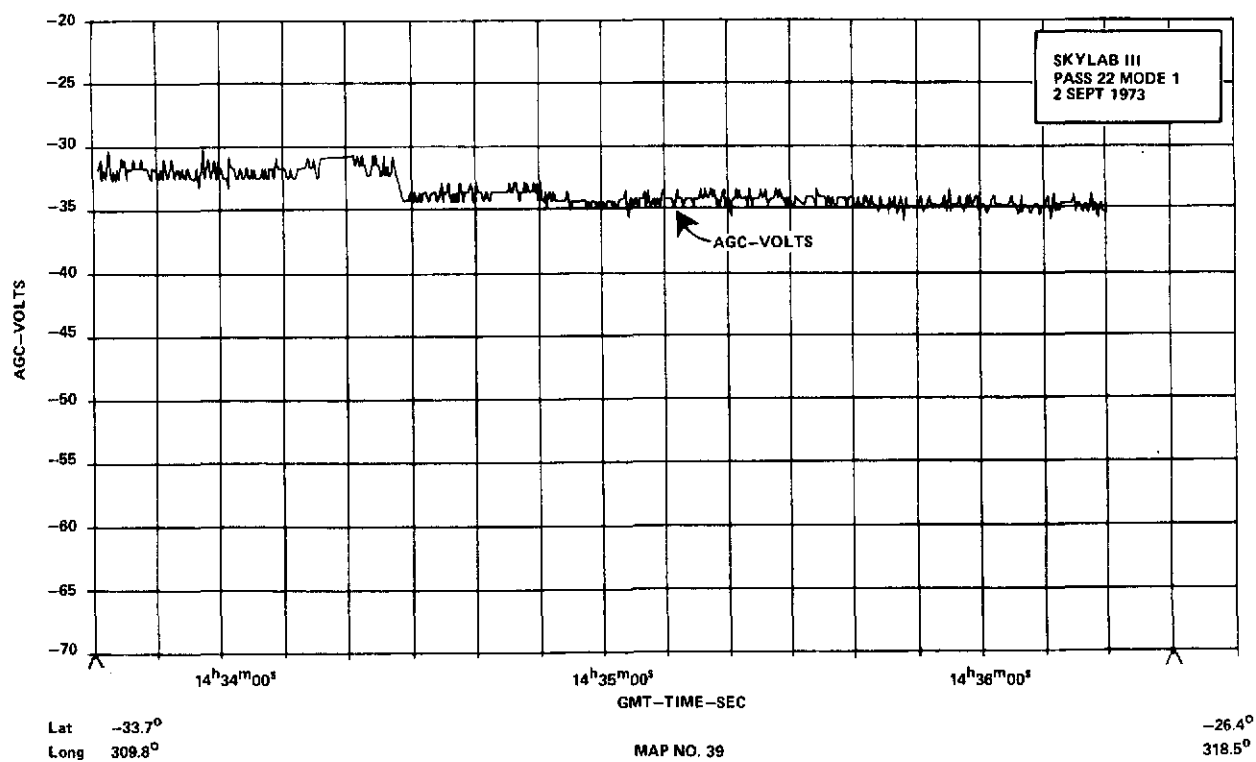
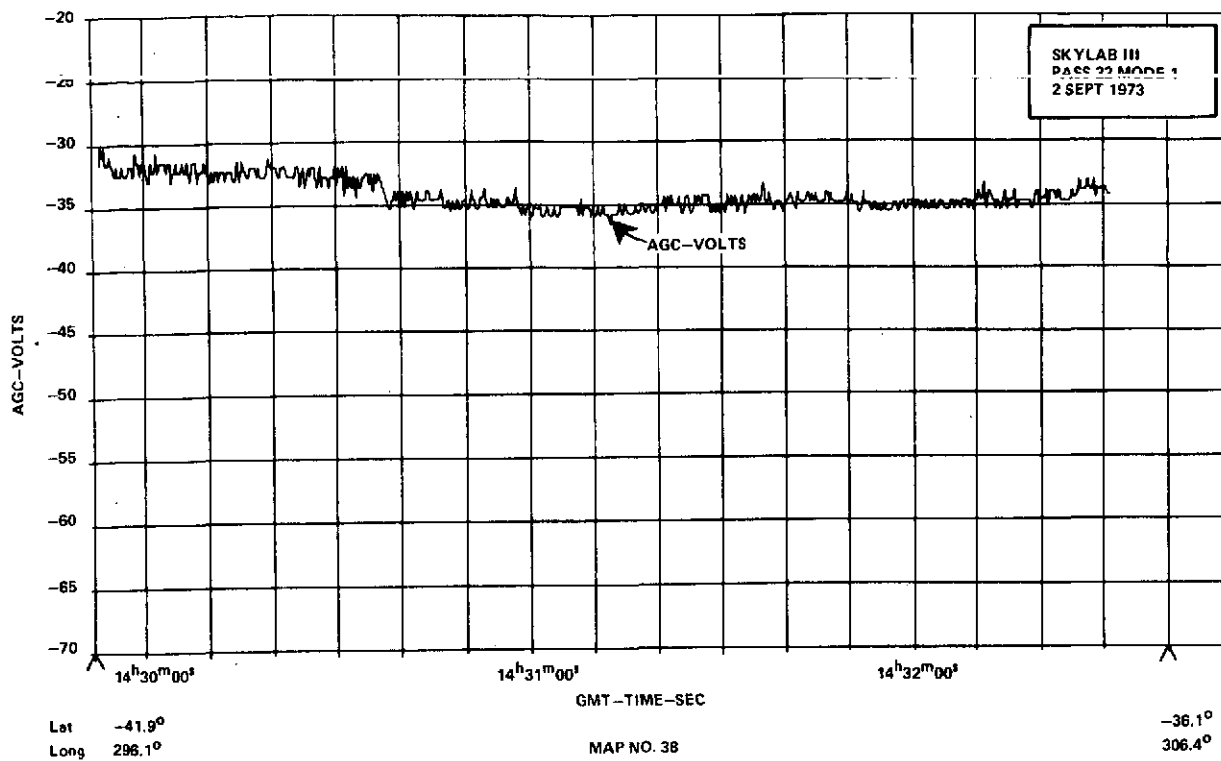


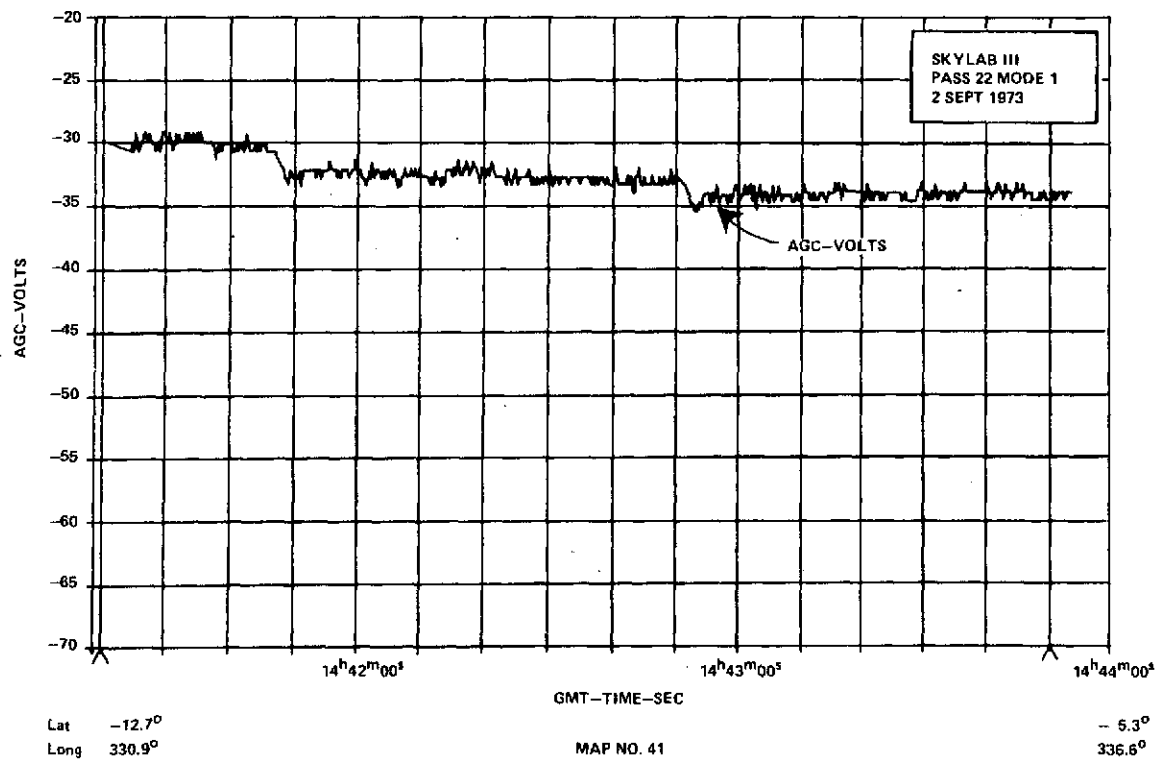
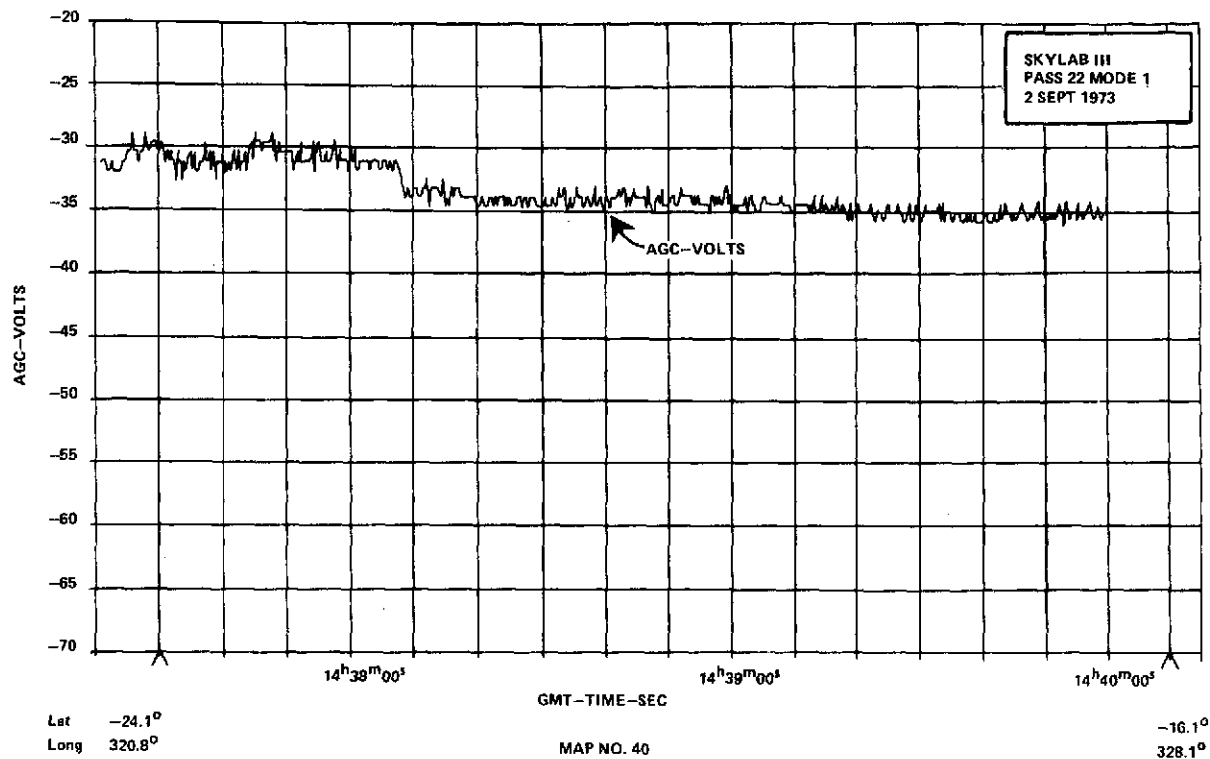


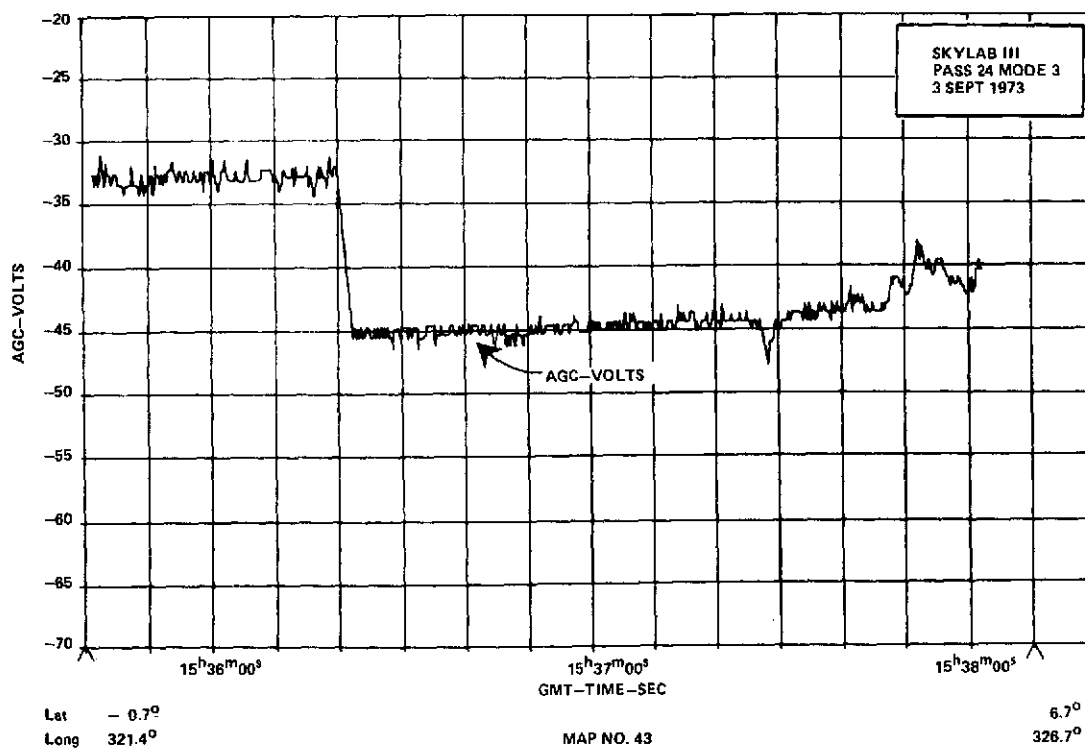
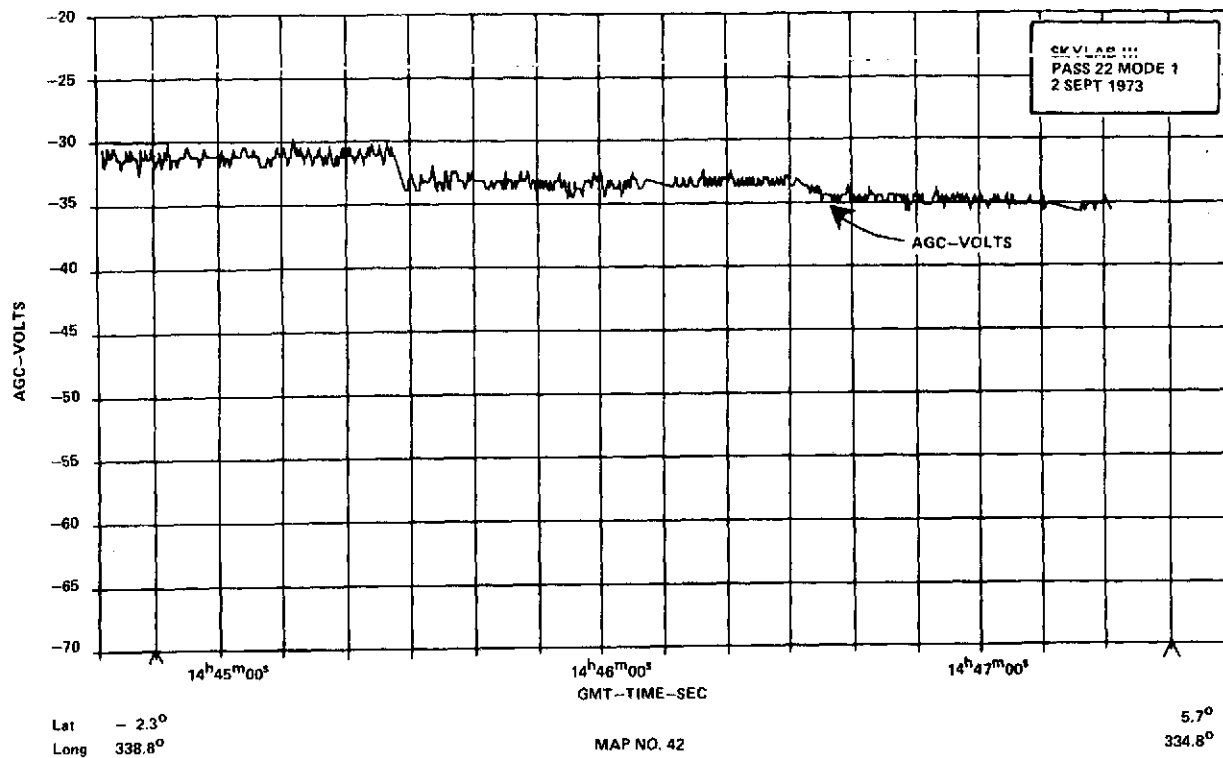


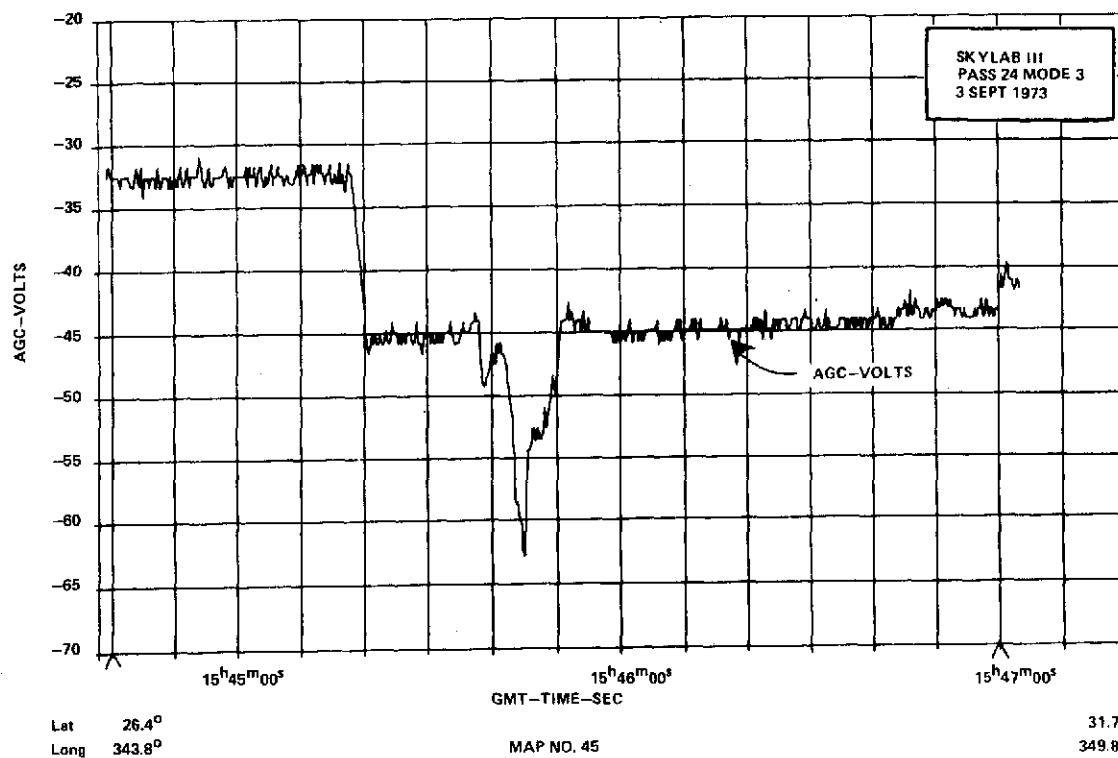
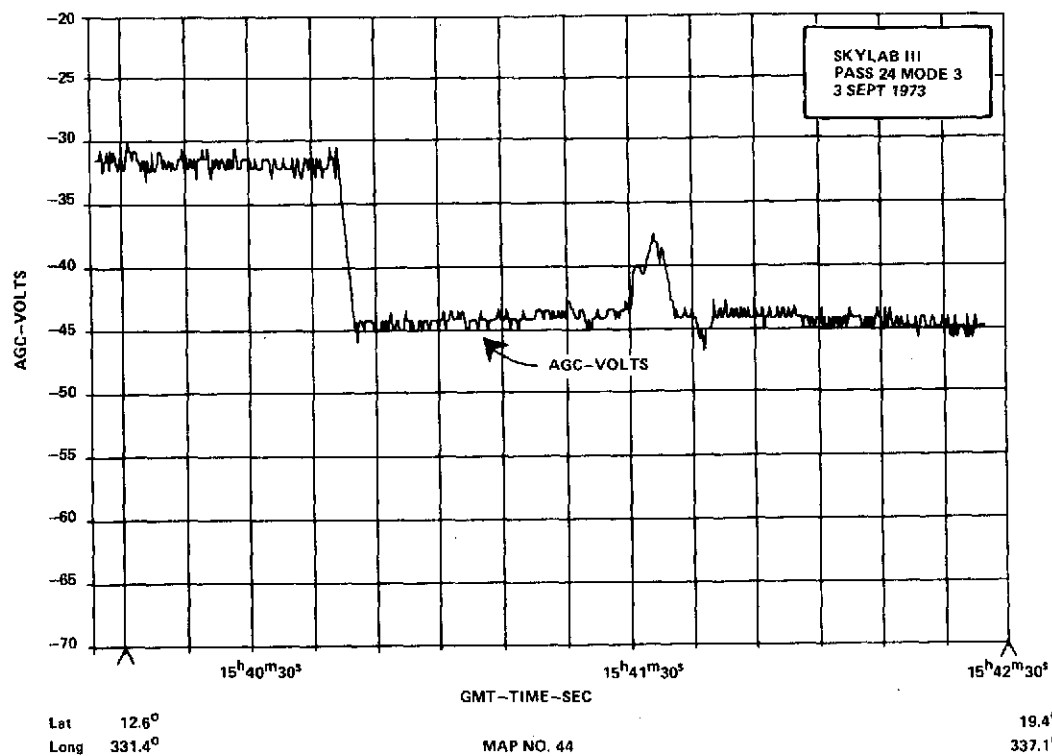


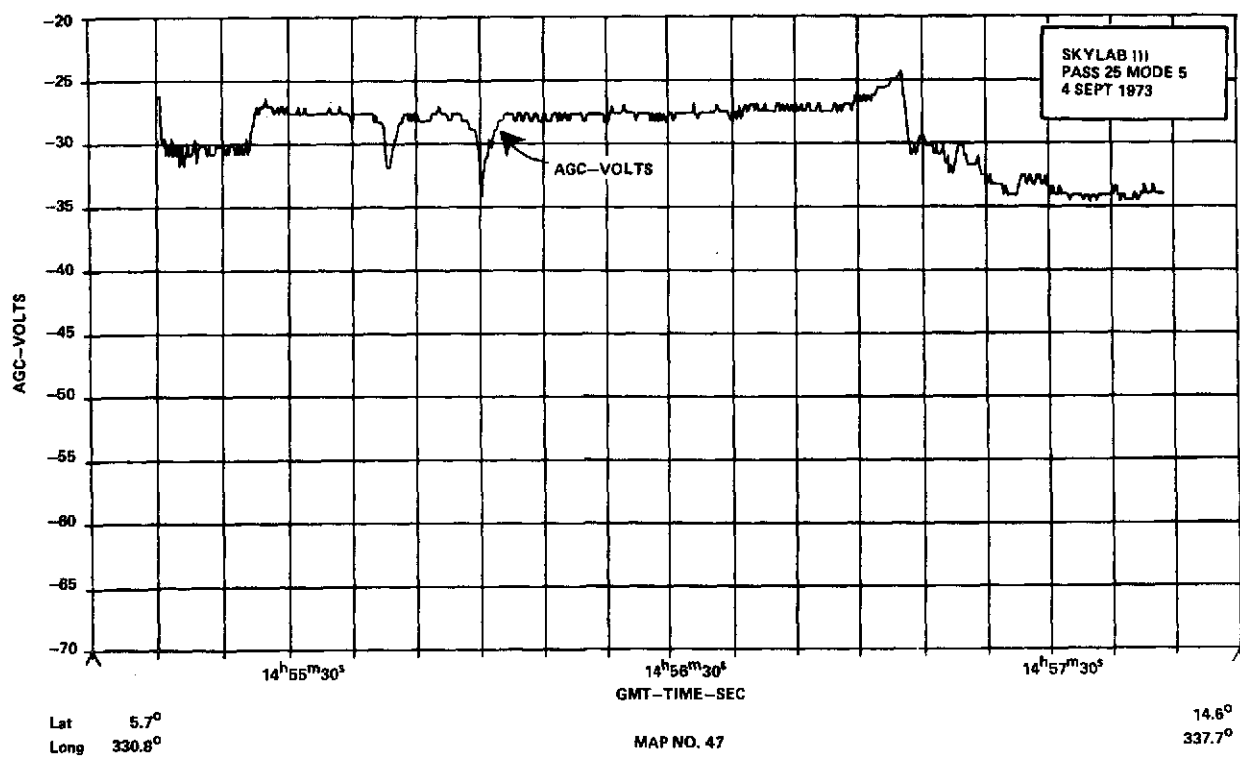
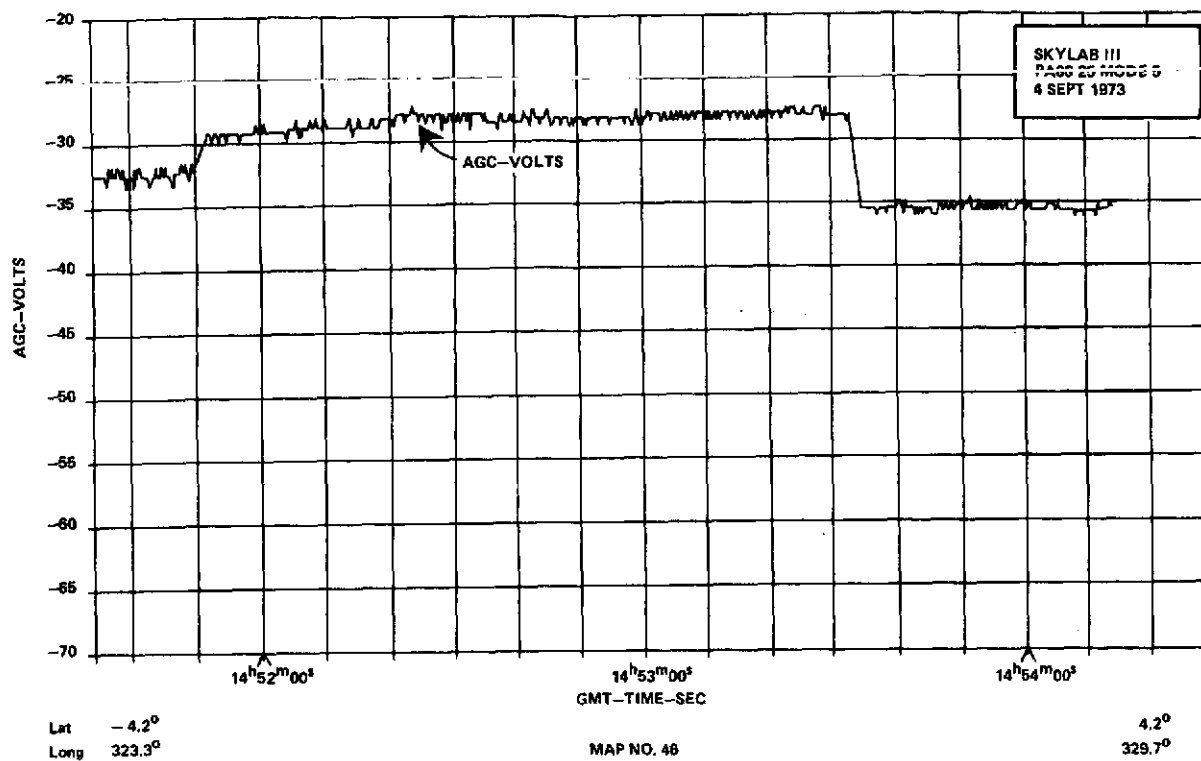


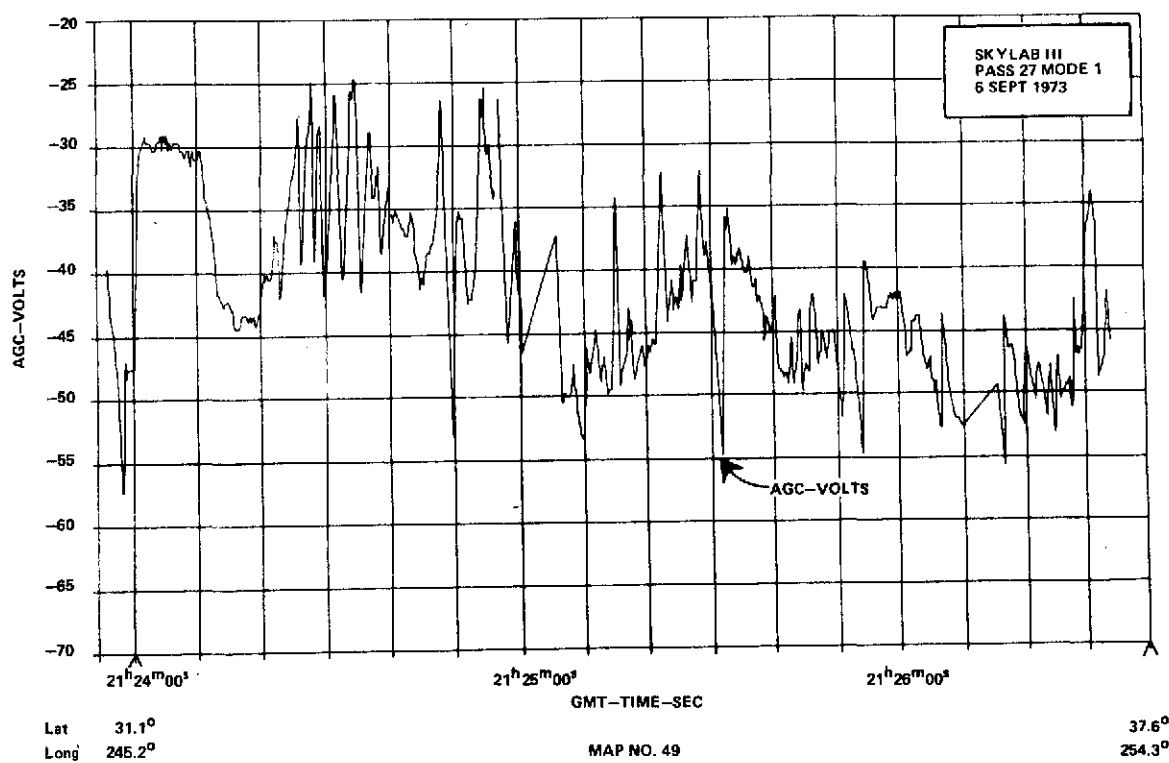
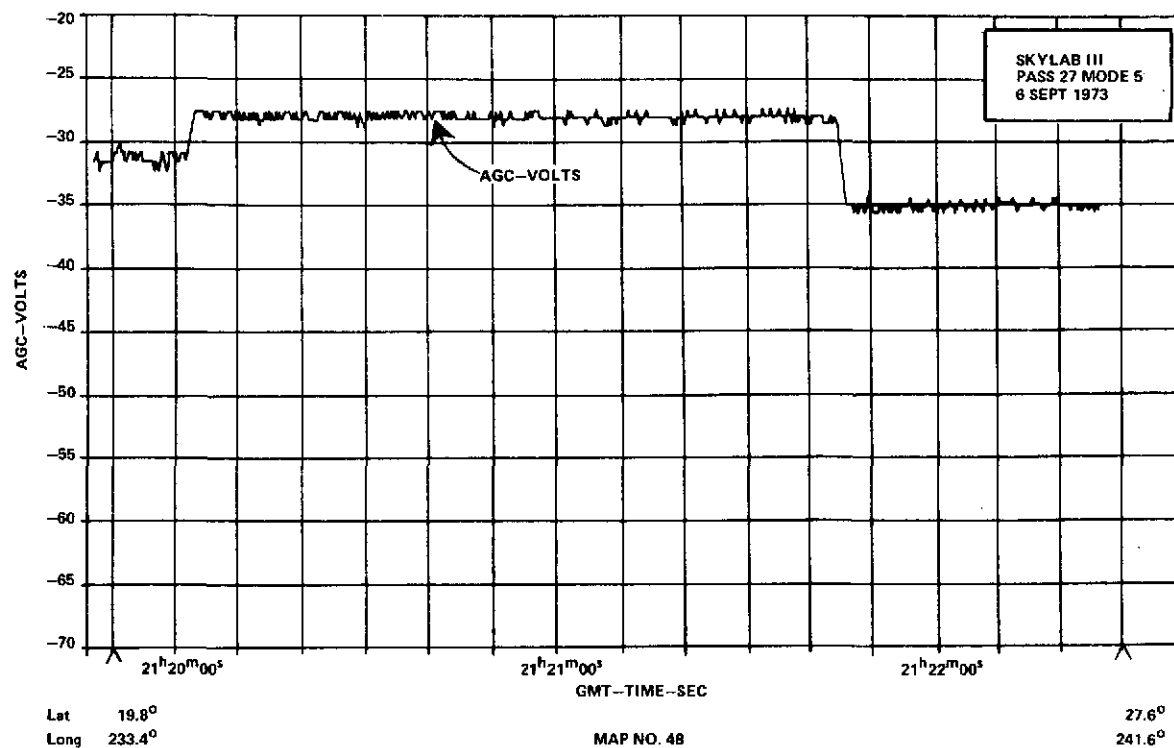


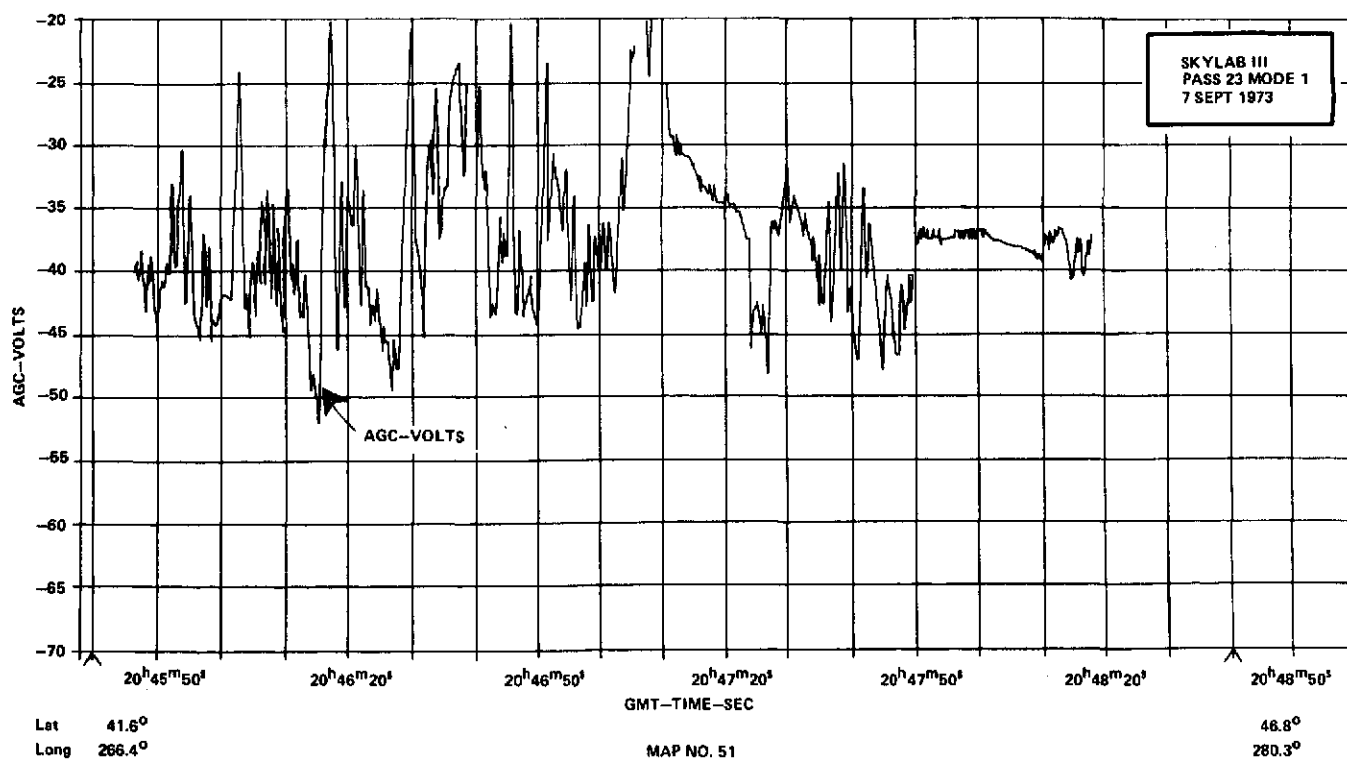
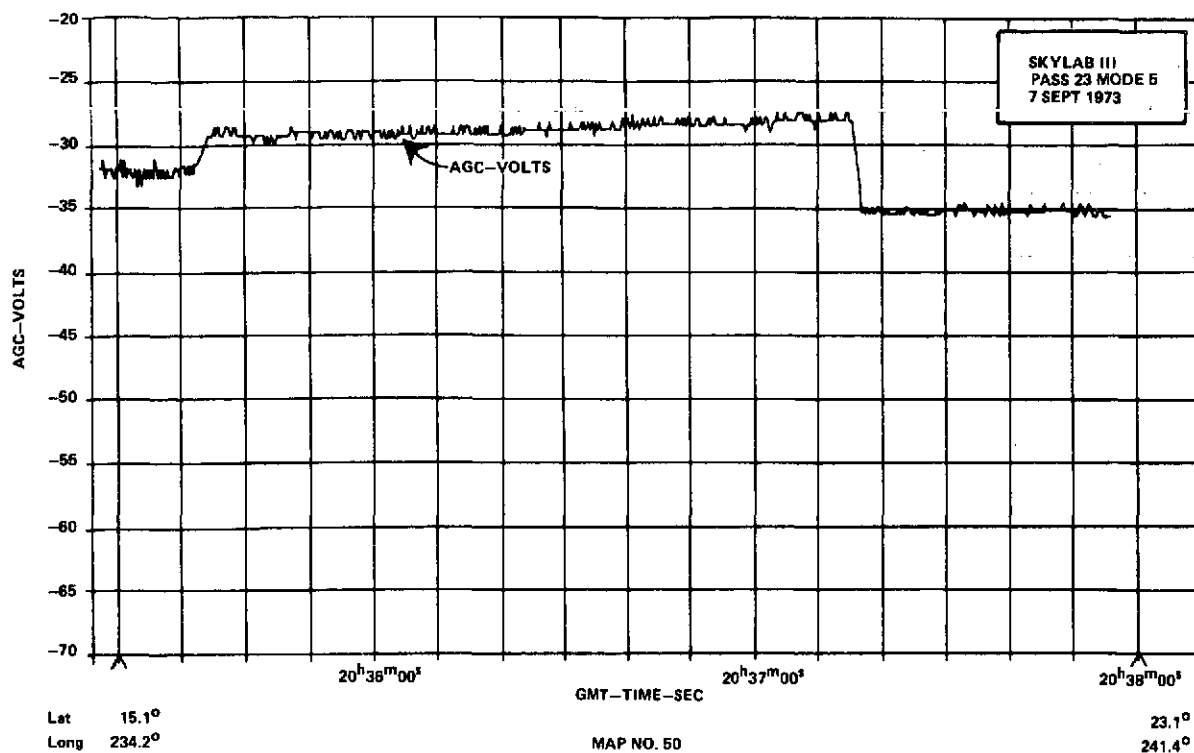


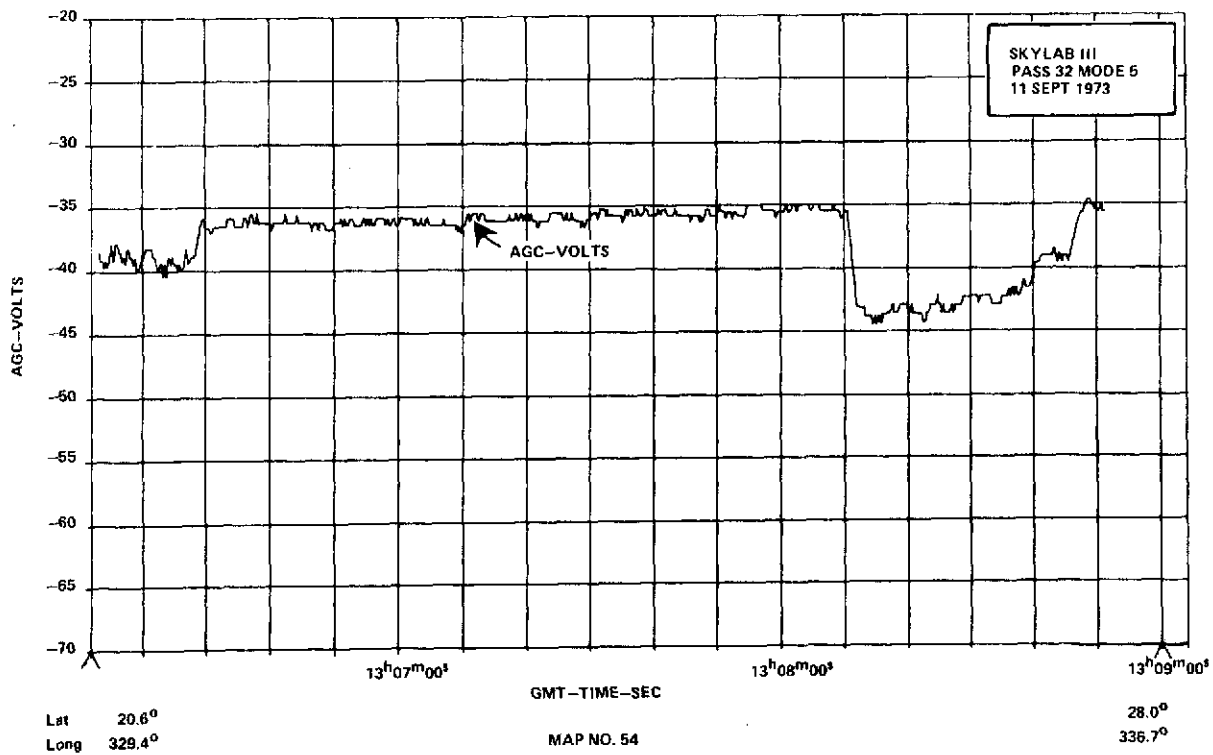
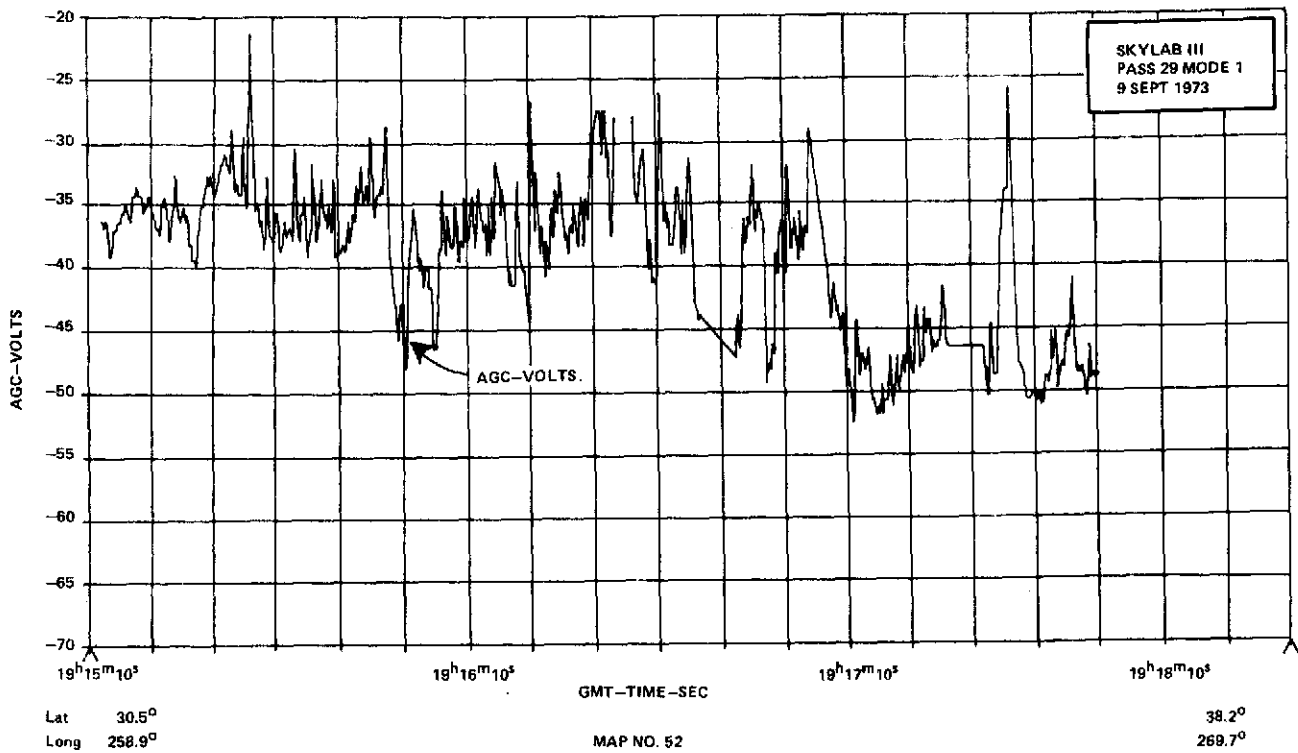


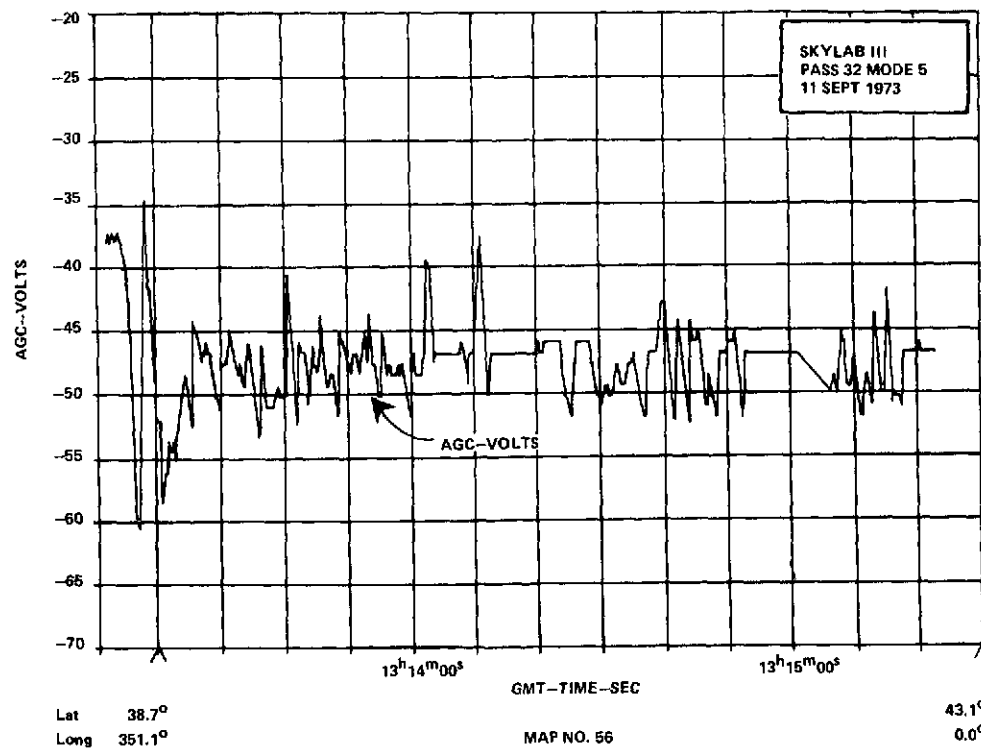
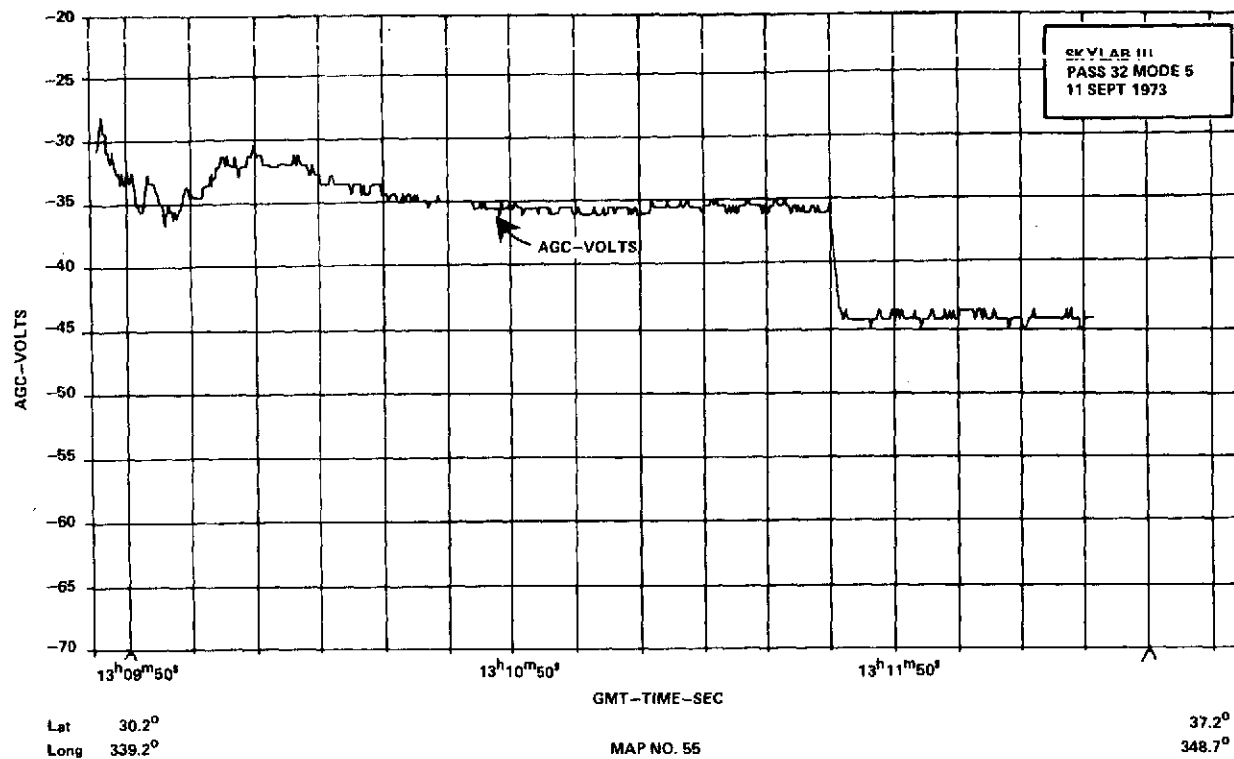


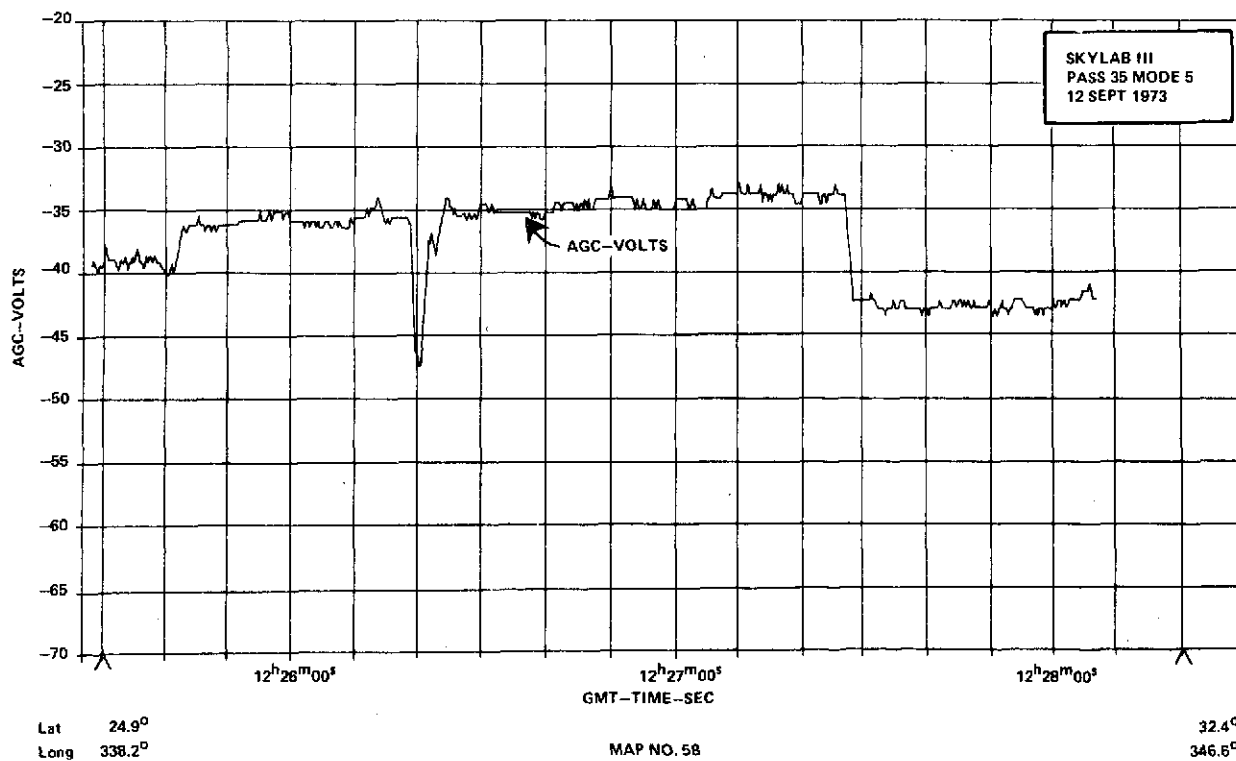
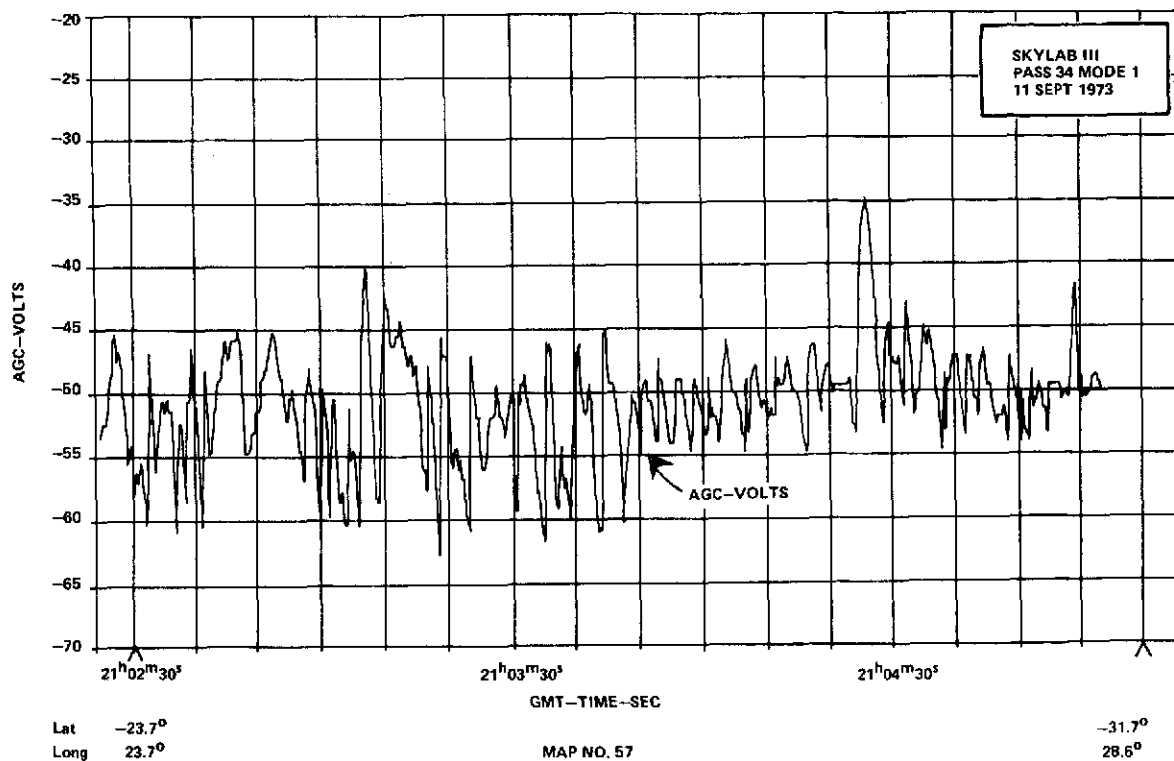


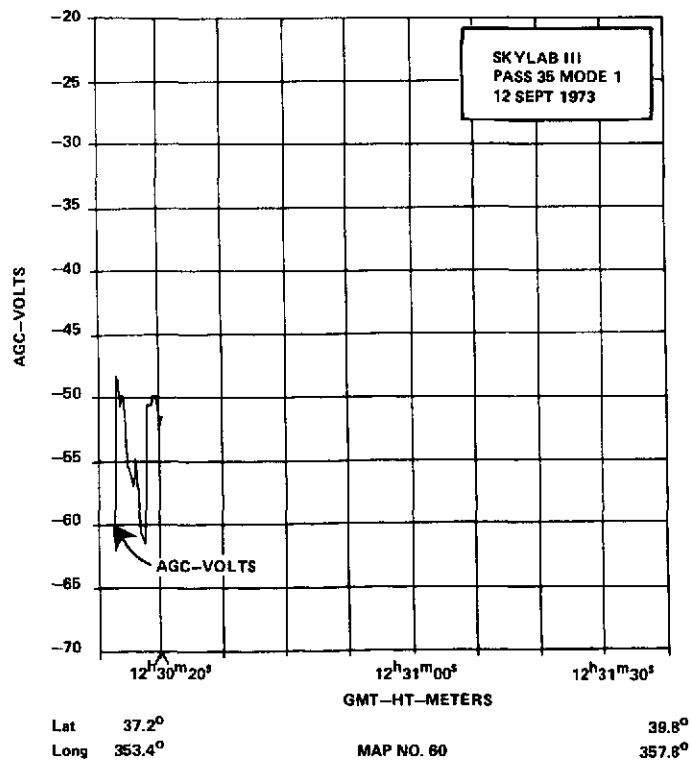
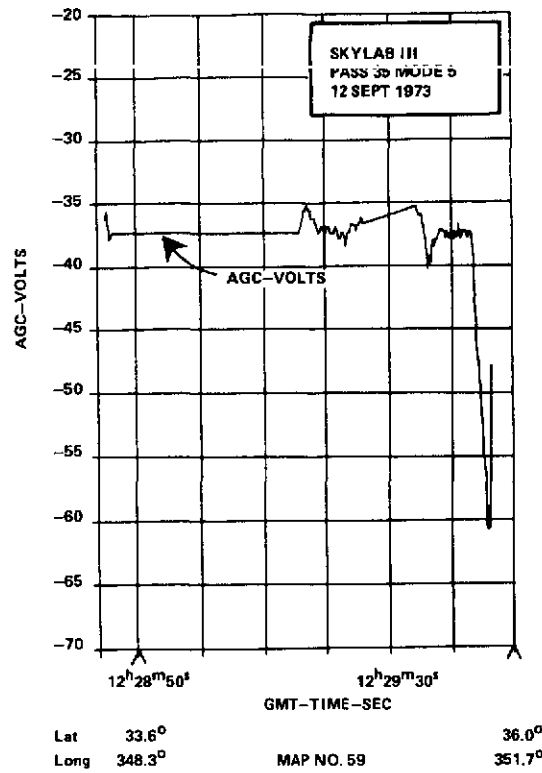


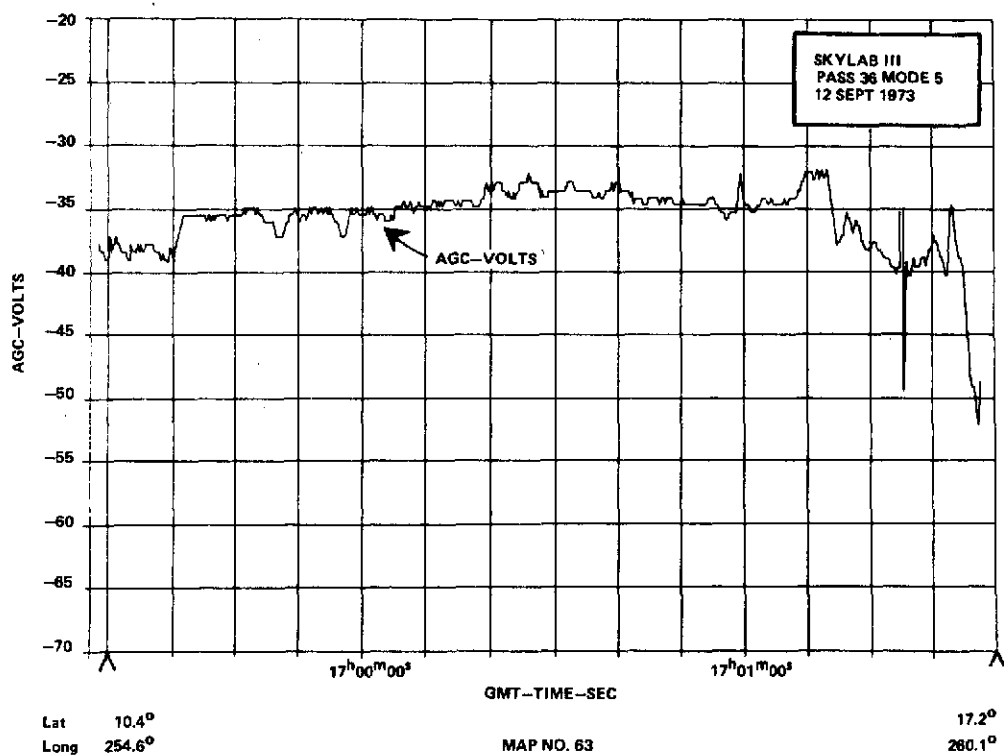
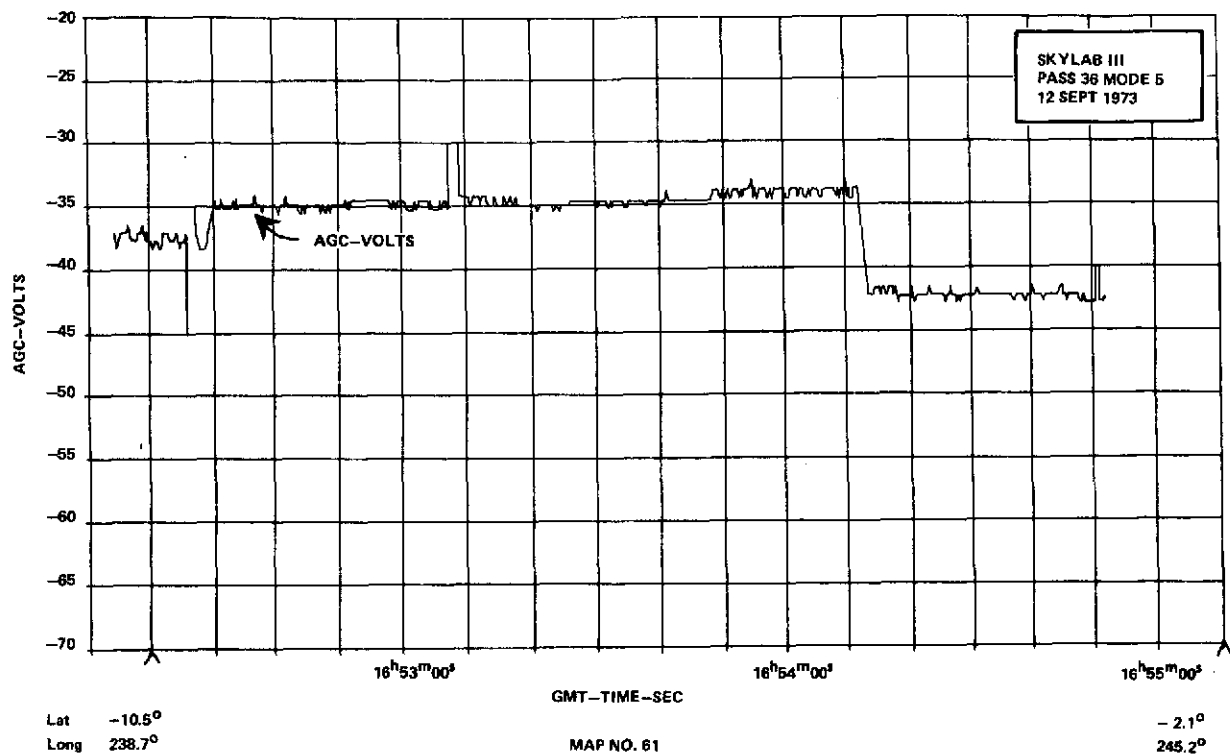


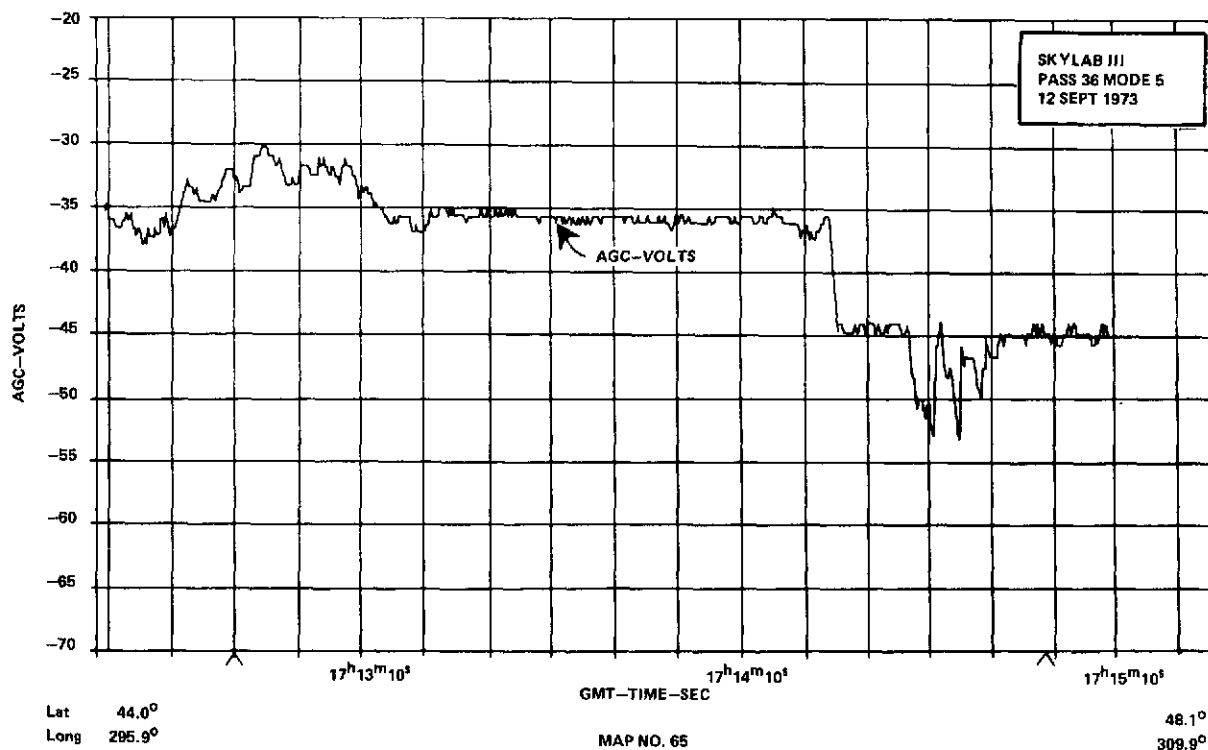
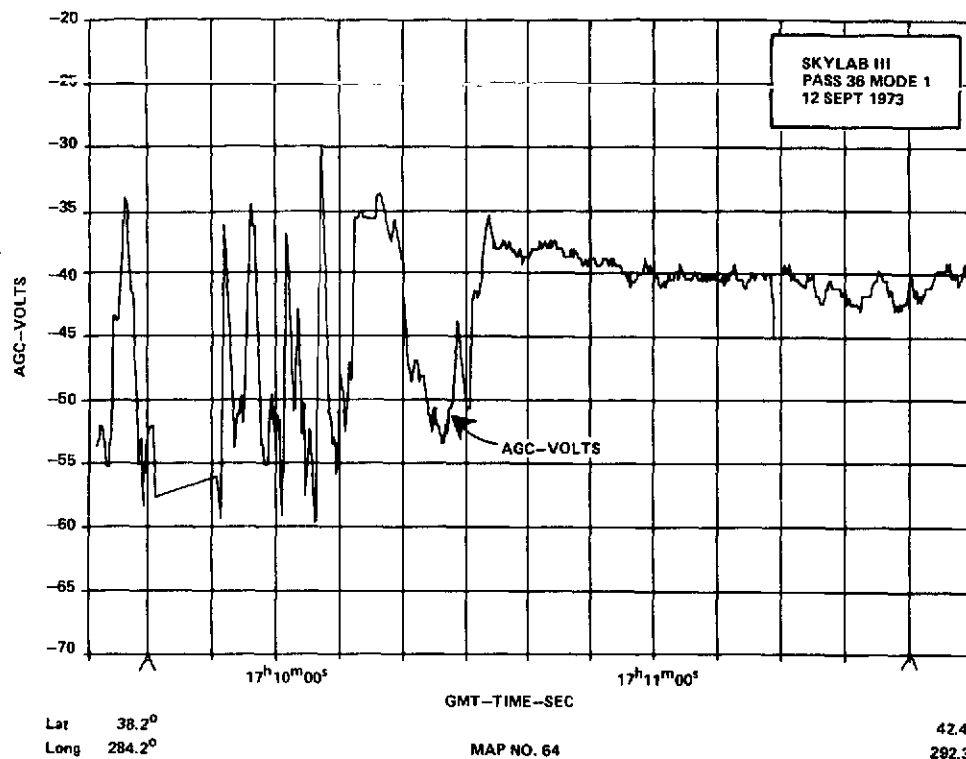


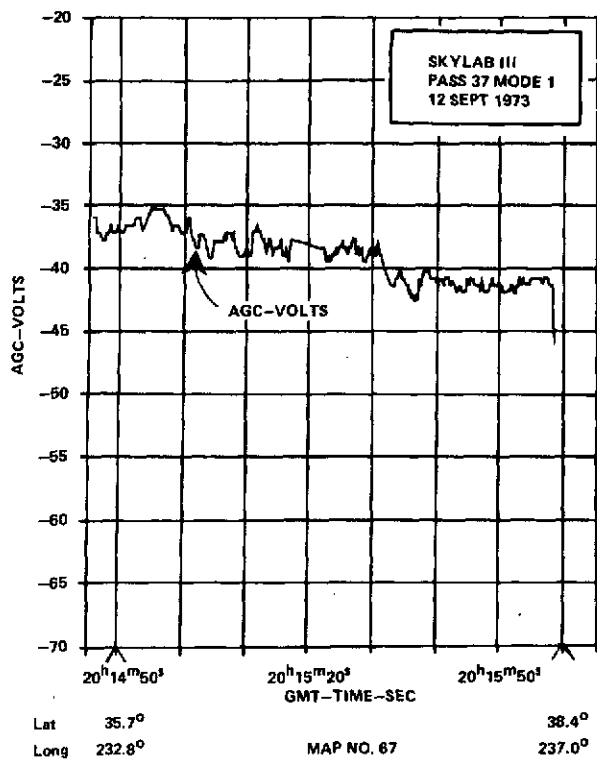
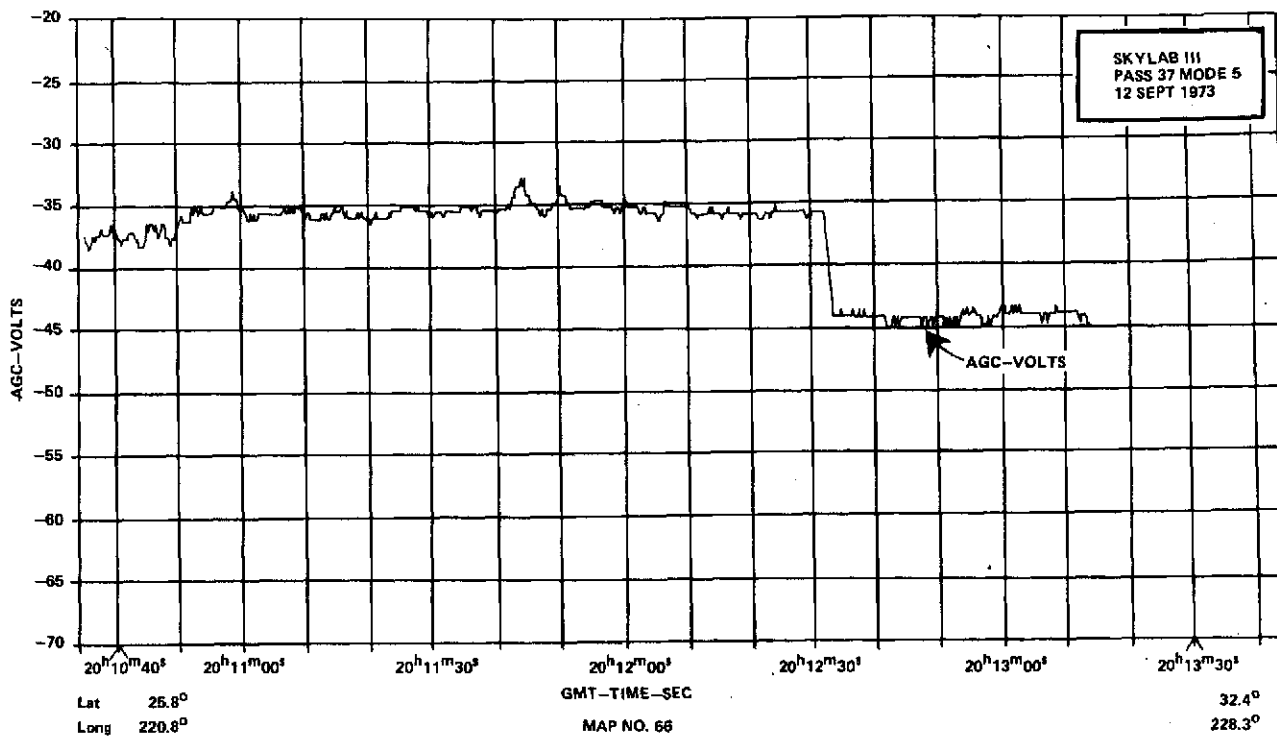


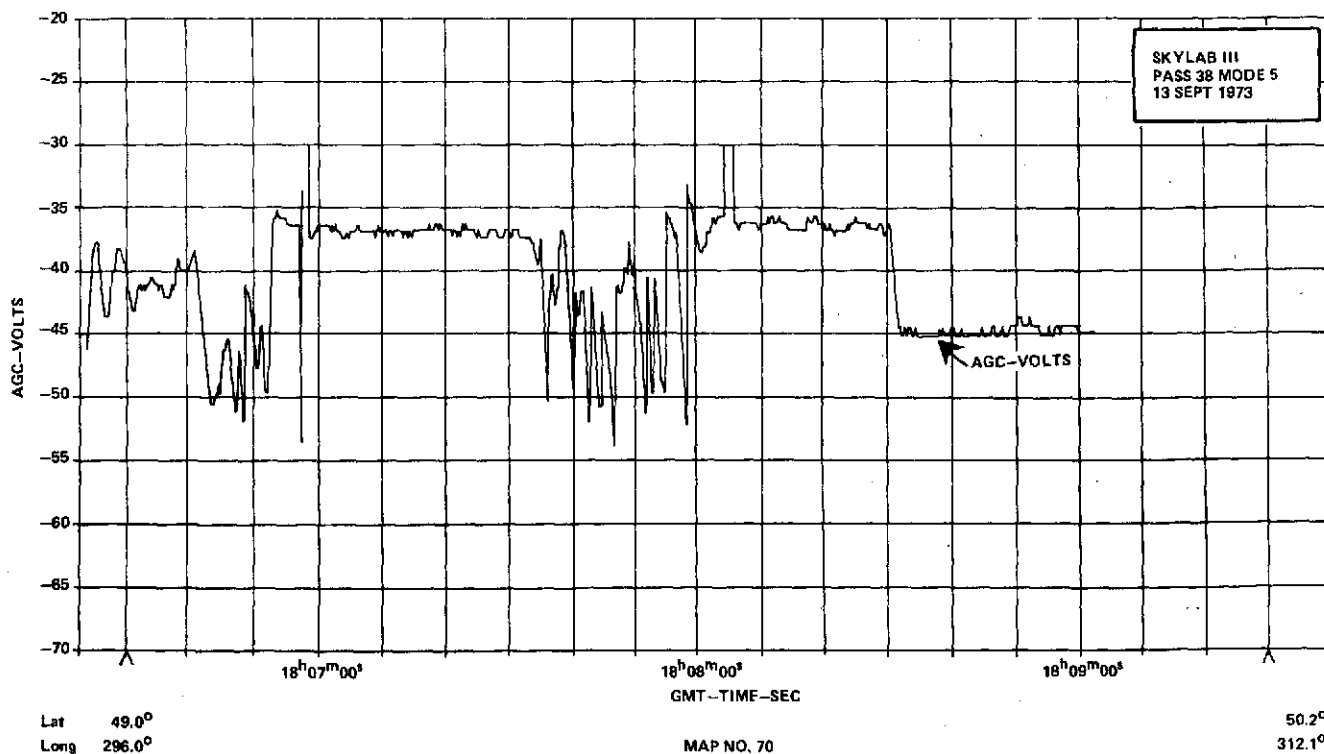
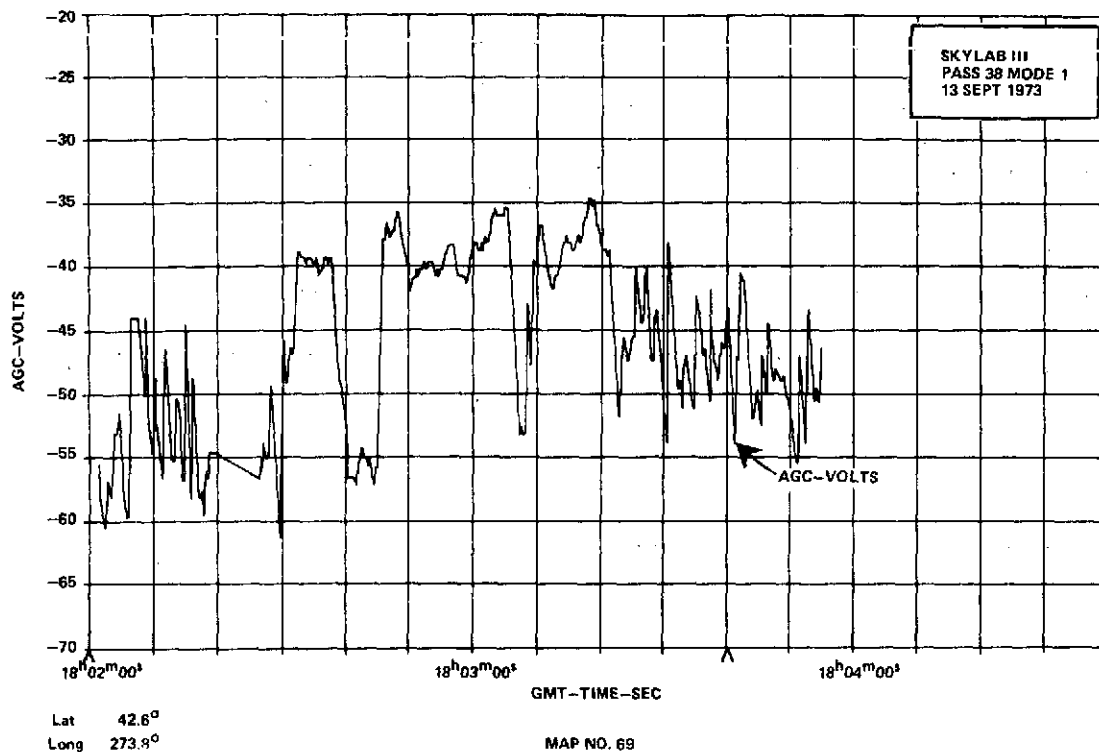


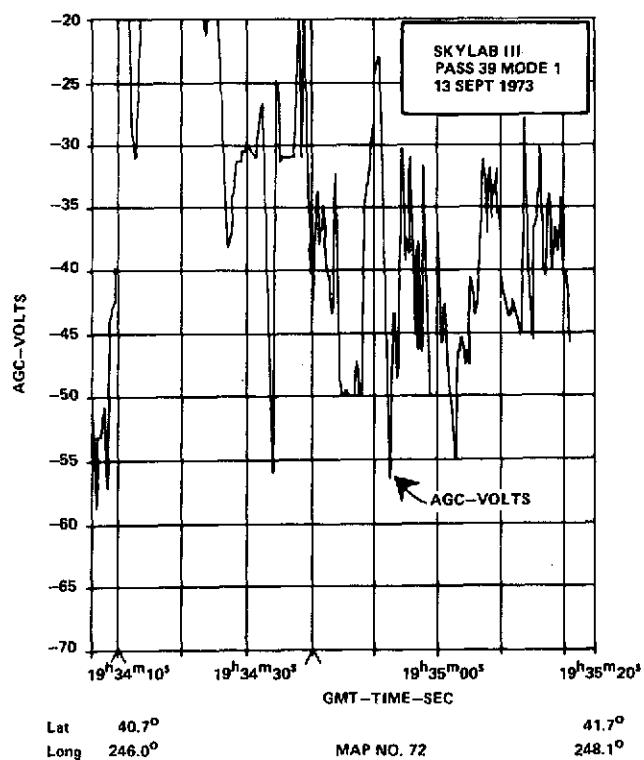
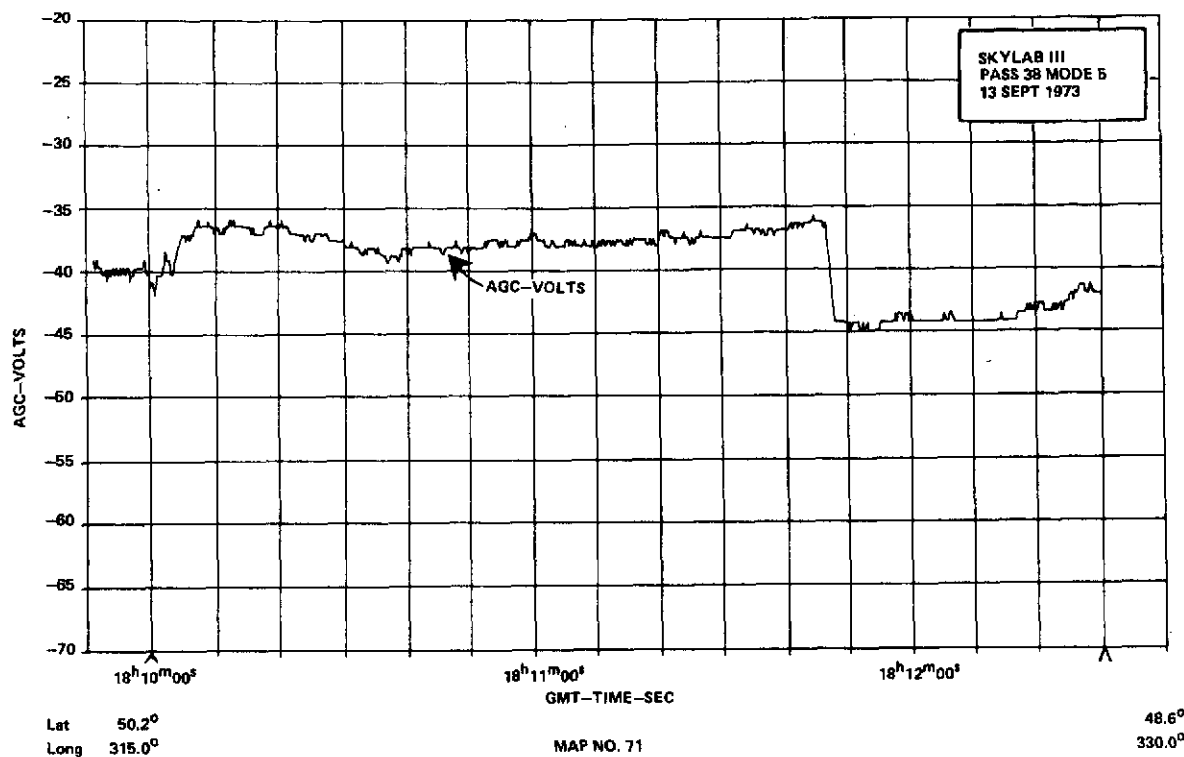


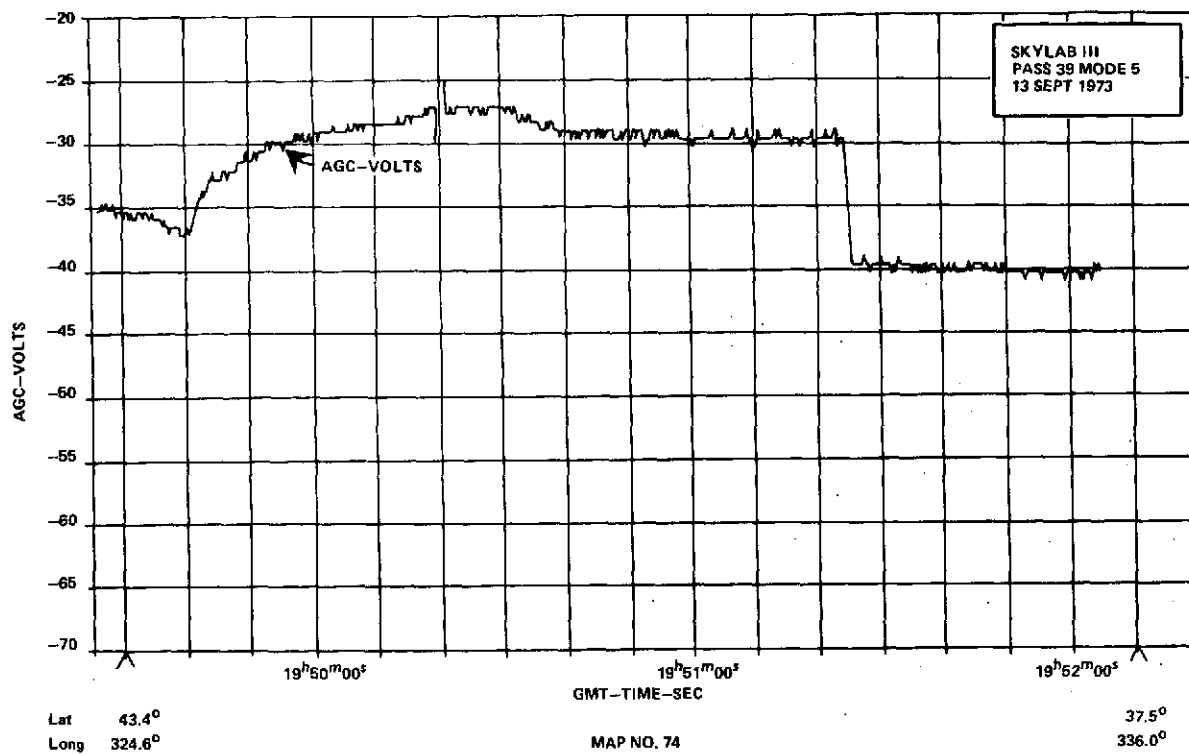
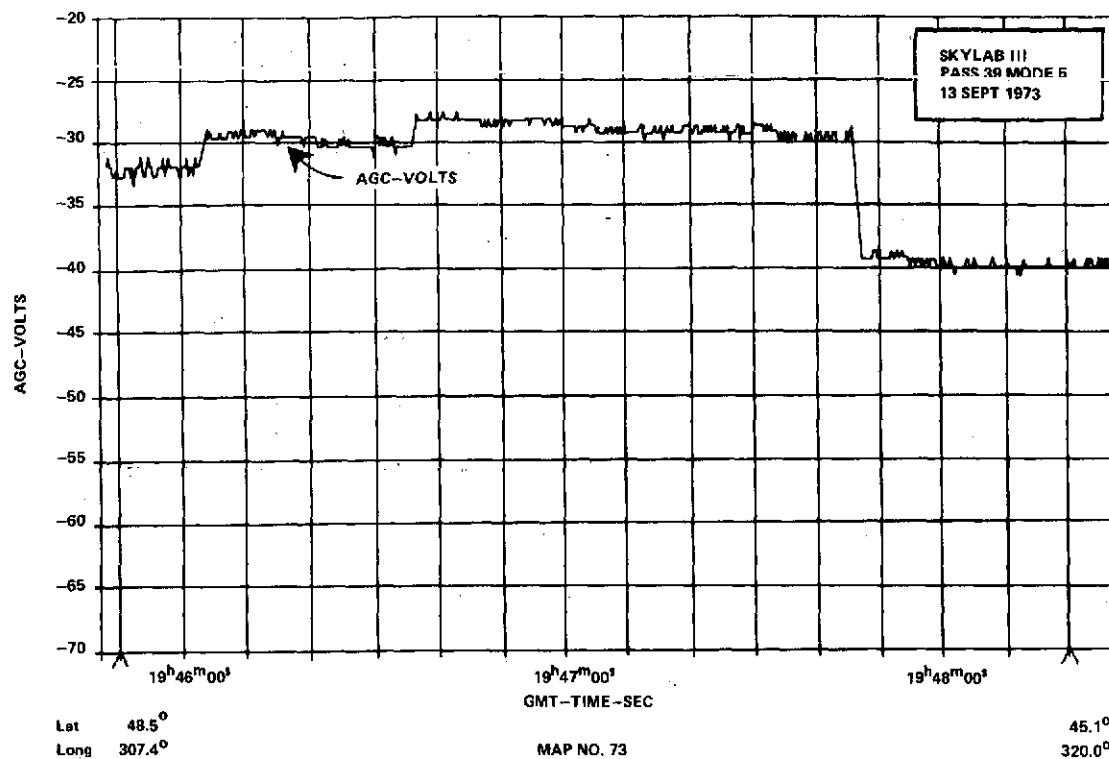


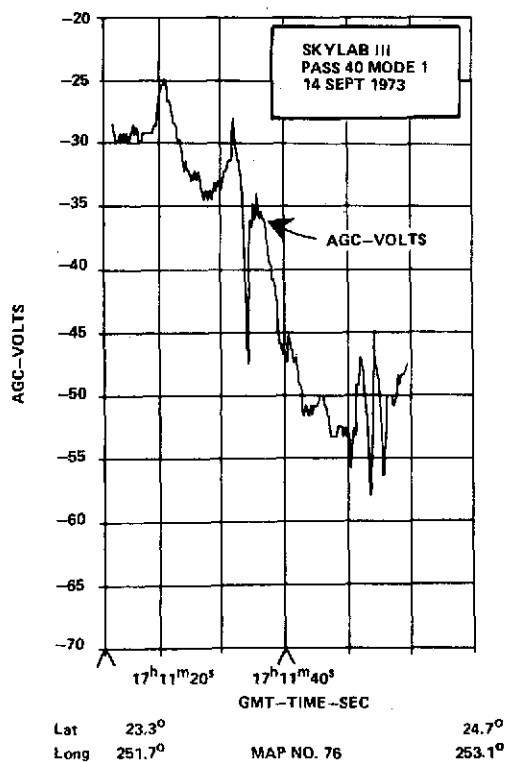
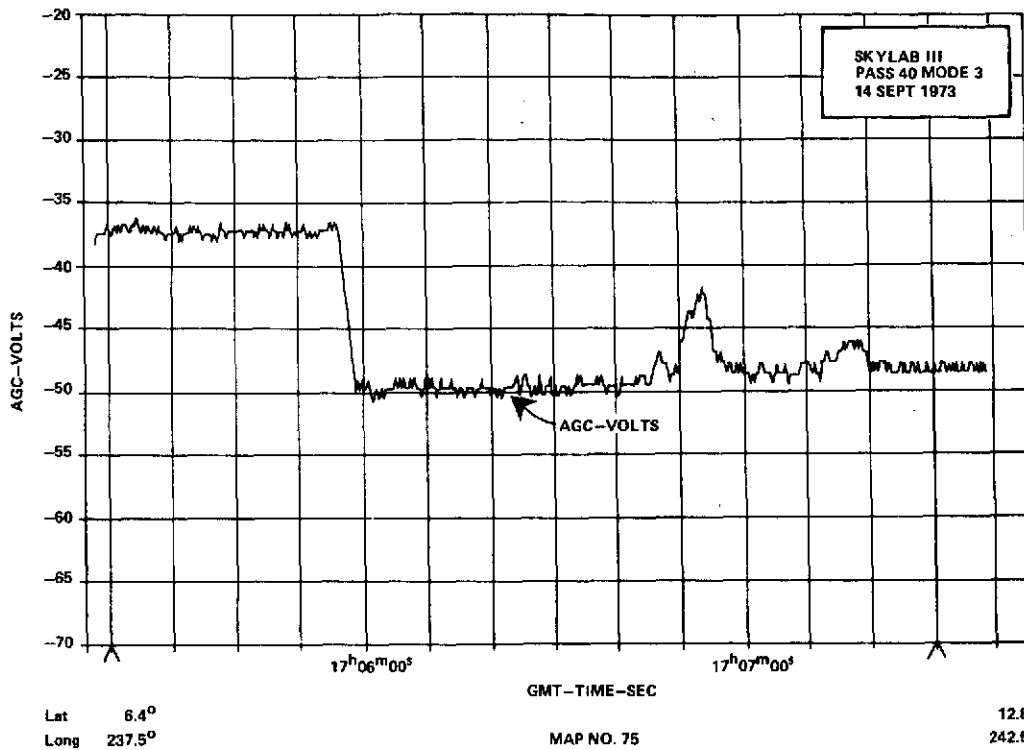


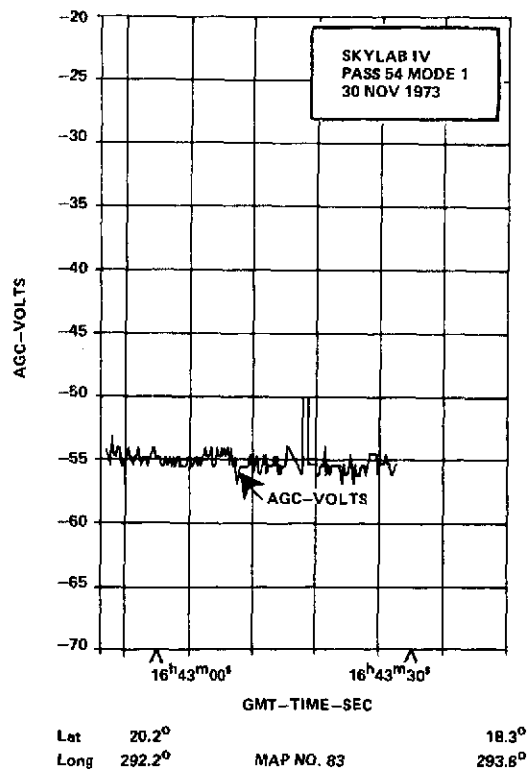
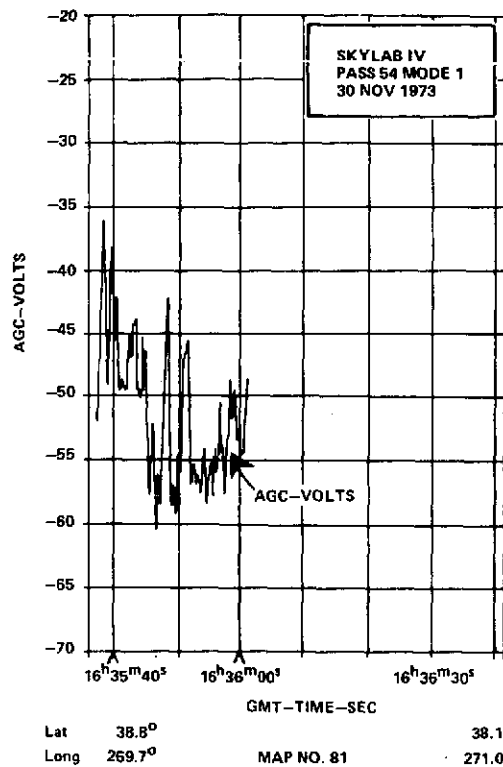


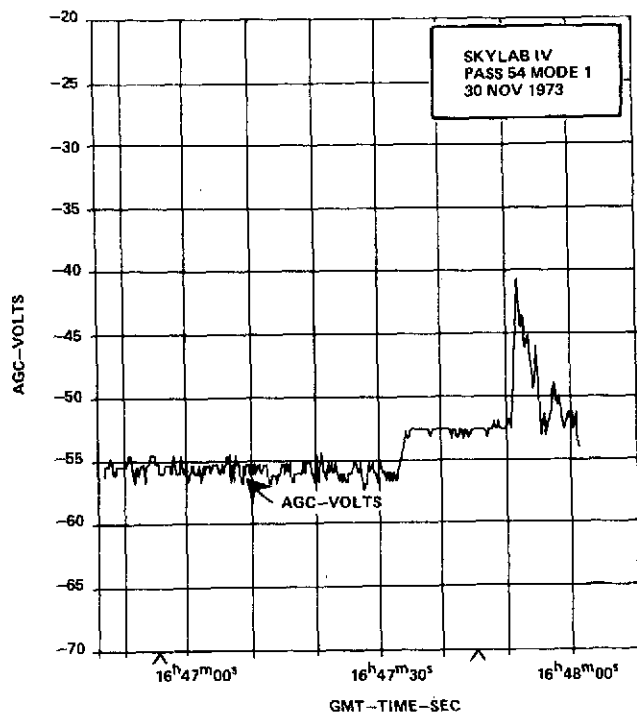






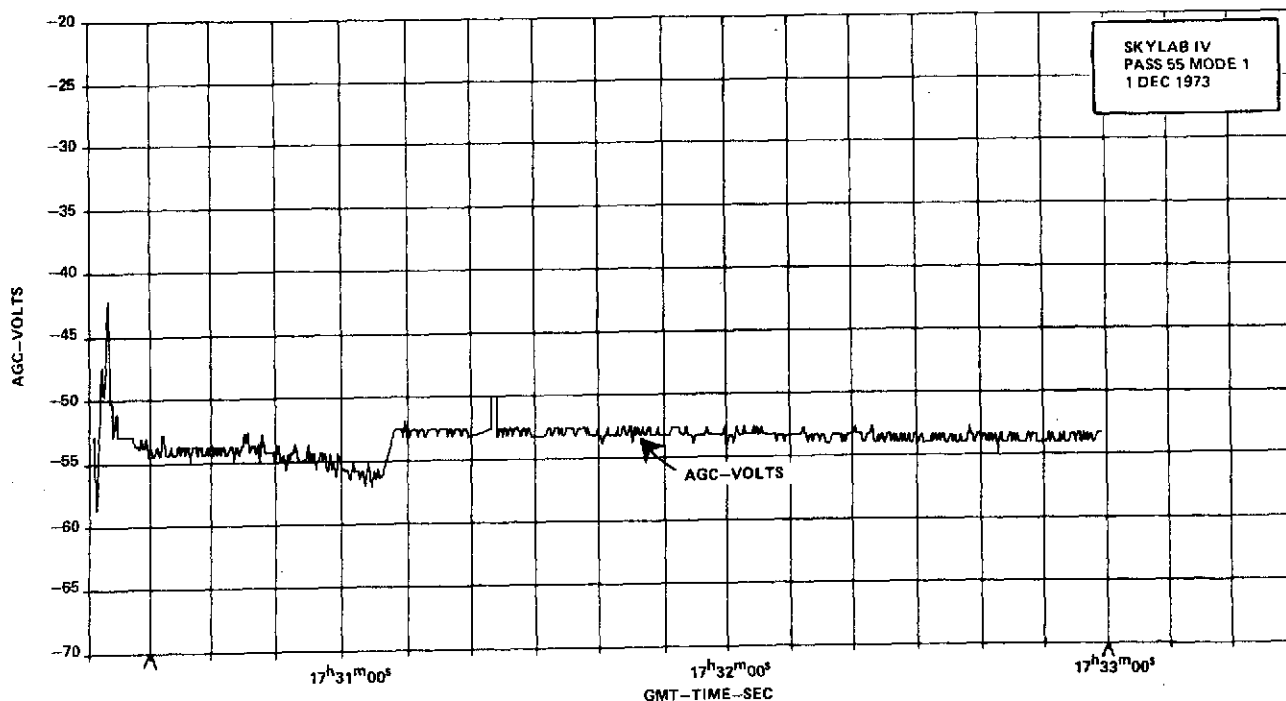






Lat 8.6° 5.2°
Long 301.8° 304.4°

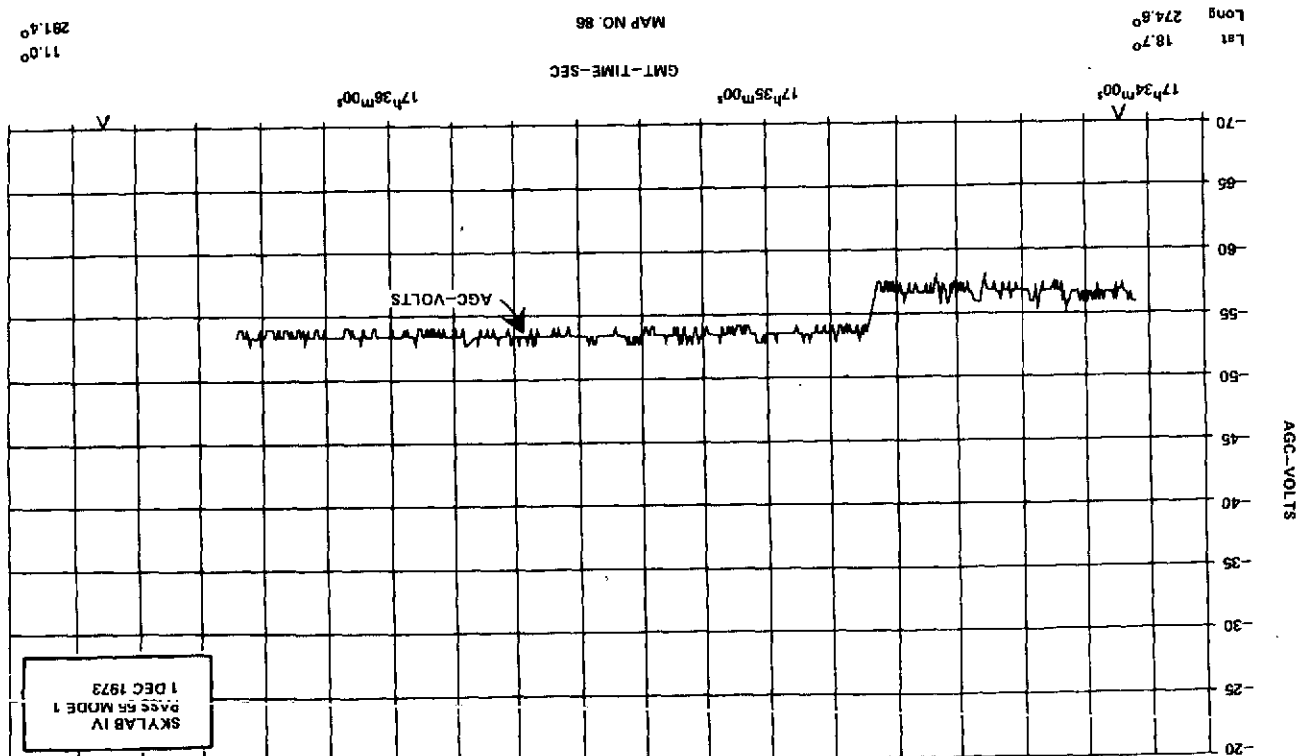
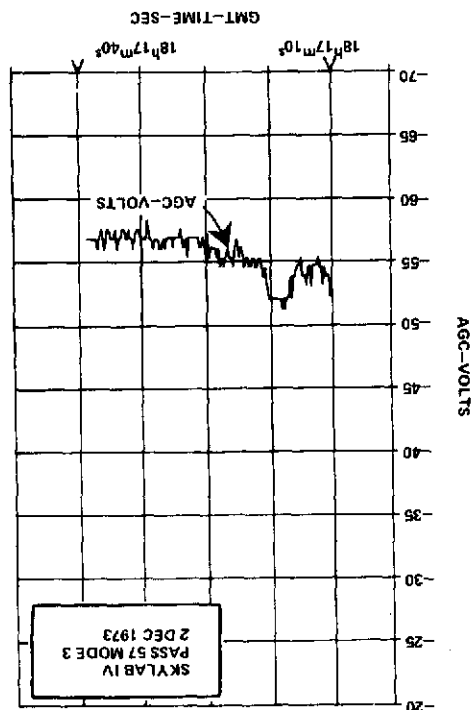
MAP NO. 84

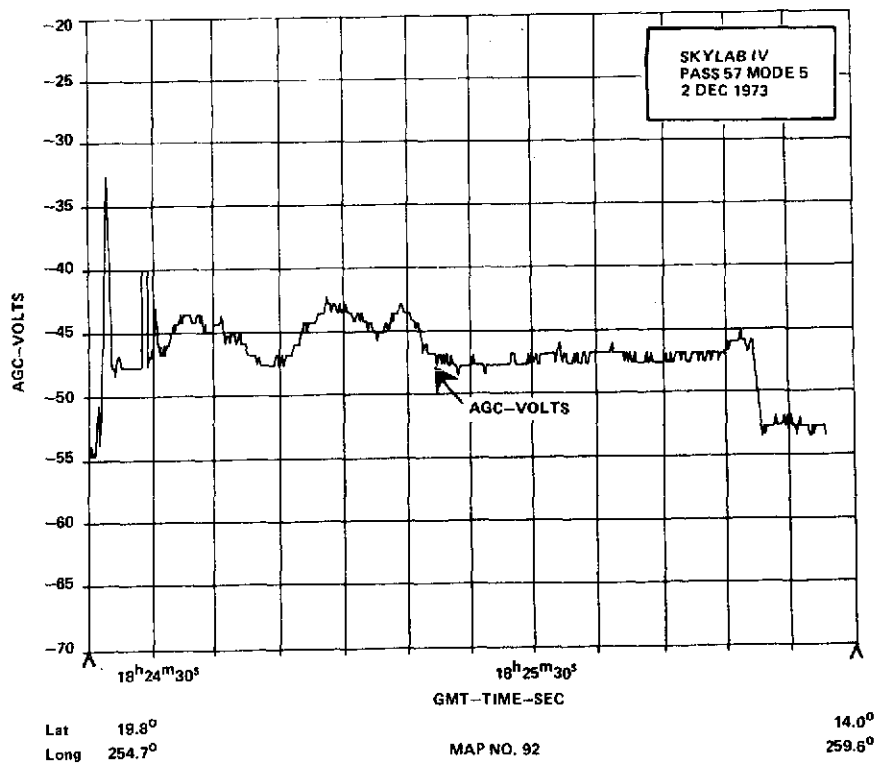
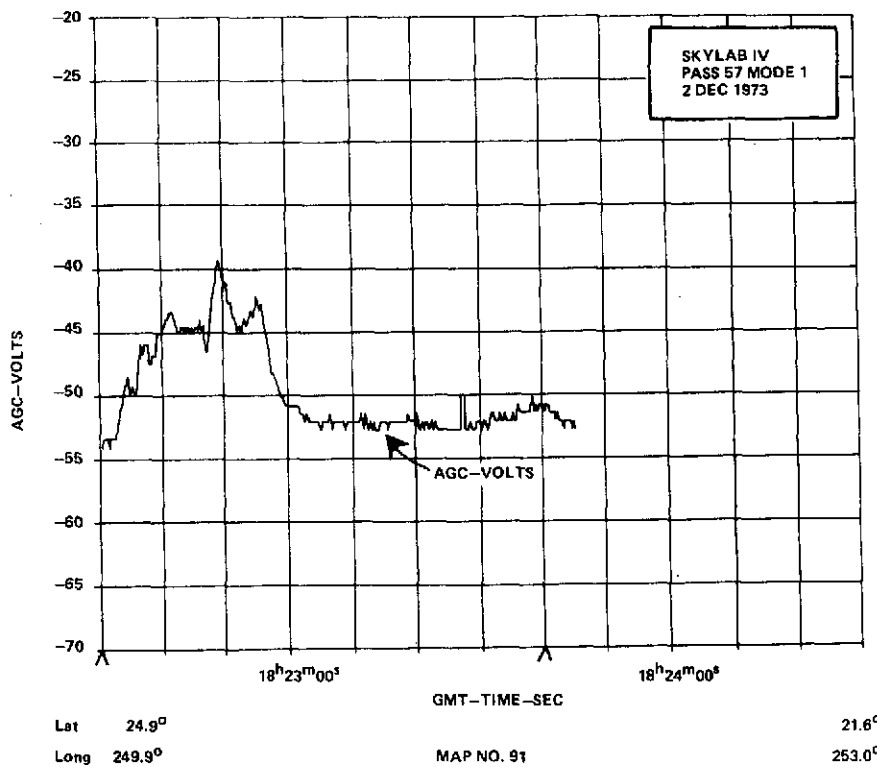


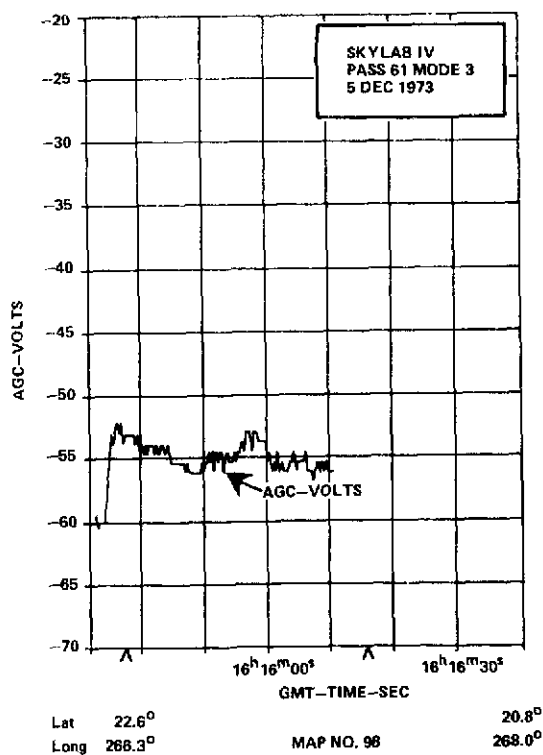
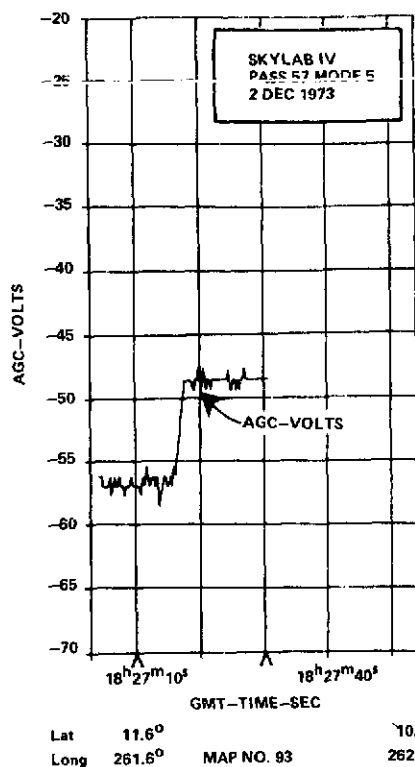
Lat 28.6° 21.8°
Long 284.9° 271.8°

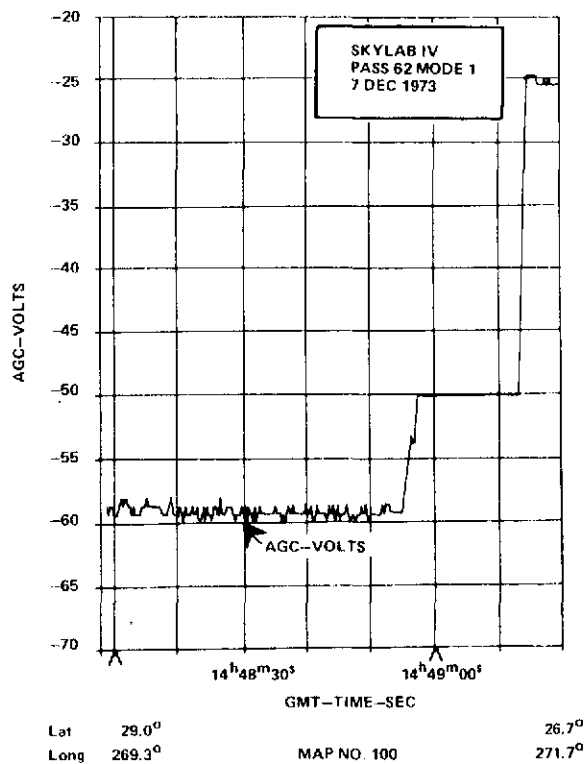
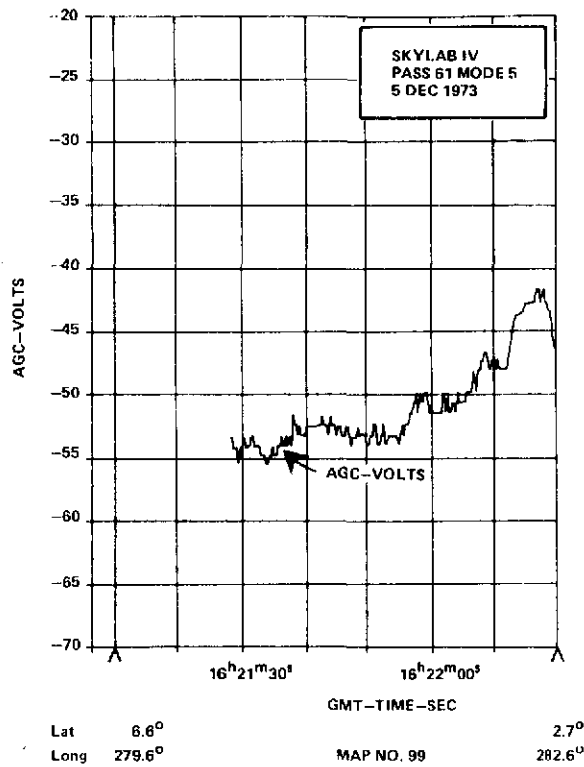
MAP NO. 85

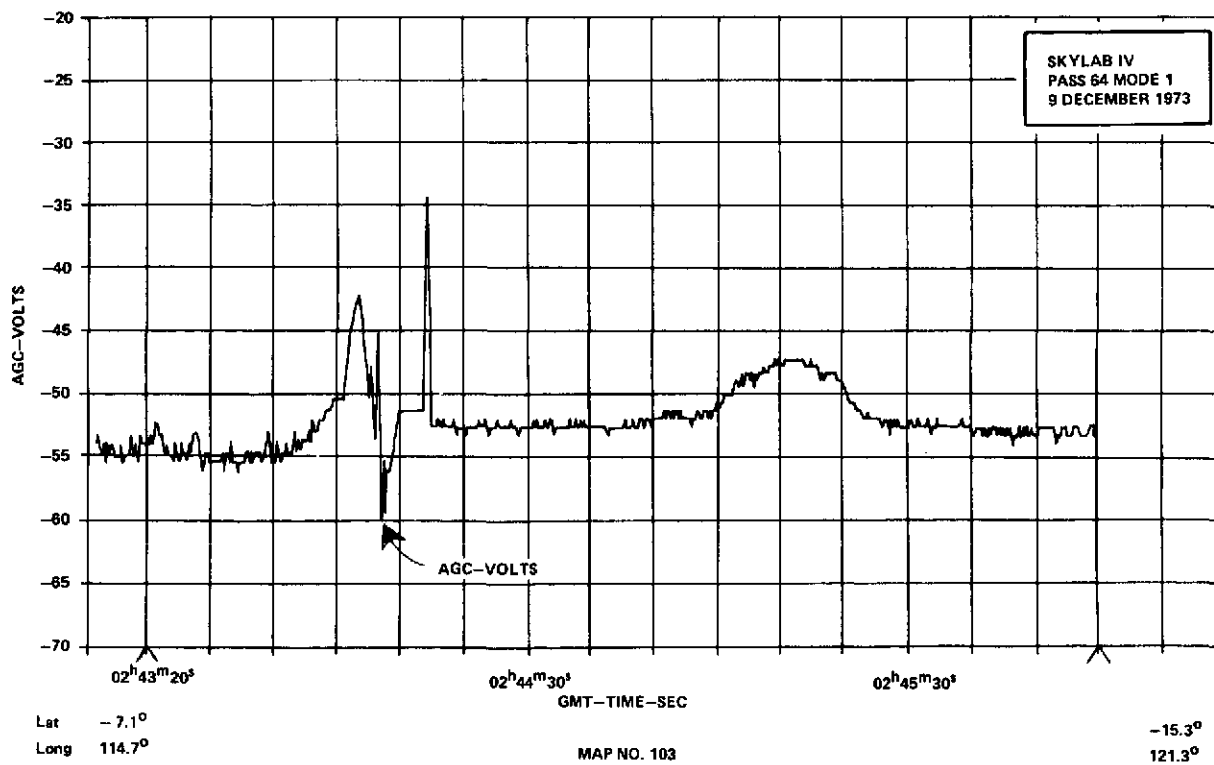
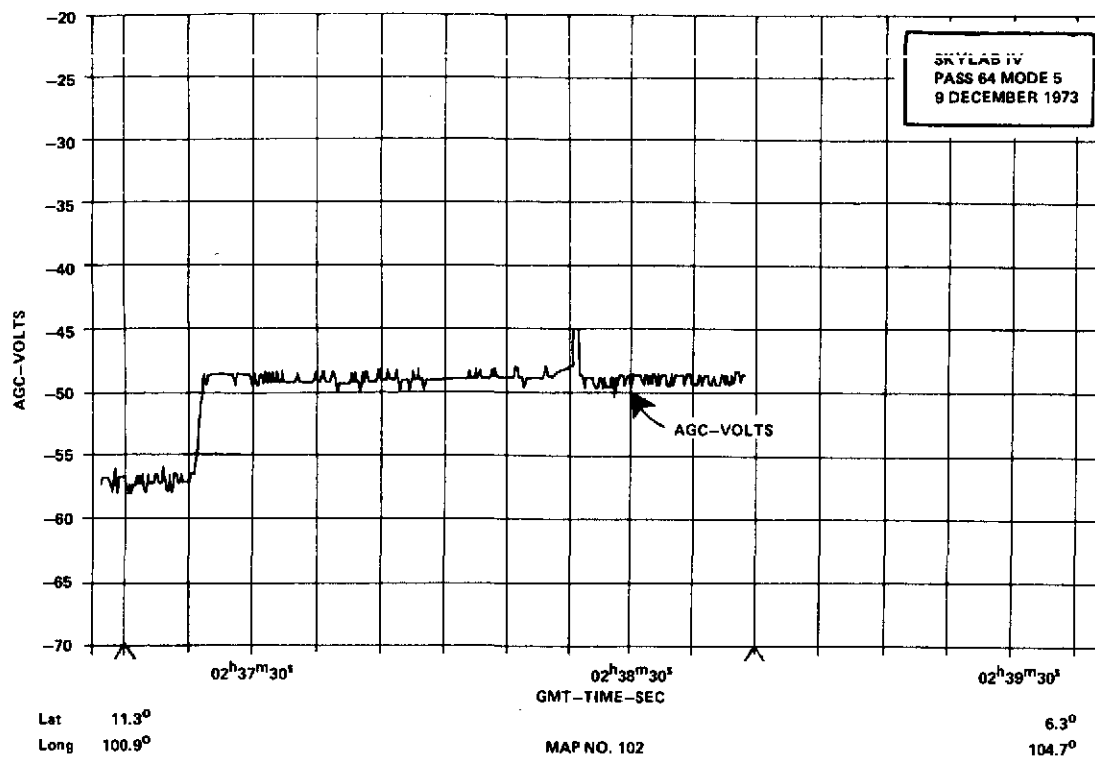
Lat 38.3° Long 232.8°
 MAP NO. 89
 38.8° 235.2°

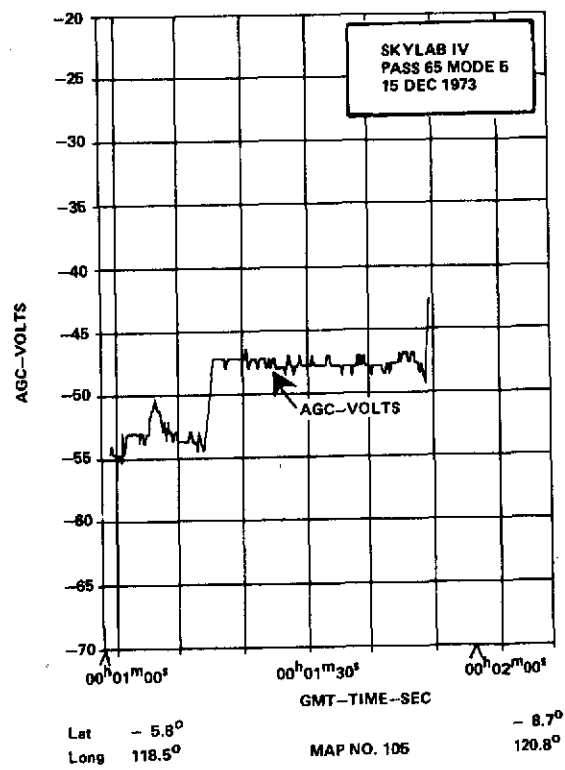
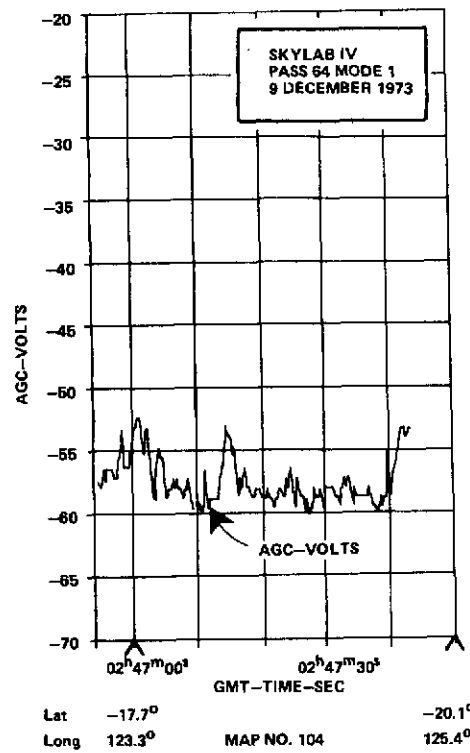


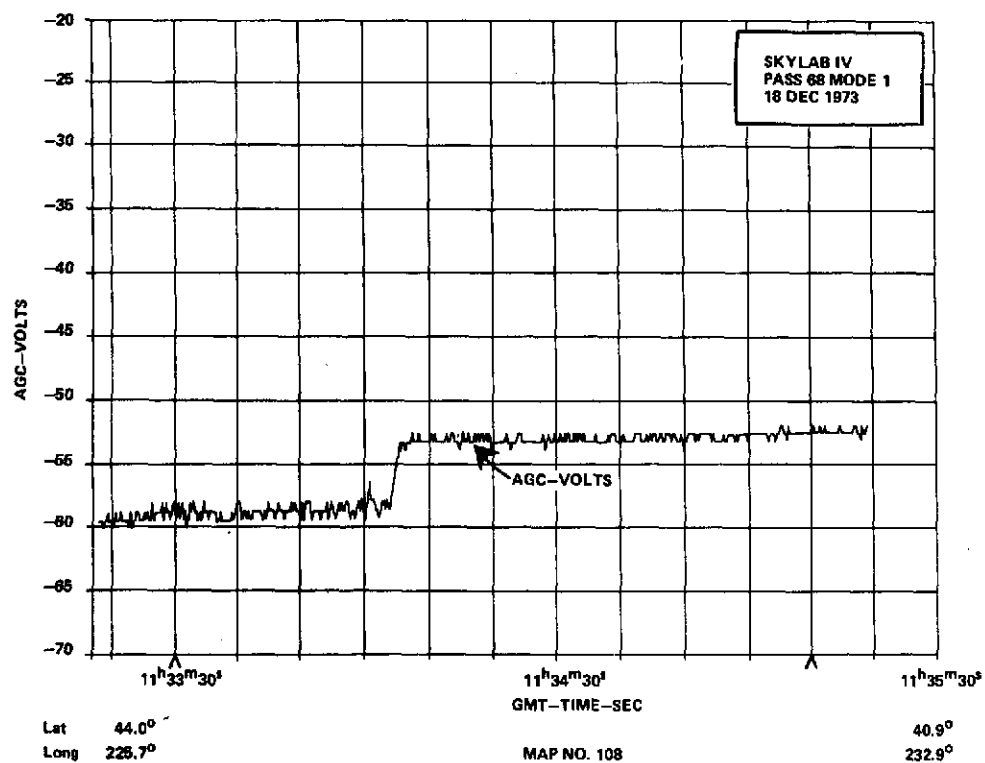
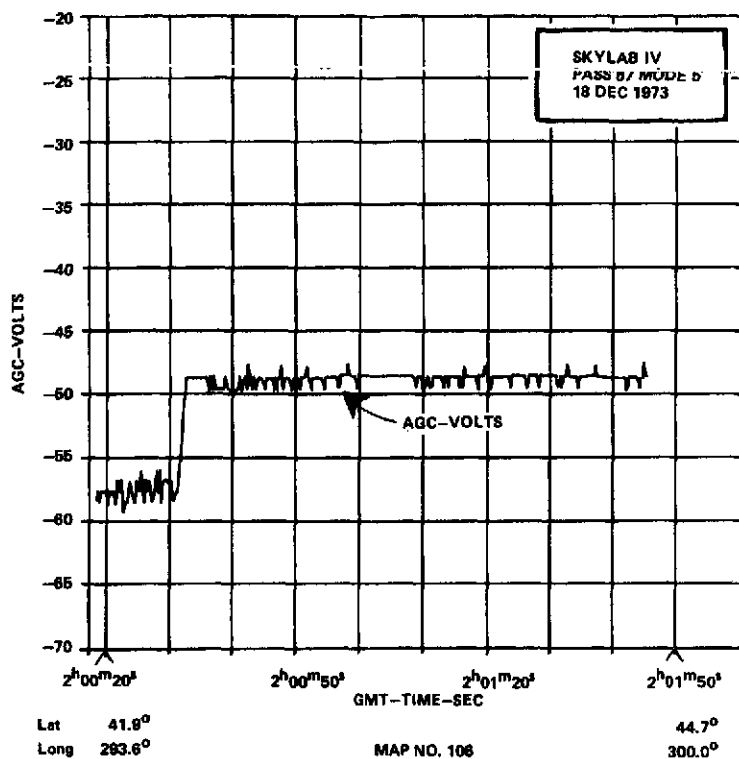


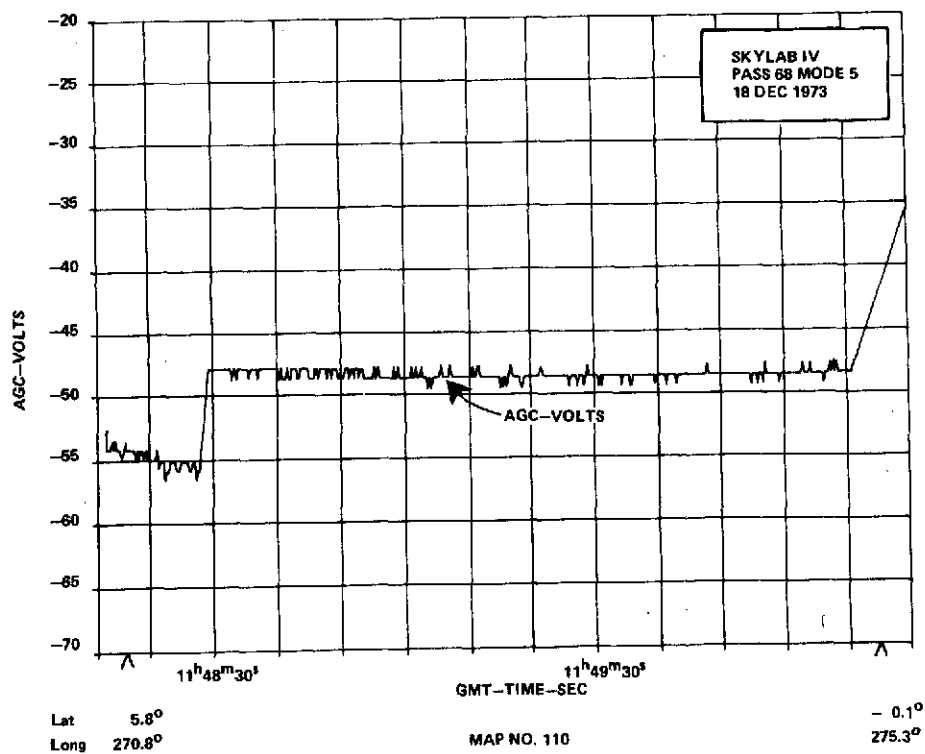
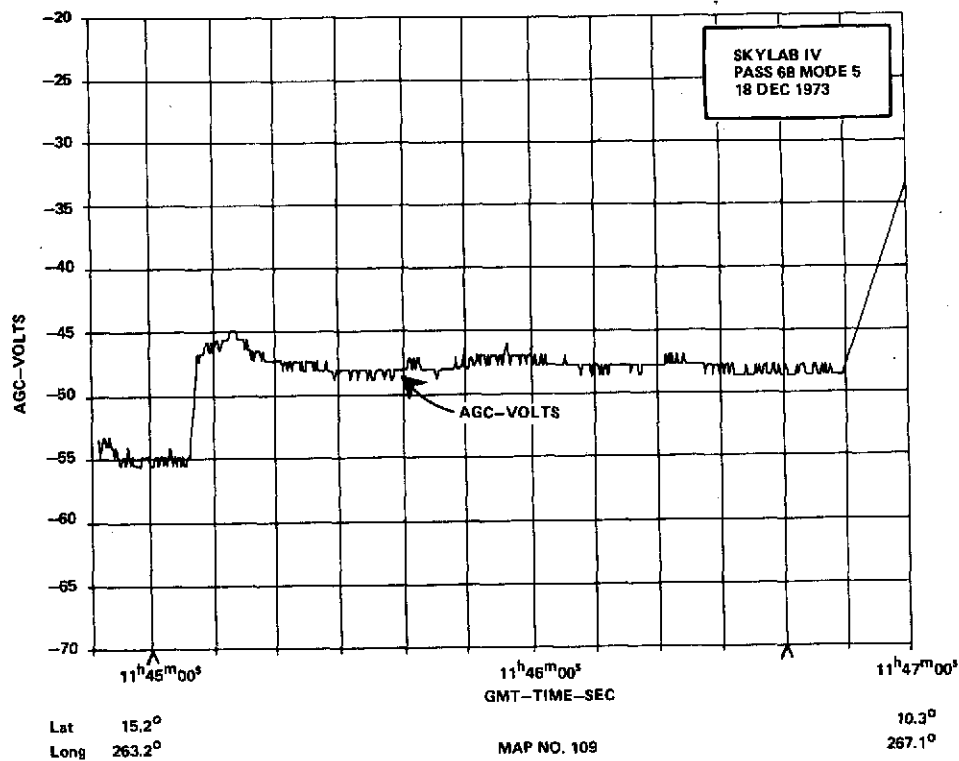


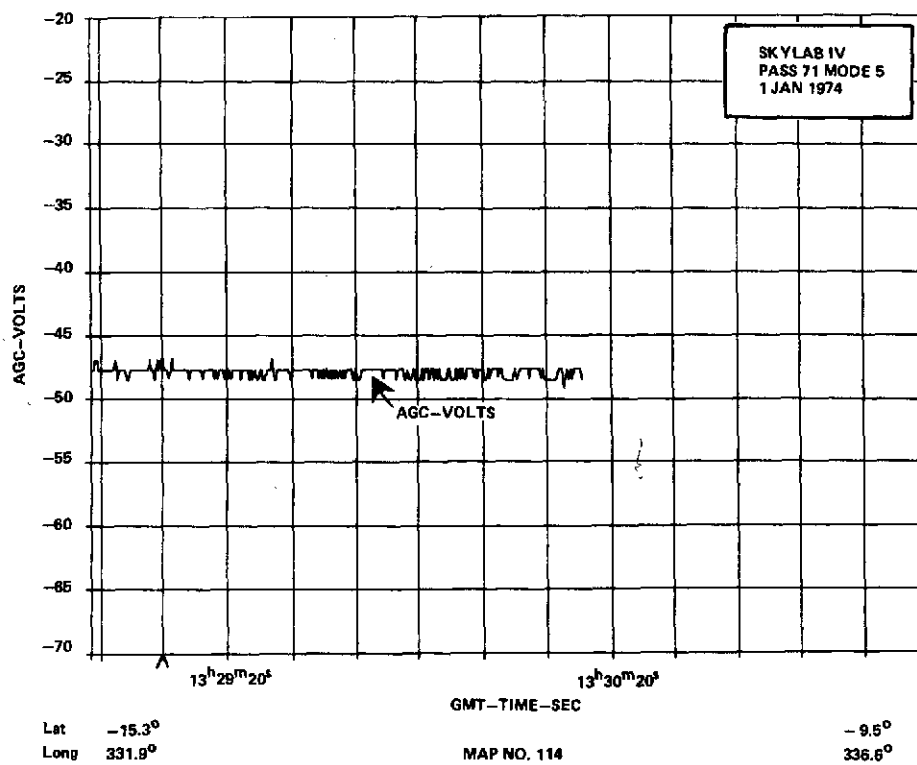
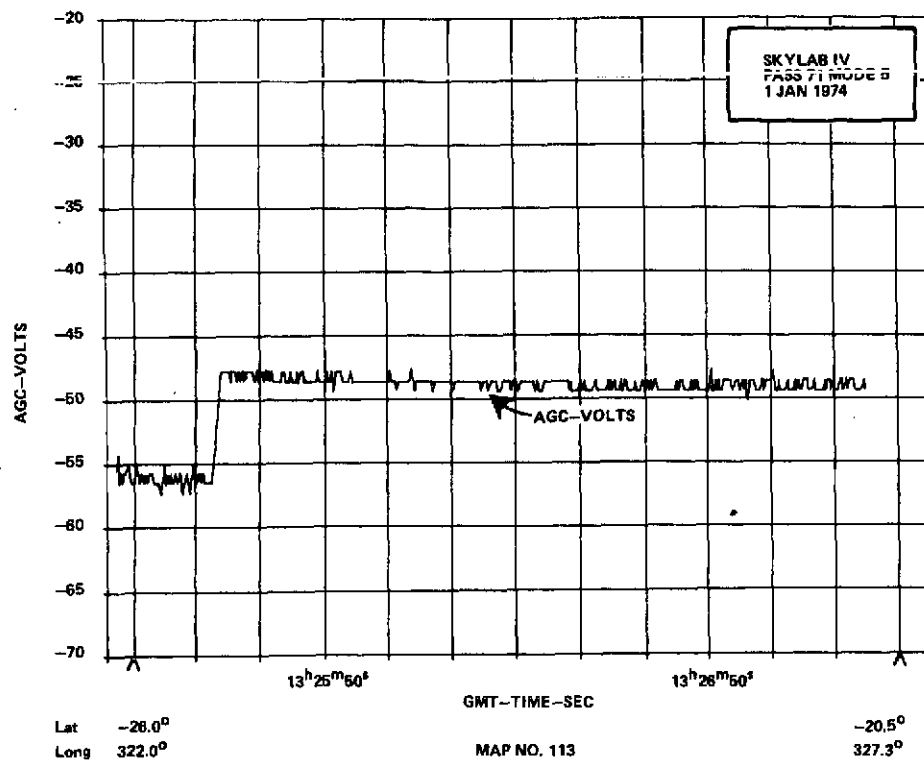


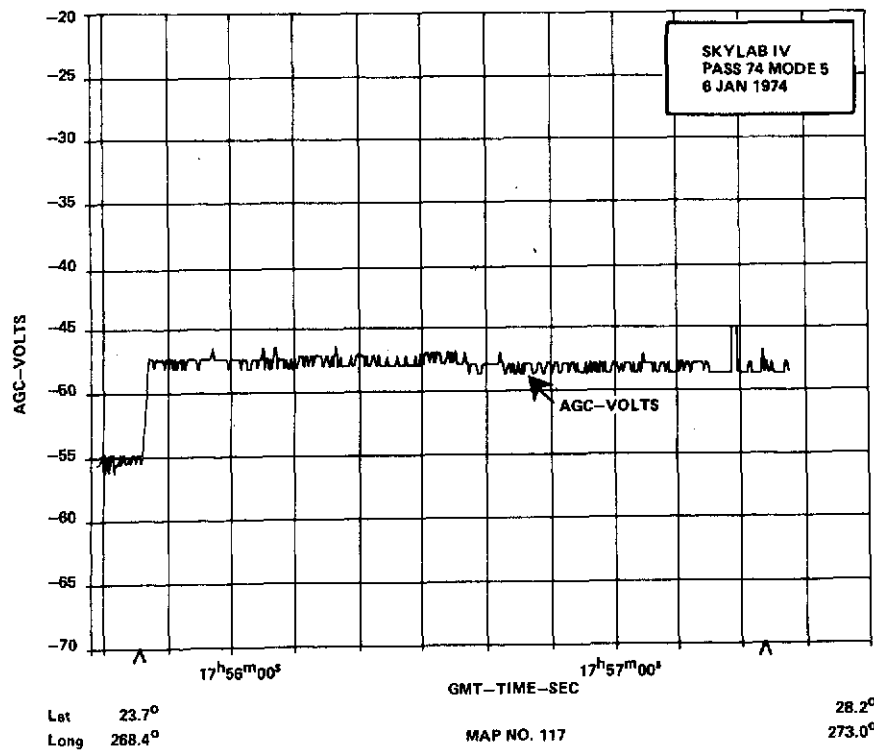
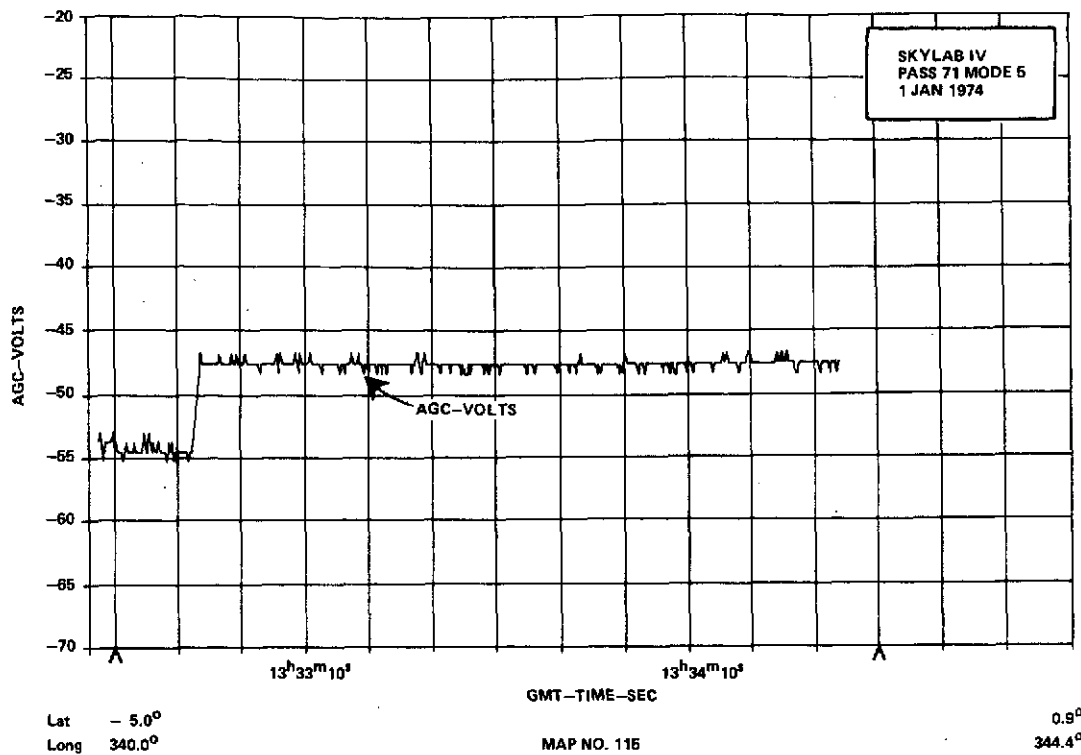


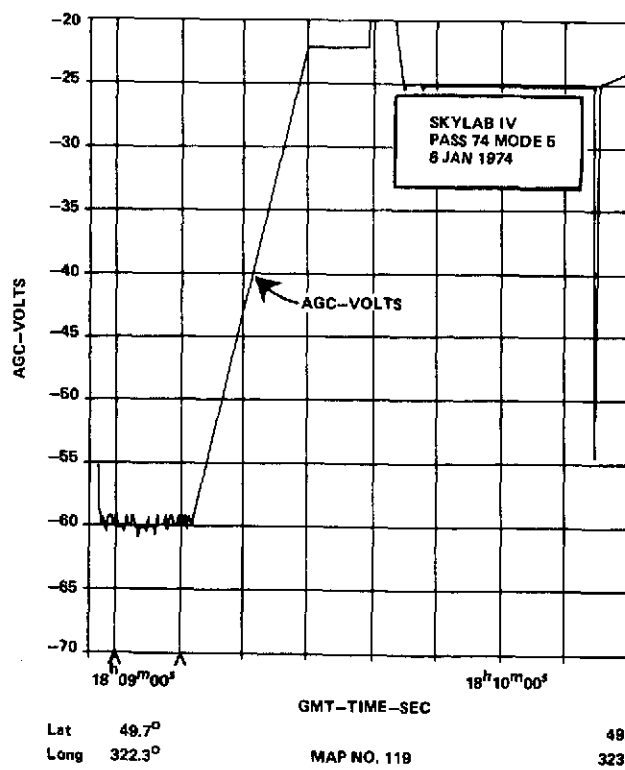
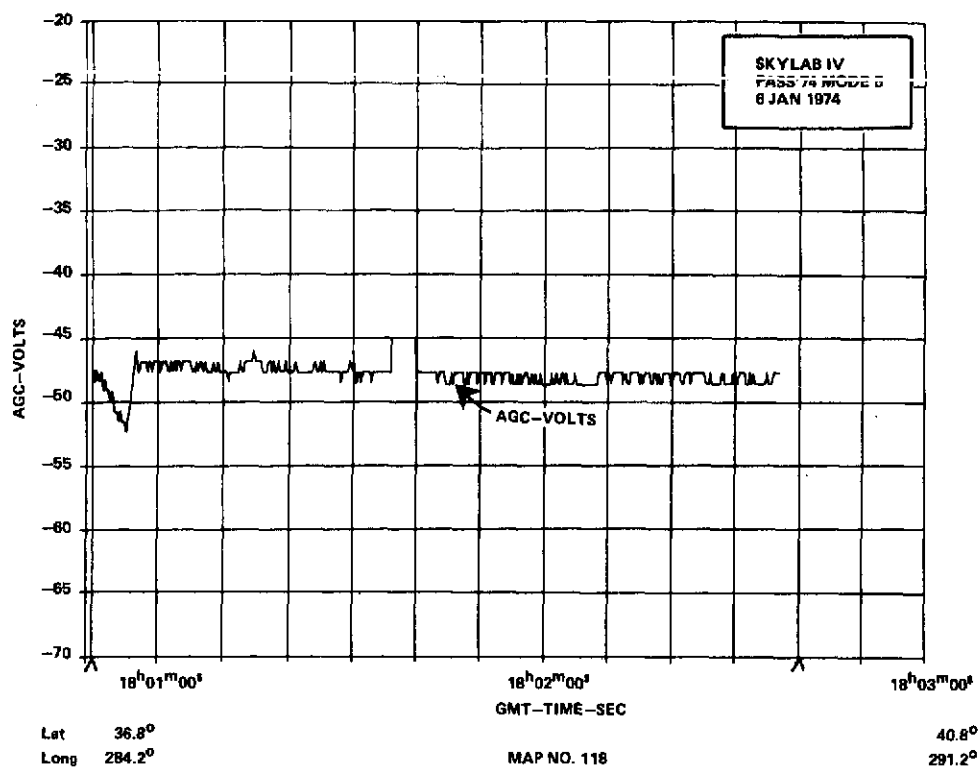


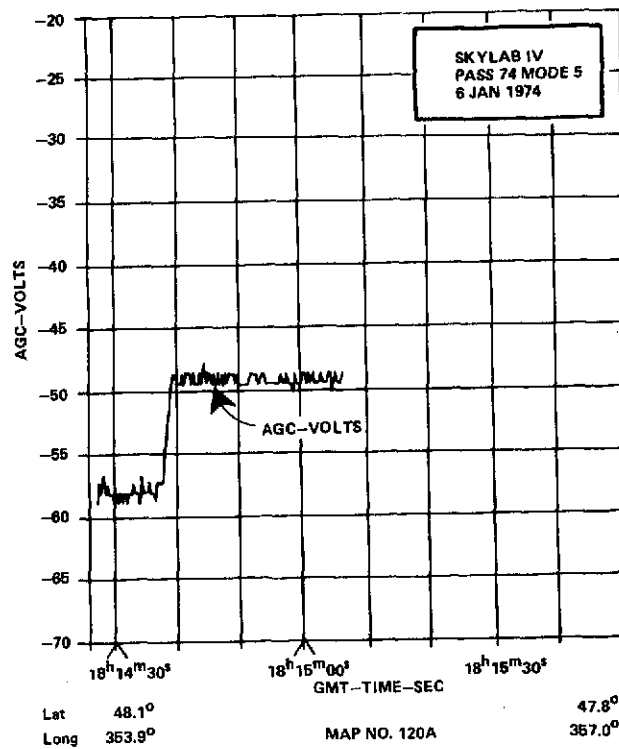
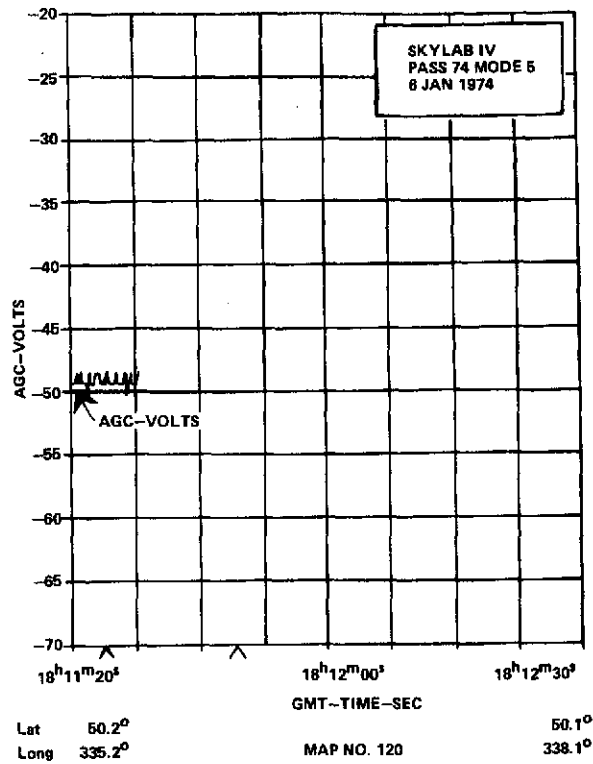


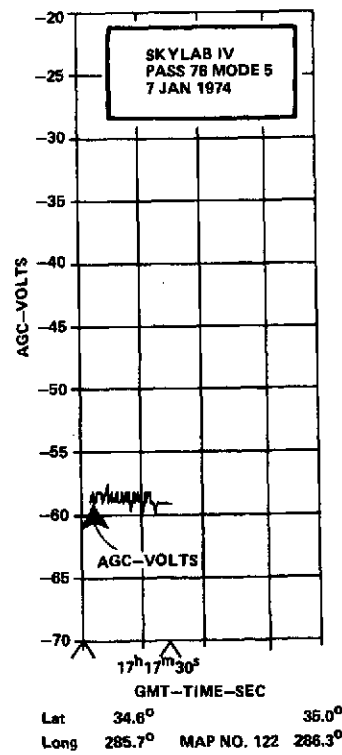
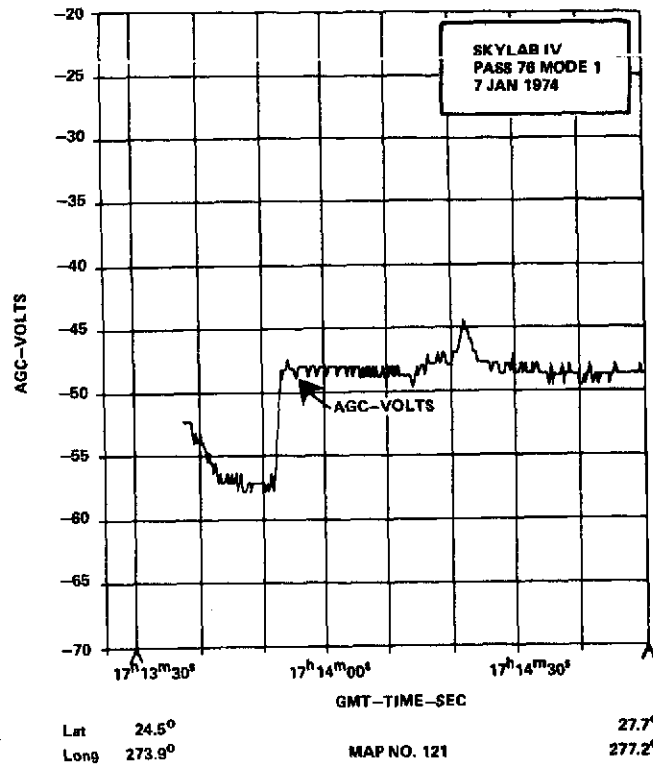


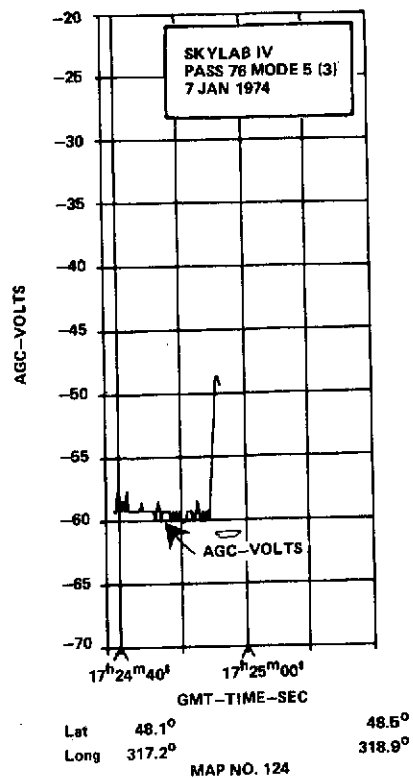
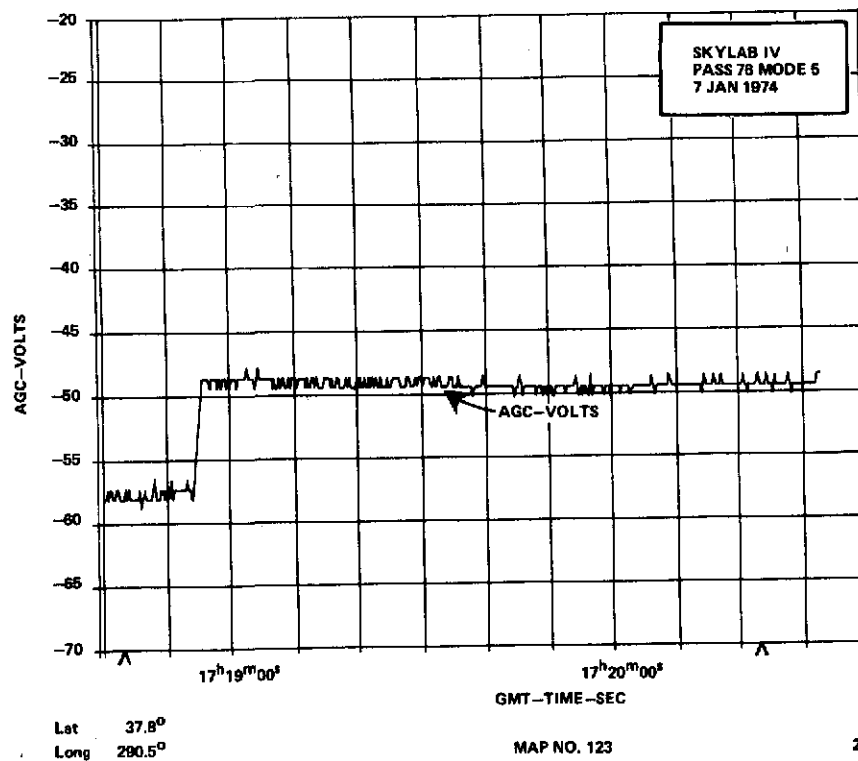


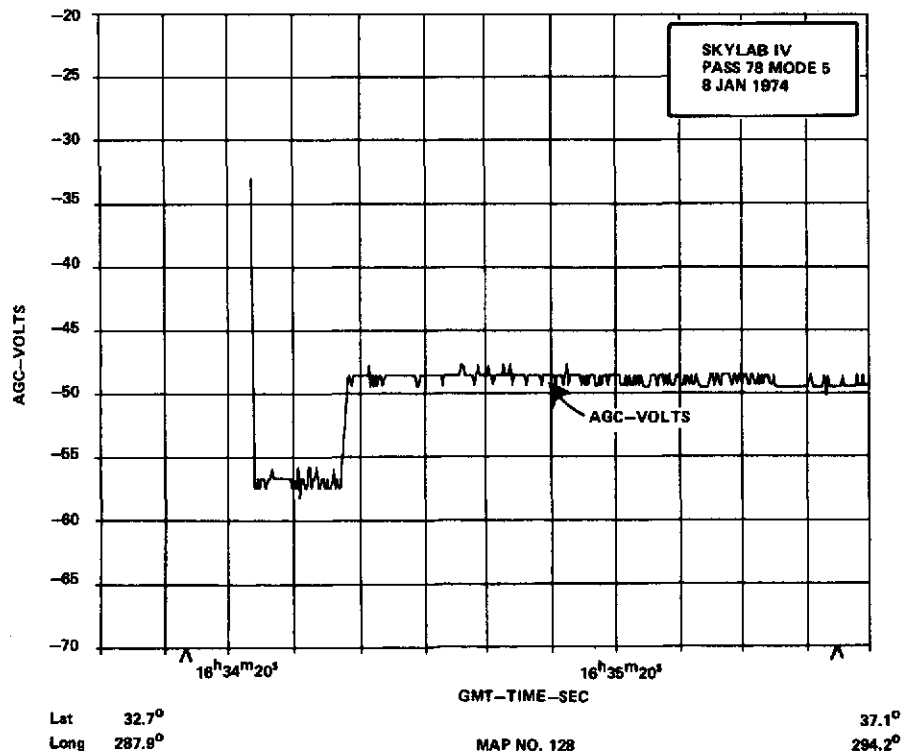
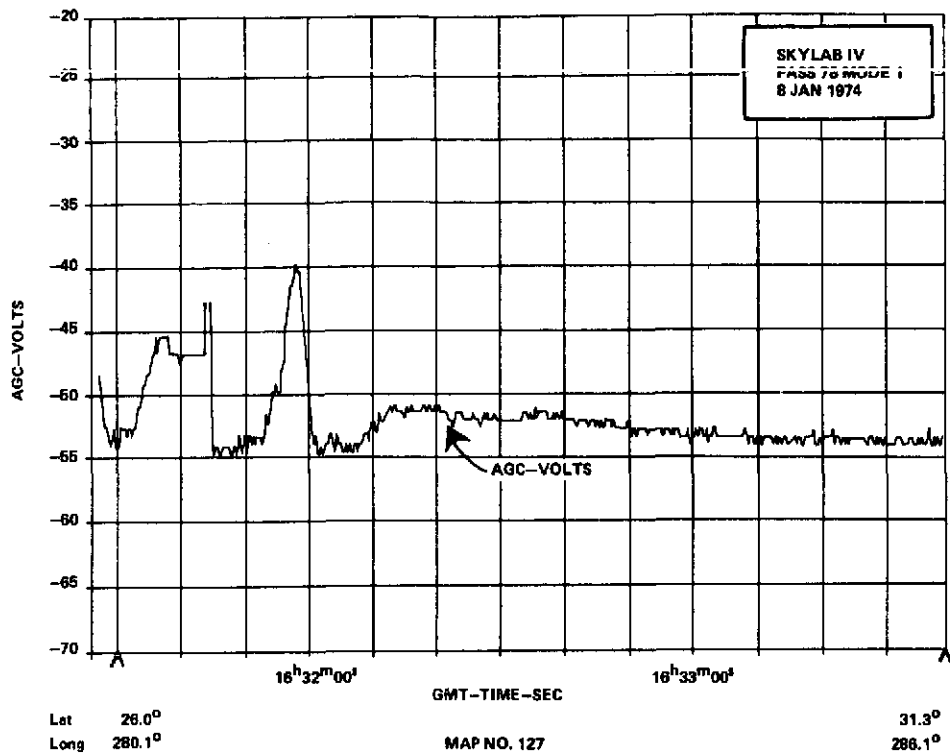


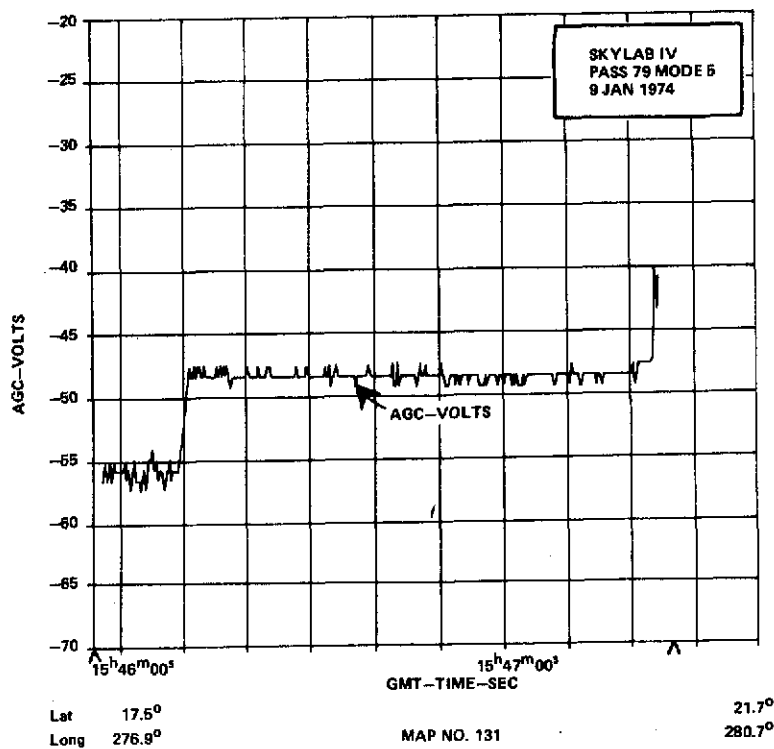
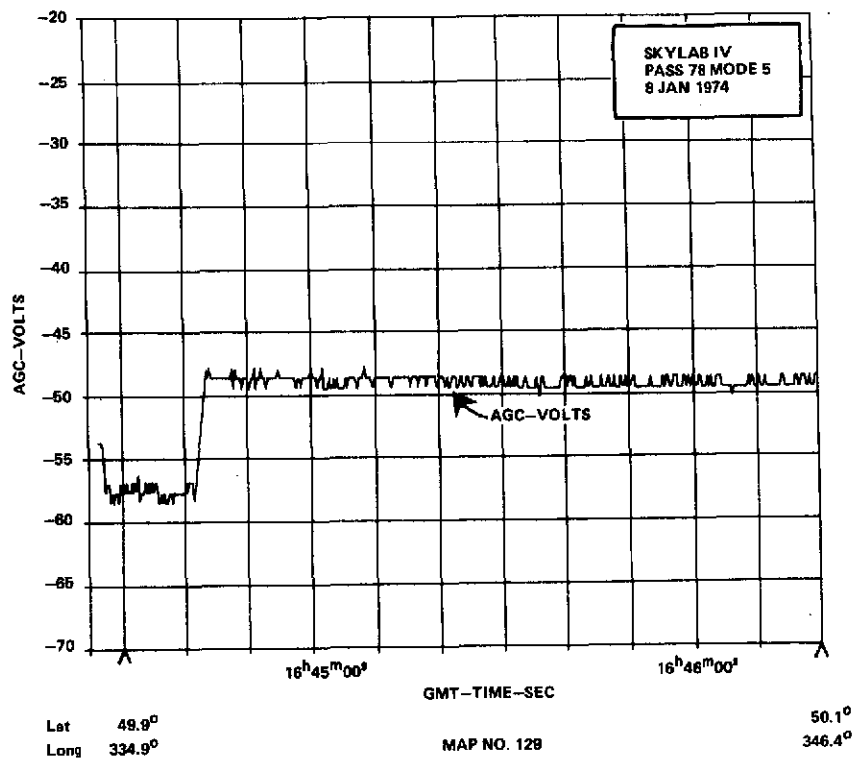


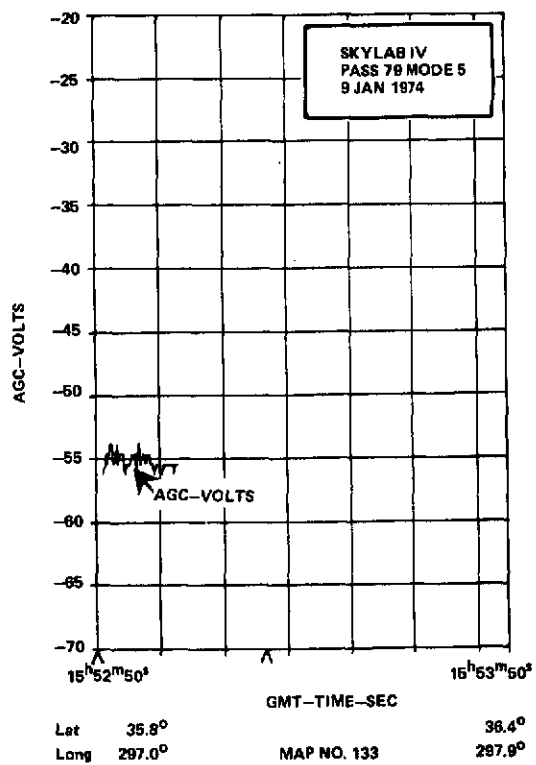
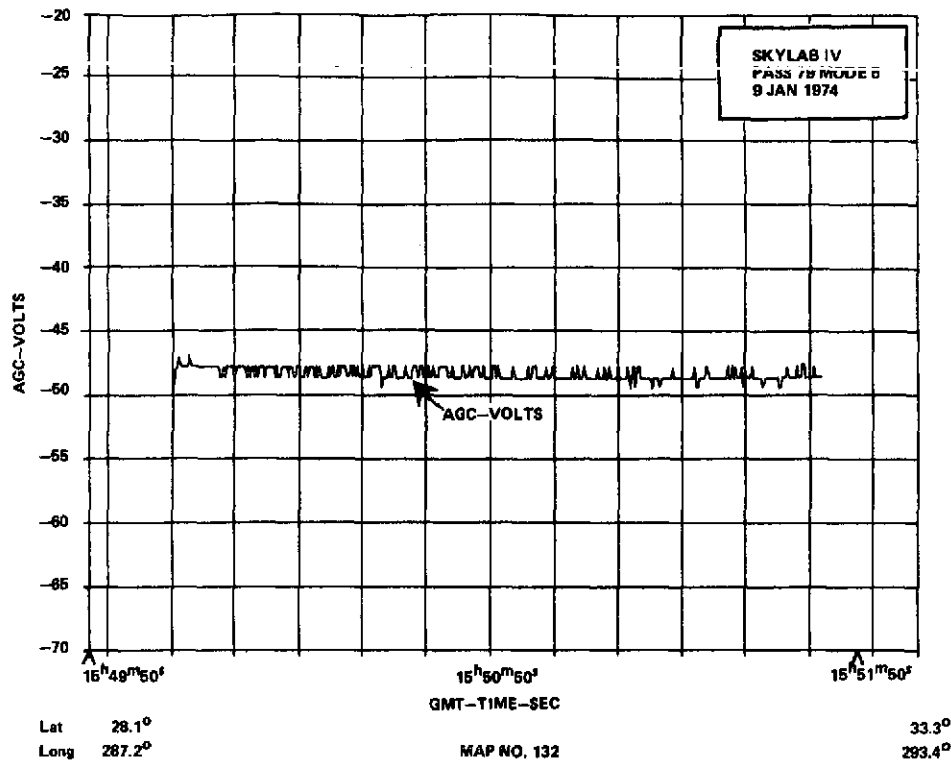


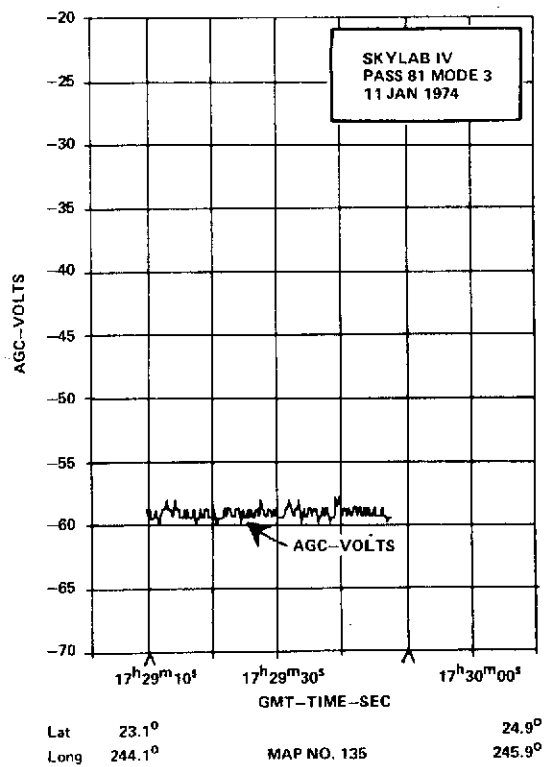
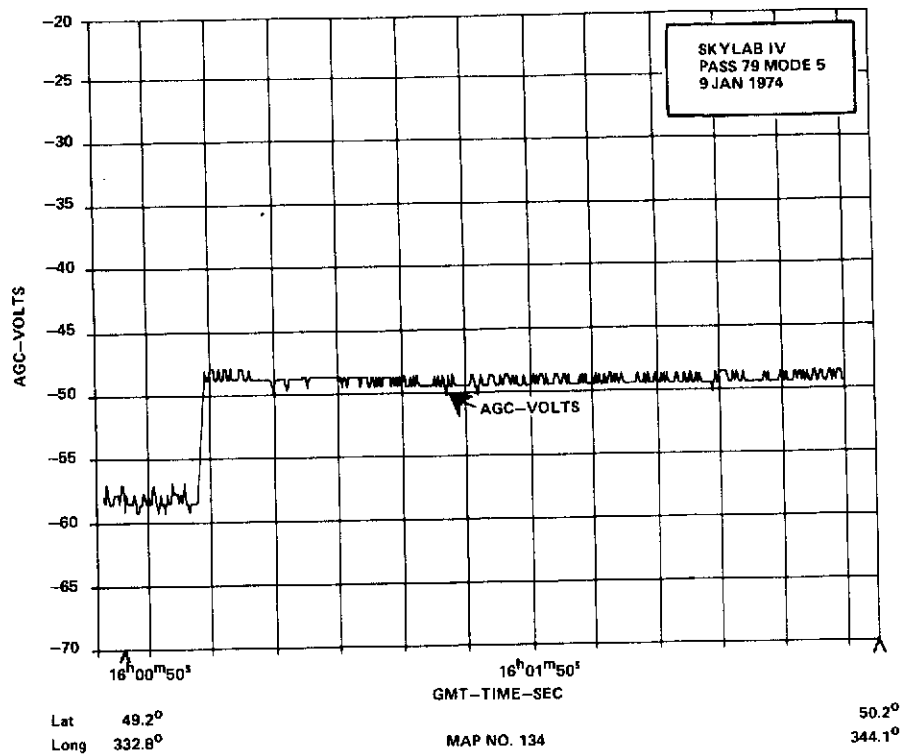


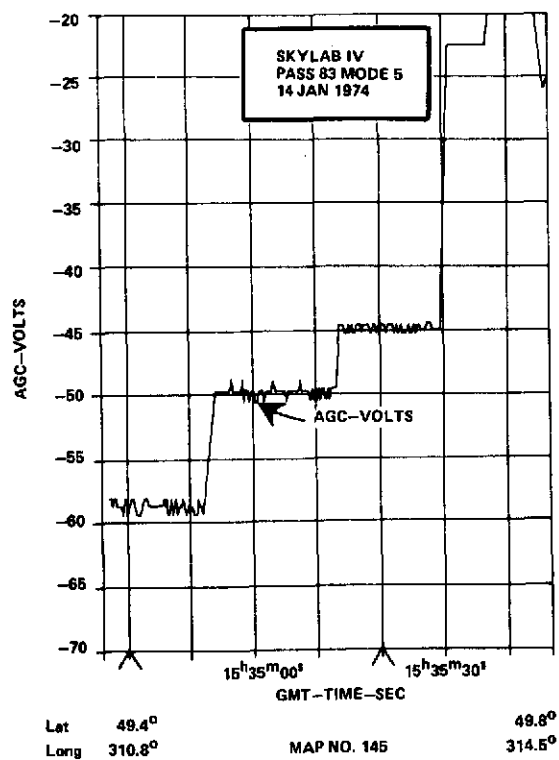
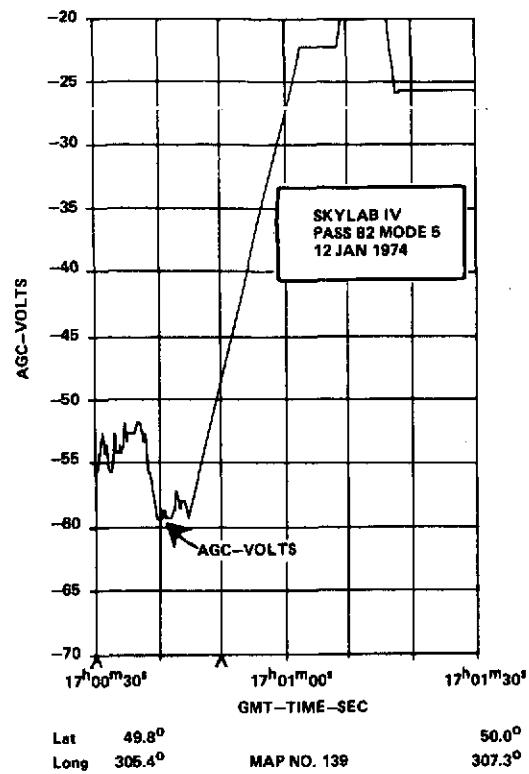


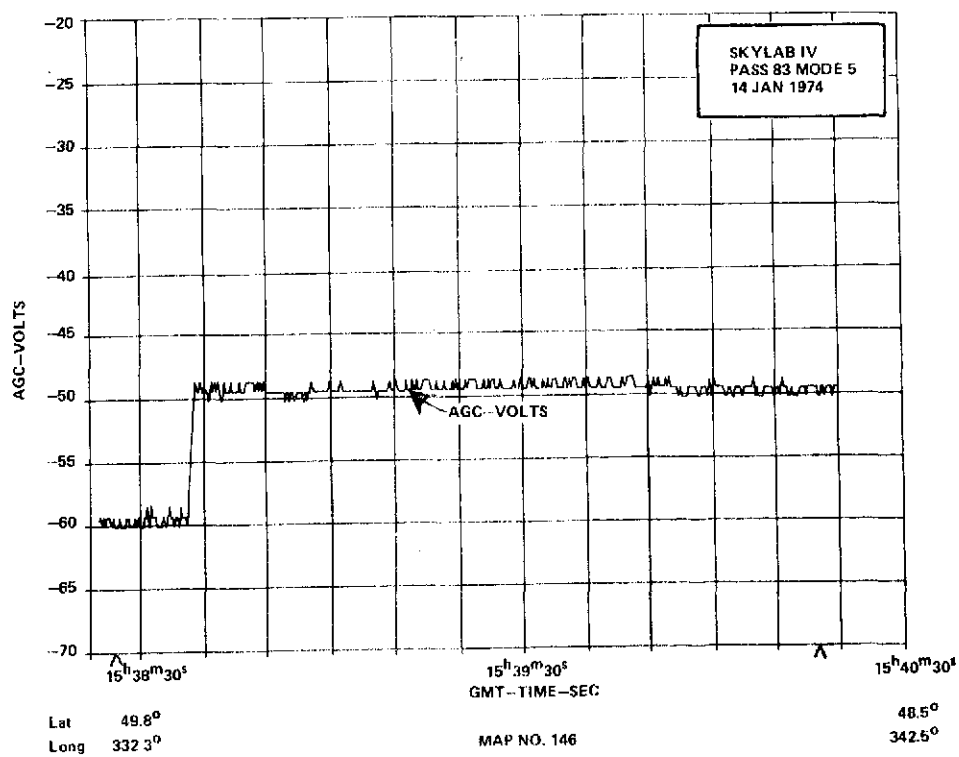
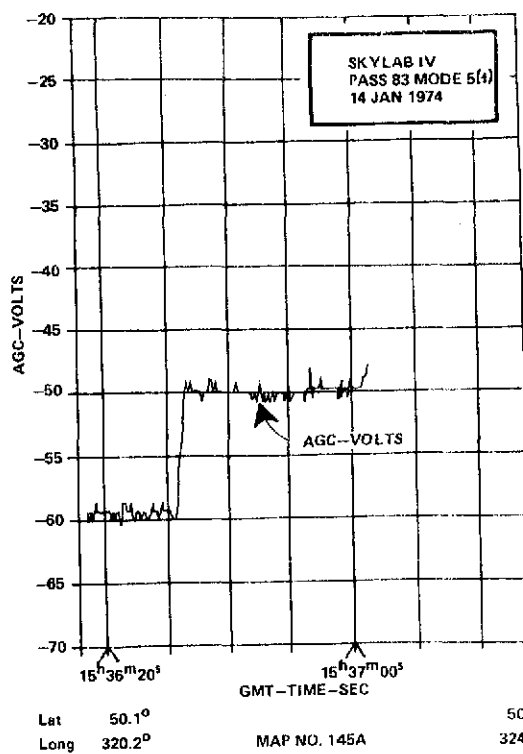


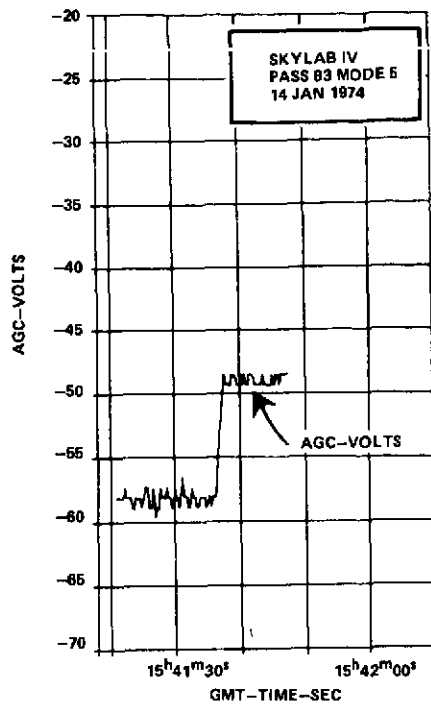




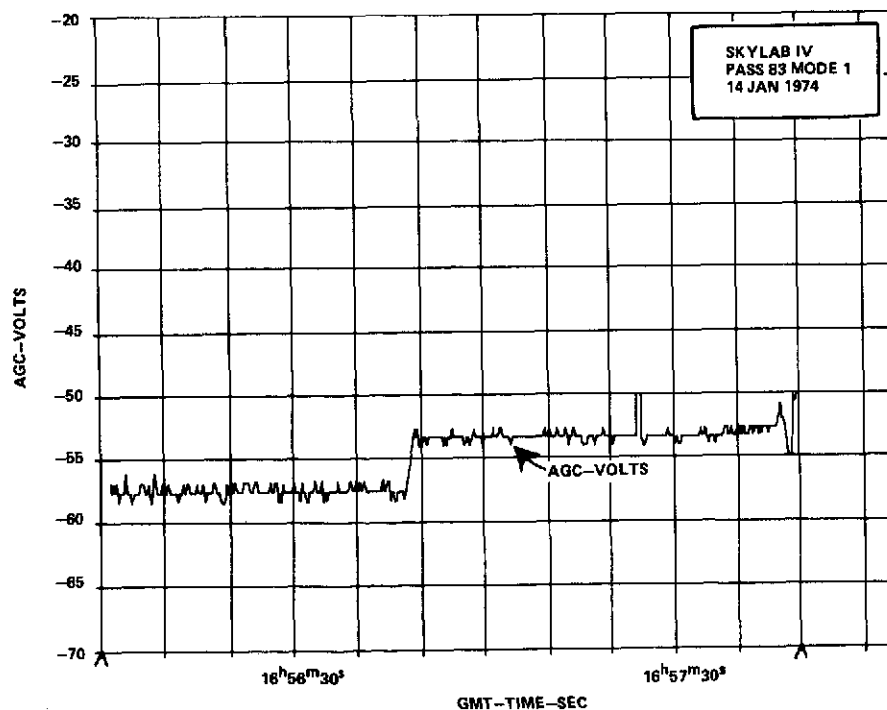




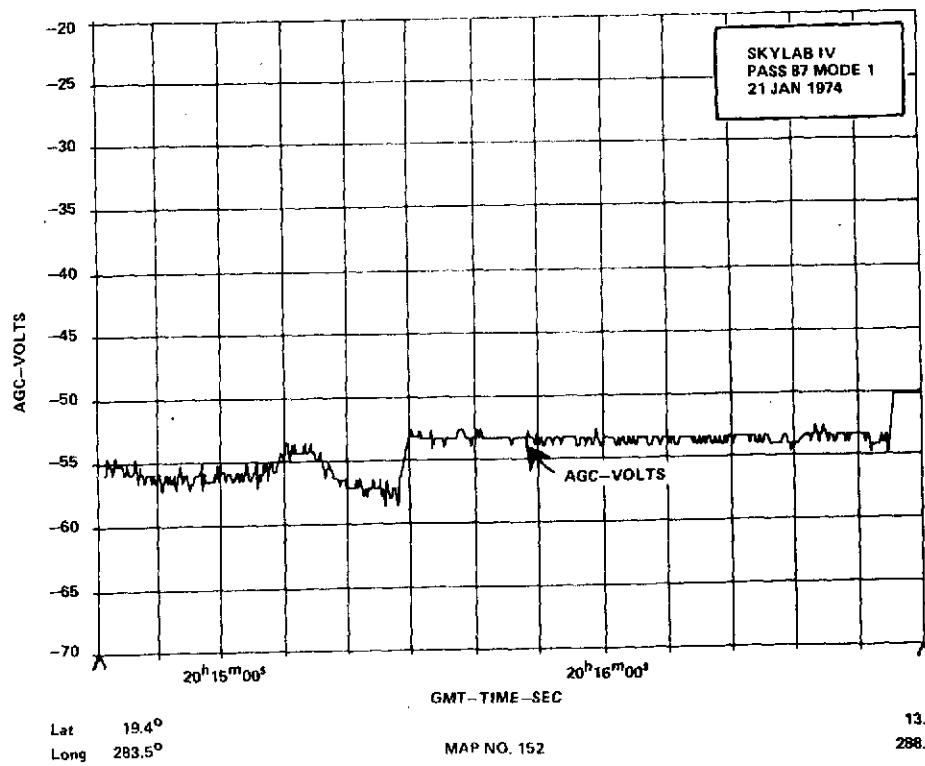
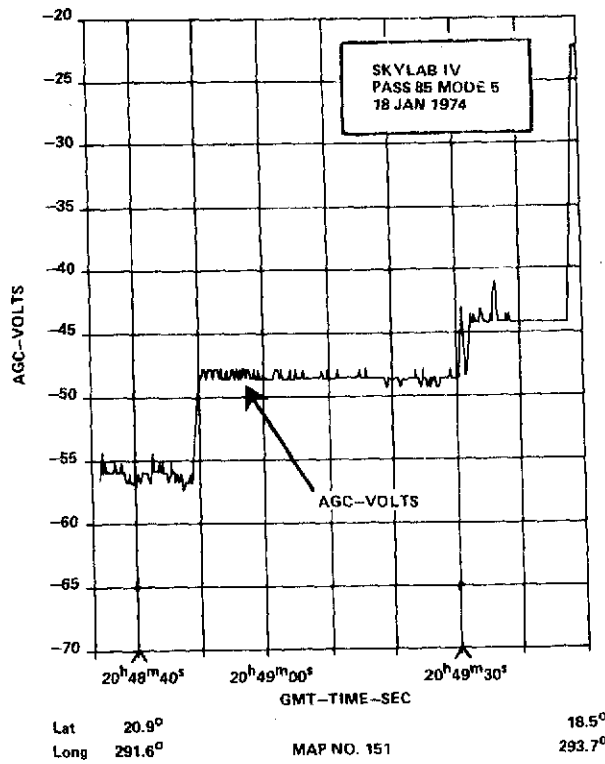




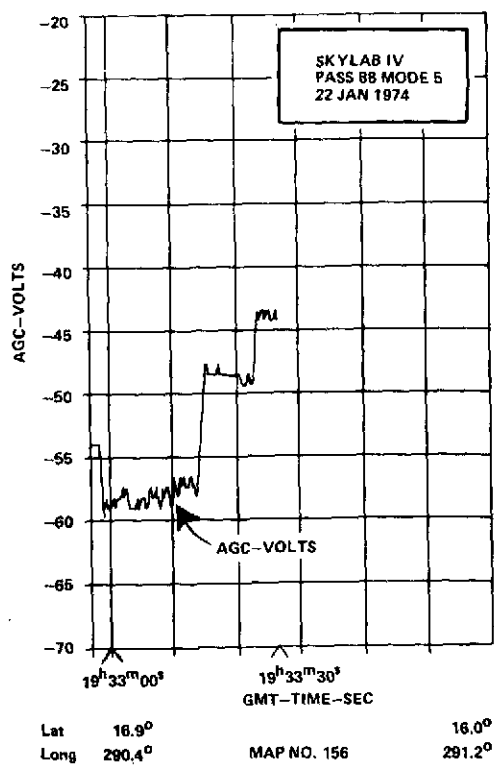
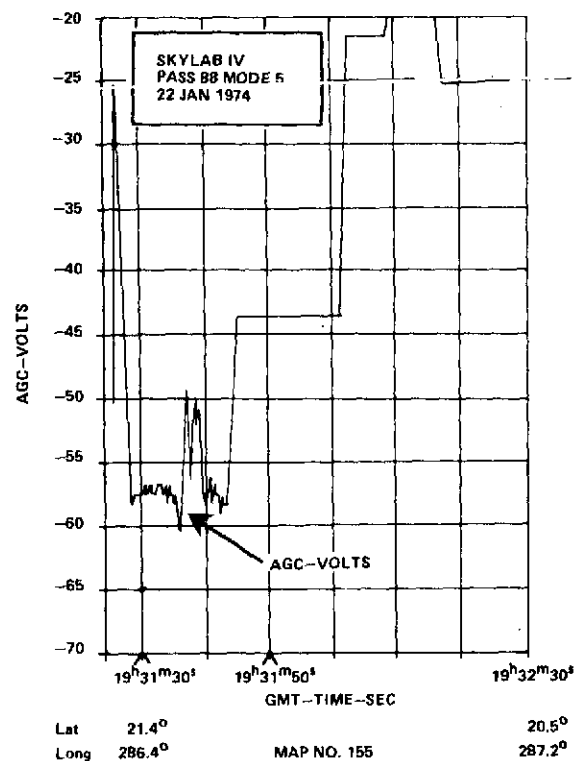
Lat 47.2° 46.8°
Long 348.3° MAP NO. 147 350.0°

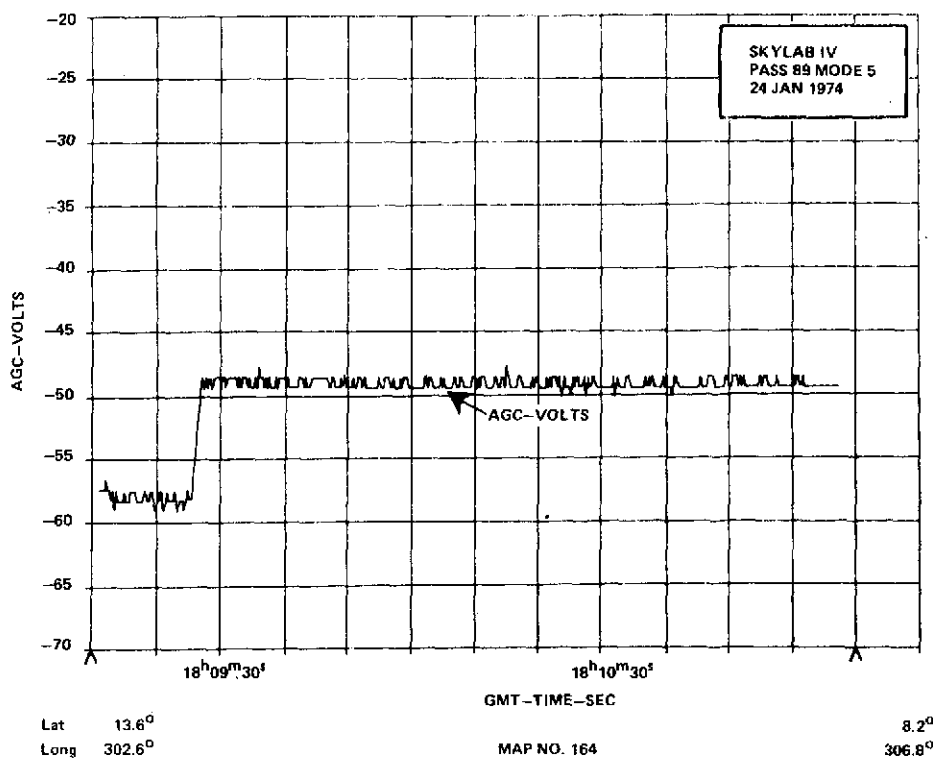
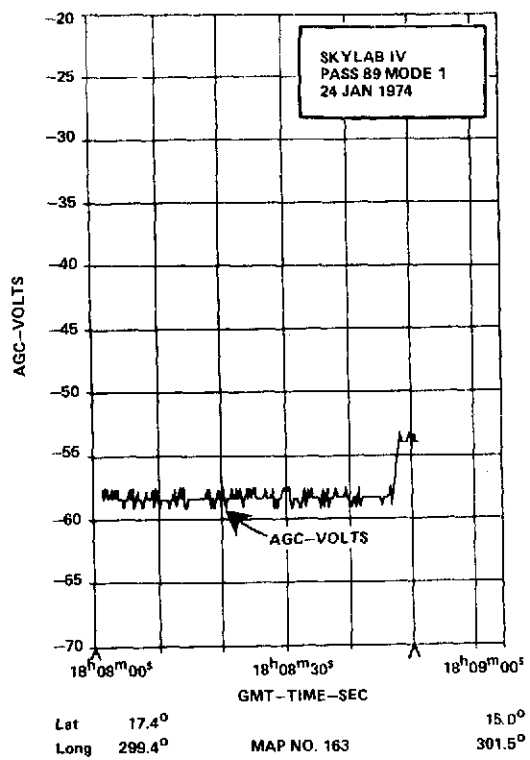


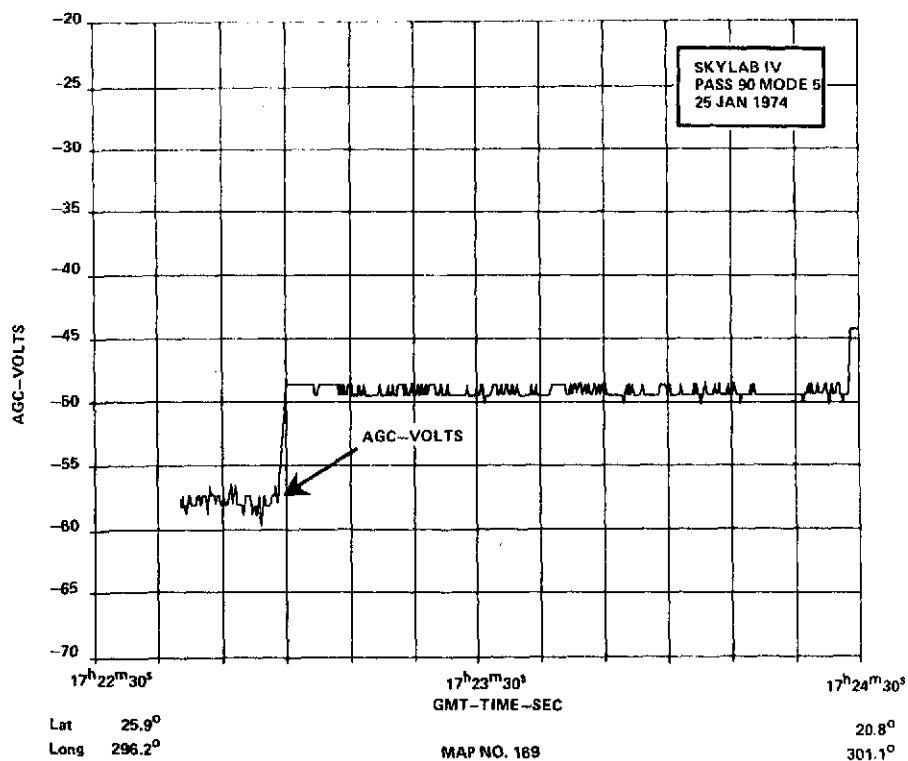
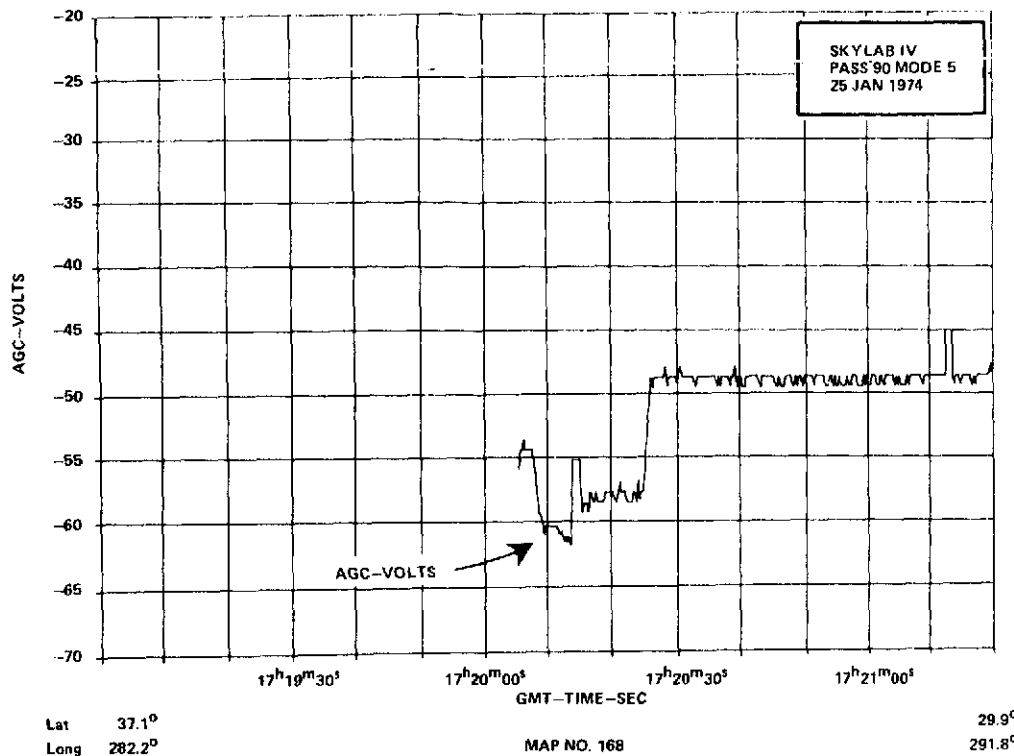
Lat 26.6° 31.5°
Long 238.2° MAP NO. 148 243.7°

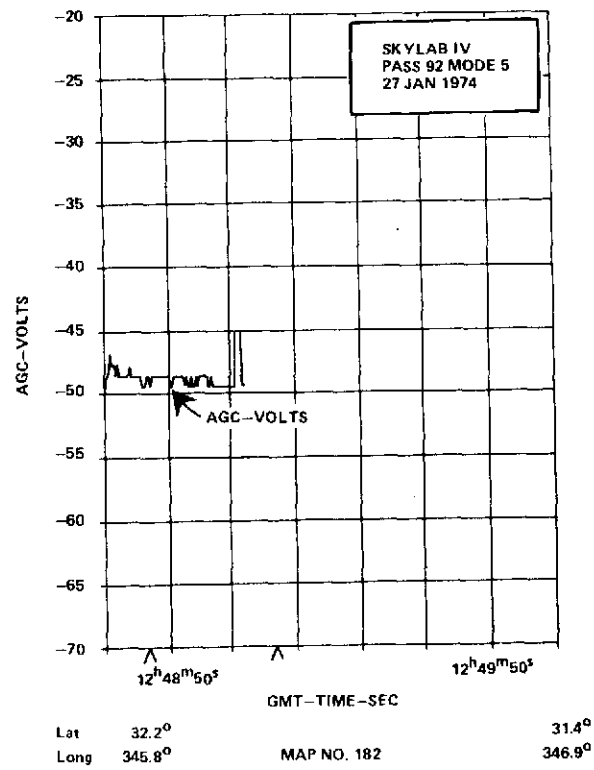
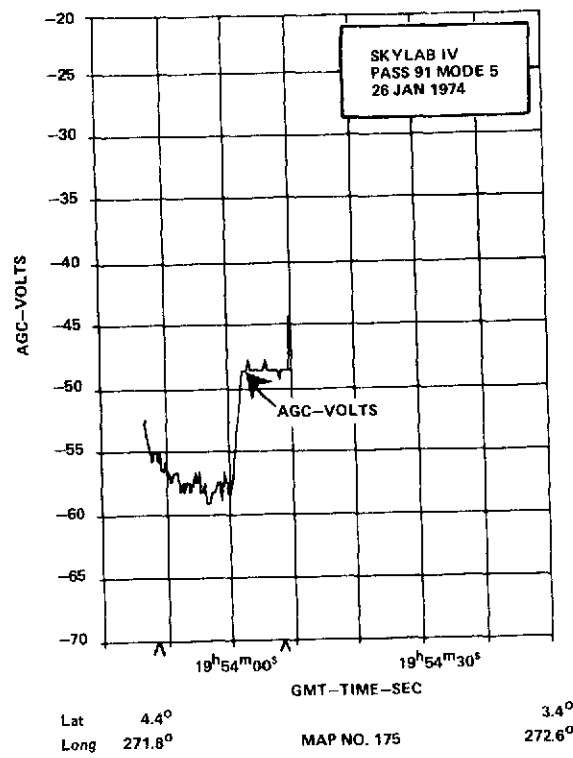


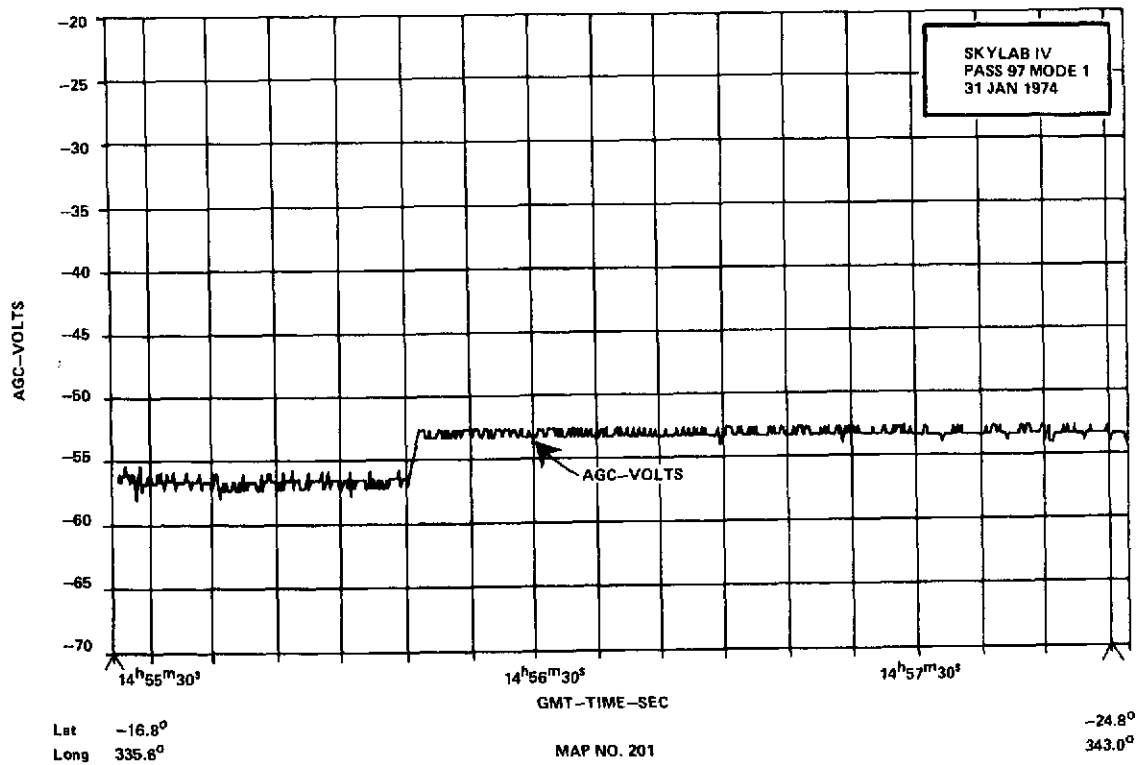
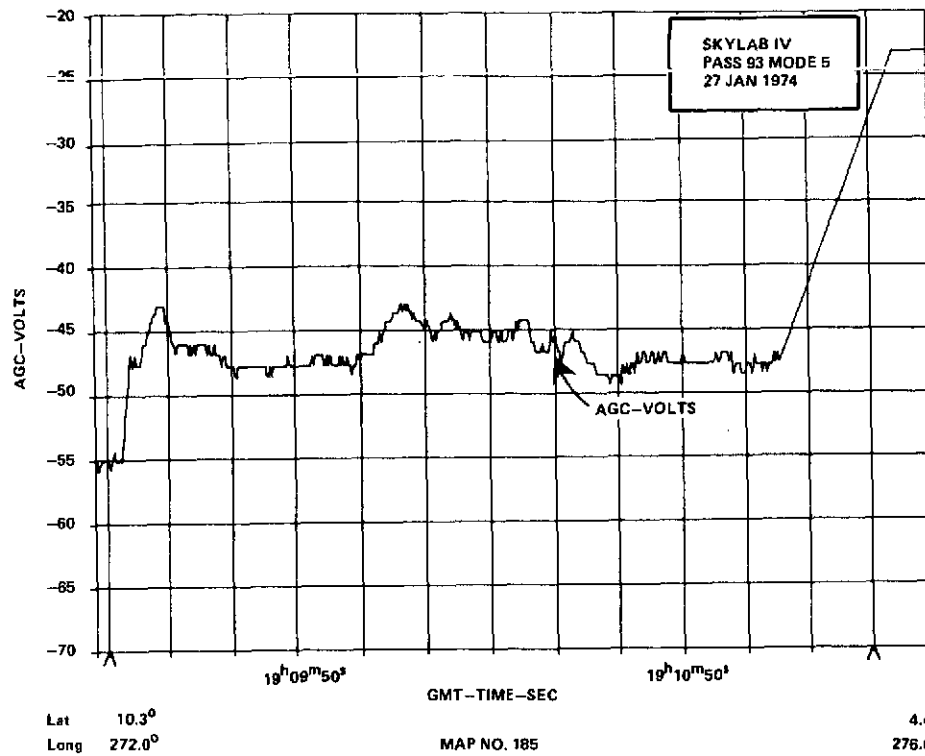
C - 4

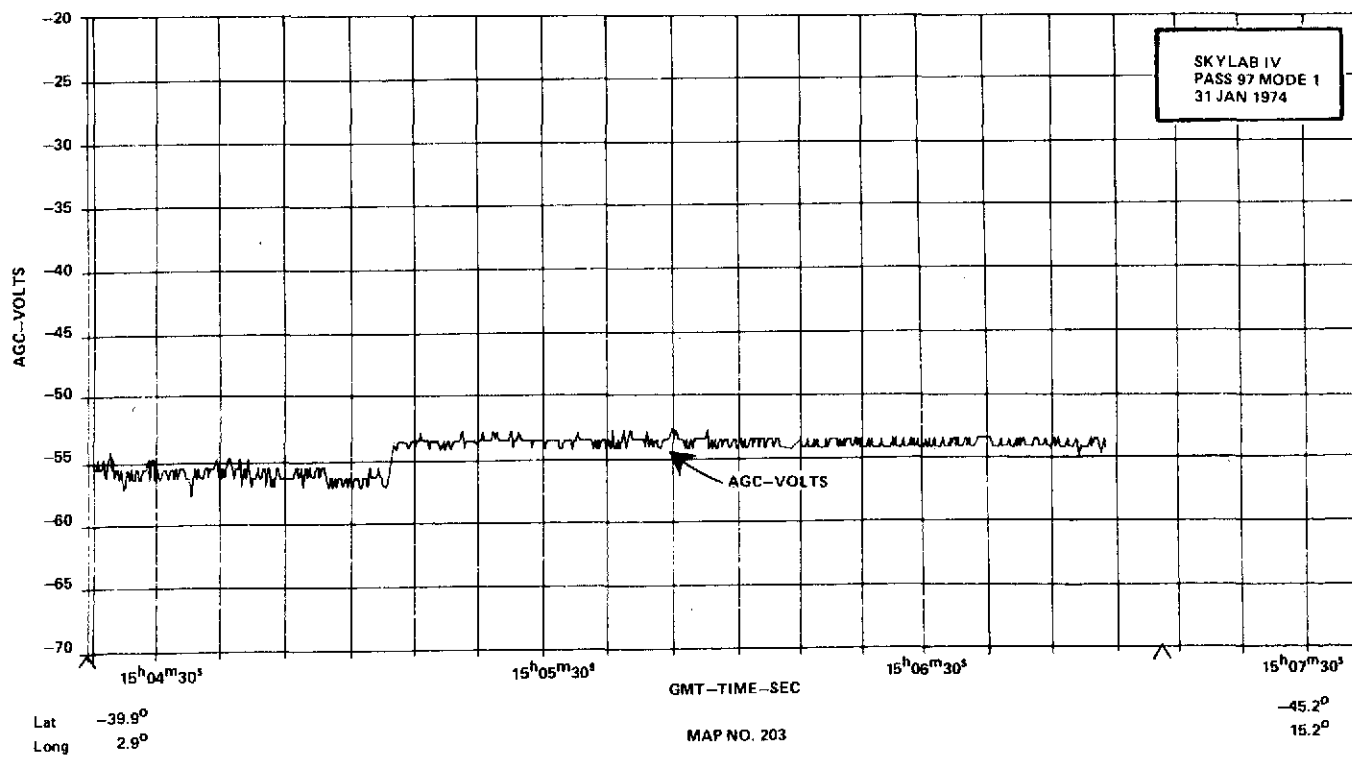
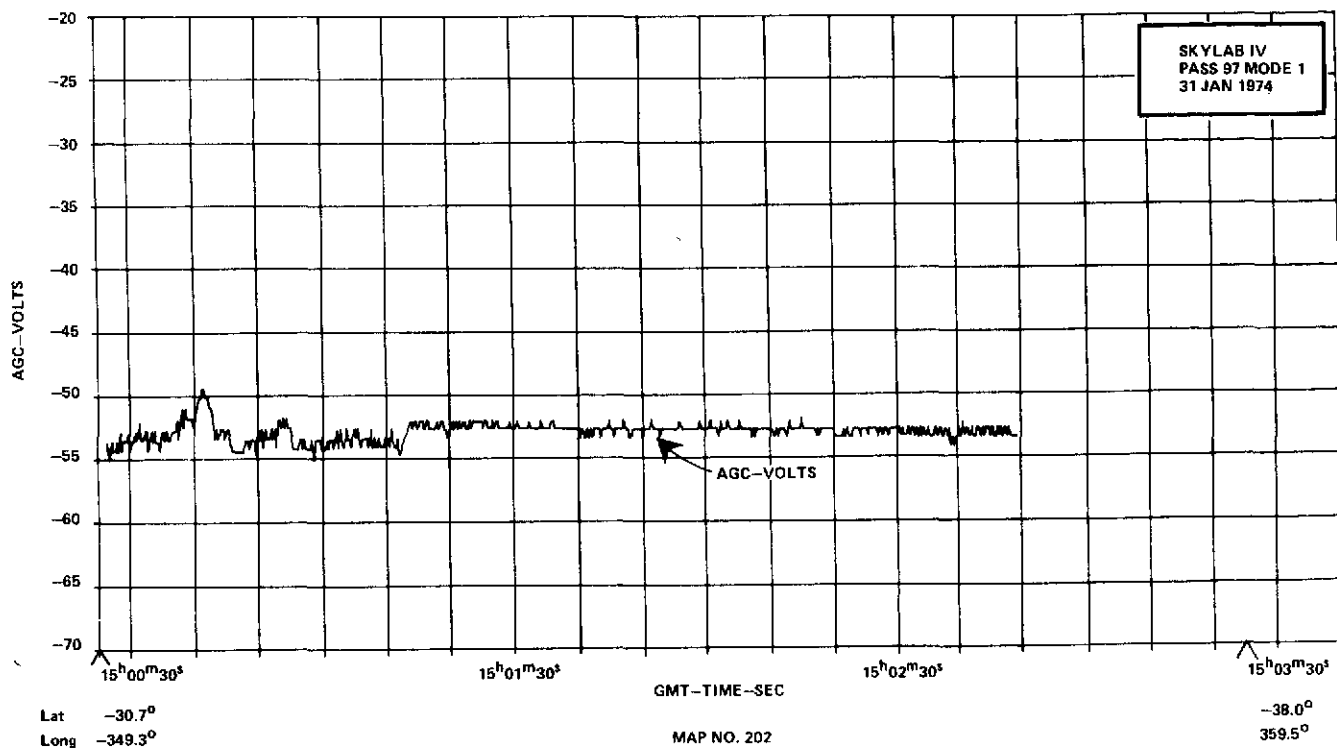


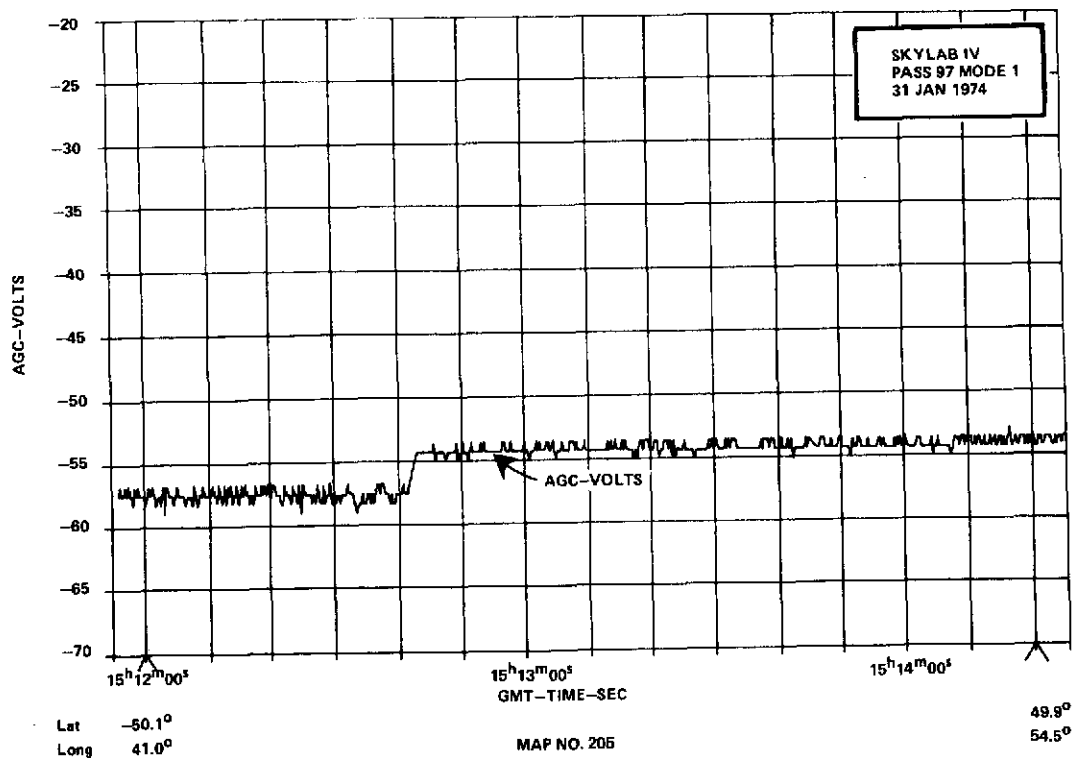
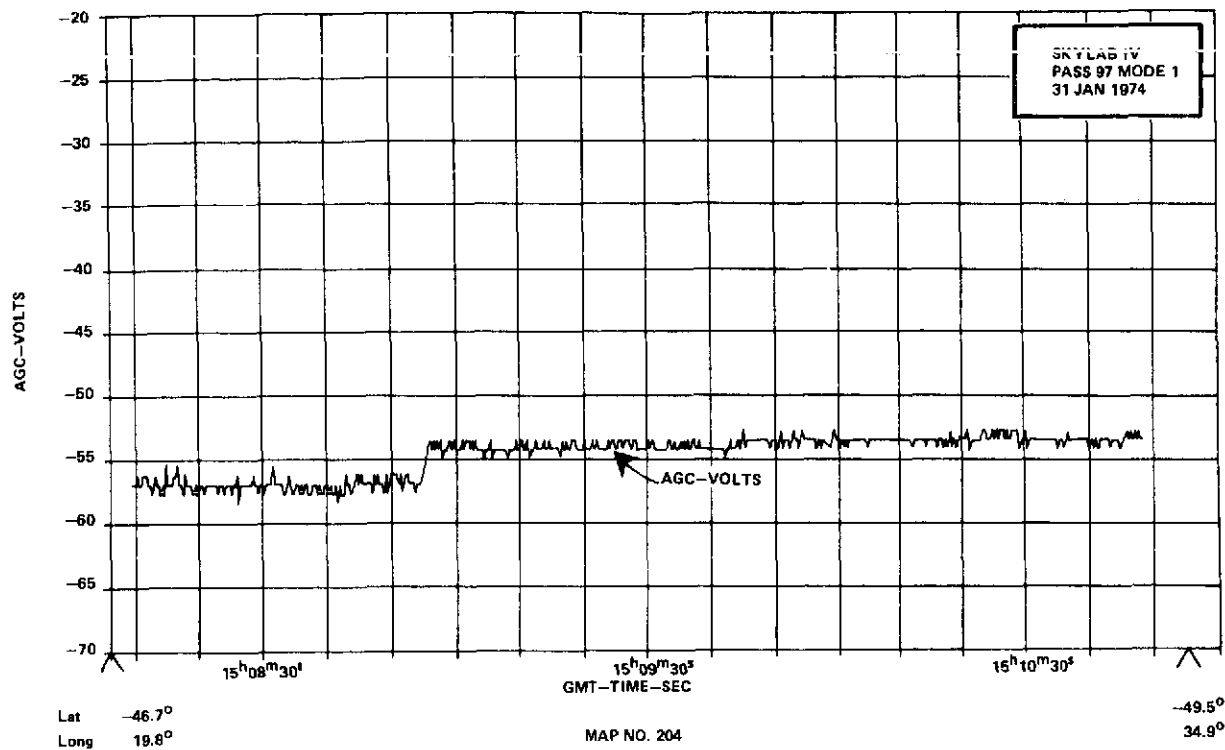


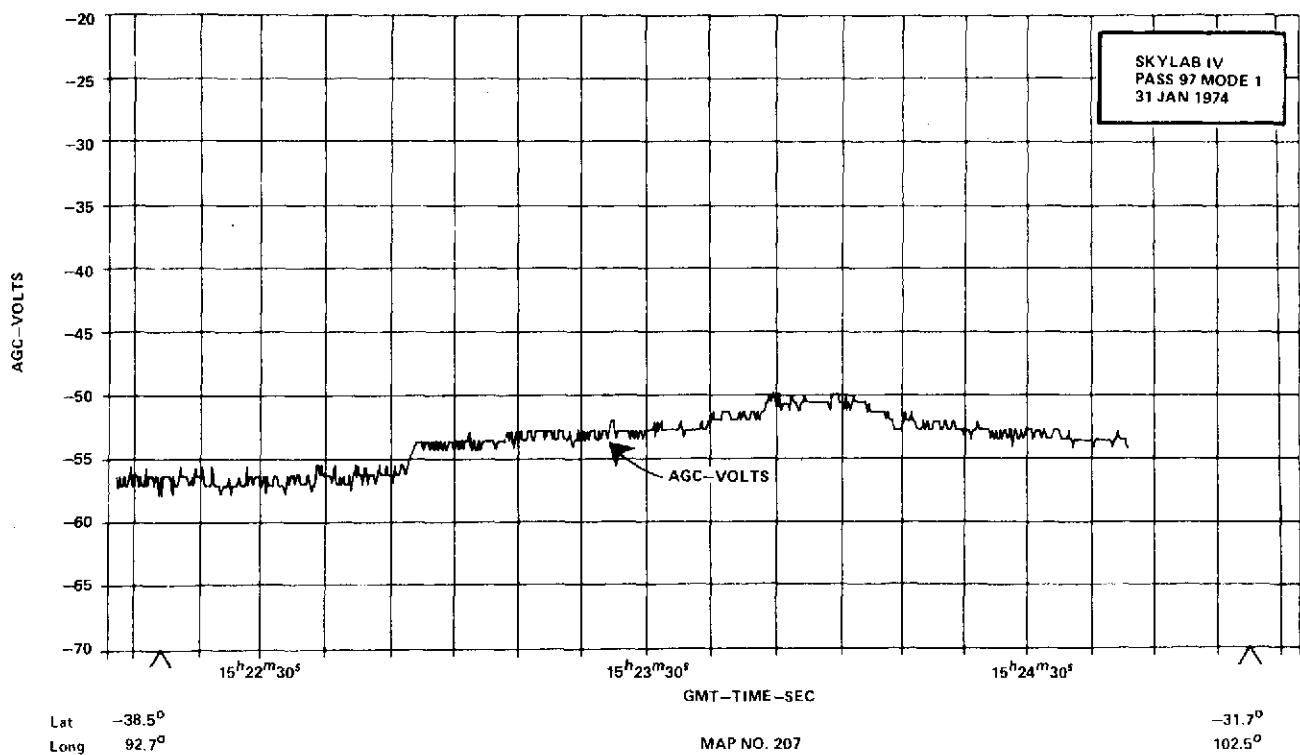
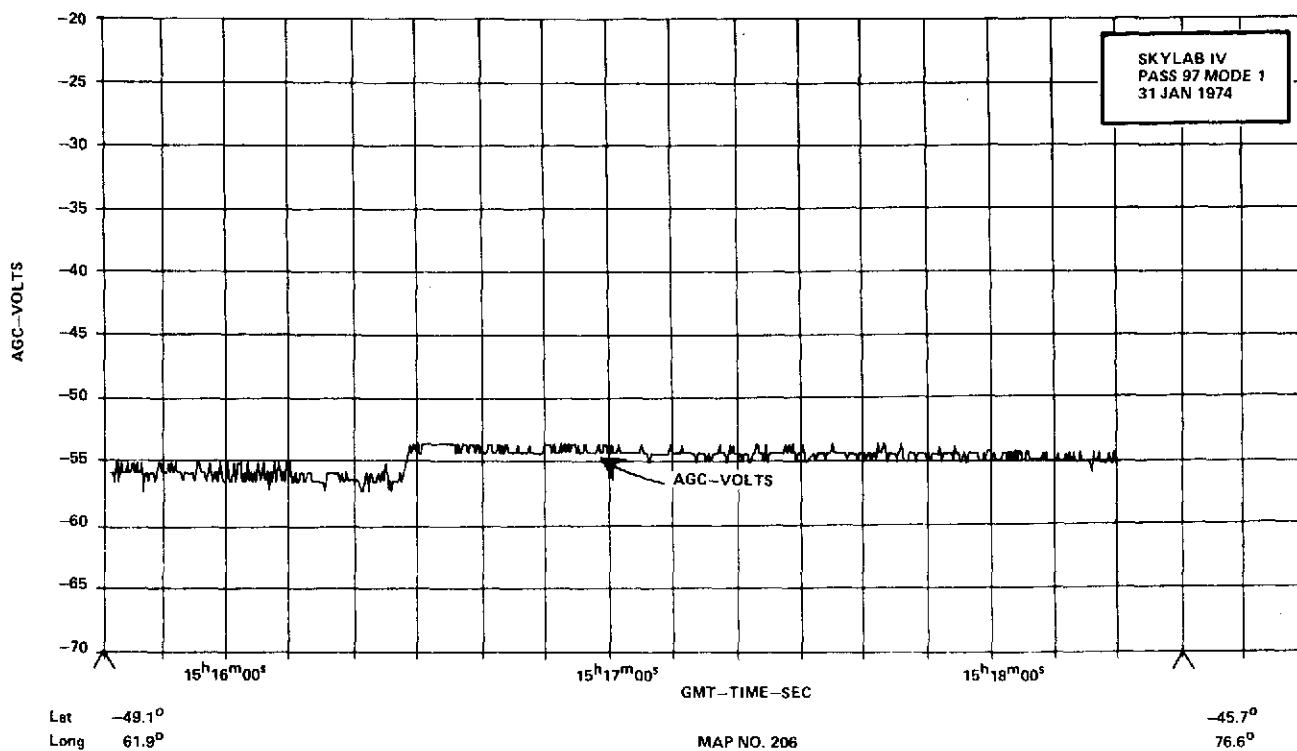


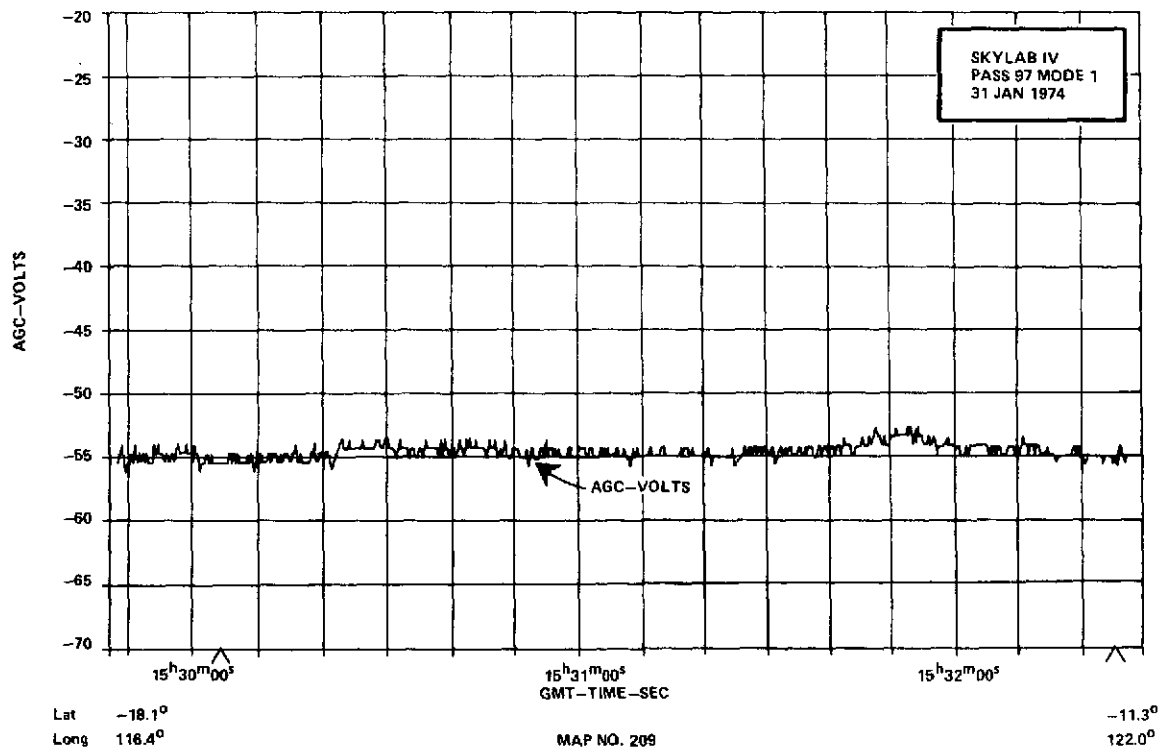
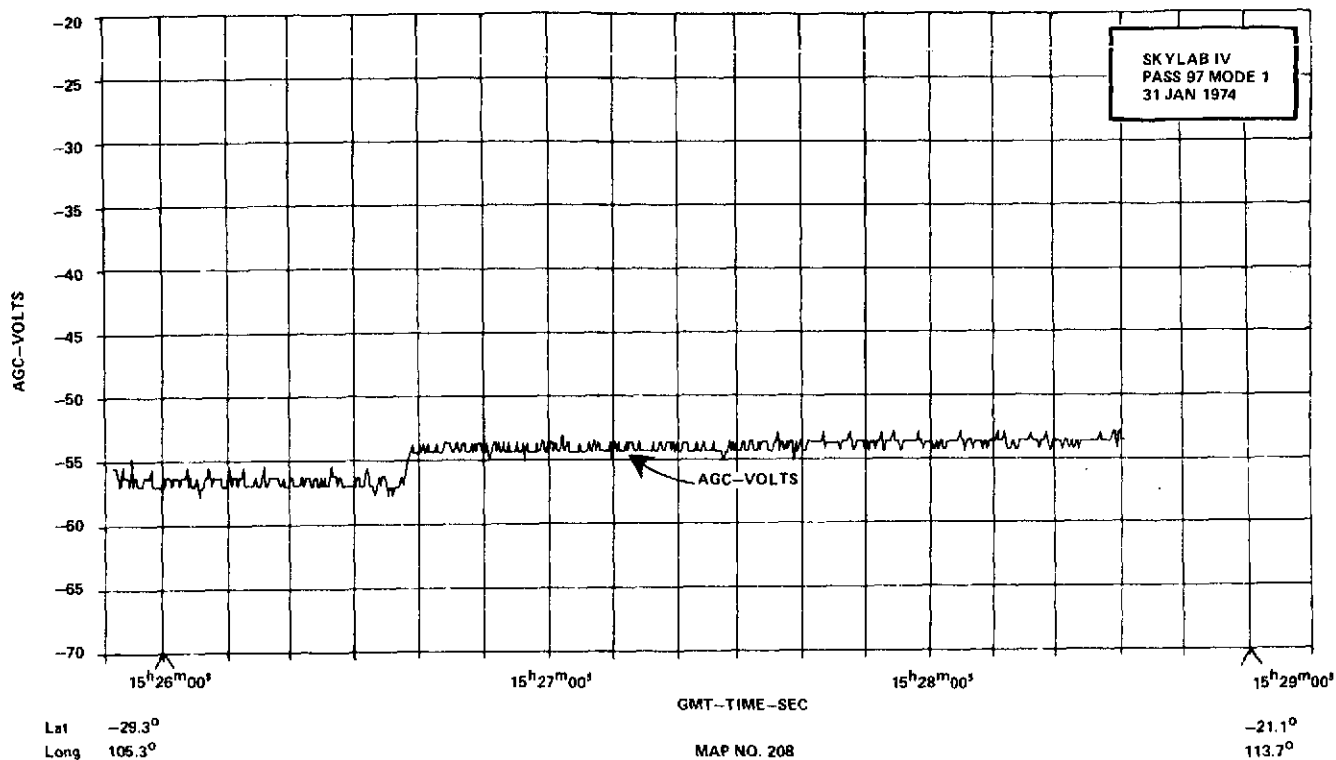


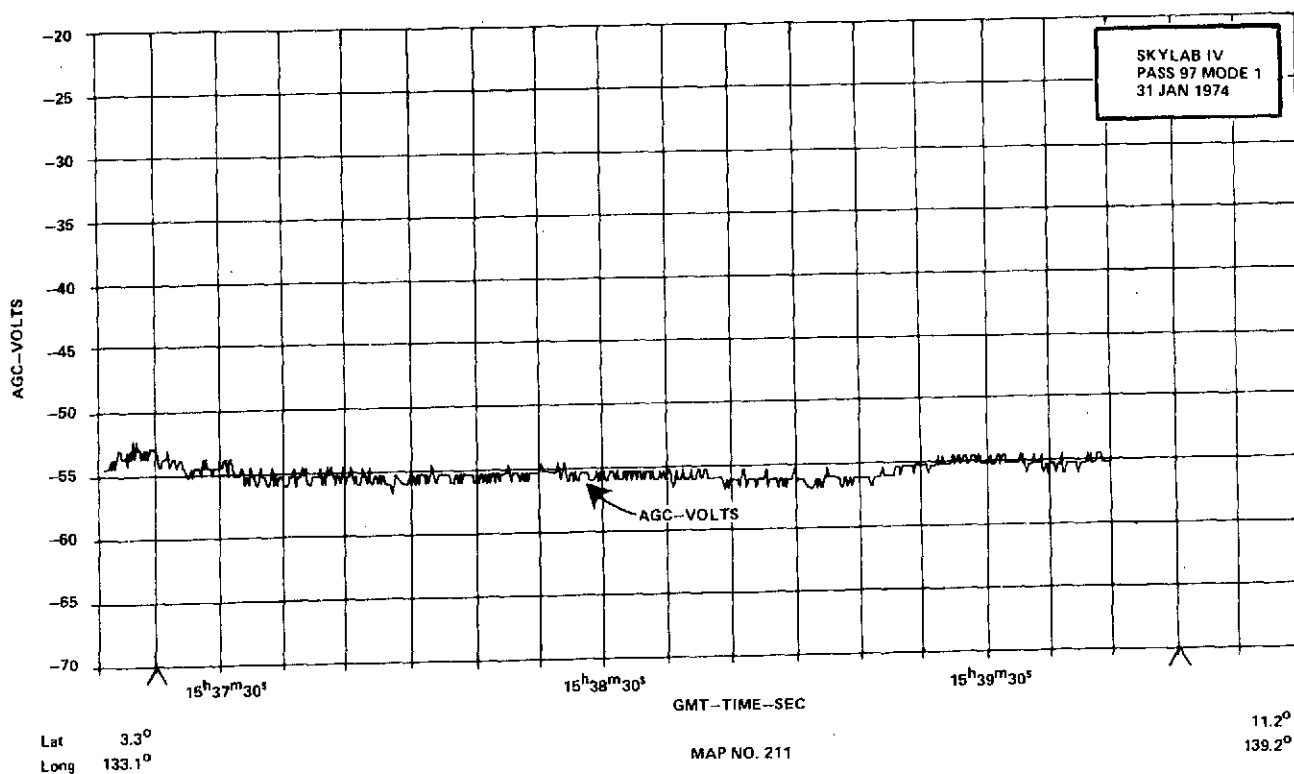
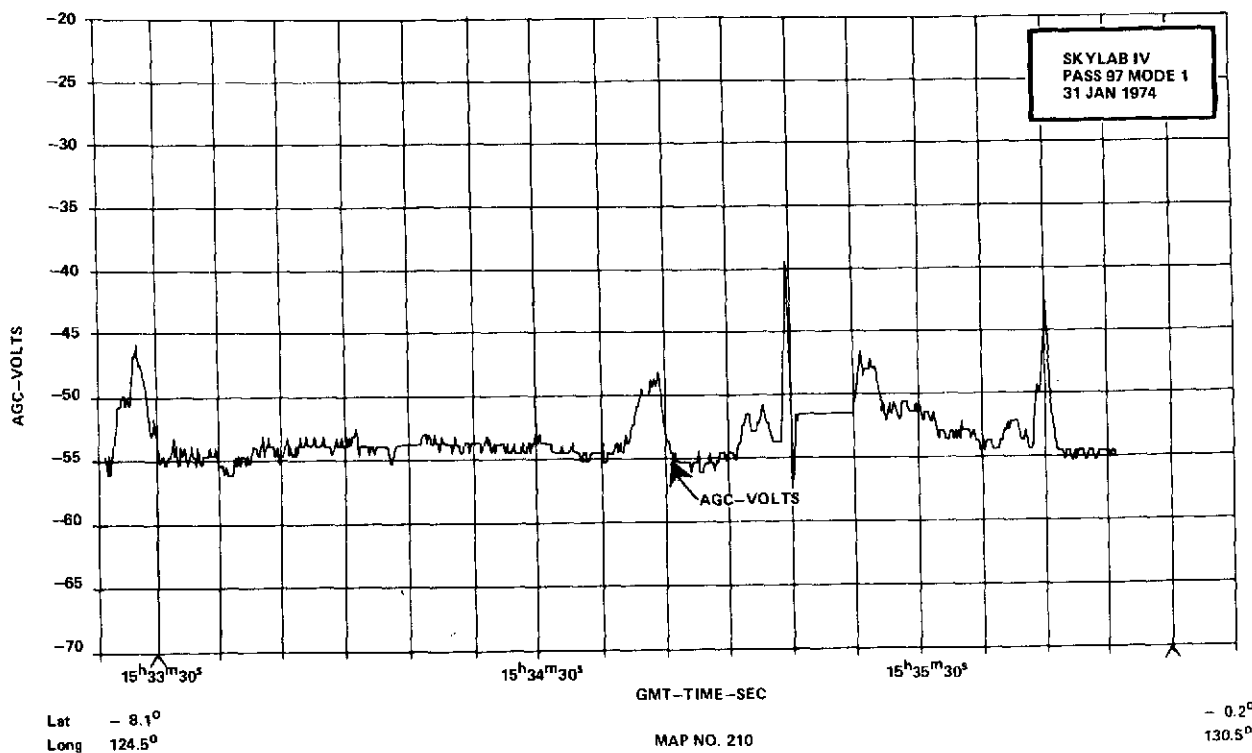


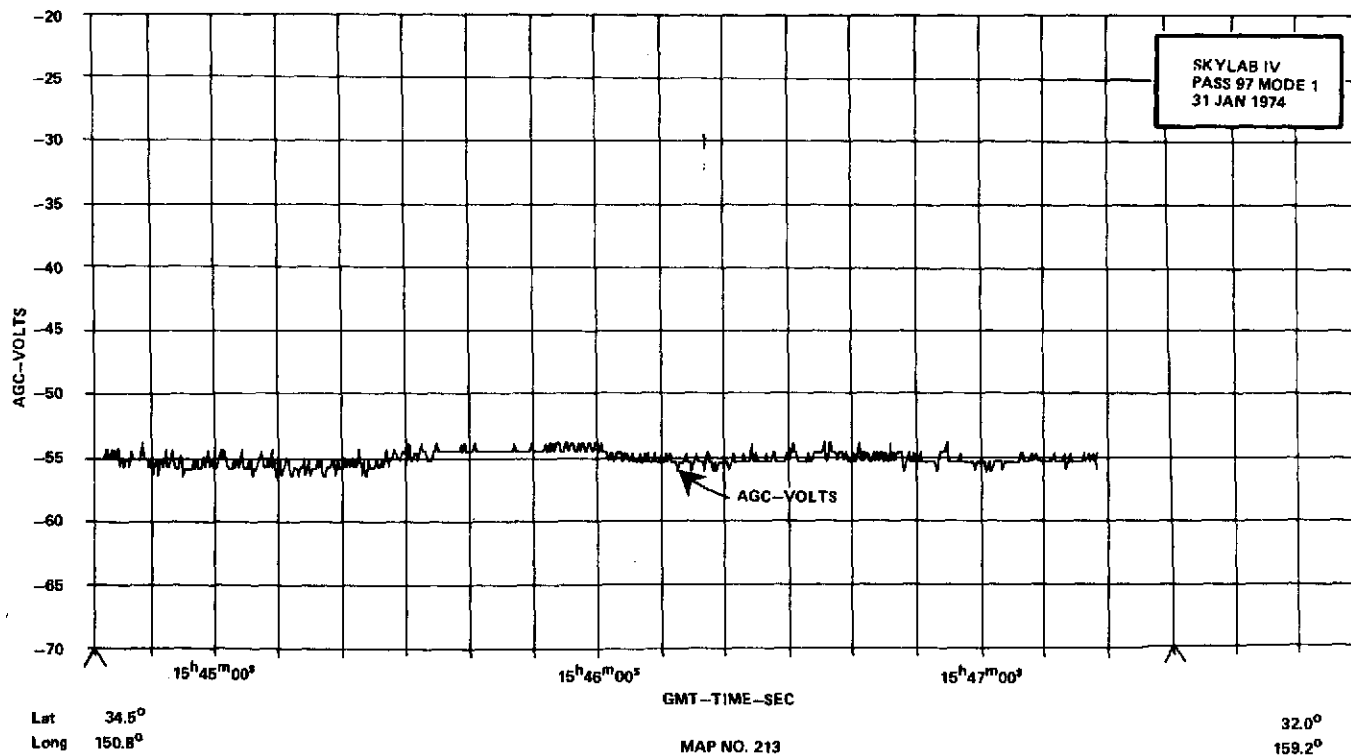
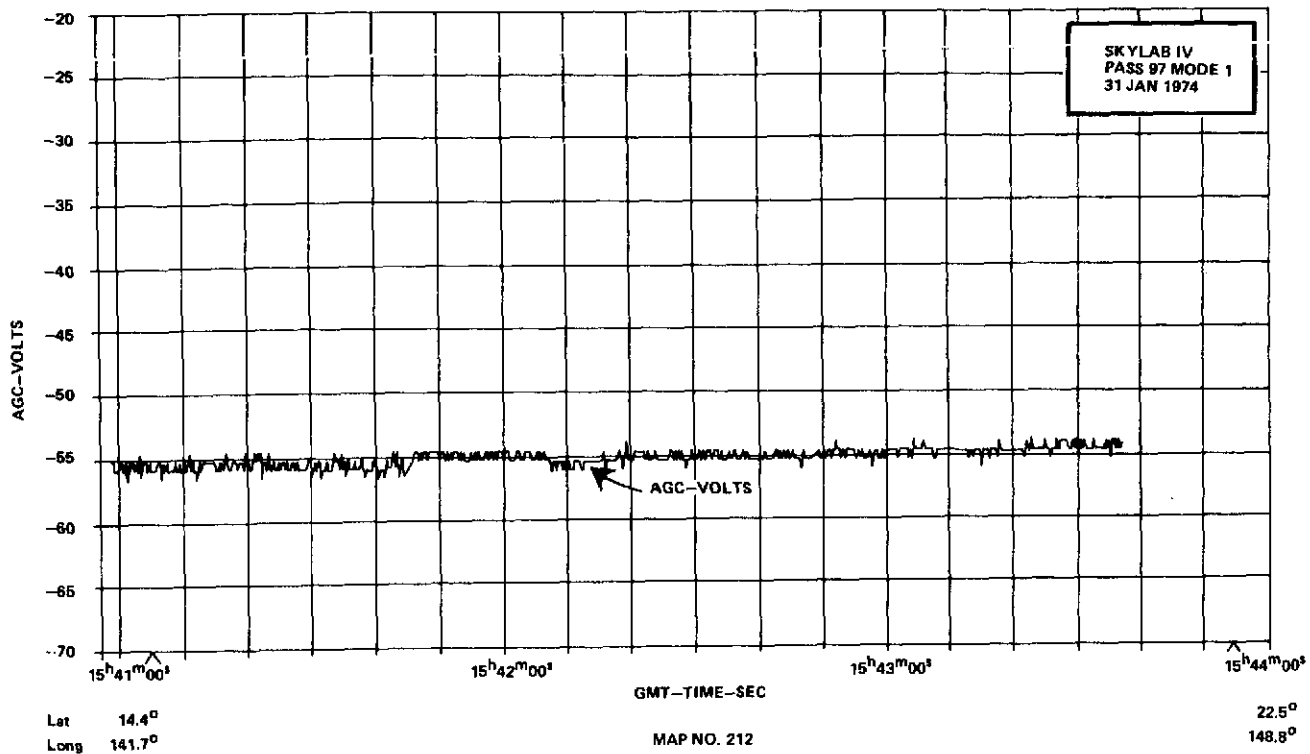


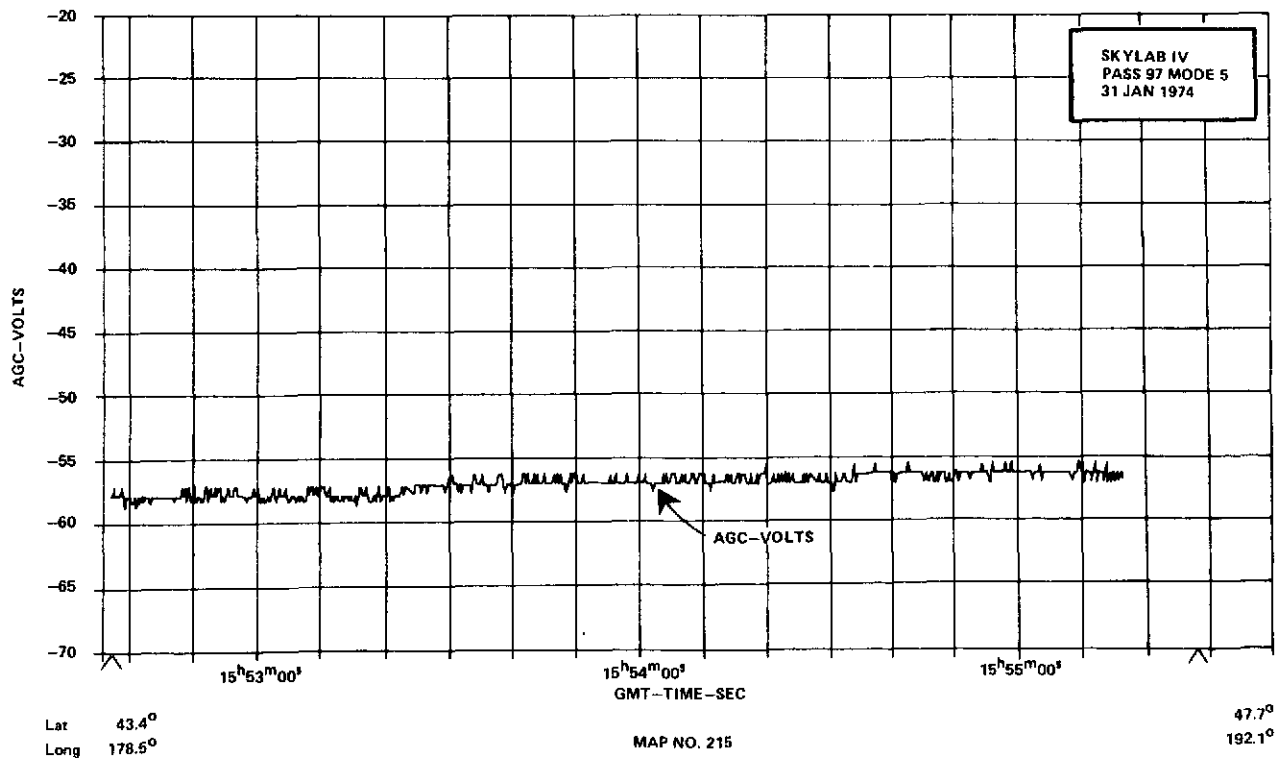
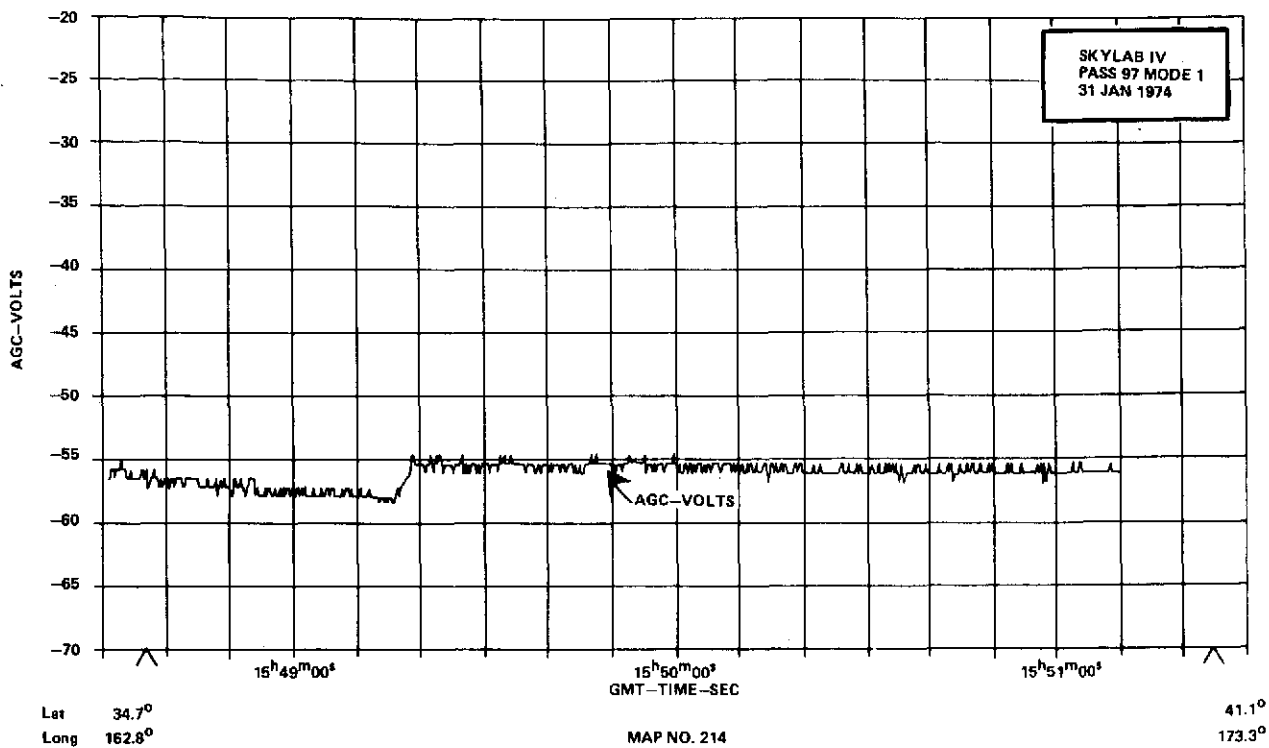


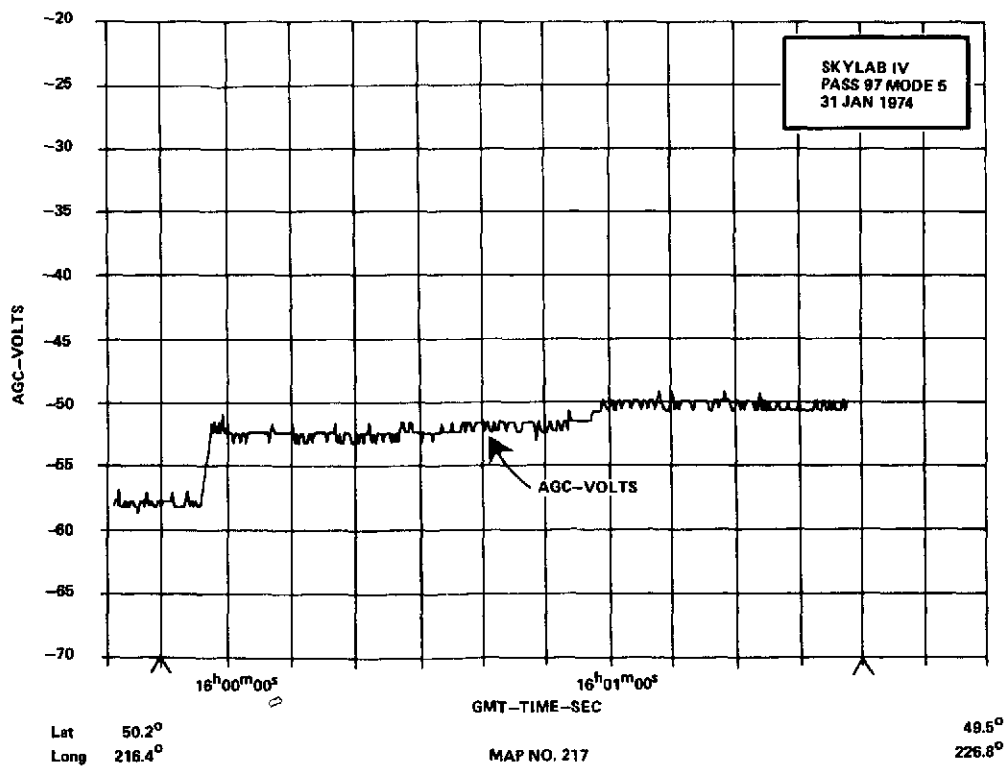
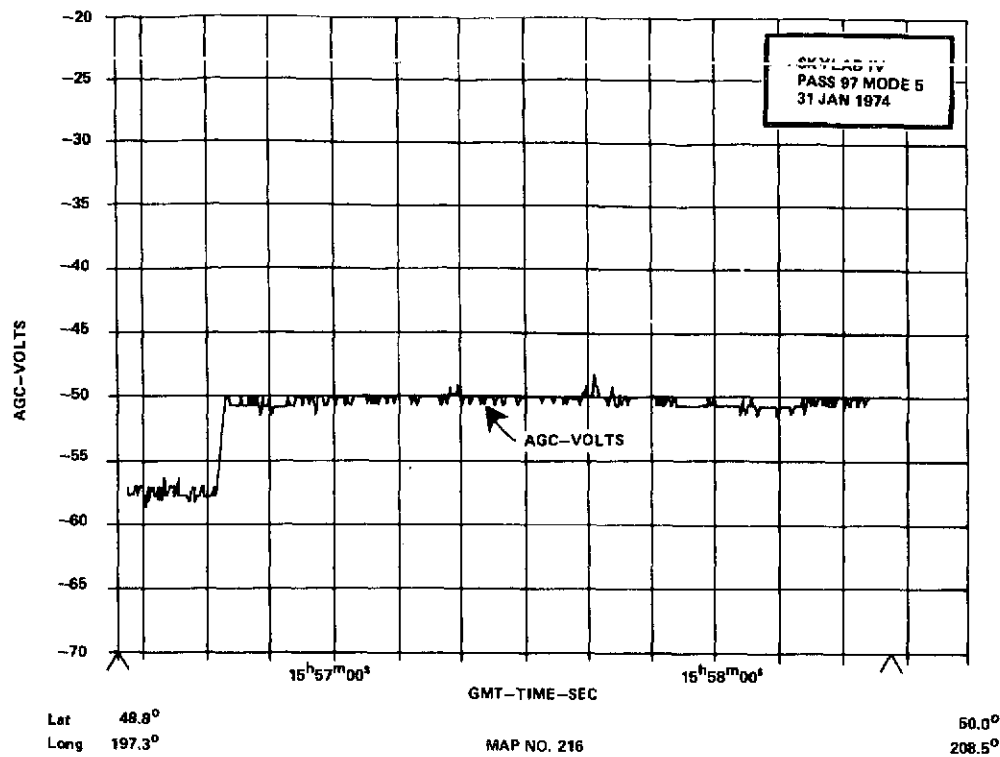


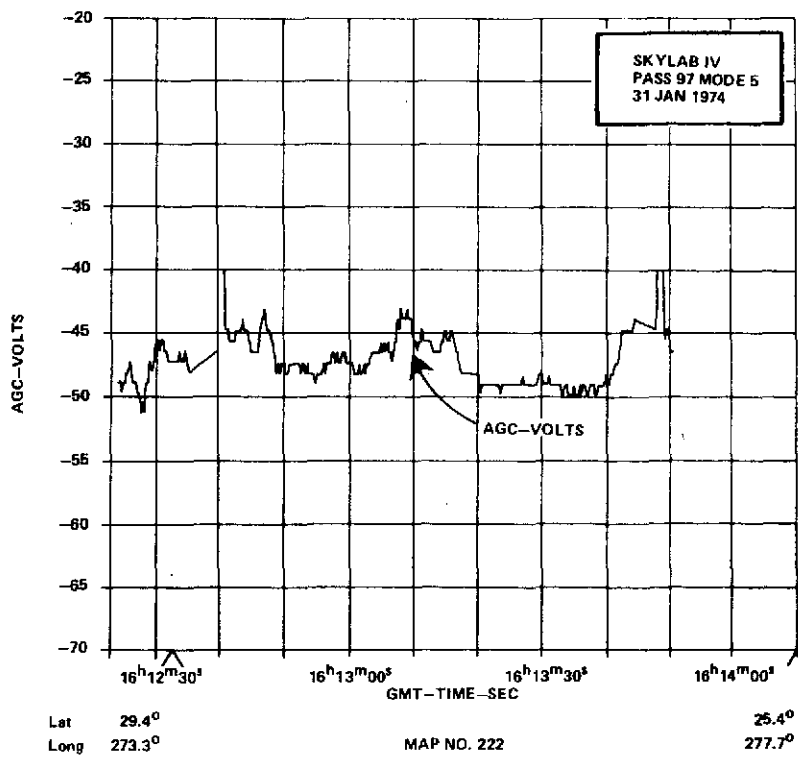
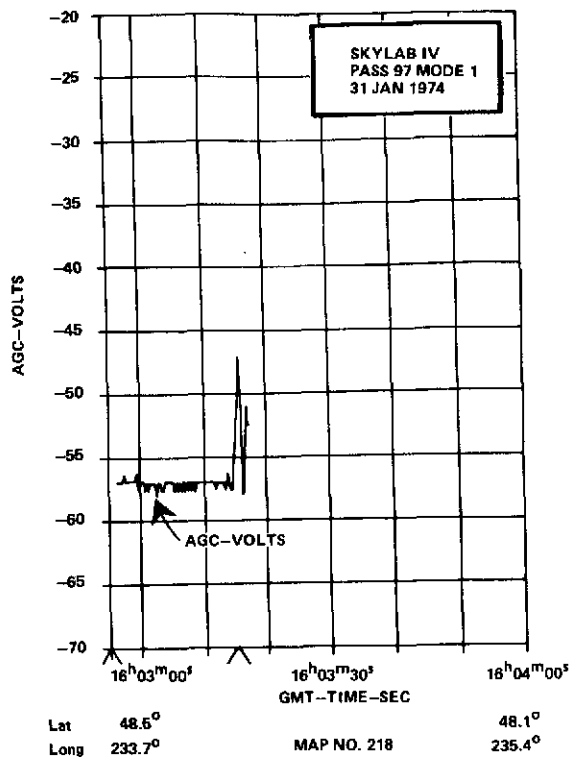


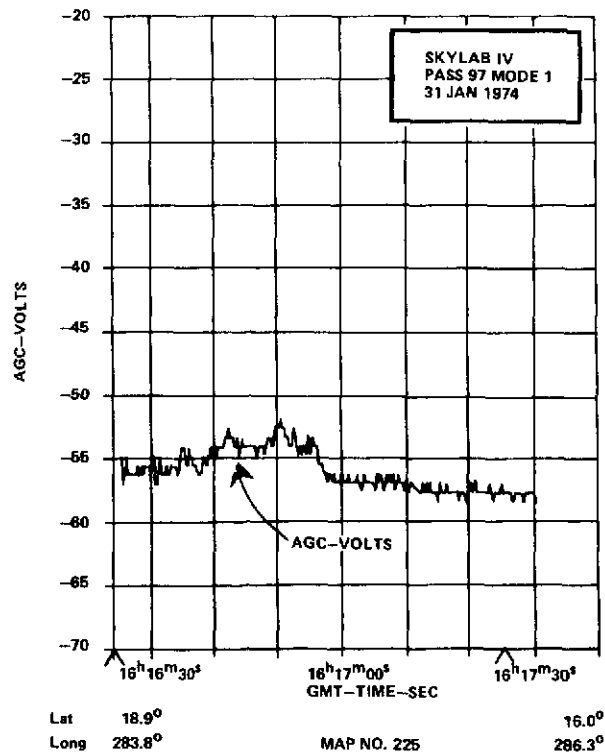
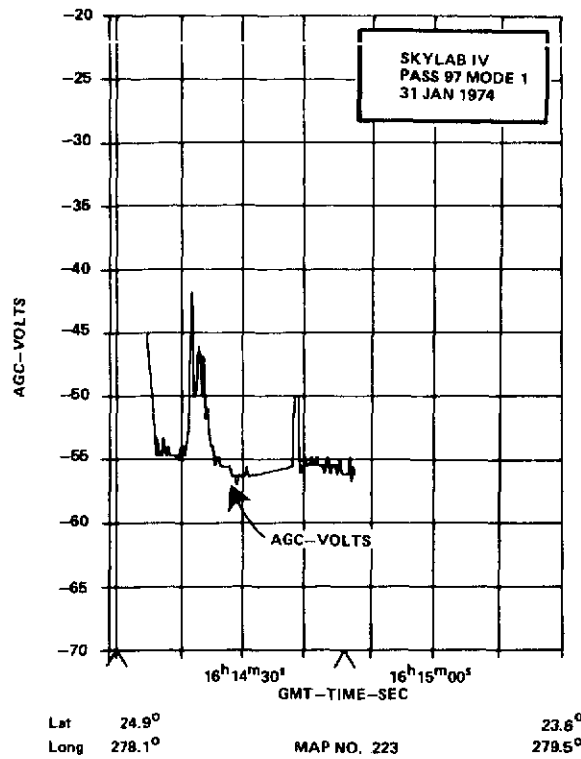


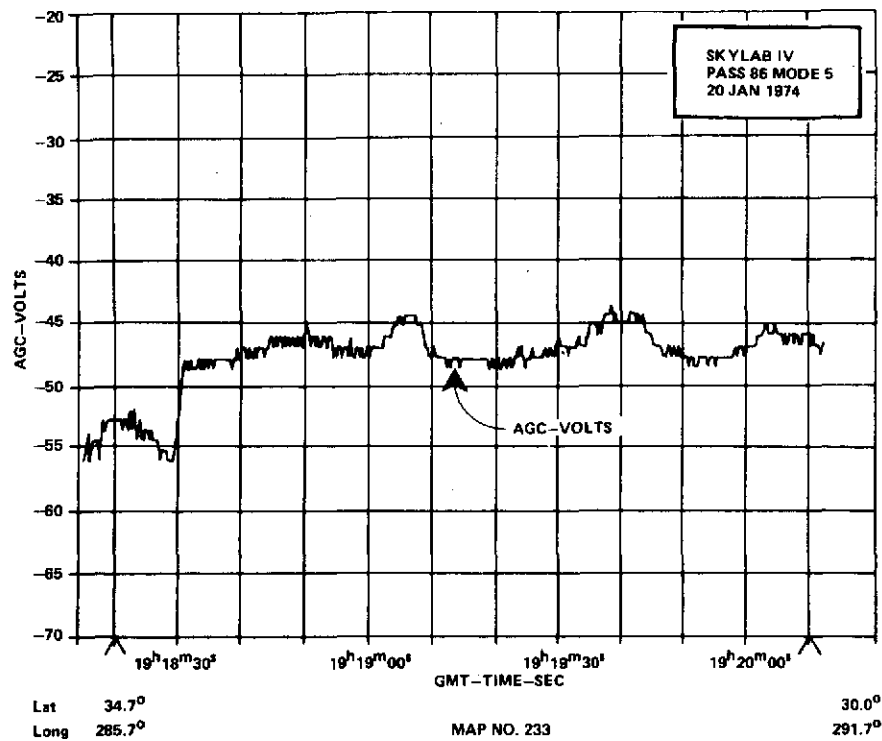
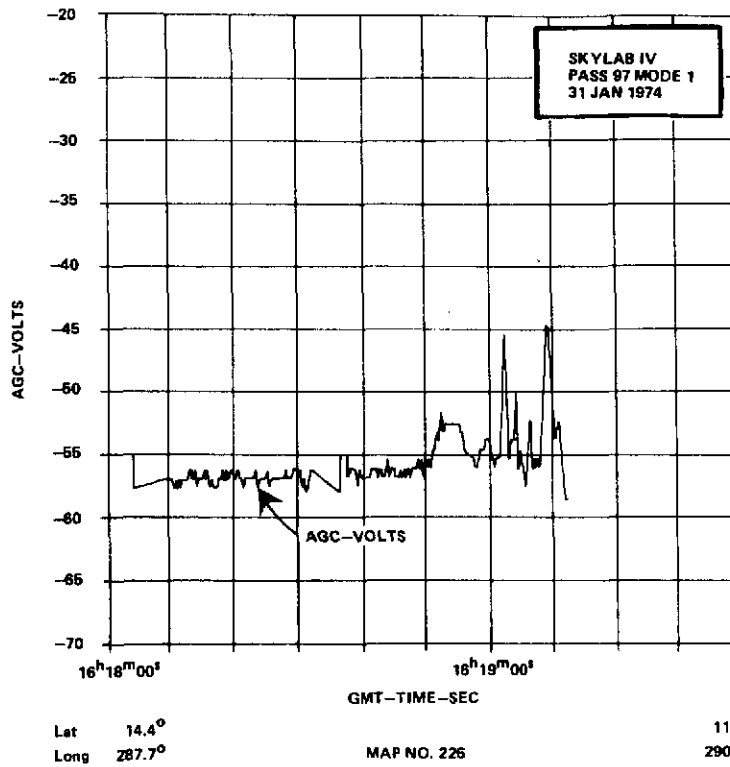












APPLICATIONS

This section contains some typical ways in which the height data can be utilized. These applications are not intended to be a complete set but are supplied as examples of uses that are readily apparent.

PRECEDING PAGE BLANK NOT FILMED

Correlation with Ocean Floor Topography

During the early phase of the SKYLAB program, the data recorded in the overwater passes off Charleston, S.C., showed abrupt changes in mean sea level which were not immediately obvious in existing geoidal data. Map No. 3 illustrates this effect. Note the 8 meter change which occurs near time $17^h 12^m 22^s$, also note the Marsh-Vincent geoidal contour. The geoidal data available for use was computed using a $1^\circ \times 1^\circ$ grid. Therefore, to place the altimeter and geoid contours on a comparative basis, the altimeter data was smoothed beyond that required for minimum-mean square error considerations and to a degree which simulates a $1^\circ \times 1^\circ$ resolution. One can easily see that the altimeter has the resolution to detect features that are caused by local topography [9]. Therefore, the altimeter can be used to determine when, where and how to consider local topography in geoid models. In this manner, a large quantity of topographic data can be utilized to improve immediately the resolution of the geoid and might later be used to fill in gaps between satellite altimeter geoid measurements. In addition, in areas where the topography is not well known, the altimeter could contribute to the improved mapping of these features.

Geological Structure

The underwater topography doesn't always correlate with the altimeter measured ocean topography. In fact, since the equipotential gravity field is being measured, the sub-surface structure can cause the surface topography to vary significantly from the sub-surface topography. This effect has been seen off the east coast of the United States and in the Gulf of Mexico.

These areas and similar ones can be geologically important for plate tectonics and geological age studies. In areas where the structure is unknown the altimeter data can be used to test an inferred structure model.

Current Detection

All three parameters (height, waveforms and radar-cross-section) measured by radar altimeters are important for the sensing of currents [2]. The slope of the sea surface perpendicular to the flow for north-south currents should be detectable in the altitude data. The Gulf Stream, for example, has a rise of 1 meter over distances of 50 to 100 km.

Long Arc Analysis

Most of the SKYLAB altimeter missions consisted of two or three individual mode operations per pass. However, one long arc mission was conducted as a climax to the altimetry experiment. This long arc (approximately one revolution, or approximately 35,000 km) pass of radar altimeter data has provided a new comparison for long wavelength features of geoids determined from existing gravity fields and new instrumentation technology for satellite altimetry.

Since the SKYLAB instrument [1,2], [4] and [7] was designed to operate in short, pre-determined modes that sequence through a routine of data taking, calibration, and automatic turn off. Therefore, the mission had to be run in a series of short arcs. For that reason the data obtained contains gaps where tracking is re-initialized. The revolution was chosen to maximize tracking coverage (to obtain good orbit determination) and to minimize overland data. However, there was a section of the pass over the United States that created an additional data gap.

The S-193 SKYLAB radar altimeter was operated in a round-the-world pass on January 31, 1974 over a ground track starting off the coast of Brazil and ending in the Caribbean Sea (figure 15). The rationale in planning this mission was that the long arc would test the instrument stability over a longer time interval and would provide an independent test of existing gravity models.

Figure 16 presents a geoid profile based upon the global altimeter pass along with detailed geoid profiles computed using the SAO-3 [10], OSU [11], and GEM-6 [8] models. For cross referencing the more detailed individual short arc altimeter residual plots, the map numbers are included in the figure. The overall level of agreement is exceptional. It should be emphasized that no adjustment of scale has been made to the altimeter for this comparison. This indicates that the altimeter geoid not only agrees well in general shape, but also it is evidently well calibrated in scale.

Previous analyses have demonstrated that the satellite altimeter could measure high frequency undulations of the geoid such as the Puerto Rico trench and sea mounts [2,12]. This around-the-world pass shows potential for measuring intermediate and low frequency geoid undulations. In addition, it can be seen that a long arc might have advantages in determining altimeter bias or for detecting trending. For future satellites where long arcs will be more prevalent, tracking coverage will almost certainly be poorly distributed for some passes. Therefore, extreme care should be used in building orbits for these passes, e.g. using altimeter data in the orbit solution. Perhaps the pass will have to be broken into a series of short arcs using a optimum set of stations for each short arc.

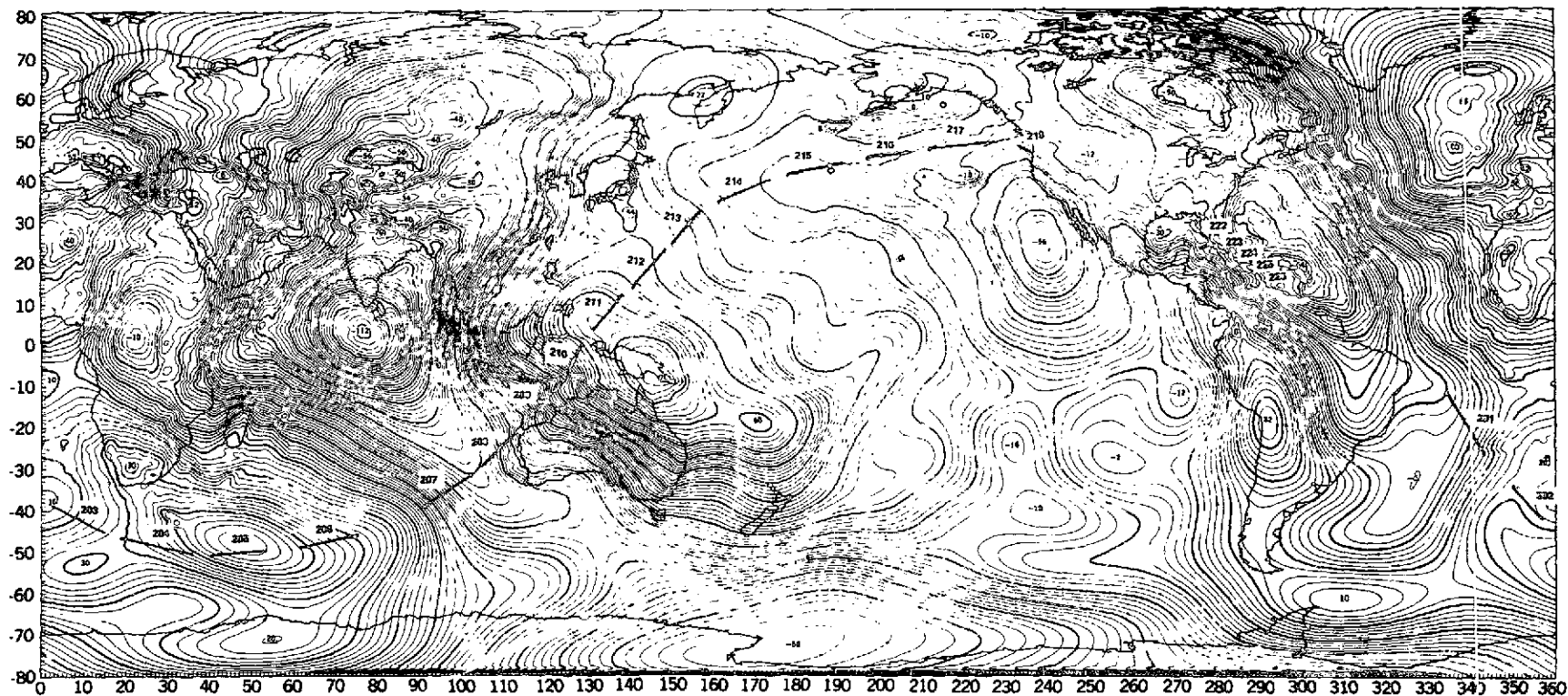


FIGURE 15. ROUND-THE-WORLD GROUND TRACK STARTING OFF THE COAST OF BRAZIL
AND ENDING IN THE CARIBBEAN SEA

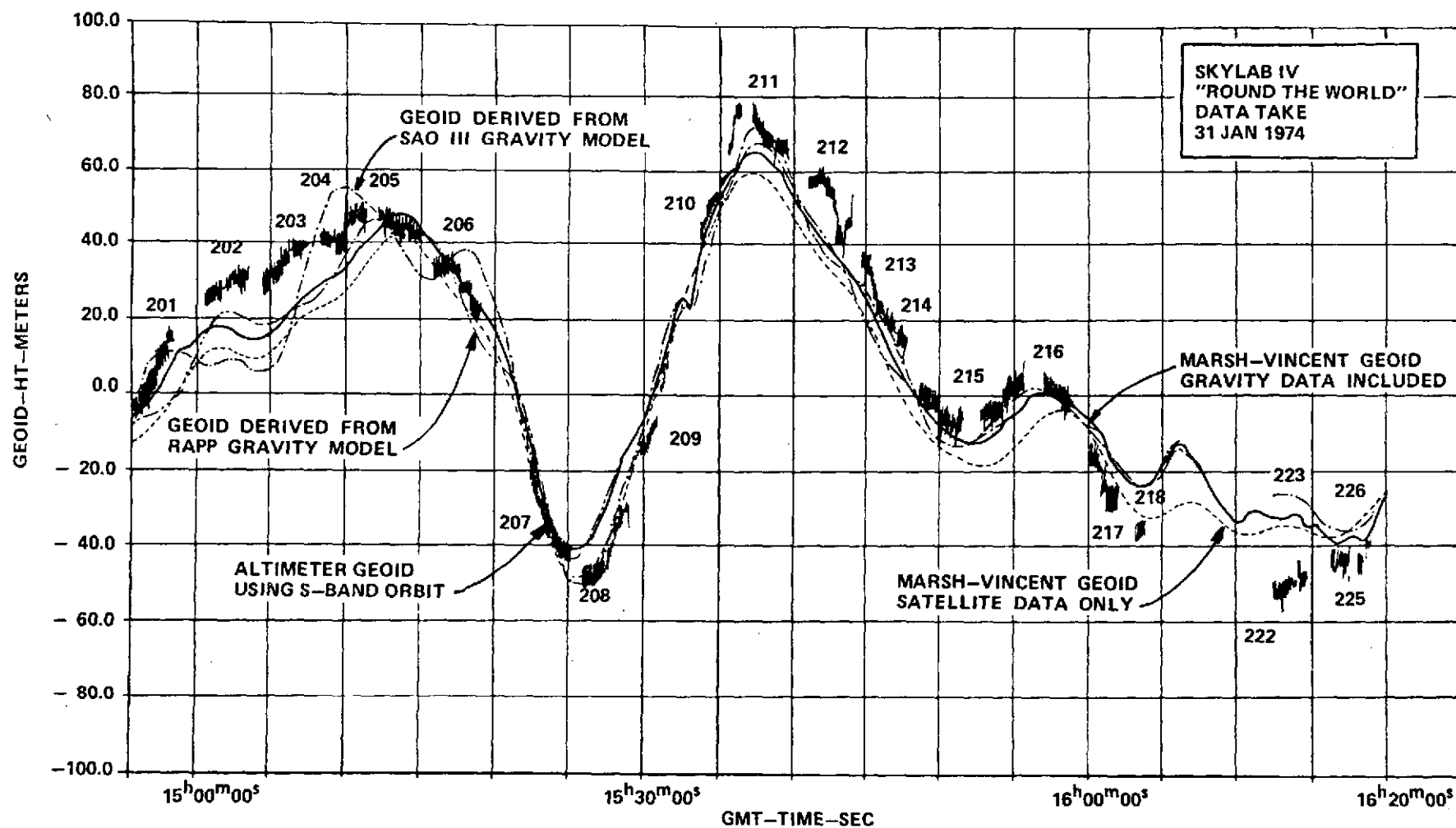


FIGURE 16. "ROUND THE WORLD" DATA TAKE

Geoid Construction

To construct a geoid from altimeter data, several techniques can be employed. The most obvious one would be to assemble the data from numerous passes and apply an interpolation scheme between the data to form a continuous topographic contour map. These contours should form the geoid. Some examples of such a geoid are shown in Figures 16 and 17. The problem in using this technique is that the geoid is very dependent on the absolute accuracy of the orbit. The ground tracks and altimeter geoid values used are shown in Figures 18 and 19, respectively.

Another way would be to lace high density altimeter data together as shown in Figure 20. In this method the altimeter data is constrained to tie-in with itself at regular intervals, and the geoid determined only depends on the orbit shape being accurate over short arcs (the interval length). The geoid constructed in this manner should be shaped correctly but might have an overall bias.

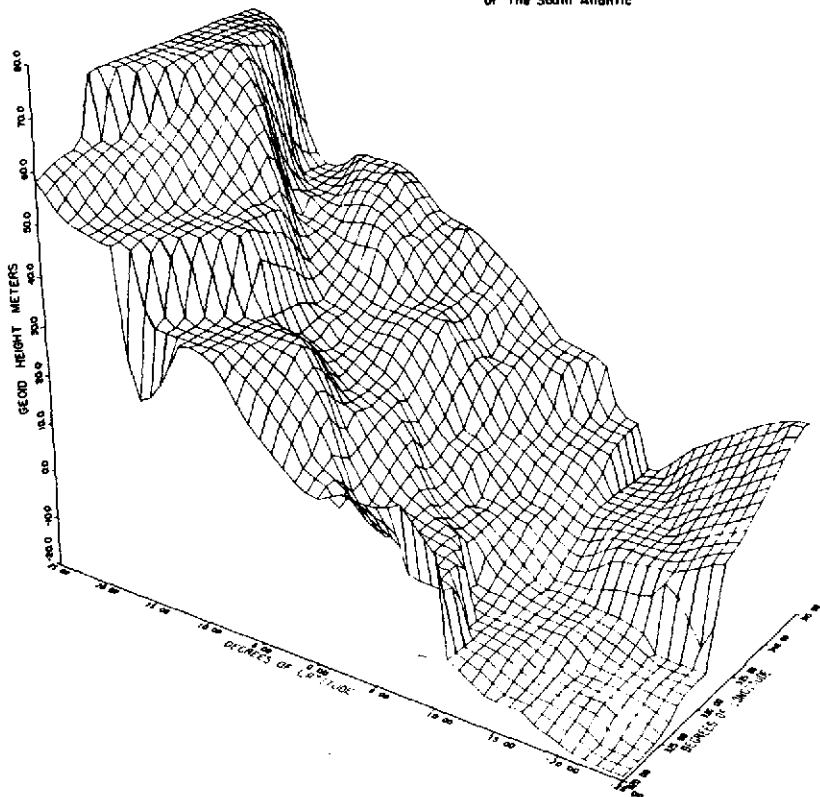
Perhaps some combination of these methods would be superior to either. In addition, one might consider using underwater topography and geological structure to improve this interpolation between the altimeter data passes.

To assess the quality of the geoid constructed, independent altimeter passes over the geoid can be used to test the shape, and a histogram of absolute heights over various grid areas will help establish the repeatability. The absolute accuracy will have to be measured in areas where a high confidence in the absolute height of the ocean surface and the orbit height can be established.

PRECEDING PAGE BLANK NOT FILMED

ORIGINAL PAGE IS
OF POOR QUALITY

SKYLAB ALTIMETER GEOD
of The South Atlantic



GEM 6 GEOD
of The South Atlantic

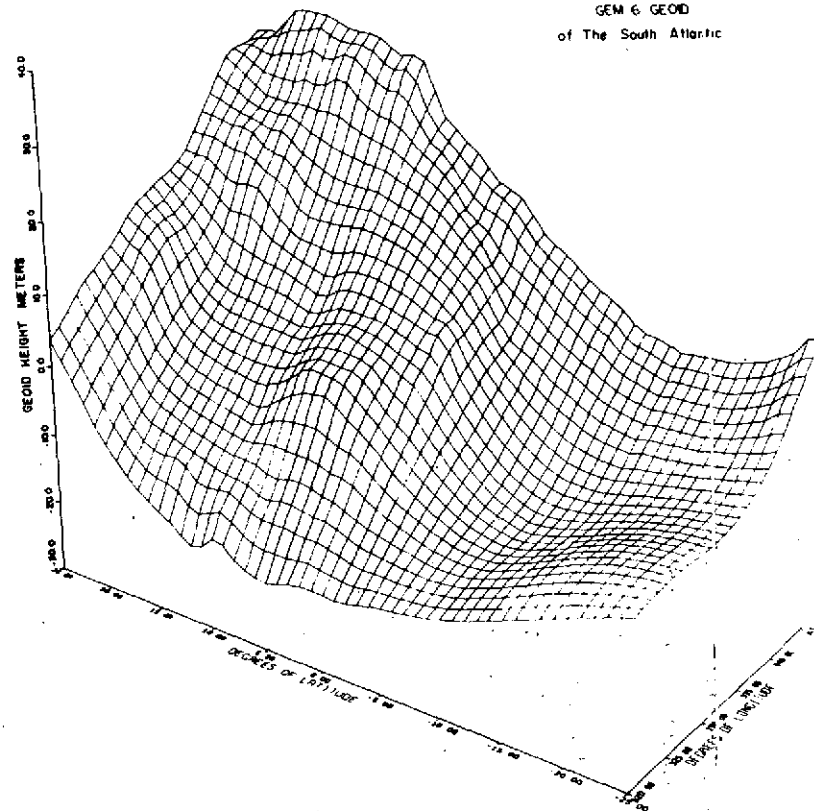


FIGURE 17. SKYLAB ALTIMETER GEOD AND GEM-6 GEOD OF THE SOUTH ATLANTIC

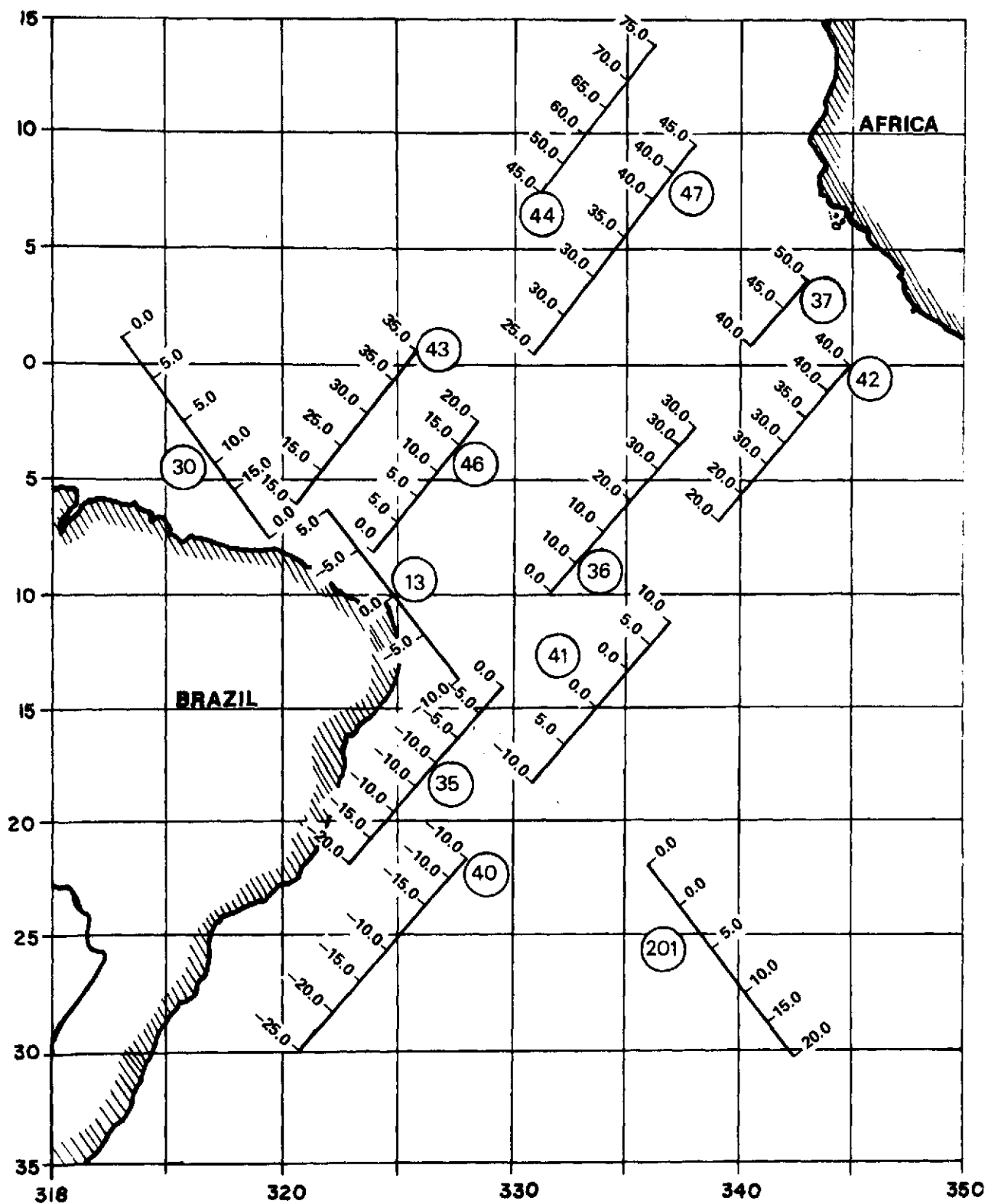


FIGURE 18. GROUND TRACKS AND ALTIMETER GEOID VALUES USED FOR DETERMINATION OF ALTIMETER GEOID FOR SOUTH ATLANTIC AREA

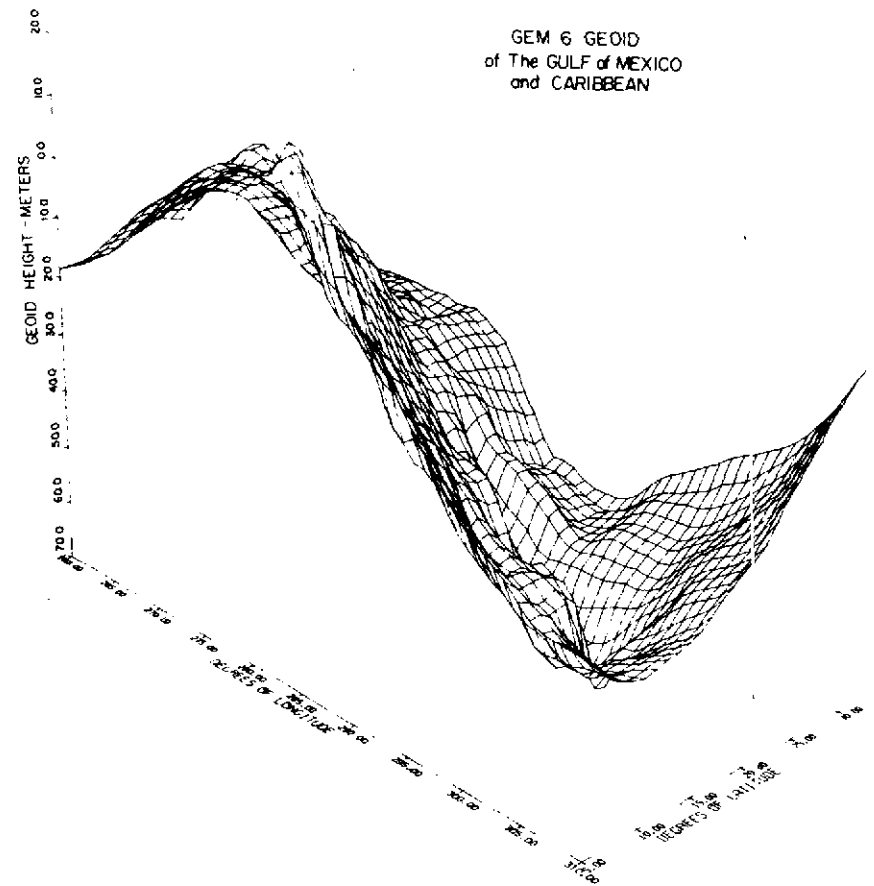
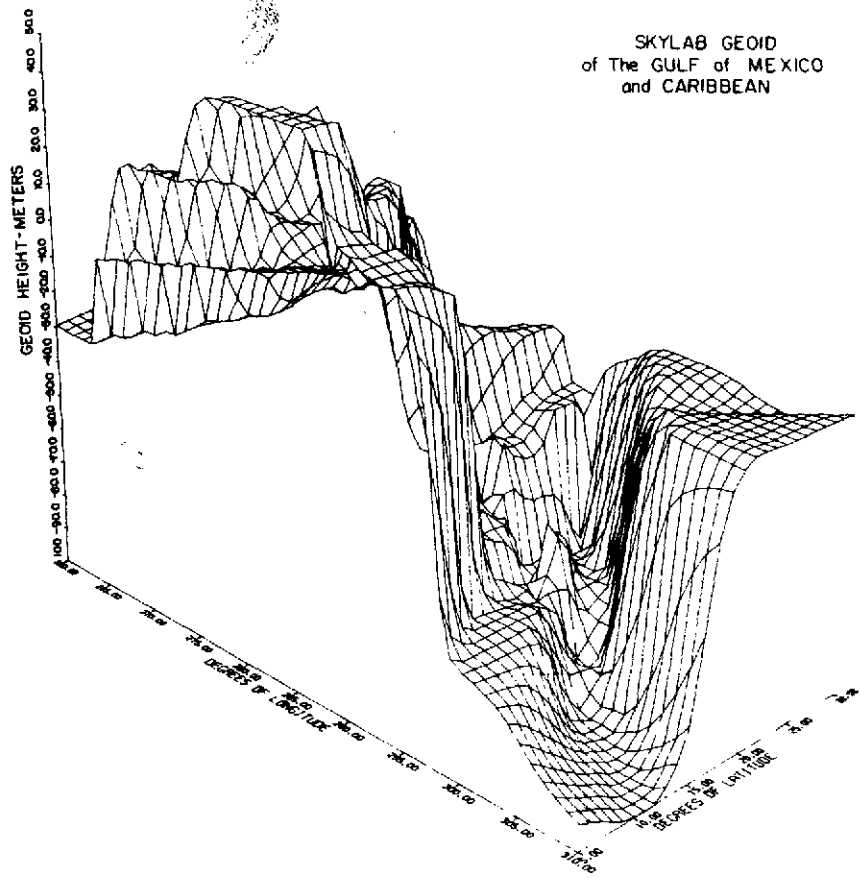


FIGURE 19. SKYLAB GEOID AND GEM-6 GEOID OF THE GULF OF MEXICO AND CARIBBEAN

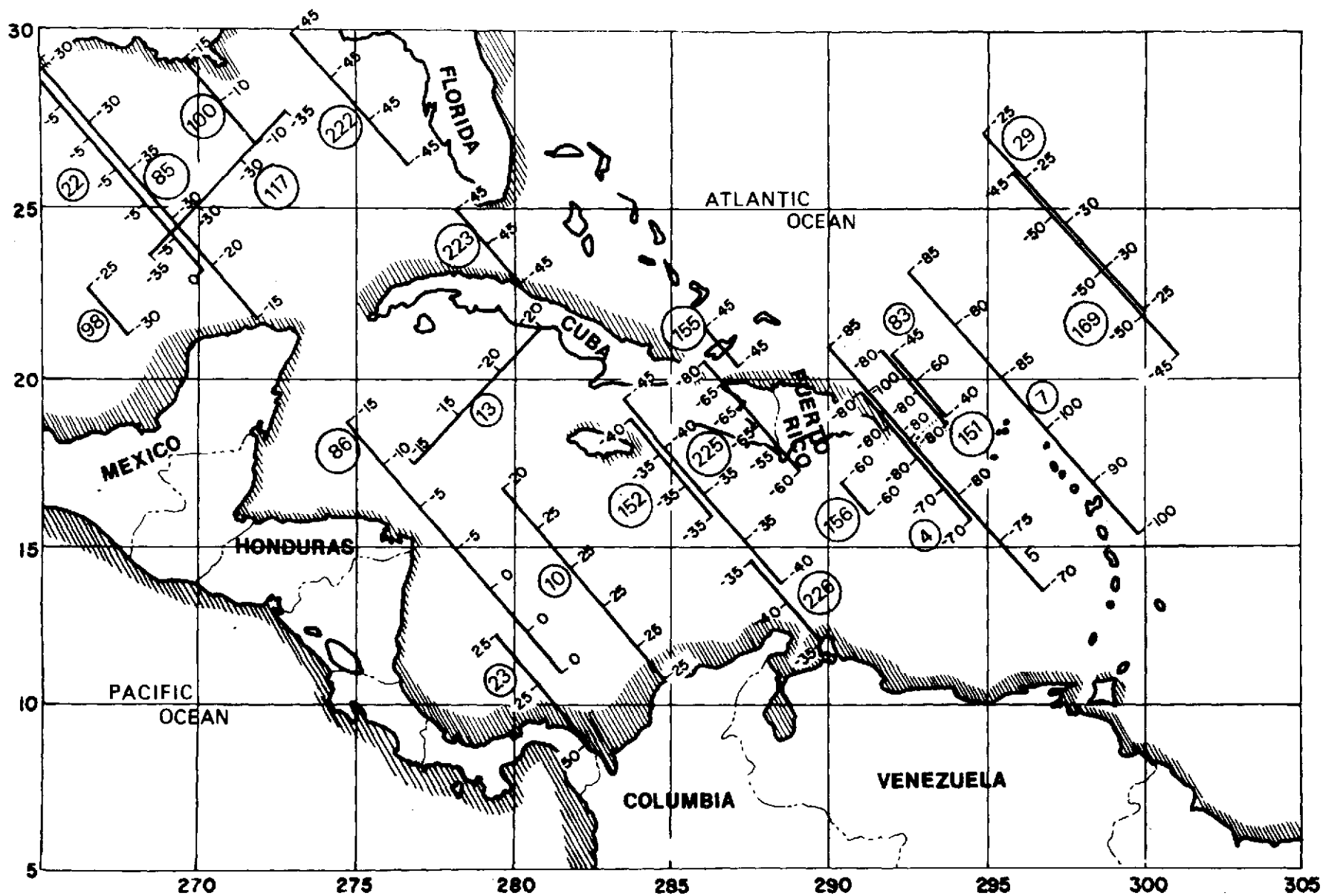


FIGURE 20. GROUND TRACKS AND ALTIMETER GEOID VALUES USED FOR DETERMINATION OF ALTIMETER GEOID FOR GULF OF MEXICO AND CARIBBEAN

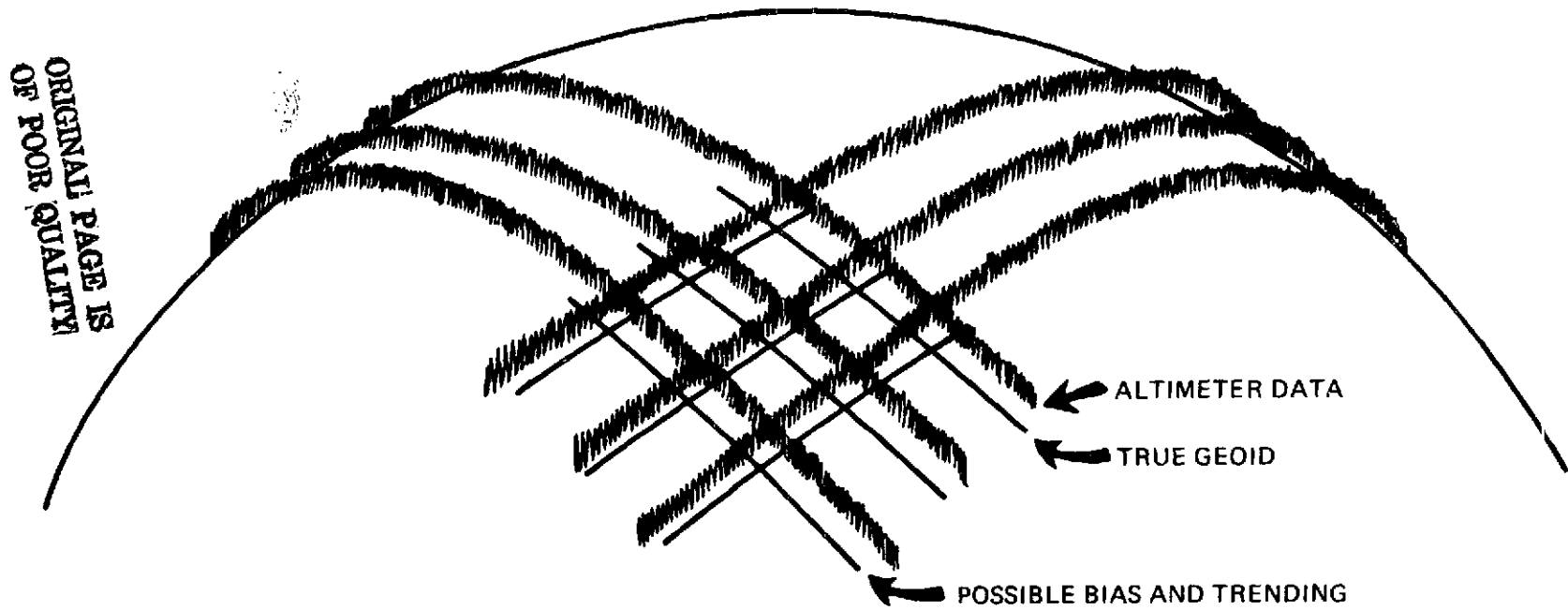


FIGURE 21. GEOID FORMED BY ADJUSTING OVERLAPPING ALTIMETER DATA

Altitude Data Filtering

The plots of altimeter measured geoid heights as a function of time, exhibit a characteristic noisy time series indicative of a typical range servo tracking a signal competing with a noise environment. An estimate of this noise has been calculated to be approximately one meter for data sets when the pointing is good.

Figure 21 displays a power spectral density computed using Fourier Transform methods and a Hanning type window. The altitude data used to compute the spectrum was obtained from SL-2, Pass 4 when the altimeter was passing over the Puerto Rico trench. The arrow corresponds to the density level for which a 3.3 Hz rectangular bandwidth white noise spectrum would yield an rms level of one meter. Since the S-193 tracker has an approximate 3.3 Hz equivalent noise bandwidth, this level is consistent with observed rms noise levels in raw data of one meter [12]. Also note that the spatial filter function [5] arising from the finite zone illuminated by the altimeter corresponds to considerably shorter wavelengths (less than 10 km) and that the calculated PSD should not be contaminated by the altimeter footprint.

The PSD data given may be used to derive altimeter data processing guidelines. Under the assumption of Gaussian statistics, or if a minimum-mean-square linear estimate is desired; the Wiener-Hopf formulation for additive noise measurements shows that the optimum filter $H_o(f)$ transfer function is

$$H_o(f) = \frac{S(f)}{S(f) + N(f)}$$

where $S(f)$ is the geoidal spectrum and $N(f)$ is the additive noise spectrum. As discussed in [13], Kaula's model of one dimensional spectral behavior behaves as f^{-3} . The observed spectrum, $S(f)$, is asymptotic to an approximation of $S(f)$ defined by

$$S(f) = \frac{5.24 \times 10^{-4}}{f^4 + 1.75 \times 10^{-3}},$$

and depicted as a dashed plot in figure 21. Solving for the half-power value of $H_o(f)$, it is found to be 0.164 Hz. Using the satellite ground track velocity, this may be expressed as a 45 km wavelength. Therefore, it is concluded that this analysis shows for geoidal regions which contain pronounced short wavelength components, that (1), the Skylab altimeter is limited by measurement noise in profiling wavelengths much below 45 km and (2), data smoothing time constants of several seconds are required to adequately reduce the random error in geoid undulation measurements. This analysis can readily be extended to yield two-sided weighting functions [14], which are applicable to smoothing solutions using both past and future observations--as is appropriate for digital computations.

Certain applications, like ocean current detection, dictate that the raw altimeter data be filtered prior to looking for the signal, since a one meter change over a 100 km wavelength is of the same order as the noise. Ocean geoid computations in general have the same problem, when short wavelength features are sought. Reference [12] shows that the lowest possible noise reduction is to 30 cm without distorting the data.

Figure 22 shows the filtered altimeter-measured geoid heights for SL-2, Pass 9, Mode 5 using a 41 point, frequency constrained, mid point filter. The altimeter was passing over the Gulf Stream at the time noted (from NOAA 2 IR data). Note the agreement of the high frequency components in the altimeter data with the GEM-6 geoid (calculated with 10 minute by 10 minute mean anomalies.) On the other hand, no distinct ocean surface elevation change is seen in the vicinity of the Gulf Stream. Therefore, one or more of the following are conjectured.

- 1) The instrument is not precise enough for the experiment,
- 2) the ocean geoid is not known well enough,
- 3) repeated data sets are required to extract a signal having such a small amplitude or
- 4) no slope exists when passing over the Gulf Stream.

Since 4 is incorrect, either one or more of the first three reasons explain the lack of obtaining a significant result.

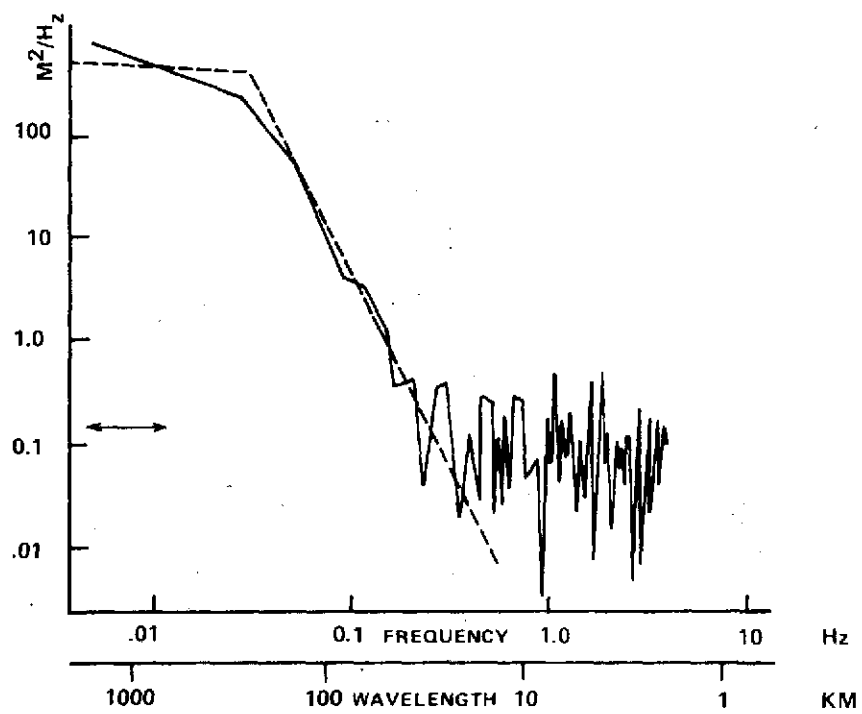


FIGURE 22. POWER SPECTRAL DENSITY COMPUTED USING FOURIER TRANSFORM METHODS AND A HANNING TYPE WINDOW

SKYLAB II
PASS 9 MODE 5
12 JUNE 1973
FILTERED (41 P)

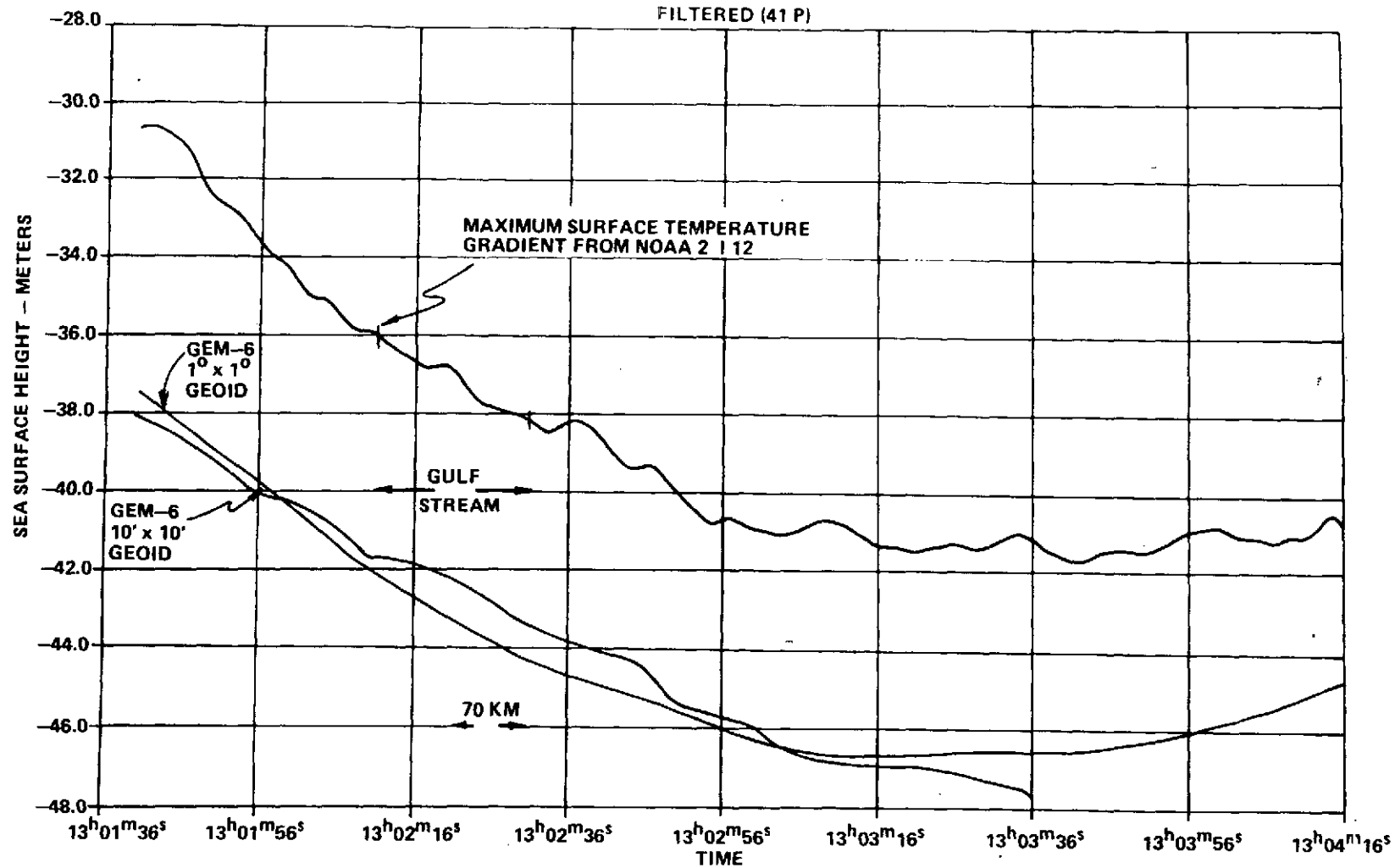


FIGURE 23. FILTERED ALTIMETER GEOID AND GEM-6 GEOID HEIGHTS

REFERENCES

1. Miller, L. S. and Hammond, D. L., "Objectives and Capabilities of the SKYLAB S-193 Altimeter Experiment," IEEE Trans. on Geosc. Elect., GE-10, NO1, pp. 73-79, January 1972.
2. McGoogan, J. T., "Precision Satellite Altimetry," 1974 IEEE Intercon Technical Papers, Earth and Ocean Physics Application Program, March 26-29, 1974.
3. Martin, C. F., "Optimum Use of Ground Stations for GEOS-C Orbit Determinations," Sea Surface Topography from Space, vol. 1, 9-1 to 9-15, NOAA TR ERL-AOML 7, 1972.
4. Lerch, F. J. et al, "Gravitational Field Models of the Earth (GEM 1 & 2)," GSFC Document X-553-72-146, May 1972.
5. McGoogan, J. T., et al, "The S-193 Radar Altimeter Experiment," Proceeding of IEEE, vol. 62, No. 6, June 1974.
6. Private Communication by Dr. L. S. Miller, Applied Sciences Associates, Apex, N.C., 1974.
7. Goad, Clyde C. and Martin, C. F., "Effects of Tropospheric and Ionospheric Refraction Errors in the Utilization of GEOS-C Altimeter Data," Planetary Sciences Department Report No. 008-74, Prepared for NASA Contract No. NAS6-2173, October 1974.
8. Vincent, S. and Marsh, J. G., "Global Detailed Gravimetric Geoid," NASA Goddard Space Flight Center, Rep. X-592-73-266, September 1973.
9. Leitao, C. D. and McGoogan, J. T., "Skylab Radar Altimeter: Short Wavelength Perturbations Detected in Ocean Surface Profiles," Science, vol. 186, September 1974.
10. Gaposchkin, E. M., "Smithsonian Standard Earth III," Presented at the American Geophysical Union Meeting, Washington, D. C., 1973.
11. Rapp, R. H., "The Earth's Gravitational Field from the Combination of Satellite and Terrestrial Data," Paper presented at the Symposium on Earth's Gravitational Field and Secular Variations in Position, Sydney, Australia, Nov. 1973 (in press), 1974.
12. McGoogan, J. T., Leitao, C. D., Miller, L. S. and Wells, W. T., "SKYLAB S-193 Altimeter Experiment Performance, Results and Applications, Presented at the International Symposium on Applications of Marine Geodesy, Columbus, Ohio, June 3-5, 1974.
13. Brown, R. D. and S. Vincent, "Power Spectra of Geoid Undulations," Presentation at the December 1972 AGU Meeting, San Francisco.
14. Merriam, C. W., "Optimization Theory and the Design of Feedback Control Systems, McGraw-Hill Book Co., New York, 1964.